

Dissertation zur Erlangung des Doktorgrades  
der Fakultät für Chemie und Pharmazie  
der Ludwig-Maximilians-Universität München



**Aliphatic and Aromatic Amines: C-H Bond  
Functionalization and Kinetics of Their  
Reactions with  $\beta$ -Lactones,  $\beta$ -Lactams, and  
Carbocationic Electrophiles**

Elija Nathan Wiedemann

aus

Augsburg

2019



# Erklärung

Diese Dissertation wurde im Sinne von § 7 der Promotionsordnung vom 28. November 2011 von Herrn PD Dr. Armin R. Ofial betreut.

## Eidesstattliche Versicherung

Diese Dissertation wurde eigenständig und ohne unerlaubte Hilfe erarbeitet.

München, den 05.11.2019

.....

(Elija Wiedemann)

Dissertation eingereicht am 05.09.2019

1. Gutachter: PD Dr. Armin R. Ofial

2. Gutachter: Prof. Dr. Oliver Trapp

Mündliche Prüfung am 02.10.2019



Für Tanja





# Danksagung

Zu allererst möchte ich mich bei Prof. Dr. Herbert Mayr und PD Dr. Armin R. Ofial bedanken. Nicht nur für die Möglichkeit, diese Dissertation in Ihrem Arbeitskreis anzufangen bzw. abzuschließen zu können, sondern auch für die Freiheiten bei der Umsetzung der Forschungsarbeit.

Bei Prof. Dr. Oliver Trapp möchte ich mich für die Zweitbegutachtung meiner Arbeit bedanken.

Dr. Sabine Schneider, Prof. Dr. Bracher und Prof. Dr. Karaghiosoff danke ich für ihre Teilnahme am Prüfungsausschuss.

Mein Dank gilt allen Angehörigen der Analytikabteilung, die unermüdlich meine Aufträge bearbeiteten. Besonders Danke ich Dr. Stephenson und Prof. Dr. Karaghiosoff für die hilfreichen Diskussionen und die Durchführung der Analysen zu jeder Tages- und Nachtzeit. Carola Draxler, Sonja Kosak und Claudia Ober für die stets schnelle Bearbeitung meiner Aufträge. Susanne Ebert, die nicht nur meine Analysen schnell bearbeitet, sondern auch das Archiv für mich noch einmal umgewälzt hat. Dafür vielen Dank.

Dr. Bernhard Kempf und Felix Kalfa für die gute Zusammenarbeit im Praktikum. Simon Matthe für die Unterstützung mit Chemikalien, Rat und Tat. Seine Hände können wahre Wunder vollbringen und müden Maschinen wieder neues Leben einhauchen.

Tanja Schmid, die mich mit ihrer positiven Art jahrelang begleitet und getragen hat. In guten wie in schlechten Zeiten. Ohne die ich dieses Studium nie abgeschlossen hätte. Unserer gemeinsamen Vorbereitung auf die POC Klausur verdanke ich meine Dissertationsstelle. Und so blicke ich zurück auf die schönsten Jahre meines Lebens. Deshalb einfach: Herzlichen Dank ♥

Bedanken möchte ich mich bei allen KollegINNen, die mir in all den Jahren geholfen und mich ermuntert. Besonders bedanken möchte ich mich bei Katharina Böck und Nathalie Hampel, die mich unermüdlich unterstützt haben und auch in tiefen Krisen stets an meiner Seite waren. Bei meinem direkten Subarbeitskreiskollegen Alexander „Der Oberunterführer“ Wagner. Bei Ivo Zenz, der mich zum JungChemikerForum gebracht hat, Francisco Corral-Bautista und Angel Puente für zahllose Stunden Frohsinn. Johannes Ammer und Tobias Nigst für die wissenschaftliche Unterstützung in jeder Form. Dominik Allgäuer, denn keiner ist unnütz. Brigitte Janker für Material und Hilfe mit den technischen Geräten. Konstantin Troshin für seinen wissenschaftlichen Input und seine Fähigkeit, Probleme (z.B. Gasflaschen, verkantete Schliffe und verbackene Flaschen) aus dem Weg zu räumen. Saloua Chelli und Sami Lakhdar und natürlich Hans Laub („Ons“), ohne dessen Premium Kinetiken das „Lazy Lab“ nicht hätte existieren können. Daniel Beck, la plej bona estro de neorganika kemio kaj bona amiko en ĉiuj situacioj.

Gökçen Savaşçı und Laurens Peters danke ich für das Aushelfen bei Computerproblemen und Durchführung von Berechnungen. Robert Mayer danke ich herzlichst für die Last-Minute Korrekturen und seine bereitwillige Unterstützung bei der Literaturrecherche und Hinweise auf Datenbanken, die ich ohne ihn nie gefunden hätte. Des Weiteren danke ich ihm für die Messung des letzten NMR Spektrums und Durchführung der letzten quantenchemischen Berechnungen. Er trug mich quasi über die Ziellinie. Ich erwarte noch viel von ihm zu hören.

Herzlichen Dank auch an all meine Forschungspraktikanten: Florian Zischka, Veit Giegold, Aaron Gerwien, Philip Watson, Korbinian Sommer, Sophia Schwarz und Andreas Locher. An meine Schülerpraktikanten Alex und Sonja, sowie meine OC-Li(gh)t-Studenten (u. a. Aaron, Adrian, Alex, Andi, Bettina, Britta, Daniel, Felix, Jakob, Jens, Henning, Kuno, Luci, Martin, Martin, Marlo, Michi, Nicole, Niklas, Philip, Sebastian, Simon, Sonja, Steffi, Susi, Tim, Thomas, Veit, Violeta).

Mein Dank gilt allen Mitgliedern und Vorständen des JungChemikerForums, mit denen ich über viele Jahre in diesem Gremium arbeiten durfte.

Alexandra Motz danke ich für ihre unermüdliche Aufbauarbeit und Carina Glas für die aufmunternden Sprüche und ihre Unterstützung bei der Prüfungsvorbereitung.

Matthias Wilhelms danke ich für die Einführung in die hohe Kunst des Brauens.

Bedanken möchte ich mich auch bei allen, die für mich einen guten Rat und ein Bett hatten. Namentlich Amelie, Anne-Marie, Caro, ChristOoph, Eva, Ines, Pascal, Martina, Martina, Martin, Micha, Michaela, Milena, Ramona, Sabine und Simon.

Besonderer Dank geht an alle, die sich für die Freiheit der Forschung und gegen die Kommerzialisierung von Forschungsergebnissen einsetzen, vor allem, wenn diese aus öffentlichen Mittel finanziert wurden. Im speziellen möchte ich dem Team von Sci-Hub ([sci-hub.tw](http://sci-hub.tw)) danken.

Meine Eltern, die mir finanziell und moralisch immer den Rücken freigehalten haben und mir die Möglichkeit gaben, dieses Studium anzutreten und durchzustehen. Meinen Großeltern, die immer für mich da waren und bei denen ich stets ein offenes Ohr gefunden habe.

All meinen Freunden, die mich immer mit einem flotten Spruch auf den Lippen angespornt haben. Ihr haltet den Erfolg hiermit in Euren Händen. Und natürlich Ihnen, liebe(r) Leser(in).

Die Reihenfolge der Nennung stellt keine Gewichtung dar. Die Liste erhebt keinen Anspruch auf Vollständigkeit.

## Publications

Kinetic and Theoretical Studies of Beta-Lactone Reactivity – A Quantitative Scale for Biological Application

Elija N. Wiedemann, Franziska A. Mandl, Iris D. Blank, Christian Ochsenfeld, Armin R. Ofial und Stephan A. Sieber, *ChemPlusChem* **2015**, *80*, 1673–1679.

## Contributions to Conferences

Kinetic Studies of Beta-Lactone Reactivity

Elija N. Wiedemann, Franziska A. Mandl, Armin R. Ofial und Stephan A. Sieber, Workshop of the Sonderforschungsbereich 749, Wildbad Kreuth (Germany), 2013.

Kinetic and Theoretical Studies of Beta-Lactone Reactivity

Elija N. Wiedemann, Franziska A. Mandl, Iris D. Blank, Christian Ochsenfeld, Armin R. Ofial und Stephan A. Sieber, Workshop of the Sonderforschungsbereich 749, Venice (Italy), 2014.

Kinetic and Theoretical Studies of Beta-Lactone Reactivity

Elija N. Wiedemann, Franziska A. Mandl, Iris D. Blank, Christian Ochsenfeld, Armin R. Ofial und Stephan A. Sieber, Workshop of the Sonderforschungsbereich 749, Munich (Germany), 2015.



# Table of Contents

Chapter 0	Introduction	1
	Summary	5
Chapter 1	Kinetic and theoretical studies of beta-lactone reactivity – a quantitative scale for biological application	13
	Supporting Information	29
Chapter 2	Transition Metal-Free C-H Functionalization of Tertiary Amines: Diisopropyl Azodicarboxylate Mediated $\alpha$ -Arylations	67
	Supporting Information	79
Chapter 3	Quantification of the Nucleophilic Reactivities of <i>N,N</i> -Dialkylated Anilines	153
	Supporting Information	211



## List of Abbreviations

2d	two-dimensional
ani	anisyl, 4-methoxyphenyl
app	apparent
Ar	aryl
benzhydrylium ion	diaryl substituted methylium ion
BBL	Beta-butyrolactone
br s	broad singlet
COSY	correlation spectroscopy
d	day; in the description of NMR spectra: doublet
DAAD	dialkyl azodicarboxylate
DEAD	diethyl azodicarboxylate
DIAD	diisopropyl azodicarboxylate
dma	4-(dimethylamino)phenyl
DMSO	dimethylsulfoxide
dpa	4-(diphenylamino)phenyl
EI	electron impact ionization
Et	ethyl
eq.	equation
equiv.	equivalent
eV	electron volt
g	gram
gHSQC	gradient HSQC
GB	gas-phase basicity
GP	general procedure
LC	liquid chromatography
h	hour
3-HBA	3-hydroxy butyric acid
HMBC	heteronuclear multiple bond correlation
HPLC	high performance liquid chromatography
HR-MS	high-resolution mass spectrometry
HSQC	heteronuclear single quantum coherence
HT	high temperature
Hz	Hertz
ind	1-methylindolin-5-yl
<i>J</i>	coupling constant
jul	julolidinyl (= 2,3,6,7-tetrahydro-1 <i>H</i> ,5 <i>H</i> -benzo[ <i>ij</i> ]quinolizin-9-yl)
L	liter
M	molar
m	multiplet
max.	maximum
3-MBA	3-(( <i>para</i> -methoxyphenyl)amino)butanoic acid
Me	methyl
mfa	4-(methyl(2,2,2-trifluoroethyl)amino)phenyl

mg	milligram
MHz	megahertz
min	minute
mL	milliliter
mmol	millimol
mor	4-morpholinophenyl
Mp	melting point
MP-11	Microperoxidase-11
mpa	4-(methyl(phenyl)amino)phenyl
MS	mass spectrometry
ms	millisecond
n. d.	not determined
NMR	nuclear magnetic resonance
ORTEP	oak ridge thermal ellipsoid plot program
3-PBA	3-(phenylamino) butyric acid
PBP	penicillin-binding-protein
PenG	penicillin G
pfa	4-(phenyl(2,2,2-trifluoroethyl)amino)phenyl
Ph	phenyl
pip	4-(piperidin-1-yl)phenyl
3-PhosBA	3-(phosphonoxy)butyric acid
pos.	positive
ppm	parts per million
pyr	4-(pyrrolidin-1-yl)phenyl
q	quartet
QM/MM	quantum mechanics/molecular mechanics
quat.	quaternary
r.t.	room temperature
ref.	reference
s	second; in the description of NMR spectra: singlet
sept	septet
<i>T</i>	temperature
<i>t</i>	time; in the description of NMR spectra: triplet
3-mTBA	3-( <i>meta</i> -tolylamino)butyric acid
3-pTBA	3-( <i>para</i> -tolylamino)butyric acid
TEA	triethanolamine
tert.	tertiary
TFA	trifluoroacetic acid
THIQ	1,2,3,4-tetrahydroisoquinoline
thq	1-methyl-1,2,3,4-tetrahydroquinolin-6-yl
tol	tolyl
Tr	trityl
TRIS	tris(hydroxymethyl)-aminomethane
UV	ultra violet
vis	visible
vol	volume
vs.	versus

## Chapter 0

### Introduction

Many attempts have been undertaken to construct a general reactivity scale that can be used to classify the reactivity of both, organic and inorganic compounds. During the recent decades, Mayr et al. have constructed a comprehensive nucleophilicity scale which is based on the kinetics of the reactions of  $\pi$ -,  $n$ -, and  $\sigma$ -nucleophiles with benzhydrylium ions, structurally related quinone methides, and diethyl benzyldenemalonates.<sup>[1]</sup>

The second-order rate constants of these reactions have been described by the linear free energy relationship (Equation 1), where  $E$  is an electrophile-specific solvent-independent parameter, and  $N$  and  $s_N$  are solvent dependent nucleophile-specific parameters.

$$\lg k_2 (20\text{ }^\circ\text{C}) = s_N (N + E) \quad (1)^{[1]}$$

Natural products comprise a rich source for bioactive molecules with medicinal relevance. Many of these contain electrophilic scaffolds that covalently bind the active sites of conserved enzymes.<sup>[2]</sup> Prominent examples include beta-lactams and beta-lactones which specifically acylate serine residues in diverse peptidases.<sup>[3]</sup> For our studies, we decided to investigate penicillin G and the beta-butyrolactone as model compounds. To quantify and dissect the differences in bioactivities, the kinetics of the reactions of beta-butyrolactam, beta-butyrolactone and penicillin G (Figure 1) with reference nucleophiles have been analyzed with a set of reference amines in pH-buffered aqueous solution at 37 °C. The relative reactivity of beta-butyrolactam, beta-butyrolactone and penicillin G could therefore be elucidated.

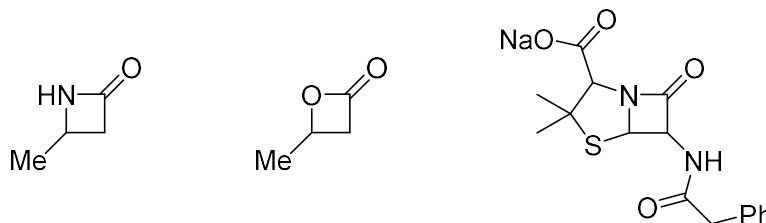
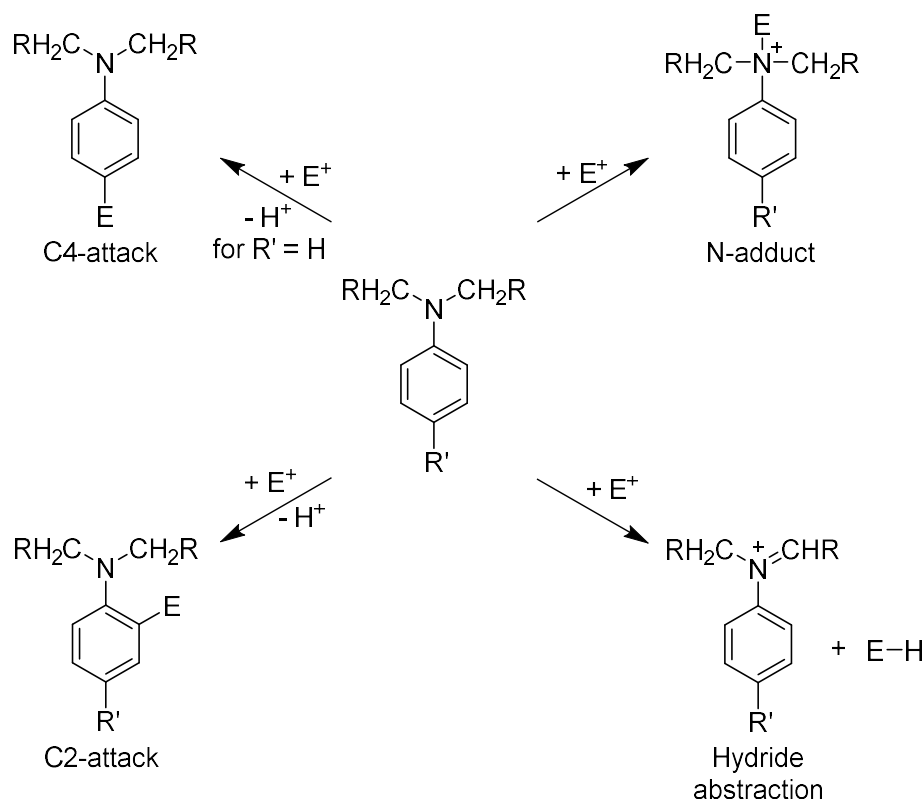


Figure 1: Beta-butyrolactone and beta-butyrolactams studied in this work.

As a second project, in this work, equation 1 was used to characterize the ambident nucleophilic reactivity of  $N,N$ -dialkylated anilines.  $N,N$ -Dialkylated anilines are highly important in organic chemistry as they are used as activator for polymerisations<sup>[4]</sup> as well as for the production of

dyes,<sup>[5]</sup> pharmaceuticals and agricultural chemicals.<sup>[6]</sup> Numerous kinetic studies on the reactivities of amines,<sup>[7]</sup> azoles,<sup>[8]</sup> and pyridines<sup>[9]</sup> have been performed, but kinetic data for the reactions of *N,N*-dialkylated anilines with carbocations are very limited to date.



Scheme 1: Possible reactions of *N,N*-dialkylated anilines with cationic electrophiles.

Using the system of Mayr et al., the reactivities of *N,N*-dialkylated anilines were studied with benzhydrylium ions in acetonitrile and dichloromethane at 20 °C.<sup>[1]</sup> *N,N*-Dialkylated anilines can react with carbocations via four different pathways (Scheme 1). Beside the reaction at the C2 and C4 ring carbon, both the attack of the nitrogen atom and hydride abstraction at the alkyl group in alpha position to the nitrogen atom are possible. In this thesis, beside *N,N*-dimethylaniline, various substitution patterns of the alkyl groups, as well as the influence of different substituents at the aromatic ring were studied (Figure 2).

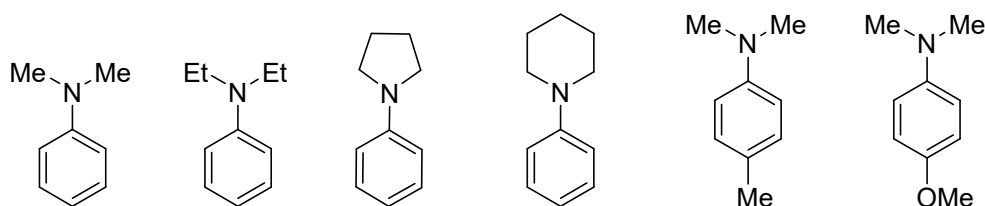
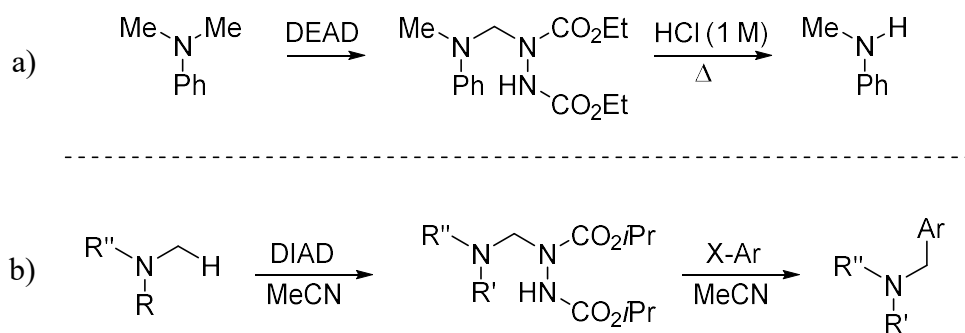


Figure 2: *N,N*-Dialkylated anilines investigated in this work.

By studying the kinetics of their reactions with benzhydrylium ions, the reactivity at the nitrogen atom of all studied *N,N*-dialkylated anilines was quantified. It was further possible to study the reactivity at the C4 carbon ring atom of *N,N*-dimethylaniline, *N,N*-diethylaniline and 1-phenylpyrrolidine as well as the selective abstraction of an hydride of *N,N*-dimethylaniline by using tritylium ions as alternative reference electrophiles.

*N,N*-Dimethylaniline is not only interesting in terms of its reactivity. Functionalization of tertiary amines at the  $sp^3$ -hybridized  $\alpha$ -carbon has been an emerging field of organic chemistry in recent years.<sup>[10]</sup> Using this synthetic method for the introduction of an aryl moiety would furnish benzylic amines, which are a common structural motif of market-relevant pharmaceuticals.<sup>[11]</sup> Beside others, the work of Diels and Paquin from 1913<sup>[12]</sup> led us to a synthetic approach (Scheme 2).



Scheme 2: a) DEAD mediated selective demethylation of *N,N*-dimethylaniline by Diels and Paquin.<sup>[12]</sup> b) Our synthetic approach for the functionalization of *N,N*-dimethylated anilines and aliphatic tertiary amines.

According to a procedure from Diels and Paquin of 1913<sup>[12]</sup> we treated *N,N*-dimethylated anilines with diisopropyl azodicarboxylate (DIAD) to generate *N*-aminomethylated hydrazine-1,2-dicarboxylates. These hydrazine-adducts react under acidic conditions with potassium aryltrifluoroborates as nucleophiles to yield the corresponding cross coupling products. In contrast to other procedures, this method works without addition of transition metal catalysts or water under acid conditions. Thus, we herein report a transition metal-free<sup>[13]</sup> two-step synthesis of  $\alpha$ -arylated amines from tertiary amines, DIAD and organotrifluoroborates.

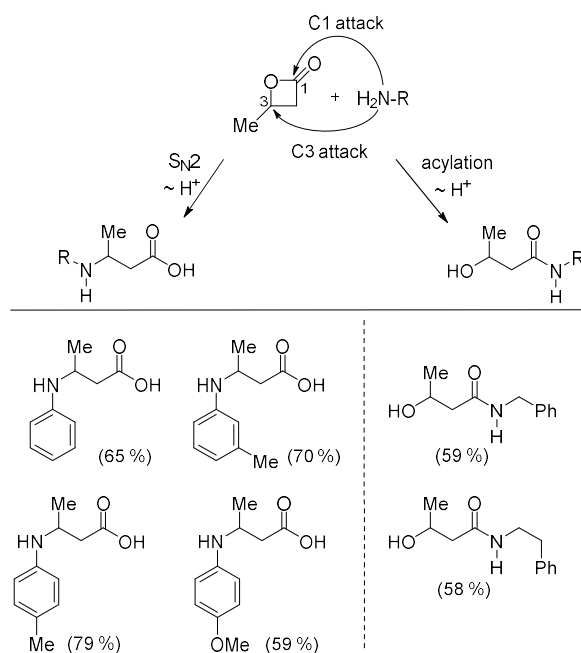
## References

- [1] H. Mayr, M. Patz, *Angew. Chem. Int. Ed.* **1994**, *33*, 938–957; *Angew. Chem.* **1994**, *106*, 990–1010.
- [2] a) M. Gersch, J. Kreuzer, S. A. Sieber, *Nat. Prod. Rep.* **2012**, *29*, 659–682; b) C. Drahl, B. F. Cravatt, E. J. Sorensen, *Angew. Chem. Int. Ed. Engl.* **2005**, *44*, 5788–5809. c) J. A. H. Schwöbel, Y. K. Koleva, S. J. Enoch, F. Bajot, M. Hewitt, J. C. Madden, D. W. Roberts, T. W. Schultz, M. T. D. Cronin, *Chem. Rev.* **2011**, *111*, 2562–2596.
- [3] D. J. Waxman, J. L. Strominger, *Annu. Rev. Biochem.* **1983**, *52*, 825–869.
- [4] a) A. Pfeil, *EP2532636* **2012**, *A2*; b) T. Bürgel, *EP2518033* **2012**, *A2*.
- [5] P. Grieb, *Chem. Ber.* **1877**, *10*, 528.
- [6] a) *National Toxicology Program. Toxicology and Carcinogenesis Studies of N,N-Dimethylaniline (CAS No. 121-69-7) in F344/N Rats and B6C3F1 Mice (Gavage Studies). TR No. 360. U.S. Department of Health and Human Services, Public Health Service, National Institutes of Health, Bethesda, MD, 1989*; b) M. Sittig, *Handbook of Toxic and Hazardous Chemicals and Carcinogens 2nd edn*, Noyes Publications, Park Ridge, NJ, **1985**; c) *U.S. Department of Health and Human Services. Hazardous Substances Data Bank (HSDB, online database). National Toxicology Information Program, National Library of Medicine, Bethesda, MD, 1993*; d) J. E. Amooore, E. Hautala, *J. Appl. Toxicol.* **1983**, *3*, 272–290.
- [7] a) C. F. Bernasconi, M. Panda, *J. Org. Chem.* **1987**, *52*, 3042–3050; b) J. P. Richard, T. L. Amyes, T. Vontor, *J. Am. Chem. Soc.* **1992**, *114*, 5626–5634; c) B. Varghese, S. Kothari, K. K. Banerji, *Int. J. Chem. Kinet.* **1999**, *31*, 245–252; d) J. P. Richard, M. M. Toteva, J. Crugeiras, *J. Am. Chem. Soc.* **2000**, *122*, 1664–1674; e) M. R. Crampton, T. A. Emokpae, C. Isanbor, *J. Phys. Org. Chem.* **2006**, *19*, 75–80; f) E. N. Wiedemann, F. A. Mandl, I. D. Blank, C. Ochsenfeld, A. R. Ofial, S. A. Sieber, *ChemPlusChem* **2015**, *80*, 1673–1679; g) F. Brotzel, Y. C. Chu, H. Mayr, *J. Org. Chem.* **2007**, *72*, 3679–3688; h) J. Ammer, M. Baidya, S. Kobayashi, H. Mayr, *J. Phys. Org. Chem.* **2010**, *23*, 1029–1035.
- [8] a) C. K. M. Heo, J. W. Bunting, *J. Chem. Soc. Perkin Trans. 2* **1994**, 2279–2290; b) A. A. Matveev, A. N. Vdovichenko, A. F. Popov, L. M. Kapkan, A. Y. Chervinskii, V. N. Matvienko, *Russ. J. Org. Chem.* **1995**, *31*, 1646–1649; c) T. B. Phan, M. Breugst, H. Mayr, *Angew. Chem. Int. Ed.* **2006**, *45*, 3869–3874; d) M. Baidya, F. Brotzel, H. Mayr, *Org. Biomol. Chem.* **2010**, *8*, 1929–1935; e) B. Maji, H. Mayr, *Angew. Chem.* **2013**, *125*, 11370–11374.
- [9] a) E. M. Arnett, R. Reich, *J. Am. Chem. Soc.* **1980**, *102*, 5892–5902; b) Y. Kondo, R. Uematsu, Y. Nakamura, S. Kusabayashi, *J. Chem. Soc. Perkin Trans. 2* **1998**, 1219–1224; c) S.-D. Yoh, D.-Y. Cheong, O.-S. Lee, *J. Phys. Org. Chem.* **2003**, *16*, 63–68; d) F. Brotzel, B. Kempf, T. Singer, H. Zipse, H. Mayr, *Chem. Eur. J.* **2007**, *13*, 336–345.
- [10]  $\alpha$ -Functionalizations of amines have been reviewed: a) K. R. Campos, *Chem. Soc. Rev.* **2007**, *36*, 1069–1084; b) K. Jones, M. Klussmann, *Synlett* **2012**, *23*, 159–162; c) E. A. Mitchell, A. Peschiulli, N. Lefevre, L. Meerpoel, B. U. W. Maes, *Chem.–Eur. J.* **2012**, *18*, 10092–10142; d) M.-X. Cheng, S.-D. Yang, *Synlett* **2017**, *28*, 159–174; e) A. Gini, T. Brandhofer, O. García Mancheño, *Org. Biomol. Chem.* **2017**, *15*, 1294–1312.
- [11] a) N. A. McGrath, M. Brichacek, J. T. Njardarson, *J. Chem. Educ.* **2010**, *87*, 1348–1349; b) F. Weber, G. Sedelmeier, *Nachr. Chem.* **2014**, *62*, 997.
- [12] O. Diels, M. Paquin, *Ber. Dtsch. Chem. Ges.* **1913**, *46*, 2000–2013.
- [13] a) S. Roscales, A. G. Csáký, *Chem. Soc. Rev.* **2014**, *43*, 8215–8225; b) F. Sánchez-Sancho, A. G. Csáký, *Synthesis* **2016**, *48*, 2165–2177.

## Summary

### Kinetic and theoretical studies of beta-lactone reactivity – a quantitative scale for biological application

The second-order rate constants ( $k_2$ ) for the reactions of beta-butyrolactone and penicillin G were studied with a set of reference amines in buffered aqueous solution at 37 °C. In case of these studies, several buffer systems were investigated. All buffers reacted with beta-butyrolactone, but smallest conversion was found with triethanolamine (TEA). Different product ratios of C1 vs. C3 attack on the beta-butyrolactone have been observed, depending on the aliphatic or aromatic nature of the standard amine used (Scheme 1). The first-order rate constants ( $k_{\text{obs}}$ ) obtained for the reaction of beta-butyrolactone with aniline were found to correlate linearly with the concentrations of the anilines and second-order rate constants ( $k_N$ ) could, therefore, be obtained with aromatic and aliphatic amines (example see Figure 1). In correspondence with their weak proteome reactivity, monocyclic beta-lactams did not react with our set of standard nucleophiles studied herein. Bicyclic beta-lactams, however, exhibited a lower activation barrier, and thus, reacted with standard nucleophiles. The experimental results were verified by theoretical studies using combined quantum mechanics/molecular mechanics (QM/MM).



Scheme 1: Products of the reactions of beta-butyrolactone with amines in  $\text{H}_2\text{O}/\text{MeCN}$  9/1 (v/v) (yields refer to isolated products).

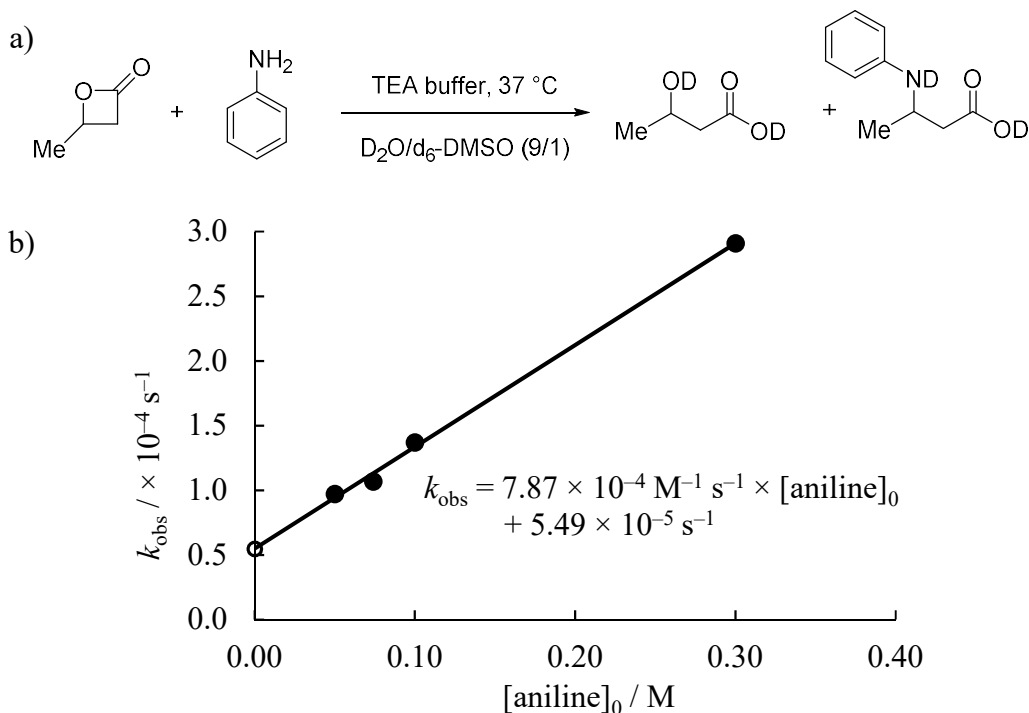


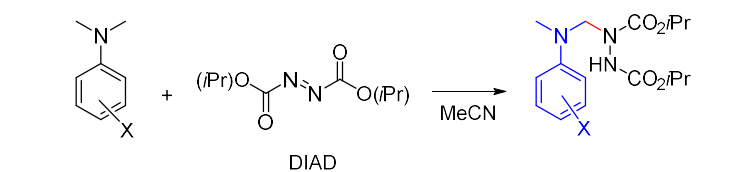
Figure 1: a) Reaction of beta-butylolactone with aniline in D<sub>2</sub>O/*d*<sub>6</sub>-DMSO 9/1 (v/v) at 37 °C. b) Linear dependence of the first-order rate constant  $k_{\text{obs}}$  for the reaction of beta-butylolactone with aniline on the concentration of aniline at 37 °C ( $k_{\text{obs}}$  for  $[\text{aniline}]_{\text{eff}} = 0$  corresponds to the hydrolysis of beta-butylolactone in triethanolamine (TEA)-buffered solution; not considered for the depicted linear correlation).

## Transition Metal-Free C-H Functionalization of Tertiary Amines: Diisopropyl Azodicarboxylate Mediated $\alpha$ -Arylations

Aromatic and aliphatic tertiary methylamines RR'NCH<sub>2</sub>-H were converted to  $\alpha$ -arylated amines RR'NCH<sub>2</sub>-Ar in two steps. In the first step, tertiary methylamines and a slight excess of diisopropyl azodicarboxylate (DIAD, 1.1 equiv.) reacted in acetonitrile to generate *N*-aminomethylated hydrazine-1,2-dicarboxylates. These amins were isolated with good yields in the range of 71–95% (Table 1). The reaction time could be shortened by heating the reaction mixture, as shown for the reaction of *N,N*-dimethyl-*para*-anisidine with DIAD (Table 1, entry 2 and 3). In an initial attempt, the *para* methyl substituted diisopropyl 1-((methyl(*p*-tolyl)amino)methyl)hydrazine-1,2-dicarboxylate was reacted with 2-methylfuran and furnished the desired  $\alpha$ -arylated amine in good yield (Scheme 2). The scope of the reaction with

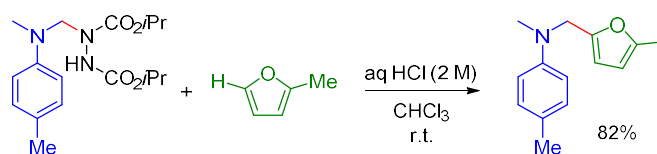
unfunctionalized arenes was, however, limited to this reaction. Reactions of these hydrazines with potassium (hetero)aryltrifluoroborates at ambient temperature in the presence of one equivalent of trifluoroacetic acid in acetonitrile furnished  $\alpha$ -arylated amines (Figure 2). Also tropinone was converted to different (hetero-aryl)methylated nortropinones (Scheme 3). Both steps of the reaction sequence occurred without addition of a metal-based catalyst.

Table 1: Addition of DIAD to *N,N*-dimethylanilines.



Aniline, X =	Hydrazine Yield <sup>[a]</sup> (%)
4-Me	95 (4 d, rt)
4-OMe	78 (2 d, rt) 81 (4 h, rflx)
H	86 (5 d, rt)
4-F	88 (2 d, rt)
4-Cl	74 (3 d, rflx)
4-Br	87 (3 d, rflx)
4-CO <sub>2</sub> Et	86 (2 d, rflx)
4-CN	71 (2 d, rt)
2,4,6-(Me) <sub>3</sub>	87 (10 h, rflx)

[a] Yield of isolated product after column chromatography.



Scheme 2: Brønsted acid mediated  $\alpha$ -arylation of diisopropyl 1-((methyl(*p*-tolyl)amino)methyl)hydrazine-1,2-dicarboxylate with 2-methylfuran.

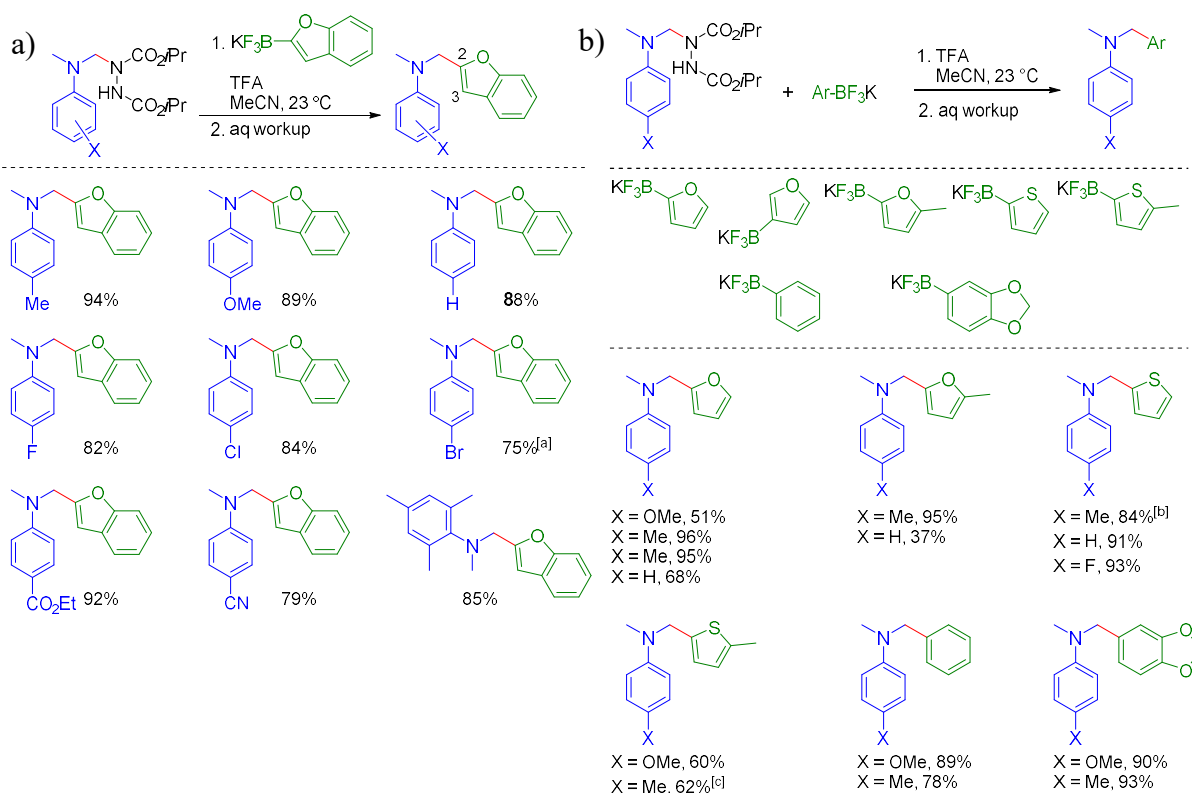
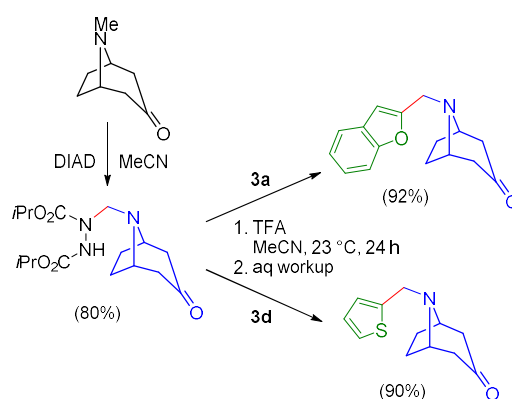


Figure 2: a) DIAD-mediated aminomethylations of potassium benzofuran-2-yl trifluoroborate by the ring-substituted *N,N*-dimethylaniline derivatives. b) DIAD-mediated  $\alpha$ -(hetero)arylations of diisopropyl hydrazine carboxylates. All yields refer to isolated products after purification by column chromatography. Reactions with the furan-2-yl trifluoroborate and the furan-3-yl trifluoroborate yield the same product. [a] Reaction at >1 mmol scale. [b] With 0.74 equiv. TFA. [c] With 0.37 equiv. TFA.



Scheme 3: Conversion of tropinone to (hetero-aryl)methylated nortropinones via DIAD-activated tropinone.

## Quantification of the Nucleophilic Reactivities of *N,N*-Dialkylated Anilines

The second-order rate constants ( $k_2$ ) for the reactions of *N,N*-dialkylated anilines were studied with benzhydrylium and tritylium ions as reference electrophiles in acetonitrile and dichloromethane at 20 °C by UV/Vis and  $^1\text{H}$  NMR spectroscopy. Product studies were performed with *para*-unsubstituted *N,N*-dialkylated anilines, yielding triarylmethanes as result of the attack at C4 carbon of the *N,N*-dialkylated anilines. The consumption of the electrophile and the formation of the according triarylmethane was followed by time-resolved  $^1\text{H}$  NMR spectroscopy. Applying UV/Vis spectroscopy, in most cases a bisexponential decay of the time-dependent absorbance of the electrophiles was observed (Figure 3).

The measured rate constants correlated linearly with the electrophilicity parameters of the respective electrophile allowing us to derive their nucleophilicity parameters  $N$  and  $s_N$  for the attack of the *N,N*-dialkylated anilin's C4 and nitrogen atom (examples are shown in Figure 4). The nucleophilic reactivities of the studied *N,N*-dialkylated anilines are in a comparable range for the attack of the C4 carbon in acetonitrile and dichloromethane, respectively. For the attack at the nitrogen atom, they cover a range of nearly 4 orders of magnitude (Figure 5). Furthermore, second-order rate constants for the selective abstraction of a hydride from the  $\text{CH}_3$  group in  $\alpha$ -position of the N atom, were measured, by studying the kinetics of the reactions with tritylium ions (Scheme 4).

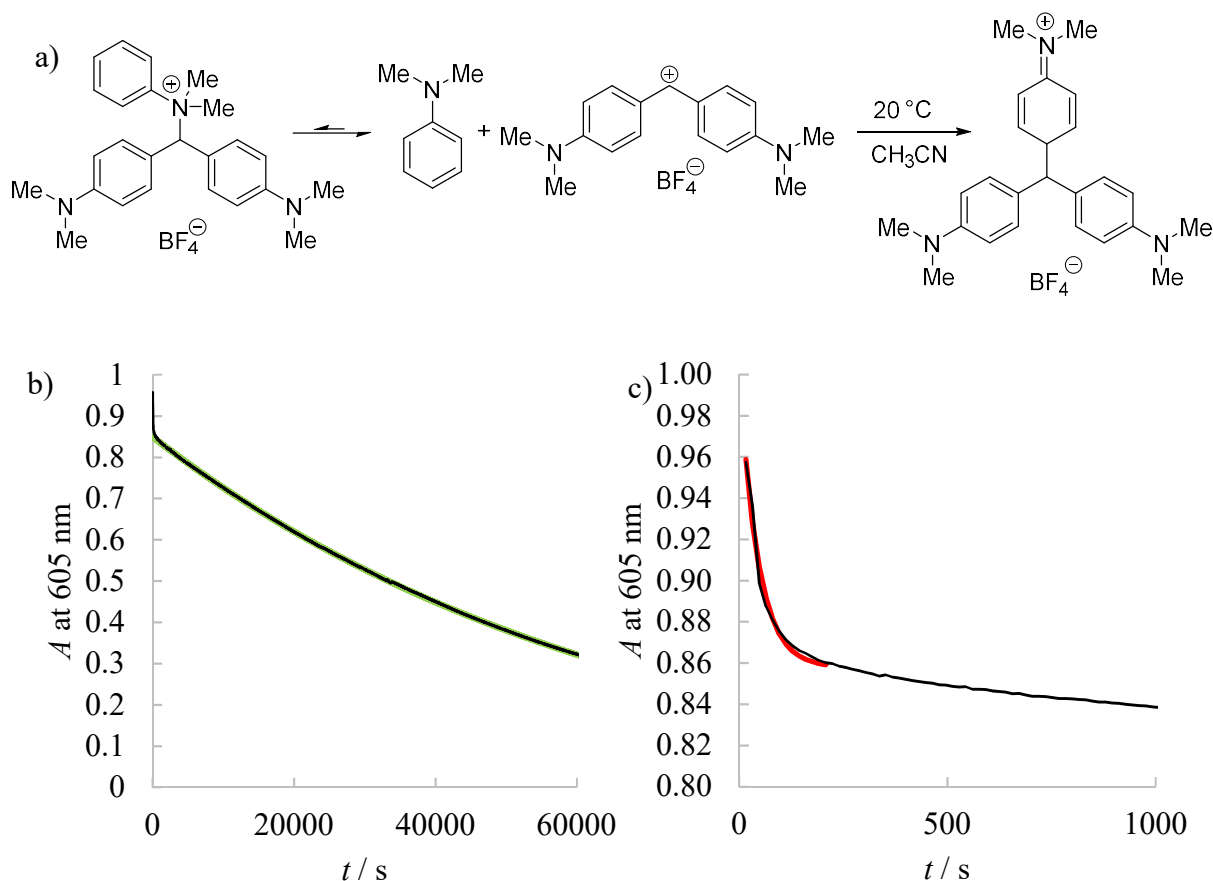


Figure 3: a) Reaction of *N,N*-dimethylaniline with  $(\text{dma})_2\text{CH}^+ \text{BF}_4^-$  in  $\text{CH}_3\text{CN}$  at  $20^\circ\text{C}$ . b) Plot of the absorbance  $A$  at 605 nm vs. time for the reaction of *N,N*-dimethylaniline ( $c = 1.67 \times 10^{-3} \text{ M}$ ) with electrophile  $(\text{dma})_2\text{CH}^+$  ( $c = 1.16 \times 10^{-5} \text{ M}$ ) in acetonitrile at  $20^\circ\text{C}$  with the calculated absorbance for the attack of the C4 carbon of *N,N*-dimethylaniline (green line;  $k_{\text{obs}} = 1.48 \times 10^{-5} \text{ s}^{-1}$ ). b) Enhancement of the first seconds. The first absorbance drop can be described by another monoexponential function and is assigned to the attack of the nitrogen atom of *N,N*-dimethylaniline (red line;  $k_{\text{obs}} = 2.28 \times 10^{-2} \text{ s}^{-1}$ ).

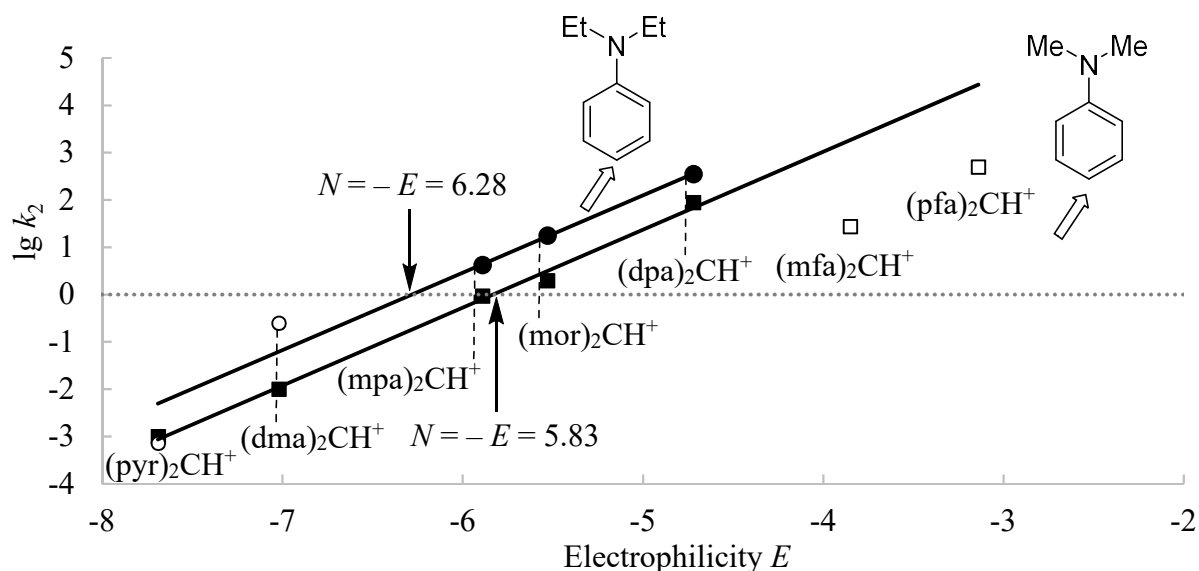
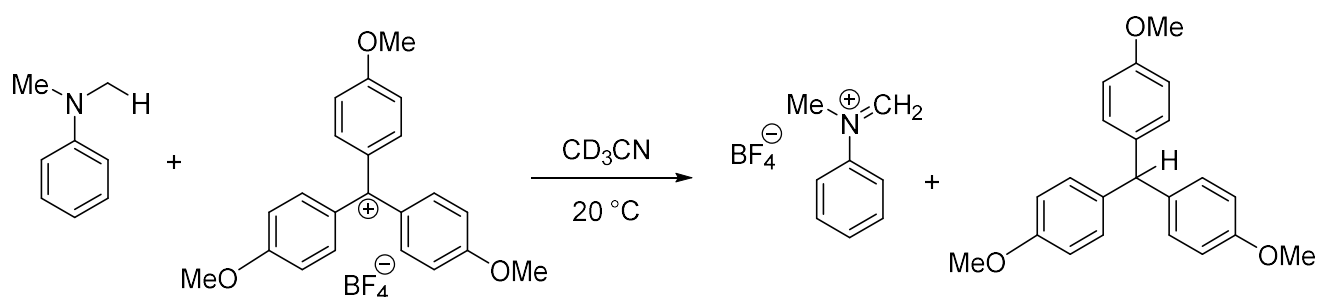


Figure 4: Correlation of the rate constants  $\lg k_2$  for the reactions of *N,N*-dimethylaniline (squares) and *N,N*-diethylaniline (circles) at the C4 ring carbon with benzhydrylium ions in acetonitrile at 20 °C with their electrophilicity parameters  $E$ . The  $N$  parameters are derived as the intercepts on the abscissa (stroked line,  $N = -E$  at  $\lg k_2 = 0$ ;  $N = 5.83$  for *N,N*-dimethylaniline and  $N = 6.28$  for *N,N*-diethylaniline), the  $s_N$  parameters are the slopes of the correlation lines ( $s_N = 1.69$  for *N,N*-dimethylaniline and  $s_N = 1.64$  for *N,N*-diethylaniline). The open symbols were not used for the calculation of the correlation line.



Scheme 4: Reaction of *N,N*-dimethylaniline with  $(\text{ani})_3\text{C}^+ \text{BF}_4^-$  in  $\text{CD}_3\text{CN}$  at 20 °C. A second-order rate constant  $k_2 = 2.71 \times 10^{-2} \text{ M}^{-1} \text{ s}^{-1}$  was obtained.

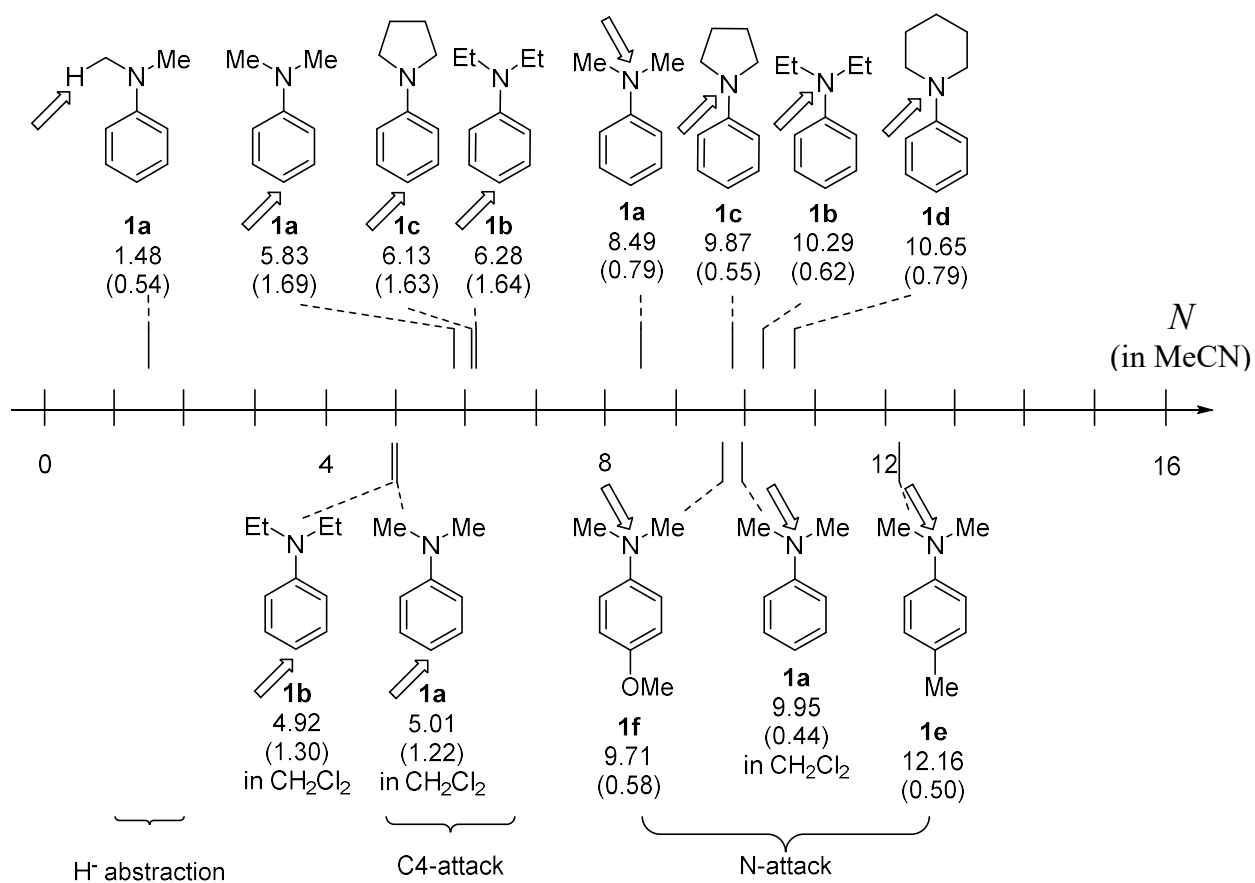


Figure 5:  $N$  and  $s_N$  parameters of the  $N,N$ -dialkylated anilines studied in this work.

## Chapter 1

# Kinetic and theoretical studies of beta-lactone reactivity – a quantitative scale for biological application

*Elija N. Wiedemann, Franziska A. Mandl, Iris D. Blank,  
Christian Ochsenfeld, Armin R. Ofial and Stephan A. Sieber*

*ChemPlusChem* **2015**, *80*, 1673–1679.

### Abstract

Natural products comprise a rich source for bioactive molecules with medicinal relevance. Many of these contain electrophilic scaffolds that bind conserved enzyme active sites covalently. Prominent examples include beta-lactams and beta-lactones, which specifically acylate serine residues in diverse peptidases. Although these scaffolds appear similar, their bioactivities and corresponding protein targets vary. To quantify and dissect these differences in bioactivities, the kinetics of the reactions of beta-butyrolactone with a set of reference amines in buffered aqueous solution at 37 °C have been analyzed. Different product ratios of C1 vs. C3 attack on the beta-butyrolactone have been observed, depending on the aliphatic or aromatic nature of the standard amine used. Quantum mechanics/molecular mechanics (QM/MM) calculations revealed that a  $\text{H}_3\text{O}^+$  molecule has a crucial role in stabilizing C3 attack by aniline, through coordination of the lactone ring oxygen. In agreement with their weak proteome reactivity, monocyclic beta-lactams did not react with our set of standard nucleophiles studied herein. Bicyclic beta-lactams, however, exhibited a lower activation barrier, and thus, reacted with standard nucleophiles. This study represents a starting point for semiquantitative reactivity scales for natural products, which, in analogy to chemical reactivity scales, will provide predictions for electrophilic modifications in biological systems.

## Introduction

Natural products frequently exhibit diverse electrophilic moieties designed to trap nucleophilic amino acid residues and thereby inhibit cellular proteins.<sup>[1]</sup> Evolution has fine-tuned these electrophiles to address a variety of cellular nucleophiles, e.g. in the active site of enzymes. These tailored scaffolds include beta-lactams, beta-lactones, epoxides and Michael acceptors, which vary in their reactivity and selectivity towards amino-, thio-, and hydroxyl-substituted amino acids (Figure 1).

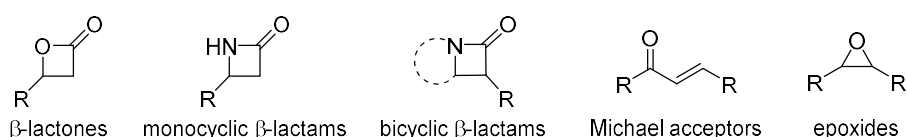


**Figure 1:** Common electrophilic motifs in natural products.

Beta-lactams are among the most potent antibiotics and they exert their cellular activity by reacting with the active site serine in penicillin-binding-proteins (PBPs), thereby inhibiting cell wall biosynthesis, and thus, bacterial viability.<sup>[2]</sup> Importantly, monocyclic beta-lactams lack pronounced protein reactivity.<sup>[3]</sup> However, scaffolds in which the lactam is activated by, for example, sulfonylation (aztreonam) or as a bicycle (penicillins), exhibit desirable reactivity and bioactivity.<sup>[4]</sup> The beta-lactones on the other hand, do not require activation in order to react with serine and cysteine residues, which suggests that monocyclic lactones and lactams show significantly different electrophilicities under physiological conditions.<sup>[5]</sup> Previous ring-opening studies with 3-alkylated beta-lactones revealed S-nucleophiles to require activation by deprotonation for an efficient C3 attack, a mixed S<sub>N</sub>2 reaction (attack at C3) and acylation (attack at C1) with amines, and C1 or C3 attack in hydrolysis reactions (Figure 2).<sup>[6,7]</sup>

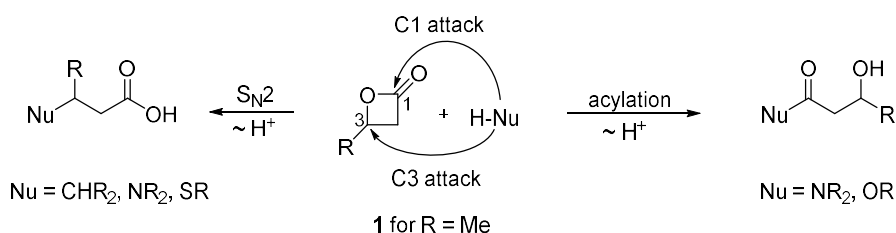


**Figure 2:** Possible beta-lactone ring-opening pathways of different nucleophiles.

Due to a lack in reliable reactivity and selectivity profiles under physiological settings, the identification of nucleophiles that distinguish between C1 vs. C3 attack, as well as an explanation for the selectivity towards these two sites, has not been possible. In order to mimic biological systems accurately, one must consider aqueous media as well as a series of

nucleophiles that imitate the reactivity of active sites. A first step in this direction was the evaluation of the alkylating potential of lactones as per their reaction rates with 4-(*p*-nitrobenzyl)pyridine in water/dioxane mixtures.<sup>[7]</sup> A crucial parameter for the determination of natural product electrophilicities is the selection of suitable nucleophiles which can be described by suitable kinetic equations. Previously, reactivities of structurally diverse carbocations and neutral electrophiles were characterized with a set of reference nucleophiles, and the corresponding second-order rate constants were evaluated according to the linear free energy relationship  $\lg k(20\text{ }^\circ\text{C}) = s_N(N + E)$ .<sup>[8]</sup> While the electrophile-independent parameter,  $N$ , is a measure of the nucleophilicity of a dissolved reactant,  $s_N$  provides information about its sensitivity towards changes in the electrophilicity of reaction partners. The electrophilicity  $E$  is a nucleophile-independent reactivity parameter. Because the same values of  $E$  is assigned to the reference electrophiles (benzhydrylium ions and quinone methides) in different solvents, all solvent effects on reactivity are considered in the nucleophilicity parameters  $N$  and  $s_N$ .

The kinetics of electrophilic compounds under physiological conditions has previously been studied by different groups, for example, to derive the carcinogenic properties of lactones or lactams from their alkylation potential.<sup>[7, 9]</sup> To determine reactivities of lactones and lactams towards nucleophiles with known  $N$  and  $s_N$  parameters,<sup>[8d]</sup> we started with investigating the reactions of beta-butyrolactone (BBL, **1**) with a set of standard amino-substituted nucleophiles (Figure 3) and determined its electrophilic reactivity, as well as the regioselectivity of nucleophilic attack with experimental and theoretical methods. In agreement with their minimal biological effects, monocyclic beta-lactams did not exhibit any reactivity with nucleophiles **6–8**, whereas reactions occurred when the beta-lactam was part of a strained bicyclic ring system. Because these reactions were performed under aqueous conditions, this study provides a basis for a rational approach to fine-tuning electrophilic scaffolds as selective inhibitors in biological applications.

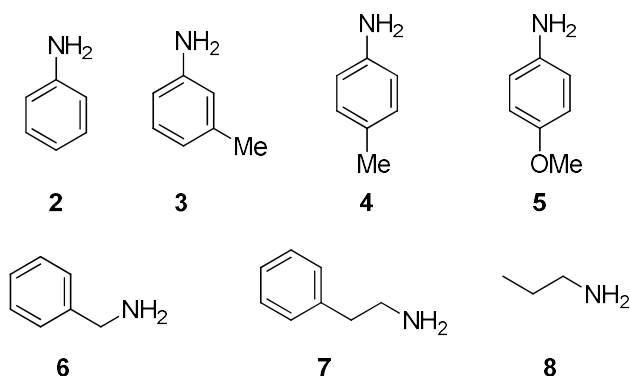


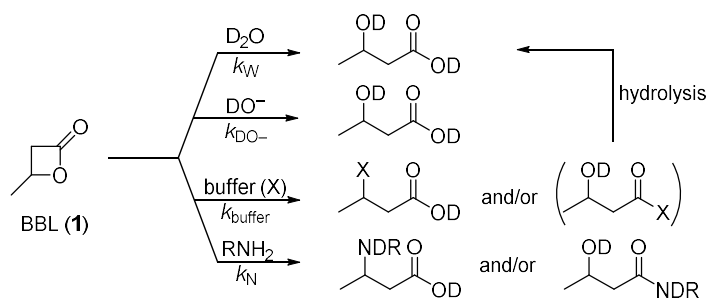
**Figure 3:** Standard amino-substituted nucleophiles used herein: aniline (**2**), *m*-toluidine (**3**), *p*-toluidine (**4**), *p*-anisidine (**5**), benzylamine (**6**), 2-phenylethylamine (**7**), *n*-propylamine (**8**).

## Results and discussion

### General considerations

To obtain a comprehensive picture of the reactivity of BBL (**1**) under physiological conditions, we used a series of primary amines (Figure 3) in aqueous solution ( $D_2O$ ) at  $37\text{ }^\circ\text{C}$  and a constant pH. In these reactions mixtures, four different nucleophiles are capable of reacting with BBL: water, hydroxide ions, the conjugate bases X of the buffer system, and the selected nucleophile (Scheme 1).

**Scheme 1.** Reactions of BBL (**1**) with amines in buffered aqueous solutions.



The rate law for the decay of the concentration of **1** (eq 1) has to consider the contributions of all four reaction channels.

$$-d[\mathbf{1}]/dt = (k_W + k_{DO^-}[DO^-] + k_{buffer}[buffer] + k_N[amine]) \cdot [\mathbf{1}] \quad (1)$$

Previous kinetic studies on the pH-dependency of BBL hydrolysis have shown that the non-catalyzed reaction of **1** with water follows a first-order rate law with a first-order rate constant,  $k_W$ . Attack by hydroxide ions ( $OH^-$ ) is only relevant at  $pH > 9$ , while acid catalysis accelerates the hydrolysis only in the region of  $pH < 1$ .<sup>[10]</sup> Blackburn and Dodds have shown that in buffered solutions, the reaction of pyridines and imidazoles with  $\beta$ -propiolactone could be described by equation 2a.<sup>[11]</sup> Significant increases in the rate of the **1** hydrolysis were only observed in the presence of highly concentrated buffers ( $> 1.5\text{ mol L}^{-1}$ ).<sup>[10b]</sup> Based on the extensive work done by Gresham on the ring opening of  $\beta$ -propiolactone by acetate or anions of inorganic acids,<sup>[12]</sup> we expected that buffers do not only participate in the stabilization of the pH but that their conjugate bases are also potential nucleophiles that are capable of attacking **1** ( $k_{buffer}[buffer]$ ).<sup>[13]</sup> As we found that the conjugate bases of the buffers indeed gave covalent adducts with **1** (see Table 1), we extended equation 2a to equation 2b.

$$k = k_W + k_{\text{DO}^-}[\text{DO}^-] + k_N[\text{amine}] \quad (2a)$$

$$k_2 = k_W + k_{\text{DO}^-}[\text{DO}^-] + k_{\text{buffer}}[\text{buffer}] + k_N[\text{amine}] \quad (2b)$$

$$k_1 = k_W + k_{\text{DO}^-}[\text{DO}^-] + k_{\text{buffer}}[\text{buffer}] \quad (3)$$

Owing the high initial concentration of water, the constant value of  $[\text{DO}^-]$  in buffered solution and only partial consumption of buffer and amine, the concentrations of all four relevant nucleophiles do not change significantly during the kinetic experiments. Consumption of **1** is, therefore, expected to follow an exponential function,  $[\mathbf{1}]_t = [\mathbf{1}]_0 e^{-kt}$ , in which  $k$  corresponds to  $k_1$  for hydrolysis of **1** in buffered aqueous solutions (eq 3) or to  $k_2$  for the reaction of **1** in buffered aqueous solutions of amines (eq 2b).

### Reactivity of **1** in aqueous buffer solutions.

In a first step, we determined the rate of the consumption of **1** in a 9:1 mixture of  $\text{D}_2\text{O}/d_6\text{-DMSO}$  in the absence of standard amine nucleophiles using time-resolved  $^1\text{H}$  NMR spectroscopy. The consumption of **1** through hydrolysis and the nucleophilic attack of different buffers (pH range from 4.75 to 8.10) was investigated (Table 1). In each case, the consumption of **1** followed a mono-exponential decay and produced a mixture of 3-hydroxybutyric acid (3-HBA) and the buffer adduct (see Supporting Information). Least squares fitting with the function  $[\mathbf{1}]_t = [\mathbf{1}]_0 \times e^{-k_1 t}$  yielded the first-order rate constants  $k_1$  as defined by equation 3, which reflect the reactivity of **1** towards the solvent at a constant pH for a 0.10 M buffer system.

The attack of **1** by buffer components was recorded by  $^1\text{H}$  NMR spectroscopy throughout kinetic experiments (right column of Table 1) and independently confirmed by LC-HRMS analysis (see Supporting Information). The presence of buffer changed the rate constant of the consumption of **1** only within a factor of  $< 1.25$  (Table 1, entries 2–5), compared with the non-buffered hydrolysis of **1** (Table 1, entry 1), which agrees with minimal formation of adducts of **1**. As illustrated in Table 1, entries 1–5, compound **1** reacted with all buffered aqueous solutions at comparable rates, we decided to proceed with aqueous TEA solutions for further kinetic investigations of reactions of **1** with primary amines. This is beneficial because the tertiary amine TEA provides a constant pH of 7.75 which is similar to physiological conditions in living cells (Table 1, entry 4).

**Table 1:** Rate constants of consumption of **1** in buffered and non-buffered mixtures of D<sub>2</sub>O/*d*<sub>6</sub>-DMSO 9/1 (v/v) at 37 °C ([**1**]<sub>0</sub> = 25 mM, [buffer]<sub>0</sub> = 0.10 M).

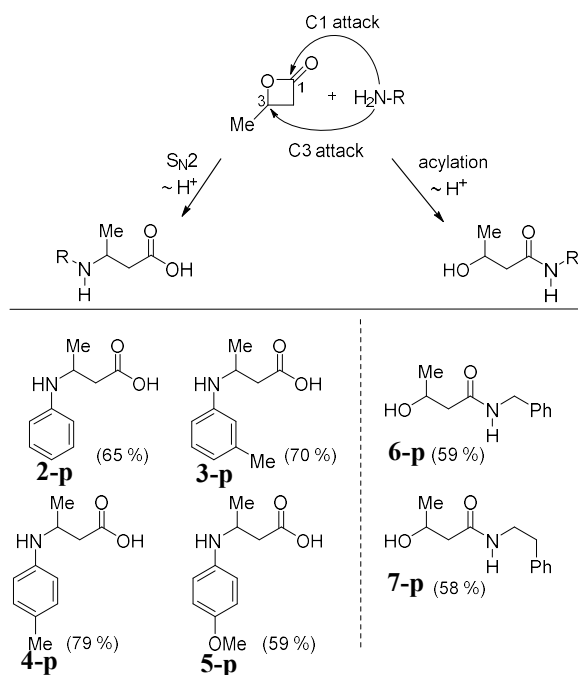
entry	buffer	pH	$k_1$ [s <sup>-1</sup> ]	$t_{1/2}$ [h]	Ratio
					3-HBA/buffer adduct
1	without buffer	–	$4.73 \times 10^{-5}$ [a]	4.1	100/–
2	acetate	4.75	$4.14 \times 10^{-5}$	4.7	96/4
3	Na <sub>2</sub> HPO <sub>4</sub> /NaH <sub>2</sub> PO <sub>4</sub>	7.00	$5.85 \times 10^{-5}$	3.3	86/14
4	TEA	7.75	$5.47 \times 10^{-5}$	3.5	83/17 → 88/12 <sup>[b]</sup>
5	TRIS	8.10	$5.79 \times 10^{-5}$	3.3	79/21

[a] Comparison with data from Ref. [14]: With  $\Delta H^\ddagger = 87.6 \text{ kJ mol}^{-1}$  and  $\Delta S^\ddagger = -77.9 \text{ J mol}^{-1} \text{ K}^{-1}$ , the second-order rate constant for the hydrolysis of **1** is calculated to be  $k(37 \text{ °C}) = 1.1 \times 10^{-6} \text{ M}^{-1} \text{ s}^{-1}$ . Multiplying  $k(37 \text{ °C})$  with [D<sub>2</sub>O] for the D<sub>2</sub>O/*d*<sub>6</sub>-DMSO 9/1 mixture in our experiment gives a first-order rate constant for the hydrolysis of **1** of  $k_w(37 \text{ °C}) = 5.5 \times 10^{-5} \text{ s}^{-1}$ , in sufficient agreement with the rate constant determined under our conditions. [b] The ratio 3-HBA/buffer adduct increased during the course of the reaction (14 h) probably because of a subsequent hydrolysis of the quaternary ammonium salt formed by C3 attack of TEA on **1** (for details see Supporting Information, Section 3.1.5). TEA = triethanolamine, TRIS = tris(hydroxymethyl)aminomethane, 3-HBA = 3-hydroxybutyric acid.

### Reactivity of **1** towards amines in aqueous solutions.

We commenced by studying the products of the reactions of **1** with a panel of nucleophilic amines (aniline (**2**), *m*-toluidine (**3**), *p*-toluidine (**4**), *p*-anisidine (**5**), benzylamine (**6**) and 2-phenylethylamine (**7**), Figure 3) in aqueous solutions. Interestingly, we observed that the amine structure directly influenced the preferred site of attack at **1**. Aromatic amines opened the lactone ring via a S<sub>N</sub>2 attack at the C3 position of **1** (O-alkyl fission), yielding the beta-amino acids, while primary aliphatic amines underwent acylation via reaction at the C1 site of **1** (O-acyl fission), forming 3-hydroxy amides (Scheme 2).

**Scheme 2.** Products (**2-p**–**7-p**) of the reactions of **1** with amines **2**–**7** in H<sub>2</sub>O/MeCN 9/1 (v/v) (yields refer to isolated products).



### QM/MM studies on the C1 versus C3 selectivity of amine attack on **1**

To explain the unexpected preference for either C1 or C3 attack of aliphatic and aromatic amines on **1**, we performed theoretical studies using a combined quantum mechanics/molecular mechanics (QM/MM) approach with linear-scaling quantum-chemical methods (QM) (see e.g. Ref. [15] and references therein).<sup>[16]</sup> The QM/MM method has been widely used to describe complex reactions. Using this strategy, reaction mechanisms were calculated using both the adiabatic mapping approach and the nudged elastic band method (for computational details see Supporting Information). The composition of the calculated systems is illustrated for the reaction of **1** with aniline (**2**) in Figure 4.

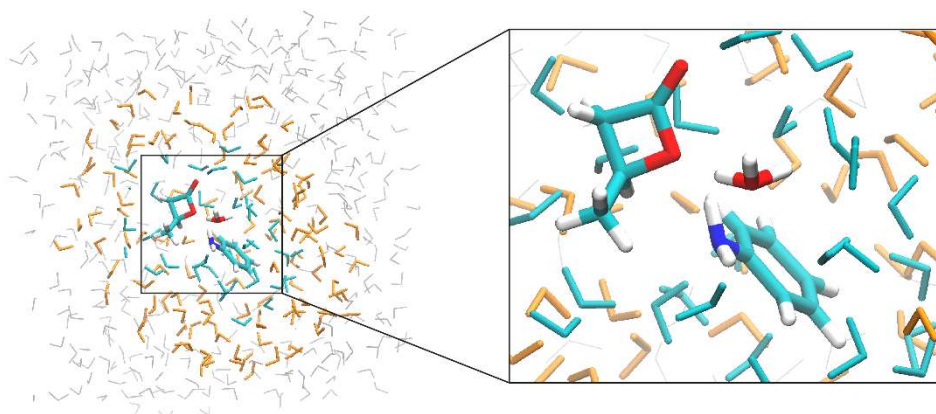


**Figure 4:** Illustration of the calculated systems obtained by using the QM/MM approach, as exemplified for the reaction of **1** with aniline (**2**). The reactants (depicted in atomic color) are part of the QM region (cyan; 156 atoms) in which chemical reactions can be described. The remaining part is described by MM (Molecular Mechanics), in which the region depicted in orange is optimized (including the QM region; overall 681 atoms) and the grey region will be held fixed (2235 atoms in total).

In this reaction,  $\text{H}_3\text{O}^+$  stabilizes the transition state of the nucleophilic attack of aniline (**2**) at C3 and thereby lowers the activation barrier by  $28 \text{ kcal mol}^{-1}$  to  $21 \text{ kcal mol}^{-1}$  (Figure 5). Specifically,  $\text{H}_3\text{O}^+$  approaches the lactone ring oxygen to a minimum distance of  $1.38 \text{ \AA}$ , forming a strong hydrogen bond (Figure 5, right), and thus, facilitating lactone ring opening. In a subsequent step, aniline (**2**) forms a covalent bond with C3 and simultaneously protonates the lactone oxygen to form a stable product ( $-17 \text{ kcal mol}^{-1}$  compared to initial state). In contrast, in the case of C1 attack,  $\text{H}_3\text{O}^+$  protonates the lactone ring oxygen instead of aniline (**2**), leaving aniline (**2**) protonated when forming the product. This product, however, is not stable ( $+13 \text{ kcal mol}^{-1}$  compared to the initial state) and immediately regenerates the starting material (Figure S7 in the Supporting Information of the publication). Owing to the dependence of this reaction on  $\text{H}_2\text{O}/\text{H}_3\text{O}^+$ , the reaction did not occur in nonaqueous solvents, such as acetonitrile and DMSO (Figure S2, S3 and Table S1 in the Supporting Information of the publication). The consumption of **1** with a rate constant of  $7.9 \times 10^{-4} \text{ M}^{-1} \text{ s}^{-1}$  was observed, however, in  $\text{D}_2\text{O}/d_6\text{-DMSO}$  9/1 (v/v) at  $37 \text{ }^\circ\text{C}$  (Table 2).

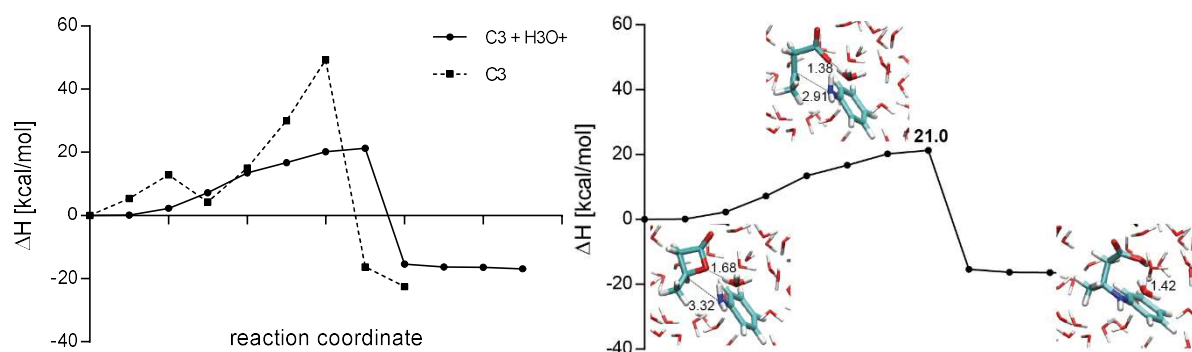


**Figure 5:** Calculated reaction profiles of the C3 attack of aniline (**2**) on **1** with (black) and without (black dashed)  $\text{H}_3\text{O}^+$  (left) with structures out of the QM/MM simulation for the starting material, transition and product state (right).

On the other hand, nucleophilic attack of the aliphatic benzylamine (**6**) at C1 does not require  $\text{H}_3\text{O}^+$  stabilization. Calculations demonstrate that attack at C1 and protonation of the lactone ring by the amine is favored (activation barrier of  $12 \text{ kcal mol}^{-1}$ ) over the attack at C3 (activation barrier of  $37 \text{ kcal mol}^{-1}$ ; Table S1 in the Supporting Information of the publication). In the transition state, the C1 atom is in a tetrahedral configuration and the lactone ring remains intact. Subsequently, proton transfer from benzylamine (**6**) to the ring oxygen induces lactone opening. If  $\text{H}_3\text{O}^+$  is considered in these simulations, the reaction also occurs via the same tetrahedral transition state, but  $\text{H}_3\text{O}^+$  protonates the ring oxygen instead. Finally, the positively charged nitrogen transfers a proton to a nearby water molecule (Figure 6).

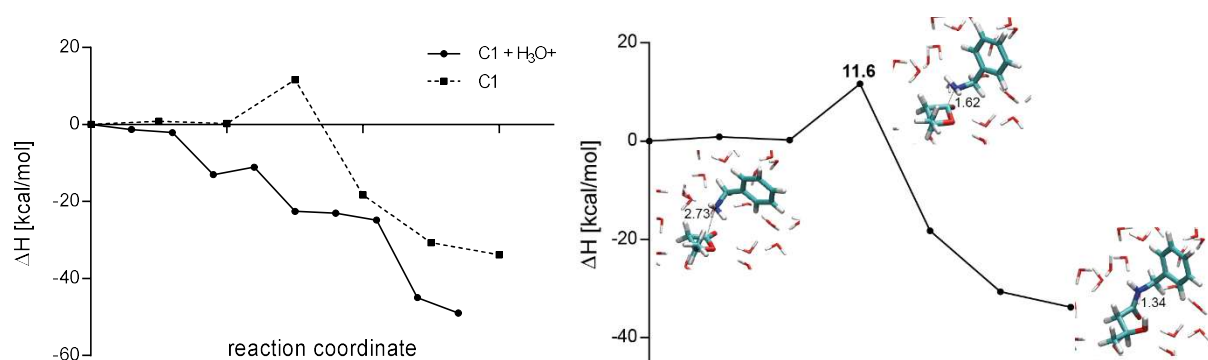


**Figure 6:** Calculated reaction profiles of the C1 attack of benzylamine (**6**) on **1** with (black) and without (black dashed)  $\text{H}_3\text{O}^+$  (left) with structures from the QM/MM simulation for the starting material, transition state and product (right). Accounting for  $\text{H}_3\text{O}^+$  in the calculated system leads to barrier-free attack at C1; however, minor product formation is also possible in the absence of  $\text{H}_3\text{O}^+$  (left).

The computational data is in line with experimental measurements of the rate constants for the reaction in the presence ( $5.8 \times 10^{-3} \text{ M}^{-1} \text{ s}^{-1}$ ) and in the absence of water ( $2.5 \times 10^{-4} \text{ M}^{-1} \text{ s}^{-1}$ )

(Figure S1 in the Supporting Information). These values demonstrate that C1 attack indeed takes place, even in absence of  $\text{H}_3\text{O}^+$  and  $\text{H}_2\text{O}$  (Figure S1 and S3 in the Supporting Information of the publication). Since almost all naturally occurring beta-lactones exhibit bulky substituents at the C3 position, the biologically relevant ring-opening reaction in enzyme active sites is likely to be at the C1 position. This is supported by cocrystal structures of the thioesterase domain of human fatty acid synthase inhibited by Orlistat<sup>[17]</sup> as well as kinetic studies that show rapid hydrolysis of the ester intermediate of lactone-bound enzyme.<sup>[18]</sup>

### Kinetic studies of the reactions of **1** with amine nucleophiles in buffered media

Next, reactivity studies were performed by following the kinetics of **1** turnover with the same set of primary aliphatic amines and ring-substituted anilines in aqueous TEA-buffered solutions (Table 2). To fully solubilize these molecules, a small amount of DMSO (10 vol%) was necessary as a co-solvent. Again, the consumption of **1** followed a mono-exponential function,  $[\mathbf{1}]_t = [\mathbf{1}]_0 e^{-k_2 t}$ , from which  $k_2$  was derived. By rearranging equation 4,  $k_N$  can be calculated from equation 5, in which  $k_1$  is the first-order rate constant of the background reactions of **1** in a mixture of TEA-buffered  $\text{D}_2\text{O}:d_6\text{-DMSO}$  (9:1) (Table 1, entry 4) and  $[\text{amine}]_{\text{eff}}$  corresponds to the concentrations of the free amines at pH 7.75.

$$k_2 = k_1 + k_N[\text{amine}]_{\text{eff}} \quad (4)$$

$$k_N = (k_2 - k_1)/[\text{amine}]_{\text{eff}} \quad (5)$$

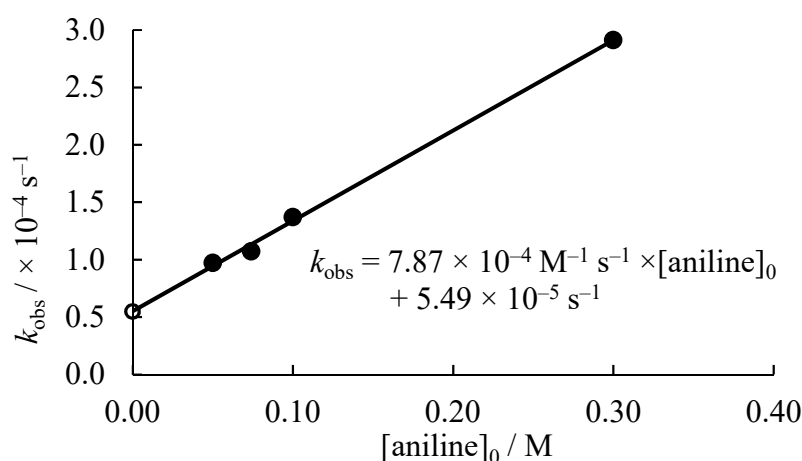


**Figure 7:** Linear dependence of the first-order rate constant  $k_2 (= k_{\text{obs}})$  for the reaction of **1** with aniline (**2**) on the concentration of **2** ( $k_{\text{obs}}$  for  $[\mathbf{2}]_0 = 0$  corresponds to the hydrolysis of **1** in TEA-buffered solution; not considered for the depicted linear correlation).

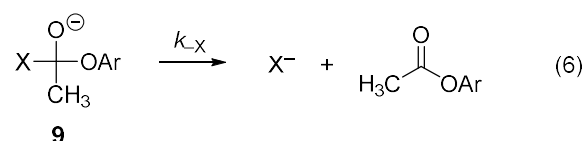
**Table 2:** Second-order rate constants of the reactions of amines with **1** in 0.10 M TEA-buffered aqueous solutions ( $[1]_0 = 25$  mM, pH 7.75 in D<sub>2</sub>O/*d*<sub>6</sub>-DMSO 9/1 (v/v), at 37 °C, determined by <sup>1</sup>H NMR spectroscopy).

nucleophile	p <i>K</i> <sub>B</sub> <sup>[a]</sup>	<i>N</i> <sup>[b]</sup>	<i>s</i> <sub>N</sub> <sup>[b]</sup>	<i>k</i> <sub>N</sub> [M <sup>-1</sup> s <sup>-1</sup> ]
aniline ( <b>2</b> )	9.4	12.99	0.73	7.9 (±0.5) × 10 <sup>-4</sup> <sup>[c]</sup>
<i>m</i> -toluidine ( <b>3</b> )	9.13	n.d.	n.d.	9.9 × 10 <sup>-4</sup>
<i>p</i> -toluidine ( <b>4</b> )	8.92	13.00	0.79	1.4 × 10 <sup>-3</sup>
<i>p</i> -anisidine ( <b>5</b> )	8.64	14.28 <sup>[d,e]</sup>	0.68 <sup>[d,e]</sup>	1.6 × 10 <sup>-3</sup>
benzylamine ( <b>6</b> )	4.64	13.44	0.55	5.8 × 10 <sup>-3</sup> <sup>[f]</sup>
phenylethylamine ( <b>7</b> )	4.11	13.40 <sup>[d]</sup>	0.57 <sup>[d]</sup>	1.1 × 10 <sup>-2</sup> <sup>[f]</sup>

[a] From Ref. [19]. [b] Reactivity parameters *N* and *s*<sub>N</sub> (as defined in eq 1) of amines in water, from Ref. [20] [c] Average *k*<sub>N</sub> of four kinetic runs at variable concentrations of **2**, the same value for *k*<sub>N</sub> is obtained from the slope of the linear correlation of *k*<sub>2</sub> vs  $[2]_0$  (see Supporting Information, Section 4.1.5). [d] This work. [e] The previously published nucleophilicity parameters for *p*-anisidine (**5**) (*N* = 16.53, *s*<sub>N</sub> = 0.50) from Ref. [20] were revised in this work (see the Supporting Information). [f] Rate constants of lower accuracy; an error of ±15 % is assumed.

The linear dependence of the first-order rate constant *k*<sub>2</sub> on the concentration of aniline (**2**) (Figure 7) is in agreement with the rate laws shown in equations 2a,b and 4. The intercept on the ordinate matches, within experimental error, the first-order rate constant *k*<sub>1</sub> (eq 3) for the background reaction in TEA-buffered solution (Table 1, entry 4), which demonstrates that the background reaction is not significantly affected by the presence of the amine. The consistency of the determined *k*<sub>N</sub> values is demonstrated by a Hammett analysis of the data for anilines, which shows a good correlation of the rate constants *k*<sub>N</sub> with the values of σ<sub>p</sub><sup>-</sup> (and σ<sub>m</sub>) of the substituents at the anilines **2–5** (lg *k*<sub>N</sub> = -1.21 σ - 3.09, R<sup>2</sup> = 0.9906, see also Figure S30 in the Supporting Information).

Ritchie characterized the relative leaving-group abilities of nucleophiles in the tetrahedral intermediates **9** (equation 6) by analyzing the rate constants for the reactions of several nucleophiles X (in water) with carbocations, N-acyl pyridinium ions and aryl esters.<sup>[21]</sup>



The relative rates for the expulsion of X are remarkably different for water and aniline (**2**) compared to those for primary aliphatic amines: relative lg *k*<sub>-X</sub>: H<sub>2</sub>O (5.20) = **2** (5.20) ≫ BuNH<sub>2</sub>

(1.21) > EtNH<sub>2</sub> (0.82).<sup>[21]</sup> These results from kinetic measurements may provide an alternative interpretation for the observed variation of regioselectivity of the attack of **1** by different nucleophiles. For water and anilines, attack at C1 of **1** is highly reversible, whereas stable products are formed by irreversible S<sub>N</sub>2 reaction at C3 of **1** (see Scheme 2). In accordance with this interpretation, the hydrolysis of (*S*)-**1** in buffered solution at pH 7 was reported to give selective inversion of the stereocenter to yield (*R*)-3-hydroxybutyric acid.<sup>[10b]</sup> Although the nucleophilicity of the primary amines **6** and **7** is in the same range as that of the anilines **2–5**, products of C1 attack at **1** were obtained with the primary alkylamines **6** and **7**. This observation is in accord with Ritchies's lg *k<sub>X</sub>* values for tetrahedral intermediates formed by nucleophilic attack on carboxylic esters, which indicate that the primary aliphatic amines are 10<sup>4</sup>-fold weaker nucleofuges than anilines or water.

Amines **2–7** employed in this study cover a relatively small range in nucleophilicity in water (12.99 < *N* < 14.28), which corresponds to a reactivity difference of only a factor of 20 towards a certain electrophile (if differences in *s<sub>N</sub>* are neglected). Because anilines attack at C3 while aliphatic amines attack at C1, rate constants for nucleophilic attack at **1** are additionally influenced to a different extent by anomeric effects.<sup>[22]</sup>

Mayr's reference electrophiles have been assigned the same value of *E* in different solvents.<sup>[8]</sup> It can be expected, however, that the use of solvent-independent *E* parameters is not possible for all electrophiles. If products with highly localized charges will be formed during nucleophilic attack solvent-dependent *E* parameters will be required.<sup>[23]</sup> In this work, the rate constant of the reaction of **1** with benzylamine (**6**) decreases by a factor of 23 when changing from aqueous solution to DMSO solution, although an increase in the rate constants by about one order of magnitude (*N/s<sub>N</sub>* for benzylamine (**6**) in DMSO: 15.28/0.65) is expected when assuming the same electrophilic reactivity of **1** in both solvents.<sup>[8d]</sup> As a consequence, it is not possible to determine a reliable *E* parameter for C1 or C3 attack on **1**. Hence, the discussion of β-lactam reactivities in the following paragraph has been based on relative rate constants towards amines.

## Electrophilic reactivity of beta-lactams

Monocyclic beta-lactams exhibit limited reactivity with enzyme active sites, while their bicyclic analogs are potent antibiotics with pronounced protein reactivity.<sup>[3]</sup> This physiological observation is in agreement with our experimental and theoretical studies, which reveal no turnover of 4-methyl-1-azetidin-2-one with nucleophiles due to an insuperable activation barrier of 40–70 kcal mol<sup>-1</sup> (Table S2 and Figure S5 and S6 in the Supporting Information of the publication). In contrast, penicillin G, which is a bicyclic beta-lactam, reacts with benzylamine (**6**), 2-phenylethylamine (**7**) and *n*-propylamine (**8**) at significantly higher rates ranging from 8 × 10<sup>-2</sup> M<sup>-1</sup> s<sup>-1</sup> (for **6**) via 9 × 10<sup>-2</sup> M<sup>-1</sup> s<sup>-1</sup> (for **7**) to 4 × 10<sup>-1</sup> M<sup>-1</sup> s<sup>-1</sup> (for **8**), a trend which was further confirmed by QM/MM calculations (Figure 8). These rates exceed those observed for monocyclic lactones. Accordingly, the acylation products **10a,b** of the reactions of penicillin G with benzylamine (**6**) and *n*-propylamine (**8**) have been isolated and characterized by NMR spectroscopy and HRMS (Scheme 3).

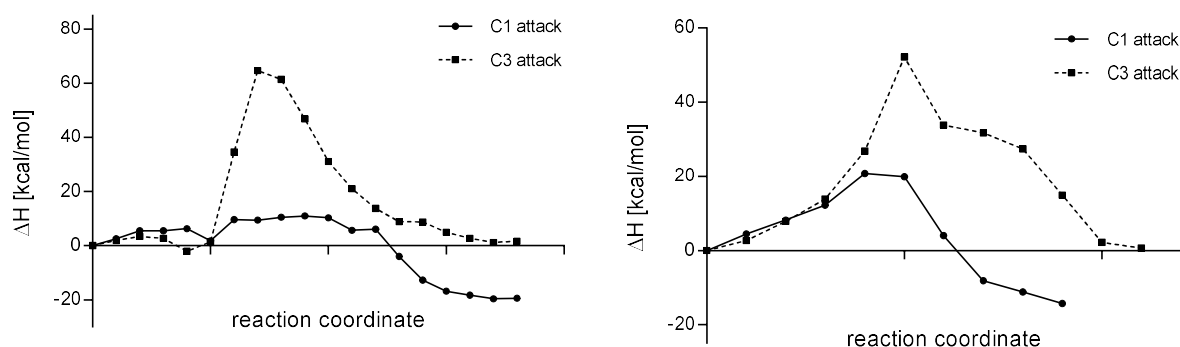
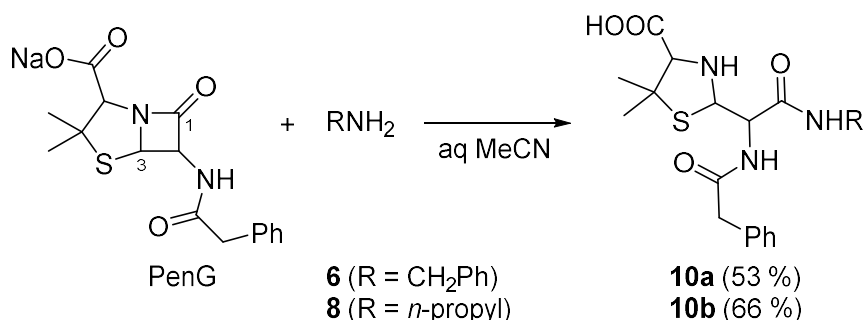


**Figure 8:** Calculated reaction profiles of *n*-propylamine (**8**) (left) and benzylamine (**6**) (right) with penicillin G. The attack at C1 is shown in black and the attack at C3 in black dashed. Left: The first barrier represents the reorientation of *n*-propylamine (**8**) during the approach towards penicillin G. The second barrier represents the nucleophilic attack at C1 and C3 respectively.

**Scheme 3.** Products of the reactions of sodium penicillin G with amines **6** and **8** in H<sub>2</sub>O/MeCN 9/1 (v/v) (yields refer to isolated products, only one diastereomer is shown).



## Conclusion

Electro- and nucleophilicity parameters have been obtained for a variety of compound classes, to provide a prognostic value for chemical reactions.<sup>[8]</sup> Natural products exhibit many electrophilic motifs that have been customized by evolution to irreversibly bind the active sites of enzymes. The corresponding biological activities are as diverse as these scaffolds and range from anticancer to antibiotic properties. Recent drug-discovery efforts have focused on natural-product-inspired covalent inhibitors; however, a quantitative scale to describe and parameterize their reactivity under physiological conditions is currently lacking. We therefore used kinetic experiments to evaluate pharmacologically relevant electrophilic scaffolds. Importantly, the ambident reactivity of beta-butyrolactone (C1 vs. C3 attack) towards anilines and primary aliphatic amines was explained by QM/MM calculations using linear-scaling QM methods. Strikingly, these calculations revealed that  $\text{H}_3\text{O}^+$  molecules are crucial for catalysis owing to their stabilizing effects on the transition state of aniline attack at the C3 position of the lactone. Although the energy path for this reaction is significantly lower than that of C1 attack, benzylamine (**6**) prefers C1 attack (with or without  $\text{H}_3\text{O}^+$  catalysis) owing to an insuperable C3 energy barrier. All of these calculations were supported by experimental data which confirmed the influence of water for the corresponding reaction rates. The value of this platform has been demonstrated in the direct comparison of beta-butyrolactone (**1**), 4-methyl-1-azetidin-2-one and penicillin G. The phenomenological observation that penicillin G and beta-lactones are reactive with protein active sites while monocyclic beta-lactams are weak binders could be proven experimentally as well as theoretically. With this proof of principle study, the scope of application can easily be expanded to other biologically-relevant electrophilic scaffolds.

## Acknowledgements

We thank Prof. Dr. H. Mayr (LMU München) for generous support and Dr. D. Stephenson (LMU München) for help with the NMR spectroscopy measurements.

We acknowledge financial support by the DFG funding initiative SFB749 (Projects A3, B1, C7), the Excellence Cluster EXC114 (CIPSM), and an ERC starting grant (250924-antibacterials).

## References

- [1] a) M. Gersch, J. Kreuzer, S. A. Sieber, *Nat. Prod. Rep.* **2012**, *29*, 659–682; b) C. Drahl, B. F. Cravatt, E. J. Sorensen, *Angew. Chem. Int. Ed. Engl.* **2005**, *44*, 5788–5809. c) J. A. H. Schwöbel, Y. K. Koleva, S. J. Enoch, F. Bajot, M. Hewitt, J. C. Madden, D. W. Roberts, T. W. Schultz, M. T. D. Cronin, *Chem. Rev.* **2011**, *111*, 2562–2596.
- [2] D. J. Waxman, J. L. Strominger, *Annu. Rev. Biochem.* **1983**, *52*, 825–869.
- [3] I. Staub, S. A. Sieber, *J. Am. Chem. Soc.* **2008**, *130*, 13400–13409.
- [4] a) M. I. Page, A. P. Laws, *Tetrahedron* **2000**, *56*, 5631–5638; b) P. Proctor, N. P. Gensmantel, M. I. Page, *J. Chem. Soc. Perkin Trans. 2* **1982**, 1185–1192.
- [5] T. Böttcher, S. A. Sieber, *MedChemComm* **2012**, *3*, 408–417.
- [6] a) A. Noel, B. Delpech, D. Crich, *Org. Biomol. Chem.* **2012**, *10*, 6480–6483; b) A. Griesbeck, D. Seebach, *Helv. Chim. Acta* **1987**, *70*, 1326–1332.
- [7] J. A. Manso, M. T. Pérez-Prior, M. d. P. García-Santos, E. Calle, J. Casado, *Chem. Res. Toxicol.* **2005**, *18*, 1161–1166.
- [8] a) H. Mayr, M. Patz, *Angew. Chem. Int. Ed. Engl.* **1994**, *33*, 938–957; b) H. Mayr, A. R. Ofial, *J. Phys. Org. Chem.* **2008**, *21*, 584–595; c) H. Mayr, T. Bug, M. F. Gotta, N. Hering, B. Irrgang, B. Janker, B. Kempf, R. Loos, A. R. Ofial, G. Remennikov, H. Schimmel, *J. Am. Chem. Soc.* **2001**, *123*, 9500–9512; d) For a comprehensive listing of nucleophilicity parameters  $N$ ,  $s_N$  and electrophilicity parameters  $E$ , see <http://www.cup.lmu.de/oc/mayr/DBintro.html>.
- [9] a) B. L. Van Duuren, B. M. Goldschmidt, *J. Med. Chem.* **1966**, *9*, 77–79; b) B. L. Van Duuren, *Ann. N. Y. Acad. Sci.* **1969**, *163*, 633–650.
- [10] a) F. A. Long, M. Purchase, *J. Am. Chem. Soc.* **1950**, *72*, 3267–3273; b) A. R. Olson, R. J. Miller, *J. Am. Chem. Soc.* **1938**, *60*, 2687–2692.
- [11] G. M. Blackburn, H. L. H. Dodds, *J. Chem. Soc. Perkin Trans. 2* **1974**, 377–382.
- [12] a) T. L. Gresham, J. E. Jansen, F. W. Shaver, J. T. Gregory, *J. Am. Chem. Soc.* **1948**, *70*, 999–1001; b) T. L. Gresham, J. E. Jansen, F. W. Shaver, *J. Am. Chem. Soc.* **1948**, *70*, 1003–1004.
- [13] For related kinetic studies of the reactions of  $\beta$ -propiolactone with anionic nucleophiles, see also P. D. Bartlett, G. Small, *J. Am. Chem. Soc.* **1950**, *72*, 4867–4869.
- [14] M. T. Pérez-Prior, J. A. Manso, M. d. P. García-Santos, E. Calle, J. Casado, *J. Org. Chem.* **2005**, *70*, 420–426.
- [15] J. Kussmann, M. Beer, C. Ochsenfeld, *Wiley Interdiscip. Rev.: Comput. Mol. Sci.* **2013**, *3*, 614–636.

- [16] a) A. Warshel, *Angew. Chem. Int. Ed.* **2014**, *53*, 10020–10031; b) H. M. Senn, W. Thiel, *Angew. Chem. Int. Ed.* **2009**, *48*, 1198–1229; *Angew. Chem.* **2009**, *121*, 1220–1254.
- [17] C. W. Pemble, L. C. Johnson, S. J. Kridel, W. T. Lowther, *Nat. Struct. Mol. Biol.* **2007**, *14*, 704–709.
- [18] M. Gersch, K. Famulla, M. Dahmen, C. Göbl, I. Malik, K. Richter, V. S. Korotkov, P. Sass, H. Rübsamen-Schaeff, T. Madl, H. Brötz-Oesterhelt, S. A. Sieber, *Nat. Commun.* **2015**, *6*, 6320.
- [19] a) Y. Altun, *J. Solution Chem.* **2004**, *33*, 479–497; b) D. Xiong, Z. Li, H. Wang, J. Wang, *Green Chem.* **2013**, *15*, 1941–1948; c) P. J. Battye, E. M. Ihsan, R. B. Moodie, *J. Chem. Soc. Perkin Trans. 2* **1980**, 741–748; d) C. H. Arrowsmith, H. X. Guo, A. J. Kresge, *J. Am. Chem. Soc.* **1994**, *116*, 8890–8894; e) R. F. Jameson, G. Hunter, T. Kiss, *J. Chem. Soc. Perkin Trans. 2* **1980**, 1105–1110.
- [20] F. Brotzel, Y. C. Chu, H. Mayr, *J. Org. Chem.* **2007**, *72*, 3679–3688.
- [21] C. D. Ritchie, *J. Am. Chem. Soc.* **1975**, *97*, 1170–1179.
- [22] T. A. Nigst, H. Mayr, *Eur. J. Org. Chem.* **2013**, 2155–2163.
- [23] H. Mayr, *Tetrahedron* **2015**, *71*, 5095–5111.

## Kinetic and theoretical studies of beta-lactone reactivity – a quantitative scale for biological application

### 1. Supporting figure

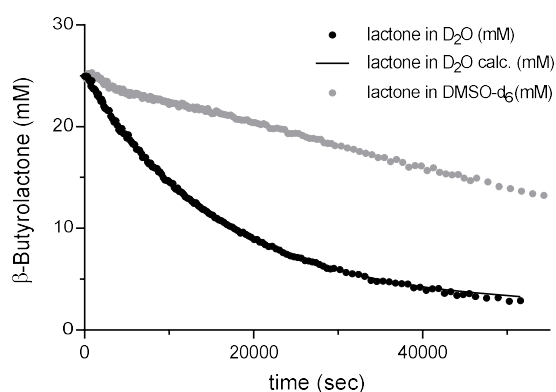


**Figure S1:** Decay of the concentration of BBL (determined by  $^1\text{H}$  NMR spectroscopy) while reacting with benzylamine in an aqueous TEA-buffered reaction mixture at 37 °C (black curve,  $[\text{BBL}]_0 = 25 \text{ mM}$ ,  $[\text{PhCH}_2\text{NH}_2]_0 = 50 \text{ mM}$ ,  $[\text{PhCH}_2\text{NH}_2]_{\text{eff}} = 1.2 \times 10^{-3} \text{ M}$ ,  $[\text{TEA}]_0 = 0.10 \text{ M}$ ,  $\text{pH} = 7.75$ , solvent  $\text{D}_2\text{O}/\text{DMSO-}d_6$  9/1 (v/v),  $k_{\text{obs}} = 6.2 \times 10^{-5} \text{ s}^{-1}$ ,  $k_{\text{N}} = 5.8 \times 10^{-3} \text{ M}^{-1} \text{ s}^{-1}$ ) and while reacting with benzylamine in  $d_6$ -DMSO at 37 °C versus time (grey curve,  $[\text{BBL}]_0 = 25 \text{ mM}$ ,  $[\text{PhCH}_2\text{NH}_2]_0 = 50 \text{ mM}$ ,  $k_{\text{N}} = 2.5 \times 10^{-4} \text{ M}^{-1} \text{ s}^{-1}$ ) is shown.

### 2. General methods and materials

**All chemical reagents and solvents** used for product studies were of reagent grade or of higher purity and used without further purification as obtained from the commercial sources Alfa-Aesar, AppliChem, Fluka/Sigma-Aldrich, Merck and Roth. **Chemical reagents and solvents** used for kinetic NMR-studies were purified by distillation. Concentrations under reduced pressure were performed by rotary evaporation at 40 °C. Yields refer to purified, dried and spectroscopically pure compounds.

$^1\text{H}$  NMR and  $^{13}\text{C}$  NMR spectra were recorded at  $(26 \pm 1) \text{ }^\circ\text{C}$  on Bruker Avance 360, Avance 500 and Avance III 500 spectrometers.  $^1\text{H}$  NMR kinetic measurements were performed on Varian VNMRS 400 or Varian 200 spectrometers at 37 °C. Chemical shifts ( $\delta$ ) were referenced

to the residual proton or carbon signal of the deuterated solvent in ppm ( $d_6$ -DMSO:  $\delta_H$  2.50,  $\delta_C$  39.52;  $CDCl_3$ :  $\delta_H$  7.26,  $\delta_C$  77.16;  $D_2O$ :  $\delta_H$  4.79).<sup>[1]</sup> Coupling constants ( $J$ ) are reported in Hertz (Hz) and multiplicity is reported as follows: s = singlet, d = doublet, t = triplet, q = quartet, m = multiplet or unresolved.

### 3. Stability of $\beta$ -butyrolactone (BBL) in different buffer systems – Determination of first-order rate constants $k_1$

#### 3.1. Kinetic data

##### 3.1.1. General

A 0.11 M buffer solution in  $D_2O$  (540  $\mu$ L) was mixed with a solution of BBL (60  $\mu$ L of a 0.25 M solution in  $d_6$ -DMSO) in an NMR tube at 37 °C to produce a 9/1 (v/v)  $D_2O/d_6$ -DMSO solvent mixture. The conversion of BBL was monitored by using time-resolved  $^1H$  NMR spectroscopy. Concentrations of BBL,  $[BBL]_t$ , were calculated from the ratio of the integral of the methyl resonances of BBL (d,  $\delta$  = 1.70 ppm) to the integral of the methyl resonances in the range  $\delta$  = 1.43–1.27 ppm.

The first-order rate constants  $k_{obs}$  (=  $k_1$  in equation (3) of the main text) were determined by least-squares fitting of the exponential function  $[BBL]_t = [BBL]_0 \cdot \exp(-k_{obs}t) + C$  to the time-dependent  $[BBL]_t$ .

$$k_{obs} = k_1 = k_W + k_{DO^-}[DO^-] + k_{buffer}[buffer] \quad (3)$$

##### 3.1.2. Hydrolysis of BBL without buffer

$D_2O$  (540  $\mu$ L) and BBL (60  $\mu$ L of a 0.25 M solution in  $d_6$ -DMSO) were mixed in an NMR tube at 37 °C. The conversion of BBL was monitored by using time-resolved  $^1H$  NMR spectroscopy. Concentrations of BBL,  $[BBL]_t$ , were calculated from the ratio of the integral of the methyl resonances of BBL (d,  $\delta$  = 1.70 ppm) to the integral of the methyl resonances assigned to 3-hydroxybutanoic acid (3-HBA: d,  $\delta$  = 1.38 ppm).

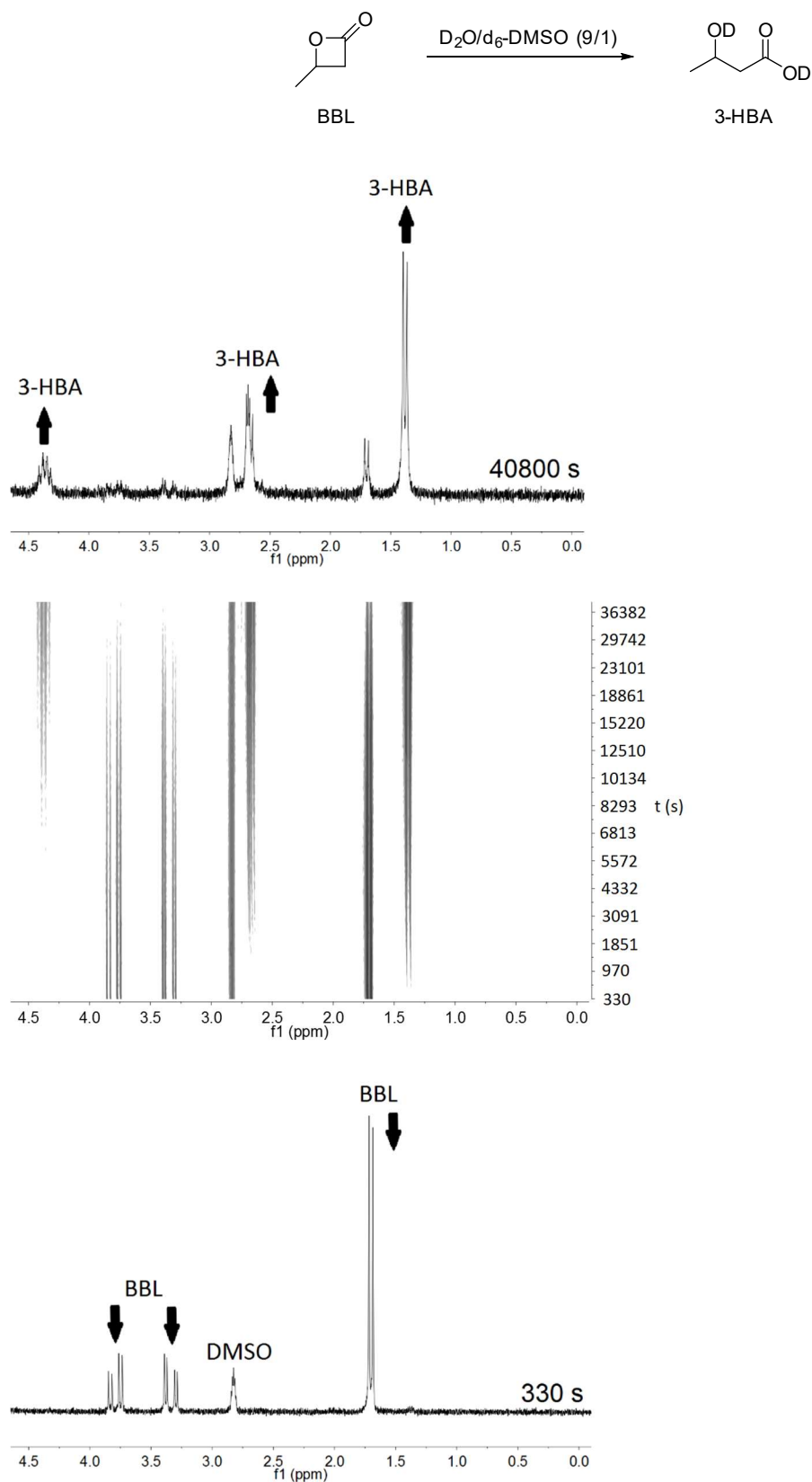


**Figure S2:** Exemplary time-resolved  $^1\text{H}$  NMR spectra of the hydrolysis of BBL in  $D_2O/d_6\text{-DMSO}$  9/1 (v/v) at 37  $^\circ\text{C}$  ( $[\text{BBL}]_0 = 25 \text{ mM}$ ). Start of the reaction (bottom), time-resolved topview of  $^1\text{H}$  NMR spectra (middle), showing the decrease of BBL resonances and increase of 3-HBA resonances, and final  $^1\text{H}$  NMR spectrum after 40800 s (top).

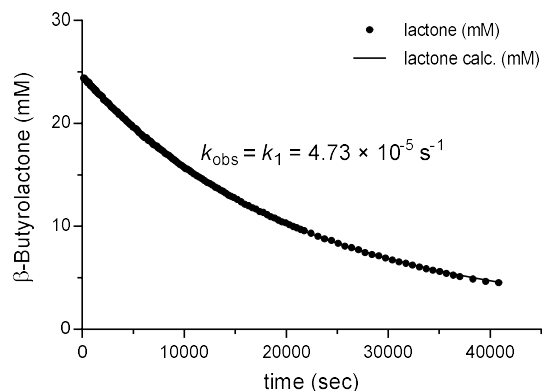


**Figure S3:** Decay of the concentration of BBL in  $D_2O/d_6$ -DMSO 9/1 (v/v) at 37 °C versus time ( $[BBL]_0 = 25$  mM,  $pH = 7.00$ ). The black line shows a mono-exponential fit of the data.

### 3.1.3. Hydrolysis of BBL in the presence of acetate buffer

Acetate buffer (540  $\mu$ L of a 0.11 M solution of NaOAc/HOAc in  $D_2O$ , pH 4.75) and BBL (60  $\mu$ L of a 0.25 M solution in  $d_6$ -DMSO) were mixed in an NMR tube at 37 °C. The conversion of BBL was monitored by using time-resolved  $^1H$  NMR spectroscopy. Concentrations of BBL,  $[BBL]_t$ , were calculated from the ratio of the integral of the methyl resonances of BBL ( $\delta = 1.70$  ppm) to the integral of the methyl resonances in the range  $\delta = 1.43$ – $1.27$  ppm.

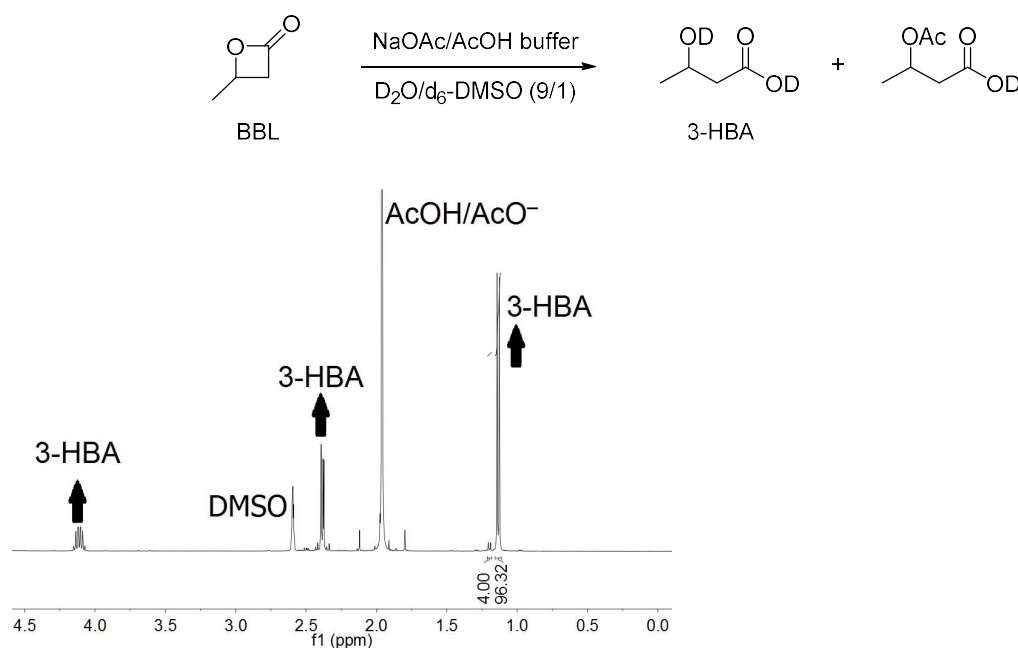


**Figure S4:**  $^1H$  NMR spectrum (400 MHz) of BBL in an acetate-buffered reaction mixture after 60 h at 37 °C ( $[BBL]_0 = 25$  mM,  $[AcOH]_0 = 0.10$  M,  $pH = 4.75$  in  $D_2O/d_6$ -DMSO 9/1 (v/v)).

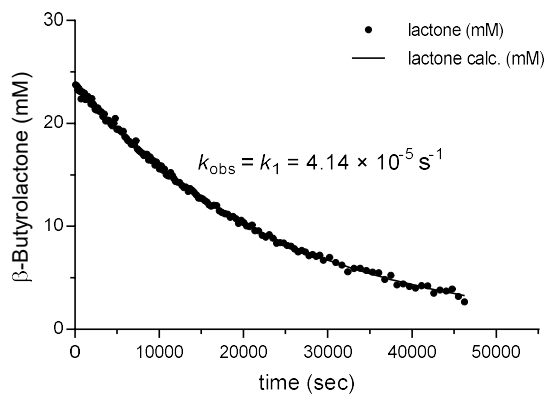
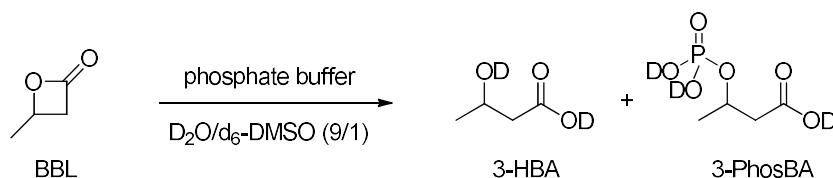


**Figure S5:** Decay of the concentration of BBL in an acetate-buffered reaction mixture at 37 °C ( $[BBL]_0 = 25$  mM,  $[AcOH]_0 = 0.10$  M,  $pH = 4.75$  in  $D_2O/d_6$ -DMSO 9/1 (v/v)). The black line shows a mono-exponential fit of the data.

### 3.1.4. Hydrolysis of BBL in the presence of phosphate buffer



Phosphate buffer (540  $\mu\text{L}$  of a 0.11 M solution of  $\text{Na}_2\text{HPO}_4/\text{NaH}_2\text{PO}_4$  in  $\text{D}_2\text{O}$ ,  $pH$  7.00) and BBL (60  $\mu\text{L}$  of a 0.25 M solution in  $d_6$ -DMSO) were mixed in an NMR tube at 37 °C. The conversion of BBL was monitored by using time-resolved  $^1\text{H}$  NMR spectroscopy. Concentrations of BBL,  $[BBL]_t$ , were calculated from the ratio of the integral of the methyl resonances of BBL ( $\delta$ ,  $\delta = 1.70$  ppm) to the integral of the methyl resonances in the range  $\delta = 1.43$ – $1.27$  ppm that were assigned to the formation of 3-HBA and 3-(phosphonoxy)butanoic acid (3-PBA, Figure S13). C-4 attack of BBL by dihydrogenphosphate or hydrogenphosphate ions to form 3-PBA is further corroborated by  $^{31}\text{P}$  NMR spectroscopic analysis of the reaction mixture, in which the resonance at  $\delta_p = 0.69$  ppm was assigned to the formation of a phosphoric acid ester (Figure S7).

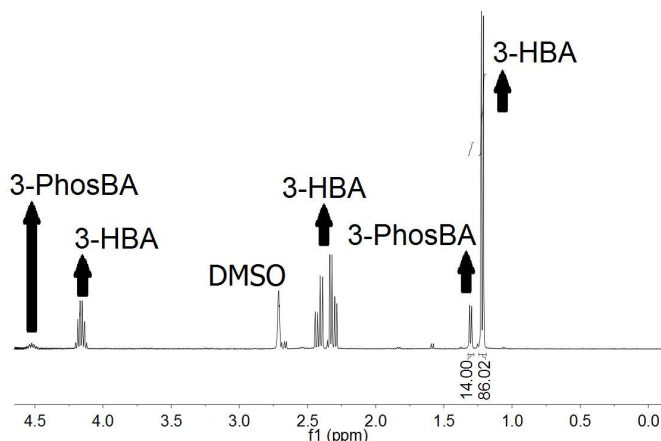


**Figure S6:**  $^1\text{H}$  NMR spectrum (400 MHz) of BBL in a phosphate-buffered reaction mixture after 49 h at 37 °C ( $[\text{BBL}]_0 = 25 \text{ mM}$ ,  $[\text{NaH}_2\text{PO}_4]_0 + [\text{Na}_2\text{HPO}_4]_0 = 0.10 \text{ M}$ ,  $\text{pH} = 7.00$  in  $\text{D}_2\text{O}/d_6\text{-DMSO}$  9/1 (v/v)).

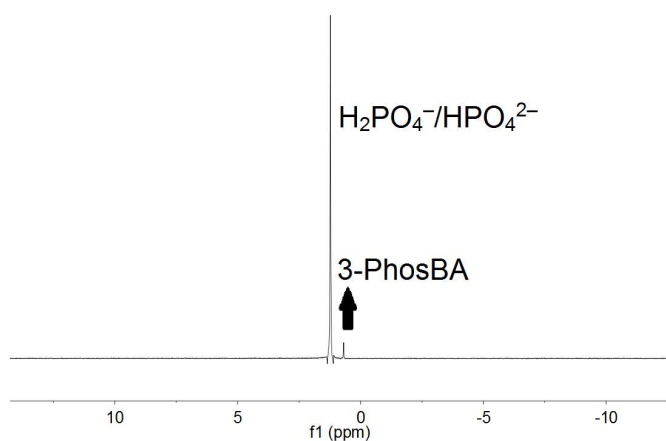


**Figure S7:**  $^{31}\text{P}\{-^1\text{H}\}$  NMR spectrum (162 MHz) of BBL in a phosphate-buffered reaction mixture after 49 h at 37 °C ( $[\text{BBL}]_0 = 25 \text{ mM}$ ,  $[\text{NaH}_2\text{PO}_4]_0 + [\text{Na}_2\text{HPO}_4]_0 = 0.10 \text{ M}$ ,  $\text{pH} = 7.00$ , solvent  $\text{D}_2\text{O}/d_6\text{-DMSO}$  9/1 (v/v)). The resonance at  $\delta = 1.23 \text{ ppm}$  is assigned to the phosphate buffer, the resonance at  $\delta = 0.69 \text{ ppm}$  is assigned to 3-(phosphonooxy)butanoic acid (3-PhosBA).

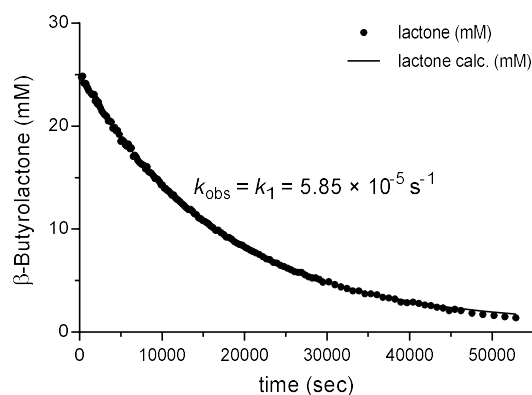
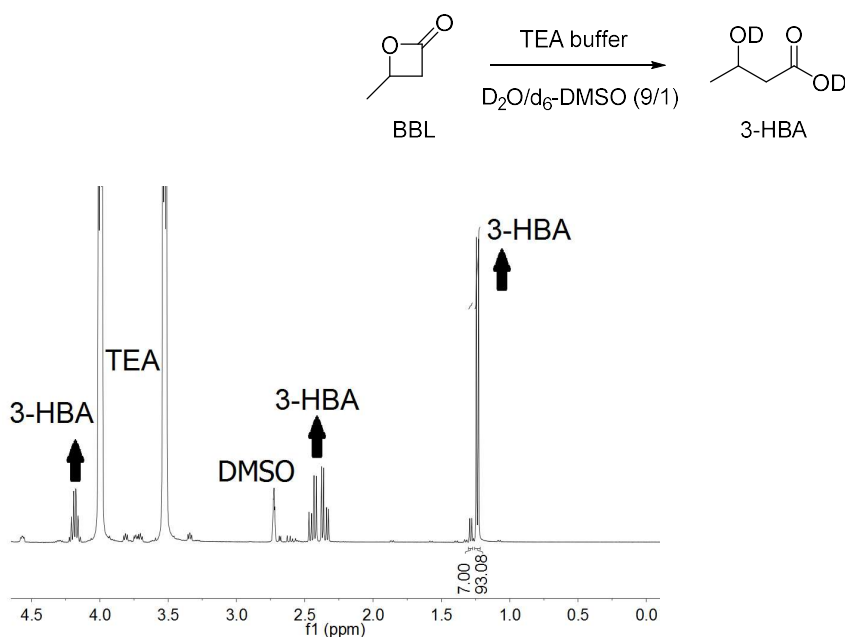


**Figure S8:** Decay of the concentration of BBL in a phosphate-buffered reaction mixture at 37 °C ( $[\text{BBL}]_0 = 25 \text{ mM}$ ,  $[\text{NaH}_2\text{PO}_4]_0 + [\text{Na}_2\text{HPO}_4]_0 = 0.10 \text{ M}$ ,  $\text{pH} = 7.00$  in  $\text{D}_2\text{O}/d_6\text{-DMSO}$  9/1 (v/v)). The black line shows a mono-exponential fit of the data.

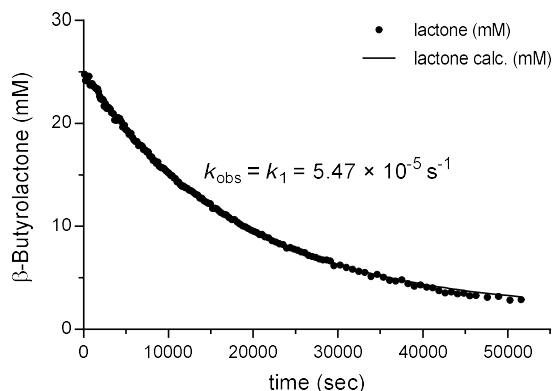
### 3.1.5. Hydrolysis of BBL in the presence of triethanolamine buffer (TEA buffer)

TEA buffer (540  $\mu\text{L}$  of a 0.11 M solution of TEA/TEA $\cdot\text{HCl}$  in  $\text{D}_2\text{O}$ , pH 7.75) and BBL (60  $\mu\text{L}$  of a 0.25 M solution in  $d_6$ -DMSO) were mixed in an NMR tube at 37  $^\circ\text{C}$ . The conversion of BBL was monitored by using time-resolved  $^1\text{H}$  NMR spectroscopy. Concentrations of BBL,  $[\text{BBL}]_t$ , were calculated from the ratio of the integral of the methyl resonances of BBL (d,  $\delta = 1.70$  ppm) to the integral of the methyl resonances in the range  $\delta = 1.43$ –1.27 ppm (Figure S9).

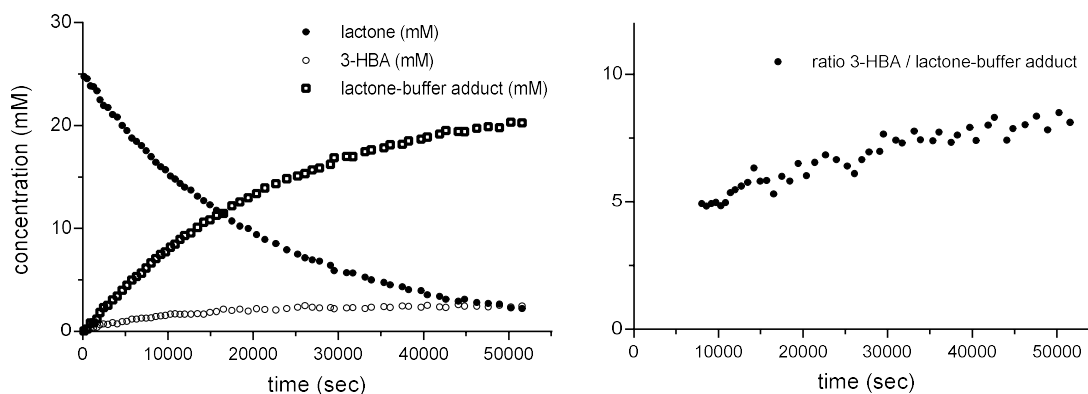
Beside 3-HBA, an adduct of BBL and TEA is formed. The 3-HBA/BBL-TEA-adduct ratio increases from 5.0 to 7.5 during the reaction (14 h, Figure S11), however reaches 13.3 after 13 days (Figure S9).



**Figure S9:**  $^1\text{H}$  NMR spectrum (400 MHz) of BBL in a TEA-buffered reaction mixture after 13 days at 37  $^\circ\text{C}$  ( $[\text{BBL}]_0 = 25$  mM,  $[\text{TEA}]_0 = 0.10$  M, pH = 7.75 in  $\text{D}_2\text{O}/d_6$ -DMSO 9/1 (v/v)).



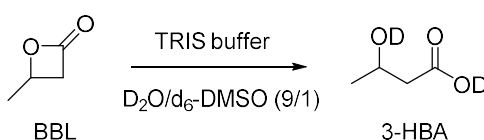
**Figure S10:** Decay of the concentration of BBL in a TEA-buffered reaction mixture at 37 °C ( $[BBL]_0 = 25$  mM,  $[TEA]_0 = 0.10$  M,  $pH = 7.75$  in  $D_2O/d_6$ -DMSO 9/1 (v/v)). The black line shows a mono-exponential fit of the data.



**Figure S11:** Concentration profiles in a TEA-buffered reaction mixture of BBL at 37 °C ( $[BBL]_0 = 25$  mM,  $[TEA]_0 = 0.10$  M,  $pH = 7.75$  in  $D_2O/d_6$ -DMSO 9/1 (v/v)) (left) and 3-HBA/BBL-buffer adduct ratio (right).

### 3.1.6. Hydrolysis of BBL in the presence of tris(hydroxymethyl)aminomethane buffer (TRIS buffer)

TRIS buffer (540  $\mu$ L of a 0.11 M solution of TRIS/TRIS·HCl in  $D_2O$ ,  $pH$  8.10) and BBL (60  $\mu$ L of a 0.25 M solution in  $d_6$ -DMSO) were mixed in an NMR tube at 37 °C. The conversion of BBL was monitored by using time-resolved  $^1H$  NMR spectroscopy. Concentrations of BBL,  $[BBL]_t$ , were calculated from the ratio of the integral of the methyl resonances of BBL ( $\delta$ ,  $\delta = 1.70$  ppm) to the integral of the methyl resonances in the range  $\delta = 1.43$ – $1.27$  ppm (Figure S11).



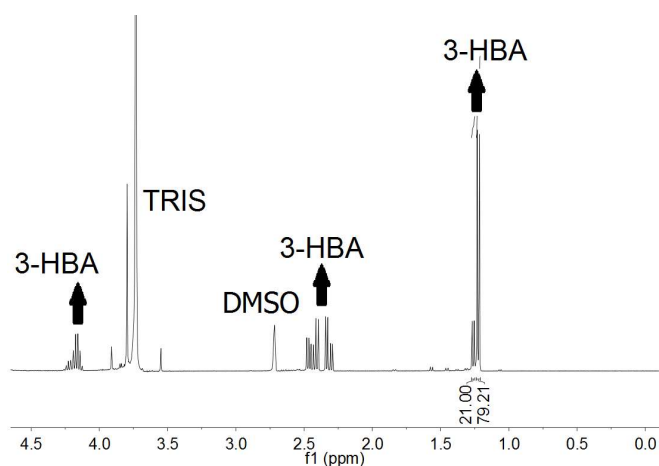


**Figure S12:**  $^1\text{H}$  NMR spectrum (400 MHz) of BBL in a TRIS-buffered reaction mixture after 9 d at 37 °C ( $[\text{BBL}]_0 = 25 \text{ mM}$ ,  $[\text{TRIS}]_0 = 0.10 \text{ M}$ ,  $\text{pH} = 8.10$  in  $\text{D}_2\text{O}/d_6\text{-DMSO}$  9/1 (v/v)).

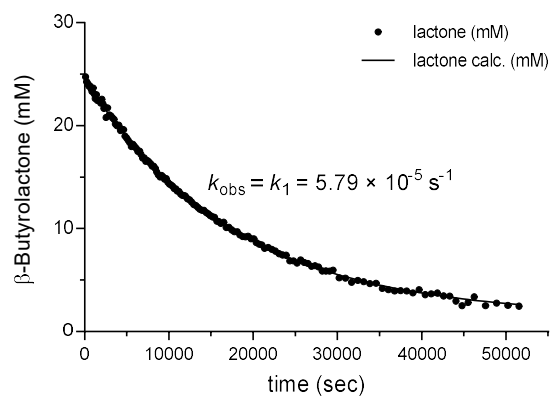


**Figure S13:** Decay of the concentration of BBL in a TRIS-buffered reaction mixture at 37 °C ( $[\text{BBL}]_0 = 25 \text{ mM}$ ,  $[\text{TRIS}]_0 = 0.10 \text{ M}$ ,  $\text{pH} = 8.10$  in  $\text{D}_2\text{O}/d_6\text{-DMSO}$  9/1 (v/v)). The black line shows a mono-exponential fit of the data.

#### 4. Kinetics of the reaction of BBL with amines in TEA-buffered D<sub>2</sub>O/*d*<sub>6</sub>-DMSO 9/1 (v/v) – Determination of second-order rate constants $k_N$

General procedure

A TEA-buffered (pH 7.75) solution of an amine (0.056 M) in D<sub>2</sub>O (540 μL) was mixed with a solution of BBL (60 μL of a 0.25 M solution in *d*<sub>6</sub>-DMSO) in an NMR tube at 37 °C to produce a 9/1 (v/v) D<sub>2</sub>O/*d*<sub>6</sub>-DMSO solvent mixture. The conversion of BBL was monitored by using time-resolved <sup>1</sup>H NMR spectroscopy. Concentrations of BBL, [BBL]<sub>*t*</sub>, were calculated from the ratio of the integral of the methyl resonances of BBL (d, δ = 1.70 ppm) to the integral of the methyl resonances in the range δ = 1.43–1.27 ppm.

The first-order rate constants  $k_{\text{obs}}$  (=  $k_2$  in equation (4) of the main text) were determined by least-squares fitting of the exponential function  $[\text{BBL}]_t = [\text{BBL}]_0 \cdot \exp(-k_{\text{obs}}t) + C$  to the time-dependent [BBL]<sub>*t*</sub>.

$$k_{\text{obs}} = k_2 = k_1 + k_N[\text{amine}]_{\text{eff}} \quad (4)$$

According to equation (5) of the main text, i.e.

$$k_N = (k_2 - k_1)/[\text{amine}]_{\text{eff}} \quad (5),$$

$k_N$  is then calculated from the experimentally determined  $k_2$ , the first-order rate constant of the BBL decay in TEA-buffered solution ( $k_1 = 5.47 \times 10^{-5} \text{ s}^{-1}$ , see Section 3.1.5) and the effective concentration of free amine at pH 7.75, [amine]<sub>eff</sub>, which is calculated according to Henderson Hasselbalch equation with  $\text{p}K_{\text{aH}^+}$  values from Ref. [2].

#### 4.1. Kinetics of the reaction of BBL with aniline in TEA-buffered D<sub>2</sub>O/d<sub>6</sub>-DMSO 9/1 (v/v)

##### 4.1.1. Reaction of BBL with [aniline]<sub>0</sub> = 50 mM

[BBL]<sub>0</sub> = 25 mM,

[PhNH<sub>2</sub>]<sub>0</sub> = 50 mM, [PhNH<sub>2</sub>]<sub>eff</sub> = 50 mM,

[TEA buffer]<sub>0</sub> = 0.10 M, pH 7.75 in D<sub>2</sub>O/d<sub>6</sub>-DMSO 9/1 (v/v), 37 °C.

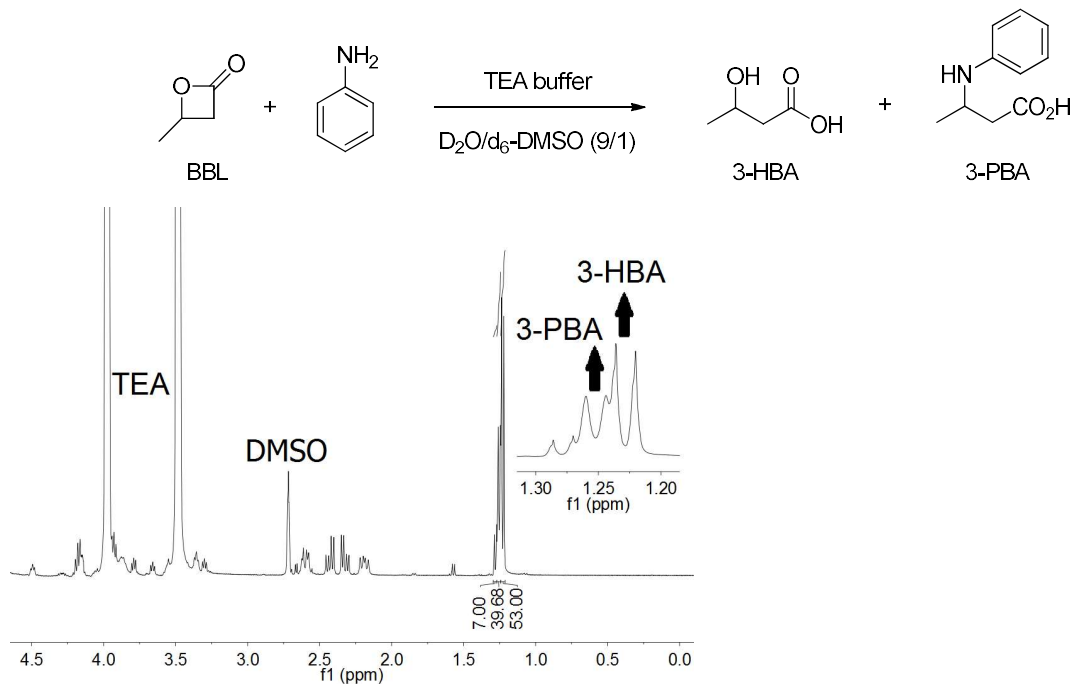


**Figure S14:** <sup>1</sup>H NMR spectrum (400 MHz) of the crude reaction mixture after completion of the reaction of BBL with aniline in a TEA-buffered D<sub>2</sub>O/d<sub>6</sub>-DMSO 9/1 (v/v) solution.

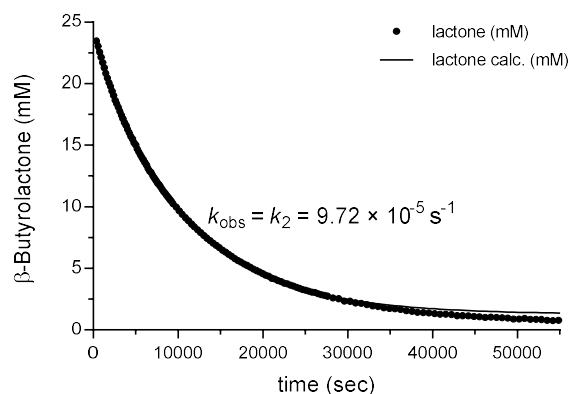


**Figure S15:** Decay of the concentration of BBL while reacting with aniline in a TEA-buffered reaction mixture at 37 °C ([aniline]<sub>0</sub> = 50 mM,  $k_{\text{N}} = 8.50 \times 10^{-4} \text{ M}^{-1} \text{ s}^{-1}$ ). The black line shows a mono-exponential fit of the data.

#### 4.1.2. Reaction of BBL with $[aniline]_0 = 74 \text{ mM}$

$[BBL]_0 = 25 \text{ mM}$ ,

$[PhNH_2]_0 = 74 \text{ mM}$ ,  $[PhNH_2]_{eff} = 74 \text{ mM}$ ,

$[TEA \text{ buffer}]_0 = 0.10 \text{ M}$ , pH 7.75 in  $D_2O/d_6\text{-DMSO}$  9/1 (v/v), 37 °C.

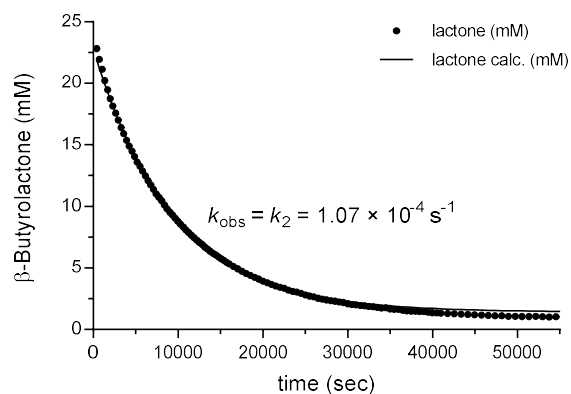


**Figure S16:** Decay of the concentration of BBL while reacting with aniline in a TEA-buffered reaction mixture at 37 °C ( $[aniline]_0 = 74 \text{ mM}$ ,  $k_N = 7.07 \times 10^{-4} \text{ M}^{-1} \text{ s}^{-1}$ ). The black line shows a mono-exponential fit of the data.

#### 4.1.3. Reaction of BBL with $[aniline]_0 = 0.10 \text{ M}$

$[BBL]_0 = 25 \text{ mM}$ ,

$[PhNH_2]_0 = 0.10 \text{ M}$ ,  $[PhNH_2]_{eff} = 0.10 \text{ M}$ ,

$[TEA \text{ buffer}]_0 = 0.10 \text{ M}$ , pH 7.75 in  $D_2O/d_6\text{-DMSO}$  9/1 (v/v), 37 °C.

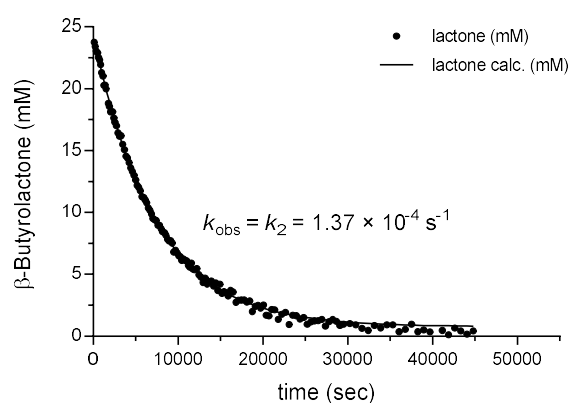


**Figure S17:** Decay of the concentration of BBL while reacting with aniline in a TEA-buffered reaction mixture at 37 °C ( $[aniline]_0 = 0.10 \text{ M}$ ,  $k_N = 8.23 \times 10^{-4} \text{ M}^{-1} \text{ s}^{-1}$ ). The black line shows a mono-exponential fit of the data.

#### 4.1.4. Reaction of BBL with [aniline]<sub>0</sub> = 0.30 M

[BBL]<sub>0</sub> = 25 mM,

[PhNH<sub>2</sub>]<sub>0</sub> = 0.30 M, [PhNH<sub>2</sub>]<sub>eff</sub> = 0.30 M,

[TEA buffer]<sub>0</sub> = 0.10 M, pH 7.75 in D<sub>2</sub>O/*d*<sub>6</sub>-DMSO 9/1 (v/v), 37 °C.

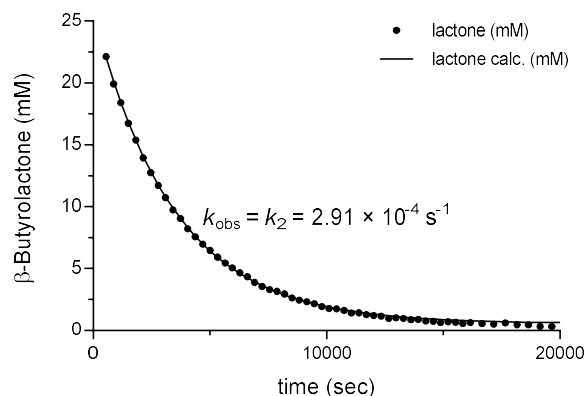


**Figure S18:** Decay of the concentration of BBL while reacting with aniline in a TEA-buffered reaction mixture at 37 °C ([aniline]<sub>0</sub> = 0.30 M,  $k_{\text{N}} = 7.88 \times 10^{-4} \text{ M}^{-1} \text{ s}^{-1}$ ). The black line shows a mono-exponential fit of the data.

#### 4.1.5. Determination of the second-order rate constant $k_{\text{N}}$ for the reaction of BBL with aniline

**Table S1:** Rate constants for the reactions of BBL with aniline at 37 °C at pH 7.75 in D<sub>2</sub>O/*d*<sub>6</sub>-DMSO 9/1 (v/v) at variable aniline concentrations.

[aniline] <sub>0</sub> (M)	$k_{\text{obs}}$ (s <sup>-1</sup> )	$k_{\text{N}}$ (M <sup>-1</sup> s <sup>-1</sup> )
$5.0 \times 10^{-2}$	$9.72 \times 10^{-5}$	$8.50 \times 10^{-4}$
$7.4 \times 10^{-2}$	$1.07 \times 10^{-4}$	$7.07 \times 10^{-4}$
$1.0 \times 10^{-1}$	$1.37 \times 10^{-4}$	$8.23 \times 10^{-4}$
$3.0 \times 10^{-1}$	$2.91 \times 10^{-4}$	$7.88 \times 10^{-4}$
averaged $k_{\text{N}}$		$7.92 \times 10^{-4}$
Standard dev		$\pm 5.4 \times 10^{-5}$

The averaged  $k_N$  is in excellent agreement with the  $k_N$  derived from the slope of the linear correlation of  $k_{obs}$  with  $[aniline]_0$  shown in Figure S19.

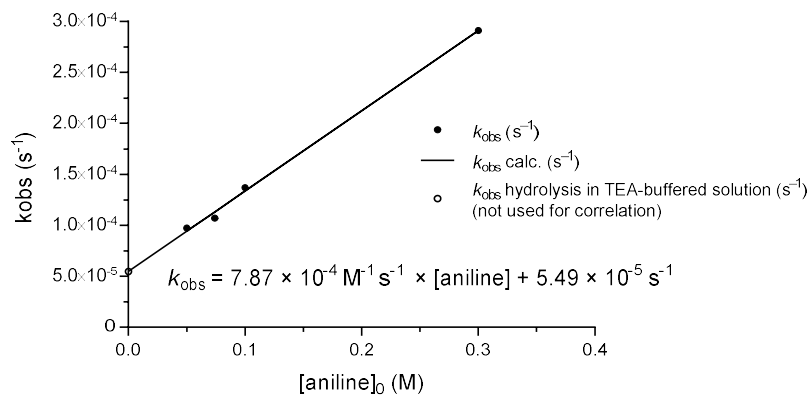


**Figure S19:** Correlation of  $k_{obs}$  with  $[aniline]_0$ . For comparison also  $k_{obs}$  of hydrolysis in TEA-buffered solution is plotted.

The average value  $k_N(aniline) = 7.92 (\pm 0.54) \times 10^{-4} M^{-1} s^{-1}$  is used in Table 3 of the main text.

4.2. Kinetics of the reaction of BBL with *m*-toluidine in TEA-buffered D<sub>2</sub>O/*d*<sub>6</sub>-DMSO 9/1 (v/v)

[BBL]<sub>0</sub> = 25 mM,  
 [m-tol-NH<sub>2</sub>]<sub>0</sub> = 50 mM, [m-tol-NH<sub>2</sub>]<sub>eff</sub> = 50 mM,  
 [TEA buffer]<sub>0</sub> = 0.10 M, pH 7.75 in D<sub>2</sub>O/*d*<sub>6</sub>-DMSO 9/1 (v/v), 37 °C.

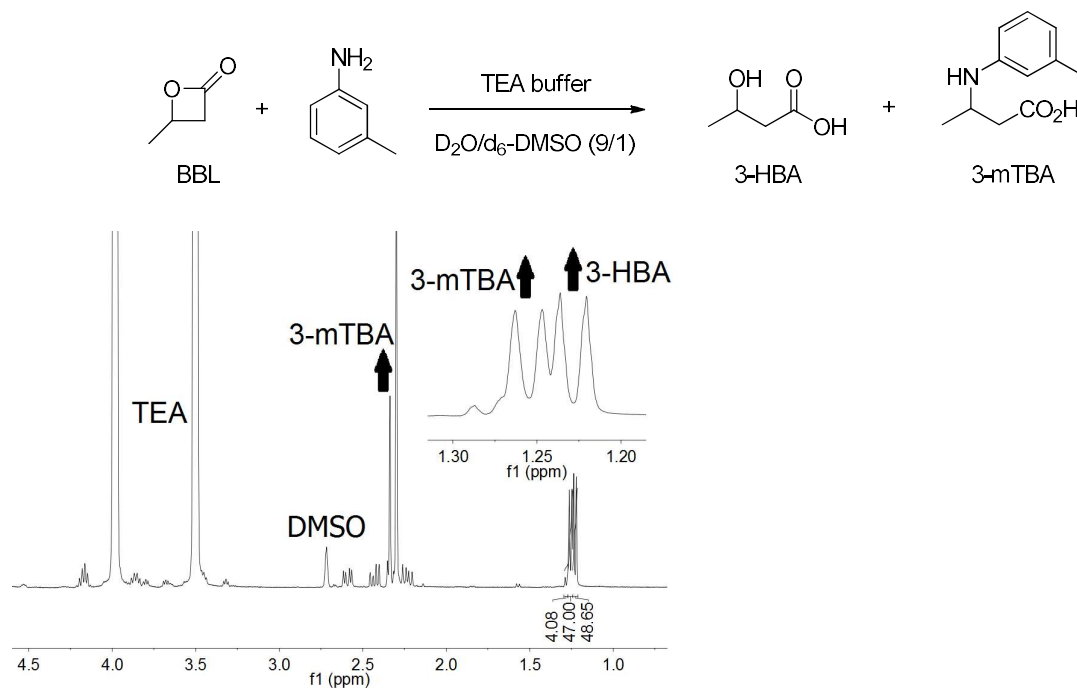


**Figure S20:** <sup>1</sup>H NMR spectrum (400 MHz) of the crude reaction mixture after completion of the reaction of BBL with *m*-toluidine in a TEA-buffered D<sub>2</sub>O/*d*<sub>6</sub>-DMSO 9/1 (v/v) solution.

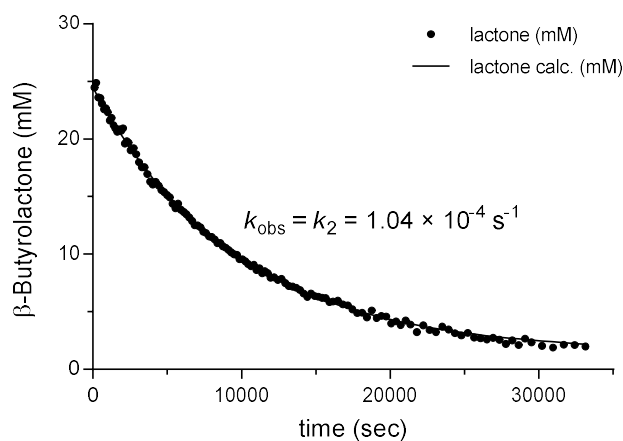


**Figure S21:** Decay of the concentration of BBL while reacting with *m*-toluidine in a TEA-buffered reaction mixture at 37 °C ( $k_N = 9.90 \times 10^{-4} \text{ M}^{-1} \text{ s}^{-1}$ ). The black line shows a mono-exponential fit of the data.

4.3. Kinetics of the reaction of BBL with *p*-toluidine in TEA-buffered D<sub>2</sub>O/*d*<sub>6</sub>-DMSO 9/1 (v/v)

[BBL]<sub>0</sub> = 25 mM,

[*p*-tol-NH<sub>2</sub>]<sub>0</sub> = 50 mM, [*p*-tol-NH<sub>2</sub>]<sub>eff</sub> = 50 mM,

[TEA buffer]<sub>0</sub> = 0.10 M, pH 7.75 in D<sub>2</sub>O/*d*<sub>6</sub>-DMSO 9/1 (v/v), 37 °C.

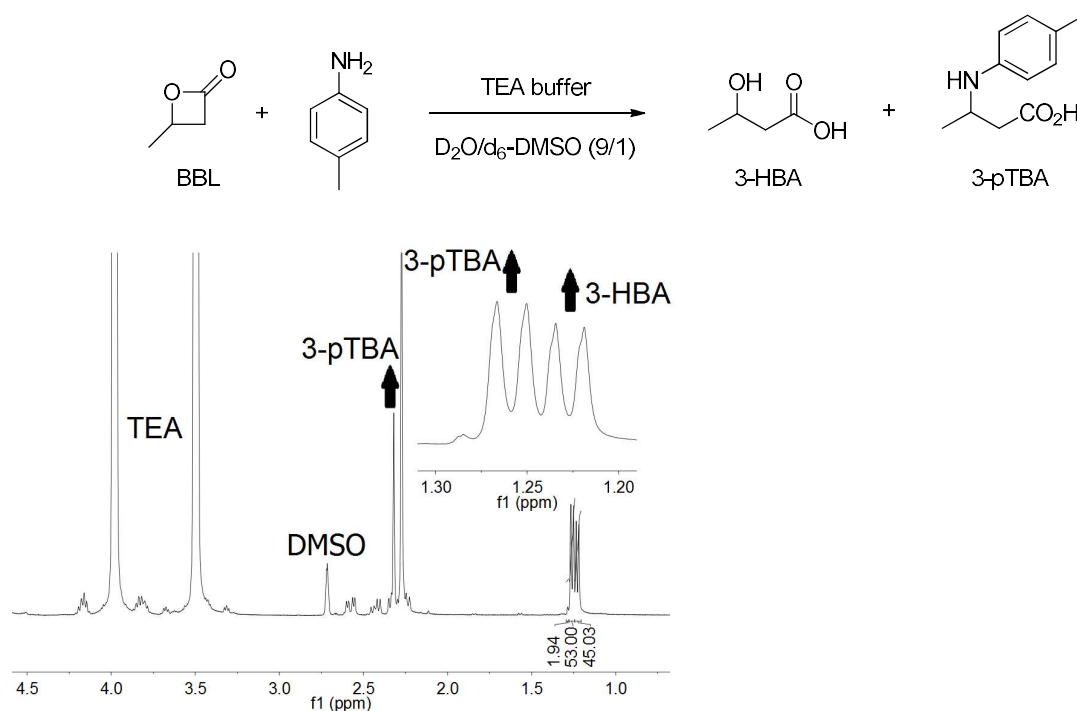


**Figure S22:** <sup>1</sup>H NMR spectrum (400 MHz) of the crude reaction mixture after completion of the reaction of BBL with *p*-toluidine in a TEA-buffered D<sub>2</sub>O/*d*<sub>6</sub>-DMSO 9/1 (v/v) solution.

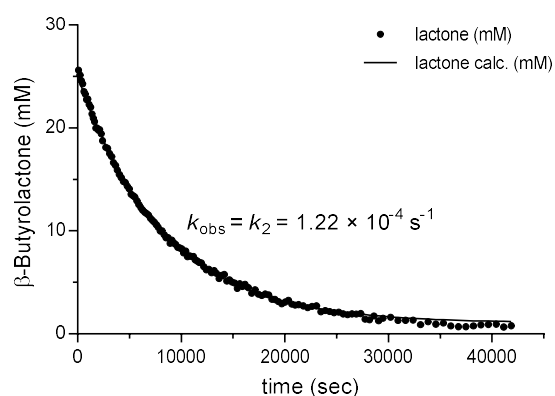


**Figure S23:** Decay of the concentration of BBL while reacting with *p*-toluidine in a TEA-buffered reaction mixture at 37 °C ( $k_{\text{N}} = 1.35 \times 10^{-3} \text{ M}^{-1} \text{ s}^{-1}$ ). The black line shows a mono-exponential fit of the data.

4.4. Kinetics of the reaction of BBL with *p*-anisidine in TEA-buffered D<sub>2</sub>O/*d*<sub>6</sub>-DMSO 9/1 (v/v)

[BBL]<sub>0</sub> = 25 mM,

[*p*-ani-NH<sub>2</sub>]<sub>0</sub> = 50 mM, [*p*-ani-NH<sub>2</sub>]<sub>eff</sub> = 50 mM,

[TEA buffer]<sub>0</sub> = 0.10 M, pH 7.75 in D<sub>2</sub>O/*d*<sub>6</sub>-DMSO 9/1 (v/v), 37 °C.

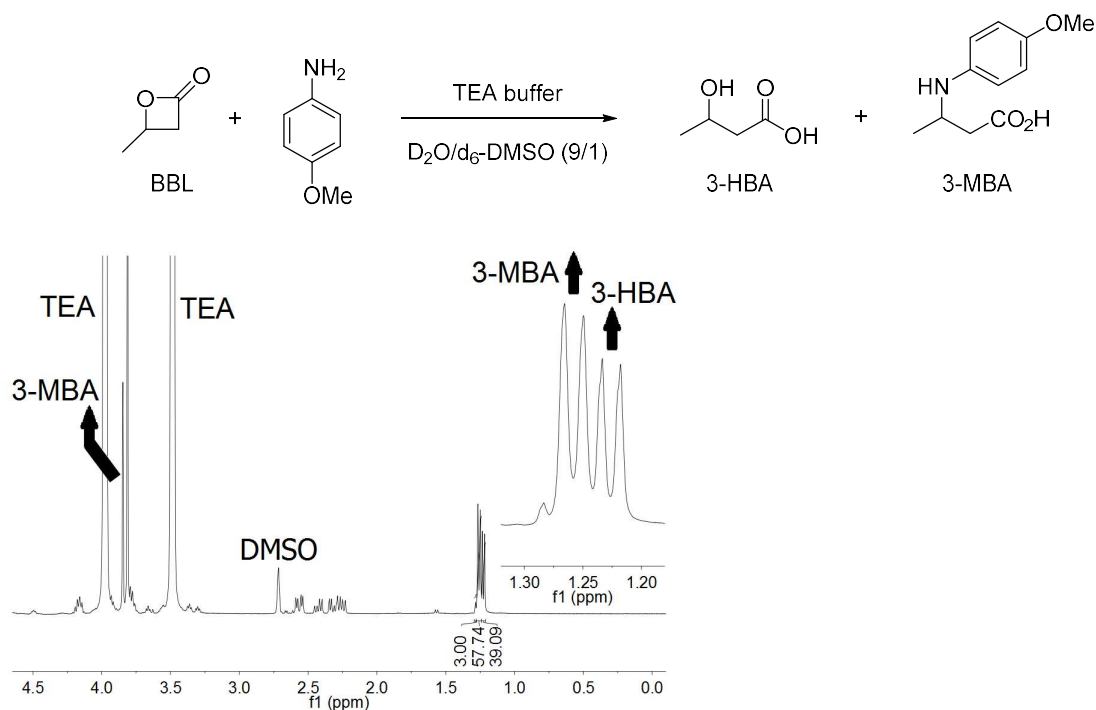


**Figure S24:** <sup>1</sup>H NMR spectrum (400 MHz) of the crude reaction mixture after completion of the reaction of BBL with *p*-anisidine in a TEA-buffered D<sub>2</sub>O/*d*<sub>6</sub>-DMSO 9/1 (v/v) solution.

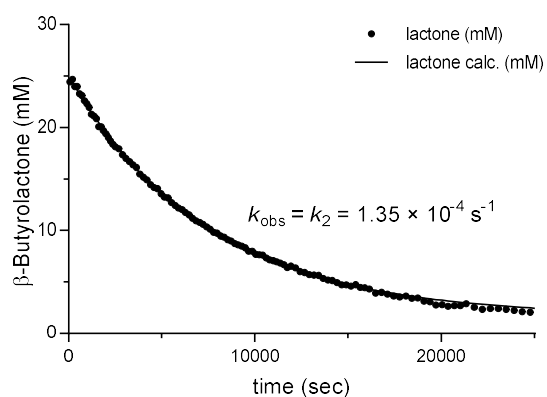


**Figure S25:** Decay of the concentration of BBL while reacting with *p*-anisidine in a TEA-buffered reaction mixture at 37 °C ( $k_{\text{N}} = 1.62 \times 10^{-3} \text{ M}^{-1} \text{ s}^{-1}$ ). The black line shows a mono-exponential fit of the data.

4.5. Kinetics of the reaction of BBL with benzylamine in TEA-buffered D<sub>2</sub>O/*d*<sub>6</sub>-DMSO 9/1 (v/v)

[BBL]<sub>0</sub> = 25 mM,

[PhCH<sub>2</sub>NH<sub>2</sub>]<sub>0</sub> = 50 mM, [PhCH<sub>2</sub>NH<sub>2</sub>]<sub>eff</sub> = 1.2 mM,

[TEA buffer]<sub>0</sub> = 0.10 M, pH 7.75 in D<sub>2</sub>O/*d*<sub>6</sub>-DMSO 9/1 (v/v), 37 °C.

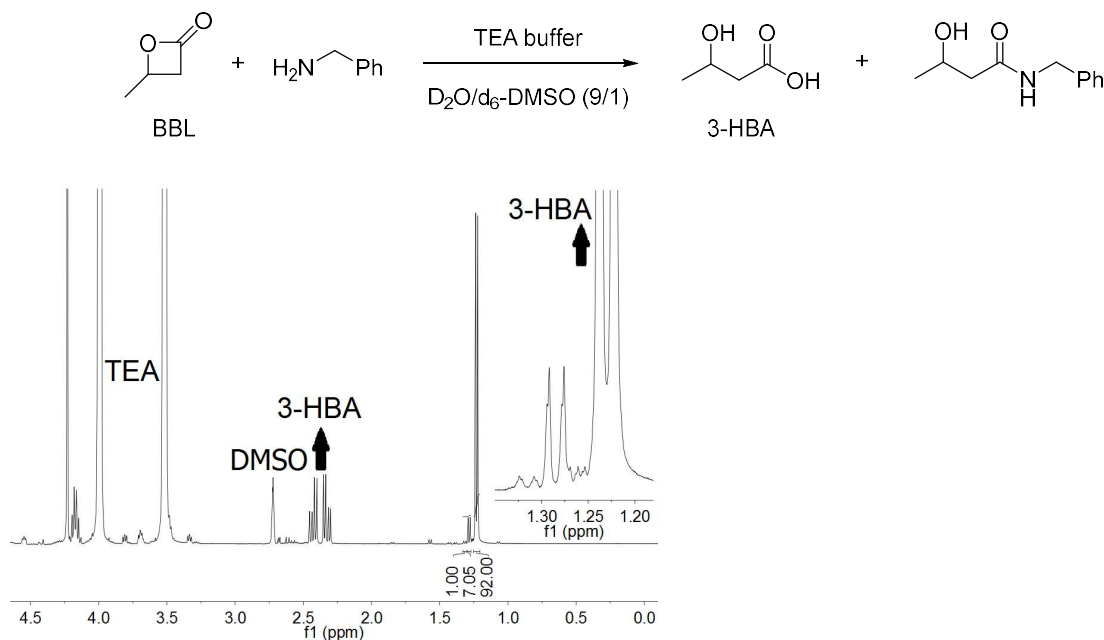


**Figure S26:** <sup>1</sup>H NMR spectrum (400 MHz) of the crude reaction mixture after completion of the reaction of BBL with benzylamine in a TEA-buffered D<sub>2</sub>O/*d*<sub>6</sub>-DMSO 9/1 (v/v) solution.

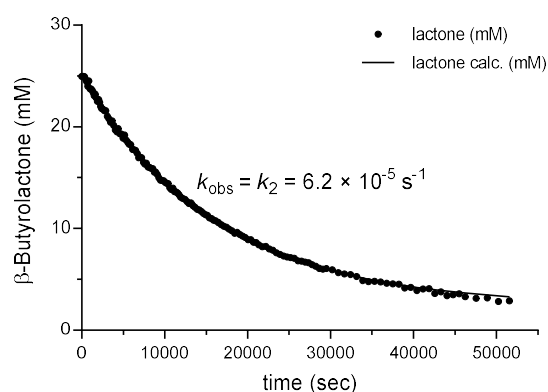


**Figure S27:** Decay of the concentration of BBL while reacting with benzylamine in a TEA-buffered reaction mixture at 37 °C ( $k_N = 5.8 \times 10^{-3} \text{ M}^{-1} \text{ s}^{-1}$ ). The black line shows a mono-exponential fit of the data.

Due to the small concentration of unprotonated benzylamine under reaction conditions, we proofed the formation of *N*-benzyl-3-hydroxybutanamide by HPLC-HRMS (ESI) analysis of the reaction mixture. Calcd. for C<sub>11</sub>H<sub>16</sub>NO<sub>2</sub> [M+H]<sup>+</sup>:  $m/z = 194.11756$ ; found:  $m/z = 194.11753$ .

4.6. Kinetics of the reaction of BBL with phenylethylamine in TEA-buffered D<sub>2</sub>O/*d*<sub>6</sub>-DMSO 9/1 (v/v)

[BBL]<sub>0</sub> = 25 mM,

[PhCH<sub>2</sub>CH<sub>2</sub>NH<sub>2</sub>]<sub>0</sub> = 50 mM, [PhCH<sub>2</sub>CH<sub>2</sub>NH<sub>2</sub>]<sub>eff</sub> = 0.36 mM,

[TEA buffer]<sub>0</sub> = 0.10 M, pH 7.75 in D<sub>2</sub>O/*d*<sub>6</sub>-DMSO 9/1 (v/v), 37 °C.

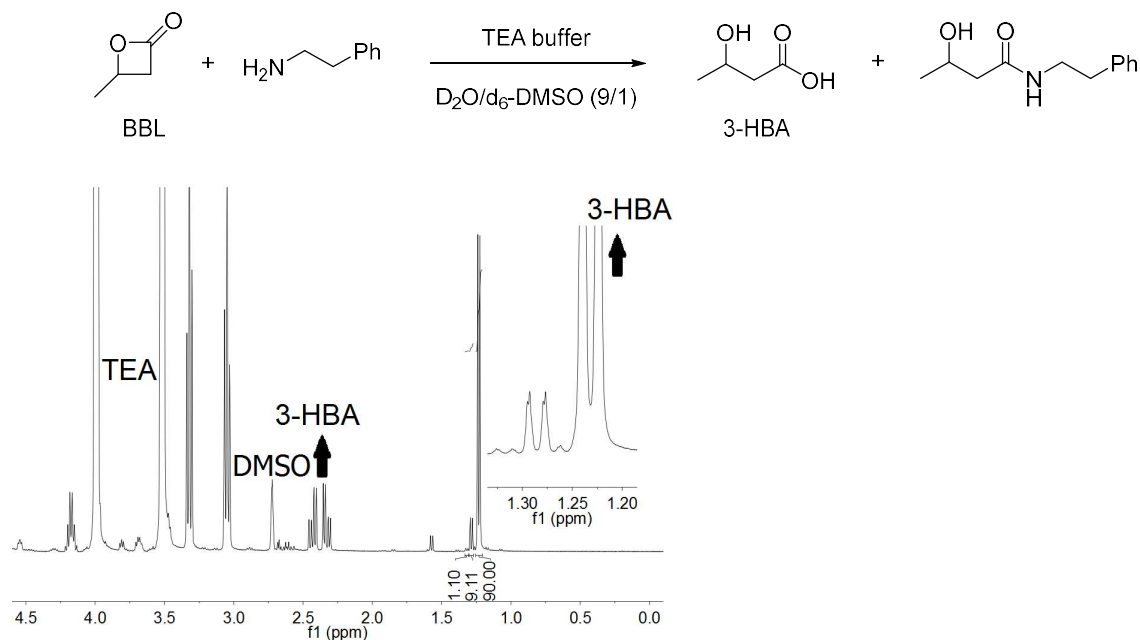


**Figure S28:** <sup>1</sup>H NMR spectrum (400 MHz) of the crude reaction mixture after completion of the reaction of BBL with phenylethylamine in a TEA-buffered D<sub>2</sub>O/*d*<sub>6</sub>-DMSO 9/1 (v/v) solution.

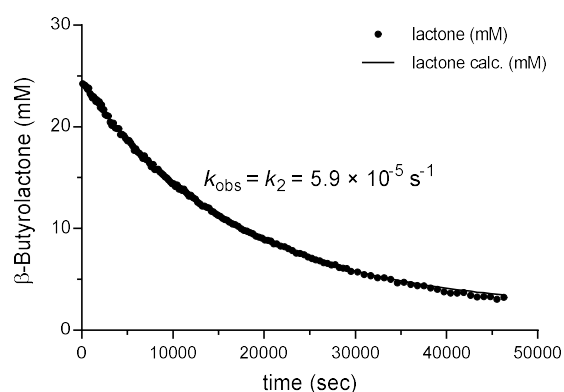


**Figure S29:** Decay of the concentration of BBL while reacting with phenylethylamine in a TEA-buffered reaction mixture at 37 °C ( $k_{\text{N}} = 1.1 \times 10^{-2} \text{ M}^{-1} \text{ s}^{-1}$ ). The black line shows a mono-exponential fit of the data.

Due to the small concentration of unprotonated phenylethylamine under reaction conditions, we proofed the formation of 3-hydroxy-*N*-phenethylbutanamide by HPLC-HRMS (ESI) analysis of the reaction mixture. Calcd. for C<sub>12</sub>H<sub>18</sub>NO<sub>2</sub> [M+H]<sup>+</sup>:  $m/z = 208.13321$ ; found:  $m/z = 208.13317$ .

#### 4.7. Rate constants for the reactions of BBL with amines

**Table S2:** Rate constants for the reactions of BBL with different amines at 37 °C and pH 7.75 in D<sub>2</sub>O/d<sub>6</sub>-DMSO 9/1 (v/v).

	aniline	<i>m</i> -toluidine	<i>p</i> -toluidine	<i>p</i> -anisidine	benzyl-amine	phenylethyl-amine
$pK_{aH^+}$	4.60	4.87	5.08	5.36	9.36	9.89
$c_{\text{eff}}$ (M)	-	$5.0 \times 10^{-2}$	$5.0 \times 10^{-2}$	$5.0 \times 10^{-2}$	$1.2 \times 10^{-3}$	$3.6 \times 10^{-4}$
$k_{\text{obs}}$ (s <sup>-1</sup> )	-	$1.04 \times 10^{-4}$	$1.22 \times 10^{-4}$	$1.35 \times 10^{-4}$	$6.2 \times 10^{-5}$	$5.9 \times 10^{-5}$
$k_N$ (M <sup>-1</sup> s <sup>-1</sup> )	$7.92 \times 10^{-4}$ [a]	$9.90 \times 10^{-4}$	$1.35 \times 10^{-3}$	$1.62 \times 10^{-3}$	$5.8 \times 10^{-3}$	$1.1 \times 10^{-2}$
$\sigma_m$ or $\sigma_p$ <sup>[b]</sup>	0	-0.07	-0.17	-0.26	-	-

[a] Average value, see Section 4.1. [b] From Ref. [3]

#### 4.8. Hammett plot for the reactions of BBL with anilines

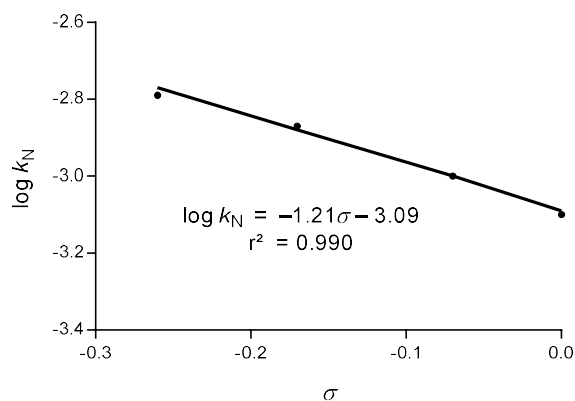


**Figure S30:** Hammett plot of the reaction of BBL with anilines at 37 °C and pH 7.75 in D<sub>2</sub>O/d<sub>6</sub>-DMSO 9/1 (v/v), with data from Table S2.

## 5. Kinetics of the reaction of BBL with benzylamine in $d_6$ -DMSO

$[BBL]_0 = 25 \text{ mM}$ ,

$[PhCH_2NH_2]_0 = 50 \text{ mM}$ , in  $d_6$ -DMSO,  $37 \text{ }^\circ\text{C}$ .

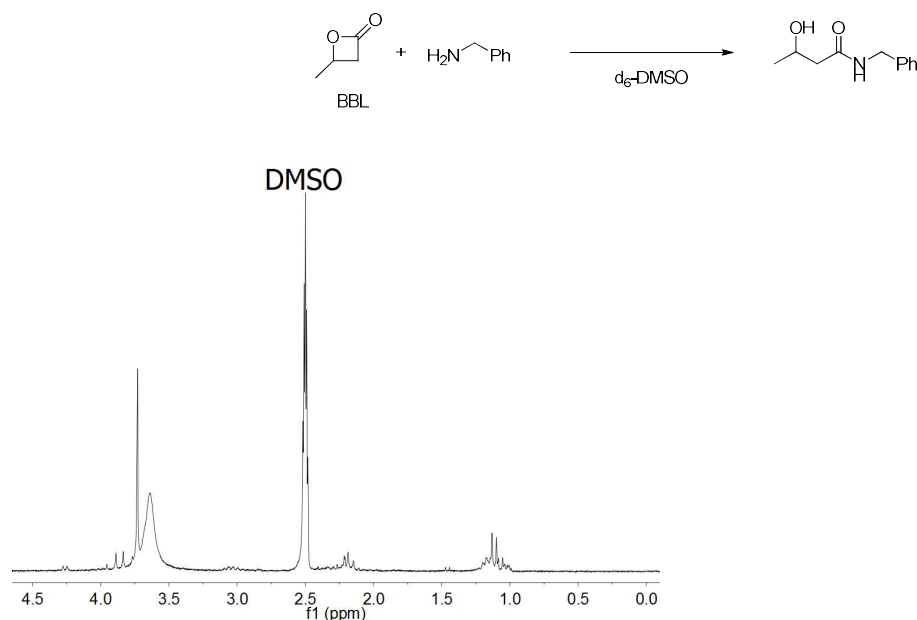


**Figure S31:**  $^1H$  NMR spectrum (200 MHz) of the crude reaction mixture after completion of the reaction of BBL with benzylamine  $d_6$ -DMSO solution.

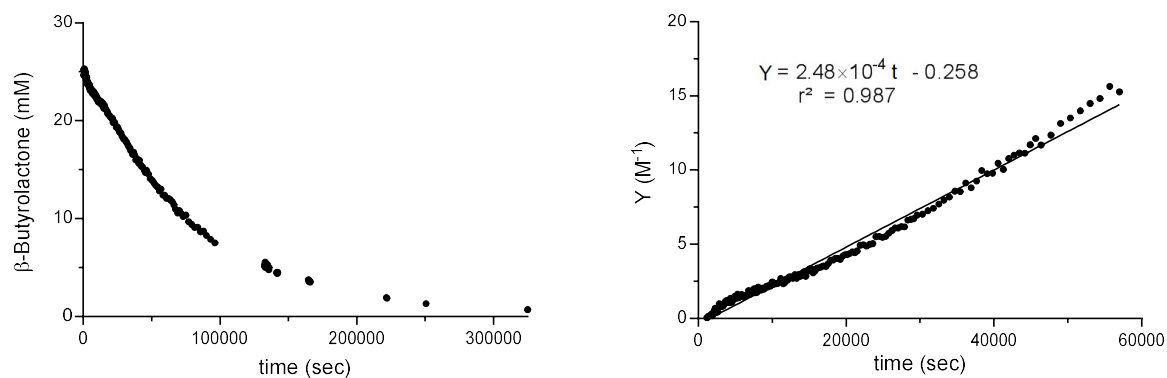


**Figure S32:** Decay of the concentration of BBL while reacting with benzylamine  $d_6$ -DMSO at  $37 \text{ }^\circ\text{C}$  (left). Determination of the second-order rate constant by plotting time versus  $Y = ([Nu]_0 - [E]_0)^{-1} \ln([E]_0/[E]_t + [Nu]_0 - [E]_0)/[Nu]_0[E]_t$  ( $k_N = 2.5 \times 10^{-4} \text{ M}^{-1} \text{ s}^{-1}$ , evaluated from data for the first half-life; right).

## 6. Determination of second-order rate constants of the reaction of sodium penicillin G with various amines in D<sub>2</sub>O/*d*<sub>6</sub>-DMSO 9/1 (v/v)

### General procedure

A TEA-buffered (pH 7.75) solution of an amine (0.056 M) in D<sub>2</sub>O (540 μL) was mixed with a solution of penicillin G (60 μL of a 0.25 M solution in *d*<sub>6</sub>-DMSO) in an NMR tube at 37 °C to produce a 9/1 (v/v) D<sub>2</sub>O/DMSO solvent mixture. The conversion of penicillin G (PenG) was monitored by using time-resolved <sup>1</sup>H NMR spectroscopy. Concentrations of PenG, [PenG]<sub>*t*</sub>, were calculated from ratio of the integral of the aromatic protons (7.63 to 7.40 ppm, m, 5 H; 15 H respectively, if the nucleophile also gave signals in this range) to all protons of the bicyclic moiety (5.67 ppm, d, *J* = 3.9 Hz, 1 H and 5.59 ppm, d, *J* = 3.8 Hz, 1 H).

The first-order rate constants *k*<sub>obs</sub> (= *k*<sub>2</sub> in equation (4) of the main text) were determined by least-squares fitting of the exponential function [PenG]<sub>*t*</sub> = [PenG]<sub>0</sub>·exp(-*k*<sub>obs</sub>*t*) + *C* to the time-dependent [PenG]<sub>*t*</sub>.

$$k_{\text{obs}} = k_2 = k_1 + k_{\text{N}}[\text{amine}]_{\text{eff}} \quad (4)$$

According to equation (5) of the main text, i.e.

$$k_{\text{N}} = (k_2 - k_1)/[\text{amine}]_{\text{eff}} \quad (5)$$

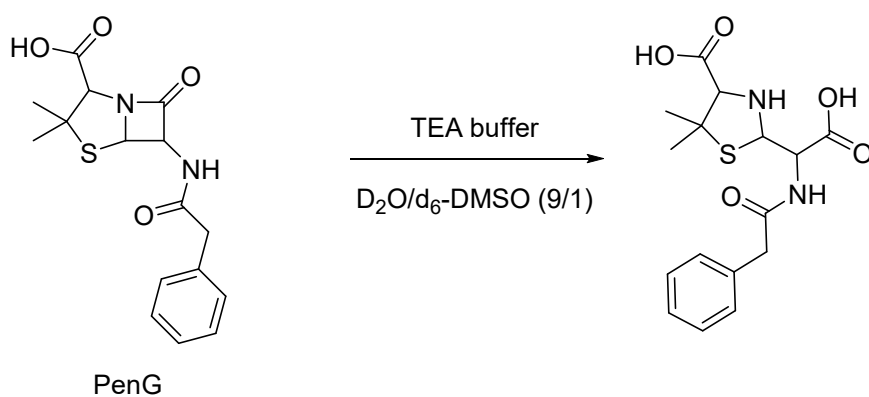
*k*<sub>N</sub> is then calculated from the experimentally determined *k*<sub>2</sub>, the first-order rate constant of the PenG decay in TEA-buffered solution (*k*<sub>1</sub> = 3.3 × 10<sup>-5</sup> s<sup>-1</sup>, see Section 7.1) and the effective concentration of free amine at pH 7.75.

6.1. Consumption of sodium penicillin G in TEA-buffered solution – Determination of the first-order rate constant  $k_1$

TEA buffer (540  $\mu\text{L}$  of a 0.11 M solution of TEA/TEA $\cdot$ HCl in  $\text{D}_2\text{O}$ , pH 7.75) and penicillin G (60  $\mu\text{L}$  of a 0.25 M solution in  $\text{d}_6$ -DMSO) were mixed in an NMR tube at 37  $^\circ\text{C}$ . The conversion of penicillin G was monitored by using time-resolved  $^1\text{H}$  NMR spectroscopy. Concentrations of penicillin G,  $[\text{PenG}]_t$ , were calculated from ratio of the integral of the aromatic protons (7.63 to 7.40 ppm, m, 5 H) to all protons of the bicyclic moiety (5.67 ppm, d,  $J = 3.9$  Hz, 1 H and 5.59 ppm, d,  $J = 3.8$  Hz, 1 H).

$[\text{PenG}]_0 = 25$  mM,

$[\text{TEA buffer}]_0 = 0.10$  M, pH 7.75 in  $\text{D}_2\text{O}/\text{d}_6\text{-DMSO}$  9/1 (v/v), 37  $^\circ\text{C}$



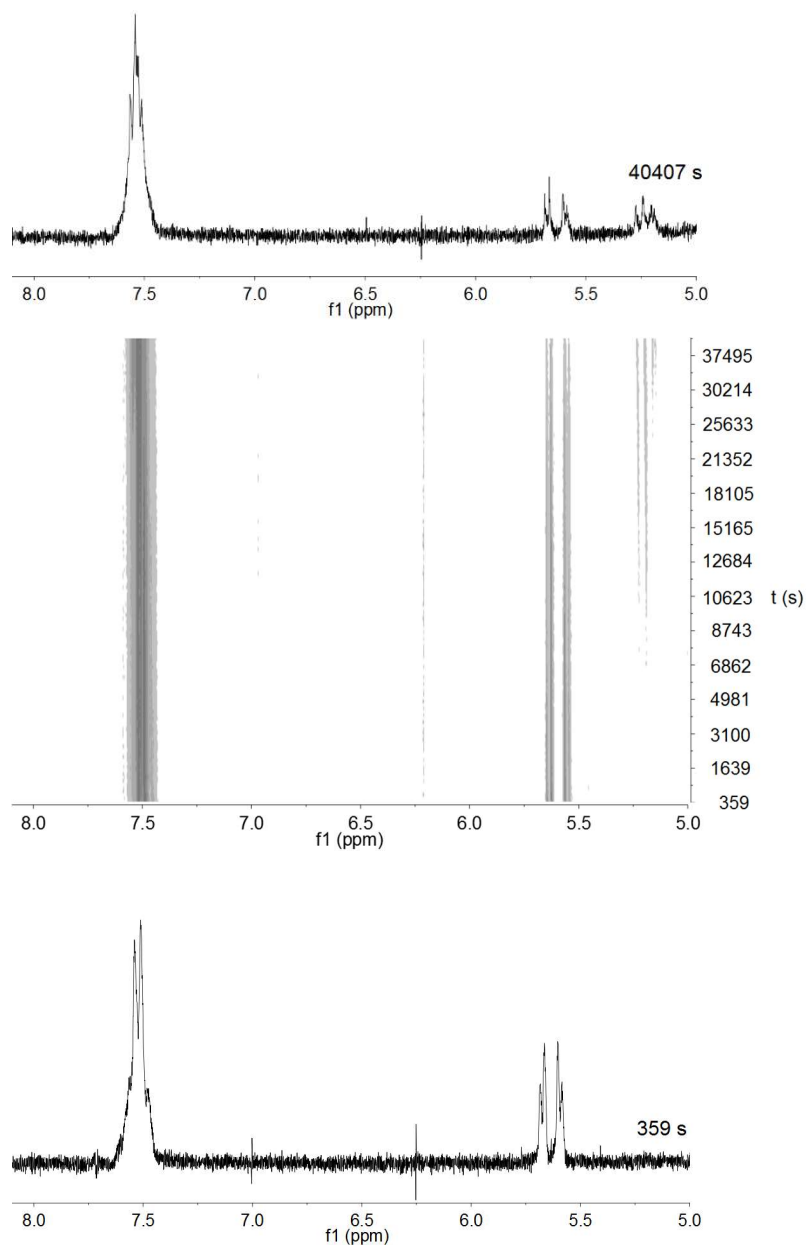


**Figure S40:** Exemplary time-resolved  $^1\text{H}$  NMR spectra of the hydrolysis of penicillin G in TEA-buffered  $\text{D}_2\text{O}/d_6\text{-DMSO}$  9/1 (v/v) at 37 °C ( $[\text{penicillin G}]_0 = 25 \text{ mM}$ ,  $\text{pH} = 7.75$ ). Start of the reaction (bottom), time-resolved topview of  $^1\text{H}$  NMR spectra showing the decrease of the followed penicillin G resonances (middle), and final  $^1\text{H}$  NMR spectrum after 40407 s (top).

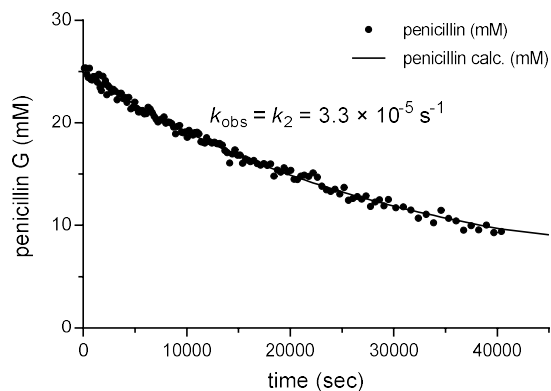


**Figure S41:** Decay of the concentration of penicillin G in a TEA-buffered reaction mixture at 37 °C. The black line shows a mono-exponential fit of the data.

## 6.2. Kinetics of the reaction of sodium penicillin G with benzylamine in TEA-buffered D<sub>2</sub>O/d<sub>6</sub>-DMSO 9/1 (v/v)

[PenG]<sub>0</sub> = 25 mM,

[PhCH<sub>2</sub>NH<sub>2</sub>]<sub>0</sub> = 50 mM, [PhCH<sub>2</sub>NH<sub>2</sub>]<sub>eff</sub> = 1.2 mM,

[TEA buffer]<sub>0</sub> = 0.10 M, pH 7.75 in D<sub>2</sub>O/d<sub>6</sub>-DMSO 9/1 (v/v), 37 °C

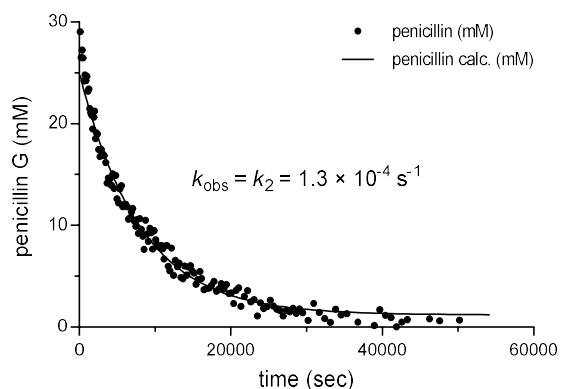
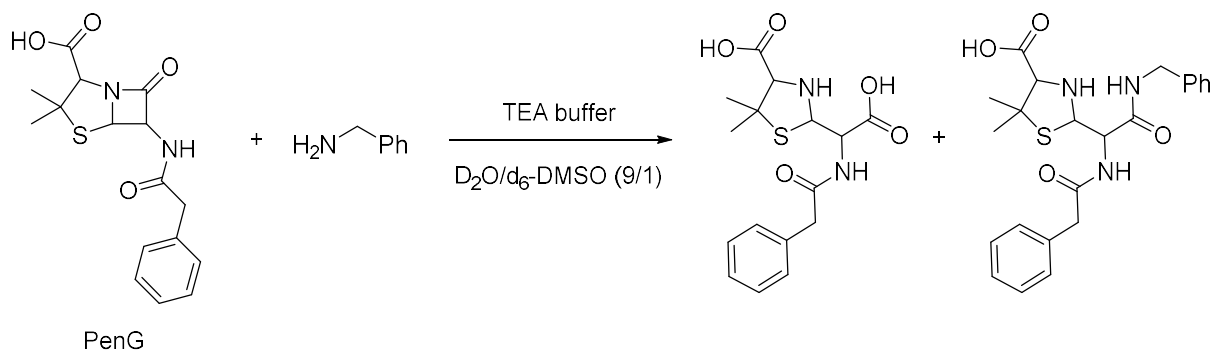


**Figure S42:** Decay of the concentration of penicillin G while reacting with benzylamine in a TEA-buffered reaction mixture at 37 °C ( $k_N = 8.1 \times 10^{-2} \text{ M}^{-1} \text{ s}^{-1}$ ). The black line shows a mono-exponential fit of the data.

6.3. Kinetics of the reaction of sodium penicillin G with phenylethylamine in TEA-buffered  $D_2O/d_6$ -DMSO 9/1 (v/v)

$[PenG]_0 = 25 \text{ mM}$ ,

$[PhCH_2CH_2NH_2]_0 = 50 \text{ mM}$ ,  $[PhCH_2CH_2NH_2]_{eff} = 0.36 \text{ mM}$ ,

$[TEA \text{ buffer}]_0 = 0.10 \text{ M}$ , pH 7.75 in  $D_2O/d_6$ -DMSO 9/1 (v/v),  $37 \text{ }^\circ\text{C}$

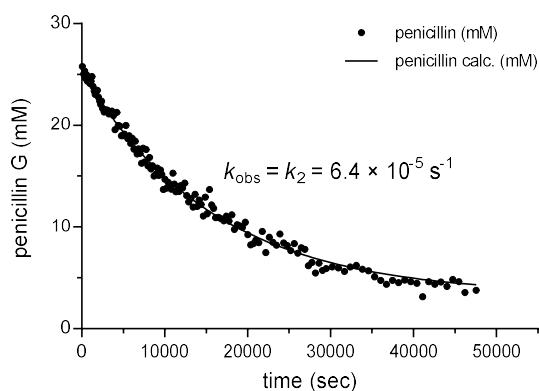
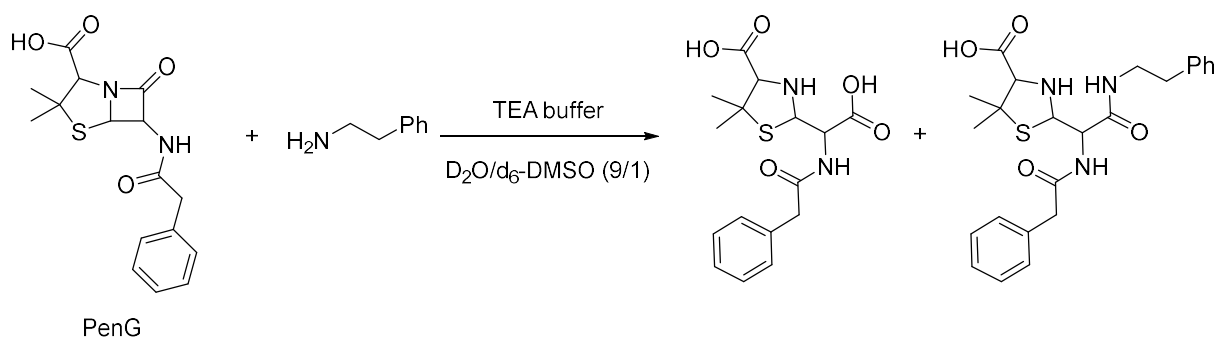


**Figure S43:** Decay of the concentration of penicillin G while reacting with phenylethylamine in a TEA-buffered reaction mixture at  $37 \text{ }^\circ\text{C}$  ( $k_N = 8.6 \times 10^{-2} \text{ M}^{-1} \text{ s}^{-1}$ ). The black line shows a mono-exponential fit of the data.

6.4. Kinetics of the reaction of sodium penicillin G with *n*-propylamine in TEA-buffered D<sub>2</sub>O/*d*<sub>6</sub>-DMSO 9/1 (v/v)

[PenG]<sub>0</sub> = 25 mM,

[*n*-PrNH<sub>2</sub>]<sub>0</sub> = 50 mM, [*n*-PrNH<sub>2</sub>]<sub>eff</sub> = 0.058 mM,

[TEA buffer]<sub>0</sub> = 0.10 M, pH 7.75 in D<sub>2</sub>O/*d*<sub>6</sub>-DMSO 9/1 (v/v), 37 °C

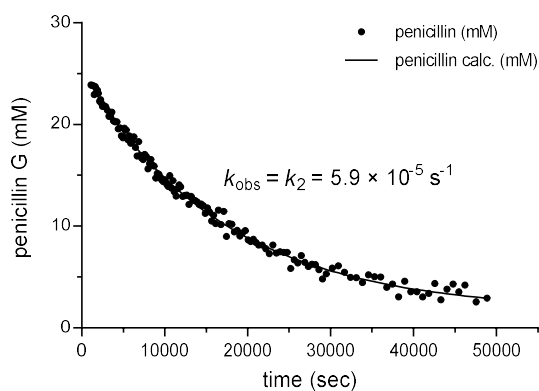
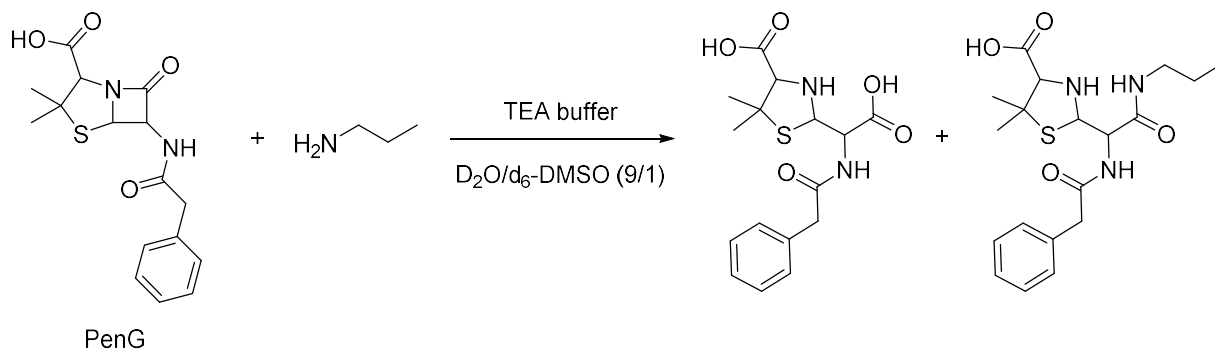


**Figure S44:** Decay of the concentration of penicillin G while reacting with *n*-propylamine in a TEA-buffered reaction mixture at 37 °C ( $k_N = 4.5 \times 10^{-1} \text{ M}^{-1} \text{ s}^{-1}$ ). The black line shows a mono-exponential fit of the data.

6.5. Rate constants for the reactions of sodium penicillin G with different aliphatic amines

**Table S3:** Rate constants for the reactions of penicillin G (PenG) with different aliphatic amines at 37 °C and pH 7.75.

	benzylamine	phenylethylamine	<i>n</i> -propylamine
$\text{p}K_{\text{aH}^+}$	9.36	9.89	10.68
$c_{\text{eff}}$ (M)	$1.2 \times 10^{-3}$	$3.6 \times 10^{-4}$	$5.8 \times 10^{-5}$
$k_{\text{obs}}$ (s <sup>-1</sup> )	$1.3 \times 10^{-4}$	$6.4 \times 10^{-5}$	$5.9 \times 10^{-5}$
$k_N$ (M <sup>-1</sup> s <sup>-1</sup> )	$8.1 \times 10^{-2}$	$8.6 \times 10^{-2}$	$4.5 \times 10^{-1}$

## 7. Determination of $N$ and $s_N$ parameters of amines in $H_2O$

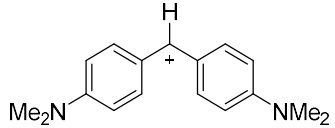
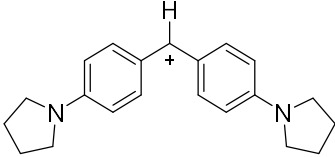
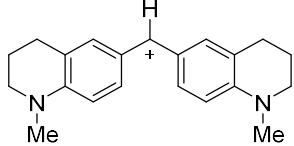
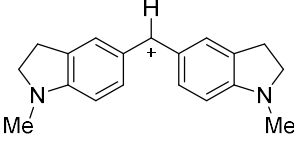
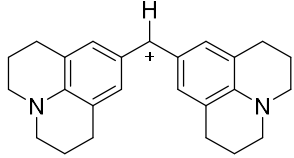
The nucleophilic reactivities of 2-phenylethylamine and *p*-anisidine in water were determined by using the benzhydrylium method as described previously.<sup>[4]</sup> Second-order rate constants for the attack of  $OH^-$  ions at the colored reference electrophiles ( $k_{2,OH^-}$ ) have previously been reported.<sup>[5]</sup> As outlined in more detail previously,<sup>[4]</sup> the second-order rate constants for the attack of the amine at the benzhydrylium ions ( $k_N$ ) in equation S1 can be obtained from the slope of a linear plot of  $k_{1\Psi}$  (equation S2) vs the amine concentration (equation S3).

$$k_{obs} = k_W + k_{2,OH^-}[OH^-] + k_N[amine] \quad (S1)$$

$$k_{1\Psi} = k_{obs} - k_{2,OH^-}[OH^-] = k_{obs} - k_{1\Psi, OH^-} \quad (S2)$$

$$k_{1\Psi} = k_W + k_N[amine] \quad (S3)$$

The following benzhydrylium tetrafluoroborates were used as reference electrophiles for the determination of the nucleophilicity parameters  $N$  and  $s_N$  of the amines according to equation (1) in the main text.

reference electrophile	abbreviation	$E$ parameter <sup>[a]</sup>
	(dma) <sub>2</sub> CH <sup>+</sup>	-7.02
	(pyr) <sub>2</sub> CH <sup>+</sup>	-7.69
	(thq) <sub>2</sub> CH <sup>+</sup>	-8.22
	(ind) <sub>2</sub> CH <sup>+</sup>	-8.76
	(jul) <sub>2</sub> CH <sup>+</sup>	-9.45

[a] from Ref. [6]

## 7.1. Phenylethylamine

**Table S4:** Reaction of phenylethylamine with  $(dma)_2CH^+BF_4^-$  (at 20 °C in water, cosolvent: 1 vol-%  $CH_3CN$ , stopped-flow, detection at 607 nm).

$E = (dma)_2CH^+BF_4^-$ ;  $Nu = \text{phenylethylamine}$

$[E]_0$ (M)	$[Nu]_0$ (M)	$[Nu]_{\text{eff}}$ (M)	$[OH^-]$ (M)	$[Nu]_{\text{eff}}/[E]_0$	$k_{\text{obs}}$ ( $s^{-1}$ )	$k_{1\psi, OH^-}$ ( $s^{-1}$ )	$k_{1\psi}$ ( $s^{-1}$ )
$7.11 \times 10^{-5}$	$5.57 \times 10^{-4}$	$3.84 \times 10^{-4}$	$1.73 \times 10^{-4}$	5	1.35	$2.26 \times 10^{-2}$	1.33
$7.11 \times 10^{-5}$	$1.67 \times 10^{-3}$	$1.35 \times 10^{-3}$	$3.23 \times 10^{-4}$	19	5.67	$4.24 \times 10^{-2}$	5.63
$7.11 \times 10^{-5}$	$2.79 \times 10^{-3}$	$2.36 \times 10^{-3}$	$4.28 \times 10^{-4}$	33	10.1	$5.60 \times 10^{-2}$	10.04
$7.11 \times 10^{-5}$	$3.90 \times 10^{-3}$	$3.39 \times 10^{-3}$	$5.13 \times 10^{-4}$	48	15.0	$6.72 \times 10^{-2}$	14.93
$7.11 \times 10^{-5}$	$5.01 \times 10^{-3}$	$4.43 \times 10^{-3}$	$5.86 \times 10^{-4}$	62	19.6	$7.68 \times 10^{-2}$	19.52

$$pK_B(\text{PhCH}_2\text{CH}_2\text{NH}_2) = 4.11^{[7]}$$

$$k_{2,OH^-} = 131 \text{ M}^{-1} \text{ s}^{-1} [5]$$

$$k_N = 4.51 \times 10^3 \text{ M}^{-1} \text{ s}^{-1}$$

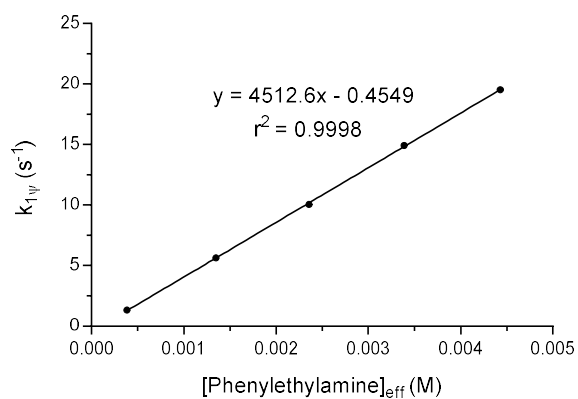


**Figure S45:** Determination of the second-order rate constant  $k_N = 4.51 \times 10^3 \text{ M}^{-1} \text{ s}^{-1}$  from the dependence of the first-order rate constant  $k_{1\psi}$  on the concentration of phenylethylamine.

**Table S5:** Reaction of phenylethylamine with  $(\text{pyr})_2\text{CH}^+\text{BF}_4^-$  (at 20 °C in water, cosolvent: 1 vol-%  $\text{CH}_3\text{CN}$ , stopped-flow, detection at 607 nm).

$E = (\text{pyr})_2\text{CH}^+\text{BF}_4^-$ ;  $\text{Nu} = \text{phenylethylamine}$

$[\text{E}]_0$ (M)	$[\text{Nu}]_0$ (M)	$[\text{Nu}]_{\text{eff}}$ (M)	$[\text{OH}^-]$ (M)	$[\text{Nu}]_{\text{eff}}/[\text{E}]_0$	$k_{\text{obs}}$ ( $\text{s}^{-1}$ )	$k_{1\psi, \text{OH}^-}$ ( $\text{s}^{-1}$ )	$k_{1\psi}$ ( $\text{s}^{-1}$ )
$1.37 \times 10^{-5}$	$4.54 \times 10^{-4}$	$3.01 \times 10^{-4}$	$1.53 \times 10^{-4}$	22	0.411	$7.41 \times 10^{-3}$	0.404
$1.37 \times 10^{-5}$	$1.36 \times 10^{-3}$	$1.07 \times 10^{-3}$	$2.88 \times 10^{-4}$	79	1.48	$1.40 \times 10^{-2}$	1.47
$1.37 \times 10^{-5}$	$2.27 \times 10^{-3}$	$1.89 \times 10^{-3}$	$3.83 \times 10^{-4}$	138	2.81	$1.86 \times 10^{-2}$	2.79
$1.37 \times 10^{-5}$	$4.09 \times 10^{-3}$	$3.56 \times 10^{-3}$	$5.26 \times 10^{-4}$	261	6.00	$2.55 \times 10^{-2}$	5.97

$\text{p}K_{\text{B}} (\text{PhCH}_2\text{CH}_2\text{NH}_2) = 4.11$

$k_{2, \text{OH}^-} = 48.5 \text{ M}^{-1} \text{ s}^{-1}$  [5]

$k_{\text{N}} = 1.73 \times 10^3 \text{ M}^{-1} \text{ s}^{-1}$

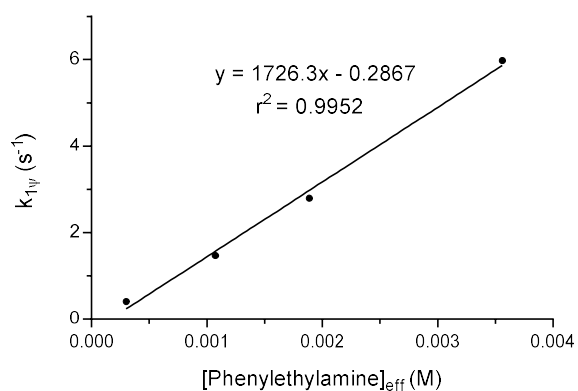


**Figure S46:** Determination of the second-order rate constant  $k_{\text{N}} = 1.73 \times 10^3 \text{ M}^{-1} \text{ s}^{-1}$  from the dependence of the first-order rate constant  $k_{1\psi}$  on the concentration of phenylethylamine.

**Table S6:** Reaction of phenylethylamine with  $(thq)_2CH^+BF_4^-$  (at 20 °C in water, cosolvent: 1 vol-%  $CH_3CN$ , stopped-flow, detection at 607 nm).

$E = (thq)_2CH^+BF_4^-$ ;  $Nu =$  phenylethylamine

$[E]_0$ (M)	$[Nu]_0$ (M)	$[Nu]_{eff}$ (M)	$[OH^-]$ (M)	$[Nu]_{eff}/[E]_0$	$k_{obs}$ ( $s^{-1}$ )	$k_{1\psi, OH^-}$ ( $s^{-1}$ )	$k_{1\psi}$ ( $s^{-1}$ )
$1.27 \times 10^{-5}$	$1.67 \times 10^{-3}$	$1.35 \times 10^{-3}$	$3.23 \times 10^{-4}$	106	1.33	$7.63 \times 10^{-3}$	1.32
$1.27 \times 10^{-5}$	$2.79 \times 10^{-3}$	$2.36 \times 10^{-3}$	$4.28 \times 10^{-4}$	185	2.32	$1.01 \times 10^{-2}$	2.31
$1.27 \times 10^{-5}$	$3.90 \times 10^{-3}$	$3.39 \times 10^{-3}$	$5.13 \times 10^{-4}$	266	3.35	$1.21 \times 10^{-2}$	3.34
$1.27 \times 10^{-5}$	$5.01 \times 10^{-3}$	$4.42 \times 10^{-3}$	$5.86 \times 10^{-4}$	347	4.62	$1.38 \times 10^{-2}$	4.61

$$pK_B(\text{PhCH}_2\text{CH}_2\text{NH}_2) = 4.11$$

$$k_{2,OH^-} = 23.6 \text{ M}^{-1} \text{ s}^{-1} [5]$$

$$k_N = 1.06 \times 10^3 \text{ M}^{-1} \text{ s}^{-1}$$

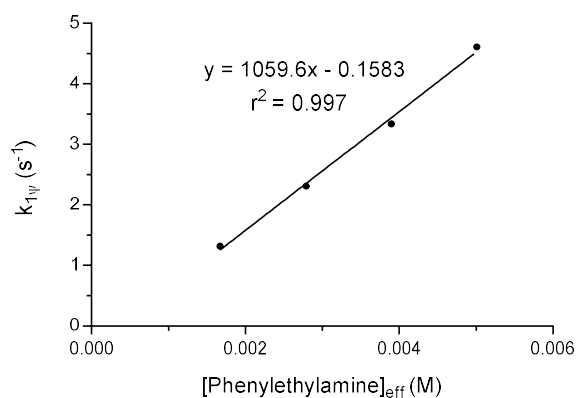


**Figure S47:** Determination of the second-order rate constant  $k_N = 1.06 \times 10^3 \text{ M}^{-1} \text{ s}^{-1}$  from the dependence of the first-order rate constant  $k_{1\psi}$  on the concentration of phenylethylamine.

**Table S7:** Reaction of phenylethylamine with  $(ind)_2CH^+BF_4^-$  (at 20 °C in water, cosolvent: 1 vol-%  $CH_3CN$ , stopped-flow, detection at 607 nm).

$E = (ind)_2CH^+BF_4^-$ ;  $Nu = \text{phenylethylamine}$

$[E]_0$ (M)	$[Nu]_0$ (M)	$[Nu]_{\text{eff}}$ (M)	$[OH^-]$ (M)	$[Nu]_{\text{eff}}/[E]_0$	$k_{\text{obs}}$ ( $s^{-1}$ )	$k_{1\psi, OH^-}$ ( $s^{-1}$ )	$k_{1\psi}$ ( $s^{-1}$ )
$1.80 \times 10^{-5}$	$5.57 \times 10^{-4}$	$3.84 \times 10^{-4}$	$1.73 \times 10^{-4}$	21	0.193	$1.87 \times 10^{-3}$	0.191
$1.80 \times 10^{-5}$	$1.67 \times 10^{-3}$	$1.35 \times 10^{-3}$	$3.23 \times 10^{-4}$	75	0.646	$3.49 \times 10^{-3}$	0.643
$1.80 \times 10^{-5}$	$2.79 \times 10^{-3}$	$2.36 \times 10^{-3}$	$4.28 \times 10^{-4}$	131	1.07	$4.62 \times 10^{-3}$	1.07
$1.80 \times 10^{-5}$	$3.90 \times 10^{-3}$	$3.39 \times 10^{-3}$	$5.13 \times 10^{-4}$	188	1.58	$5.54 \times 10^{-3}$	1.57
$1.80 \times 10^{-5}$	$5.01 \times 10^{-3}$	$4.42 \times 10^{-3}$	$5.86 \times 10^{-4}$	246	2.09	$6.33 \times 10^{-3}$	2.08

$$pK_B (\text{PhCH}_2\text{CH}_2\text{NH}_2) = 4.11$$

$$k_{2,OH^-} = 10.8 \text{ M}^{-1} \text{ s}^{-1} [5]$$

$$k_N = 466 \text{ M}^{-1} \text{ s}^{-1}$$

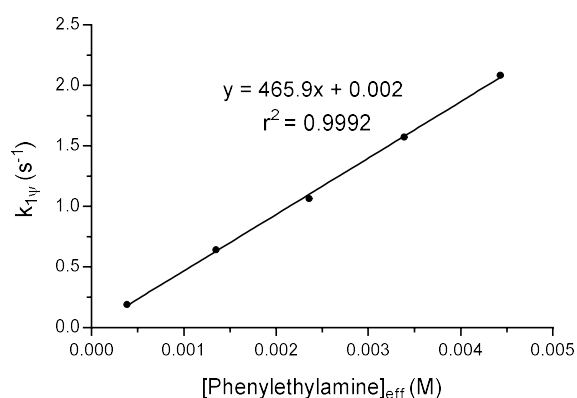


**Figure S48:** Determination of the second-order rate constant  $k_N = 466 \text{ M}^{-1} \text{ s}^{-1}$  from the dependence of the first-order rate constant  $k_{1\psi}$  on the concentration of phenylethylamine.

**Table S8:** Reaction of phenylethylamine with  $(jul)_2CH^+BF_4^-$  (at 20 °C in water, cosolvent: 1 vol-%  $CH_3CN$ , stopped-flow, detection at 630 nm).

$E = (jul)_2CH^+BF_4^-$ ;  $Nu =$  phenylethylamine

$[E]_0$ (M)	$[Nu]_0$ (M)	$[Nu]_{eff}$ (M)	$[OH^-]$ (M)	$[Nu]_{eff}/[E]_0$	$k_{obs}$ ( $s^{-1}$ )	$k_{1\psi, OH^-}$ ( $s^{-1}$ )	$k_{1\psi}$ ( $s^{-1}$ )
$2.77 \times 10^{-5}$	$5.57 \times 10^{-4}$	$3.84 \times 10^{-4}$	$1.73 \times 10^{-4}$	14	0.0621	$5.94 \times 10^{-4}$	$6.15 \times 10^{-2}$
$2.77 \times 10^{-5}$	$1.67 \times 10^{-3}$	$1.35 \times 10^{-3}$	$3.23 \times 10^{-4}$	49	0.233	$1.11 \times 10^{-3}$	$2.32 \times 10^{-1}$
$2.77 \times 10^{-5}$	$2.79 \times 10^{-3}$	$2.36 \times 10^{-3}$	$4.28 \times 10^{-4}$	85	0.378	$1.47 \times 10^{-3}$	$3.77 \times 10^{-1}$
$2.77 \times 10^{-5}$	$5.01 \times 10^{-3}$	$4.42 \times 10^{-3}$	$5.86 \times 10^{-4}$	160	0.774	$2.02 \times 10^{-3}$	$7.72 \times 10^{-1}$

$$pK_B (\text{PhCH}_2\text{CH}_2\text{NH}_2) = 4.11$$

$$k_{2,OH^-} = 3.44 \text{ M}^{-1} \text{ s}^{-1} [5]$$

$$k_N = 175 \text{ M}^{-1} \text{ s}^{-1}$$

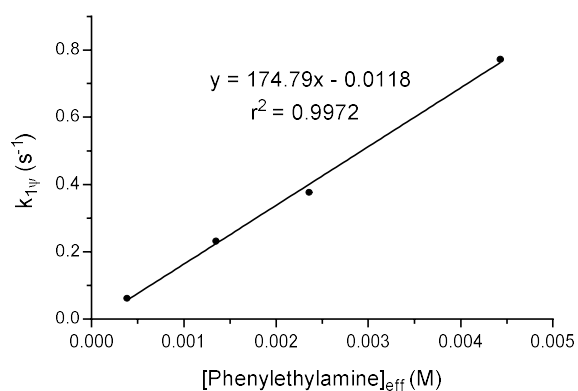


**Figure S49:** Determination of the second-order rate constant  $k_N = 175 \text{ M}^{-1} \text{ s}^{-1}$  from the dependence of the first-order rate constant  $k_{1\psi}$  on the concentration of phenylethylamine.

**Table S9:** Rate Constants for the reactions of phenylethylamine with different benzhydrylium ions as reference electrophiles (20 °C, in water).

reference electrophile	<i>E</i> parameter	<i>k<sub>N</sub></i> (20 °C) (M <sup>-1</sup> s <sup>-1</sup> )
(dma) <sub>2</sub> CH <sup>+</sup>	-7.02	4.51 × 10 <sup>3</sup>
(pyr) <sub>2</sub> CH <sup>+</sup>	-7.69	1.73 × 10 <sup>3</sup>
(thq) <sub>2</sub> CH <sup>+</sup>	-8.22	1.06 × 10 <sup>3</sup>
(ind) <sub>2</sub> CH <sup>+</sup>	-8.76	4.66 × 10 <sup>2</sup>
(jul) <sub>2</sub> CH <sup>+</sup>	-9.45	1.75 × 10 <sup>2</sup>

Reactivity parameters for phenylethylamine (in water): *N* = 13.40; *s<sub>N</sub>* = 0.57

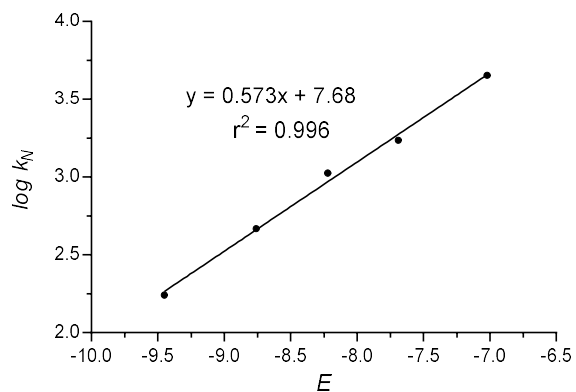


**Figure S50:** Plot of *log k<sub>N</sub>* vs. the electrophilicity parameters *E* for the reactions of benzhydrylium ions with phenylethylamine.

## 7.2. *p*-Anisidine

**Table S10:** Reaction of *p*-anisidine with  $(dma)_2CH^+BF_4^-$  (at 20 °C in water, cosolvent: 1 vol-%  $CH_3CN$ , stopped-flow, detection at 607 nm).

E =  $(dma)_2CH^+BF_4^-$ ; Nu = *p*-anisidine

[E] <sub>0</sub> (M)	[Nu] <sub>0</sub> (M)	[Nu] <sub>eff</sub>	[OH <sup>-</sup> ] (M)	[Nu] <sub>eff</sub> /[E] <sub>0</sub>	<i>k</i> <sub>obs</sub> (s <sup>-1</sup> )	<i>k</i> <sub>1ψ, OH<sup>-</sup></sub> (s <sup>-1</sup> )	<i>k</i> <sub>1ψ</sub> (s <sup>-1</sup> )
$1.90 \times 10^{-4}$	$1.33 \times 10^{-3}$	$1.33 \times 10^{-3}$	$1.63 \times 10^{-6}$	7	106	$2.13 \times 10^{-4}$	$1.06 \times 10^2$
$1.90 \times 10^{-4}$	$3.98 \times 10^{-3}$	$3.98 \times 10^{-3}$	$2.82 \times 10^{-6}$	21	351	$3.69 \times 10^{-4}$	$3.51 \times 10^2$
$1.90 \times 10^{-4}$	$6.64 \times 10^{-3}$	$6.64 \times 10^{-3}$	$3.64 \times 10^{-6}$	35	587	$4.77 \times 10^{-4}$	$5.87 \times 10^2$
$1.90 \times 10^{-4}$	$9.29 \times 10^{-3}$	$9.29 \times 10^{-3}$	$4.30 \times 10^{-6}$	49	856	$5.64 \times 10^{-4}$	$8.56 \times 10^2$

$$pK_B = 8.70^{[2a]}$$

$$k_{2,OH^-} = 131 \text{ M}^{-1} \text{ s}^{-1} [5]$$

$$k_N = 9.37 \times 10^4 \text{ M}^{-1} \text{ s}^{-1}$$

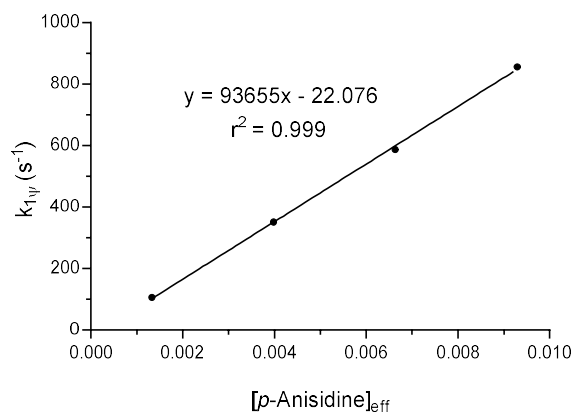


**Figure S51:** Determination of the second-order rate constant  $k_N = 9.37 \times 10^4 \text{ M}^{-1} \text{ s}^{-1}$  from the dependence of the first-order rate constant  $k_{1\psi}$  on the concentration of *p*-anisidine.

**Table S11:** Reaction of *p*-anisidine with  $(\text{pyr})_2\text{CH}^+\text{BF}_4^-$  (at 20 °C in water, cosolvent: 1 vol-%  $\text{CH}_3\text{CN}$ , stopped-flow, detection at 607 nm).

$E = (\text{pyr})_2\text{CH}^+\text{BF}_4^-$ ;  $\text{Nu} = p\text{-anisidine}$

$[\text{E}]_0$ (M)	$[\text{Nu}]_0$ (M)	$[\text{Nu}]_{\text{eff}}$	$[\text{OH}^-]$ (M)	$[\text{Nu}]_{\text{eff}}/[\text{E}]_0$	$k_{\text{obs}}$ ( $\text{s}^{-1}$ )	$k_{1\psi, \text{OH}^-}$ ( $\text{s}^{-1}$ )	$k_{1\psi}$ ( $\text{s}^{-1}$ )
$2.95 \times 10^{-5}$	$1.33 \times 10^{-3}$	$1.33 \times 10^{-3}$	$1.63 \times 10^{-6}$	45	14.6	$7.90 \times 10^{-5}$	$1.46 \times 10^1$
$2.95 \times 10^{-5}$	$3.98 \times 10^{-3}$	$3.98 \times 10^{-3}$	$2.82 \times 10^{-6}$	135	93.3	$1.37 \times 10^{-4}$	$9.33 \times 10^1$
$2.95 \times 10^{-5}$	$6.64 \times 10^{-3}$	$6.64 \times 10^{-3}$	$3.64 \times 10^{-6}$	225	167	$1.76 \times 10^{-4}$	$1.67 \times 10^2$
$2.95 \times 10^{-5}$	$9.29 \times 10^{-3}$	$9.29 \times 10^{-3}$	$4.30 \times 10^{-6}$	315	229	$2.09 \times 10^{-4}$	$2.29 \times 10^2$
$2.95 \times 10^{-5}$	$1.19 \times 10^{-2}$	$1.19 \times 10^{-2}$	$4.87 \times 10^{-6}$	405	288	$2.36 \times 10^{-4}$	$2.88 \times 10^2$

$$\text{p}K_{\text{B}} = 8.70$$

$$k_{2, \text{OH}^-} = 48.5 \text{ M}^{-1} \text{ s}^{-1[5]}$$

$$k_{\text{N}} = 2.57 \times 10^4 \text{ M}^{-1} \text{ s}^{-1}$$

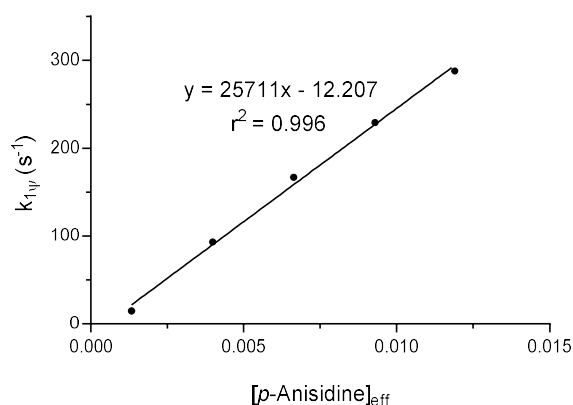


**Figure S52:** Determination of the second-order rate constant  $k_{\text{N}} = 2.57 \times 10^4 \text{ M}^{-1} \text{ s}^{-1}$  from the dependence of the first-order rate constant  $k_{1\psi}$  on the concentration of *p*-anisidine.

**Table S12:** Reaction of *p*-anisidine with  $(ind)_2CH^+BF_4^-$  (at 20 °C in water, cosolvent: 1 vol-%  $CH_3CN$ , stopped-flow, detection at 607 nm).

$E = (ind)_2CH^+BF_4^-$ ;  $Nu = p$ -anisidine

$[E]_0$ (M)	$[Nu]_0$ (M)	$[Nu]_{eff}$	$[OH^-]$ (M)	$[Nu]_{eff}/[E]_0$	$k_{obs}$ ( $s^{-1}$ )	$k_{1\psi, OH^-}$ ( $s^{-1}$ )	$k_{1\psi}$ ( $s^{-1}$ )
$3.23 \times 10^{-5}$	$1.33 \times 10^{-3}$	$1.33 \times 10^{-3}$	$1.63 \times 10^{-6}$	41	13.0	$1.76 \times 10^{-5}$	13.0
$3.23 \times 10^{-5}$	$3.98 \times 10^{-3}$	$3.98 \times 10^{-3}$	$2.82 \times 10^{-6}$	123	28.8	$3.04 \times 10^{-5}$	28.6
$3.23 \times 10^{-5}$	$6.64 \times 10^{-3}$	$6.64 \times 10^{-3}$	$3.64 \times 10^{-6}$	205	48.1	$3.93 \times 10^{-5}$	48.1
$3.23 \times 10^{-5}$	$9.29 \times 10^{-3}$	$9.29 \times 10^{-3}$	$4.31 \times 10^{-6}$	288	62.7	$4.65 \times 10^{-5}$	62.7
$3.23 \times 10^{-5}$	$1.19 \times 10^{-2}$	$1.19 \times 10^{-2}$	$4.87 \times 10^{-6}$	370	75.1	$5.26 \times 10^{-5}$	75.1

$$pK_B = 8.70$$

$$k_{2,OH^-} = 10.8 \text{ M}^{-1} \text{ s}^{-1[5]}$$

$$k_N = 5.96 \times 10^3 \text{ M}^{-1} \text{ s}^{-1}$$

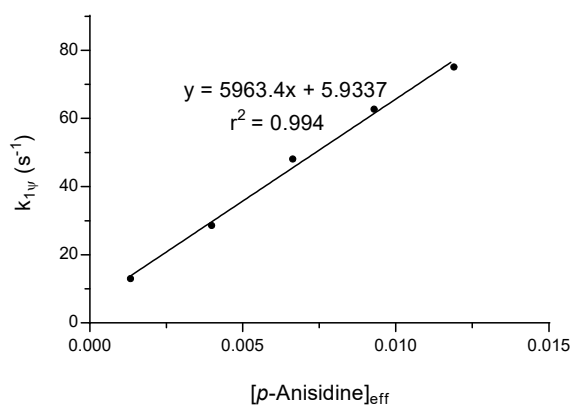


**Figure S53:** Determination of the second-order rate constant  $k_N = 5.96 \times 10^3 \text{ M}^{-1} \text{ s}^{-1}$  from the dependence of the first-order rate constant  $k_{1\psi}$  on the concentration of *p*-anisidine.

**Table S13:** Rate constants for the reactions of *p*-anisidine with different electrophiles (20 °C).

reference electrophile	<i>E</i> parameter	$k_N$ (20 °C) (M <sup>-1</sup> s <sup>-1</sup> )
(dma) <sub>2</sub> CH <sup>+</sup>	-7.02	9.37 × 10 <sup>4</sup>
(pyr) <sub>2</sub> CH <sup>+</sup>	-7.69	2.57 × 10 <sup>4</sup>
(ind) <sub>2</sub> CH <sup>+</sup>	-8.76	5.96 × 10 <sup>3</sup>

Reactivity parameters for *p*-anisidine (in water):  $N = 14.28$ ;  $s_N = 0.68$

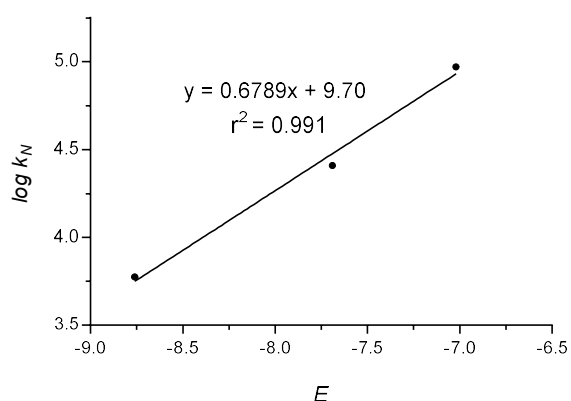


**Figure S54:** Plot of  $\log k_N$  vs. the electrophilicity parameters *E* for the reactions of benzhydrylium ions with *p*-anisidine.

## 8. References

- [1] H. E. Gottlieb, V. Kotlyar, A. Nudelman, *J. Org. Chem.* **1997**, *62*, 7512-7515.
- [2] a) Y. Altun, *J. Solution Chem.* **2004**, *33*, 479-497; b) K. K. R. Poduval, M. Stobiecka, W. F. A. Dehaen, W. Dehaen, H. Radecka, J. Radecki, *Supramol. Chem.* **2010**, *22*, 413-419.
- [3] C. Hansch, A. Leo, R. W. Taft, *Chem. Rev.* **1991**, *91*, 165-195.
- [4] F. Brotzel, Y. C. Chu, H. Mayr, *J. Org. Chem.* **2007**, *72*, 3679-3688.
- [5] S. Minegishi, H. Mayr, *J. Am. Chem. Soc.* **2003**, *125*, 286-295.
- [6] H. Mayr, T. Bug, M. F. Gotta, N. Hering, B. Irrgang, B. Janker, B. Kempf, R. Loos, A. R. Ofial, G. Remennikov, H. Schimmel, *J. Am. Chem. Soc.* **2001**, *123*, 9500-9512.
- [7] R. F. Jameson, G. Hunter, T. Kiss, *J. Chem. Soc. Perkin Trans. 2* **1980**, 1105-1110.

## Chapter 2

# Transition Metal-Free C-H Functionalization of Tertiary Amines: Diisopropyl Azodicarboxylate Mediated $\alpha$ -Arylations

### Abstract

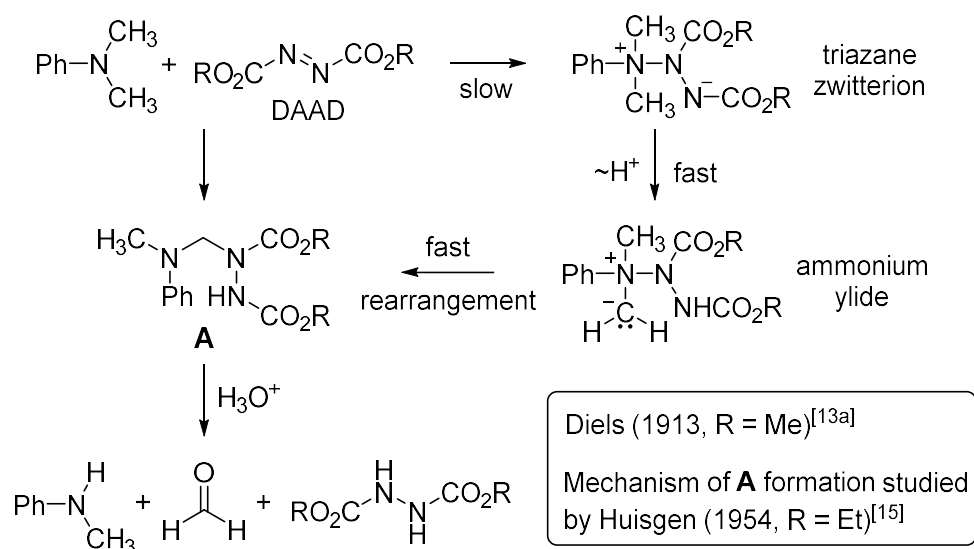
Aromatic and aliphatic tertiary methylamines  $RR'NCH_2-H$  were converted to  $\alpha$ -arylated amines  $RR'NCH_2-Ar$  in two steps. In the first step, tertiary methylamines and diisopropyl azodicarboxylate (DIAD) reacted in acetonitrile to generate *N*-aminomethylated hydrazine-1,2-dicarboxylates. Reactions of these hydrazines with potassium (hetero)aryltrifluoroborates at ambient temperature in the presence of one equivalent of trifluoroacetic acid in acetonitrile furnished  $\alpha$ -arylated amines. Both steps of the reaction sequence occurred without addition of a metal-based catalyst.

### Introduction

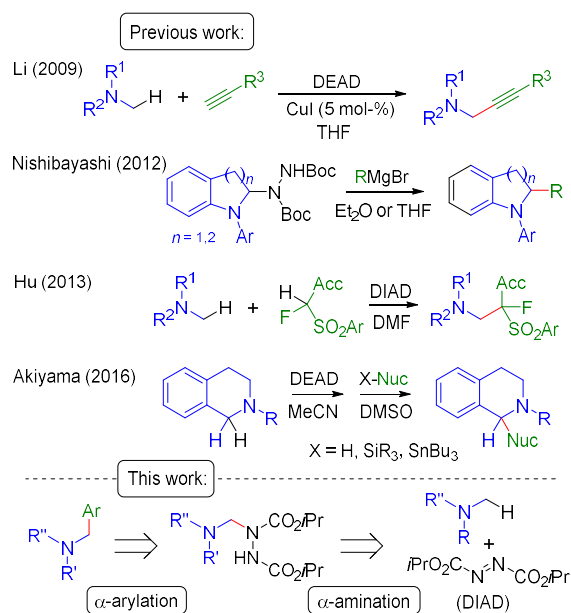
Functionalization of tertiary amines at the  $sp^3$ -hybridized  $\alpha$ -carbon has been an emerging field of organic chemistry in recent years.<sup>[1]</sup> Using this synthetic method for the introduction of an aryl moiety would furnish benzylic amines, which are a common structural motif of market-relevant pharmaceuticals.<sup>[2]</sup> Several methods for the arylation of amines were developed, therefore, which generally rely on the use of stoichiometric or catalytic amounts of metal salts or nucleophilic organometallics.<sup>[3-6]</sup> With exception of a few reports, which focus on oxidative cross couplings of 1,2,3,4-tetrahydroisoquinolines (THIQs) with indoles and phenols,<sup>[7]</sup> to the best of our knowledge, metal-free  $\alpha$ -CH-arylations of tertiary amines under mild conditions have not been reported.<sup>[1d,8-11]</sup>

In this context, dialkyl azodicarboxylates (DAADs) appeared attractive reagents because they possess electrophilic as well as oxidative properties.<sup>[12]</sup> This combination of features had already been used by Diels and Paquin in 1913, who demethylated *N,N*-dimethylaniline by addition of dimethyl azodicarboxylate to form aminal **A**, which was then hydrolyzed (Scheme 1).<sup>[13-16]</sup>

*N*-Demethylation of tertiary amines and alkaloids<sup>[13,17]</sup> remained the sole application of the oxidative  $\alpha$ -amination of tertiary amines by DAADs for many decades.<sup>[18]</sup>



**Scheme 1.** Demethylation of *N,N*-dimethylaniline through addition of dialkyl azodicarboxylates (DAADs) and subsequent hydrolysis.



**Scheme 2.** Intermolecular CC bond-forming reactions upon DAAD-mediated oxidation of tertiary amines.

In 2009, first examples of intermolecular CC bond-forming reactions were disclosed by Li and Xu, who successfully applied oxidative C(sp<sup>3</sup>)-H bond amination by diethyl azodicarboxylate (DEAD) for CuI-catalyzed alkynylations of aliphatic tertiary methylamines (Scheme 2).<sup>[19]</sup> Transition metal catalysis was found to be dispensable when acidic pronucleophiles or otherwise activated nucleophiles were used for DAAD-mediated  $\alpha$ -functionalizations of

tertiary amines.<sup>[20]</sup> Nishibayshi exploited the Lewis acidity of Grignard reagents (2.2 equiv.) in azodicarboxylate-mediated  $\alpha$ -arylations of cyclic tertiary amines.<sup>[21]</sup> Hu showed that a mixture of diisopropyl azodicarboxylate (DIAD) and CH acidic acceptor-substituted fluoromethylsulfones selectively fluoromethylated NCH<sub>3</sub> groups of tertiary aliphatic amines.<sup>[22]</sup> DMSO as a highly polar solvent turned out to be beneficial when Akiyama and co-workers used structurally diverse nucleophiles (silylated enol ethers, CH acids, allylstannanes etc.) in combination with DEAD as the oxidant to functionalize the C-1 position of THIQs. These authors suggested that the basicity of the dicarboxyhydrazide anion was a further crucial factor for achieving high yielding reactions of the THIQ-DEAD addition products with the investigated (pro)nucleophiles.<sup>[23]</sup>

Herein, we report on a transition metal-free<sup>[24]</sup> two-step synthesis of  $\alpha$ -arylated amines from tertiary amines, DIAD, and organotrifluoroborates (Scheme 2).

## Results and Discussion

In agreement with a recent study,<sup>[23]</sup> the amins **2a–i** were isolated with good yields in the range of 71–95% when the ring-substituted *N,N*-dimethylanilines **1a–i** and a slight excess of DIAD (1.1 equiv.) were combined in acetonitrile (Table 1).<sup>[25]</sup> Heating the reaction mixture to reflux shortened the reaction time for the generation of **2b** from two days to 4 h and was helpful when preparing the  $\alpha$ -aminated anilines that carried electron-withdrawing groups.

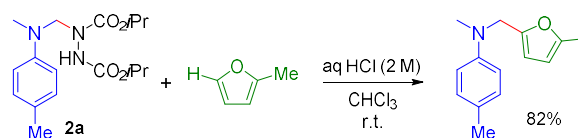
As typically observed for amides or carbamates,<sup>[23,26]</sup> the broad, unresolved signals in the <sup>1</sup>H and <sup>13</sup>C NMR spectra (CDCl<sub>3</sub>, 27 °C) of hydrazine-1,2-dicarboxylates **2a–i** indicate hindered rotations around the N-C bonds in (H)NN-CO and (R)(N)N-CO groups. Significantly improved resolutions and signal-to-noise ratios of the resonances were achieved when the NMR spectra of the hydrazine-1,2-dicarboxylates **2a–i** were acquired in *d*<sub>6</sub>-DMSO at 90 °C (Supporting Information).

**Table 1.** Addition of DIAD to *N,N*-dimethylanilines **1a-i**.

Aniline	X =	Hydrazine	Yield <sup>a)</sup> (%)
<b>1a</b>	4-Me	<b>2a</b>	95 (4 d, rt)
<b>1b</b>	4-OMe	<b>2b</b>	78 (2 d, rt) 81 (4 h, reflux)
<b>1c</b>	H	<b>2c</b>	86 (5 d, rt)
<b>1d</b>	4-F	<b>2d</b>	88 (2 d, rt)
<b>1e</b>	4-Cl	<b>2e</b>	74 (3 d, reflux)
<b>1f</b>	4-Br	<b>2f</b>	87 (3 d, reflux)
<b>1g</b>	4-CO <sub>2</sub> Et	<b>2g</b>	86 (2 d, reflux)
<b>1h</b>	4-CN	<b>2h</b>	71 (2 d, rt)
<b>1i</b>	2,4,6-(Me) <sub>3</sub>	<b>2i</b>	87 (10 h, reflux)

<sup>a)</sup> Yield of isolated product after column chromatography.

Previous work by Nishibayashi showed that acidic conditions facilitate the formation of electrophilic species from amins, [27] such as **2**, which should be interceptable in CC bond-forming reactions by sufficiently nucleophilic arenes. [28] In an initial attempt, 2-methylfuran and **2a** were used as substrates to probe the formation of an  $\alpha$ -arylated amine. The 5-aminomethylated 2-methylfuran was isolated in 82% yield when aq HCl (2 M) was added to an equimolar solution of the reactants in chloroform (Scheme 3).

**Scheme 3.** Brønsted acid mediated  $\alpha$ -arylation of **2a** with 2-methylfuran.

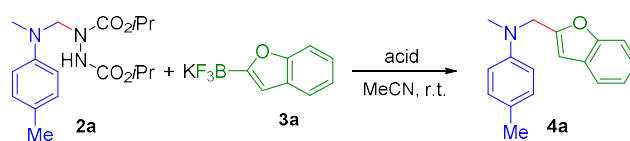
However, further studies with indoles, thiophenes and methoxy-substituted benzenes, signalled a very limited scope of this transformation. Aminomethylated arenes were only obtained in yields of <35%. In addition, diarylmethanes formed as major by-products owing either to

subsequent reactions of the initially formed  $\alpha$ -arylated amines or to the presence of formaldehyde in the solutions caused by decomposition of **2a**.

Kinetic investigations by Berionni, Mayr, and co-workers had shown that the reactivities of arenes Ar-H increased by more than three orders of magnitude when a trifluoroborate substituent was introduced at the  $\pi$ -system.<sup>[29]</sup> The fact that potassium aryltrifluoroborates Ar-BF<sub>3</sub>K are generally synthesized from ArB(OR)<sub>2</sub> and KHF<sub>2</sub> at low pH provides evidence for the stability of the Ar-BF<sub>3</sub><sup>-</sup> ions under acidic reaction conditions.<sup>[30-32]</sup> Both properties of ArBF<sub>3</sub>K, enhanced reactivity of the  $\pi$ -system and their stability towards Brønsted acids, led us to hypothesize that potassium aryltrifluoroborates might be suitable substrates for transition metal-free reactions with the DIAD-activated anilines **2**.<sup>[33]</sup>

In a first series of experiments, hydrazine-1,2-dicarboxylate **2a** was combined with potassium benzofuran-2-yltrifluoroborate (**3a**) in presence of stoichiometric amounts of Brønsted or Lewis acids (Table 2). The  $\alpha$ -arylated *N,N*-dimethyl-*p*-toluidine **4a** formed in the presence of all examined acids and was isolated in 70 to 94% yield (Table 2, entries 1–5). Changing from aqueous hydrochloric acid to an ethereal HCl solution shortened the reaction time and increased the yield of **4a** from good to excellent (entries 1,2). When trifluoroacetic acid (TFA) was used as the acid, the reactants were quantitatively converted within 2 h at ambient temperature and **4a** was isolated in 94% yield (entry 3). The  $\alpha$ -arylations of **2a** to form **4a** could also be achieved when the Lewis acids ZnBr<sub>2</sub> or BF<sub>3</sub>·OEt<sub>2</sub> were used. The yields of the Lewis acid mediated reactions were, however, considerably lower than those for the Brønsted acid mediated versions (entries 4,5). Nevertheless, it is noteworthy that 59% of **4a** were obtained when only 25 mol-% of BF<sub>3</sub>·OEt<sub>2</sub> were employed (entry 6), which indicates a potential for developing catalytic versions of this transformation.

**Table 2.** Optimization of the  $\alpha$ -arylation of **2a** by potassium benzofuran-2-yltrifluoroborate (**3a**) to yield **4a**.<sup>a)</sup>



Entry	Acid	Reaction time	Yield <sup>b)</sup> (%)
1	aq HCl (2 M)	24 h	70
2	HCl (2 M in Et <sub>2</sub> O)	12 h	94
3	CF <sub>3</sub> COOH	2 h	94
4	ZnBr <sub>2</sub>	2 h	90
5	BF <sub>3</sub> ·OEt <sub>2</sub>	24 h	79
6	BF <sub>3</sub> ·OEt <sub>2</sub> <sup>c)</sup>	24 h	59

<sup>a)</sup> Reaction conditions: **2a**, **3a**, acid (1 equiv.), MeCN, ambient temperature.

<sup>b)</sup> Yield of isolated product after column chromatography.

<sup>c)</sup> With 25 mol-% of BF<sub>3</sub>·OEt<sub>2</sub>.

Under the optimized reaction conditions (Table 2, entry 3), we tested the scope of further *N*-aminomethylated hydrazines **2** in the reaction with potassium benzofuran-2-yltrifluoroborate (**3a**). Electron-donating or electron-withdrawing groups at the para-position of the phenyl rings in **2a–h** did not significantly affect the efficiency of the arylation by **3a** (Figure 1). The arylation was scalable as demonstrated by the good yield obtained for the *p*-bromo-derivative **4f** (isolated in 75% yield when starting with 1.5 mmol educts). Hydrazine-1,2-dicarboxylates **2g** and **2h** selectively underwent aminomethylation reactions with the trifluoroborate **3a** to give **4g** and **4h**, respectively, which showed that the electrophilic sites of CO<sub>2</sub>Et and CN groups were compatible with our standard reaction conditions. The success of the 2,4,6-trimethylaniline derivative **2i** to generate product **4i** when treated with **3a** exemplifies the robustness of this  $\alpha$ -functionalization of tertiary amines towards steric hindrance in the vicinity of the amino group's nitrogen.

Exclusive *ipso*-substitutions of the BF<sub>3</sub>K group in the reactions of **3a** with **2a–i** were indicated by the diagnostic NMR chemical shift of  $\delta(\text{C-3}) = 103.8\text{--}104.4$  ppm in the aminomethylated benzofurans **4a–i**, which contrasts with the observation that bis(*p*-methoxyphenyl)methyl cations reacted preferentially with the 3-position of benzofuran-2-yl trifluoroborate (**3a**).<sup>[29b]</sup>

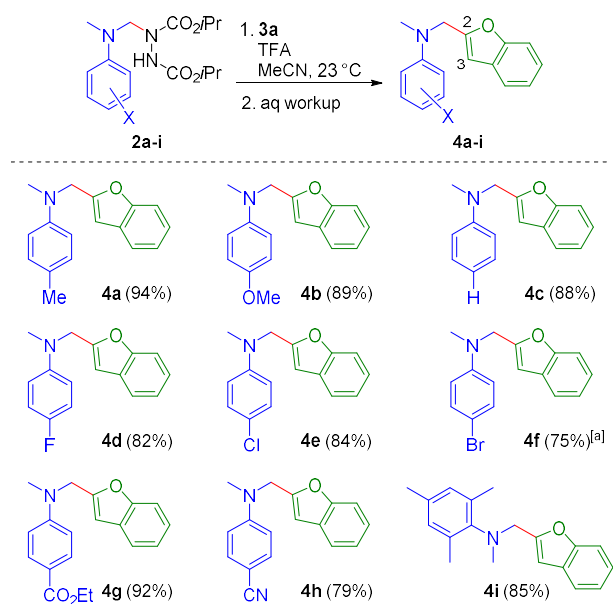


**Figure 1.** DIAD-mediated aminomethylations of potassium benzofuran-2-yl trifluoroborate (**3a**) by the ring-substituted *N,N*-dimethylaniline derivatives **2a-i**. [a] Reaction at >1 mmol scale (see Experimental).

To define the scope of the potassium aryltrifluoroborates that can be used for substituting the hydrazine moiety in **2**, we studied further reactions of furyl, thienyl and phenyl derivatives under the standard conditions (Figure 2).<sup>[34]</sup>

The reaction of **2a-c** with potassium furan-2-yltrifluoroborate (**3b**) furnished moderate to good yields of the 2-aminomethylated furans **5a-c**. The 2-substituted furan **5b** was also isolated when **2a** was combined with potassium furan-3-yltrifluoroborate (**3b'**), a constitutional isomer of **3b**. This observation is in accord with previous reports on the attack of electrophiles at remote positions of furanyl trifluoroborates.<sup>[29b]</sup> Instead of undergoing *ipso*-substitution different types of carbocations reacted at C-H groups of the  $\pi$ -systems, that is, at the 5-position of **3b** or the 2-position of **3b'**. Subsequent protodeborylations then led in both cases to 2-substituted furans. Analogously, the formation of **5b** from both **3b** and **3b'** as well as the formation of **5f-h** by C-5 attack of **2a,c,d** at **3d** can be explained.

While 5-methyl substituted 2-thienyltrifluoroborate (**3e**) gave only moderate yields of its reactions with hydrazine derivatives **2a,b** ( $\rightarrow$  **5i,j**), the successful reactions of the same electrophiles with phenyltrifluoroborates **3f,g** to form products **5k-n** further widened the scope of this arylation reaction.

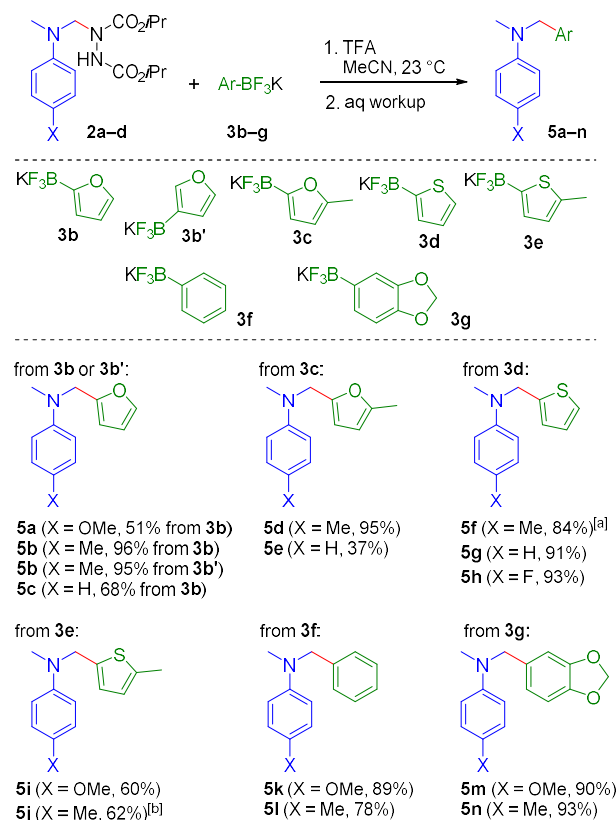
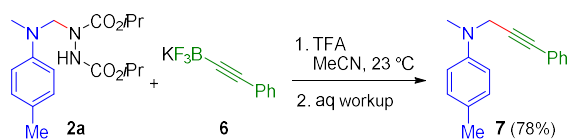


**Figure 2.** DIAD-mediated  $\alpha$ -(hetero)arylations of diisopropyl hydrazine carboxylates (yields refer to isolated products after purification by column chromatography). [a] With 0.74 equiv. TFA. [b] With 0.37 equiv. TFA.

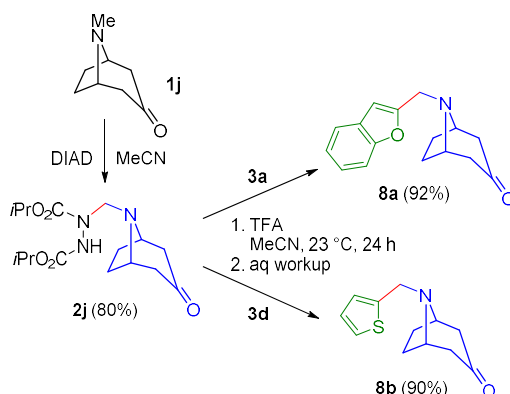
Carbon-carbon bond-forming reactions between DIAD-activated anilines and organotrifluoroborates were also extended to C(sp<sup>3</sup>)-C(sp) cross couplings. The alkylation of **2a** by potassium phenylethynyltrifluoroborate (**6**) furnished propargylamine **7** (78% yield, Scheme 4), which was previously obtained from **1a** by using transition-metal catalysis.<sup>[23,35]</sup>



**Scheme 4.**  $\alpha$ -Alkylation of DIAD-activated *N,N*-dimethyl-*p*-toluidine (**2a**).

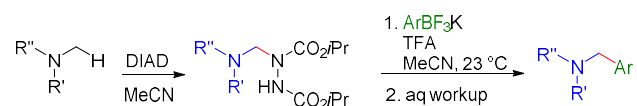
Derivatization of natural products, such as alkaloids, is of particular interest for the development of pharmaceuticals.<sup>[5g,22]</sup> We have, therefore, isolated **2j**, the addition product of DIAD and tropinone (Scheme 5). Substitution of the hydrazine moiety of **2j** by the benzofuranyl group of **3a** furnished within 24 h the (heteroaryl)methylated nortropinone **8a** in 92% yield.

Analogously, the reaction of **2j** with **3d** at ambient temperature delivered the 9-(2-thienyl)-functionalized tropinone **8b** (90% yield).



**Scheme 5.** Conversion of tropinone (**1j**) to (hetero-aryl)methylated nortropinones **8a,b** via DIAD-activated tropinone (**2j**).

In summary, additions of diisopropyl azodicarboxylate (DIAD) to aromatic and aliphatic tertiary amines in acetonitrile generated aminomethylated hydrazine-1,2-dicarboxylates. The insertion of DIAD in the C-H bond of an NCH<sub>3</sub> group thus provided  $\alpha$ -aminations of tertiary amines under mild conditions. The high reactivities of heteroaryl- and aryltrifluoroborates, ArBF<sub>3</sub>K, as well as their stability under acidic conditions allowed us to transform the DIAD-amine addition products to a series of  $\alpha$ -arylated amines (Scheme 6).



**Scheme 6.** DIAD-amine addition products as relays for the transition metal-free  $\alpha$ -arylation of tertiary amines.

Several functional groups in the amine tolerated the arylation reactions with organotrifluoroborates. Chloro- and bromoanilines could, thus, be used for further classical palladium-catalyzed cross-couplings or functionalization reactions, while carboxylic ester or cyano groups may serve as electrophilic sites for the addition of nucleophiles.

Both steps of the amination/arylation sequence from unfunctionalized to  $\alpha$ -arylated amines were efficient without adding a transition metal catalyst. The thus developed arylation method

was also successfully applied for the introduction of heteroaromatic groups at C-9 of tropinone, which underscores its potential for selective *N*-methyl functionalizations of alkaloids.<sup>[5g]</sup>

## Experimental Section

Typical procedure: The hydrazine-1,2-dicarboxylate **2f** (619 mg, 1.54 mmol) was dissolved in acetonitrile (5 mL). Subsequently, the potassium aryltrifluoroborate **3a** (345 mg, 1.54 mmol) and trifluoroacetic acid (120  $\mu$ L, 1.57 mmol) were added dropwise within 1–5 min. The reaction mixture was stirred at room temperature for 2 h. Then, the solvent was removed under reduced pressure. The residue was treated with 2 M aq ammonia (20 mL) and extracted with CH<sub>2</sub>Cl<sub>2</sub> (3  $\times$  20 mL). The combined organic layers were dried (Na<sub>2</sub>SO<sub>4</sub>), filtered, and volatiles were removed under reduced pressure. Finally, the crude product was purified by flash column chromatography (SiO<sub>2</sub>, acetone/pentane gradient from 1/200 to 1/20): **4f** (363 mg, 75%), light yellow oil. See Supporting Information for product characterization.

## Acknowledgements

We thank Professor Herbert Mayr for continued support and helpful discussions. We are grateful to Prof. Dr. Konstantin Karaghiosoff, Dr. David S. Stephenson and Claudia Ober for support with the HT-NMR experiments and to Dr. Guillaume Berionni for providing **3c** and **3e** and general advice for the preparation of potassium organotrifluoroborates.

## References

- [1]  $\alpha$ -Functionalizations of amines have been reviewed: a) K. R. Campos, *Chem. Soc. Rev.* **2007**, *36*, 1069–1084; b) K. Jones, M. Klusmann, *Synlett* **2012**, *23*, 159–162; c) E. A. Mitchell, A. Peschiulli, N. Lefevre, L. Meerpoel, B. U. W. Maes, *Chem.–Eur. J.* **2012**, *18*, 10092–10142; d) M.-X. Cheng, S.-D. Yang, *Synlett* **2017**, *28*, 159–174; e) A. Gini, T. Brandhofer, O. García Mancheño, *Org. Biomol. Chem.* **2017**, *15*, 1294–1312.
- [2] a) N. A. McGrath, M. Brichacek, J. T. Njardarson, *J. Chem. Educ.* **2010**, *87*, 1348–1349; b) F. Weber, G. Sedelmeier, *Nachr. Chem.* **2014**, *62*, 997.
- [3] a) Z. Li, D. S. Bohle, C.-J. Li, *Proc. Natl. Acad. Sci. U. S. A.* **2006**, *103*, 8928–8933; b) C.-J. Li, *Acc. Chem. Res.* **2009**, *42*, 335–344; c) S. A. Girard, T. Knauber, C.-J. Li, *Angew. Chem. Int. Ed.* **2014**, *53*, 74–100; d) X. Zheng, Z. Li in *From C-H to CC-bonds: Cross-Dehydrogenative-Couplings* (Ed.: C.-J. Li), RSC Green Chemistry Series Vol. 26, Royal Society of Chemistry, Cambridge, UK, **2015**, pp. 55–66.
- [4] a) C. S. Yeung, V. M. Dong, *Chem. Rev.* **2011**, *111*, 1215–1292; b) Z. Li, R. Yu in *Handbook of Green Chemistry Volume 7: Green Synthesis, First Edition* (Ed.: C.-J. Li),

- Wiley-VCH, Weinheim, **2012**, pp. 335–367; c) *C-H Bond Activation in Organic Synthesis* (Ed.: J. J. Li), Boca Raton, FL, **2015**.
- [5] a) A. McNally, C. K. Prier, D. W. C. MacMillan, *Science* **2011**, *334*, 1114–1117; b) C. K. Prier, D. W. C. MacMillan, *Chem. Sci.* **2014**, *3*, 4173–4178; c) M. H. Shaw, V. W. Shurtleff, J. A. Terrett, J. D. Cuthbertson, D. W. C. MacMillan, *Science* **2016**, *352*, 1304–1308; d) Q. Li, C. W. Liskey, J. F. Hartwig, *J. Am. Chem. Soc.* **2014**, *136*, 8755–8765; e) C. Yan, L. Li, Y. Liu, Q. Wang, *Org. Lett.* **2016**, *18*, 4686–4689; f) D. T. Ahnemann, A. G. Doyle, *Chem. Sci.* **2016**, *7*, 7002–7006; g) J. P. Barham, M. P. John, J. A. Murphy, *J. Am. Chem. Soc.* **2016**, *138*, 15482–15487.
- [6] W. Muramatsu, K. Nakano, C.-J. Li, *Org. Biomol. Chem.* **2014**, *12*, 2189–2192.
- [7] a) J. Dhineshkumar, M. Lamani, K. Alagiri, K. R. Prabhu, *Org. Lett.* **2013**, *15*, 1092–1095; b) H. Ueda, K. Yoshida, H. Tokuyama, *Org. Lett.* **2014**, *16*, 4194–4197; c) C. Huo, C. Wang, M. Wu, X. Jia, X. Wang, Y. Yuan, H. Xie, *Org. Biomol. Chem.* **2014**, *12*, 3123–3128.
- [8] R. Rohlmann, O. García Mancheño, *Synlett* **2013**, *24*, 6–10.
- [9] C.-L. Sun, Z.-J. Shi, *Chem. Rev.* **2014**, *114*, 9219–9280.
- [10] C. Liu, J. Yuan, M. Gao, S. Tang, W. Li, R. Shi, A. Lei, *Chem. Rev.* **2015**, *115*, 12138–12204.
- [11] R. Narayan, K. Matcha, A. P. Antonchick, *Chem. Eur. J.* **2015**, *21*, 14678–14693.
- [12] J. Košmrlj, M. Kočevár, S. Polanc, *Synlett* **2009**, 2217–2235.
- [13] a) O. Diels, M. Paquin, *Ber. Dtsch. Chem. Ges.* **1913**, *46*, 2000–2013; b) O. Diels, E. Fischer, *Ber. Dtsch. Chem. Ges.* **1914**, *47*, 2043–2047; c) O. Diels, *Justus Liebigs Ann. Chem.* **1922**, *429*, 1–55.
- [14] a) G. W. Kenner, R. J. Stedman, *J. Chem. Soc.* **1952**, 2089–2094; b) G. H. Kerr, O. Meth-Cohn, E. B. Mullock, H. Suschitzky, *J. Chem. Soc. Perkin Trans. 1* **1974**, 1614–1619.
- [15] a) R. Huisgen, F. Jakob, *Justus Liebigs Ann. Chem.* **1954**, *590*, 37–54; b) A slightly different reaction mechanism, involving the formation of an iminium ion pair, was suggested in: R. Huisgen, *The Adventure Playground of Mechanisms and Novel Reactions*, American Chemical Society, Washington DC, **1994**, pp. 51–52.
- [16] Reviews: a) G. S. Kaitmazova, N. P. Gambaryan, E. M. Rokhlin, *Russ. Chem. Rev.* **1989**, *58*, 1145–1156; b) V. Nair, A. T. Biju, S. C. Mathew, B. Pattoorpadu Babu, *Chem. Asian J.* **2008**, *3*, 810–820.
- [17] a) K. Heß, *Ber. Dtsch. Chem. Ges.* **1919**, *52*, 964–1004; b) E. J. Fornefeld, H. R. Sullivan Jr., W. E. Thompson (Eli Lilly and Co.), **1965**, US Pat. 3213128; c) E. E. Smisman, A. Makriyannis, *J. Org. Chem.* **1973**, *38*, 1652–1657; d) L. S. Schwab, *J. Med. Chem.* **1980**, *23*, 698–702; e) J. Marton, C. Simon, S. Hosztafi, Z. Szabó, Á. Márki, A. Borsodi, S. Makleit, *Bioorg. Med. Chem.* **1997**, *5*, 369–382; f) Review: S. Thavaneswaran, K. McCamley, P. J. Scammells, *Nat. Prod. Commun.* **2006**, *1*, 885–897.
- [18] For a diisopropyl azodicarboxylate-mediated cyclization of an allylic amine and a phenolic moiety: G. Vincent, Y. Chen, J. W. Lane, R. M. Williams, *Heterocycles* **2007**, *72*, 385–398.
- [19] a) X. Xu, X. Li, *Org. Lett.* **2009**, *11*, 1027–1029; b) See also: K. N. Singh, P. Singh, A. Kaur, P. Singh, *Synlett* **2012**, *23*, 760–764.
- [20] A. M. Zhirov, A. V. Aksenov, *Russ. Chem. Rev.* **2014**, *83*, 502–522.

- [21] a) Y. Miyake, K. Nakajima, Y. Nishibayashi, *Chem. Eur. J.* **2012**, *18*, 16473–16477; b) For further examples of reactions with aryl magnesium bromides (6 equiv): K. N. Singh, S. V. Kessar, P. Singh, P. Singh, M. Kaur, A. Batra, *Synthesis* **2014**, *46*, 2644–2650.
- [22] W. Huang, C. Ni, Y. Zhao, J. Hu, *New. J. Chem.* **2013**, *37*, 1684–1687.
- [23] T. Suga, S. Iizuka, T. Akiyama, *Org. Chem. Front.* **2016**, *3*, 1259–1264.
- [24] a) S. Roscales, A. G. Csáký, *Chem. Soc. Rev.* **2014**, *43*, 8215–8225; b) F. Sánchez-Sancho, A. G. Csáký, *Synthesis* **2016**, *48*, 2165–2177.
- [25] In contrast, it was reported that **1c** reacts with bis(2,2,2-trichloroethyl) azodicarboxylate in 3 M LiClO<sub>4</sub>-diethyl ether solution to form a *p*-substituted aryl hydrazide: I. Zaltsgendler, Y. Leblanc, M. A. Bernstein, *Tetrahedron Lett.* **1993**, *34*, 2441–2444.
- [26] a) C. Cox, T. Lectka, *J. Org. Chem.* **1998**, *63*, 2426–2427; b) P. R. Rablen, *J. Org. Chem.* **2000**, *65*, 7930–7937; c) M. J. Deetz, C. C. Forbes, M. Jonas, J. P. Malerich, B. D. Smith, O. Wiest, *J. Org. Chem.* **2002**, *67*, 3949–3952.
- [27] One TsOH-catalyzed (20 mol-%) reaction between an azodicarboxylate-activated *N*-(*t*-butylphenyl)-1,2,3,4-tetrahydroquinoline and indole was reported in ref [21a].
- [28] a) H. Mayr, T. Bug, M. F. Gotta, N. Hering, B. Irrgang, B. Janker, B. Kempf, R. Loos, A. R. Ofial, G. Remennikov, H. Schimmel, *J. Am. Chem. Soc.* **2001**, *123*, 9500–9512; b) B. Kempf, N. Hampel, A. R. Ofial, H. Mayr, *Chem. Eur. J.* **2003**, *9*, 2209–2218; c) H. Mayr, B. Kempf, A. R. Ofial, *Acc. Chem. Res.* **2003**, *36*, 66–77; d) S. Lakhdar, M. Westermaier, F. Terrier, R. Goumont, T. Boubaker, A. R. Ofial, H. Mayr, *J. Org. Chem.* **2006**, *71*, 9088–9095; e) T. A. Nigst, M. Westermaier, A. R. Ofial, H. Mayr, *Eur. J. Org. Chem.* **2008**, 2369–2374; f) J. Ammer, C. Nolte, H. Mayr, *J. Am. Chem. Soc.* **2012**, *134*, 13902–13911.
- [29] a) G. Berionni, B. Maji, P. Knochel, H. Mayr, *Chem. Sci.* **2012**, *3*, 878–882; b) G. Berionni, V. Morozova, M. Heininger, P. Mayer, P. Knochel, H. Mayr, *J. Am. Chem. Soc.* **2013**, *135*, 6317–6324.
- [30] G. A. Molander, N. Ellis, *Acc. Chem. Res.* **2007**, *40*, 275–286.
- [31] a) R. Ting, C. W. Harwig, J. Lo, Y. Li, M. J. Adam, T. J. Ruth, D. M. Perrin, *J. Org. Chem.* **2008**, *73*, 4662–4670; b) D. M. Perrin, *Acc. Chem. Res.* **2016**, *49*, 1333–1343.
- [32] K. M. Fisher, Y. Bolshan, *J. Org. Chem.* **2015**, *80*, 12676–12685.
- [33] For  $\alpha$ -CH-arylations of carbamates by organoboranes, see: a) Z. Xie, L. Liu, W. Chen, H. Zheng, Q. Xu, H. Yuan, H. Lou, *Angew. Chem.* **2014**, *126*, 3985–3989; *Angew. Chem. Int. Ed.* **2014**, *53*, 3904–3908; b) X. Liu, S. Sun, Z. Meng, H. Lou, L. Liu, *Org. Lett.* **2015**, *17*, 2396–2399; c) X. Liu, Z. Meng, C. Li, H. Lou, L. Liu, *Angew. Chem.* **2015**, *127*, 6110–6113; *Angew. Chem. Int. Ed.* **2015**, *54*, 6012–6015; d) G. Wang, Y. Mao, L. Liu, *Org. Lett.* **2016**, *18*, 6476–6479; e) Y. Sun, G. Wang, J. Chen, C. Liu, M. Cai, R. Zhu, H. Huang, W. Li, L. Liu, *Org. Biomol. Chem.* **2016**, *14*, 9431–9438.
- [34] For an iron-catalyzed oxidative C–H/C–H cross-coupling of thiophenes with methylamines, see: M. Ohta, M. P. Quick, J. Yamaguchi, B. Wünsch, K. Itami, *Chem. Asian J.* **2009**, *4*, 1416–1419.
- [35] a) S. Murata, K. Teramoto, M. Miura, M. Nomura, *J. Chem. Res. (S)* **1993**, 434; b) Z. Li, C.-J. Li, *J. Am. Chem. Soc.* **2004**, *126*, 11810–11811; c) C. M. Rao Volla, P. Vogel, *Org. Lett.* **2009**, *11*, 1701–1704; d) P. Liu, C.-Y. Zhou, S. Xiang, C.-M. Che, *Chem. Commun.* **2010**, *46*, 2739–2741; e) G. H. Dang, D. T. Nguyen, D. T. Le, T. Truong, N. T. S. Phan, *J. Mol. Catal. A* **2014**, *395*, 300–306; f) S. Kaur, M. Kumar, V. Bhalla, *Chem. Commun.* **2015**, *51*, 16327–16330; g) F. Alonso, A. Arroyo, I. Martín-García, Y. Moglie, *Adv. Synth. Catal.* **2015**, *357*, 3549–3561.

## Transition Metal-Free C-H Functionalization of Tertiary Amines: Diisopropyl Azodicarboxylate Mediated $\alpha$ -Arylations

### 1. General

#### Analytcs

$^1\text{H}$  NMR (600, 400, or 300 MHz),  $^{13}\text{C}$  NMR (151, 101, or 75.5 MHz), and  $^{19}\text{F}$  NMR spectra (376 MHz) were recorded on Varian or Bruker NMR systems in  $d_6$ -DMSO or  $\text{CDCl}_3$ . Chemical shifts in ppm refer to the solvent residual signal in  $d_6$ -DMSO ( $\delta_{\text{H}}$  2.50,  $\delta_{\text{C}}$  39.52 ppm)<sup>[S1]</sup> or  $\text{CDCl}_3$  ( $\delta_{\text{H}}$  7.26,  $\delta_{\text{C}}$  77.16 ppm)<sup>[S1]</sup> as internal standard or to external  $\text{CFCl}_3$  ( $\delta_{\text{F}}$  0.0 ppm), respectively. The following abbreviations are used to describe the mutiplicities of  $^1\text{H}$  resonances: br s = broad singlet, s = singlet, d = doublet, t = triplet, q = quartet, sept = septet, m = multiplet, app = apparent. NMR signal assignments are based on additional 2D-NMR experiments (COSY, HSQC, and HMBC).

#### Materials

Commercially available acetonitrile (Acros, 99.9%, Extra Dry, AcroSeal) was used as received.

Diisopropyl azodicarboxylate (DIAD; 94%, ABCR or Apollo) was purchased and used as received.

The following commercially available potassium aryl- or alkynyltrifluoroborates were used as received: Potassium 3-furanyltrifluoroborate **3b'** (97%, Aldrich), potassium 2-thienyltrifluoroborate **3d** (Aldrich), potassium phenyltrifluoroborate **3f** (98%, Apollo), potassium 3,4-(methylenedioxy)phenyltrifluoroborate **3g** (97%, Aldrich), and potassium (phenylethynyl)trifluoroborate **6** (95%, Aldrich). Potassium benzofuran-2-yltrifluoroborate **3a** (90%, Aldrich) was recrystallized from acetone/diethyl ether.

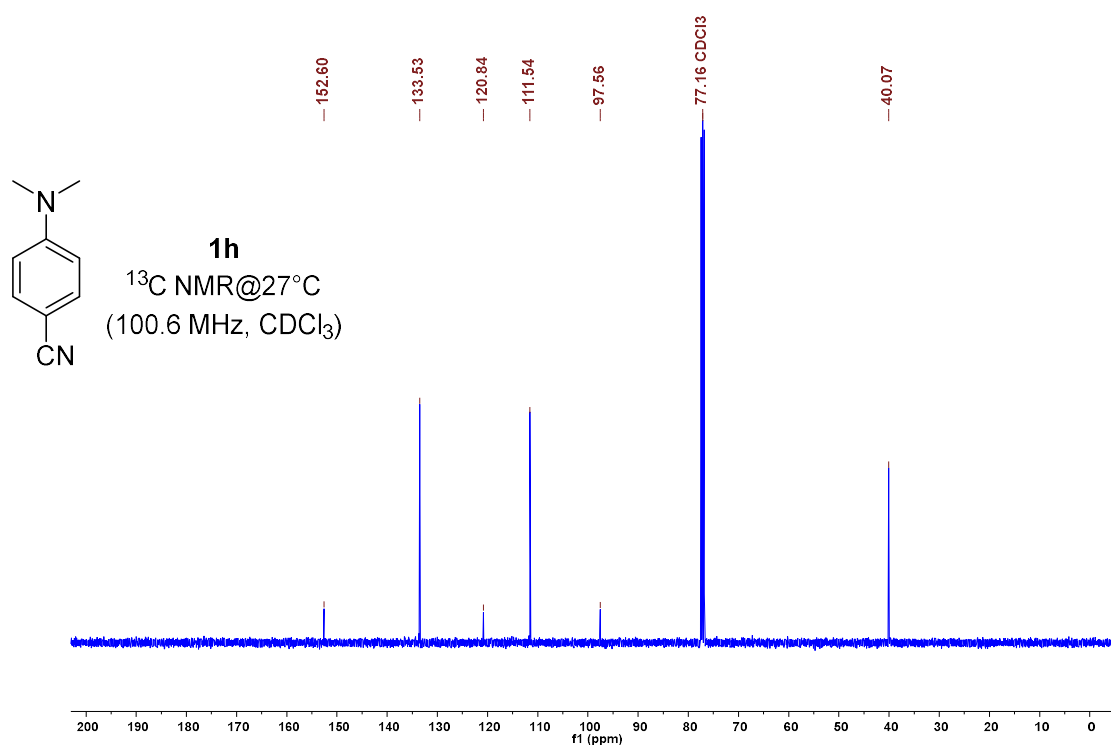
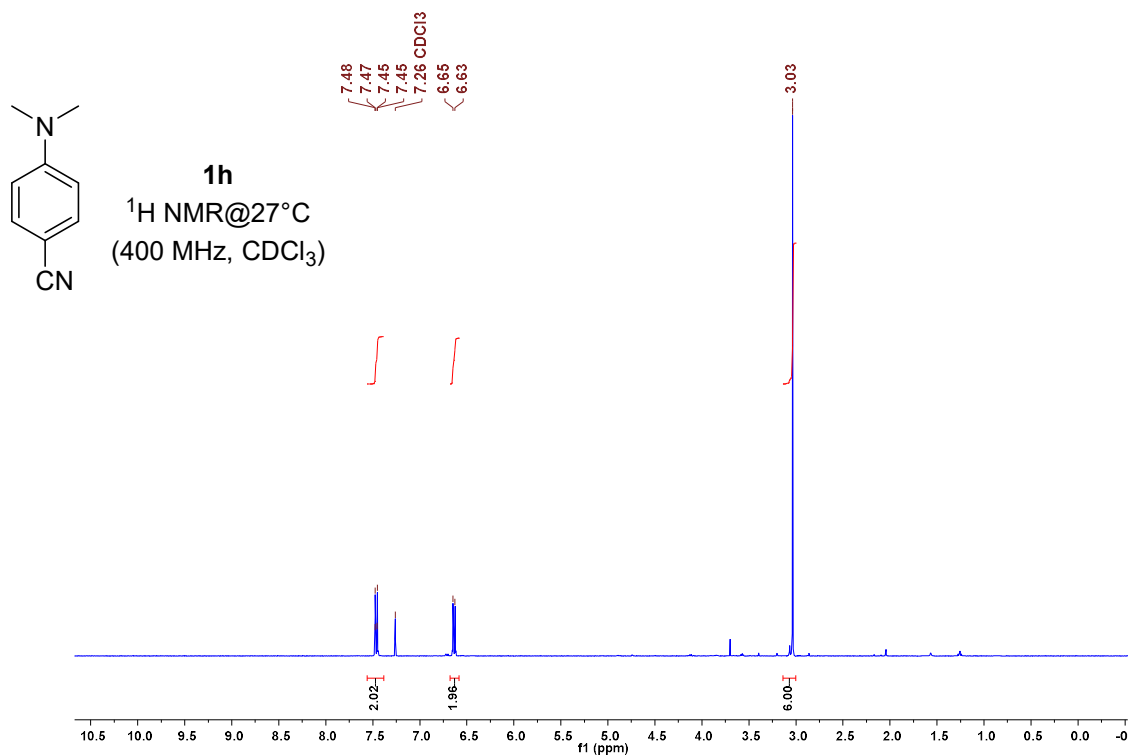
Potassium 2-furanyltrifluoroborate **3b**, potassium trifluoro(5-methylfuran-2-yl)borate **3c** and potassium trifluoro(5-methylfuran-2-yl)borate **3e** were synthesized from the parent heteroarenes by subsequent treatment with *n*-BuLi,  $\text{B}(\text{OiPr})_3$ , and  $\text{KHF}_2$  (6 equiv.) in analogy to a procedure described in ref. [S2] The crude products were purified by recrystallization from acetone/diethyl ether.

Commercially available substituted *N,N*-dimethylanilines and tropinone were used as received. *N,N*-Dimethyl-*p*-anisidine was prepared as described in ref. [S3]

4-(Dimethylamino)benzotrile (**1h**) was synthesized from 4-aminobenzotrile by reductive methylation:<sup>[S4]</sup> 4-Aminobenzotrile (1.0 g, 8.5 mmol) was dissolved in 1,4-dioxane (100 mL). Zinc powder (7.0 g) and 30% aq formaldehyde solution (3.5 mL, 38 mmol) were added. Subsequently, acetic acid (12 mL, 0.21 mol) was added to the reaction mixture via a dropping funnel. The exothermic reaction was controlled by cooling the reaction solution with an ice bath (0 °C). After another 12 h of stirring at ambient temperature, the solution was neutralized by addition of aq NaOH solution. Solid

residues were then removed by filtration. The aqueous phase was extracted with chloroform. The combined organic layers were then dried ( $\text{Na}_2\text{SO}_4$ ), filtered, and concentrated in the vacuum, which caused precipitation of **1h** (1.20 g, 97%).  $^1\text{H}$  and  $^{13}\text{C}$  NMR data were in accord with those reported in ref. [S5].

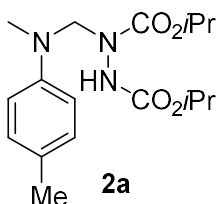
$^1\text{H}$  NMR (400 MHz,  $\text{CDCl}_3$ ):  $\delta$  3.03 (s, 6 H,  $\text{NMe}_2$ ), 6.63–6.65 (m, 2 H, ArH), 7.45–7.48 (m, 2 H, ArH).  $^{13}\text{C}$  NMR (101 MHz,  $\text{CDCl}_3$ ):  $\delta$  40.1, 97.6, 111.5, 120.8, 133.5, 152.6.



## 2. Preparation of 2a–j

*General Procedure (GP1):* The amine **1** was dissolved in MeCN and diisopropyl azodicarboxylate (DIAD) was added dropwise under stirring. The reaction mixture was then stirred at room temperature, if not indicated otherwise, for the indicated time. After the removal of volatiles under reduced pressure, the crude product was purified by flash column chromatography by applying an acetone/pentane (or acetone/isohexane) gradient (1/100 to 1/10).

**Diisopropyl 1-((methyl(*p*-tolyl)amino)methyl)hydrazine-1,2-dicarboxylate (2a).** According to GP1, **2a** was prepared from *N,N*-dimethyl-*p*-toluidine **1a** (10 mL, 69 mmol) and DIAD (16 mL, 76 mmol) in MeCN (50 mL) by stirring the reaction mixture at ambient temperature for 4 days. After purification by column chromatography (silica gel, acetone/isohexane 1/10;  $R_f = 0.33$ ) **2a** was obtained as a slightly orange colored viscous liquid (22.1 g, 95%).



$^1\text{H NMR}$  (400 MHz,  $d_6$ -DMSO, 90 °C):  $\delta$  1.14 (br d,  $J = 6.2$  Hz, 6 H,  $\text{OCH}(\text{CH}_3)_2$ ), 1.22 (d,  $J = 6.2$  Hz, 6 H,  $\text{OCH}(\text{CH}_3)_2$ ), 2.19 (s, 3 H, Ar-Me), 2.92 (s, 3 H, NMe), 4.76 (sept,  $J = 6.2$  Hz, 1 H,  $\text{OCH}(\text{CH}_3)_2$ ), 4.84 (sept,  $J = 6.2$  Hz, 1 H,  $\text{OCH}(\text{CH}_3)_2$ ), 4.95 (br s, 2 H,  $\text{NCH}_2\text{N}$ ), 6.72–6.76 (m, 2 H, ArH), 6.95–6.99 (m, 2 H, ArH).

$^{13}\text{C NMR}$  (101 MHz,  $d_6$ -DMSO, 90 °C):  $\delta$  19.3 ( $\text{CH}_3$ , Ar-Me), 21.2 ( $\text{CH}_3$ , OiPr), 21.3 ( $\text{CH}_3$ , OiPr), 37.0 ( $\text{CH}_3$ , NMe), 66.0 ( $\text{CH}_2$ ,  $\text{NCH}_2\text{N}$ ), 67.7 (CH, OiPr), 68.7 (CH, OiPr), 112.8 (CH), 125.3 (C), 128.7 (CH), 145.8 (C), 154.8 (C,  $\text{CO}_2i\text{Pr}$ ).

**Diisopropyl 1-(((4-methoxyphenyl)(methyl)amino)methyl)hydrazine-1,2-dicarboxylate (2b).**

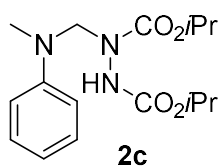
According to GP1, **2b** was prepared from *N,N*-dimethyl-*p*-anisidine **1b** (3.09 g, 20.5 mmol) and DIAD (4.6 mL, 22 mmol) in MeCN (20 mL) by stirring the reaction mixture at reflux temperature for 4 h. After purification by column chromatography **2b** was obtained as a brown viscous liquid (5.86 g, 81%).

$^1\text{H NMR}$  (400 MHz,  $d_6$ -DMSO, 90 °C):  $\delta$  1.14 (br d,  $J = 6.2$  Hz, 6 H,  $\text{OCH}(\text{CH}_3)_2$ ), 1.21 (d,  $J = 6.2$  Hz, 6 H,  $\text{OCH}(\text{CH}_3)_2$ ), 2.90 (s, 3 H, NMe), 3.68 (s, 3 H, OMe), 4.77 (sept,  $J = 6.2$  Hz, 1 H,  $\text{OCH}(\text{CH}_3)_2$ ), 4.83 (sept,  $J = 6.2$  Hz, 1 H,  $\text{OCH}(\text{CH}_3)_2$ ), 4.92 (br s, 2 H,  $\text{NCH}_2\text{N}$ ), 6.79 (app s, 4 H, ArH).

$^{13}\text{C NMR}$  (101 MHz,  $d_6$ -DMSO, 90 °C):  $\delta$  21.3 ( $\text{CH}_3$ , OiPr), 37.2 ( $\text{CH}_3$ , NMe), 55.1 ( $\text{CH}_3$ , Ar-OMe), 66.8 ( $\text{CH}_2$ ,  $\text{NCH}_2\text{N}$ ), 67.7 (CH, OiPr), 68.7 (CH, OiPr), 114.2 (CH), 114.4 (CH), 142.4 (C), 151.6 (C), 154.8 (C,  $\text{CO}_2i\text{Pr}$ ).

**HR-MS** (EI, 70 eV):  $m/z$   $[\text{M}]^{*+}$  Calcd for  $[\text{C}_{17}\text{H}_{27}\text{N}_3\text{O}_5]^{*+}$  353.1945; Found 353.1951.

**Diisopropyl 1-((methyl(phenyl)amino)methyl)hydrazine-1,2-dicarboxylate (2c).** According to



GP1, **2c** was prepared from *N,N*-dimethyl-aniline **1c** (2.7 mL, 21 mmol) and DIAD (5.0 mL, 24 mmol) in MeCN (20 mL) by stirring the reaction mixture at ambient temperature for 5 days. After purification by column chromatography **2c** was obtained as a yellow viscous liquid (5.86 g, 86%).

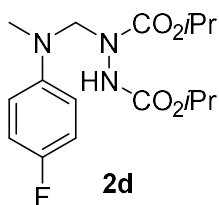
**<sup>1</sup>H NMR** (400 MHz, *d*<sub>6</sub>-DMSO, 90 °C): δ 1.14 (br d, *J* = 6.3 Hz, 6 H, OCH(CH<sub>3</sub>)<sub>2</sub>), 1.22 (d, *J* = 6.3 Hz, 6 H, OCH(CH<sub>3</sub>)<sub>2</sub>), 2.96 (s, 3 H, NMe), 4.76 (sept, *J* = 6.3 Hz, 1 H, OCH(CH<sub>3</sub>)<sub>2</sub>), 4.86 (sept, *J* = 6.3 Hz, 1 H, OCH(CH<sub>3</sub>)<sub>2</sub>), 5.00 (br s, 2 H, NCH<sub>2</sub>N), 6.67–6.70 (m, 1 H, ArH), 6.82–6.85 (m, 2 H, ArH), 7.14–7.18 (m, 2 H, ArH), 8.94 (br s, <1 H, NH).

**<sup>13</sup>C NMR** (101 MHz, *d*<sub>6</sub>-DMSO, 90 °C): δ 21.25 (CH<sub>3</sub>, *OiPr*), 21.27 (CH<sub>3</sub>, *OiPr*), 36.9 (CH<sub>3</sub>, NMe), 65.7 (CH<sub>2</sub>, NCH<sub>2</sub>N), 67.7 (CH, *OiPr*), 68.8 (CH, *OiPr*), 112.5 (CH), 116.6 (CH), 128.2 (CH), 147.9 (C), 154.8 (C, CO<sub>2</sub>*iPr*).

**HR-MS** (EI, 70 eV): *m/z* [M]<sup>+</sup> Calcd for [C<sub>16</sub>H<sub>25</sub>N<sub>3</sub>O<sub>4</sub>]<sup>+</sup> 323.1840; Found 323.1853.

**Elemental Analysis:** Calcd: C 59.42, H 7.79, N 12.99; Found: C 59.04, H 7.70, N 12.77.

**Diisopropyl 1-(((4-fluorophenyl)(methyl)amino)methyl)hydrazine-1,2-dicarboxylate (2d).**



According to GP1, **2d** was prepared from 4-fluoro-*N,N*-dimethyl-aniline **1d** (4.9 g, 35 mmol) and DIAD (8.0 mL, 38 mmol) in MeCN (25 mL) by stirring the reaction mixture at ambient temperature for 48 h. After purification by column chromatography **2d** was obtained as a brownish solid (10.5 g, 88%).

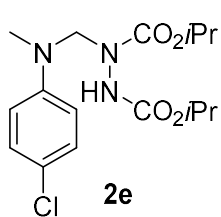
**<sup>1</sup>H NMR** (400 MHz, *d*<sub>6</sub>-DMSO, 90 °C): δ 1.13 (br d, *J* = 6.2 Hz, 6 H, OCH(CH<sub>3</sub>)<sub>2</sub>), 1.21 (d, *J* = 6.2 Hz, 6 H, OCH(CH<sub>3</sub>)<sub>2</sub>), 2.93 (s, 3 H, NMe), 4.76 (sept, *J* = 6.2 Hz, 1 H, OCH(CH<sub>3</sub>)<sub>2</sub>), 4.84 (sept, *J* = 6.2 Hz, 1 H, OCH(CH<sub>3</sub>)<sub>2</sub>), 4.96 (br s, 2 H, NCH<sub>2</sub>N), 6.81–6.84 (m, 2 H, ArH), 6.94–6.99 (m, 2 H, ArH), 8.90 (br s, <1 H, NH).

**<sup>13</sup>C NMR** (101 MHz, *d*<sub>6</sub>-DMSO, 90 °C): δ 21.2 (CH<sub>3</sub>, *OiPr*), 37.3 (CH<sub>3</sub>, NMe), 66.4 (CH<sub>2</sub>, NCH<sub>2</sub>N), 67.7 (CH, *OiPr*), 68.8 (CH, *OiPr*), 114.0 (CH, d, *J*<sub>C,F</sub> = 7.5 Hz), 114.4 (CH, d, *J*<sub>C,F</sub> = 21.9 Hz), 144.7 (C, d, *J*<sub>C,F</sub> = 1.5 Hz), 154.8 (C, CO<sub>2</sub>*iPr*), 154.9 (C, d, <sup>1</sup>*J*<sub>C,F</sub> = 234 Hz).

**<sup>19</sup>F NMR** (376 MHz, *d*<sub>6</sub>-DMSO, 90 °C) δ –128.5 (br s).

**HR-MS** (EI, 70 eV): *m/z* [M]<sup>+</sup> Calcd for [C<sub>16</sub>H<sub>24</sub>FN<sub>3</sub>O<sub>4</sub>]<sup>+</sup> 341.1745; Found 341.1747.

**Elemental Analysis:** Calcd: C 56.29, H 7.09, N 12.31; Found: C 56.16, H 7.13, N 12.23.

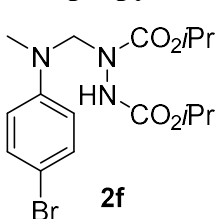
**Diisopropyl 1-(((4-chlorophenyl)(methyl)amino)methyl)hydrazine-1,2-dicarboxylate (2e).**

According to GP1, **2e** was prepared from 4-chloro-*N,N*-dimethylaniline **1e** (2.10 g, 13.4 mmol) and DIAD (3.1 mL, 15 mmol) in MeCN (10 mL) by stirring the reaction mixture at reflux temperature for 72 h. After purification by column chromatography **2e** was obtained as a brown viscous liquid (3.52 g, 74 %).

$^1\text{H NMR}$  (400 MHz,  $d_6$ -DMSO, 90 °C):  $\delta$  1.13 (br d,  $J = 6$  Hz, 6 H,  $\text{OCH}(\text{CH}_3)_2$ ), 1.22 (d,  $J = 6.2$  Hz, 6 H,  $\text{OCH}(\text{CH}_3)_2$ ), 2.94 (s, 3 H, NMe), 4.75 (sept,  $J = 6.2$  Hz, 1 H,  $\text{OCH}(\text{CH}_3)_2$ ), 4.84 (sept,  $J = 6.2$  Hz, 1 H,  $\text{OCH}(\text{CH}_3)_2$ ), 4.98 (br s, 2 H,  $\text{NCH}_2\text{N}$ ), 6.80–6.84 (m, 2 H, ArH), 7.14–7.18 (m, 2 H, ArH).

$^{13}\text{C NMR}$  (101 MHz,  $d_6$ -DMSO, 90 °C):  $\delta$  21.2 ( $\text{CH}_3$ , OiPr), 21.3 ( $\text{CH}_3$ , OiPr), 37.1 ( $\text{CH}_3$ , NMe), 65.7 ( $\text{CH}_2$ ,  $\text{NCH}_2\text{N}$ ), 67.7 (CH, OiPr), 68.9 (CH, OiPr), 114.1 (CH), 120.6 (C), 127.8 (CH), 146.8 (C), 154.8 (C,  $\text{CO}_2i\text{Pr}$ ).

**HR-MS** (EI, 70 eV):  $m/z$   $[\text{M}]^{*+}$  Calcd for  $[\text{C}_{16}\text{H}_{24}\text{ClN}_3\text{O}_4]^{*+}$  357.1450; Found 357.1449.

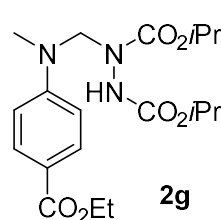
**Diisopropyl 1-(((4-bromophenyl)(methyl)amino)methyl)hydrazine-1,2-dicarboxylate (2f).**

According to GP1, **2f** was prepared from 4-bromo-*N,N*-dimethylaniline **1f** (1.7 g, 8.4 mmol) and DIAD (1.9 mL, 9.0 mmol) in MeCN (10 mL) by stirring the reaction mixture at reflux temperature for 72 h. After purification by column chromatography **2f** was obtained as a brown viscous liquid (2.95 g, 87%).

$^1\text{H NMR}$  (400 MHz,  $d_6$ -DMSO, 90 °C):  $\delta$  1.13 (br d,  $J = 6$  Hz, 6 H,  $\text{OCH}(\text{CH}_3)_2$ ), 1.22 (d,  $J = 6.2$  Hz, 6 H,  $\text{OCH}(\text{CH}_3)_2$ ), 2.94 (s, 3 H, NMe), 4.75 (sept,  $J = 6.2$  Hz, 1 H,  $\text{OCH}(\text{CH}_3)_2$ ), 4.84 (sept,  $J = 6.2$  Hz, 1 H,  $\text{OCH}(\text{CH}_3)_2$ ), 4.98 (br s, 2 H,  $\text{NCH}_2\text{N}$ ), 6.77–6.80 (m, 2 H, ArH), 7.27–7.30 (m, 2 H, ArH), 8.93 (br s, <1 H, NH).

$^{13}\text{C NMR}$  (101 MHz,  $d_6$ -DMSO, 90 °C):  $\delta$  21.2 ( $\text{CH}_3$ , OiPr), 21.3 ( $\text{CH}_3$ , OiPr), 37.1 ( $\text{CH}_3$ , NMe), 65.5 ( $\text{CH}_2$ ,  $\text{NCH}_2\text{N}$ ), 67.7 (CH, OiPr), 68.9 (CH, OiPr), 108.0 (C), 114.6 (CH), 130.7 (CH), 147.2 (C), 154.8 (C,  $\text{CO}_2i\text{Pr}$ ).

**HR-MS** (EI, 70 eV):  $m/z$   $[\text{M}]^{*+}$  Calcd for  $[\text{C}_{16}\text{H}_{24}^{79}\text{BrN}_3\text{O}_4]^{*+}$  401.0945; Found 401.0948.

**Diisopropyl 1-(((4-(ethoxycarbonyl)phenyl)(methyl)amino)methyl)hydrazine-1,2-dicarboxylate (2g).**

According to GP1, **2g** was prepared from ethyl 4-(dimethylamino)benzoate **1g** (1.95 g, 9.99 mmol) and DIAD (2.0 mL, 9.5 mmol) in MeCN (5 mL) by stirring the reaction mixture at reflux temperature for 48 h. Then pentane was added and the mixture was heated at 35 °C. After cooling to ambient temperature a (heavy) liquid layer formed, which was separated from the apolar layer. This extraction of unreacted starting materials by pentane was repeated (2 ×). After removing

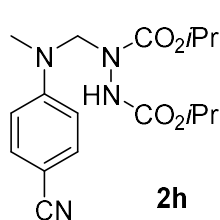
volatiles in the vacuum, **2g** was obtained as a yellow oil (3.22 g, 86%).

**<sup>1</sup>H NMR** (400 MHz, *d*<sub>6</sub>-DMSO, 90 °C): δ 1.12 (br d, *J* = 6 Hz, 6 H, OCH(CH<sub>3</sub>)<sub>2</sub>), 1.23 (d, *J* = 6.2 Hz, 6 H, OCH(CH<sub>3</sub>)<sub>2</sub>), 1.30 (t, *J* = 7.1 Hz, 3 H, OCH<sub>2</sub>CH<sub>3</sub>), 3.03 (s, 3 H, NMe), 4.26 (q, *J* = 7.1 Hz, 2 H, OCH<sub>2</sub>CH<sub>3</sub>), 4.75 (sept, *J* = 6.2 Hz, 1 H, OCH(CH<sub>3</sub>)<sub>2</sub>), 4.86 (sept, *J* = 6.2 Hz, 1 H, OCH(CH<sub>3</sub>)<sub>2</sub>), 5.07 (br s, 2 H, NCH<sub>2</sub>N), 6.86–6.89 (m, 2 H, ArH), 7.75–7.79 (m, 2 H, ArH).

**<sup>13</sup>C NMR** (101 MHz, *d*<sub>6</sub>-DMSO, 90 °C): δ 13.8 (CH<sub>3</sub>, OEt), 21.2 (CH<sub>3</sub>, *OiPr*), 21.3 (CH<sub>3</sub>, *OiPr*), 37.1 (CH<sub>3</sub>, NMe), 59.2 (CH<sub>2</sub>, OEt), 65.0 (CH<sub>2</sub>, NCH<sub>2</sub>N), 67.8 (CH, *OiPr*), 69.1 (CH, *OiPr*), 111.4 (CH), 117.8 (C), 130.0 (CH), 151.6 (C), 154.8 (C, CO<sub>2</sub>*iPr*), 165.3 (C, CO<sub>2</sub>Et).

**HR-MS** (EI, 70 eV): *m/z* [M]<sup>+</sup> Calcd for [C<sub>19</sub>H<sub>29</sub>N<sub>3</sub>O<sub>6</sub>]<sup>+</sup> 395.2051; Found 395.2060.

**Diisopropyl 1-(((4-cyanophenyl)(methyl)amino)methyl)hydrazine-1,2-dicarboxylate (2h).**



According to GP1, **2h** was prepared from 4-(dimethylamino)benzotrile **1h** (1.33 g, 9.01 mmol) and DIAD (2.1 mL, 10 mmol) in MeCN (5 mL) by stirring the reaction mixture at ambient temperature for 48 h. After purification by column chromatography **2h** was obtained as a colorless solid (2.22 g, 71%).

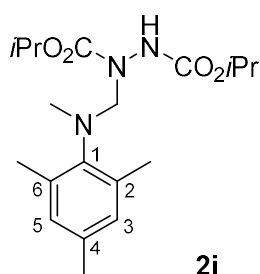
**<sup>1</sup>H NMR** (400 MHz, CDCl<sub>3</sub>, 27 °C): δ 1.22–1.26 (m, 12 H, 2 × OCH(CH<sub>3</sub>)<sub>2</sub>), 3.11 (s, 3 H, NMe), 4.90–5.15 (m, 4 H, 2 × OCH(CH<sub>3</sub>)<sub>2</sub> and NCH<sub>2</sub>N), 6.38 (br s, 1 H, NH), 6.84 (app d, *J* = 8.8 Hz, 2 H, ArH), 7.47 (app d, *J* = 8.8 Hz, 2 H, ArH). The additional resonance at δ = 2.16 ppm is caused by trace amounts of acetone.

**<sup>13</sup>C NMR** (101 MHz, CDCl<sub>3</sub>, 27 °C): δ 22.0 (CH<sub>3</sub>, *OiPr*), 22.1 (CH<sub>3</sub>, *OiPr*), 38.8 (CH<sub>3</sub>, NMe), 65.9 (CH<sub>2</sub>, NCH<sub>2</sub>N), 70.3 (CH, *OiPr*), 71.0 (CH, *OiPr*), 99.7 (C, CN), 112.6 (CH), 120.3 (C), 133.6 (CH), 151.0 (C), 155.7 (C). Additional resonances at δ = 31.1 and 207.1 ppm are caused by trace amounts of acetone.

**HR-MS** (EI, 70 eV): *m/z* [M]<sup>+</sup> Calcd for [C<sub>17</sub>H<sub>24</sub>N<sub>4</sub>O<sub>4</sub>]<sup>+</sup> 348.1792; Found 348.1793.

**Elemental Analysis:** Calcd: C 58.61, H 6.94, N 16.08; Found C 58.36, H 6.95, N 15.94.

**Diisopropyl 1-((mesityl(methyl)amino)methyl)hydrazine-1,2-dicarboxylate (2i).**



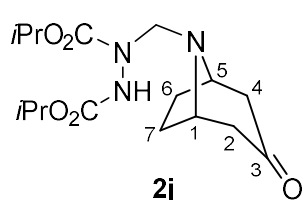
According to GP1, **2i** was prepared from *N,N*,2,4,6-pentamethylaniline **1i** (0.82 g, 5.0 mmol) and DIAD (1.0 mL, 4.7 mmol) in MeCN (1 mL) by stirring the reaction mixture at reflux temperature for 10 h. After recrystallization **2i** was obtained as a colorless solid (1.50 g, 87%); mp 94–96 °C. Partial decomposition of **2i** in *d*<sub>6</sub>-DMSO at 90 °C hindered the unequivocal assignment of resonances. Therefore, the NMR data for a solution of **2i** in CDCl<sub>3</sub> at 27 °C are reported.

**<sup>1</sup>H NMR** (400 MHz, CDCl<sub>3</sub>, 27 °C): δ 1.23 (br d, *J* = 6.3 Hz, 6 H, OCH(CH<sub>3</sub>)<sub>2</sub>), 1.26 (br d, *J* = 6.3 Hz, 6 H, OCH(CH<sub>3</sub>)<sub>2</sub>), 2.23 (app s, 9 H, 2,4,6-(CH<sub>3</sub>)<sub>3</sub>), 2.82 (s, 3 H, NMe), 4.72–4.98 (m, 4 H, 2 × OCH(CH<sub>3</sub>)<sub>2</sub> and NCH<sub>2</sub>N), 6.59 (br s, 1 H, NH), 6.82 (s, 2 H, 3-H and 5-H).

$^{13}\text{C}$  NMR (101 MHz,  $\text{CDCl}_3$ , 27 °C):  $\delta$  18.9 ( $\text{CH}_3$ , 2- $\text{CH}_3$  and 6- $\text{CH}_3$ ), 20.8 ( $\text{CH}_3$ , 4- $\text{CH}_3$ ), 22.01 ( $\text{CH}_3$ , *OiPr*), 22.03 ( $\text{CH}_3$ , *OiPr*), 39.6 ( $\text{CH}_3$ , br, NMe), 69.6–71.2 (superimposed CH and  $\text{CH}_2$ , *OiPr* and  $\text{NCH}_2\text{N}$ ), 129.5 (CH, C-3 and C-5), 135.2 (C), 136.8 (C), 145.1 (C), 155.9 and 156.5 (C,  $\text{CO}_2i\text{Pr}$ ).

**HR-MS** (EI, 70 eV):  $m/z$   $[\text{M} - \text{H}]^+$  Calcd for  $[\text{C}_{19}\text{H}_{30}\text{N}_3\text{O}_4]^+$  364.2231; Found 364.2230.

**Diisopropyl 1-((3-oxo-8-azabicyclo[3.2.1]octan-8-yl)methyl)hydrazine-1,2-dicarboxylate (2j).**



According to GP1, **2j** was prepared from tropinone **1j** (0.47 g, 3.4 mmol) and DIAD (0.77 mL, 3.7 mmol) in MeCN (10 mL) by stirring the reaction mixture at ambient temperature for 24 h. After purification by column chromatography **2j** was obtained as a brown solid (0.93 g, 80%); mp 92–95 °C.

$^1\text{H}$  NMR (400 MHz,  $\text{CDCl}_3$ , 27 °C):  $\delta$  1.14–1.16 (m, 12 H,  $\text{OCH}(\text{CH}_3)_2$ ), 1.54–1.57 (m, 2 H, 6-H and 7-H), 2.02 (br s, 2 H, 6-H and 7-H), 2.13–2.17 (m, 2 H, 2-H and 4-H), 2.58–2.61 (m, 2 H, 2-H and 4-H), 3.51 (br s, 2 H, 1-H and 5-H), 4.23 (br s, 2 H,  $\text{NCH}_2\text{N}$ ), 4.82–4.86 (m, 2 H,  $2 \times \text{OCH}(\text{CH}_3)_2$ ).

$^{13}\text{C}$  NMR (101 MHz,  $\text{CDCl}_3$ , 27 °C):  $\delta$  21.9 ( $\text{CH}_3$ , *OiPr*), 22.0 ( $\text{CH}_3$ , *OiPr*), 27.6 ( $\text{CH}_2$ , C-6 and C-7), 48.5 ( $\text{CH}_2$ , C-2 and C-4), 57.4 (CH, C-1 and C-5), 65.9 ( $\text{CH}_2$ ,  $\text{NCH}_2\text{N}$ ), 69.2 (CH, *iPr*), 69.6 (CH, *iPr*), 154.9 and 156.4 (C,  $\text{CO}_2i\text{Pr}$ ), 208.8 (C, C-3).

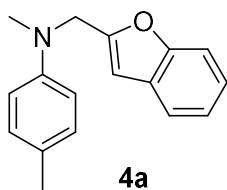
**HR-MS** (EI, 70 eV):  $m/z$   $[\text{M}]^{*+}$  Calcd for  $[\text{C}_{16}\text{H}_{27}\text{N}_3\text{O}_5]^{*+}$  341.1945; Found 341.1948.

**Elemental Analysis:** Calcd.: C 56.29, H 7.97, N 12.31; Found: C 56.19, H 7.89, N 12.38.

### 3. Preparation of $\alpha$ -Aryl Amines

*General Procedure (GP2):* The hydrazine-1,2-dicarboxylate **2** was dissolved in acetonitrile. Subsequently, potassium aryltrifluoroborate **3** and trifluoroacetic acid were added dropwise within 1–5 min. The reaction mixture was stirred at room temperature for the indicated time. At the end of the reaction time, the solvent was removed under reduced pressure. The residue was treated with aq ammonia (2 M, 20 mL) and extracted with dichloromethane ( $3 \times 20$  mL). The combined organic layers were dried over  $\text{Na}_2\text{SO}_4$ , filtered, and volatiles were removed under reduced pressure. Finally, the crude product was purified by flash column chromatography with acetone/pentane mixtures (gradient from 1/200 to 1/20).

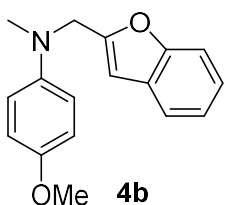
***N*-(Benzofuran-2-ylmethyl)-*N*,4-dimethylaniline (4a).** According to GP2, **2a** (173 mg, 0.513 mmol) was dissolved in MeCN (5 mL). Potassium benzofuran-2-yltrifluoroborate **3a** (115 mg, 0.513 mmol) and trifluoroacetic acid (40  $\mu\text{L}$ , 0.51 mmol) were added, and the mixture was stirred for 2 h. After column chromatography **4a** (121 mg, 94%) was obtained as a colorless liquid;  $R_f = 0.92$  (silica gel, acetone/isohexane = 1/10).



$^1\text{H NMR}$  (600 MHz,  $\text{CDCl}_3$ ):  $\delta$  2.36 (s, 3 H, 4- $\text{CH}_3$ ), 3.11 (s, 3 H, NMe), 4.65 (s, 2 H,  $\text{NCH}_2$ ), 6.56 (q,  $J = 1$  Hz, 1 H), 6.85–6.87 (m, 2 H), 7.14–7.16 (m, 2 H), 7.25–7.32 (m, 2 H), 7.52–7.55 (m, 2 H).

$^{13}\text{C NMR}$  (150.6 MHz,  $\text{CDCl}_3$ ):  $\delta$  20.4 ( $\text{CH}_3$ , 4- $\text{CH}_3$ ), 38.9 ( $\text{CH}_3$ , NMe), 50.9 ( $\text{CH}_2$ ,  $\text{NCH}_2$ ), 104.0 (CH), 111.2 (CH), 113.4 (CH), 120.8 (CH), 122.7 (CH), 123.8 (CH), 126.7 (C), 128.5 (C), 129.8 (CH), 147.2 (C), 155.0 (C), 155.4 (C).

***N*-(Benzofuran-2-ylmethyl)-4-methoxy-*N*-methylaniline (4b).** According to GP2, **2b** (157 mg, 0.444 mmol) was dissolved in MeCN (10 mL). Potassium benzofuran-2-yltrifluoroborate **3a** (100 mg, 0.446 mmol) and TFA (35  $\mu\text{L}$ , 0.46 mmol) were added, and the mixture was stirred for 24 h. After column chromatography **4b** (106 mg, 89%) was obtained as a colorless liquid.

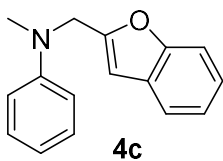


$^1\text{H NMR}$  (400 MHz,  $\text{CDCl}_3$ ):  $\delta$  3.02 (s, 3 H, NMe), 3.79 (s, 3 H, OMe), 4.55 (s, 2 H,  $\text{NCH}_2$ ), 6.51–6.52 (m, 1 H), 6.87 (br s, 4 H), 7.19–7.28 (m, 2 H), 7.45–7.52 (m, 2 H).

$^{13}\text{C NMR}$  (100.6 MHz  $\text{CDCl}_3$ ):  $\delta$  39.5 ( $\text{CH}_3$ , NMe), 51.9 ( $\text{CH}_2$ ,  $\text{NCH}_2$ ), 55.8 ( $\text{CH}_3$ , OMe), 104.3 (CH), 111.2 (CH), 114.8 (CH), 115.5 (CH), 120.8 (CH), 122.8 (CH), 123.9 (CH), 128.5 (C), 144.1 (C), 152.5 (C), 155.0 (C), 155.4 (C).

**HR-MS** (EI, 70 eV):  $m/z$   $[\text{M}]^{+\cdot}$  Calcd for  $[\text{C}_{17}\text{H}_{17}\text{NO}_2]^{+\cdot}$  267.1254; Found 267.1254.

***N*-(Benzofuran-2-ylmethyl)-*N*-methylaniline (4c).** According to GP2, **2c** (171 mg, 0.529 mmol) was dissolved in MeCN (10 mL). Potassium benzofuran-2-yltrifluoroborate **3a** (118 mg, 0.527 mmol) and TFA (41  $\mu$ L, 0.54 mmol) were added, and the mixture was stirred for 24 h. After column chromatography **4c** (110 mg, 88%) was obtained as a colorless liquid. Known compound, the NMR spectroscopic data are in accord with those given in ref.<sup>[S6]</sup>

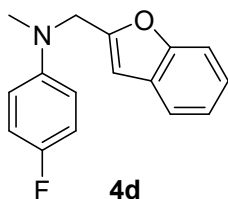


<sup>1</sup>H NMR (300 MHz, CDCl<sub>3</sub>):  $\delta$  3.10 (s, 3 H, NMe), 4.63 (s, 2 H, NCH<sub>2</sub>), 6.51–6.52 (m, 1 H), 6.78–6.82 (m, 1 H), 6.86–6.89 (m, 2 H), 7.19–7.31 (m, 4 H), 7.46–7.51 (m, 1 H).

<sup>13</sup>C NMR (75.5 MHz, CDCl<sub>3</sub>):  $\delta$  38.7 (CH<sub>3</sub>, NMe), 50.6 (CH<sub>2</sub>, NCH<sub>2</sub>), 104.0 (CH), 111.2 (CH), 113.0 (CH), 117.4 (CH), 120.8 (CH), 122.8 (CH), 123.9 (CH), 128.5 (C), 129.3 (CH), 149.2 (C), 155.1 (C), 155.3 (C).

HR-MS (EI, 70 eV):  $m/z$  [M]<sup>+</sup> Calcd for [C<sub>16</sub>H<sub>15</sub>NO]<sup>+</sup> 237.1148; Found 237.1148.

***N*-(Benzofuran-2-ylmethyl)-4-fluoro-*N*-methylaniline (4d).** According to GP2, **2d** (270 mg, 0.791 mmol) was dissolved in MeCN (5 mL). Potassium benzofuran-2-yltrifluoroborate **3a** (178 mg, 0.795 mmol) and TFA (62  $\mu$ L, 0.81 mmol) were added, and the mixture was stirred for 2 h. After column chromatography **4d** (165 mg, 82%) was obtained as a yellow liquid.

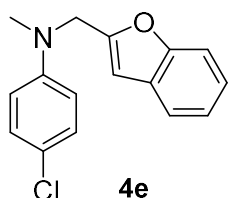


<sup>1</sup>H NMR (400 MHz, CDCl<sub>3</sub>):  $\delta$  3.08 (s, 3 H, NMe), 4.60 (s, 2 H, NCH<sub>2</sub>), 6.55 (br s, 1 H), 6.82–6.86 (m, 2 H), 7.01–7.05 (m, 2 H), 7.25–7.34 (m, 2 H), 7.52–7.57 (m, 2 H).

<sup>13</sup>C NMR (100.6 MHz CDCl<sub>3</sub>):  $\delta$  39.2 (CH<sub>3</sub>, NMe), 51.3 (CH<sub>2</sub>, NCH<sub>2</sub>), 104.2 (CH), 111.2 (CH), 114.4 (CH, d,  $J_{C,F}$  = 7.3 Hz), 115.6 (CH, d,  $J_{C,F}$  = 22.1 Hz), 120.8 (CH), 122.8 (CH), 124.0 (CH), 128.4 (C), 146.0 (C, d,  $J_{C,F}$  = 1.9 Hz), 155.03 (C), 155.05 (C), 156.0 (C, d,  $^1J_{C,F}$  = 236.0 Hz).

<sup>19</sup>F NMR (376 MHz, CDCl<sub>3</sub>):  $\delta$  -127.88 (tt,  $J$  = 8.5, 4.4 Hz).

***N*-(Benzofuran-2-ylmethyl)-4-chloro-*N*-methylaniline (4e).** According to GP2, **2e** (40 mg, 0.11 mmol) was dissolved in MeCN (1 mL). Potassium benzofuran-2-yltrifluoroborate **3a** (25 mg, 0.11 mmol) and TFA (9  $\mu$ L, 0.1 mmol) were added, and the solution was stirred for 2 h. After column chromatography **4e** (25 mg, 84%) was obtained as a yellowish liquid.

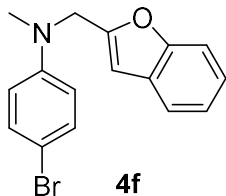


<sup>1</sup>H NMR (400 MHz, CDCl<sub>3</sub>):  $\delta$  3.07 (s, 3 H, NMe), 4.59 (s, 2 H, NCH<sub>2</sub>), 6.48 (br s, 1 H), 6.74–6.77 (m, 2 H), 7.17–7.27 (m including residual CHCl<sub>3</sub>, 4 H), 7.43–7.50 (m, 2 H).

<sup>13</sup>C NMR (100.6 MHz CDCl<sub>3</sub>):  $\delta$  39.0 (CH<sub>3</sub>, NMe), 50.7 (CH<sub>2</sub>, NCH<sub>2</sub>), 104.2 (CH), 111.2 (CH), 114.2 (CH), 120.9 (CH), 122.3 (C), 122.9 (CH), 124.0 (CH), 128.4 (C), 129.1 (CH), 147.8 (C), 154.7 (C), 155.1 (C).

**HR-MS** (EI, 70 eV):  $m/z$   $[M]^{+}$  Calcd for  $[C_{16}H_{14}^{35}ClNO]^{+}$  271.0758; Found 271.0762.

***N*-(Benzofuran-2-ylmethyl)-4-bromo-*N*-methylaniline (4f)**. Following GP2, **2f** (619 mg, 1.54 mmol) and potassium benzofuran-2-yltrifluoroborate **3a** (345 mg, 1.54 mmol) were dissolved in MeCN (5.0 mL). After the addition of TFA (120  $\mu$ L, 1.57 mmol), the solution was stirred at room temperature for 2 h. After column chromatography **4f** (363 mg, 75%) was obtained as a light yellow oil.

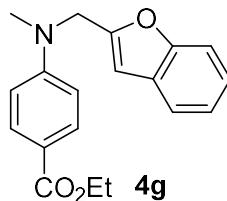


**$^1H$  NMR** (400 MHz,  $CDCl_3$ ):  $\delta$  3.00 (s, 3 H, NMe), 4.53 (s, 2 H, NCH<sub>2</sub>), 6.42 (br s, 1 H), 6.63–6.66 (m, 2 H), 7.12–7.21 (m, 2 H), 7.24–7.27 (m, 2 H), 7.37–7.44 (m, 2 H).

**$^{13}C$  NMR** (100.6 MHz,  $CDCl_3$ ):  $\delta$  38.9 (CH<sub>3</sub>, NMe), 50.5 (CH<sub>2</sub>, NCH<sub>2</sub>), 104.2 (CH), 109.4 (C), 111.2 (CH), 114.6 (CH), 120.9 (CH), 122.9 (CH), 124.0 (CH), 128.4 (C), 132.0 (CH), 148.2 (C), 154.6 (C), 155.1 (C).

**HR-MS** (EI, 70 eV):  $m/z$   $[M]^{+}$  Calcd for  $[C_{16}H_{14}^{79}BrNO]^{+}$  315.0253; Found 315.0249.

**Ethyl 4-((benzofuran-2-ylmethyl)(methyl)amino)benzoate (4g)**. According to GP2, **2g** (0.12 g, 0.30 mmol) was dissolved in MeCN (5 mL). Potassium benzofuran-2-yltrifluoroborate **3a** (68 mg, 0.30 mmol) and TFA (23  $\mu$ L, 0.30 mmol) were added, and the solution was stirred for 2 h. After column chromatography **4g** (85 mg, 92%) was obtained as a slightly yellowish liquid.



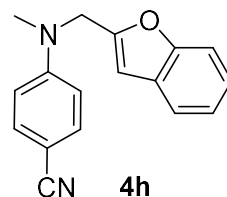
**$^1H$  NMR** (600 MHz,  $CDCl_3$ ):  $\delta$  1.38 (t,  $J$  = 7.1 Hz, 3 H,  $OCH_2CH_3$ ), 3.17 (s, 3 H, NMe), 4.34 (q,  $J$  = 7.1 Hz, 2 H,  $OCH_2CH_3$ ), 4.68 (s, 2 H, NCH<sub>2</sub>), 6.50–6.51 (m, 1 H), 6.79–6.81 (m, 2 H), 7.19–7.27 (m including residual  $CHCl_3$ , 2 H), 7.44–7.50 (m, 2 H), 7.94–7.96 (m, 2 H).

**$^{13}C$  NMR** (100.6 MHz,  $CDCl_3$ ):  $\delta$  14.6 (CH<sub>3</sub>,  $OCH_2CH_3$ ), 38.8 (CH<sub>3</sub>, NMe), 49.9 (CH<sub>2</sub>, NCH<sub>2</sub>), 60.3 (CH<sub>2</sub>,  $OCH_2CH_3$ ), 104.2 (CH), 111.2 (CH), 111.4 (CH), 118.6 (C), 120.9 (CH), 122.9 (CH), 124.1 (CH), 128.3 (C), 131.4 (CH), 152.3 (C), 154.1 (C), 155.1 (C), 166.9 (C).

**HR-MS** (EI, 70 eV):  $m/z$   $[M]^{+}$  Calcd for  $[C_{19}H_{19}NO_3]^{+}$  309.1359; Found 309.1359.

**Elemental Analysis**: Calcd: C 73.77, H 6.19, N 4.53. Found: C 73.52, H 6.24, N 4.53.

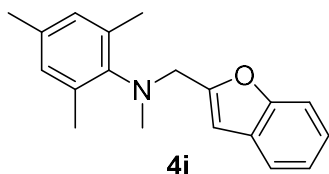
**4-((Benzofuran-2-ylmethyl)(methyl)amino)benzonitrile (4h)**. According to GP2, **2h** (32 mg, 0.092 mmol) was dissolved in MeCN (5 mL). Potassium benzofuran-2-yltrifluoroborate **3a** (21 mg, 0.094 mmol) and TFA (7  $\mu$ L, 0.09 mmol) were added, and the solution was stirred for 24 h. After column chromatography **4h** (19 mg, 79%) was obtained as a colorless liquid.



**$^1H$  NMR** (400 MHz,  $CDCl_3$ ):  $\delta$  3.17 (s, 3 H, NMe), 4.67 (s, 2 H, NCH<sub>2</sub>), 6.51 (br s, 1 H), 6.79–6.81 (m, 2 H), 7.19–7.28 (m, 2 H), 7.43–7.51 (m, 2 H).

<sup>13</sup>C NMR (100.6 MHz, CDCl<sub>3</sub>): δ 38.8 (CH<sub>3</sub>, NMe), 49.9 (CH<sub>2</sub>, NCH<sub>2</sub>), 98.8 (C, CN), 104.4 (CH), 111.3 (CH), 112.2 (CH), 120.5 (C), 121.0 (CH), 123.1 (CH), 124.4 (CH), 128.2 (C), 133.7 (CH), 151.6 (C), 153.5 (C), 155.1 (C).

***N*-(Benzofuran-2-ylmethyl)-*N*,2,4,6-tetramethylaniline (4i)**. According to GP2, **2i** (122 mg, 0.33 mmol) was dissolved in MeCN (5 mL). Potassium benzofuran-2-yltrifluoroborate **3a** (75 mg, 0.33 mmol) and TFA (26 μL, 0.34 mmol) were added, and the solution was stirred for 2 h. After column chromatography **4i** (78 mg, 85%) was obtained as a slightly yellowish liquid.

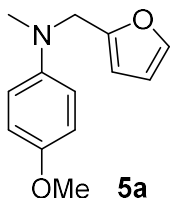


<sup>1</sup>H NMR (400 MHz, CDCl<sub>3</sub>): δ 2.30 (s, 3 H, 4-CH<sub>3</sub>), 2.36 (s, 6 H, 2,6-(CH<sub>3</sub>)<sub>2</sub>), 2.86 (s, 3 H, NMe), 4.31 (s, 2 H, NCH<sub>2</sub>), 6.65–6.66 (m, 1 H), 6.89 (br s, 2 H), 7.24–7.28 (m, 2 H), 7.48–7.50 (m, 1 H), 7.56–7.58 (m, 1 H).

<sup>13</sup>C NMR (100.6 MHz, CDCl<sub>3</sub>): δ 19.2 (CH<sub>3</sub>, 2,6-(CH<sub>3</sub>)<sub>2</sub>), 20.9 (CH<sub>3</sub>, 4-CH<sub>3</sub>), 40.2 (CH<sub>3</sub>, NMe), 53.3 (CH<sub>2</sub>, NCH<sub>2</sub>), 103.8 (CH), 111.2 (CH), 120.7 (CH), 122.6 (CH), 123.6 (CH), 128.8 (C), 129.7 (CH), 135.0 (C), 137.3 (C), 146.7 (C), 155.1 (C), 157.6 (C).

HR-MS (EI, 70 eV): *m/z* [M]<sup>+</sup> Calcd for [C<sub>19</sub>H<sub>21</sub>NO]<sup>+</sup> 279.1618; Found 279.1633.

***N*-(Furan-2-ylmethyl)-4-methoxy-*N*-methylaniline (5a)**. Following GP2, **2b** (210 mg, 0.594 mmol) and potassium 2-furanyltrifluoroborate **3b** (103 mg, 0.592 mmol) were dissolved in MeCN (5 mL). After the addition of TFA (46 μL, 0.60 mmol), the solution was stirred at room temperature for 1 h. After column chromatography **5a** (66 mg, 51%) was obtained as a colorless oil. Known compound.<sup>[S7]</sup>

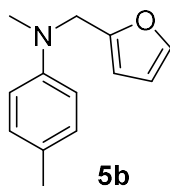


<sup>1</sup>H NMR (400 MHz, CDCl<sub>3</sub>): δ 2.91 (s, 3 H, NMe), 3.78 (s, 3 H, OMe), 4.38 (s, 2 H, NCH<sub>2</sub>), 6.13–6.14 (m, 1 H), 6.30–6.31 (m, 1 H), 6.85 (br s, 4 H), 7.36–7.37 (m, 1 H).

<sup>13</sup>C NMR (100.6 MHz, CDCl<sub>3</sub>): δ 39.1 (CH<sub>3</sub>, NMe), 51.3 (CH<sub>2</sub>, NCH<sub>2</sub>), 55.8 (CH<sub>3</sub>, OMe), 107.5 (CH), 110.2 (CH), 114.7 (CH), 115.6 (CH), 141.9 (CH), 144.4 (C), 152.4 (C), 152.6 (C).

HR-MS (EI, 70 eV): *m/z* [M]<sup>+</sup> Calcd for [C<sub>13</sub>H<sub>15</sub>NO<sub>2</sub>]<sup>+</sup> 217.1097; Found 217.1096.

***N*-(Furan-2-ylmethyl)-*N*,4-dimethylaniline (5b) from 3b**. According to GP2, **2a** (92 mg, 0.27 mmol) was dissolved in MeCN (5 mL). Potassium 2-furanyltrifluoroborate **3b** (48 mg, 0.28 mmol) and TFA (22 μL, 0.29 mmol) were added, and the mixture was stirred for 2 h. After column chromatography **5b** (52 mg, 96%) was obtained as a colorless liquid; *R<sub>f</sub>* = 0.85 (silica gel, acetone/isohexane = 1/10).



**<sup>1</sup>H NMR** (600 MHz, CDCl<sub>3</sub>): δ 2.31 (s, 3 H, 4-CH<sub>3</sub>), 2.98 (s, 3 H, NMe), 4.46 (s, 2 H, NCH<sub>2</sub>), 6.16–6.17 (m, 1 H), 6.32–6.33 (m, 1 H), 6.80–6.81 (m, 2 H), 7.09–7.10 (m, 2 H), 7.377–7.383 (m, 1 H).

**<sup>13</sup>C NMR** (150.6 MHz, CDCl<sub>3</sub>): δ 20.4 (CH<sub>3</sub>, 4-CH<sub>3</sub>), 38.6 (CH<sub>3</sub>, NMe), 50.3 (CH<sub>2</sub>, NCH<sub>2</sub>), 107.3 (CH), 110.2 (CH), 113.6 (CH), 126.6 (C), 129.7 (CH), 141.9 (CH), 147.5 (C), 152.6 (C).

**HR-MS** (EI, 70 eV): *m/z* [M]<sup>+</sup> Calcd for [C<sub>13</sub>H<sub>15</sub>NO]<sup>+</sup> 201.1148; Found 201.1151.

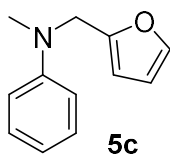
***N*-(Furan-2-ylmethyl)-*N*,4-dimethylaniline (5b) from 3b'**. According to GP2, **2a** (116 mg, 0.344 mmol) was dissolved in MeCN (10 mL). Potassium 3-furanyltrifluoroborate **3b'** (60 mg, 0.34 mmol) and TFA (30 μL, 0.39 mmol) were added, and the mixture was stirred for 24 h. After column chromatography **5b** (65 mg, 95 %) was obtained as a colorless liquid.

**<sup>1</sup>H NMR** (400 MHz, CDCl<sub>3</sub>): δ 2.31 (s, 3 H, 4-CH<sub>3</sub>), 2.99 (s, 3 H, NMe), 4.46 (s, 2 H, NCH<sub>2</sub>), 6.16–6.18 (m, 1 H), 6.32–6.34 (m, 1 H), 6.79–6.83 (m, 2 H), 7.08–7.12 (m, 2 H), 7.38–7.39 (m, 1 H).

**<sup>13</sup>C NMR** (100.6 MHz, CDCl<sub>3</sub>): δ 20.4 (CH<sub>3</sub>, 4-CH<sub>3</sub>), 38.6 (CH<sub>3</sub>, NMe), 50.4 (CH<sub>2</sub>, NCH<sub>2</sub>), 107.3 (CH), 110.2 (CH), 113.6 (CH), 126.6 (C), 129.7 (CH), 141.9 (CH), 147.5 (C), 152.6 (C).

**HR-MS** (EI, 70 eV): *m/z* [M]<sup>+</sup> Calcd for [C<sub>13</sub>H<sub>15</sub>NO]<sup>+</sup> 201.1148; Found 201.1142.

***N*-(Furan-2-ylmethyl)-*N*-methylaniline (5c)**. According to GP2, **2c** (180 mg, 0.557 mmol) and potassium 2-furanyltrifluoroborate **3b** (97 mg, 0.56 mmol) were dissolved in MeCN (5 mL). Then TFA (43 μL, 0.56 mmol) was added, and the reaction mixture was stirred for 2 h. After column chromatography **5c** (71 mg, 68%) was obtained as a colorless oil. Known compound, the NMR spectroscopic data are in accord with those given in ref.<sup>[S8]</sup>

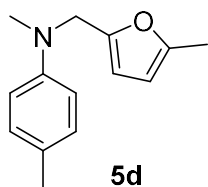


**<sup>1</sup>H NMR** (400 MHz, CDCl<sub>3</sub>): δ 2.97 (s, 3 H, NMe), 4.45 (s, 2 H, NCH<sub>2</sub>), 6.12–6.13 (m, 1 H), 6.27–6.29 (m, 1 H), 6.72–6.76 (m, 1 H), 6.81–6.83 (m, 2 H), 7.21–7.25 (m, 2 H), 7.33–7.34 (m, 1 H).

**<sup>13</sup>C NMR** (100.6 MHz, CDCl<sub>3</sub>): δ 38.4 (CH<sub>3</sub>, NMe), 50.0 (CH<sub>2</sub>, NCH<sub>2</sub>), 107.3 (CH), 110.3 (CH), 113.2 (CH), 117.2 (CH), 129.2 (CH), 141.9 (CH), 149.5 (C), 152.5 (C).

**HR-MS** (EI, 70 eV): *m/z* [M]<sup>+</sup> Calcd for [C<sub>12</sub>H<sub>13</sub>NO]<sup>+</sup> 187.0992; Found 187.0988.

***N*,4-Dimethyl-*N*-((5-methylfuran-2-yl)methyl)aniline (5d)**. According to GP2, **2a** (190 mg, 0.563 mmol) was dissolved in MeCN (5 mL). Potassium (5-methylfuran-2-yl)trifluoroborate **3c** (106 mg, 0.564 mmol) and TFA (45 μL, 0.59 mmol) were added, and the solution was stirred for 2 h. After column chromatography **5d** (115 mg, 95%) was obtained as a colorless liquid.

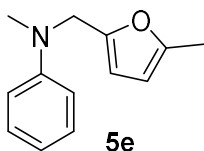


**<sup>1</sup>H NMR** (600 MHz, CDCl<sub>3</sub>): δ 2.27 (s, 6 H, 4-CH<sub>3</sub> and furyl 5-Me), 2.95 (s, 3 H, NMe), 4.36 (s, 2 H, NCH<sub>2</sub>), 5.86–5.87 (m, 1 H), 6.00 (m, 1 H), 6.76–6.78 (m, 2 H), 7.05–7.06 (m, 2 H).

$^{13}\text{C}$  NMR (150.6 MHz,  $\text{CDCl}_3$ ):  $\delta$  13.7 ( $\text{CH}_3$ , furyl 5-Me), 20.4 ( $\text{CH}_3$ , 4- $\text{CH}_3$ ), 38.6 ( $\text{CH}_3$ , NMe), 50.5 ( $\text{CH}_2$ ,  $\text{NCH}_2$ ), 106.1 (CH), 108.2 (CH), 113.7 (CH), 126.5 (C), 129.7 (CH), 147.7 (C), 150.6 (C), 151.5 (C).

**HR-MS** (EI, 70 eV):  $m/z$   $[\text{M}]^{*+}$  Calcd for  $[\text{C}_{14}\text{H}_{17}\text{NO}]^{*+}$  215.1305; Found 215.1312.

***N*-Methyl-*N*-((5-methylfuran-2-yl)methyl)aniline (5e)**. According to GP2, potassium trifluoro(5-methylfuran-2-yl)borate **3c** (112 mg, 0.596 mmol) and **2c** (193 mg, 0.597 mmol) were dissolved in MeCN (5 mL). After the addition of TFA (47  $\mu\text{L}$ , 0.61 mmol), the reaction mixture was stirred for 72 h. After column chromatography **5e** (44 mg, 37%) was obtained as a colorless liquid.

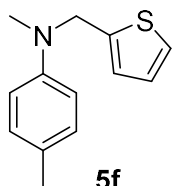


$^1\text{H}$  NMR (400 MHz,  $\text{CDCl}_3$ ):  $\delta$  2.30 (s, 3 H, furyl 5-Me), 3.02 (s, 3 H, NMe), 4.43 (s, 2 H,  $\text{NCH}_2$ ), 5.89–5.90 (m, 1 H), 6.04 (d,  $J = 3.0$  Hz, 1 H), 6.75–6.79 (m, 1 H), 6.85–6.89 (m, 2 H), 7.27–7.30 (m, 2 H).

$^{13}\text{C}$  NMR (100.6 MHz,  $\text{CDCl}_3$ ):  $\delta$  13.7 ( $\text{CH}_3$ , furyl 5-Me), 38.3 ( $\text{CH}_3$ , NMe), 50.1 ( $\text{CH}_2$ ,  $\text{NCH}_2$ ), 106.1 (CH), 108.1 (CH), 113.2 (CH), 117.1 (CH), 129.2 (CH), 149.6 (C), 150.5 (C), 151.5 (C).

**HR-MS** (EI, 70 eV):  $m/z$   $[\text{M}]^{*+}$  Calcd for  $[\text{C}_{13}\text{H}_{15}\text{NO}]^{*+}$  201.1148; Found 201.1144.

***N*,4-Dimethyl-*N*-(thiophen-2-ylmethyl)aniline (5f)**. According to GP2, **2a** (120 mg, 0.356 mmol) was dissolved in MeCN (10 mL). Potassium 2-thienyltrifluoroborate **3d** (83 mg, 0.44 mmol) and TFA (20  $\mu\text{L}$ , 0.26 mmol) were added, and the solution was stirred for 24 h. After column chromatography **5f** (65 mg, 84%) as a colorless liquid;  $R_f = 0.88$  (silica gel, acetone/isohexane = 1/10).

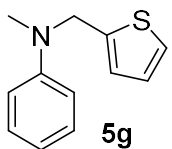


$^1\text{H}$  NMR (300 MHz,  $\text{CDCl}_3$ ):  $\delta$  2.27 (s, 3 H, 4- $\text{CH}_3$ ), 2.94 (s, 3 H, NMe), 4.63 (s, 2 H,  $\text{NCH}_2$ ), 6.74–6.79 (m, 2 H), 6.89–6.95 (m, 2 H), 7.05–7.08 (m, 2 H), 7.16–7.18 (m, 1 H).

$^{13}\text{C}$  NMR (75.5 MHz,  $\text{CDCl}_3$ ):  $\delta$  20.4 ( $\text{CH}_3$ , 4- $\text{CH}_3$ ), 38.5 ( $\text{CH}_3$ , NMe), 52.6 ( $\text{CH}_2$ ,  $\text{NCH}_2$ ), 113.8 (CH), 124.4 (CH), 125.0 (CH), 126.8 (CH), 126.8 (C), 129.8 (CH), 142.4 (C), 147.4 (C).

**HR-MS** (EI, 70 eV):  $m/z$   $[\text{M}]^{*+}$  Calcd for  $[\text{C}_{13}\text{H}_{15}\text{NS}]^{*+}$  217.0920; Found 217.0915.

***N*-Methyl-*N*-(thiophen-2-ylmethyl)aniline (5g)**. Following GP2, **2c** (167 mg, 0.516 mmol) and potassium 2-thienyltrifluoroborate **3d** (99 mg, 0.52 mmol) were dissolved in MeCN (5 mL). Then, TFA (40  $\mu\text{L}$ , 0.52 mmol) was added dropwise. The reaction proceeded smoothly within 24 h to give **5g** (95 mg, 91%) as a light yellowish oil.  $^{13}\text{C}$  NMR data are in accord with resonances reported for the trideuterated analogue *N*-methyl-*N*-(thiophene-2-yl-5- $d_1$ -methyl- $d_2$ )aniline.<sup>[S9]</sup>

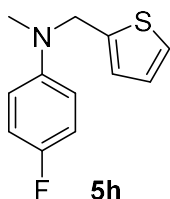


**<sup>1</sup>H NMR** (400 MHz, CDCl<sub>3</sub>): δ 3.04 (s, 3 H, NMe), 4.73 (s, 2 H, NCH<sub>2</sub>), 6.82–6.85 (m, 1 H), 6.90 (d, *J* = 8.4 Hz, 2 H), 6.98–7.01 (m, 2 H), 7.22–7.23 (m, 1 H), 7.30–7.34 (m, 2 H).

**<sup>13</sup>C NMR** (100.6 MHz, CDCl<sub>3</sub>): δ 38.3 (CH<sub>3</sub>, NMe), 52.2 (CH<sub>2</sub>, NCH<sub>2</sub>), 113.3 (CH), 117.4 (CH), 124.4 (CH), 125.0 (CH), 126.8 (CH), 129.3 (CH), 142.2 (C), 149.3 (C).

**HR-MS** (EI, 70 eV): *m/z* [M]<sup>+</sup> Calcd for [C<sub>12</sub>H<sub>13</sub>NS]<sup>+</sup> 203.0763; Found 203.0765.

**4-Fluoro-*N*-methyl-*N*-(thiophen-2-ylmethyl)aniline (5h)**. According to GP2, **2d** (225 mg, 0.659 mmol) was dissolved in MeCN (5 mL). Potassium 2-thienyltrifluoroborate **3d** (125 mg, 0.658 mmol) and TFA (52 μL, 0.68 mmol) were added, and the mixture was stirred for 2 h. After column chromatography **5h** (136 mg, 93%) was obtained as a colorless liquid.



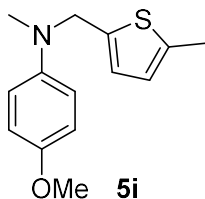
**<sup>1</sup>H NMR** (400 MHz, CDCl<sub>3</sub>): δ 2.93 (s, 3 H, NMe), 4.61 (s, 2 H, NCH<sub>2</sub>), 6.75–6.78 (m, 2 H), 6.89–6.90 (m, 1 H), 6.93–6.97 (m, 3 H), 7.17–7.19 (m, 1 H).

**<sup>13</sup>C NMR** (100.6 MHz, CDCl<sub>3</sub>): δ 38.9 (CH<sub>3</sub>, NMe), 53.1 (CH<sub>2</sub>, NCH<sub>2</sub>), 114.9 (CH, d, *J*<sub>C,F</sub> = 7.4 Hz), 115.7 (CH, d, *J*<sub>C,F</sub> = 22.0 Hz), 124.5 (CH), 125.2 (CH), 126.8 (CH), 141.9 (C), 146.1 (C, d, *J*<sub>C,F</sub> = 2.0 Hz), 156.1 (C, d, <sup>1</sup>*J*<sub>C,F</sub> = 236.2 Hz).

**<sup>19</sup>F NMR** (376 MHz, CDCl<sub>3</sub>): δ -127.93 (tt, *J* = 8.5, 4.4 Hz).

**HR-MS** (EI, 70 eV): *m/z* [M]<sup>+</sup> Calcd for [C<sub>12</sub>H<sub>12</sub>FNS]<sup>+</sup> 221.0669; Found 221.0659.

**4-Methoxy-*N*-methyl-*N*-((5-methylthiophen-2-yl)methyl)aniline (5i)**. According to GP2, **2b** (199 mg, 0.563 mmol) was dissolved in MeCN (5 mL). Potassium (5-methyl-2-thienyl)trifluoroborate **3e** (115 mg, 0.564 mmol) and TFA (44 μL, 0.57 mmol) were added, and the mixture was stirred for 2 h. After column chromatography **5i** (83 mg, 60%) was obtained as a colorless liquid.

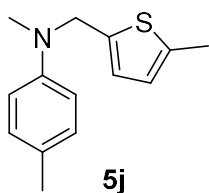


**<sup>1</sup>H NMR** (400 MHz, CDCl<sub>3</sub>): δ 2.44 (s, 3 H, 5-Me), 2.90 (s, 3 H, NMe), 3.79 (s, 3 H, OMe), 4.52 (s, 2 H, NCH<sub>2</sub>), 6.59–6.60 (m, 1 H), 6.70 (d, *J* = 3.3 Hz, 1 H), 6.83–6.89 (m, 4 H).

**<sup>13</sup>C NMR** (100.6 MHz, CDCl<sub>3</sub>): δ 15.4 (CH<sub>3</sub>), 38.8 (CH<sub>3</sub>, NMe), 53.6 (CH<sub>2</sub>, NCH<sub>2</sub>), 55.8 (CH<sub>3</sub>, OMe), 114.7 (CH), 115.7 (CH), 124.6 (CH), 125.2 (CH), 138.9 (C), 139.6 (C), 144.3 (C), 152.4 (C).

**HR-MS** (EI, 70 eV): *m/z* [M]<sup>+</sup> Calcd for [C<sub>14</sub>H<sub>17</sub>NOS]<sup>+</sup> 247.1025; Found 247.1024.

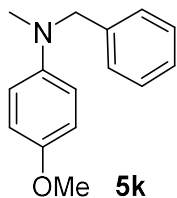
***N*,4-Dimethyl-*N*-((5-methylthiophen-2-yl)methyl)aniline (5j).** According to GP2, **2a** (240 mg, 0.711 mmol) was dissolved in MeCN (10 mL). Potassium (5-methyl-2-thienyl)trifluoroborate **3e** (175 mg, 0.858 mmol) and TFA (20  $\mu$ L, 0.26 mmol) were added, and the mixture was stirred for 24 h. After column chromatography **5j** (102 mg, 62%) was obtained as a colorless liquid;  $R_f$  = 0.87 (silica gel, acetone/isohexane = 1/10).



**$^1\text{H NMR}$**  (300 MHz,  $\text{CDCl}_3$ ):  $\delta$  2.25 (s, 3 H, 4- $\text{CH}_3$ ), 2.41 (s, 3 H), 2.91 (s, 3 H, NMe), 4.54 (s, 2 H, N $\text{CH}_2$ ), 6.55–6.56 (m, 1 H), 6.66–6.67 (m, 1 H), 6.73–6.76 (m, 2 H), 7.03–7.06 (m, 2 H).

**$^{13}\text{C NMR}$**  (75.5 MHz,  $\text{CDCl}_3$ ):  $\delta$  15.5 ( $\text{CH}_3$ ), 20.4 ( $\text{CH}_3$ , 4- $\text{CH}_3$ ), 38.4 ( $\text{CH}_3$ , NMe), 52.7 ( $\text{CH}_2$ , N $\text{CH}_2$ ), 113.7 (CH), 124.7 (CH), 125.0 (CH), 126.7 (C), 129.8 (CH), 138.9 (C), 139.8 (C), 147.4 (C).

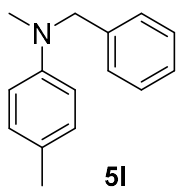
***N*-Benzyl-4-methoxy-*N*-methylaniline (5k).** According to GP2, **2b** (161 mg, 0.456 mmol) was dissolved in MeCN (10 mL). Potassium phenyltrifluoroborate **3f** (84 mg, 0.46 mmol) and TFA (35  $\mu$ L, 0.46 mmol) were added, and the mixture was stirred for 24 h. After column chromatography **5k** (92 mg, 89%) was obtained as a colorless liquid. Known compound, the NMR spectroscopic data are in accord with those given in ref.<sup>[S10]</sup>



**$^1\text{H NMR}$**  (400 MHz,  $\text{CDCl}_3$ ):  $\delta$  2.88 (s, 3 H, NMe), 3.71 (s, 3 H, OMe), 4.39 (s, 2 H, N $\text{CH}_2$ ), 6.69–6.82 (m, 4 H), 7.21–7.30 (m, 5 H).

**$^{13}\text{C NMR}$**  (100.6 MHz,  $\text{CDCl}_3$ ):  $\delta$  39.1 ( $\text{CH}_3$ , NMe), 55.8 ( $\text{CH}_3$ , OMe), 58.1 ( $\text{CH}_2$ , N $\text{CH}_2$ ), 114.6 (CH), 114.8 (CH), 126.9 (CH), 127.2 (CH), 128.5 (CH), 139.3 (C), 144.9 (C), 151.9 (C).

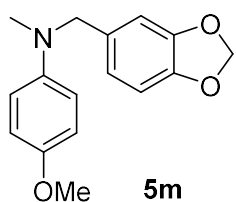
***N*-Benzyl-*N*,4-dimethylaniline (5l).** According to GP2, **2a** (116 mg, 0.344 mmol) was dissolved in MeCN (5 mL). Potassium phenyltrifluoroborate **3f** (64 mg, 0.35 mmol) and TFA (27  $\mu$ L, 0.35 mmol) were added, and the mixture was stirred for 24 h. After column chromatography **5l** (57 mg, 78%) was obtained as a colorless liquid,  $R_f$  = 0.92 (silica gel, acetone/isohexane = 1/10). Known compound, the NMR spectroscopic data are in accord with those given in ref.<sup>[S11]</sup>



**$^1\text{H NMR}$**  (400 MHz,  $\text{CDCl}_3$ ):  $\delta$  2.23 (s, 3 H, 4- $\text{CH}_3$ ), 2.94 (s, 3 H, NMe), 4.46 (s, 2 H, N $\text{CH}_2$ ), 6.64–6.68 (m, 2 H), 6.99–7.03 (m, 2 H), 7.19–7.22 (m, 3 H), 7.26–7.30 (m, 2 H).

**$^{13}\text{C NMR}$**  (100.6 MHz,  $\text{CDCl}_3$ ):  $\delta$  20.4 ( $\text{CH}_3$ , 4- $\text{CH}_3$ ), 38.8 ( $\text{CH}_3$ , NMe), 57.2 ( $\text{CH}_2$ , N $\text{CH}_2$ ), 112.9 (CH), 125.9 (C), 126.9 (CH), 127.0 (CH), 128.6 (CH), 129.8 (CH), 139.4 (C), 148.0 (C).

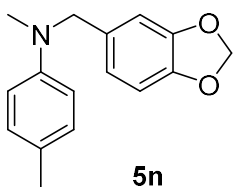
***N*-(Benzo[*d*][1,3]dioxol-5-ylmethyl)-4-methoxy-*N*-methylaniline (5m).** According to GP2, **2b** (150 mg, 0.424 mmol) was dissolved in MeCN (10 mL). Potassium 3,4-(methylenedioxy)phenyltrifluoroborate **3g** (99 mg, 0.43 mmol) and TFA (33  $\mu$ L, 0.43 mmol) were added, and the mixture was stirred for 48 h. After column chromatography **5m** (103 mg, 90%) was obtained as a colorless liquid.



<sup>1</sup>H NMR (400 MHz, CDCl<sub>3</sub>):  $\delta$  2.91 (s, 3 H, NMe), 3.78 (s, 3 H, OMe), 4.34 (s, 2 H, NCH<sub>2</sub>), 5.94 (s, 2 H, OCH<sub>2</sub>O), 6.72–6.87 (m, 7 H).

<sup>13</sup>C NMR (100.6 MHz, CDCl<sub>3</sub>):  $\delta$  39.1 (CH<sub>3</sub>, NMe), 55.8 (CH<sub>3</sub>, OMe), 58.0 (CH<sub>2</sub>, NCH<sub>2</sub>), 101.0 (CH<sub>2</sub>, OCH<sub>2</sub>O), 107.8 (CH), 108.2 (CH), 114.8 (CH), 114.9 (CH), 120.3 (CH), 133.2 (C), 144.8 (C), 146.6 (C), 147.9 (C), 152.0 (C).

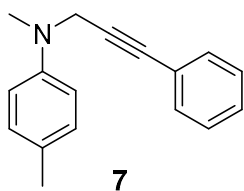
***N*-(Benzo[*d*][1,3]dioxol-5-ylmethyl)-*N*,4-dimethylaniline (5n).** According to GP2, **2a** (231 mg, 0.675 mmol) was dissolved in MeCN (10 mL). Potassium 3,4-(methylenedioxy)phenyltrifluoroborate (158 mg, 0.693 mmol) and TFA (54  $\mu$ L, 0.71 mmol) were added, and the mixture was stirred for 24 h. After column chromatography **5n** (161 mg, 93%) was obtained as a colorless liquid, *R*<sub>f</sub> = 0.90 (silica gel, acetone/isohexane = 1/10).



<sup>1</sup>H NMR (400 MHz, CDCl<sub>3</sub>):  $\delta$  2.29 (s, 3 H, 4-CH<sub>3</sub>), 2.97 (s, 3 H, NMe), 4.41 (s, 2 H, NCH<sub>2</sub>), 5.94 (s, 2 H, OCH<sub>2</sub>O), 6.71–6.79 (m, 5 H), 7.06–7.08 (m, 2 H).

<sup>13</sup>C NMR (100.6 MHz, CDCl<sub>3</sub>):  $\delta$  20.4 (CH<sub>3</sub>, 4-CH<sub>3</sub>), 38.6 (CH<sub>3</sub>, NMe), 57.0 (CH<sub>2</sub>, NCH<sub>2</sub>), 101.0 (OCH<sub>2</sub>O), 107.6 (CH), 108.3 (CH), 113.0 (CH), 120.0 (CH), 126.0 (C), 129.8 (CH), 133.3 (C), 146.6 (C), 147.9 (C), 148.0 (C).

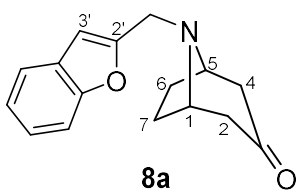
***N*,4-Dimethyl-*N*-(3-phenylprop-2-yn-1-yl)aniline (7).** According to GP2, **2a** (214 mg, 0.634 mmol) was dissolved in MeCN (10 mL). Potassium (phenylethynyl)trifluoroborate **6** (137 mg, 0.656 mmol) and TFA (50  $\mu$ L, 0.65 mmol) were added, and the mixture was stirred for 24 h. After column chromatography **7** (115 mg, 78%) was obtained as a colorless liquid. Known compound, the NMR spectroscopic data are in accord with those given in ref.<sup>[S12]</sup>



<sup>1</sup>H NMR (300 MHz, CDCl<sub>3</sub>):  $\delta$  2.34 (s, 3 H, 4-Me), 3.05 (s, 3 H, NMe), 4.27 (s, 2 H, NCH<sub>2</sub>), 6.89–6.92 (m, 2 H), 7.13–7.16 (m, 2 H), 7.30–7.32 (m, 3 H), 7.42–7.45 (m, 2 H).

<sup>13</sup>C NMR (75.5 MHz, CDCl<sub>3</sub>):  $\delta$  20.5 (CH<sub>3</sub>), 39.1 (CH<sub>3</sub>, NMe), 43.8 (CH<sub>2</sub>, NCH<sub>2</sub>), 84.4 (C), 85.2 (C), 115.1 (CH), 123.2 (C), 127.8 (C), 128.1 (CH), 128.3 (CH), 129.7 (CH), 131.8 (CH), 147.4 (C).

**8-(Benzofuran-2-ylmethyl)-8-azabicyclo[3.2.1]octan-3-one (8a).** According to GP2, **2j** (48 mg, 0.14 mmol) was dissolved in MeCN (10 mL). Potassium benzofuran-2-yltrifluoroborate **3a** (32 mg, 0.14 mmol) and TFA (11  $\mu$ L, 0.14 mmol) were added, and the mixture was stirred for 24 h. After column chromatography **8a** (33 mg, 92%) was obtained as a colorless liquid.

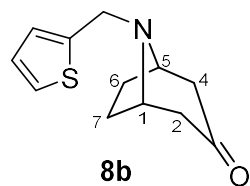


**$^1\text{H NMR}$**  (400 MHz,  $\text{CDCl}_3$ ):  $\delta$  1.64–1.70 (m, 2 H, 6-H and 7-H), 2.13–2.17 (m, 2 H, 6-H and 7-H), 2.25 (br d,  $^2J = 16$  Hz, 2 H, 2-H and 4-H), 2.75 (dd,  $^2J = 16.2$  Hz,  $^3J = 4.4$  Hz, 2 H, 2-H and 4-H), 3.62 (br s, 2 H, 1-H and 5-H), 3.89 (d,  $J = 0.9$  Hz, 2 H,  $\text{NCH}_2$ ), 6.66 (q,  $J = 0.9$  Hz, 1 H, 3'-H), 7.20–7.29 (m, 2 H), 7.48–7.55 (m, 2 H).

**$^{13}\text{C NMR}$**  (100.6 MHz,  $\text{CDCl}_3$ ):  $\delta$  27.8 ( $\text{CH}_2$ , C-6 and C-7), 48.3 ( $\text{CH}_2$ , C-2 and C-4), 48.7 ( $\text{CH}_2$ ,  $\text{NCH}_2$ ), 59.1 (CH, C-1 and C-5), 104.9 (CH, C-3'), 111.4 (CH), 120.9 (CH), 122.9 (CH), 124.2 (CH), 128.4 (C), 155.2 (C), 155.7 (C), 209.7 (C,  $\text{C}=\text{O}$ ).

**HR-MS** (EI, 70 eV):  $m/z$   $[\text{M}]^{+\cdot}$  Calcd for  $[\text{C}_{16}\text{H}_{17}\text{NO}_2]^{+\cdot}$  255.1254; Found 255.1252.

**8-(Thiophen-2-ylmethyl)-8-azabicyclo[3.2.1]octan-3-one (8b).** According to GP2, **2j** (183 mg, 0.536 mmol) was dissolved in MeCN (5 mL). Potassium 2-thienyltrifluoroborate **3d** (102 mg, 0.542 mmol) and TFA (42  $\mu$ L, 0.55 mmol) were added, and the reaction mixture was stirred for 24 h. After purification **8b** (107 mg, 90%) was obtained as a light yellow liquid.<sup>[S13]</sup>



**$^1\text{H NMR}$**  (400 MHz,  $\text{CDCl}_3$ ):  $\delta$  1.61–1.67 (m, 2 H, 6-H and 7-H), 2.08–2.12 (m, 2 H, 6-H and 7-H), 2.20–2.25 (m, 2 H, 2-H and 4-H), 2.70 (dd,  $^2J = 16$  Hz,  $^3J = 4.6$  Hz, 2 H, 2-H and 4-H), 3.56 (br s, 2 H, 1-H and 5-H), 3.92 (br s, 2 H,  $\text{NCH}_2$ ), 6.94–6.97 (m, 2 H), 7.24–7.26 (m, 1 H).

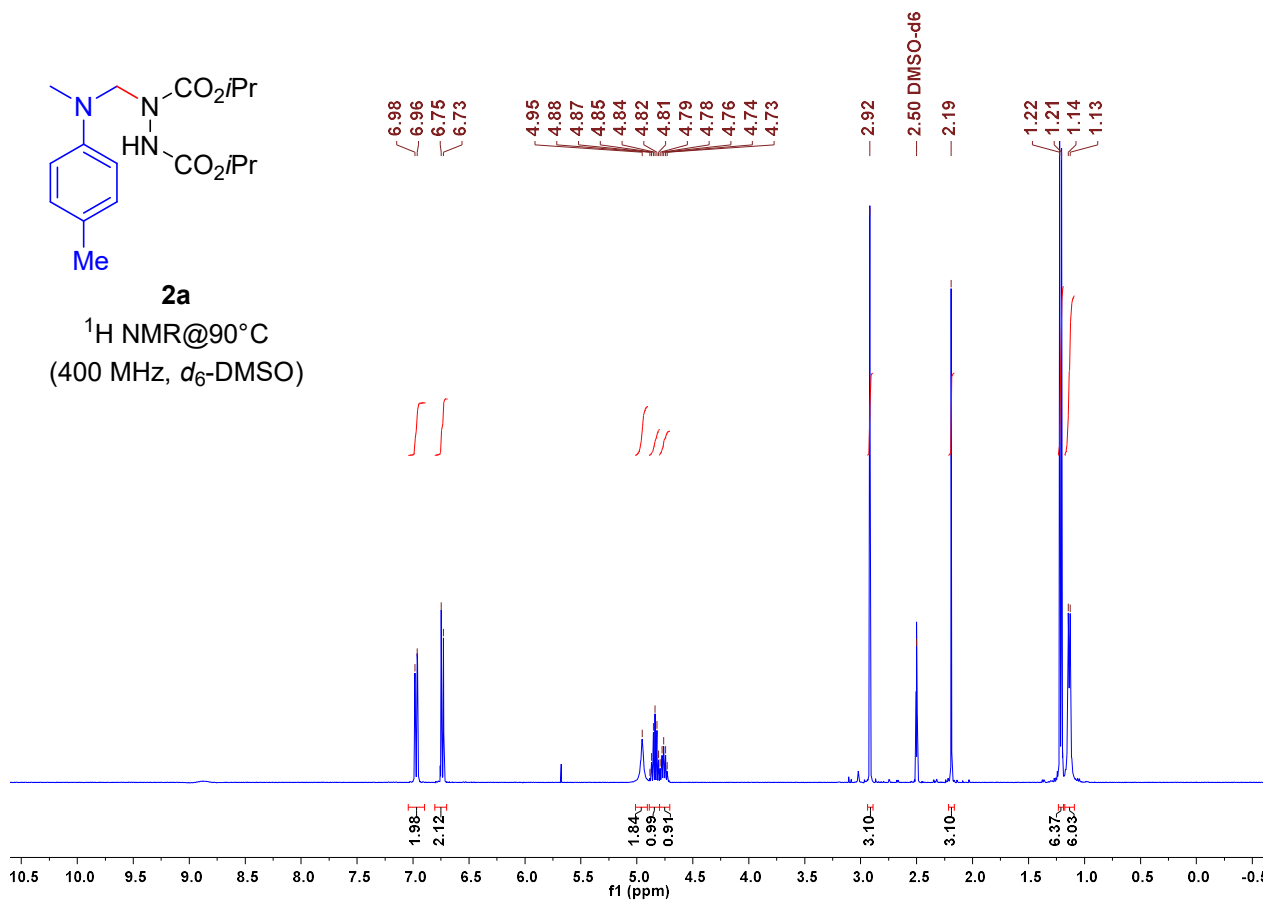
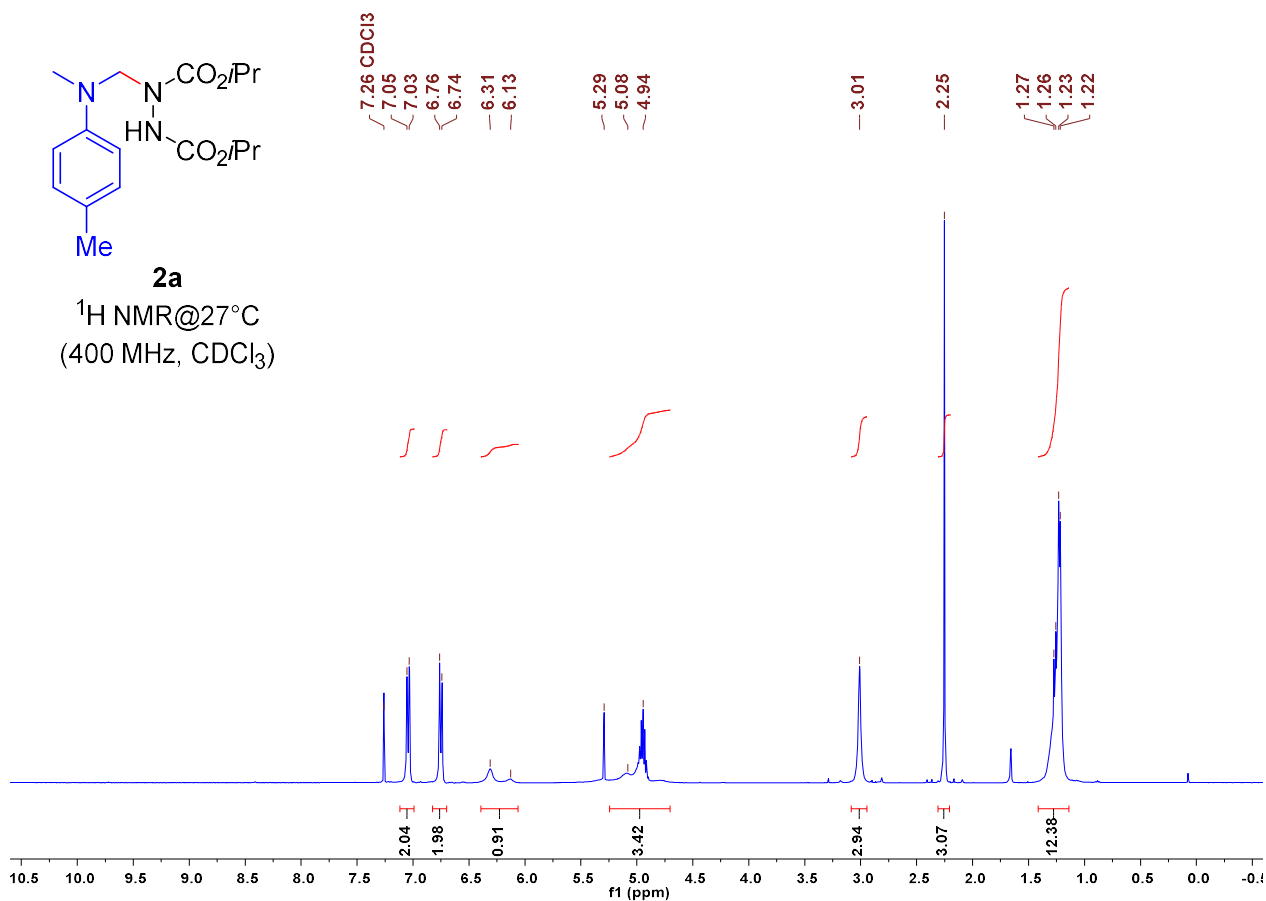
**$^{13}\text{C NMR}$**  (100.6 MHz,  $\text{CDCl}_3$ ):  $\delta$  27.8 ( $\text{CH}_2$ , C-6 and C-7), 48.7 ( $\text{CH}_2$ , C-2 and C-4), 50.7 ( $\text{CH}_2$ ,  $\text{NCH}_2$ ), 58.8 (CH, C-1 and C-5), 124.9 (CH), 125.0 (CH), 126.6 (CH), 144.0 (C), 210.3 (C,  $\text{C}=\text{O}$ ).

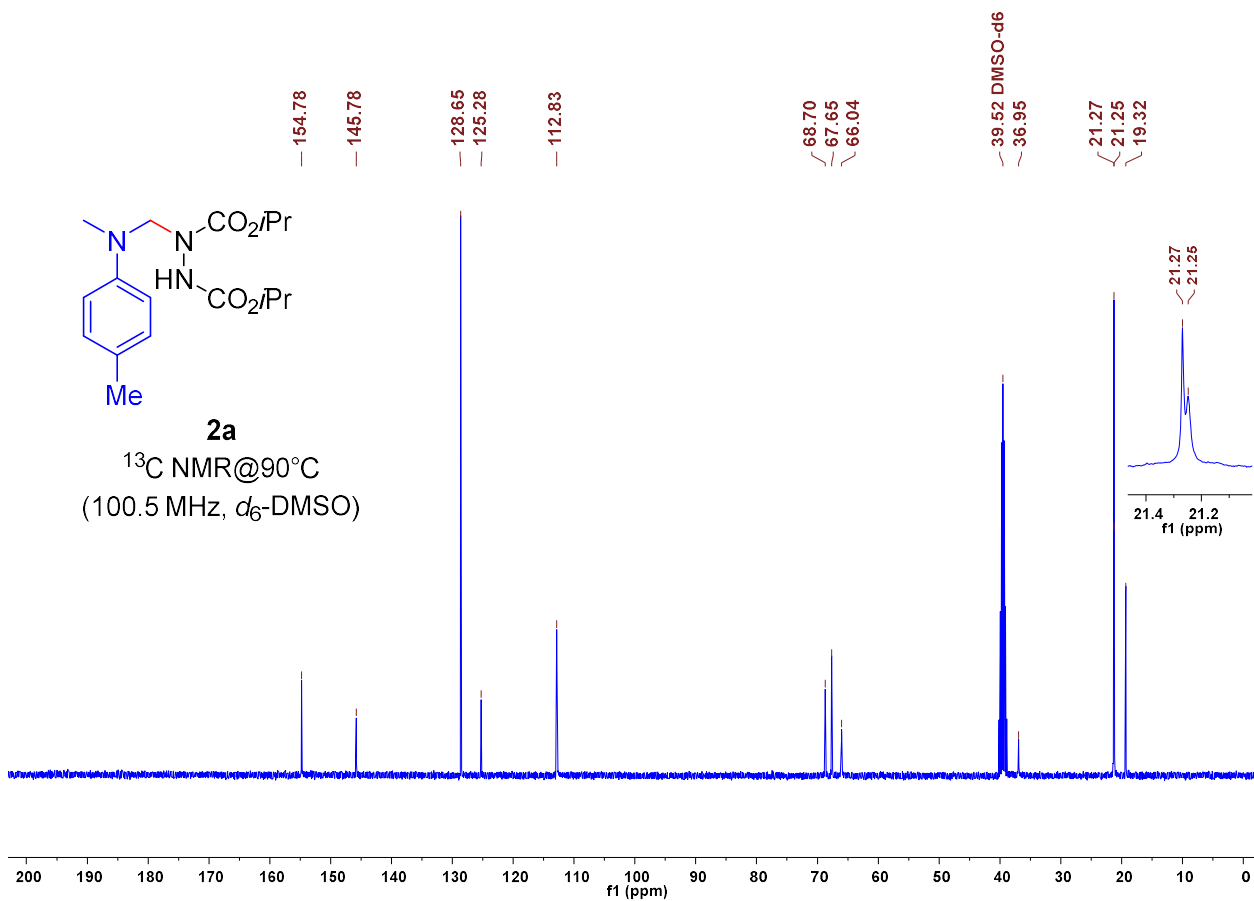
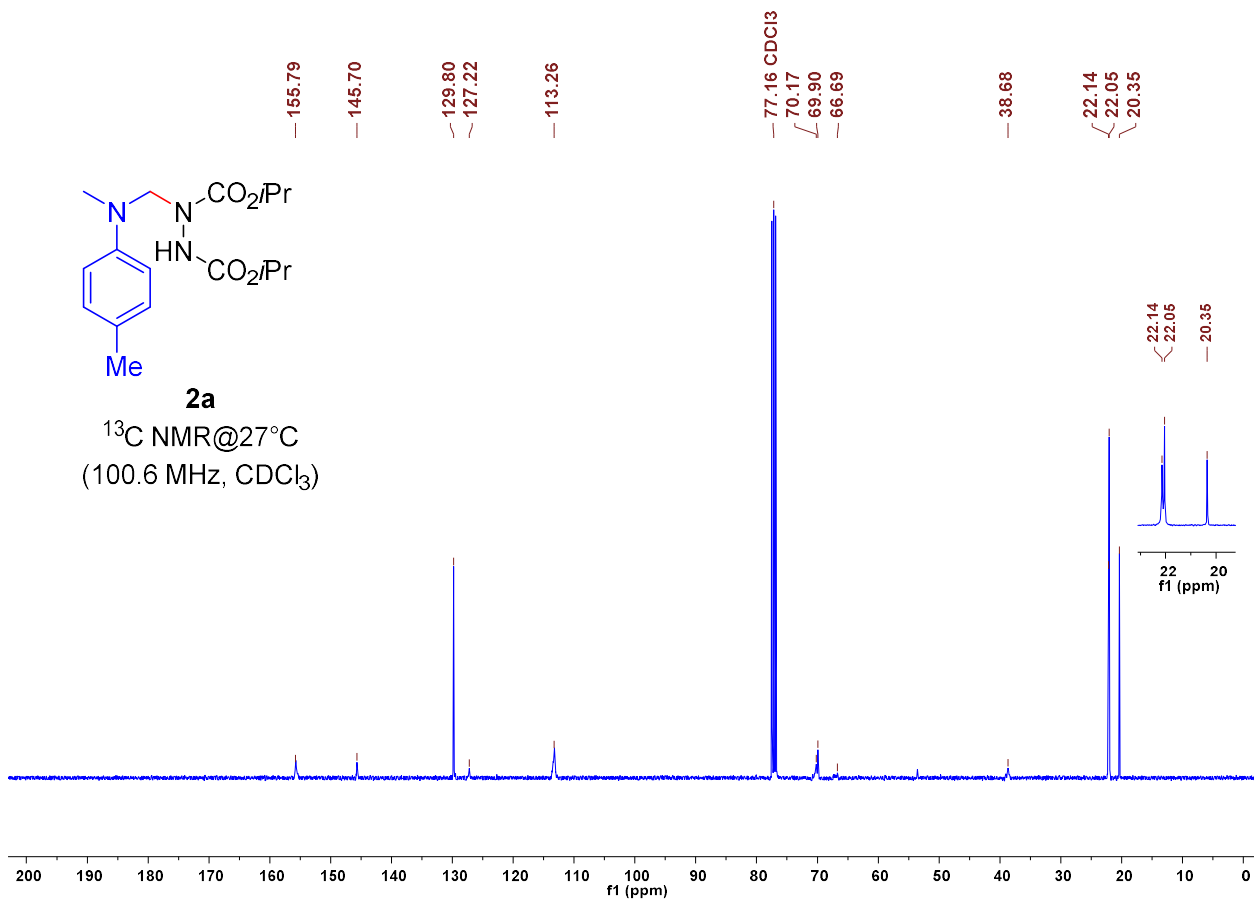
**HR-MS** (EI, 70 eV):  $m/z$   $[\text{M}]^{+\cdot}$  Calcd for  $[\text{C}_{12}\text{H}_{15}\text{NOS}]^{+\cdot}$  221.0869; Found 221.0869.

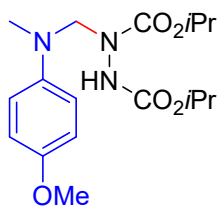
#### 4. References

- [S1] G. R. Fulmer, A. J. M. Miller, N. H. Sherden, H. E. Gottlieb, A. Nudelman, B. M. Stoltz, J. E. Bercaw, K. I. Goldberg, *Organometallics* **2010**, *29*, 2176–2179.
- [S2] (a) G. Berionni, V. Morozova, M. Heininger, P. Mayer, P. Knochel, H. Mayr, *J. Am. Chem. Soc.* **2013**, *135*, 6317–6324; (b) G. Berionni, private communication, 2016.
- [S3] J. A. Hodges, R. T. Raines, *Org. Lett.* **2006**, *8*, 4695–4697.
- [S4] R. A. da Silva, I. H. S. Estevam, L. W. Bieber, *Tetrahedron Lett.* **2007**, *48*, 7680–7682.
- [S5] X. Jiang, C. Wang, Y. Wei, D. Xue, Z. Liu, J. Xiao, *Chem. Eur. J.* **2014**, *20*, 58–63.
- [S6] G. W. Kabalka, L.-L. Zhou, L. Wang, R. M. Pagni, *Tetrahedron* **2006**, *62*, 857–867.
- [S7] D. Bilović, V. Hahn, *Croat. Chem. Acta* **1967**, *39*, 189–197.
- [S8] a) O. S. Nayal, V. Bhatt, S. Sharma, N. Kumar, *J. Org. Chem.* **2015**, *80*, 5912–5918; b) O. S. Nayal, M. S. Thakur, V. Bhatt, M. Kumar, N. Kumar, B. Singh, U. Sharma, *Chem. Commun.* **2016**, *52*, 9648–9651.
- [S9] a) Y. Hu, L. Liang, W.-t. Wei, X. Sun, X.-j. Zhang, M. Yan, *Tetrahedron* **2015**, *71*, 1425–1430; b) See also: A. Giumanini, G. Lercker, *Gazz. Chim. Ital.* **1974**, *104*, 415–424.
- [S10] D. Maiti, B. P. Fors, J. L. Henderson, Y. Nakamura, S. L. Buchwald, *Chem. Sci.* **2011**, *2*, 57–68.
- [S11] R. Nishio, M. Sugiura, S. Kobayashi, *Chem. Asian J.* **2007**, *2*, 983–995.
- [S12] Z. Li, C. J. Li, *J. Am. Chem. Soc.* **2004**, *126*, 11810–11811.
- [S13] Previously, the hydrochloride **8b**·HCl was characterized: N. Willand, B. Folléas, C. Boutillon, L. Verbraeken, J.-C. Gesquière, A. Tartar, B. Deprez, *Tetrahedron Lett.* **2007**, *48*, 5007–5011.

## **5. Copies of NMR Spectra of Products 2, 4, 5, 7, and 8**

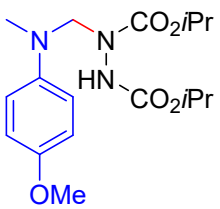
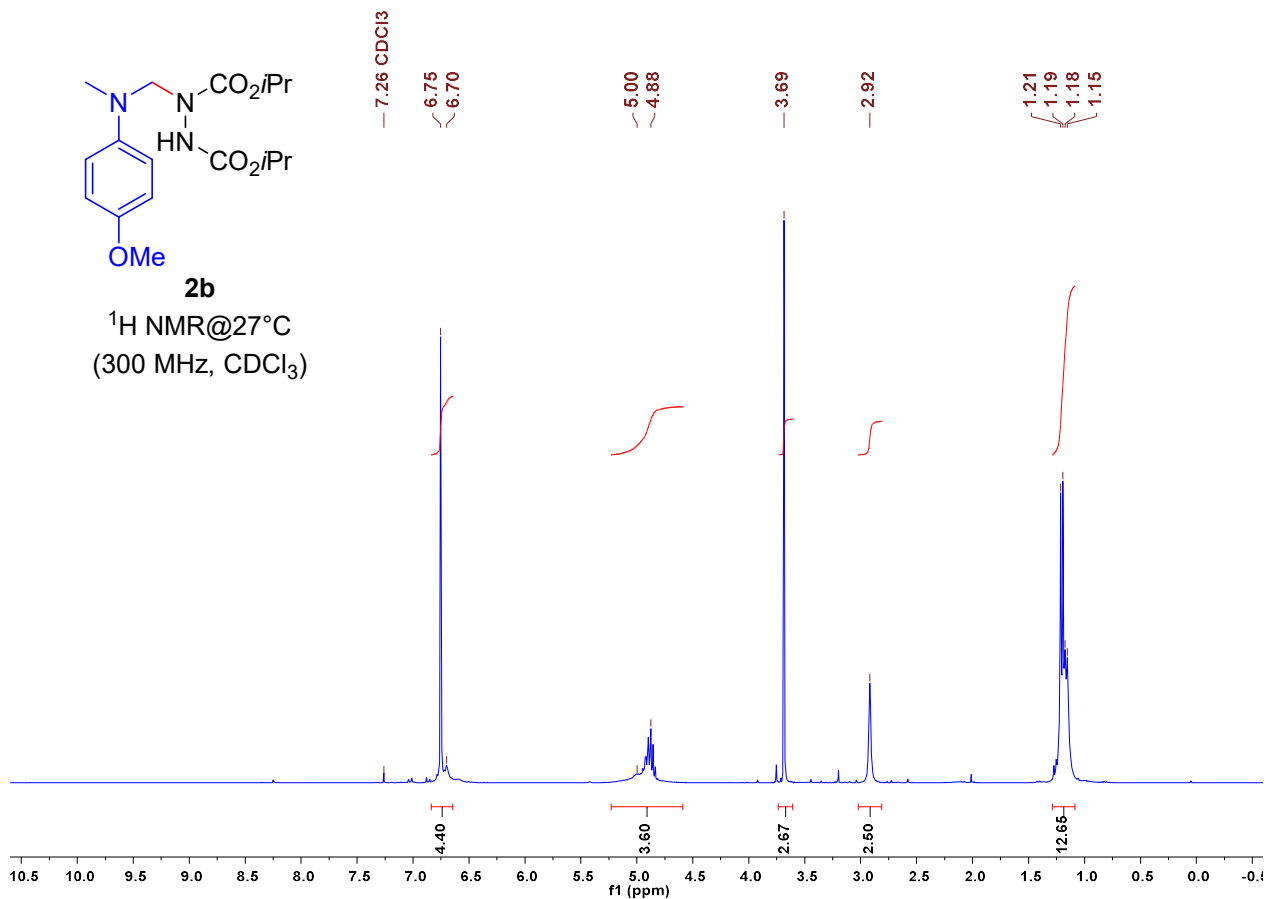






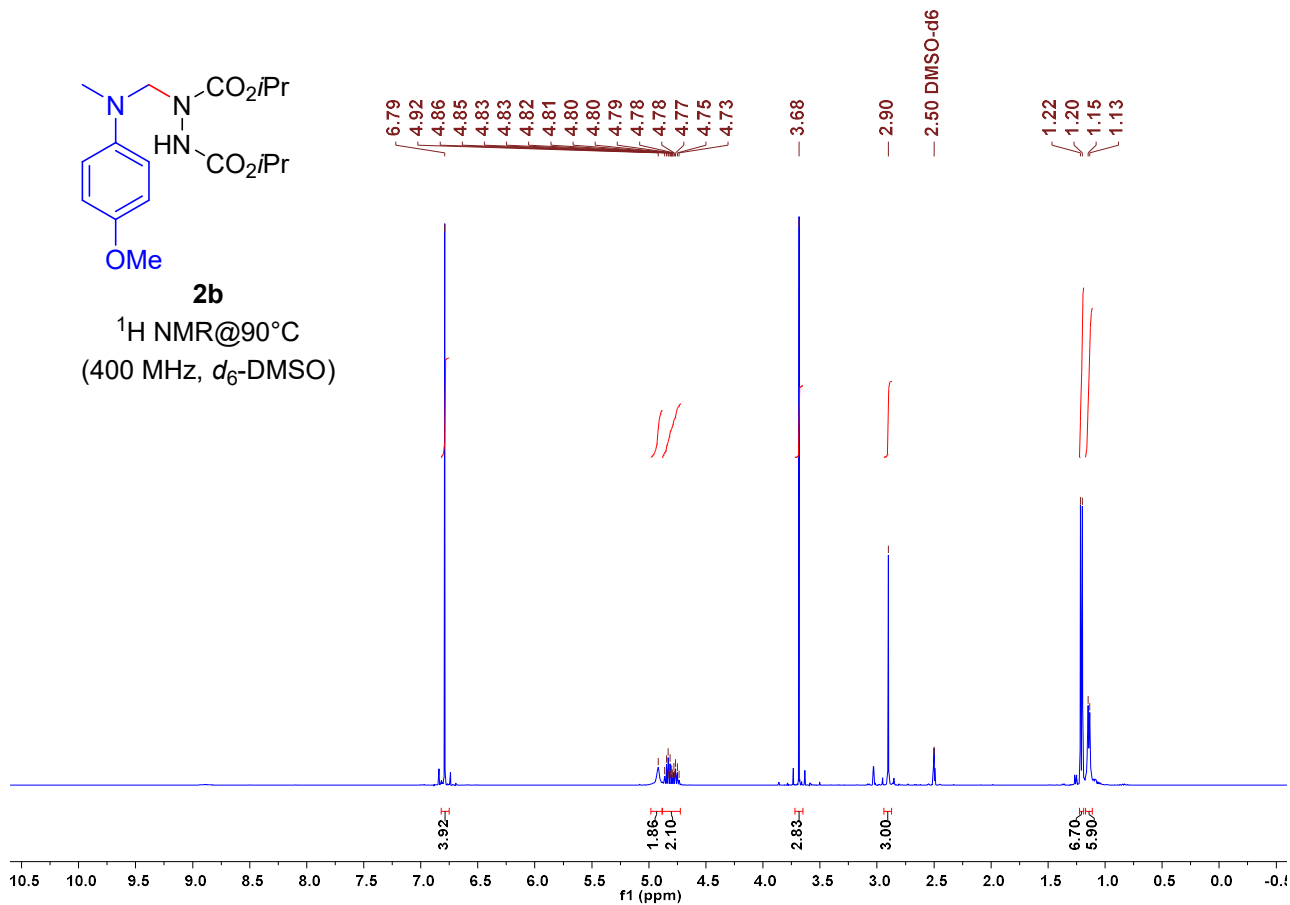
**2b**

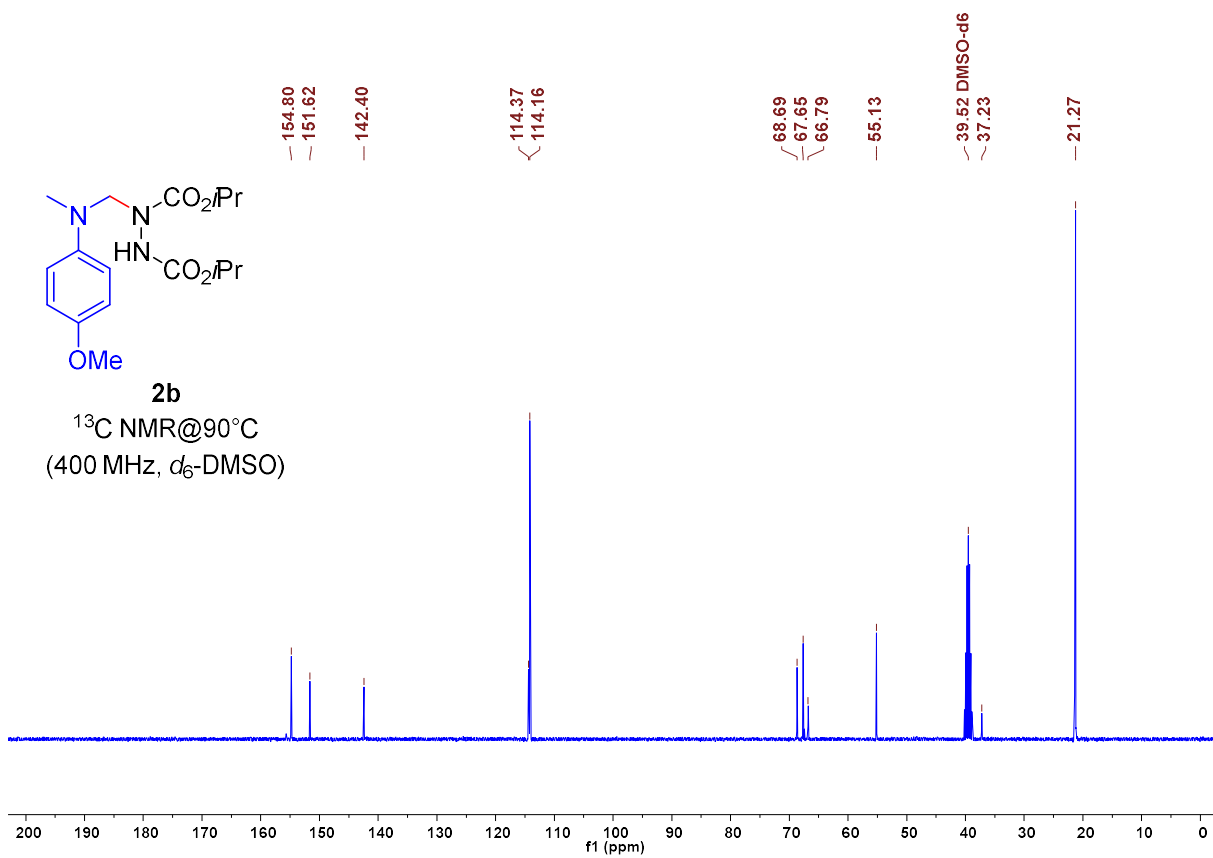
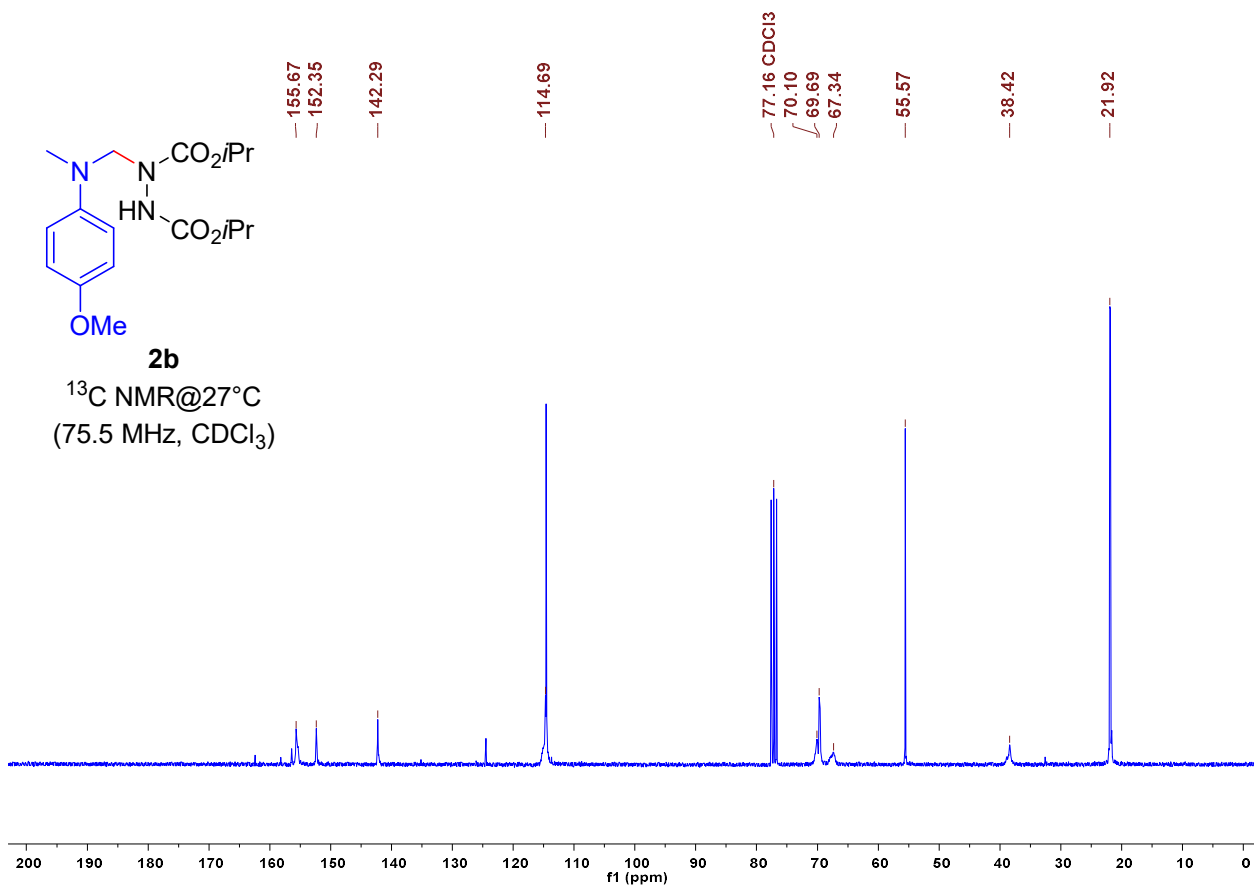
$^1\text{H NMR}$  @27°C  
(300 MHz,  $\text{CDCl}_3$ )

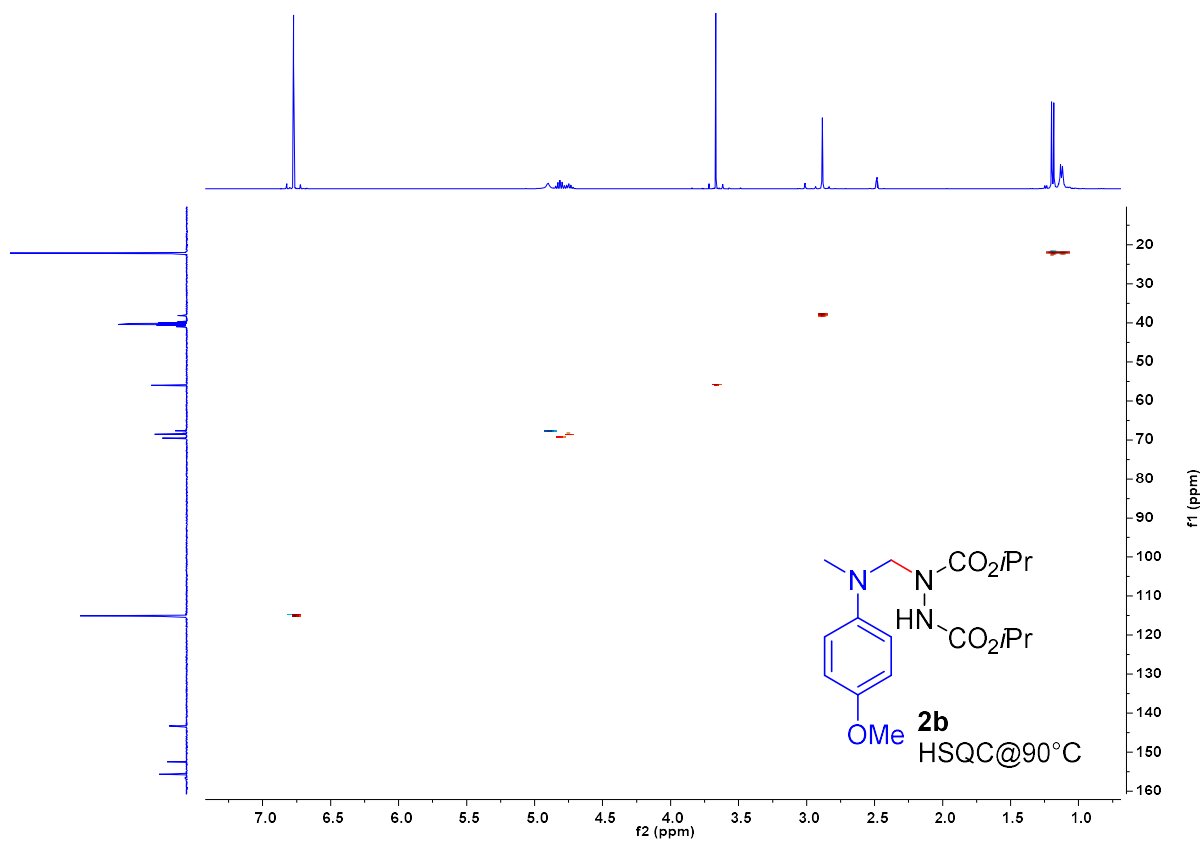


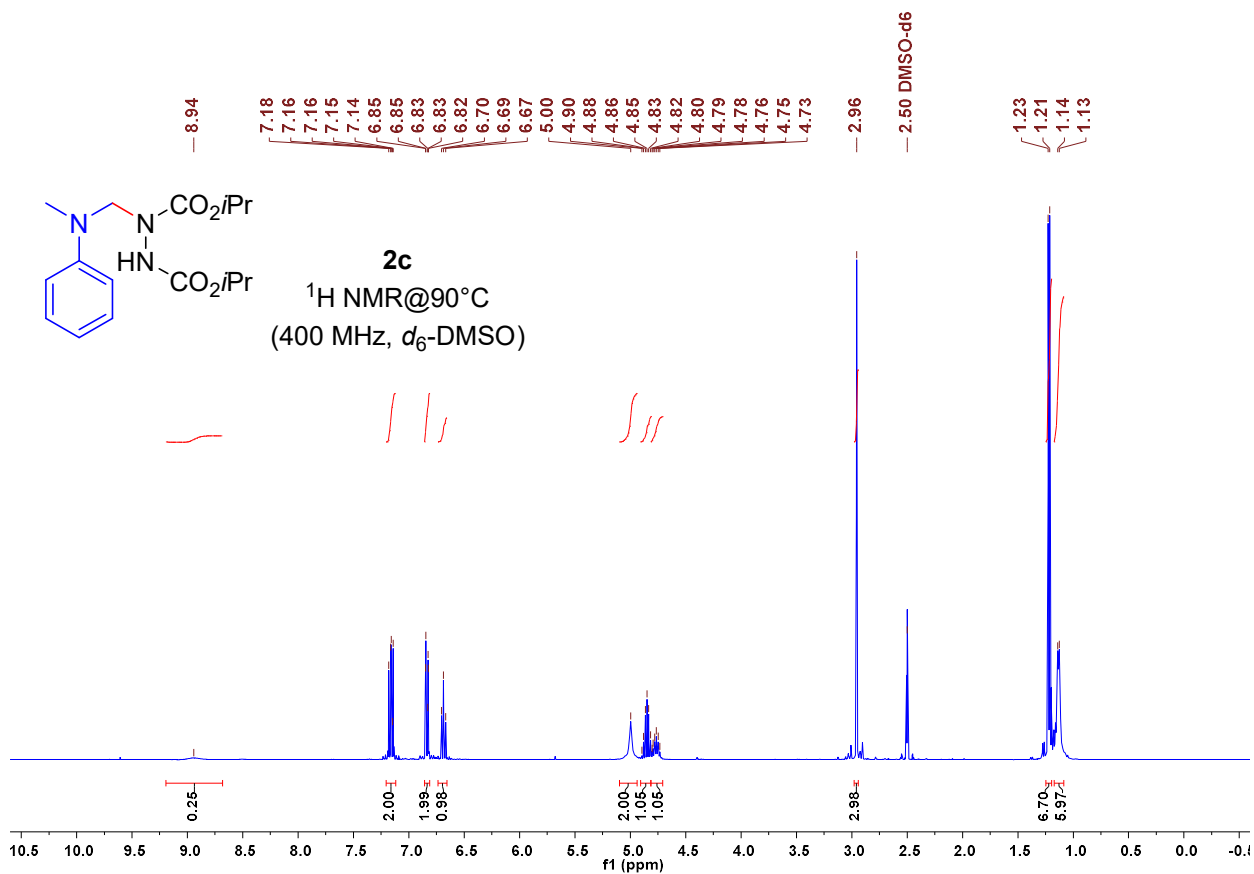
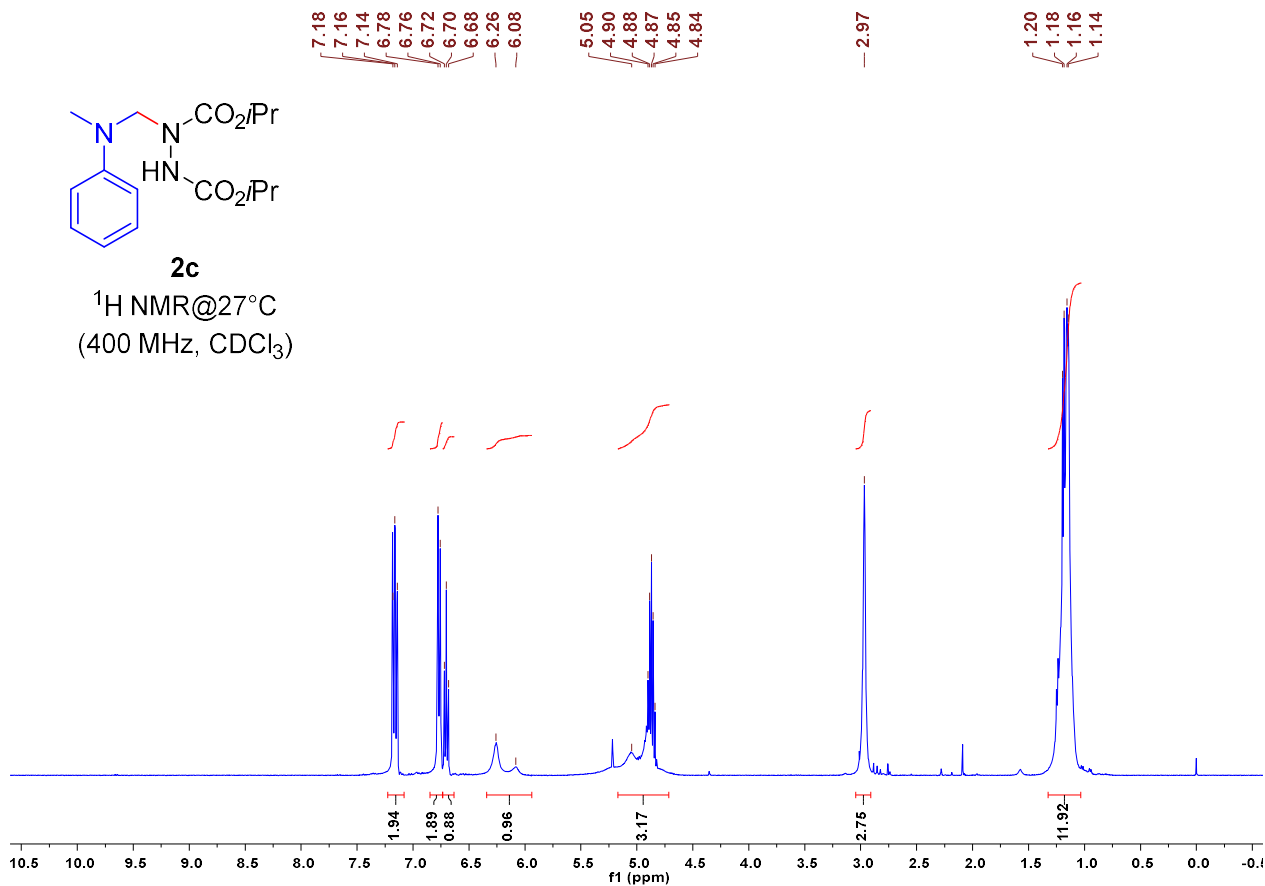
**2b**

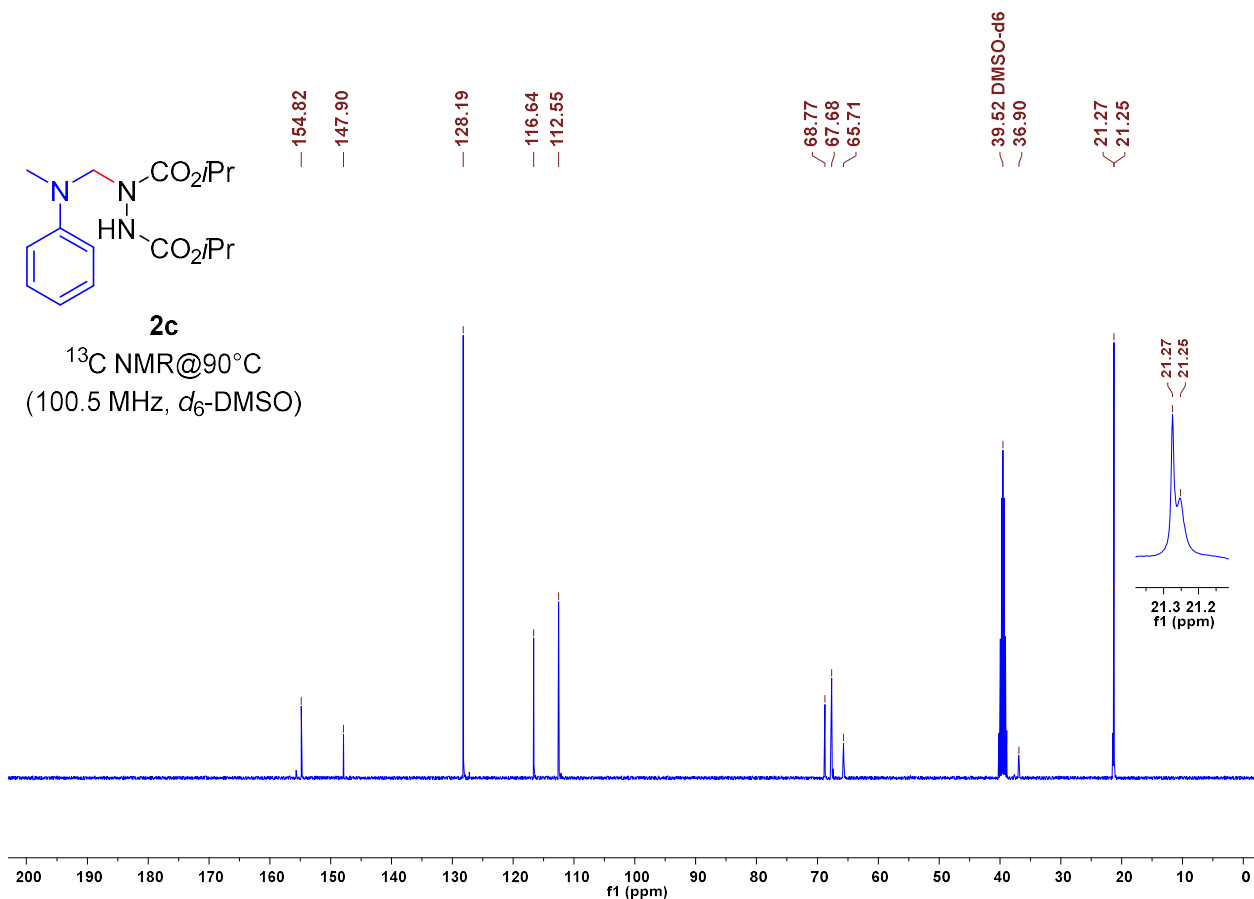
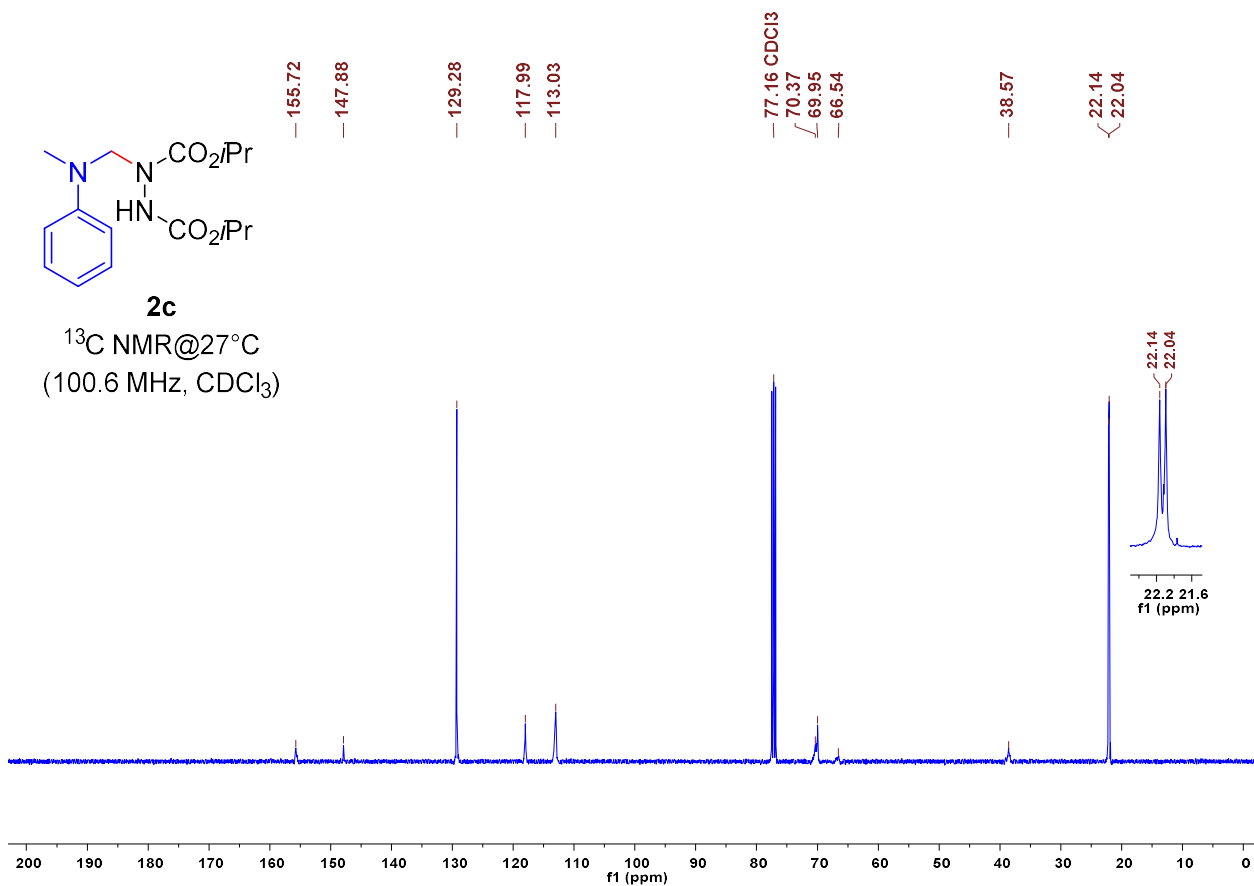
$^1\text{H NMR}$  @90°C  
(400 MHz,  $d_6$ -DMSO)

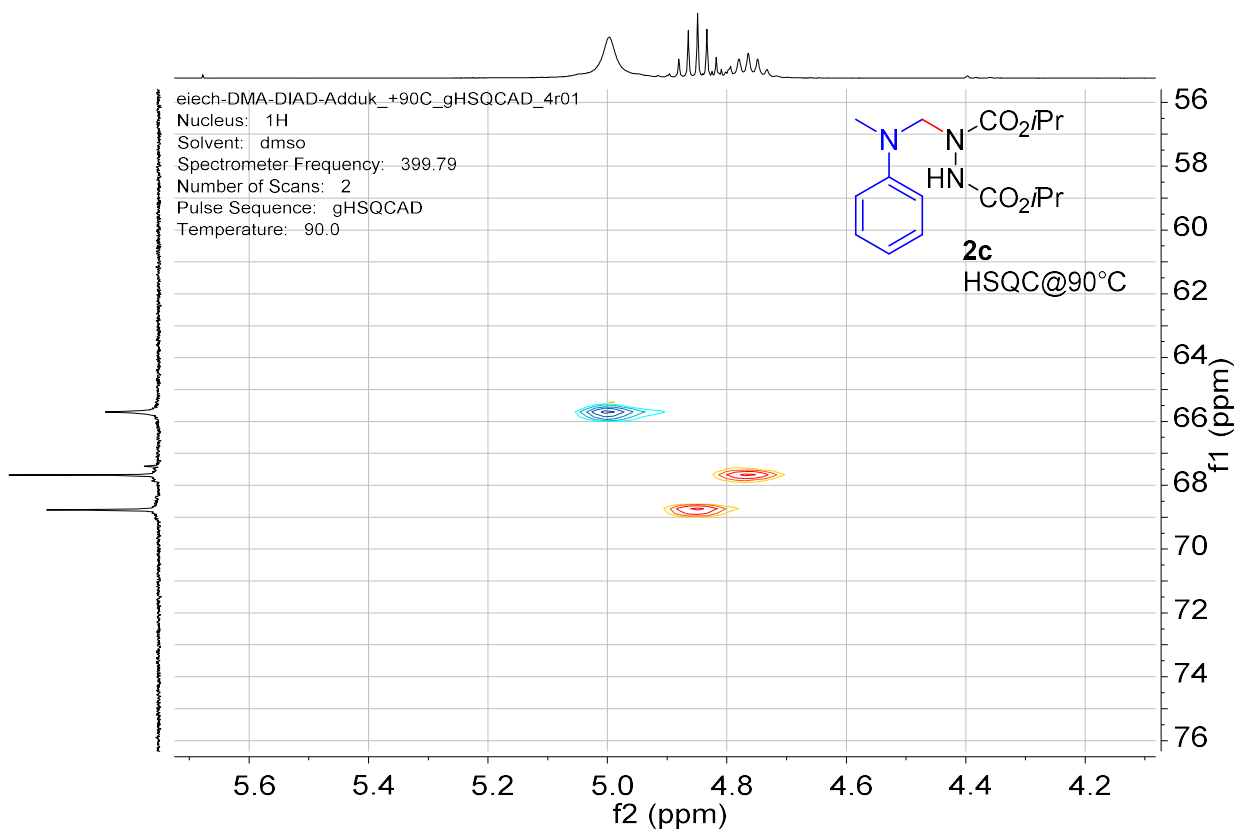


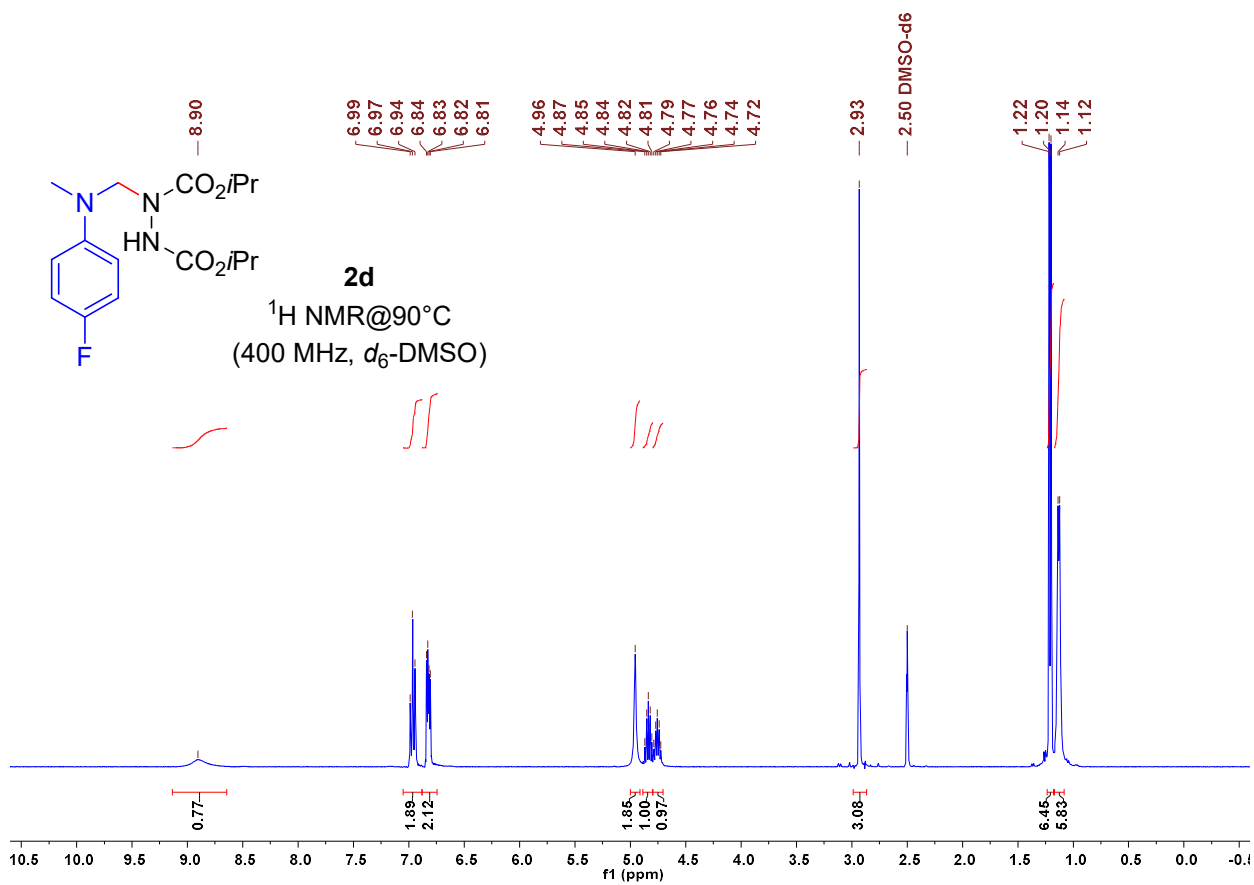
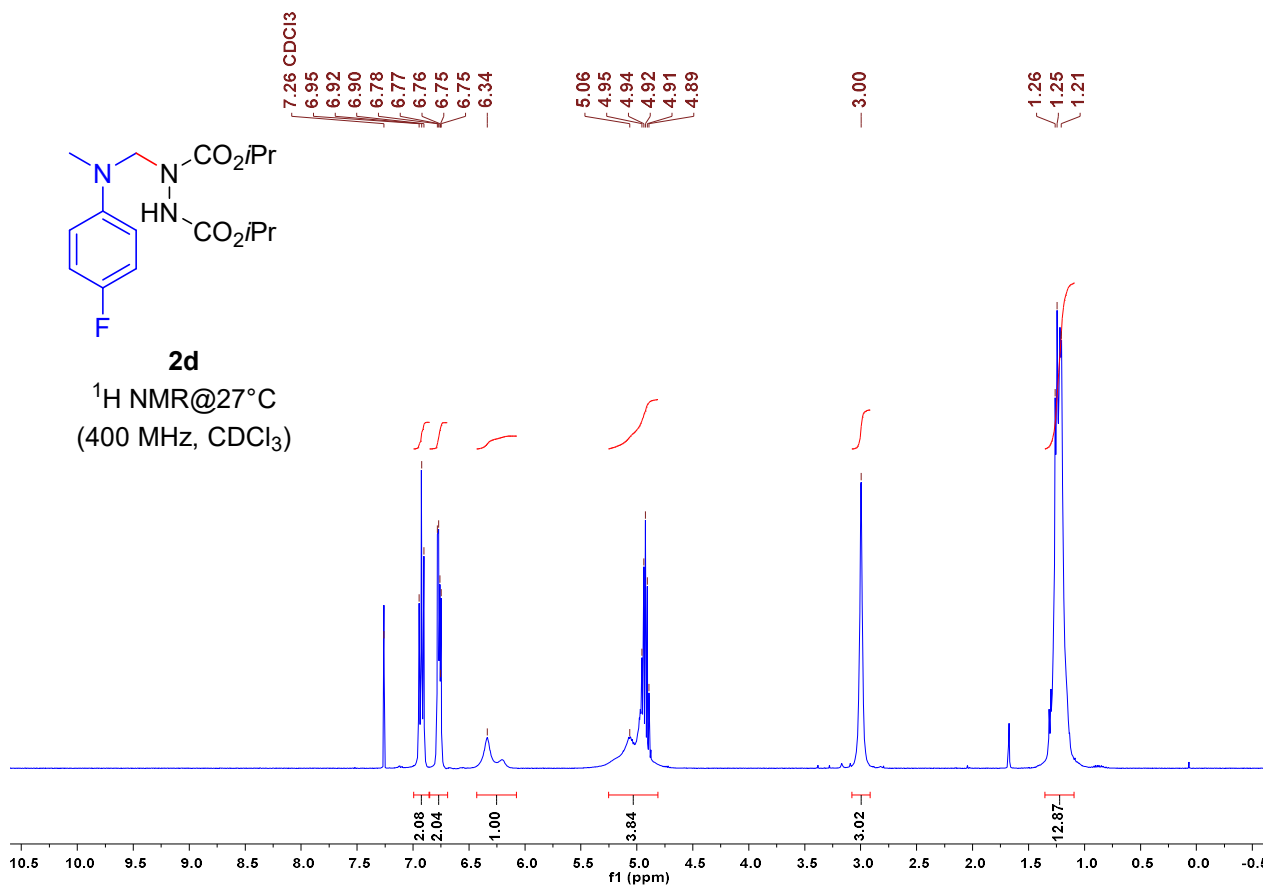


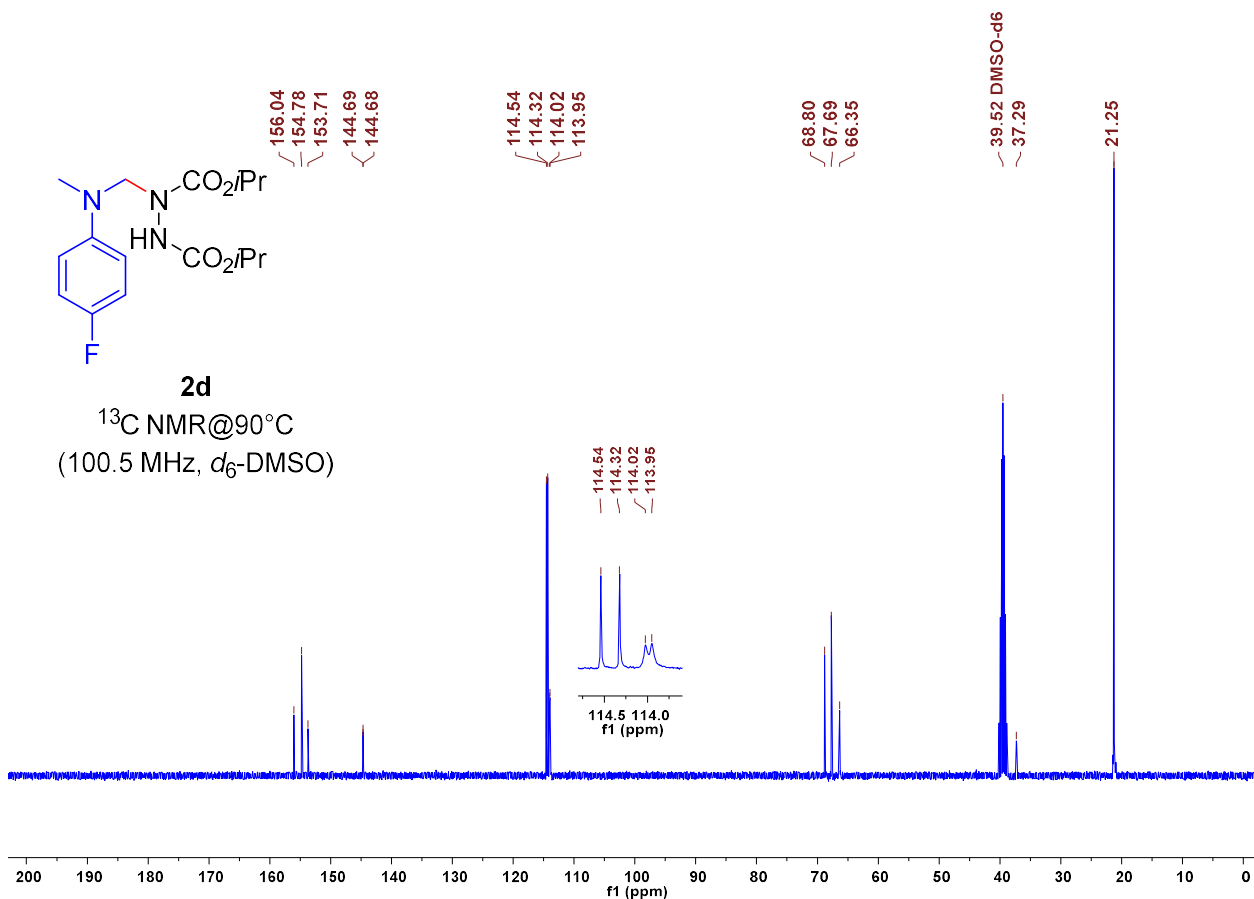
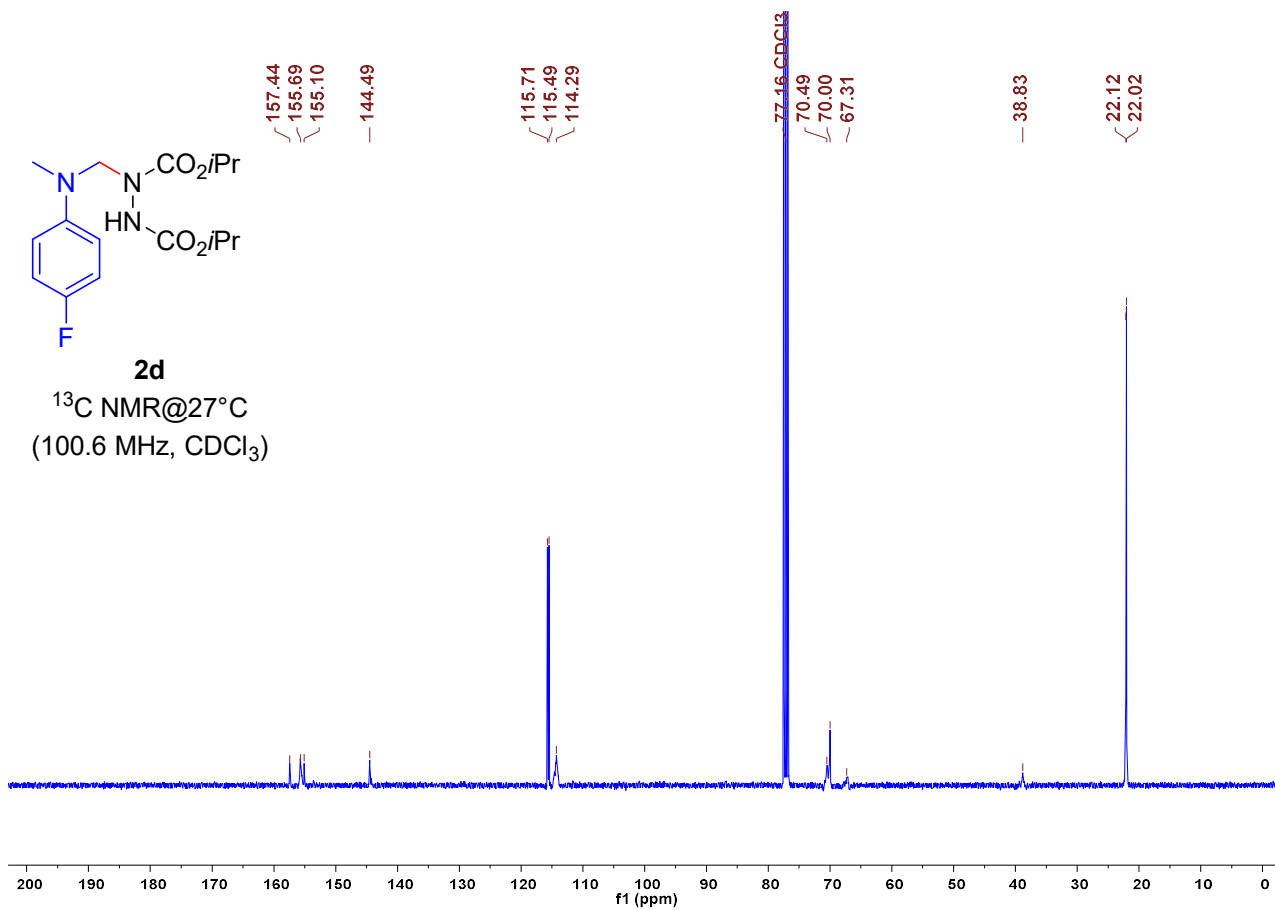


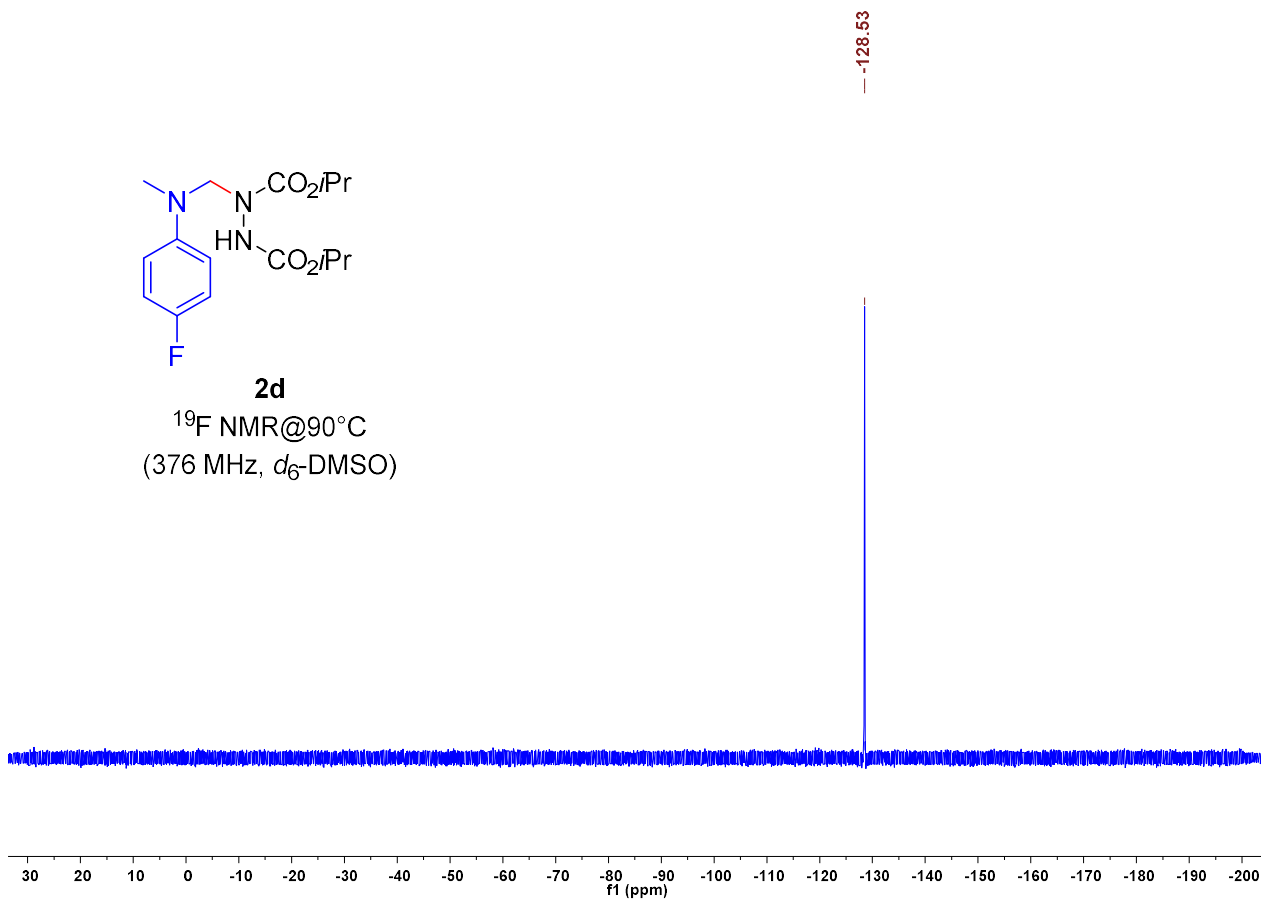
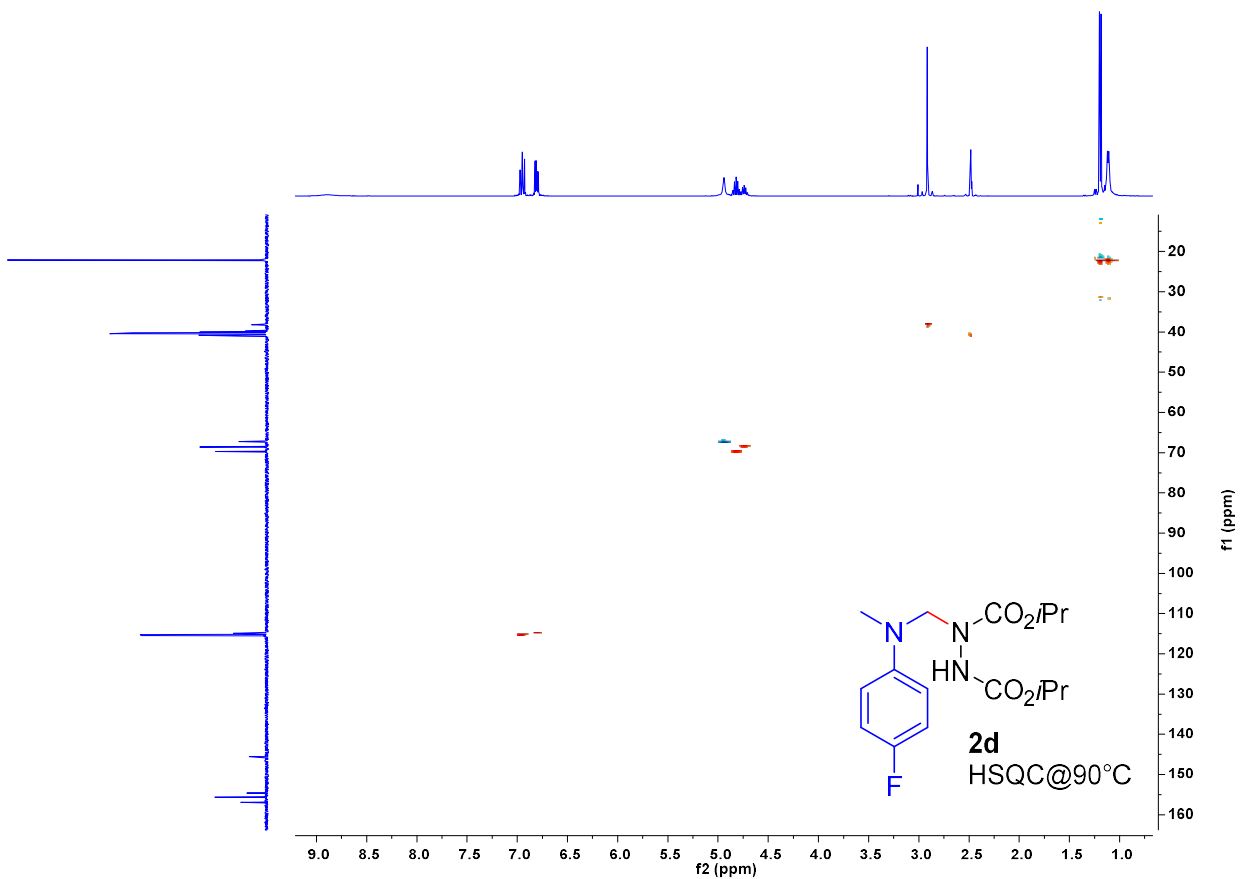


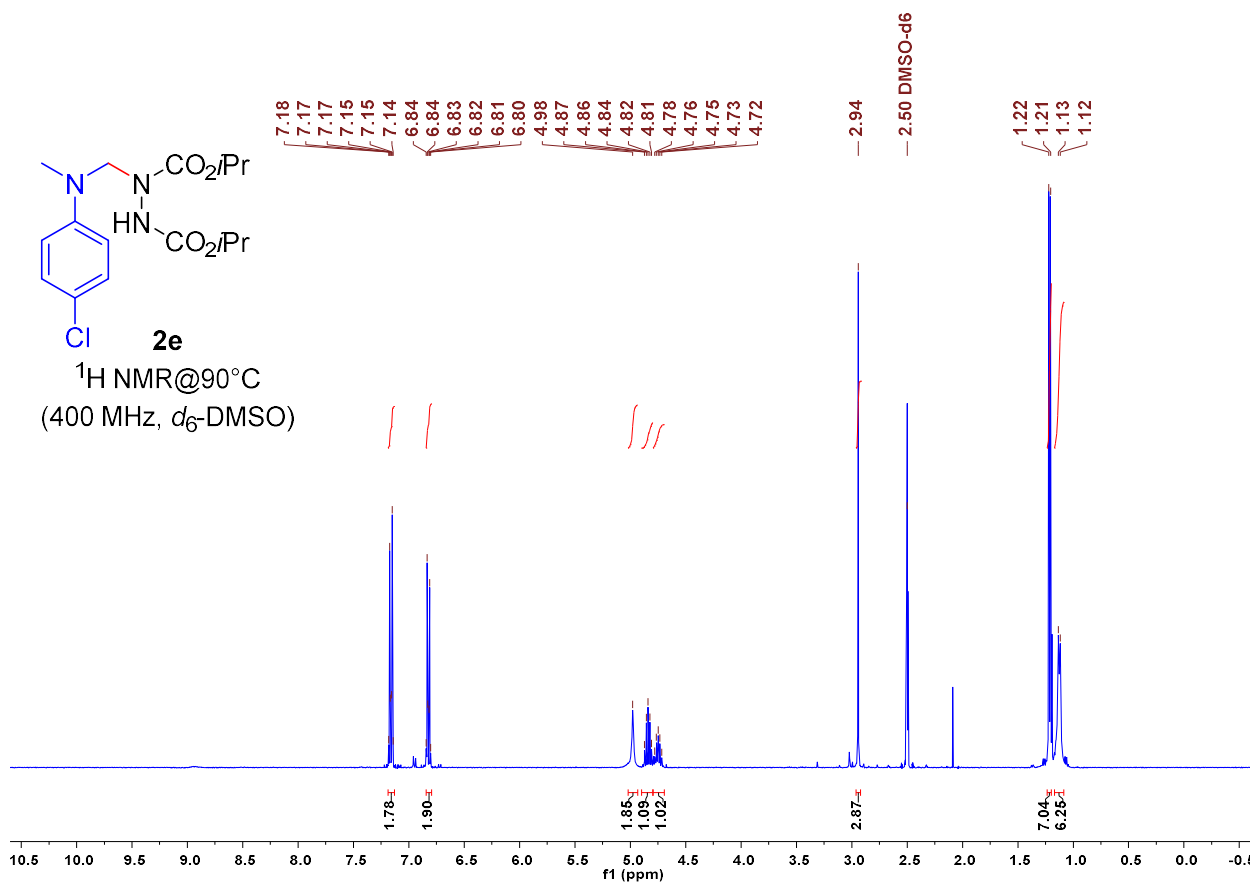
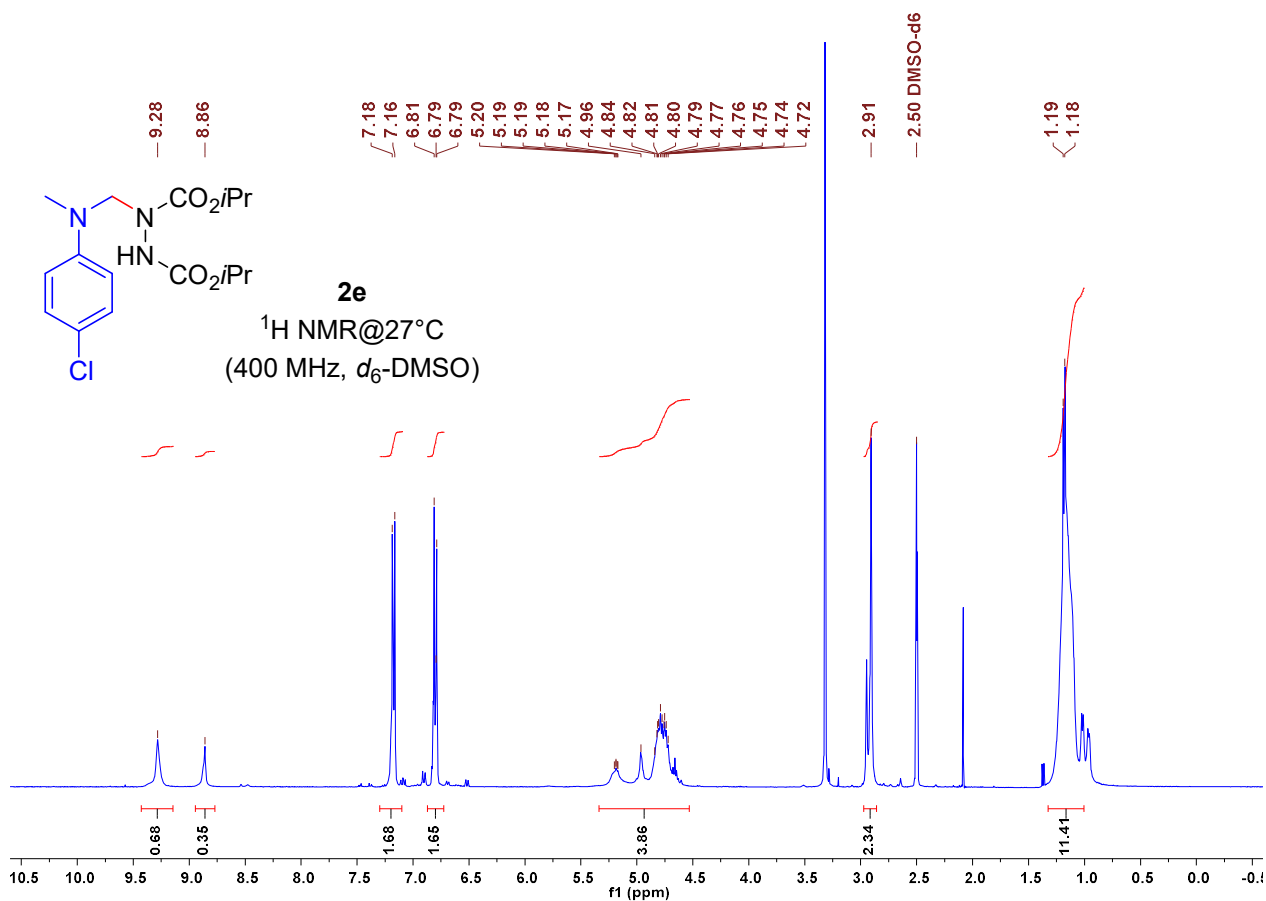


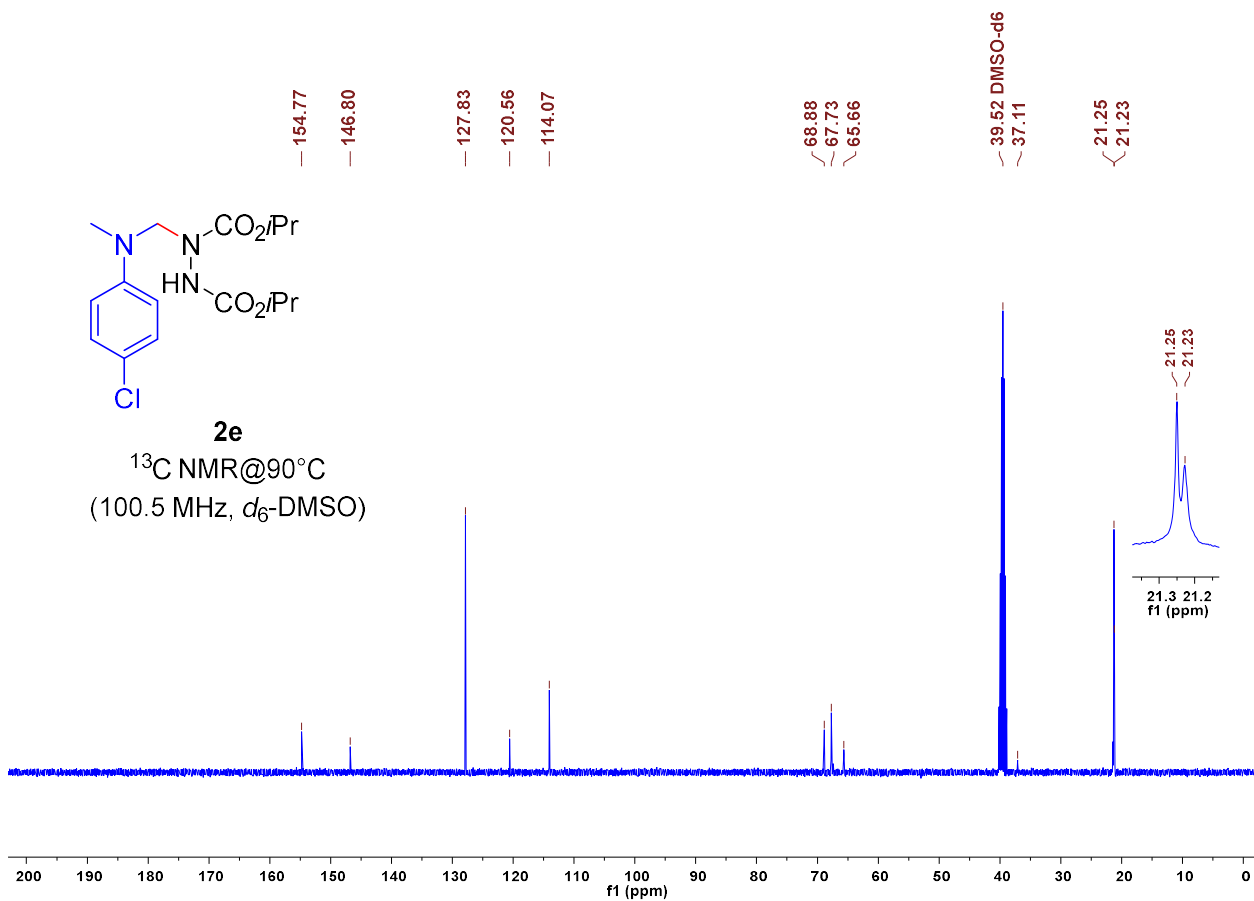
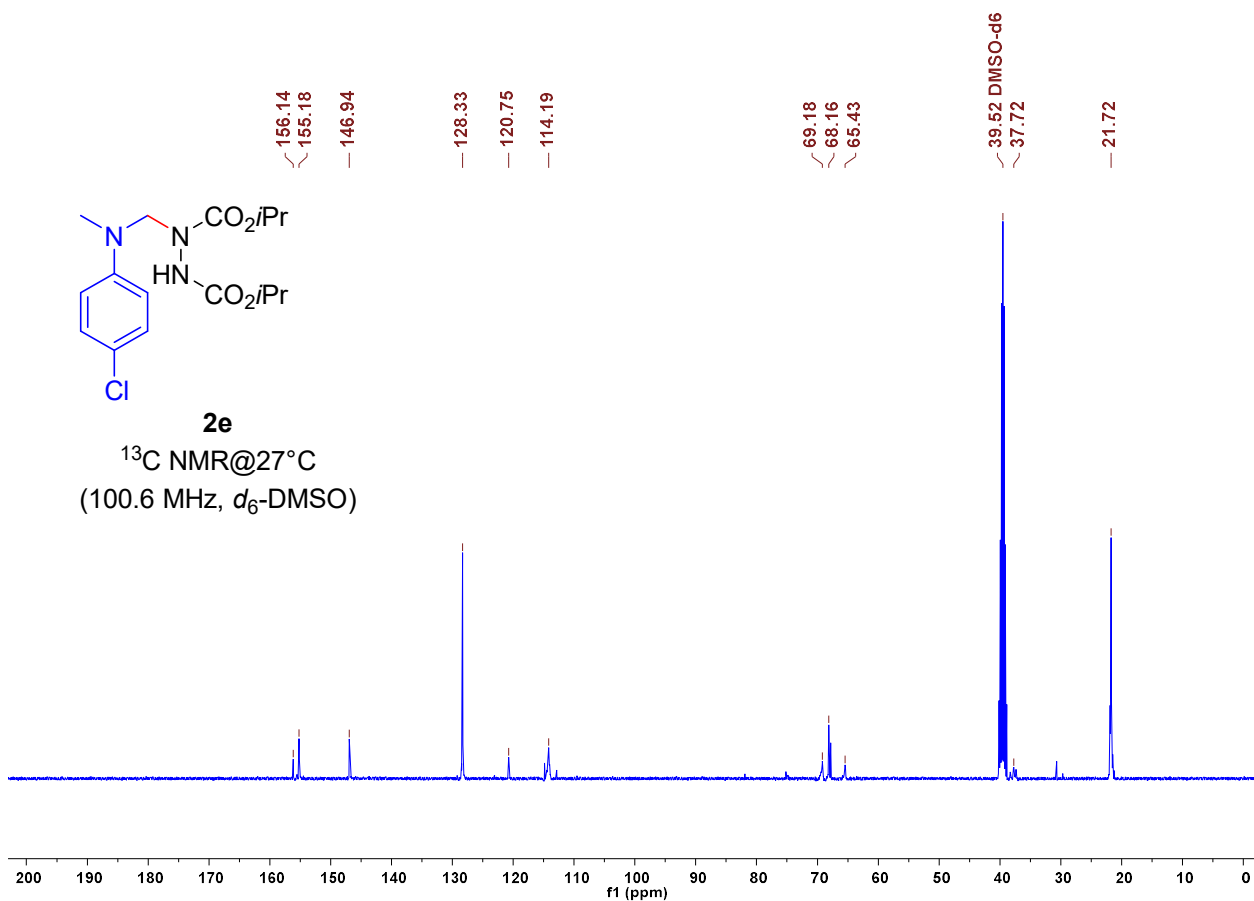


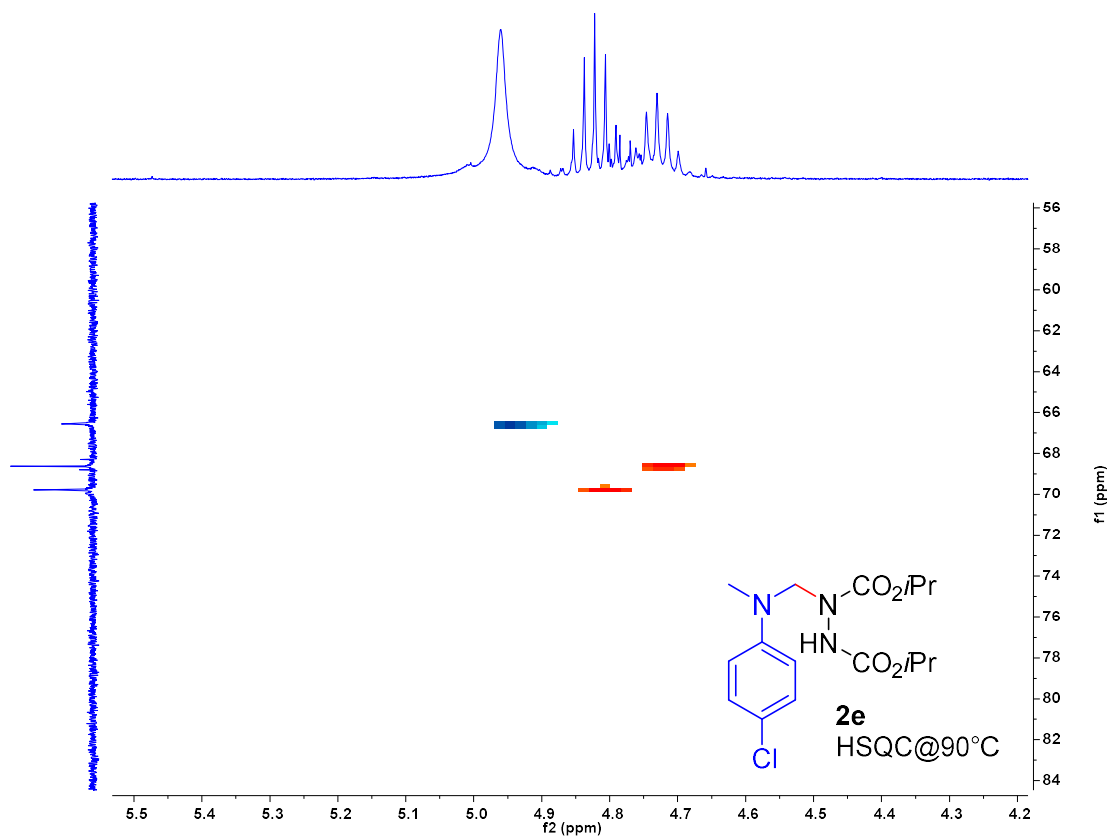


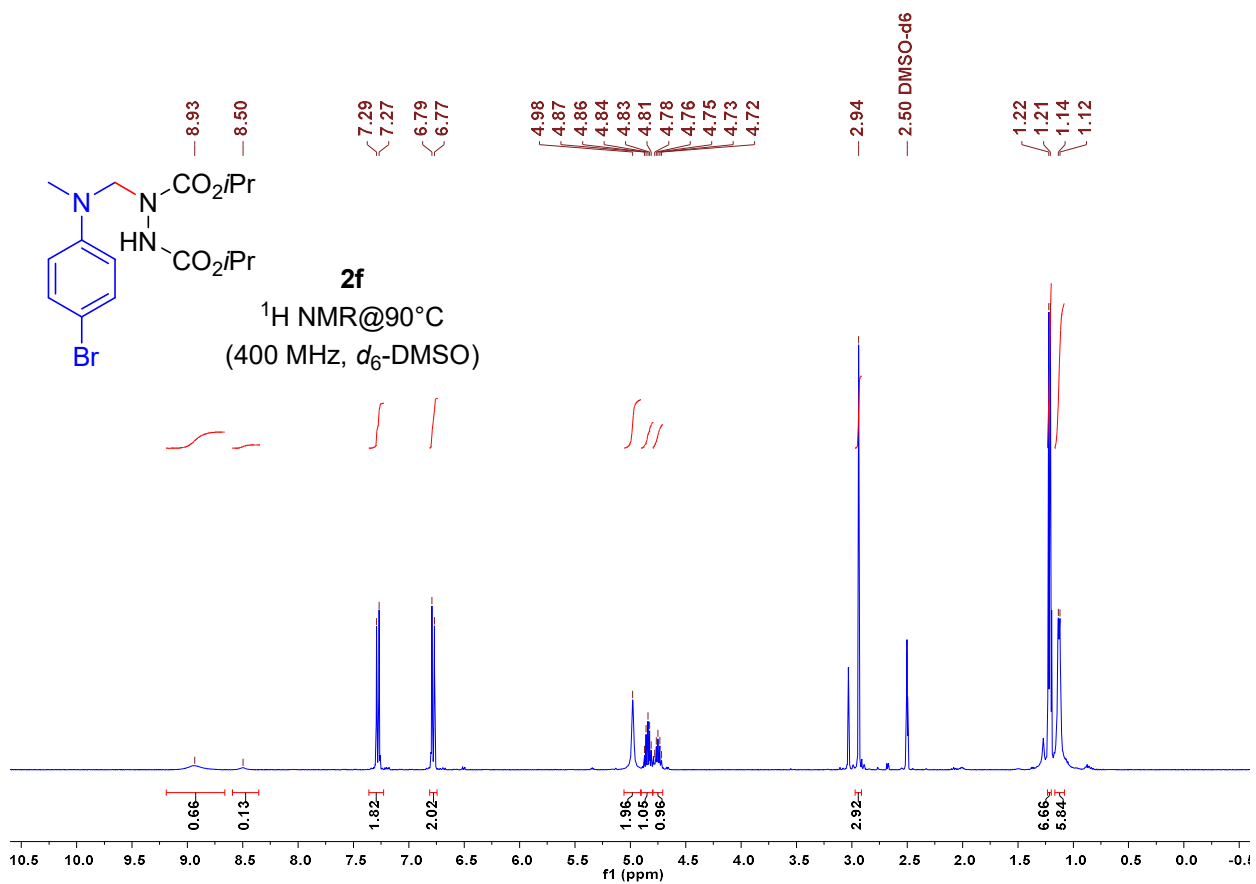
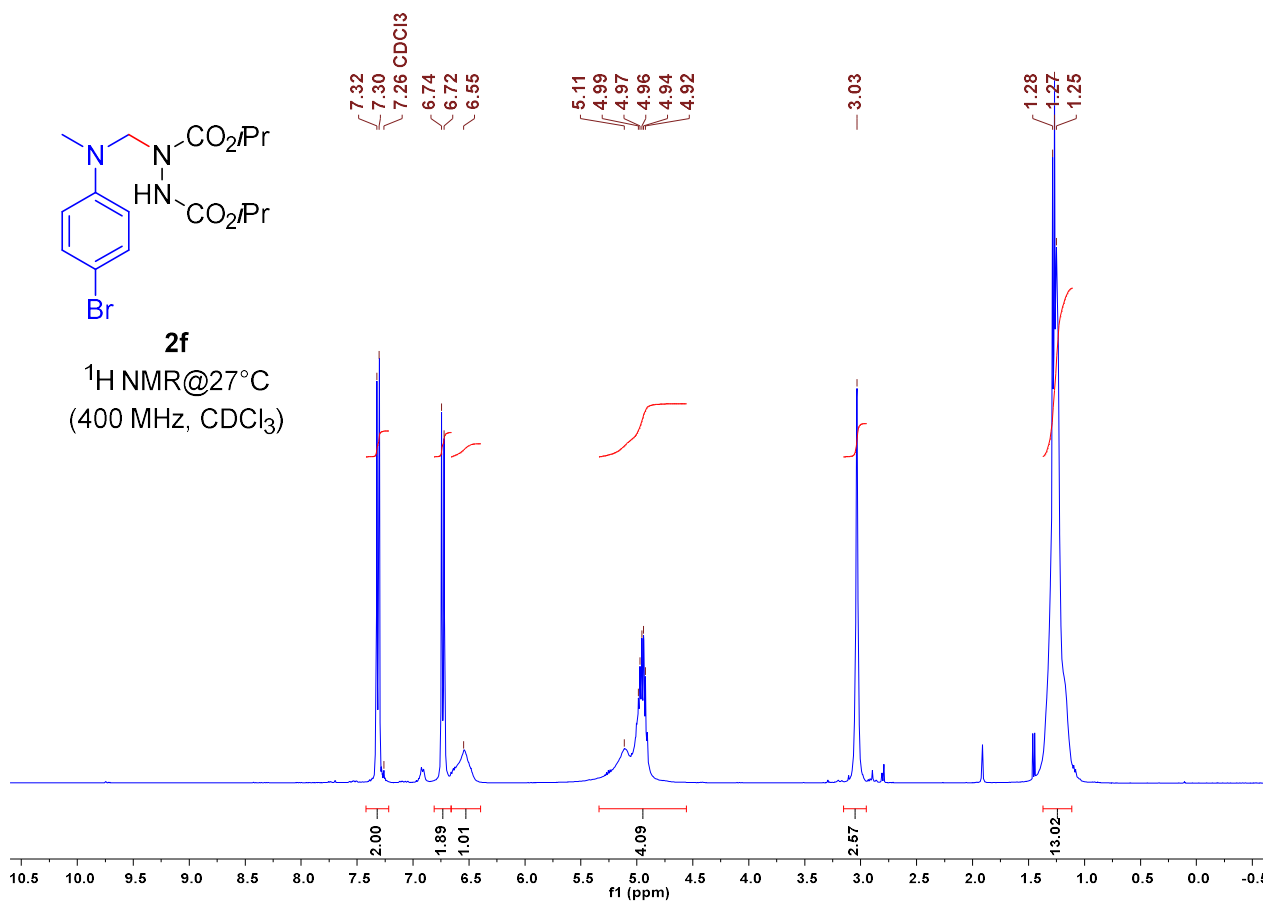


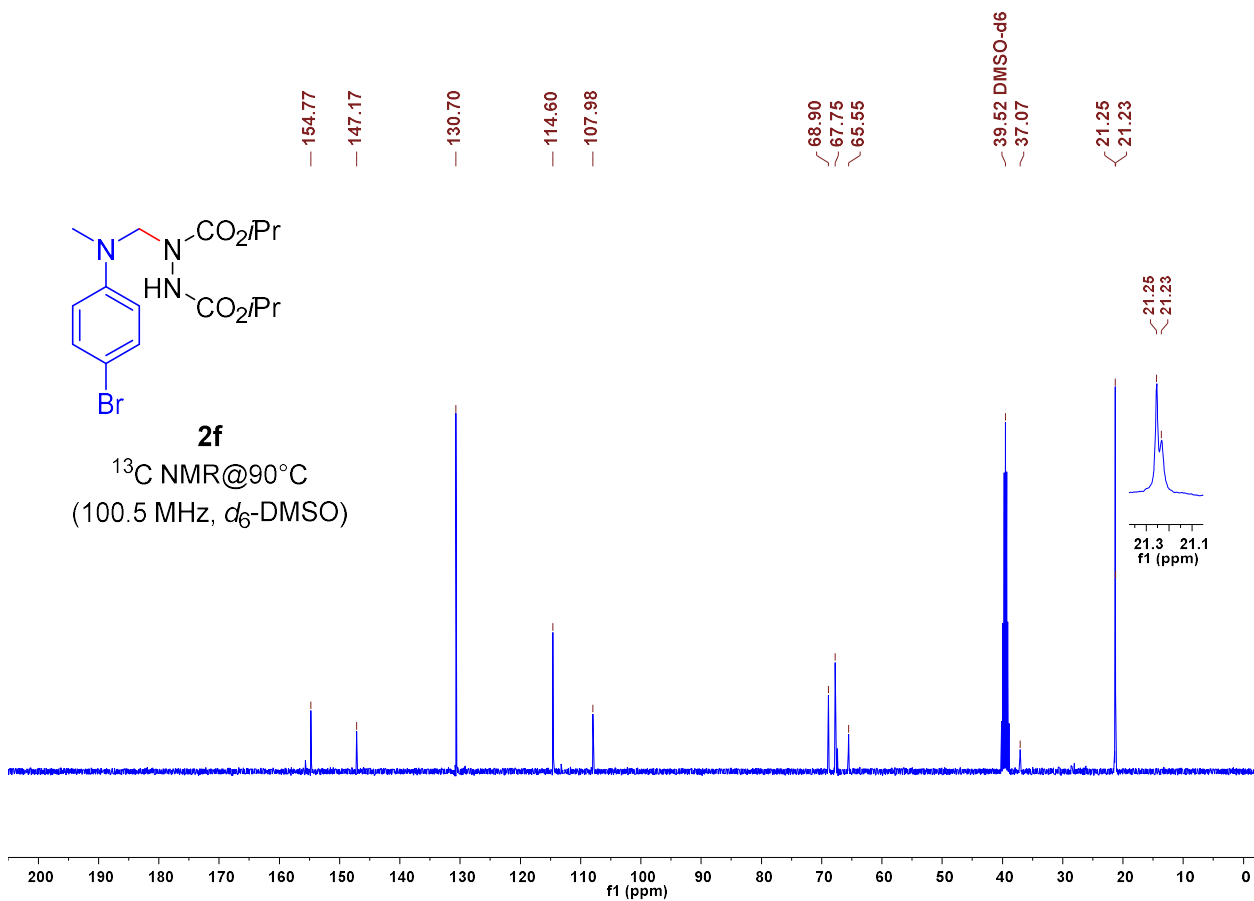
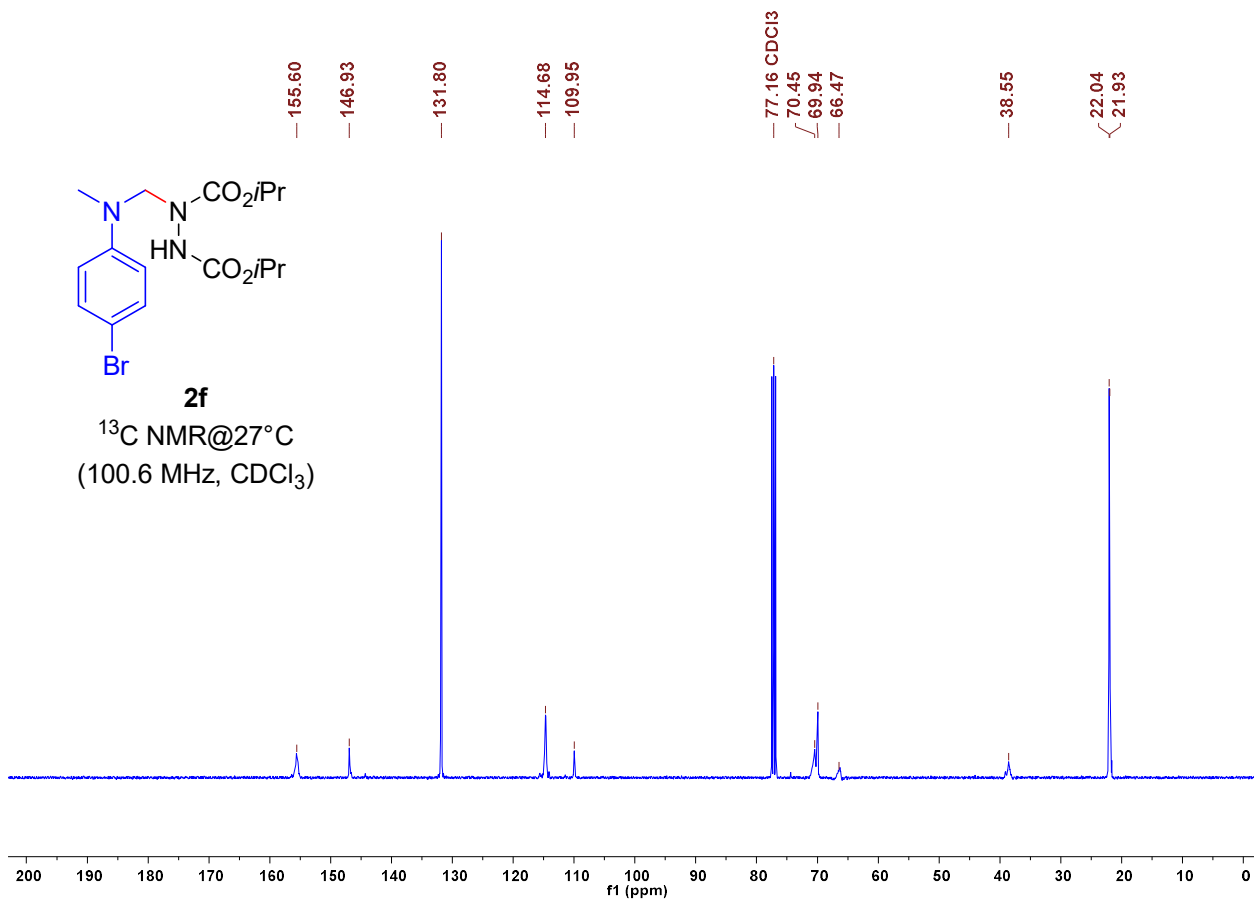


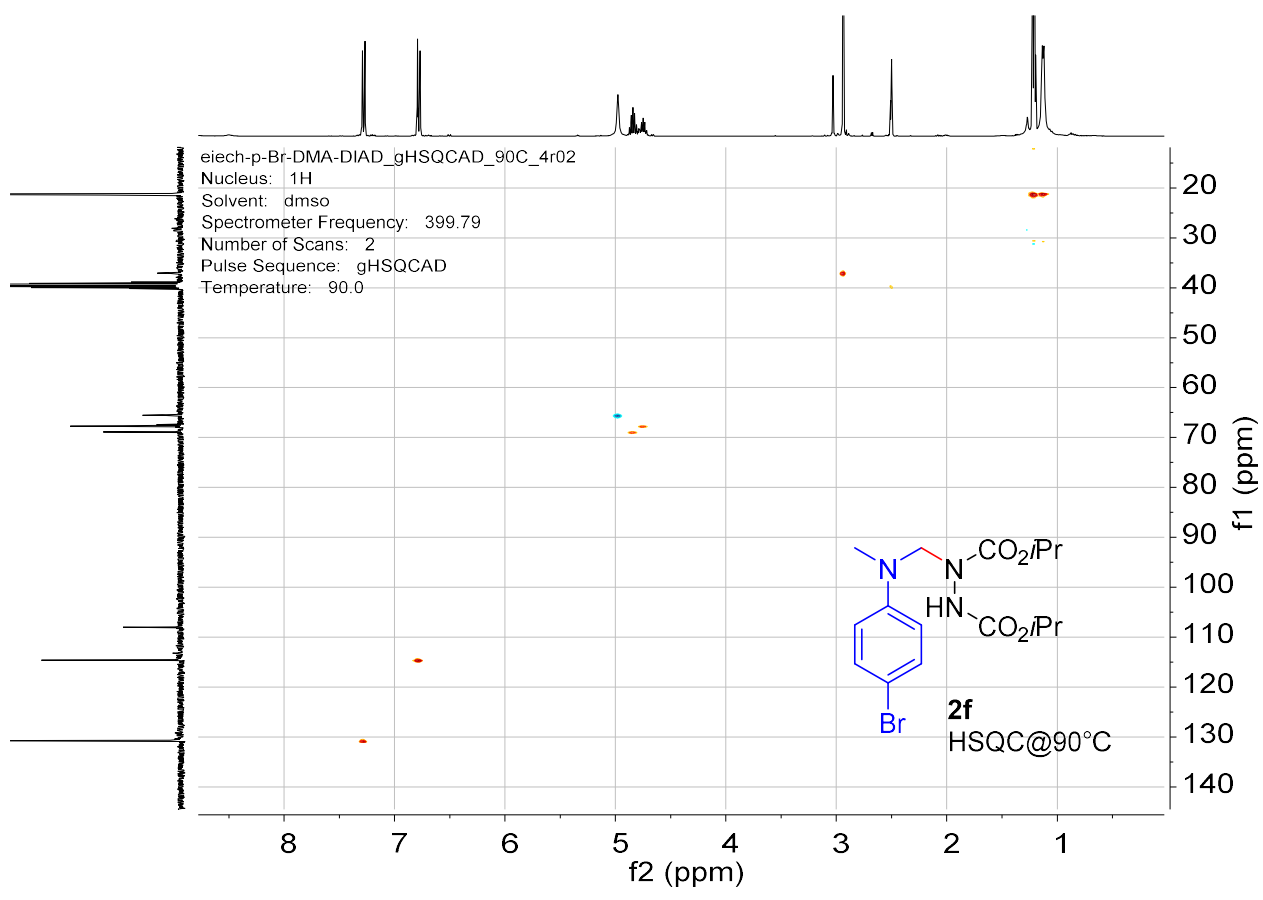


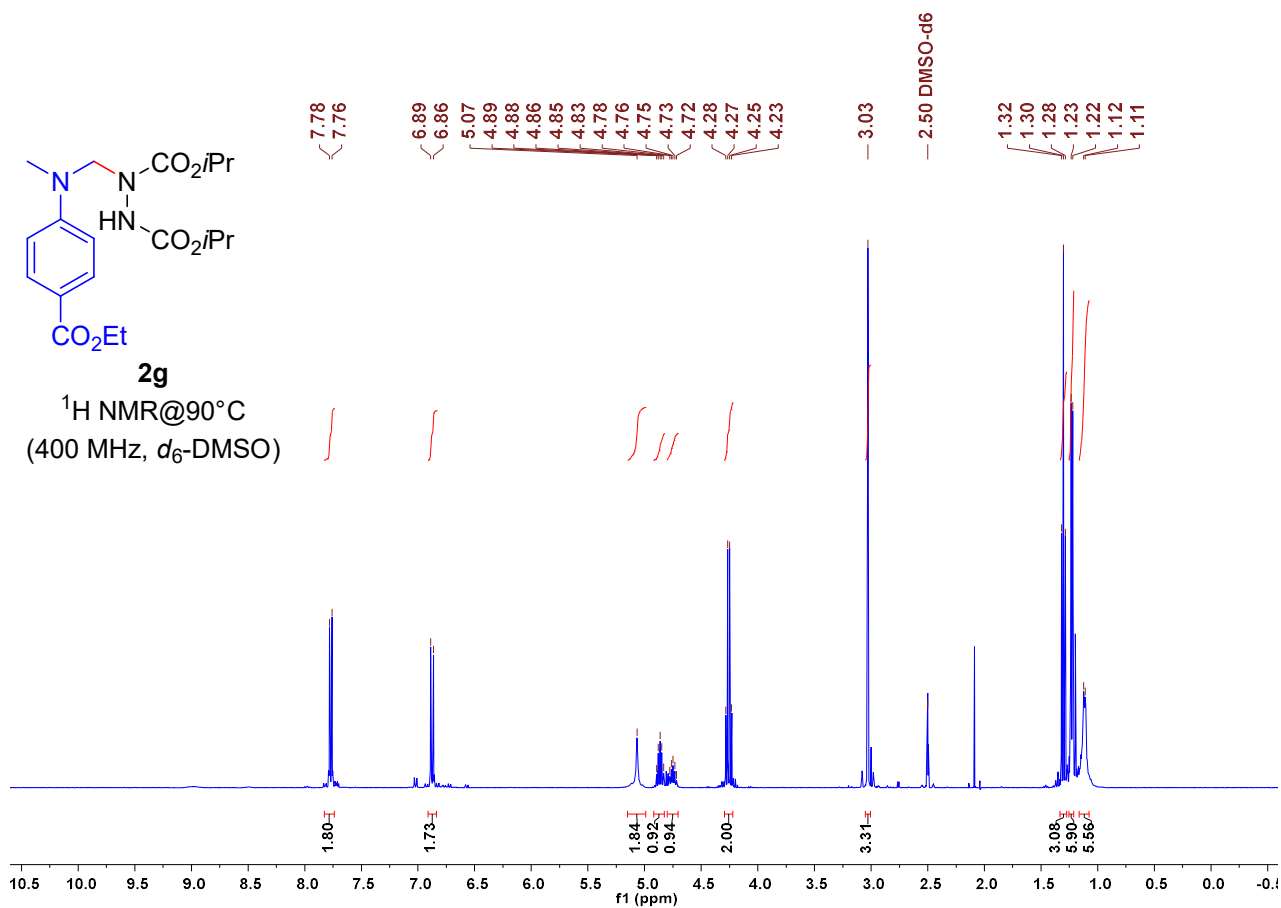
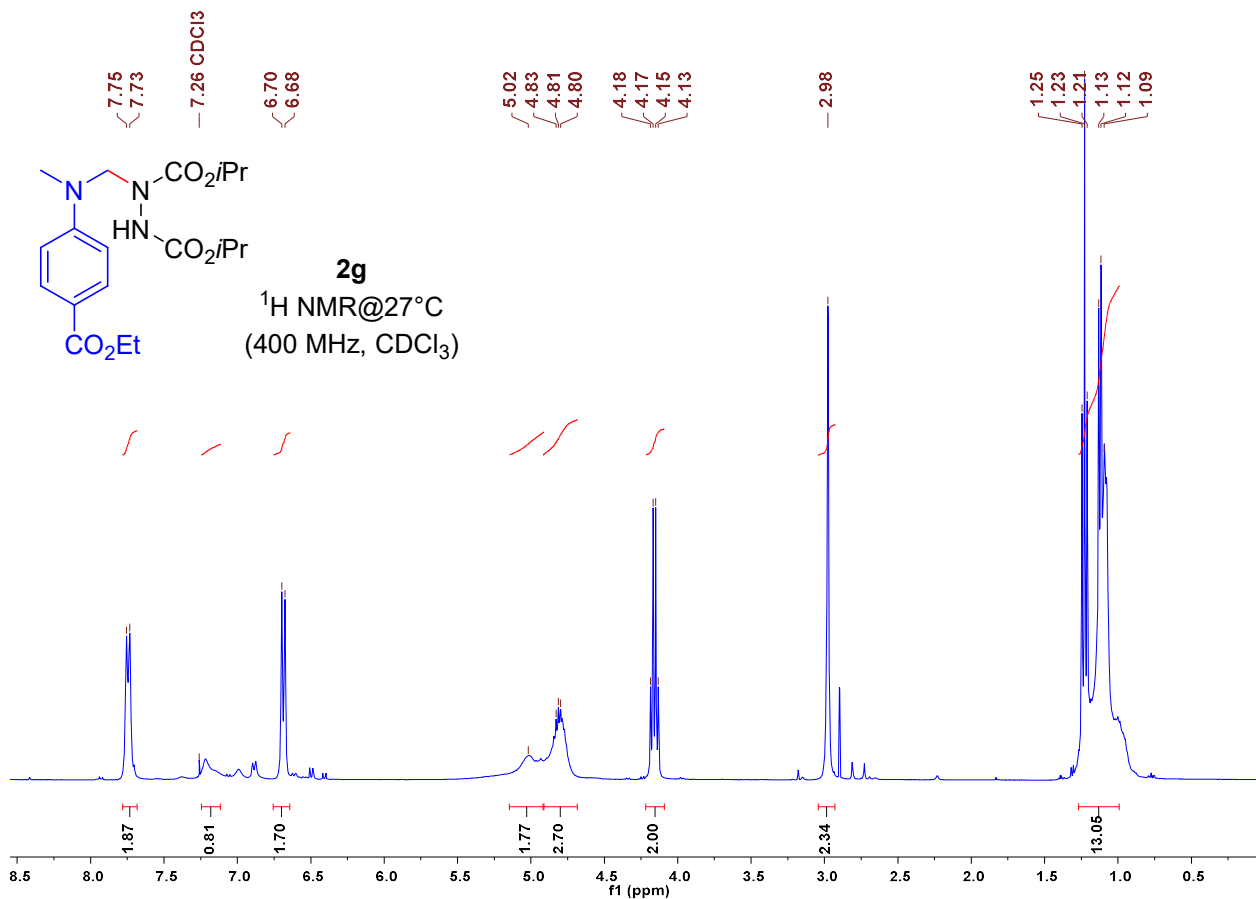


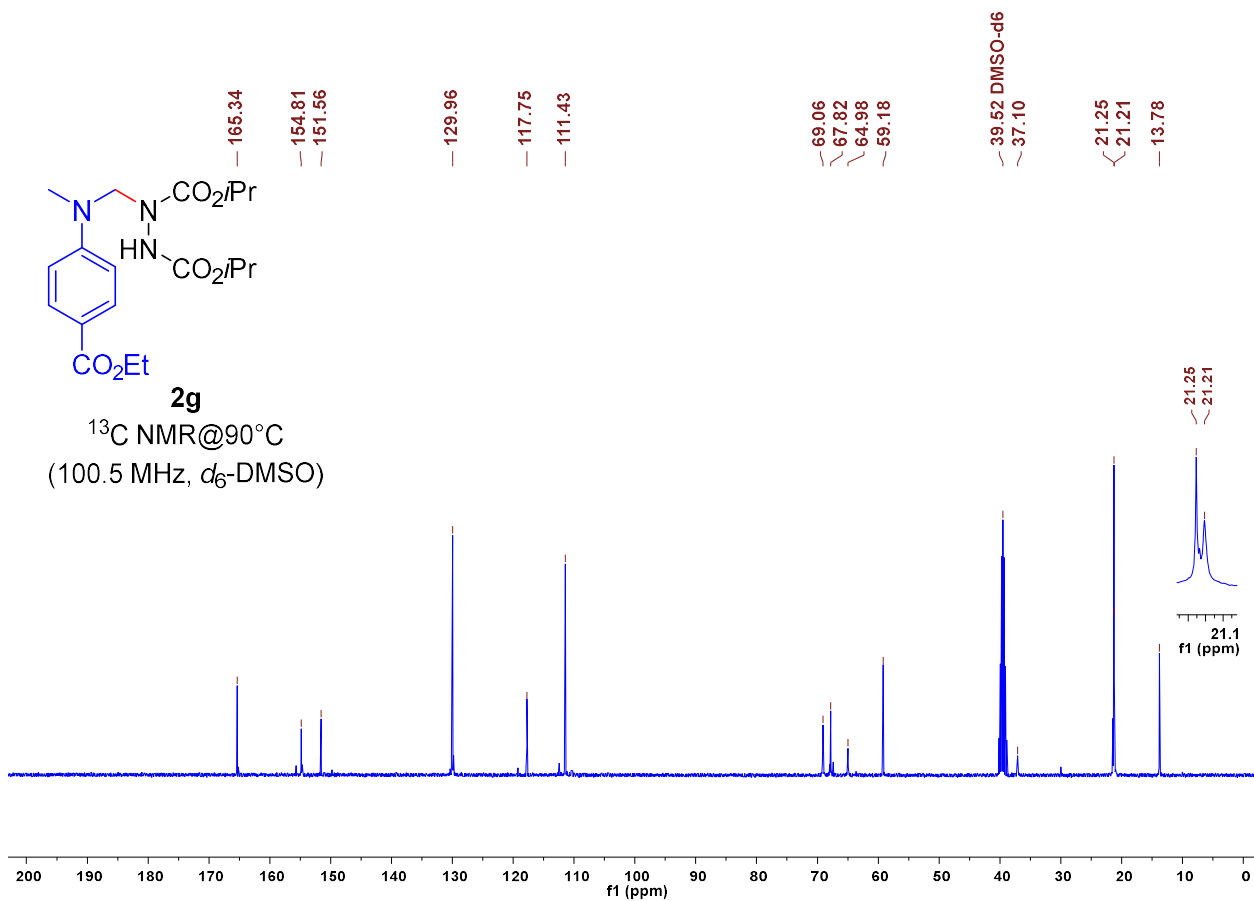
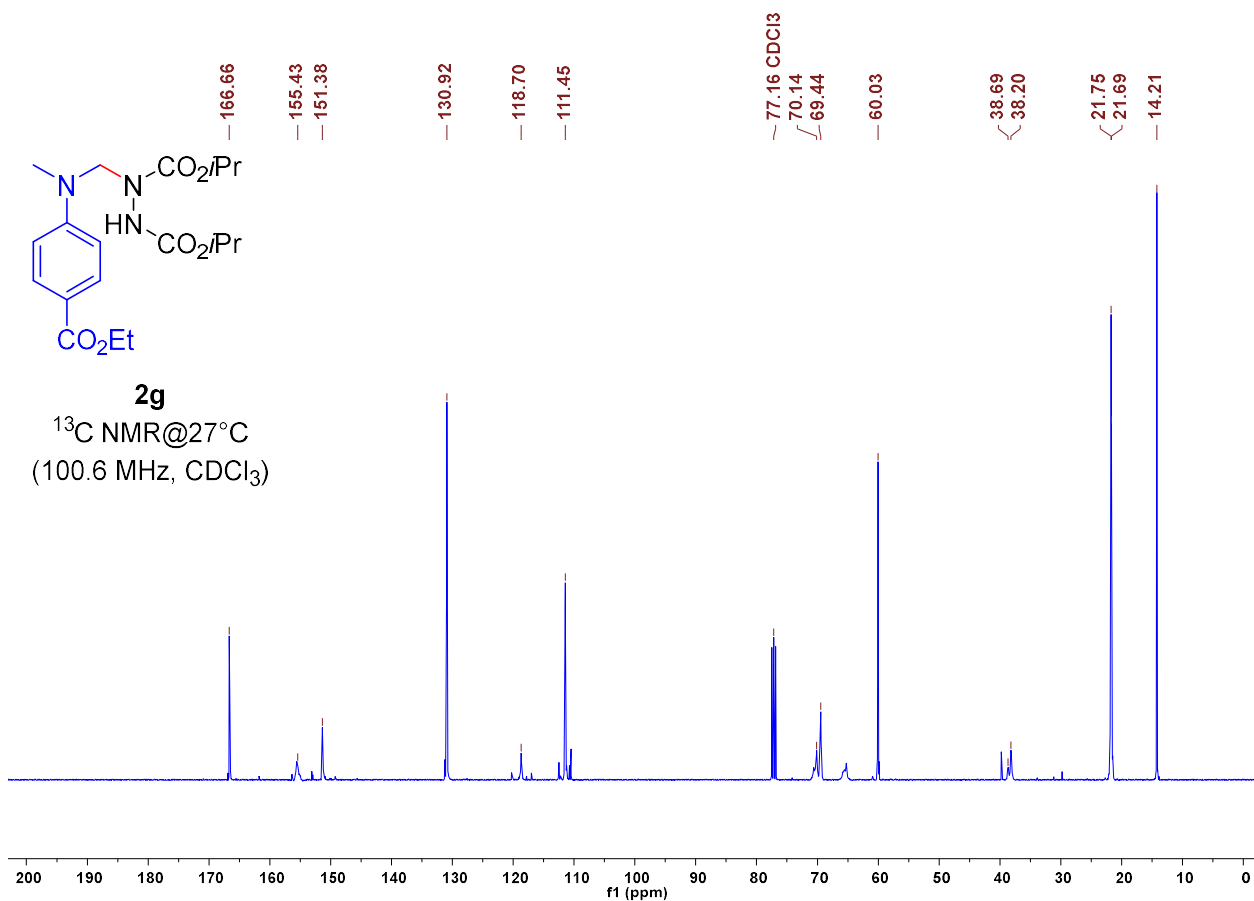


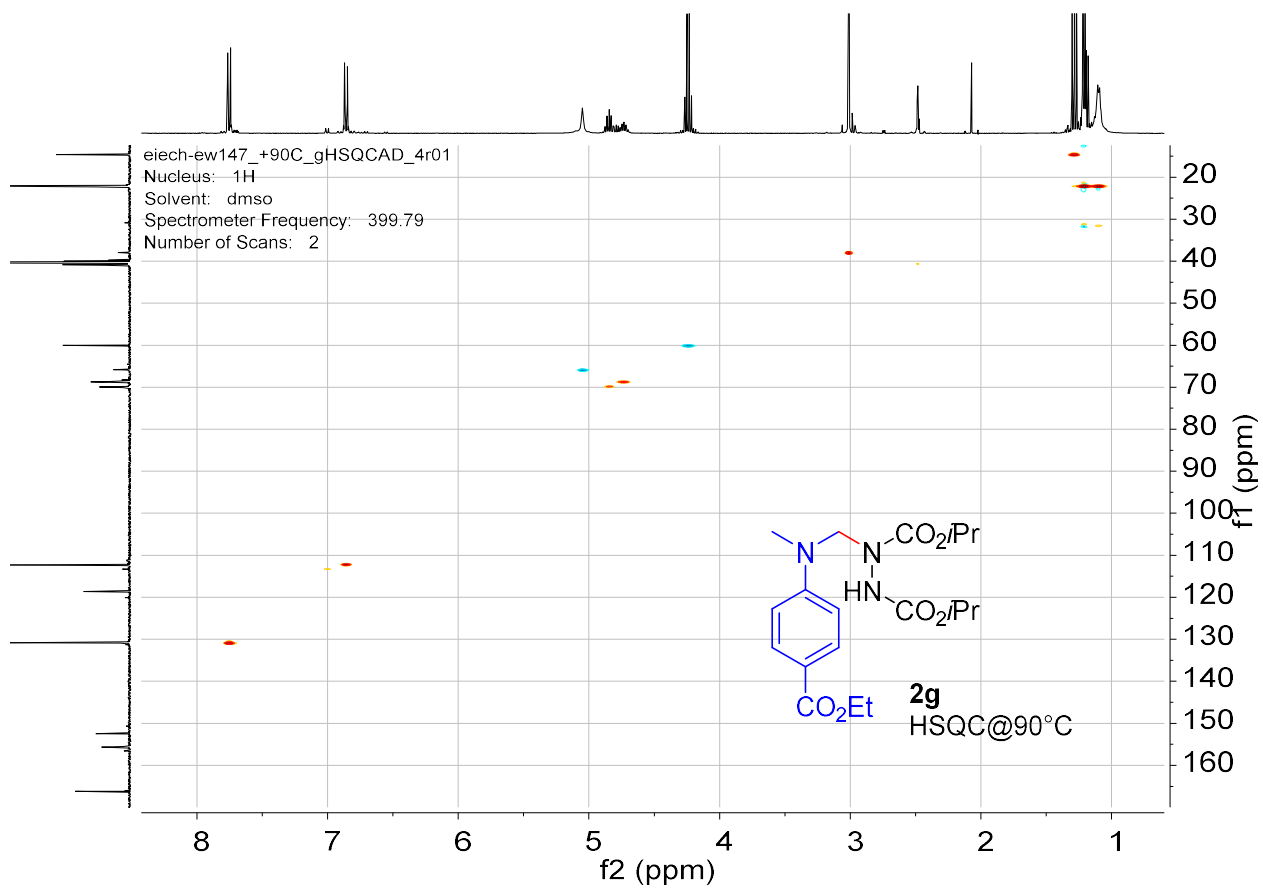


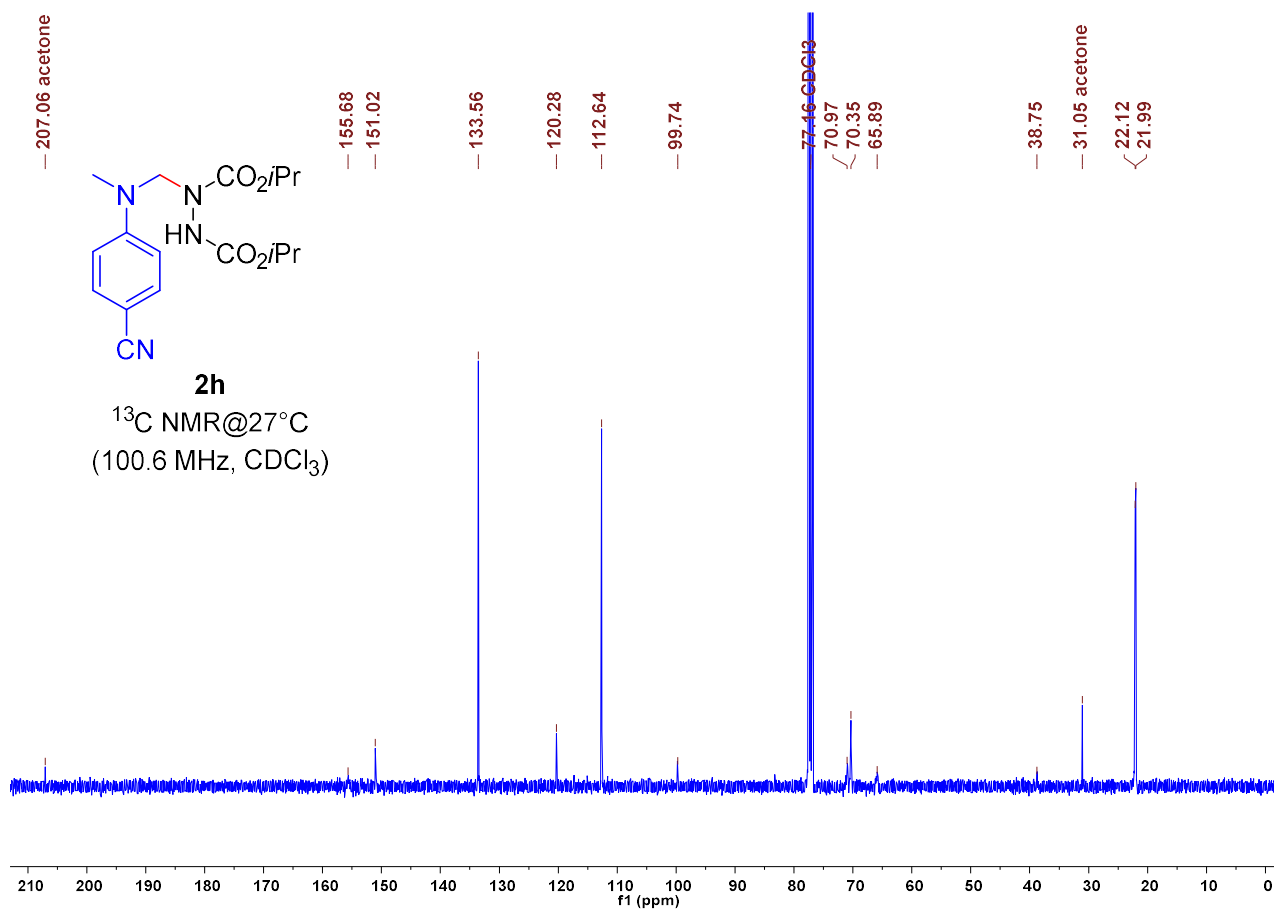
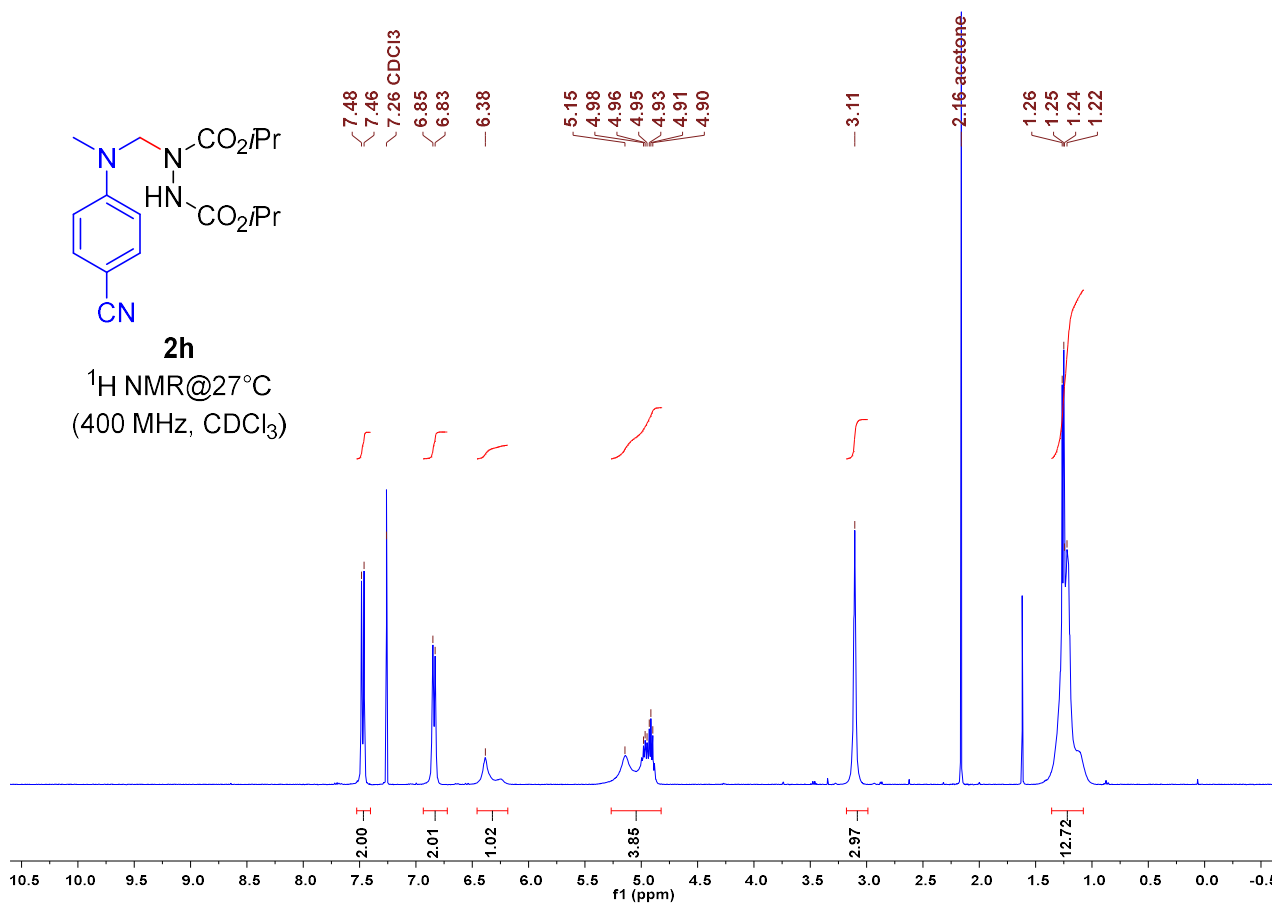


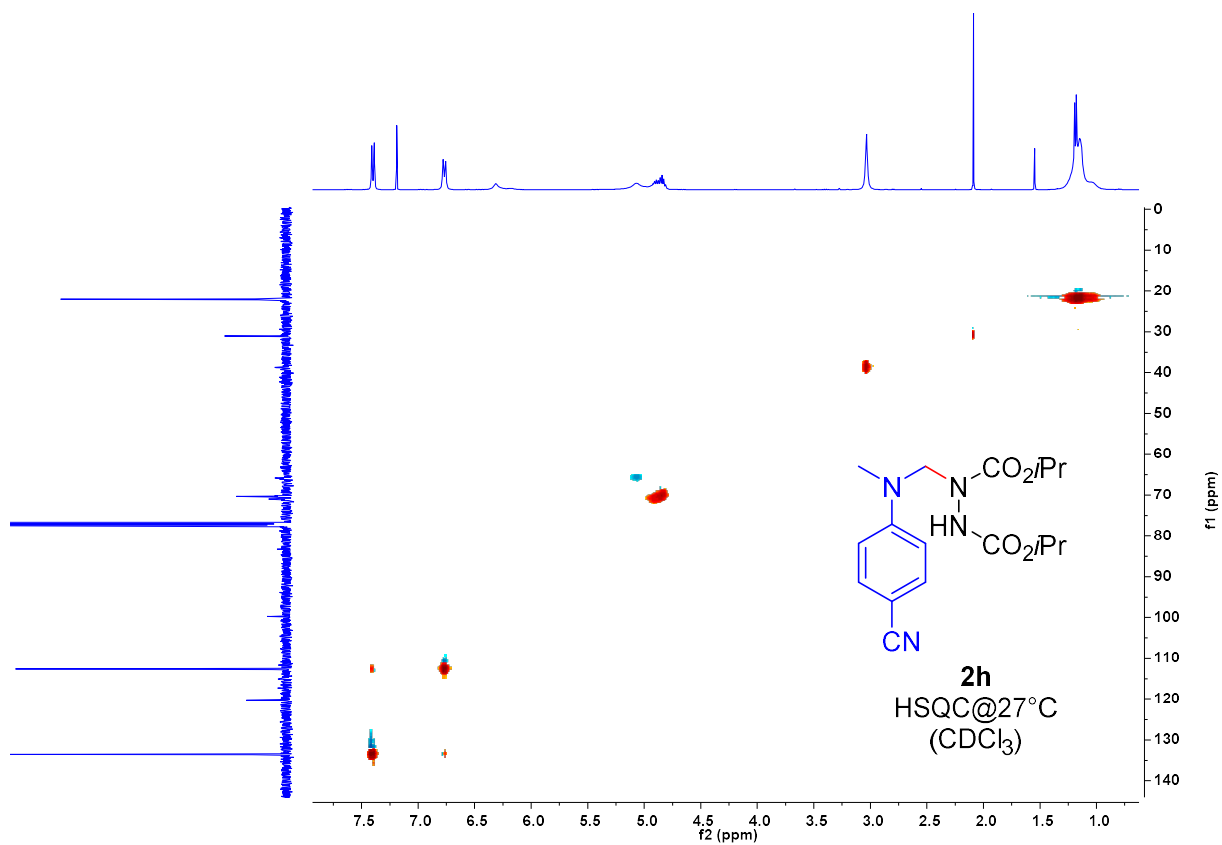


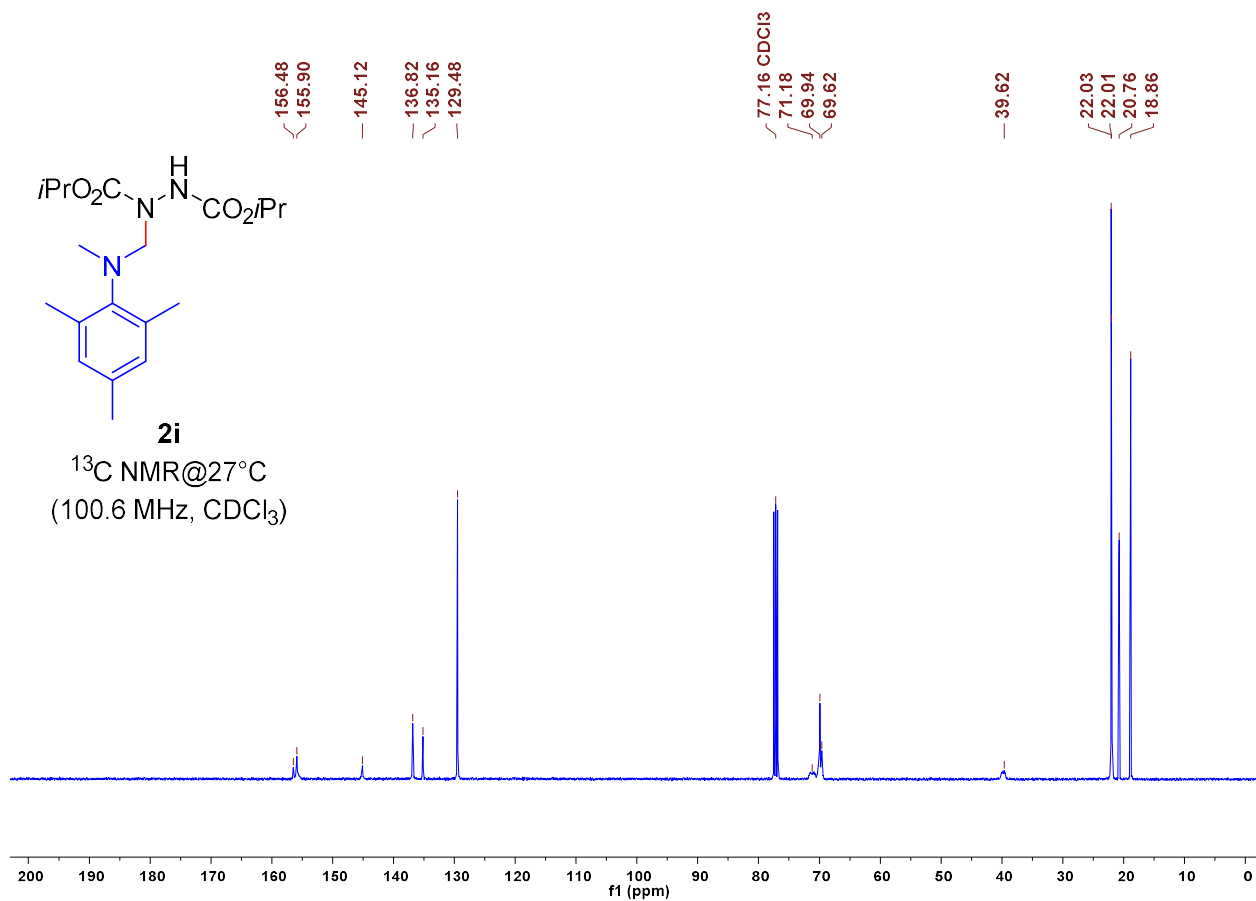
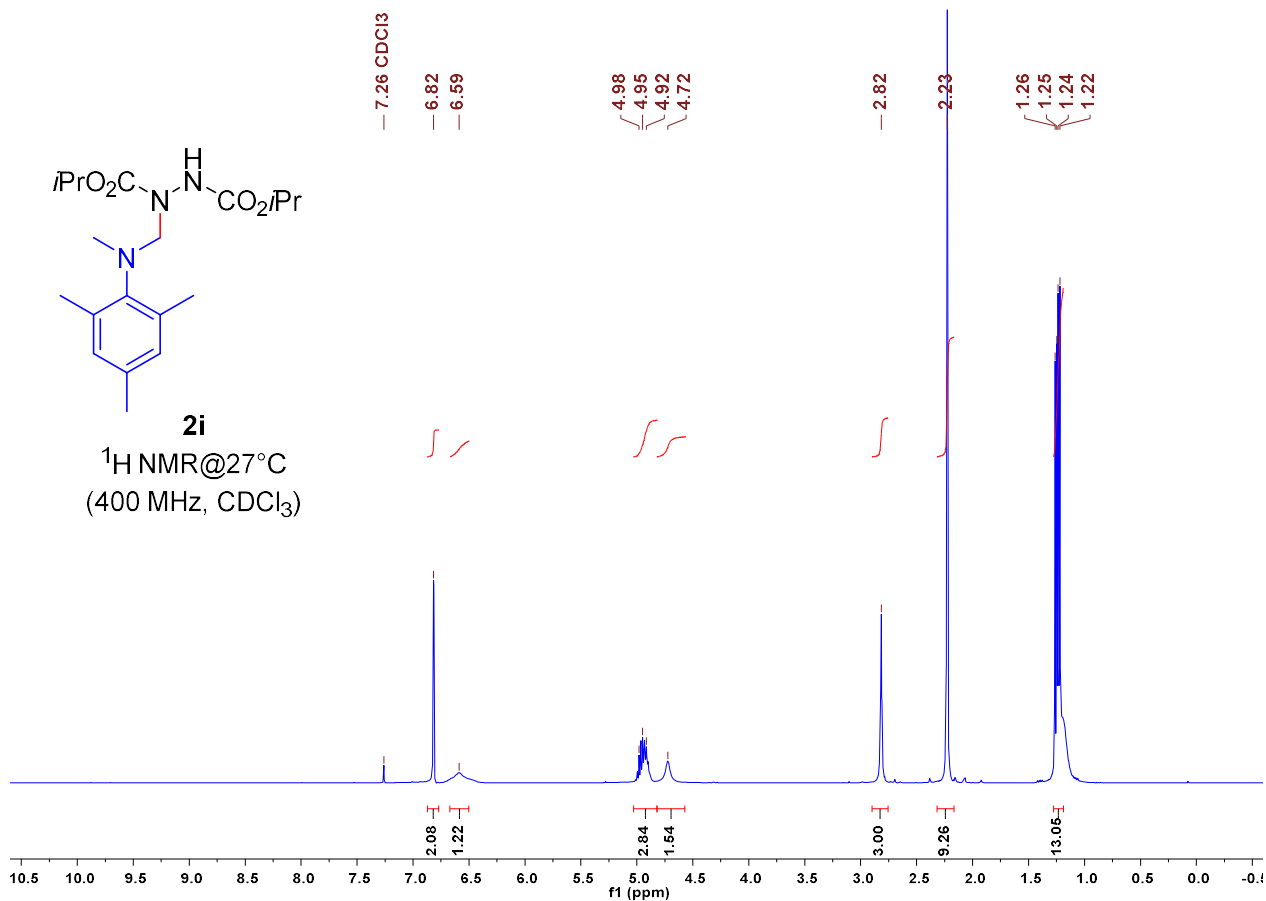


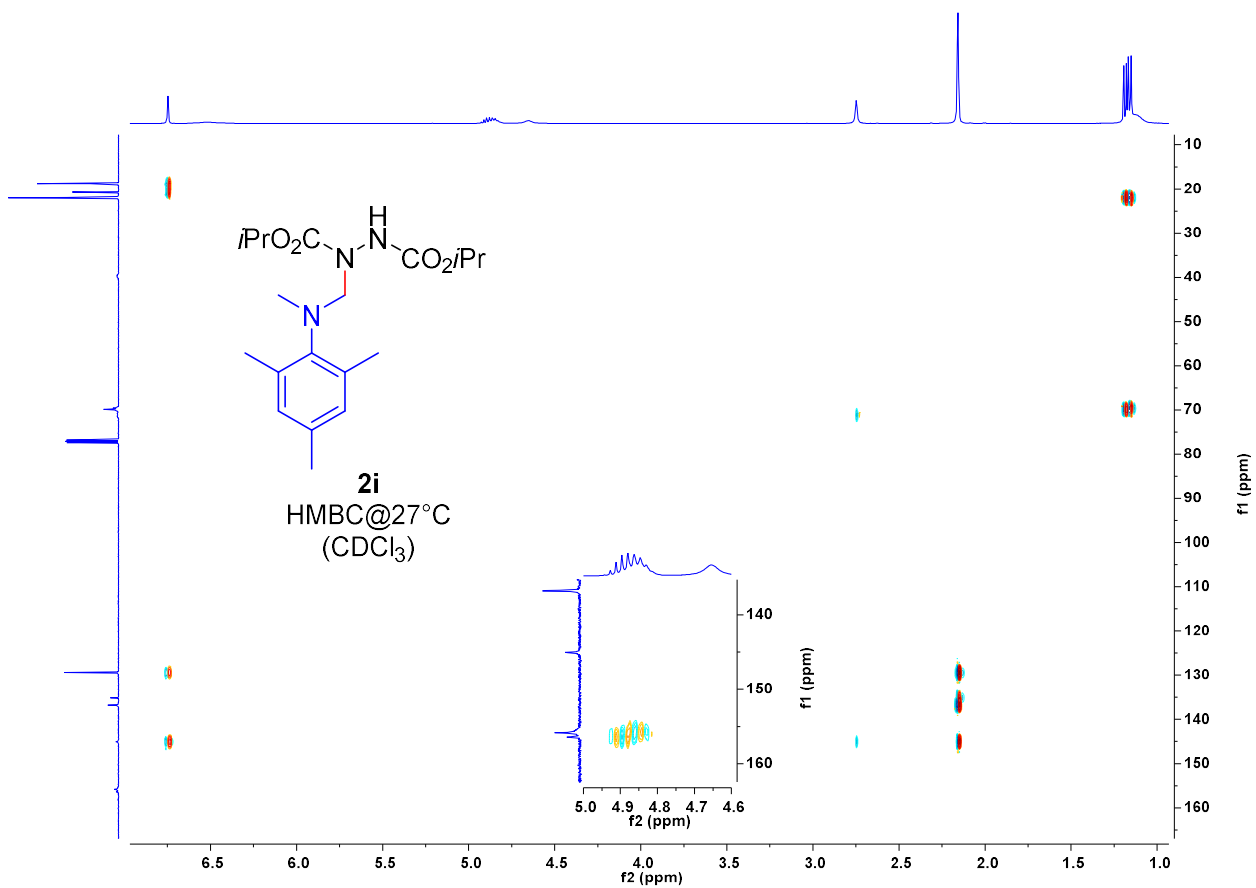
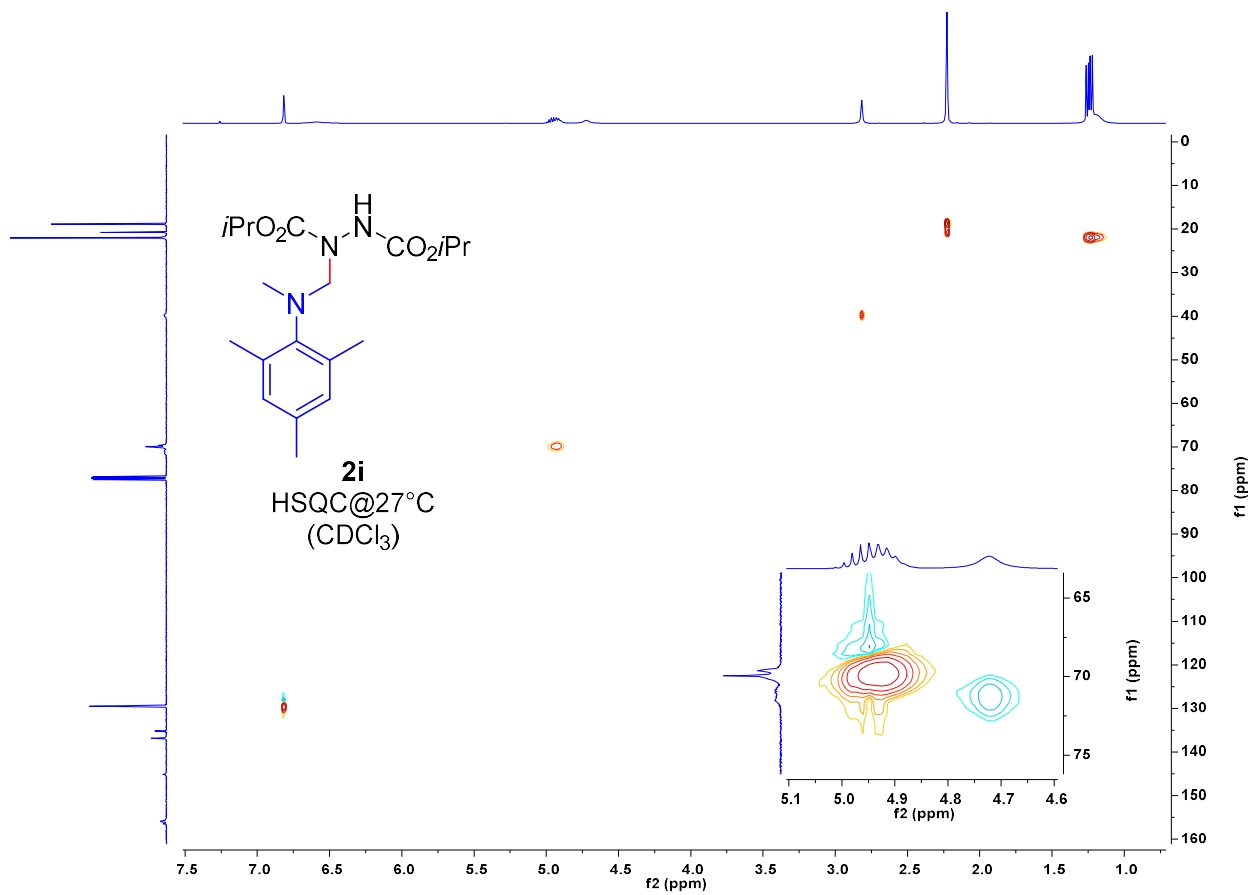


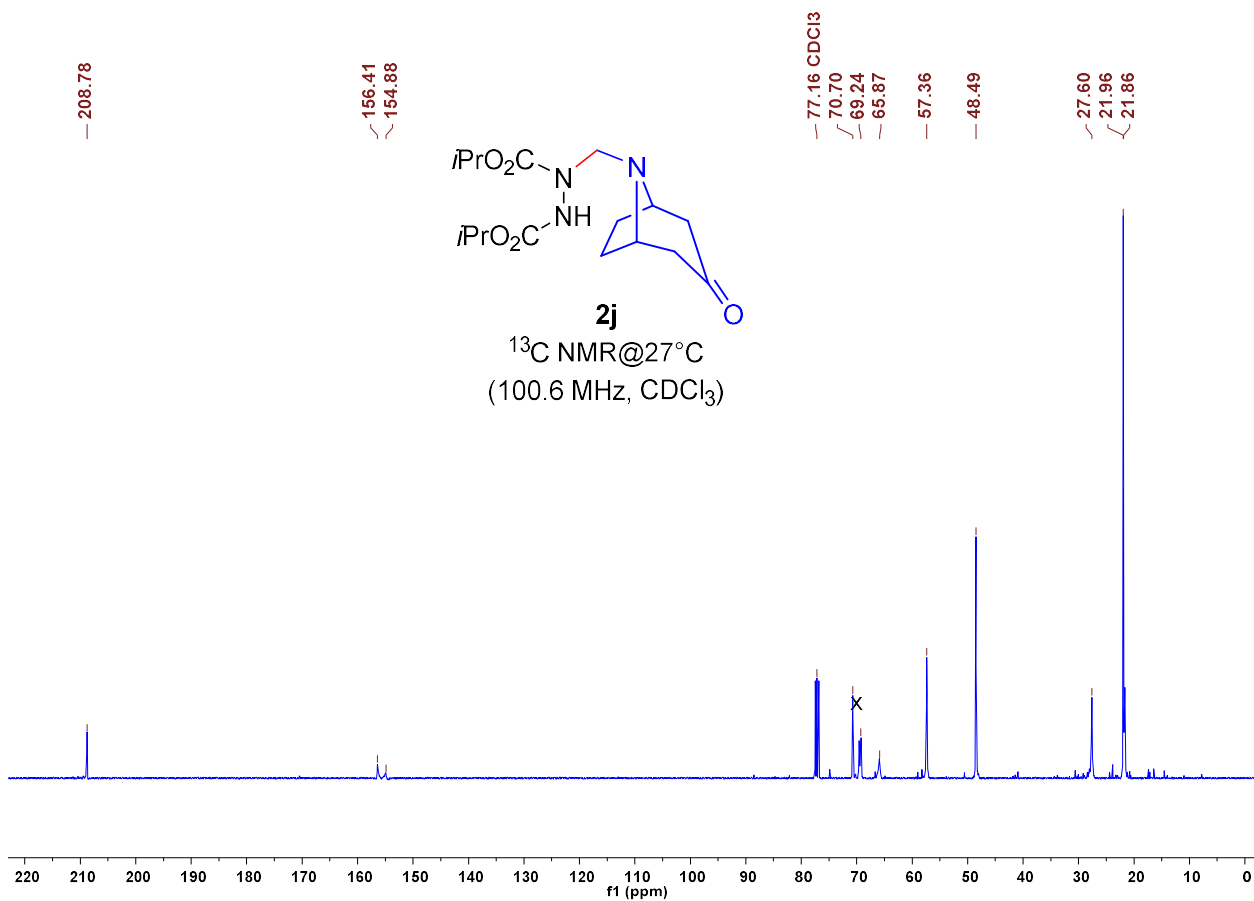
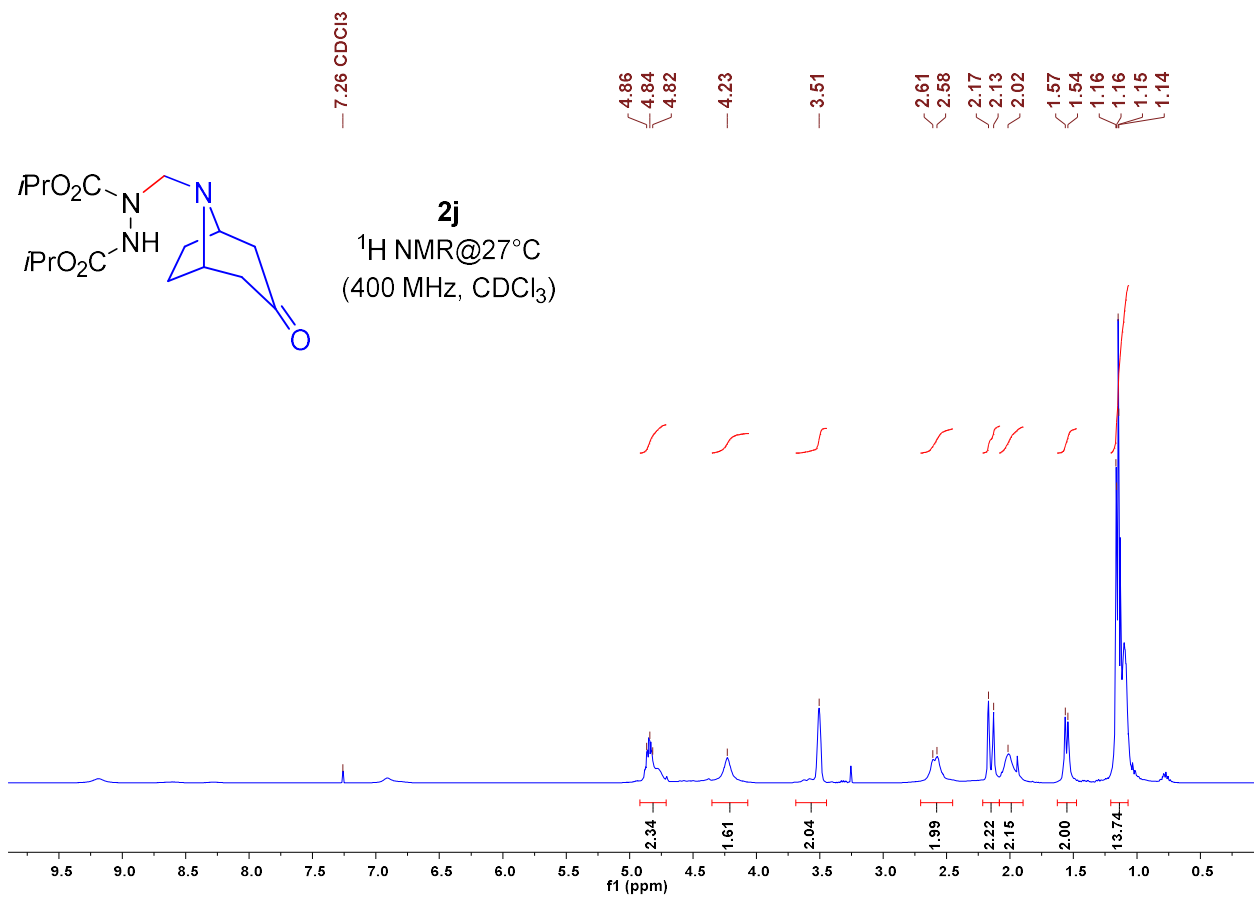


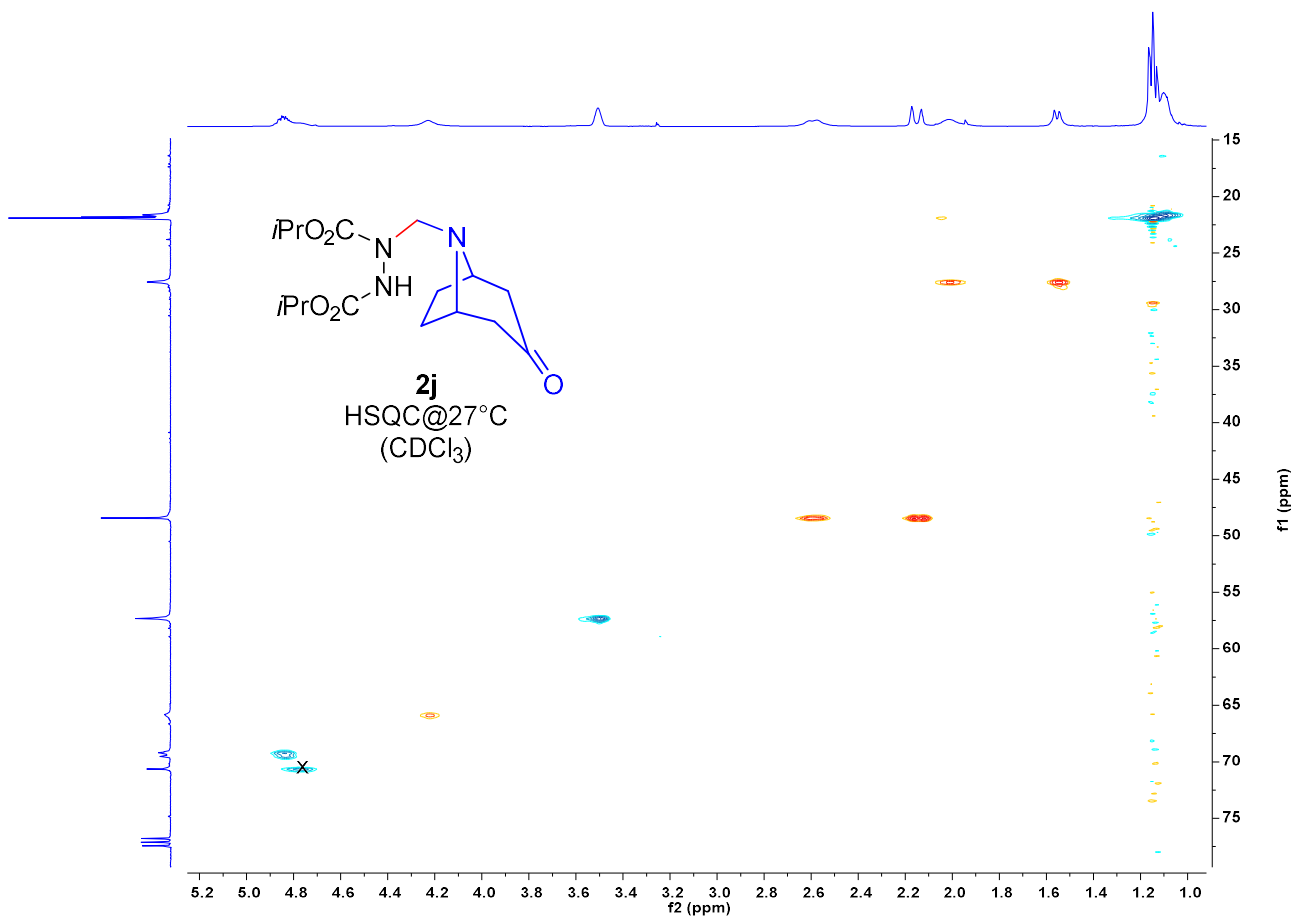


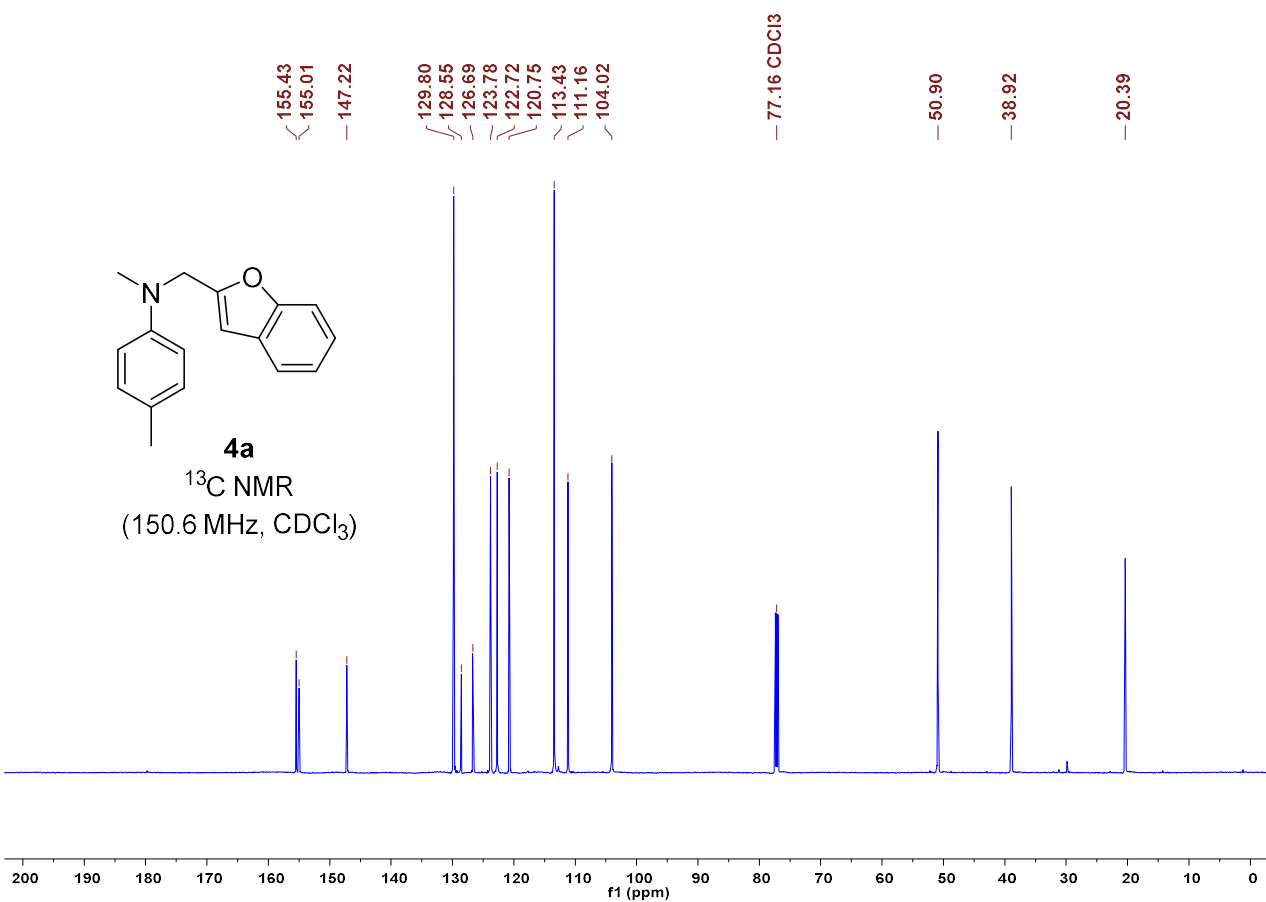
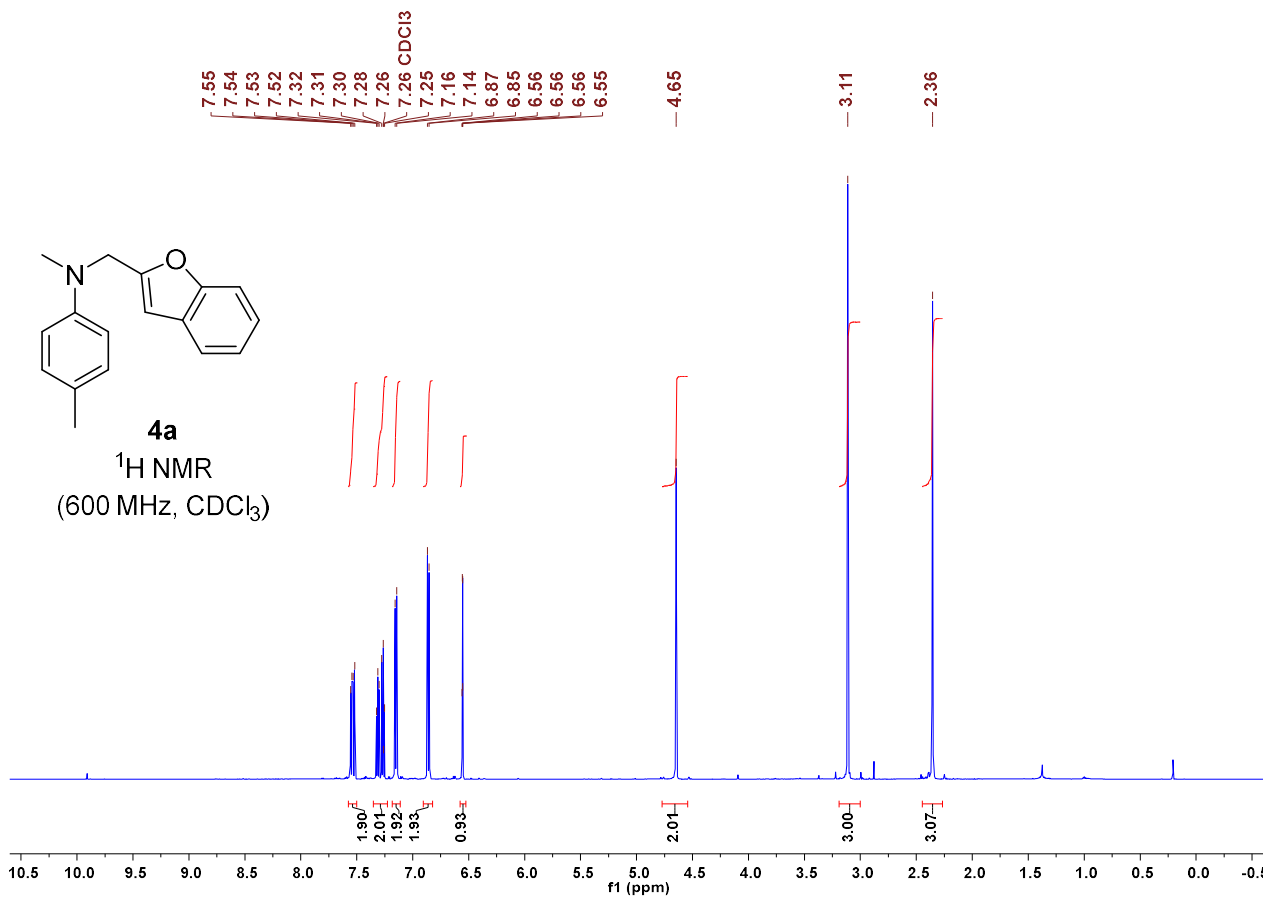


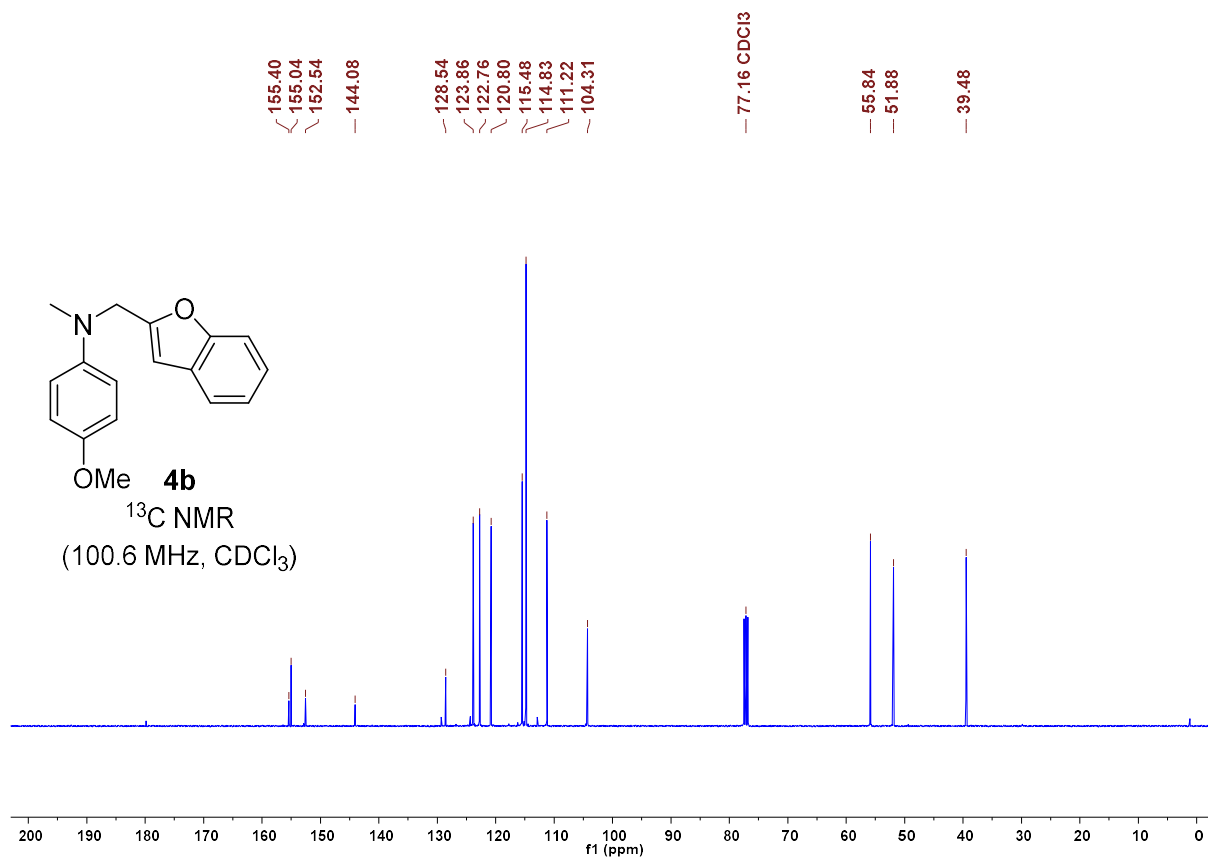
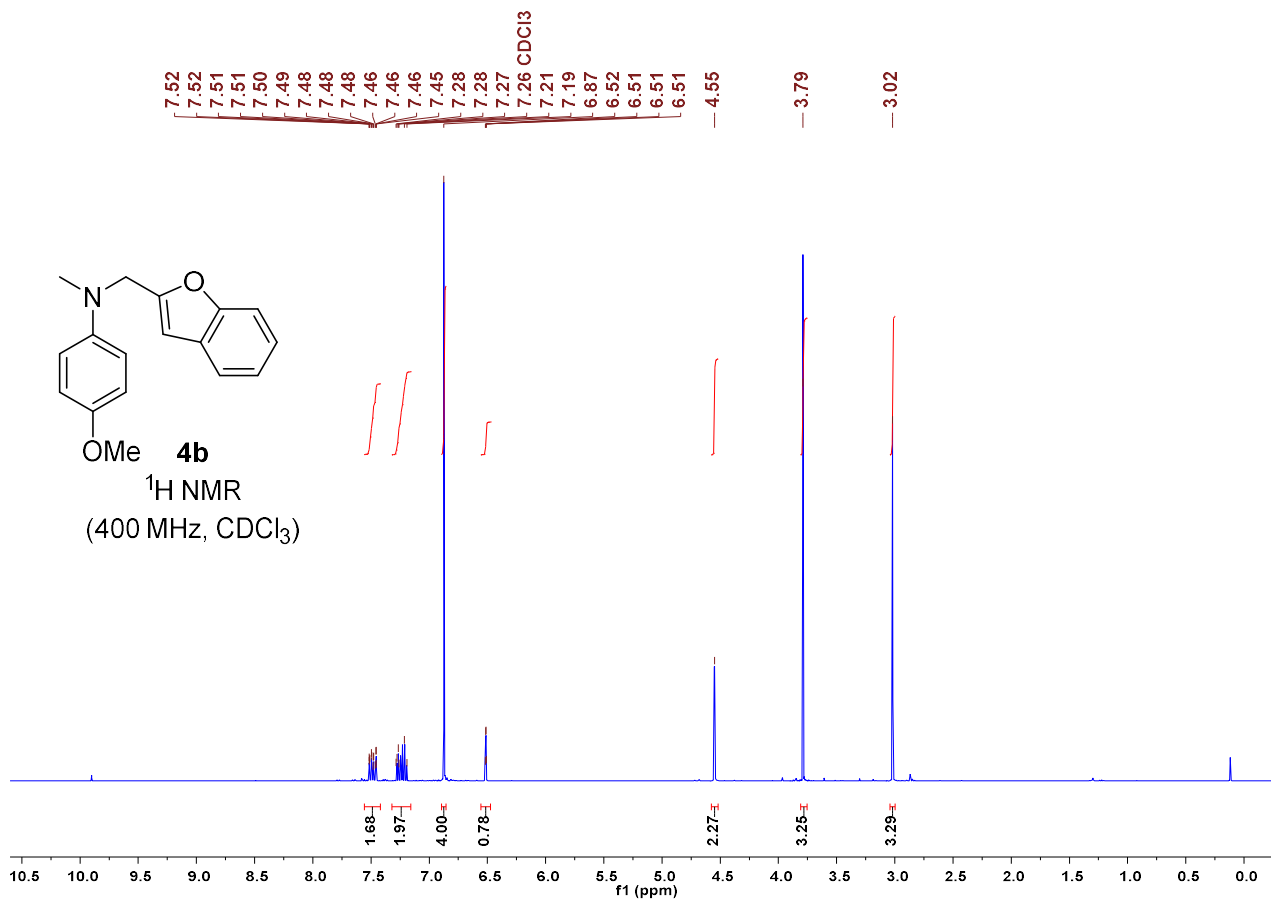


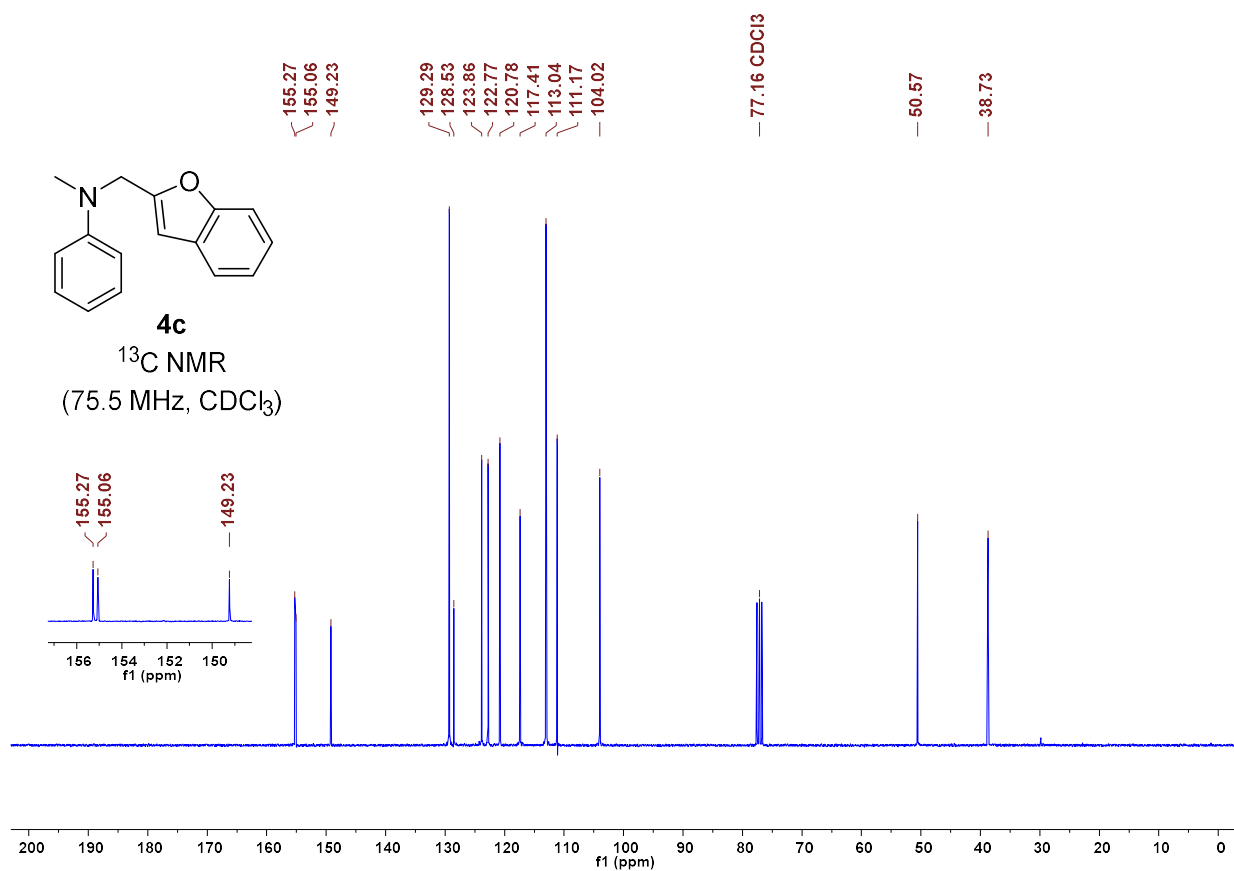
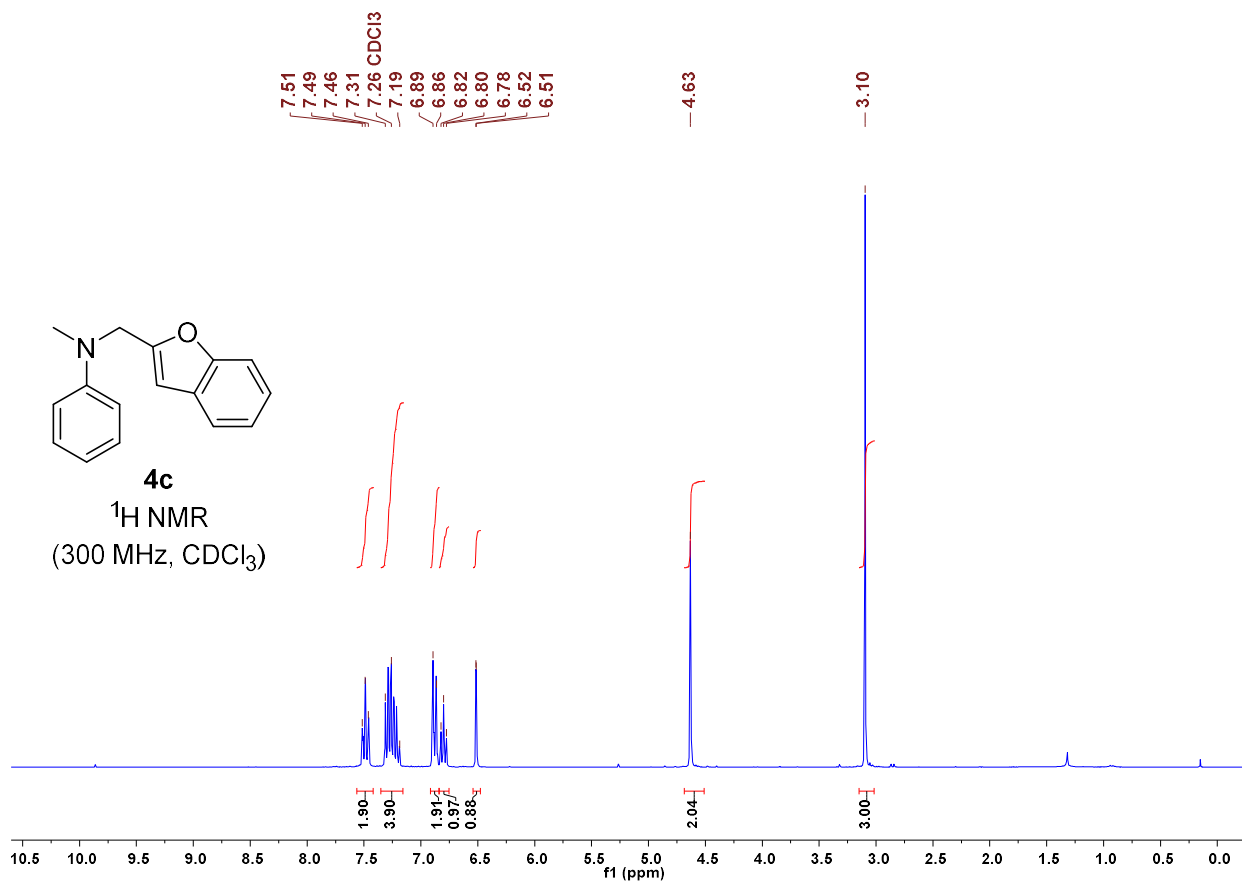


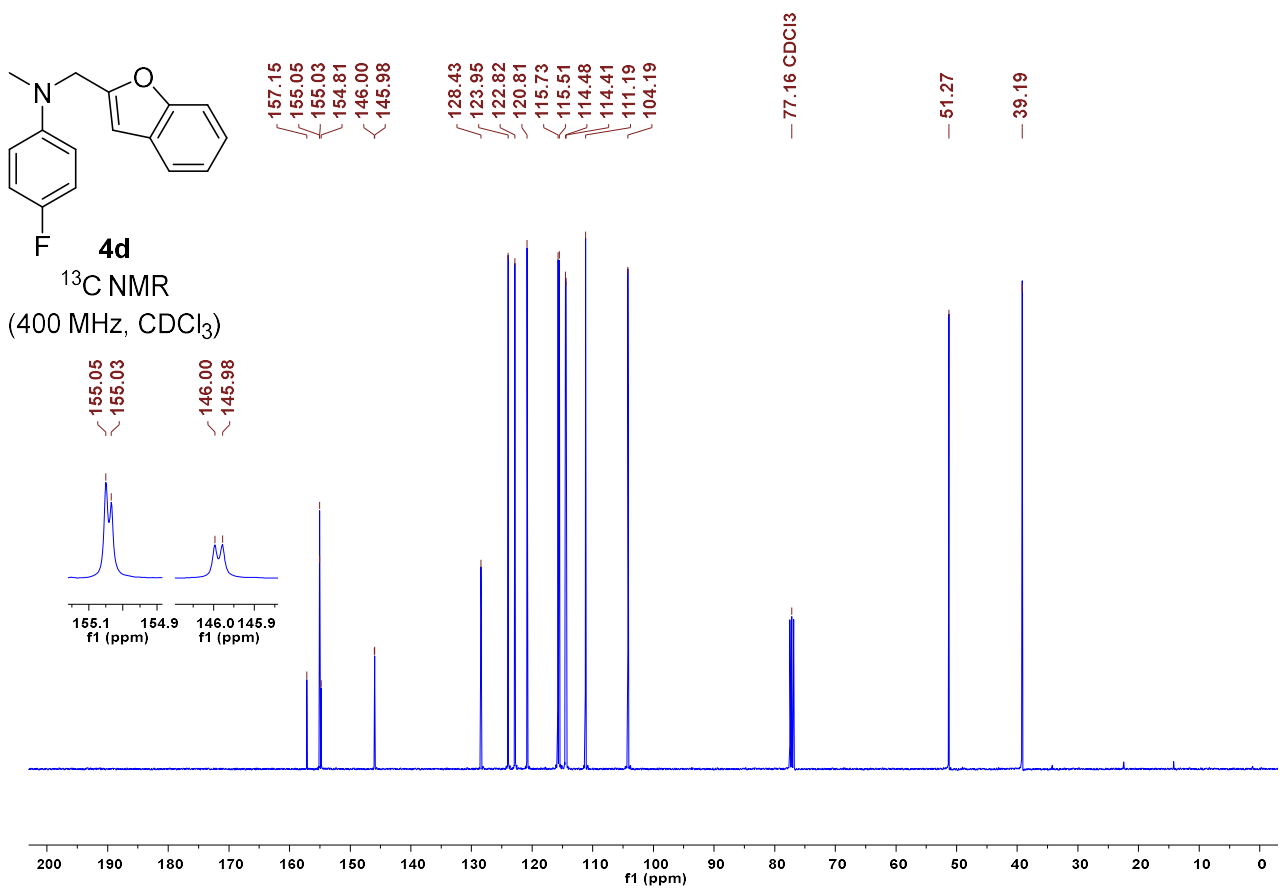
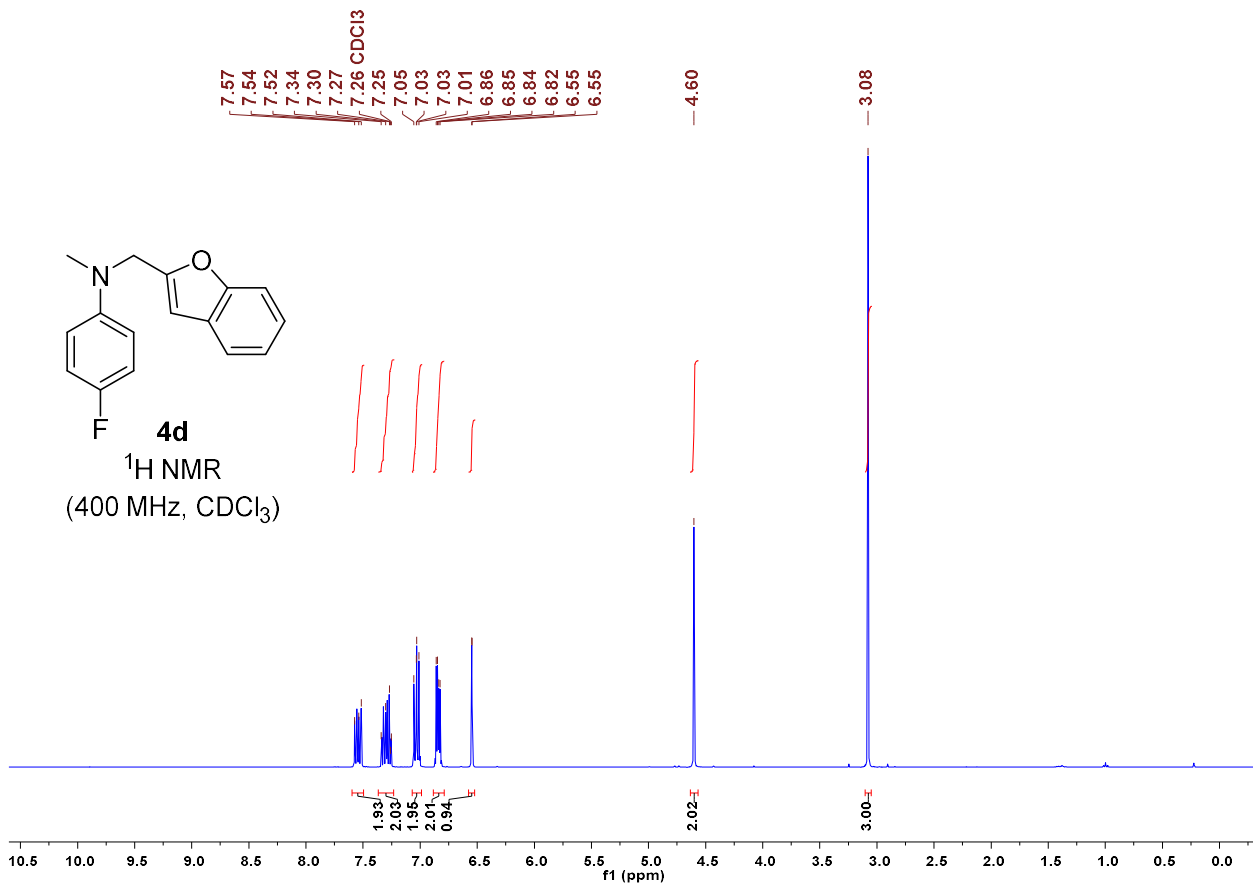


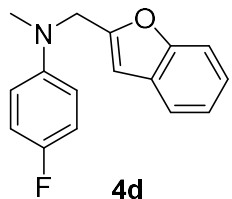




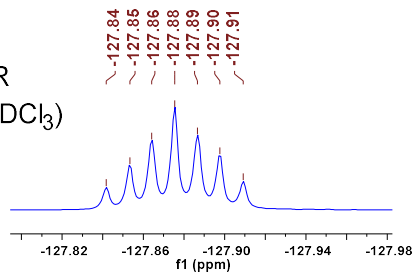




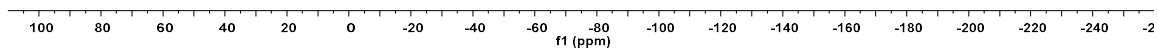


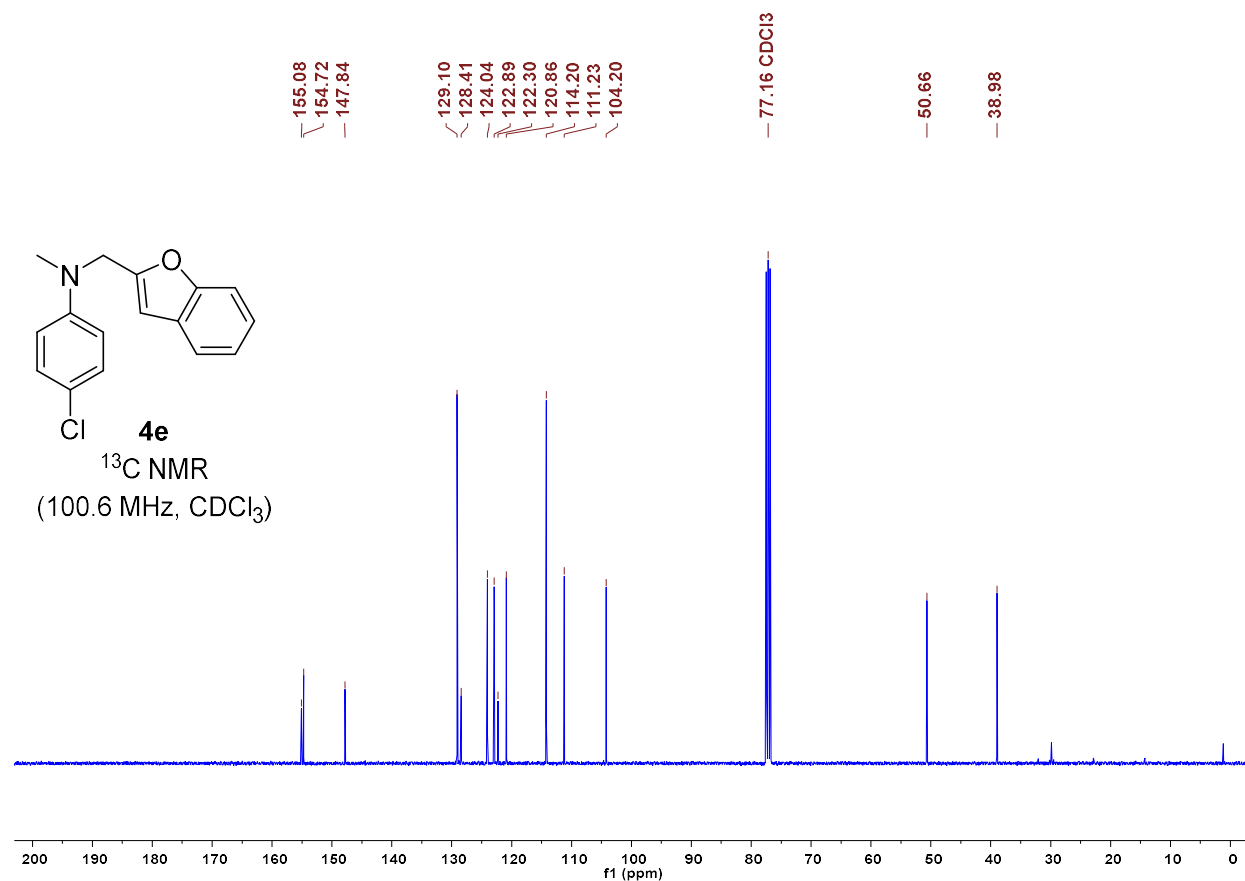
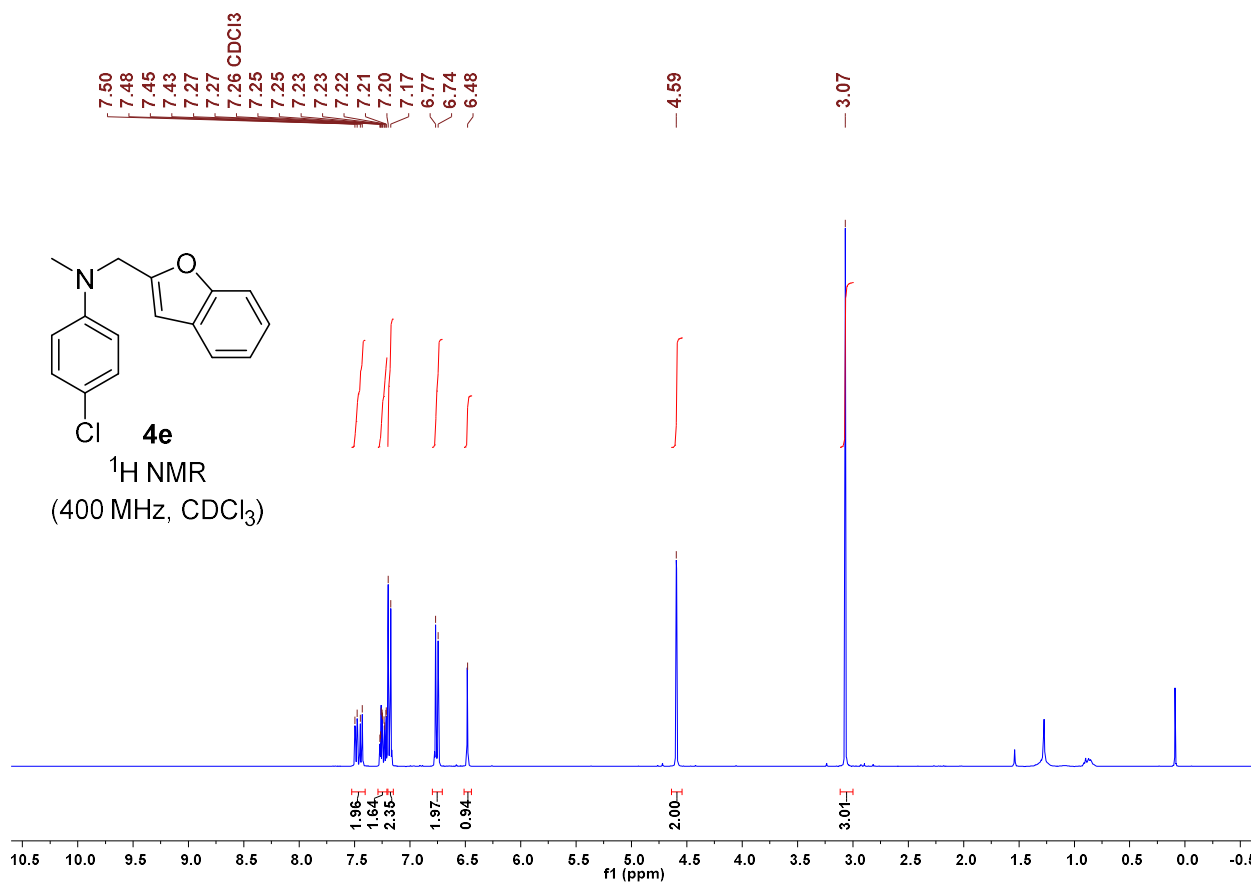


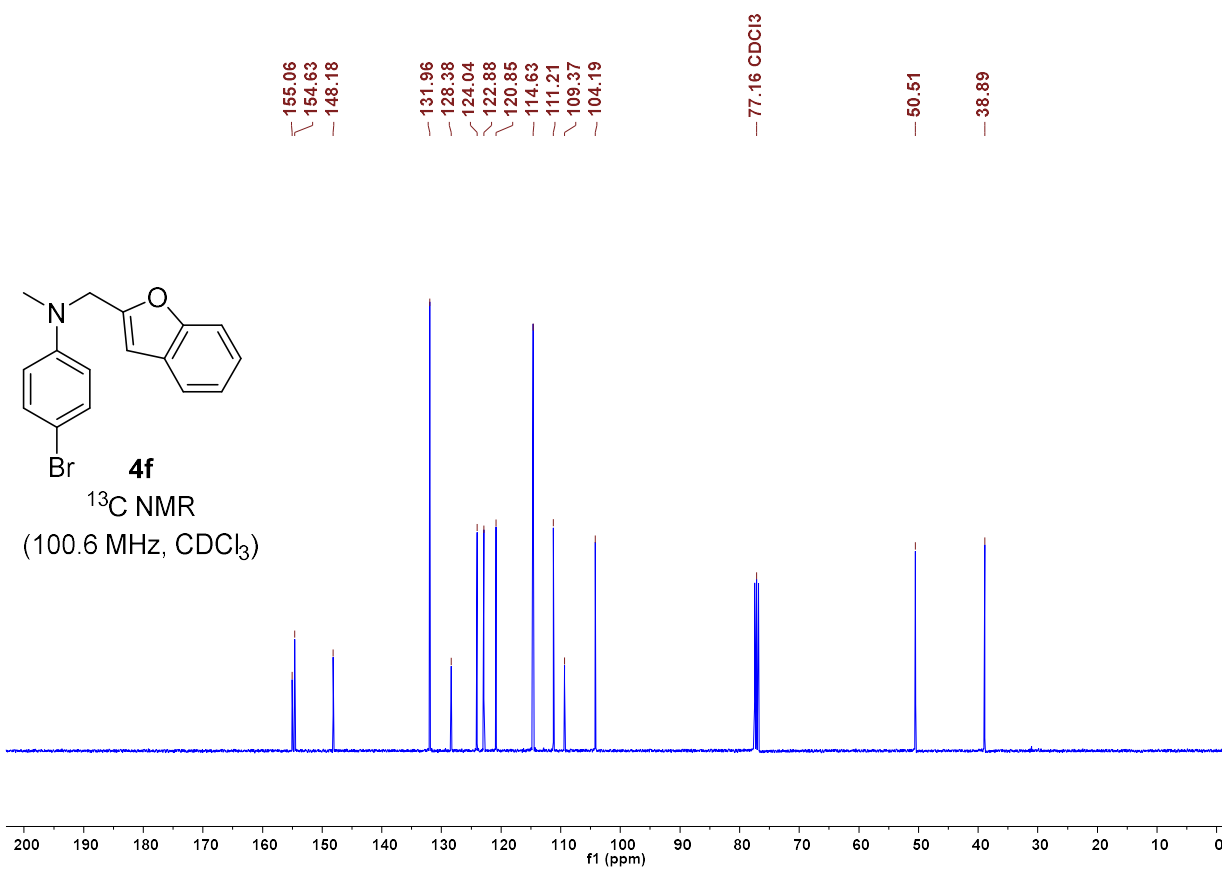
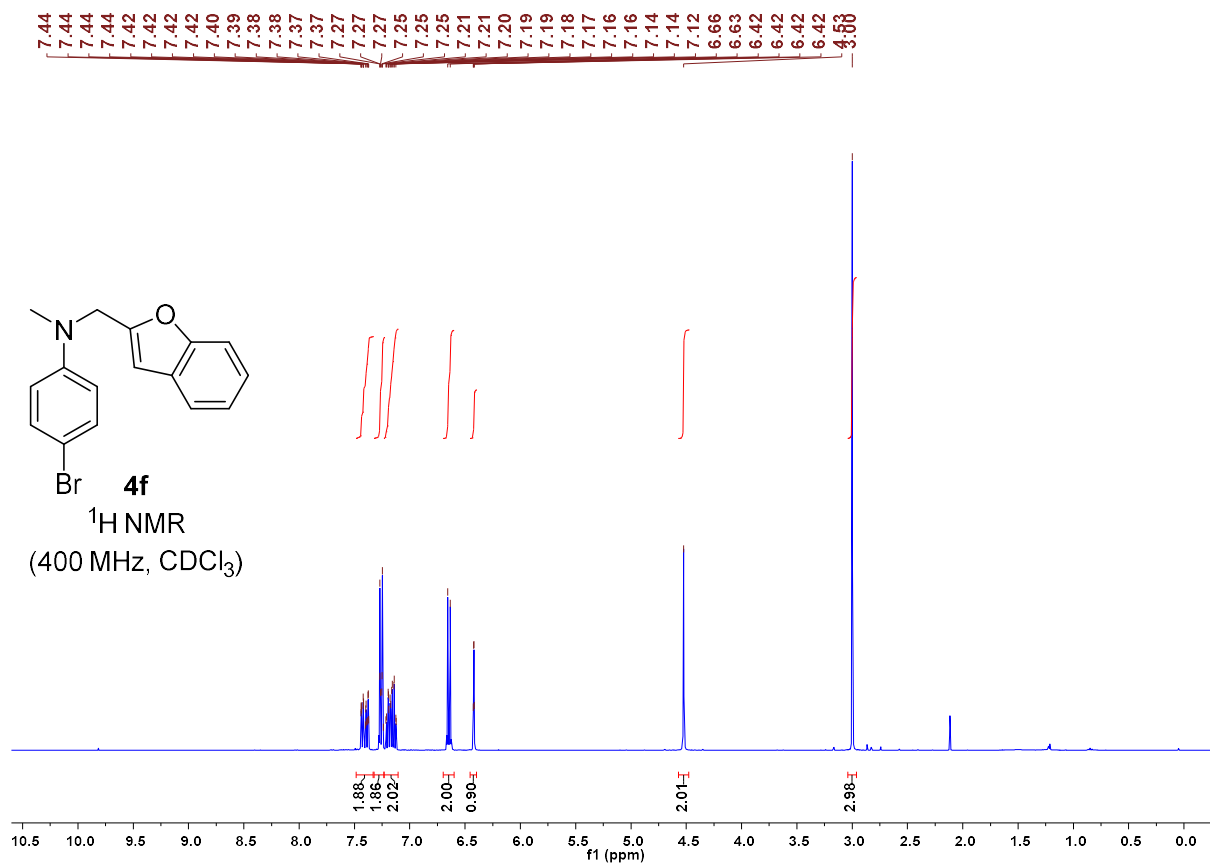
<sup>19</sup>F NMR  
(376 MHz, CDCl<sub>3</sub>)

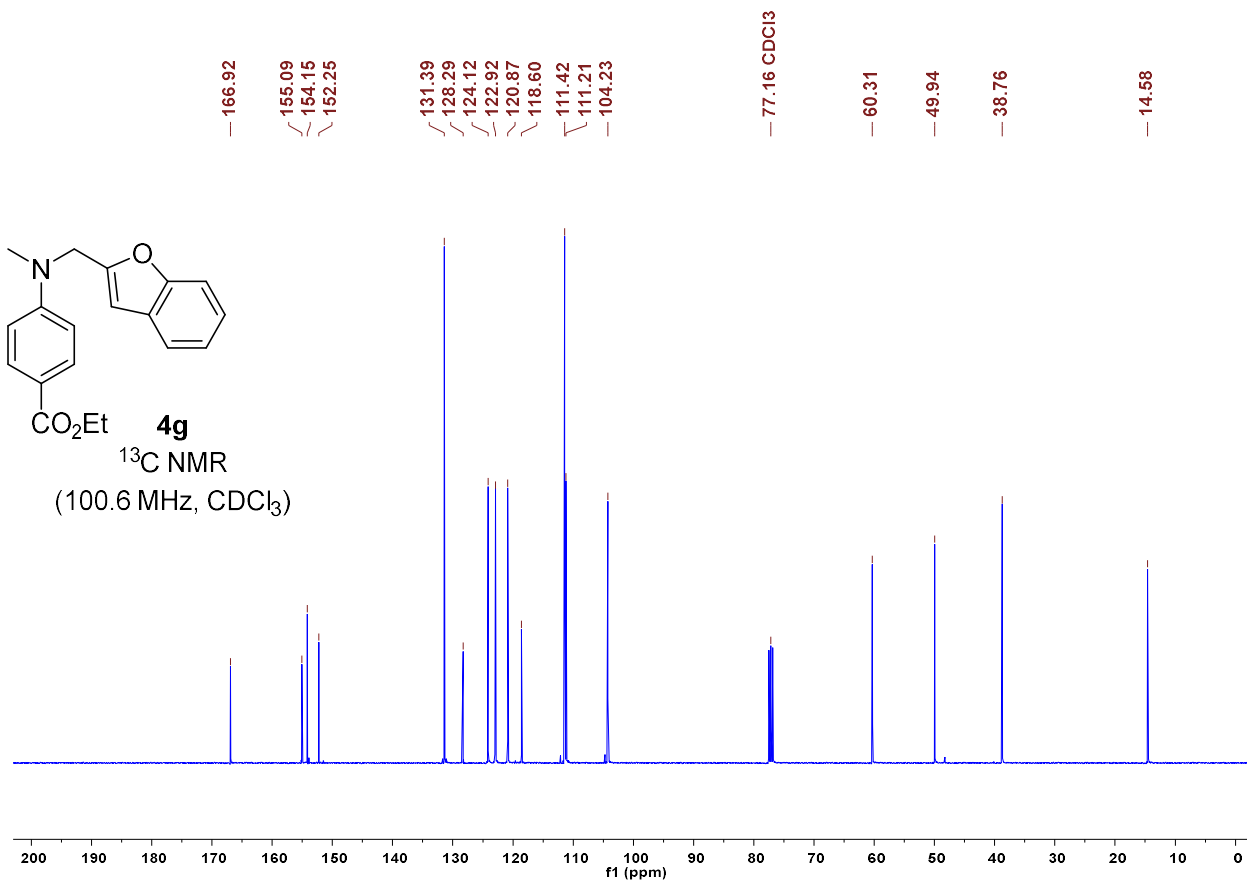
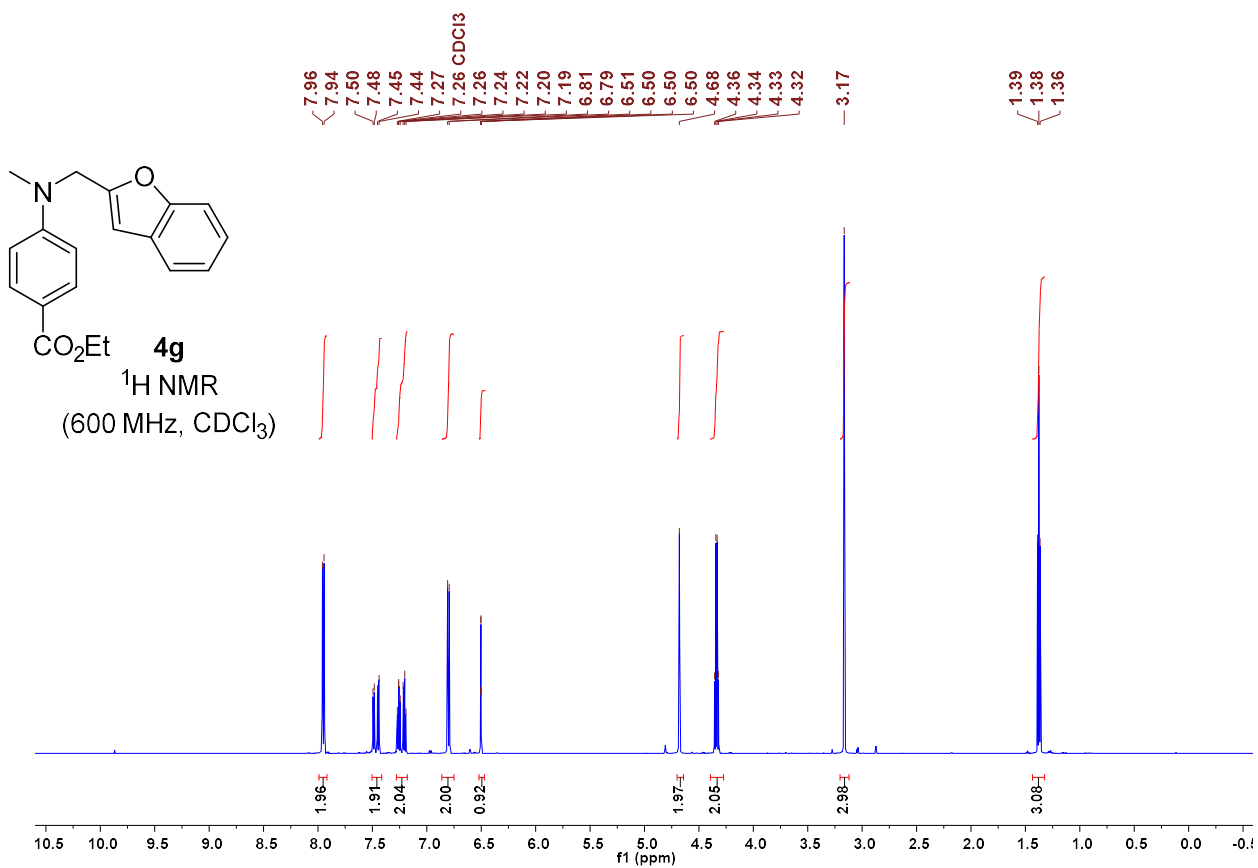


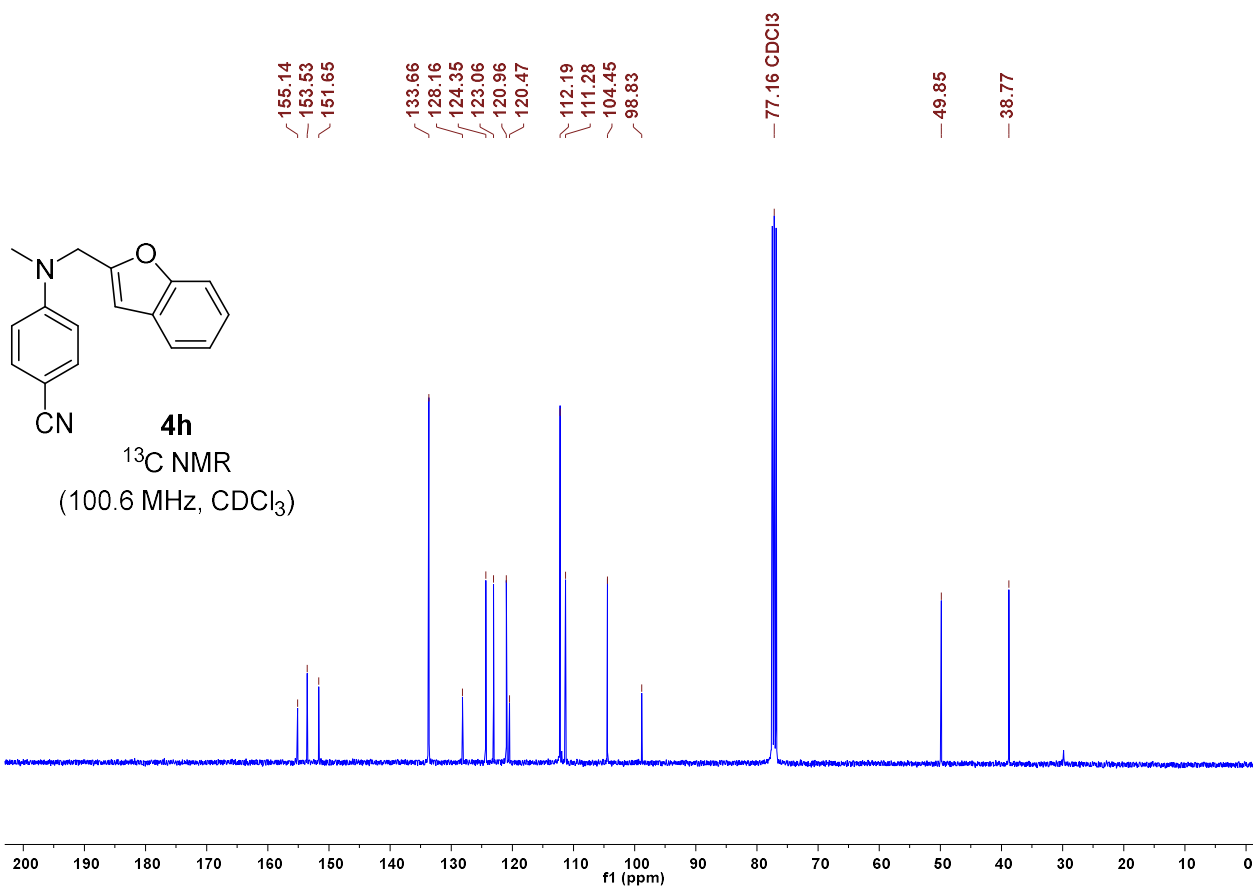
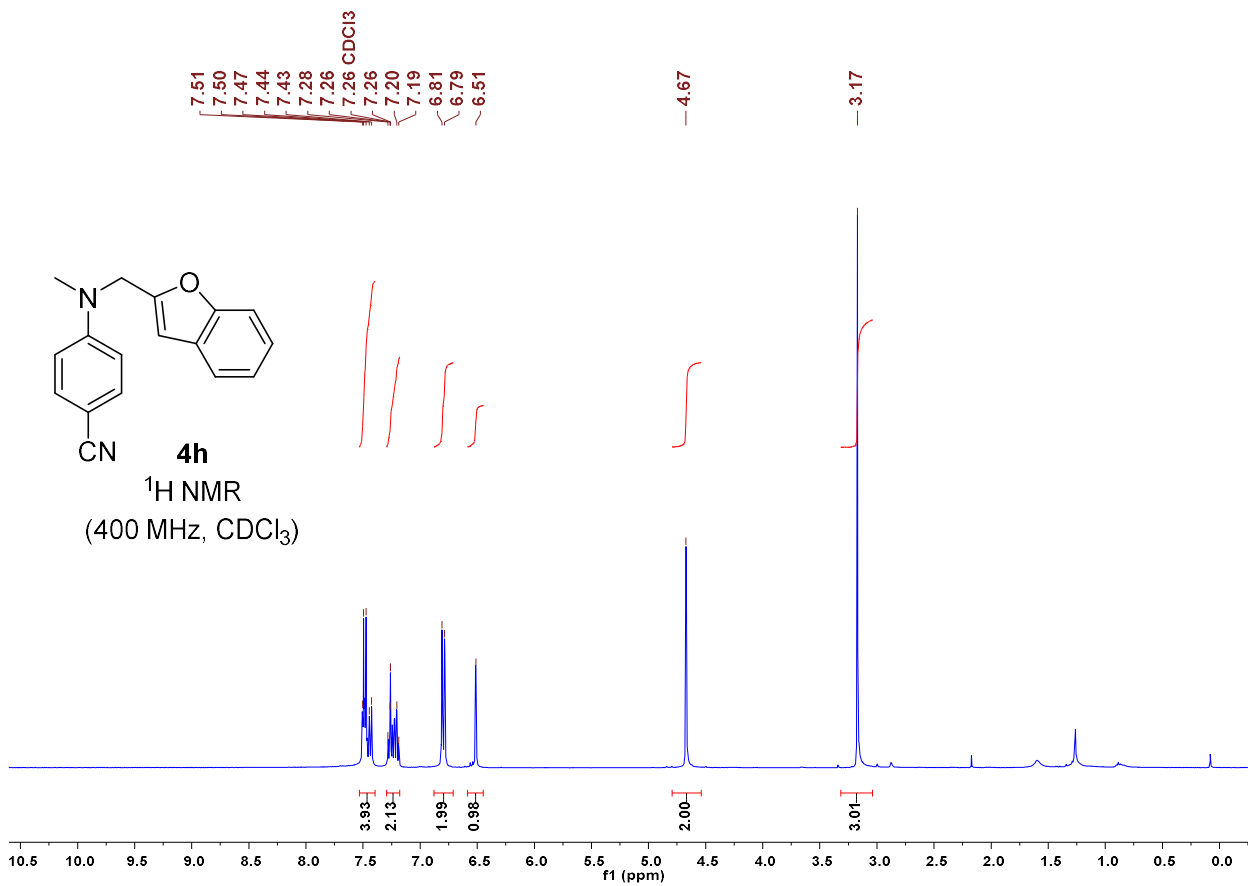
-127.84  
-127.85  
-127.86  
-127.88  
-127.89  
-127.90  
-127.91

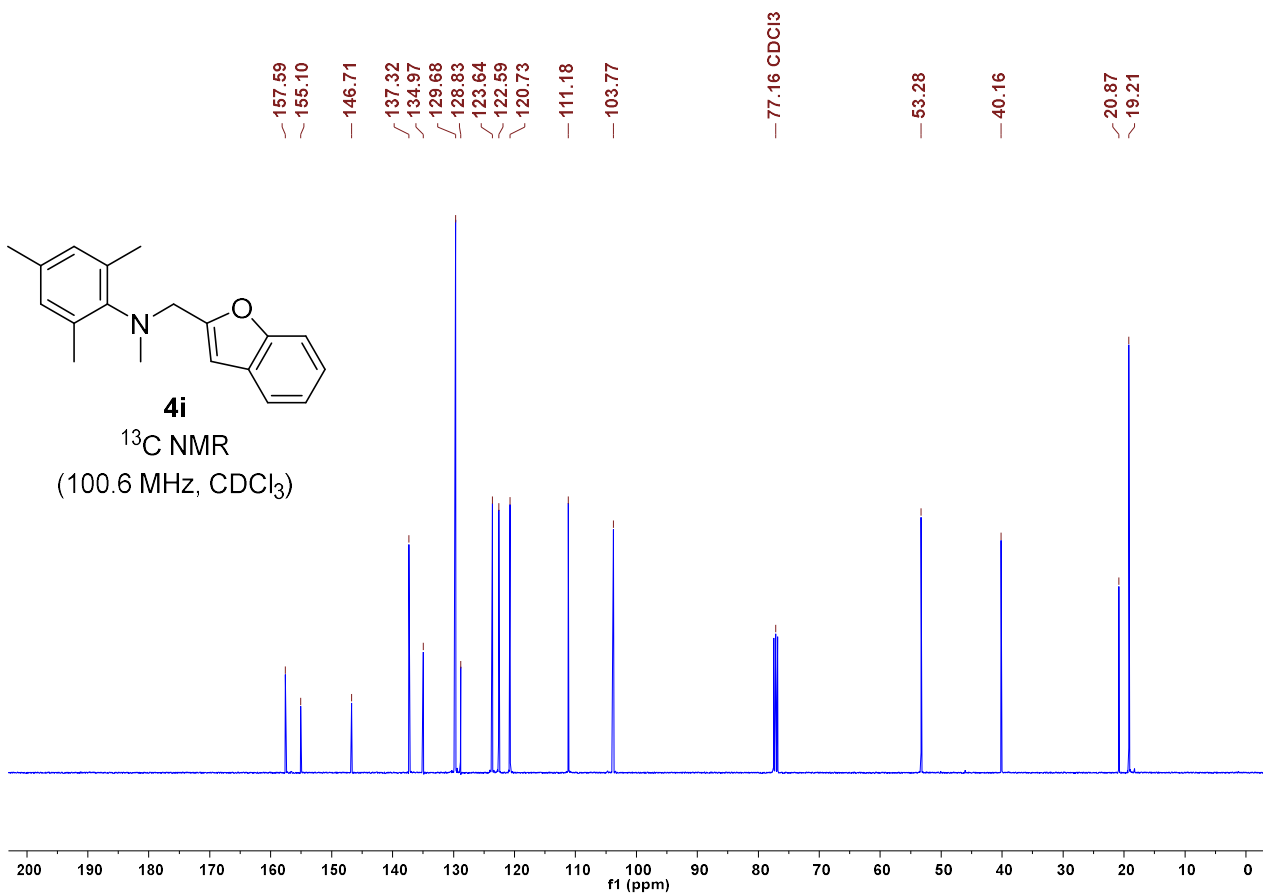
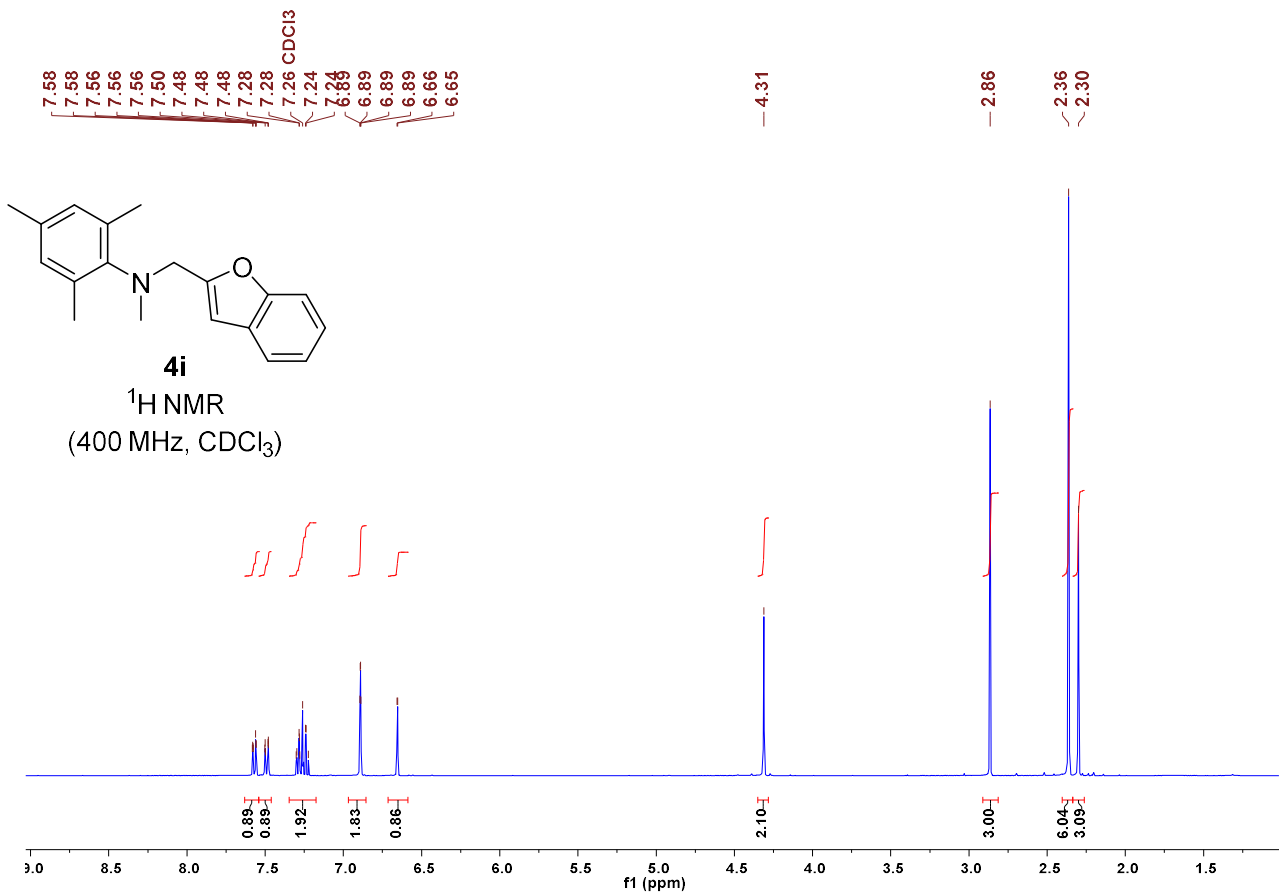


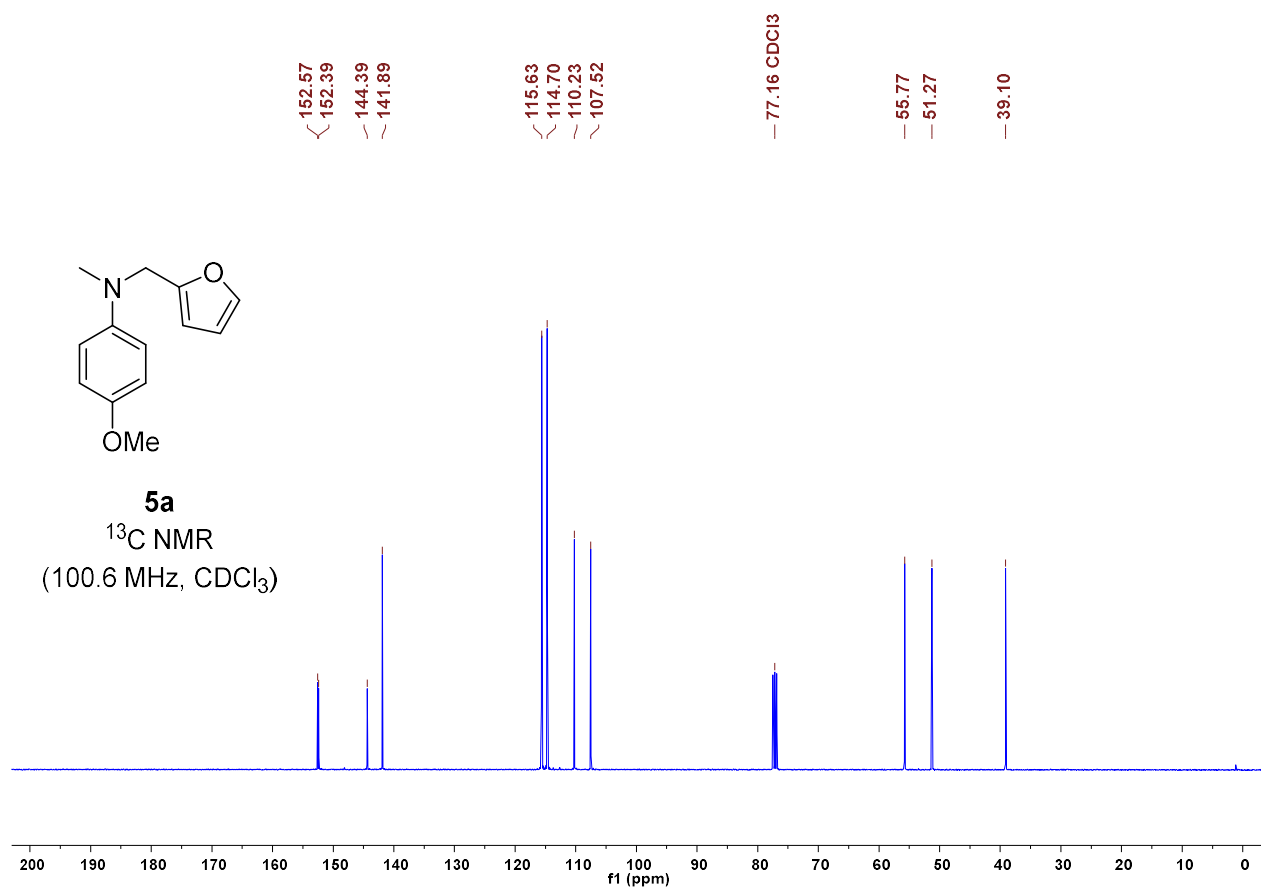
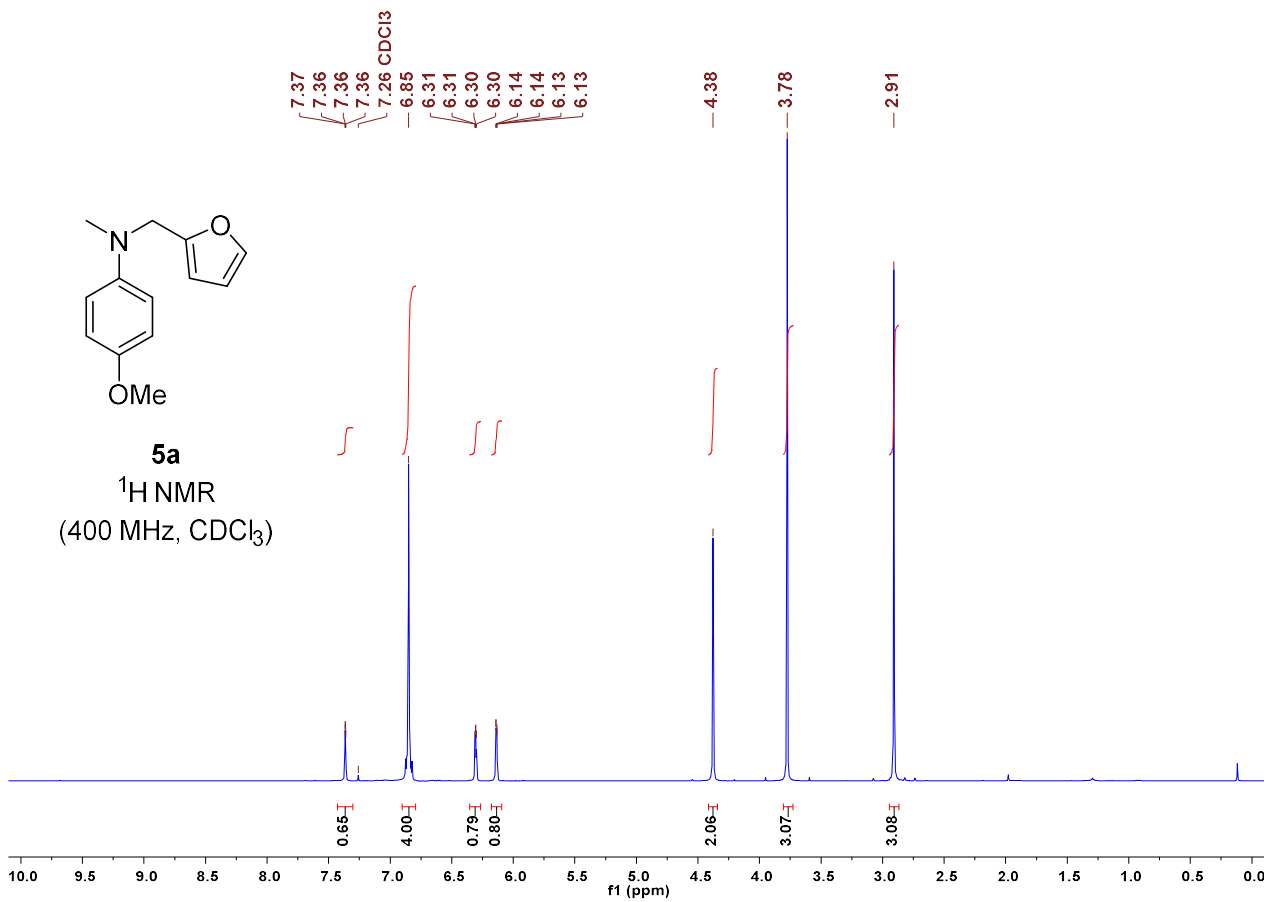


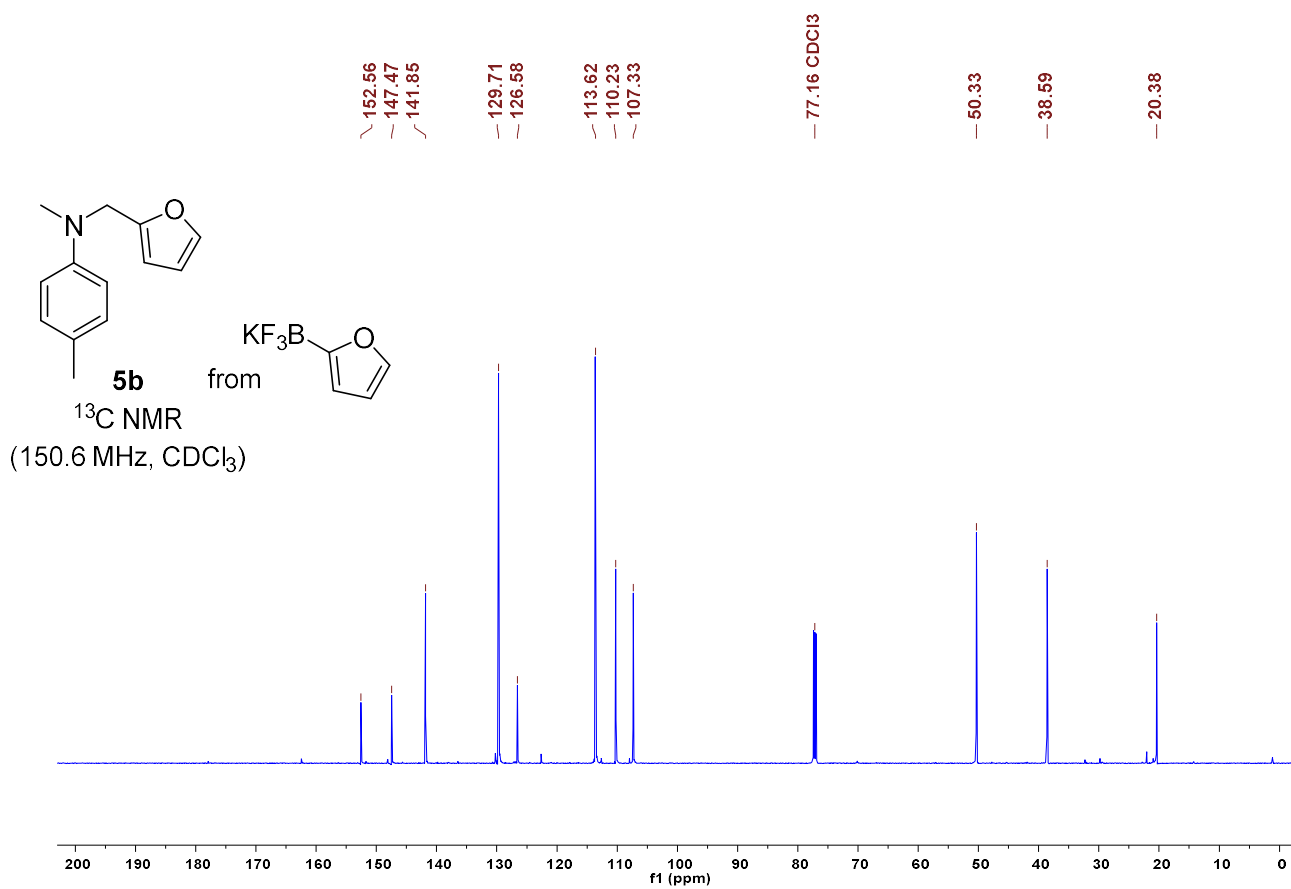
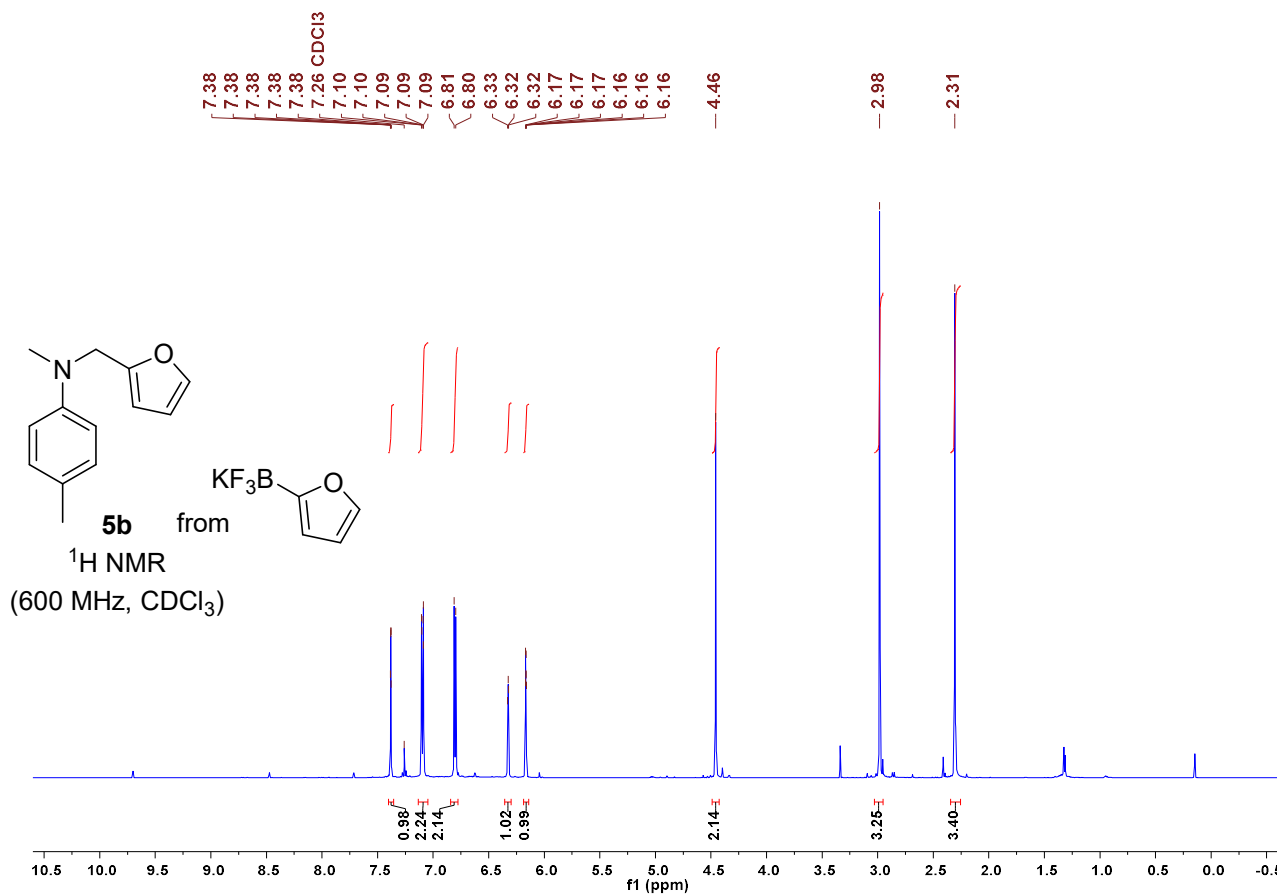


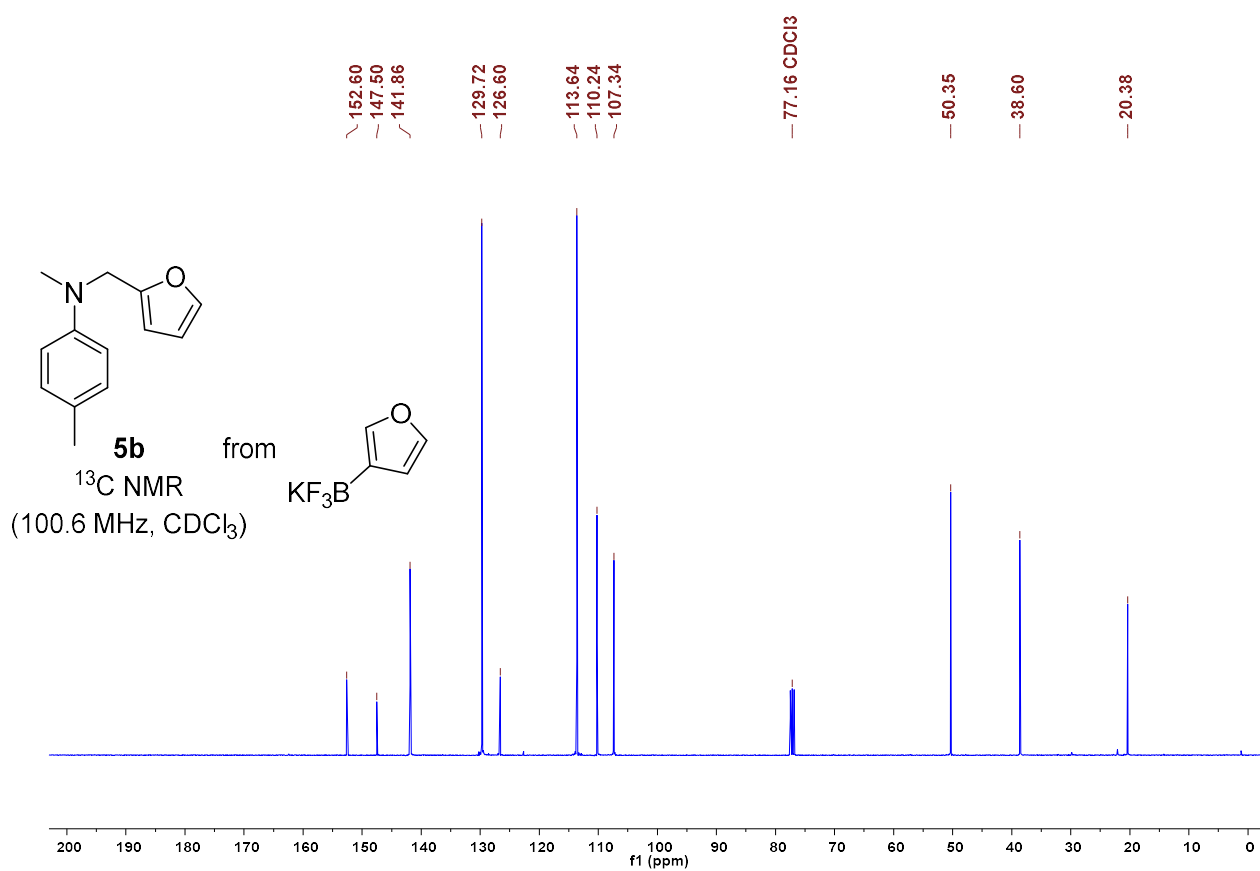
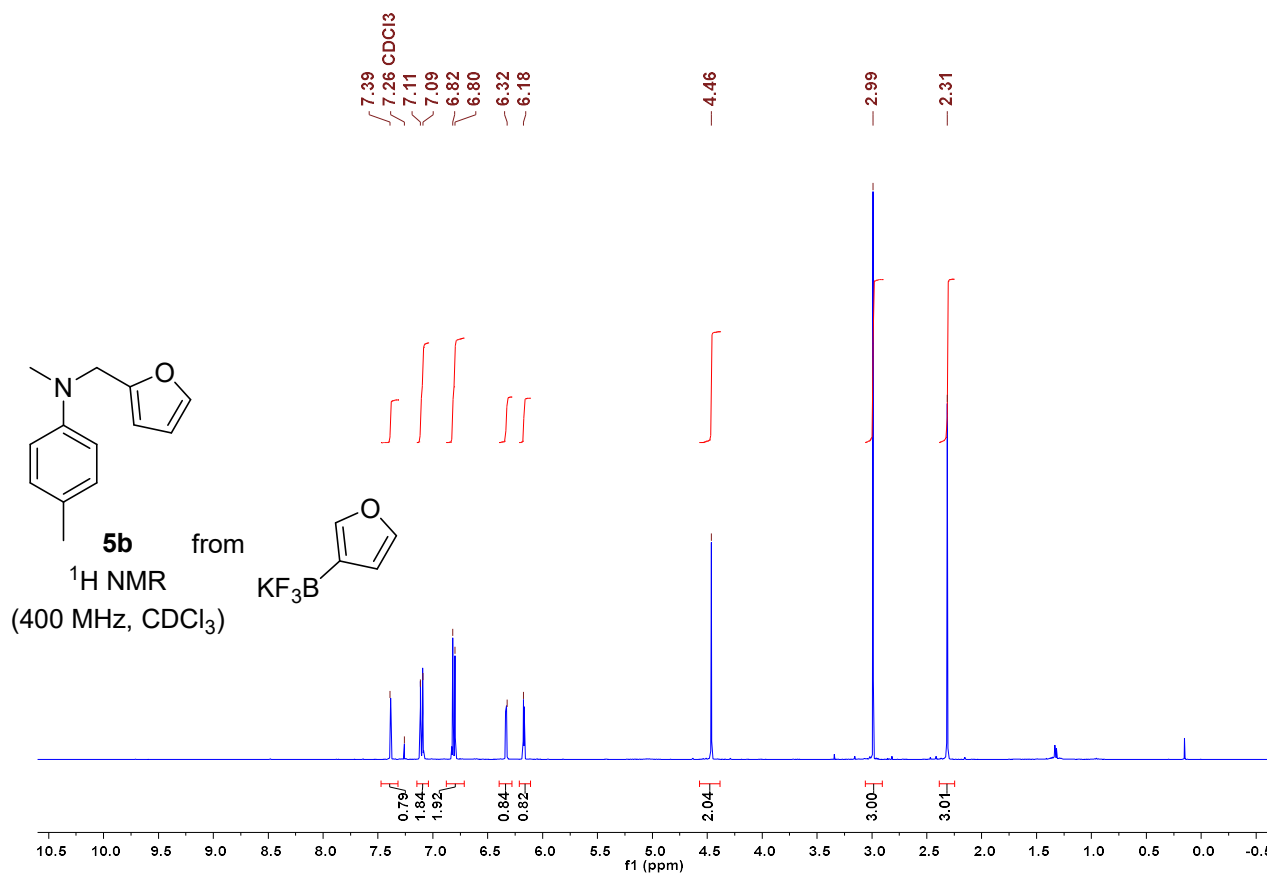


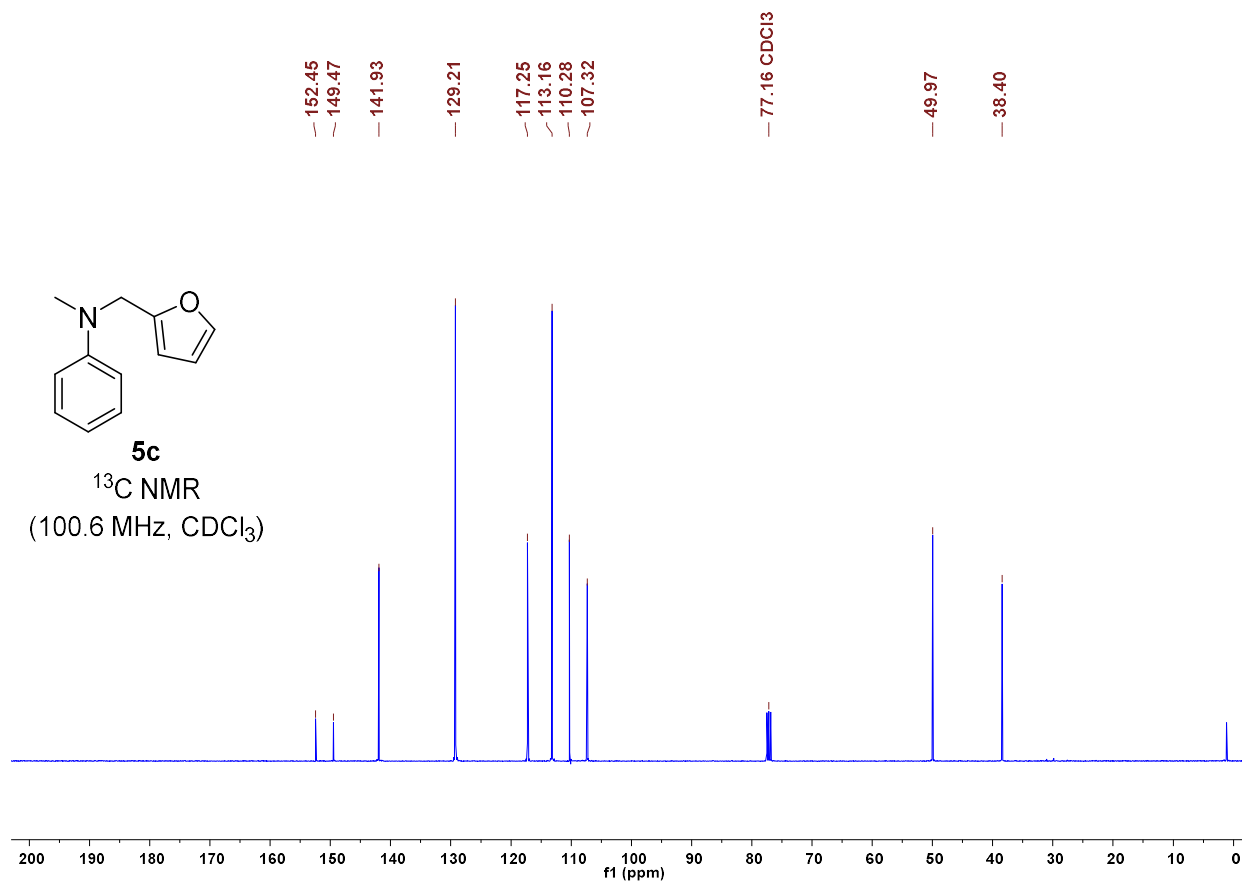
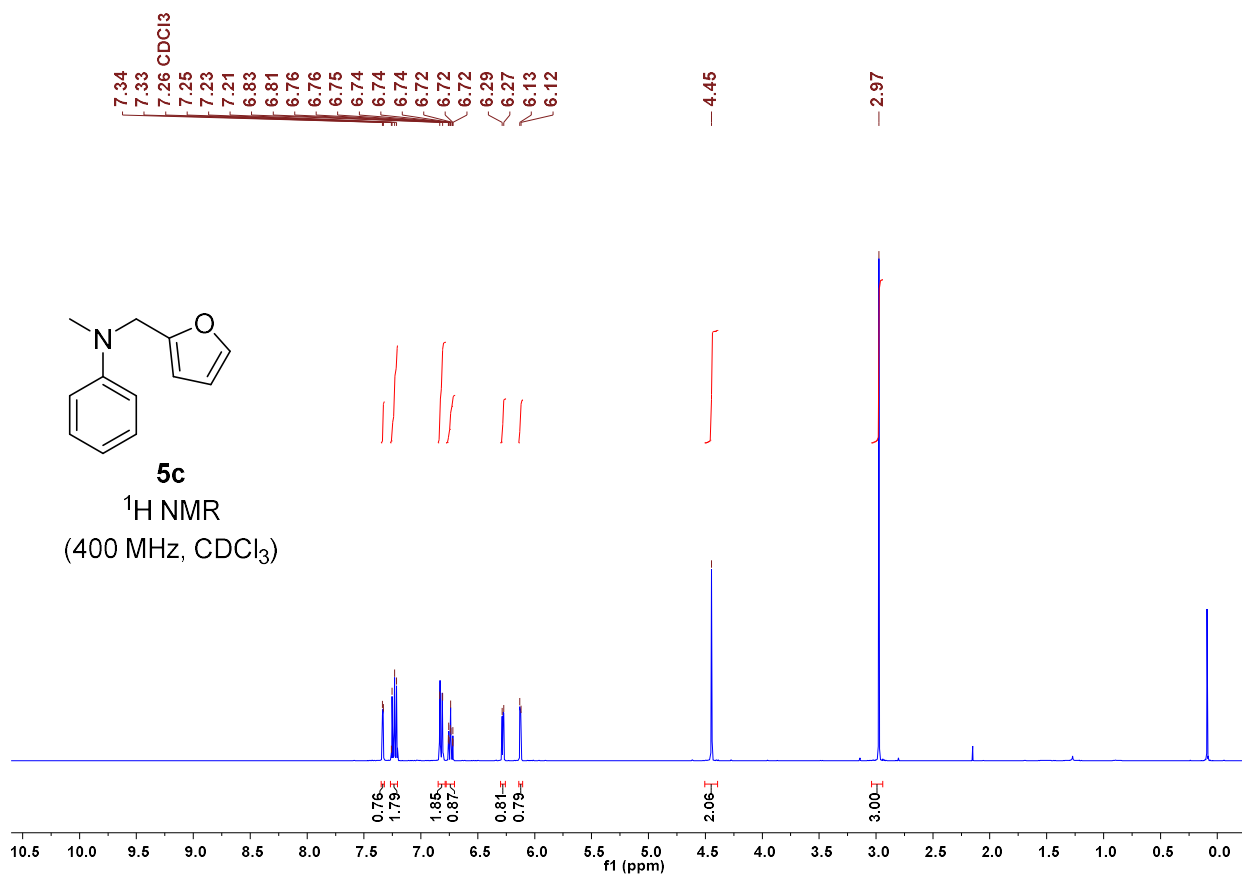


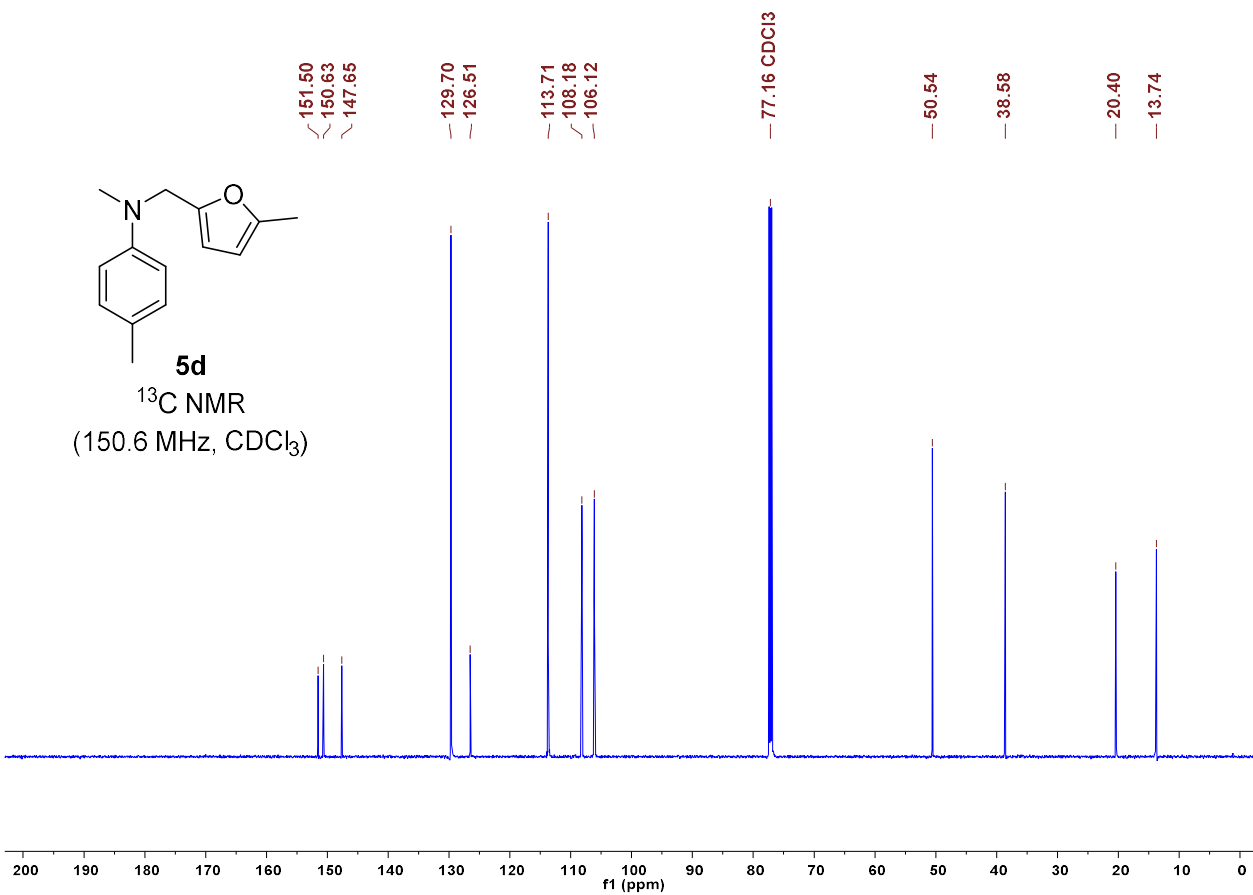
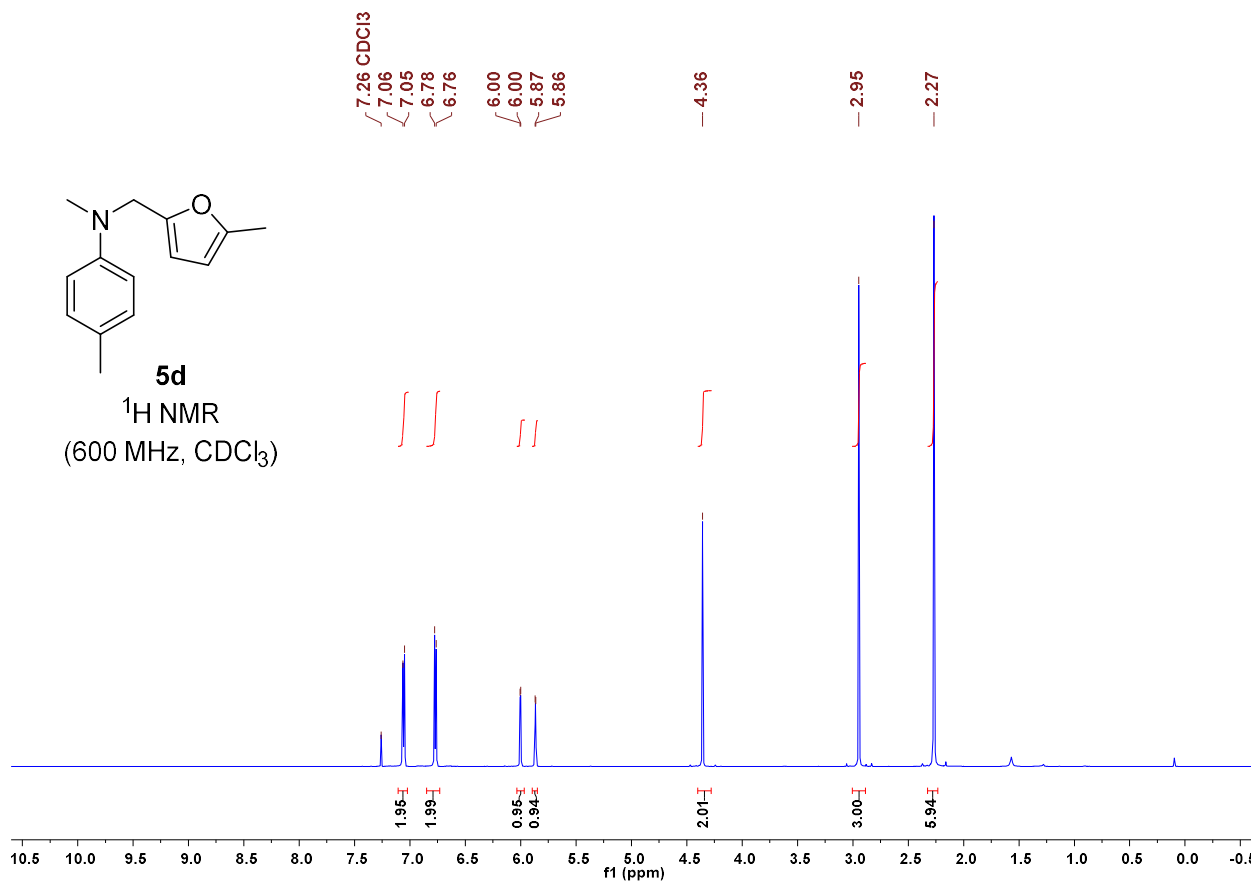


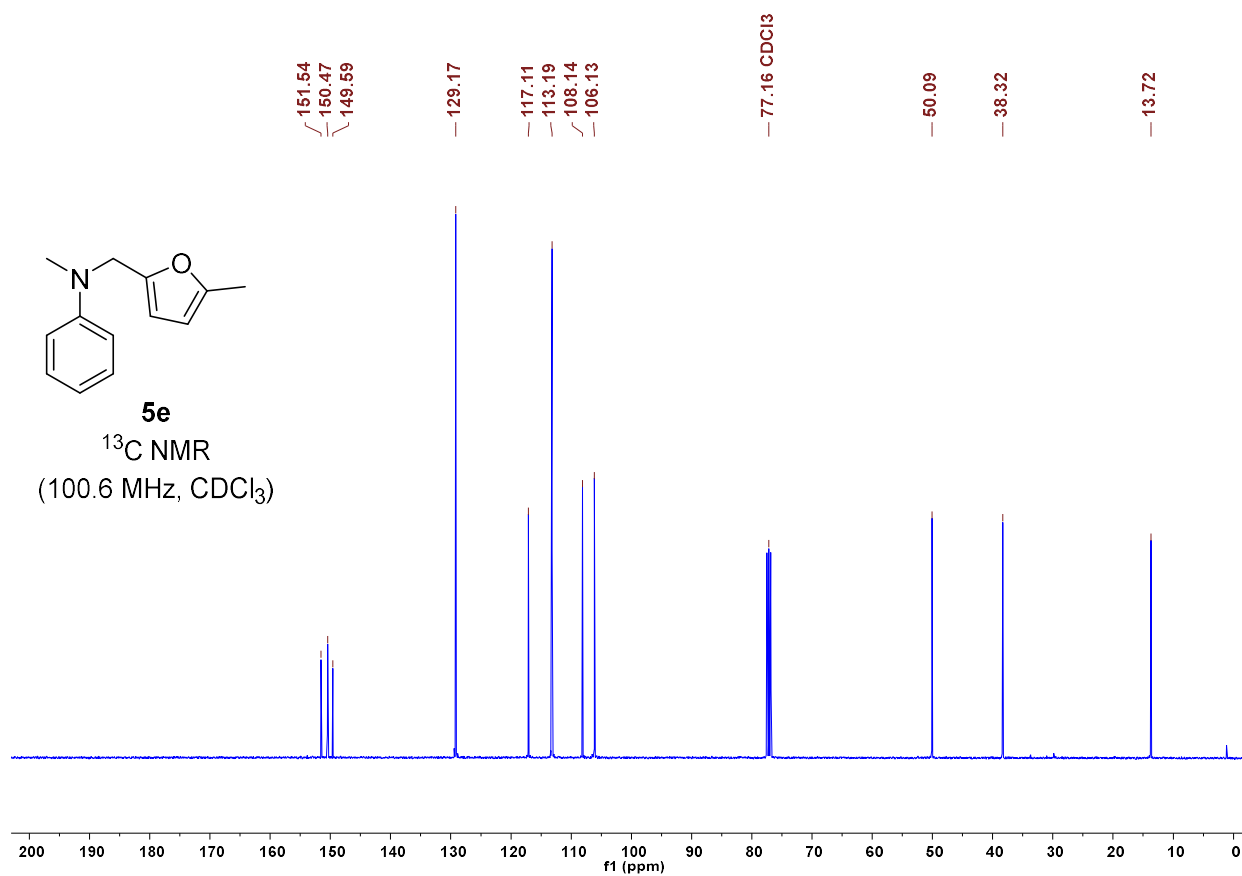
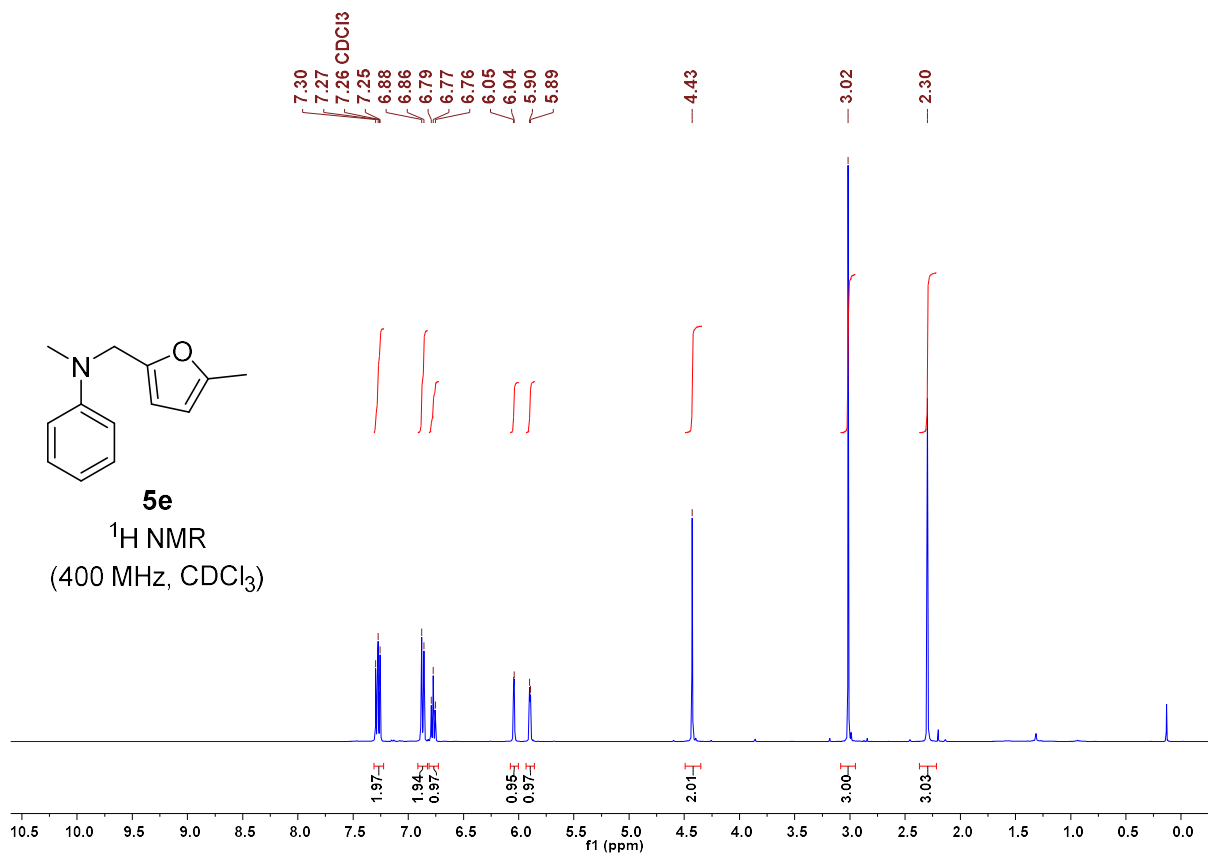


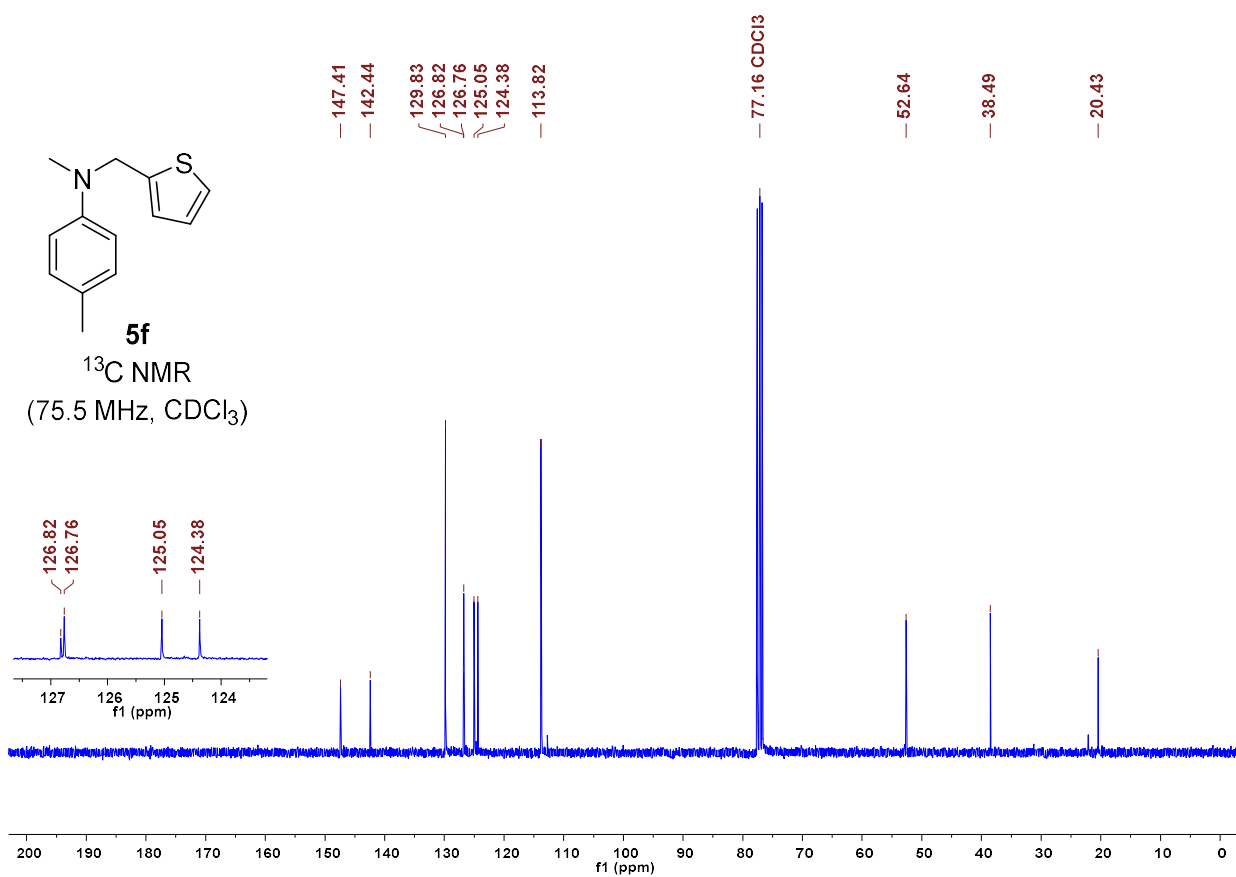
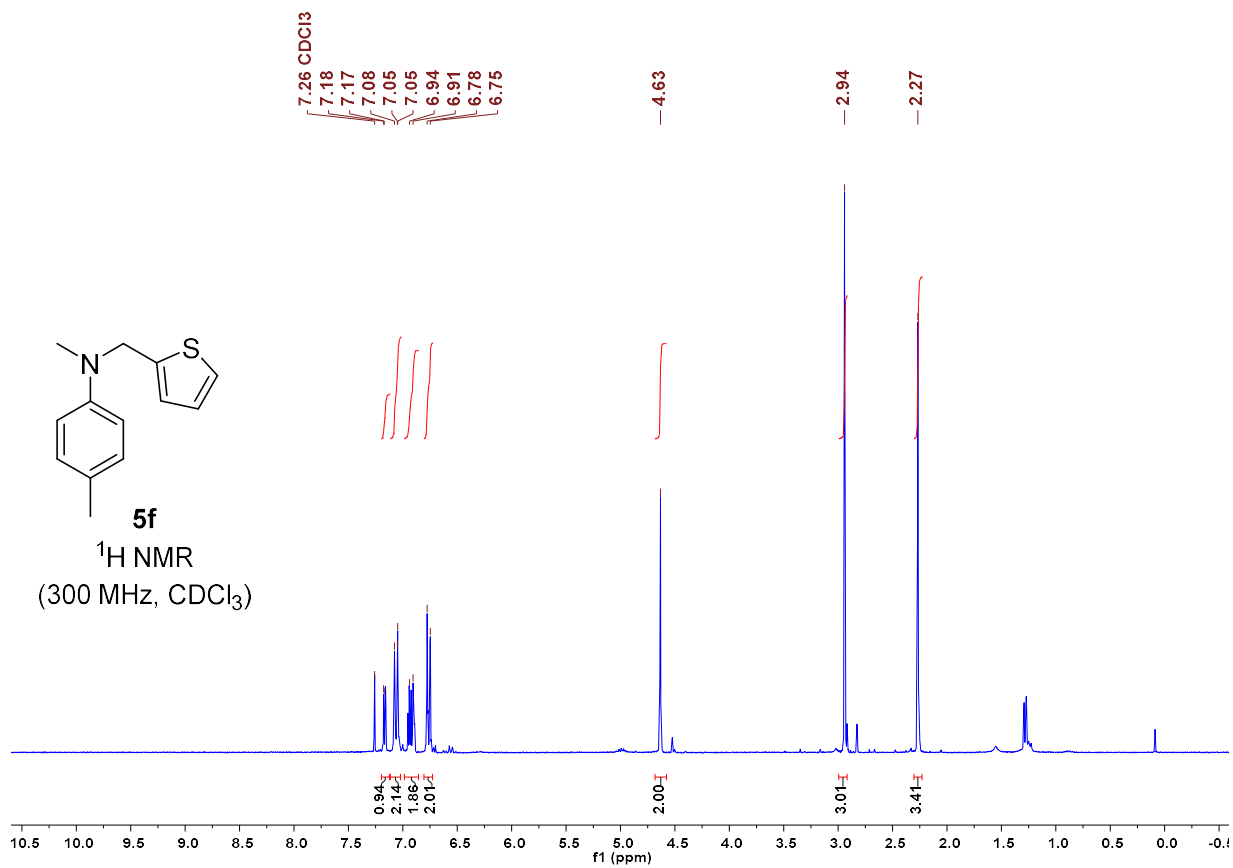


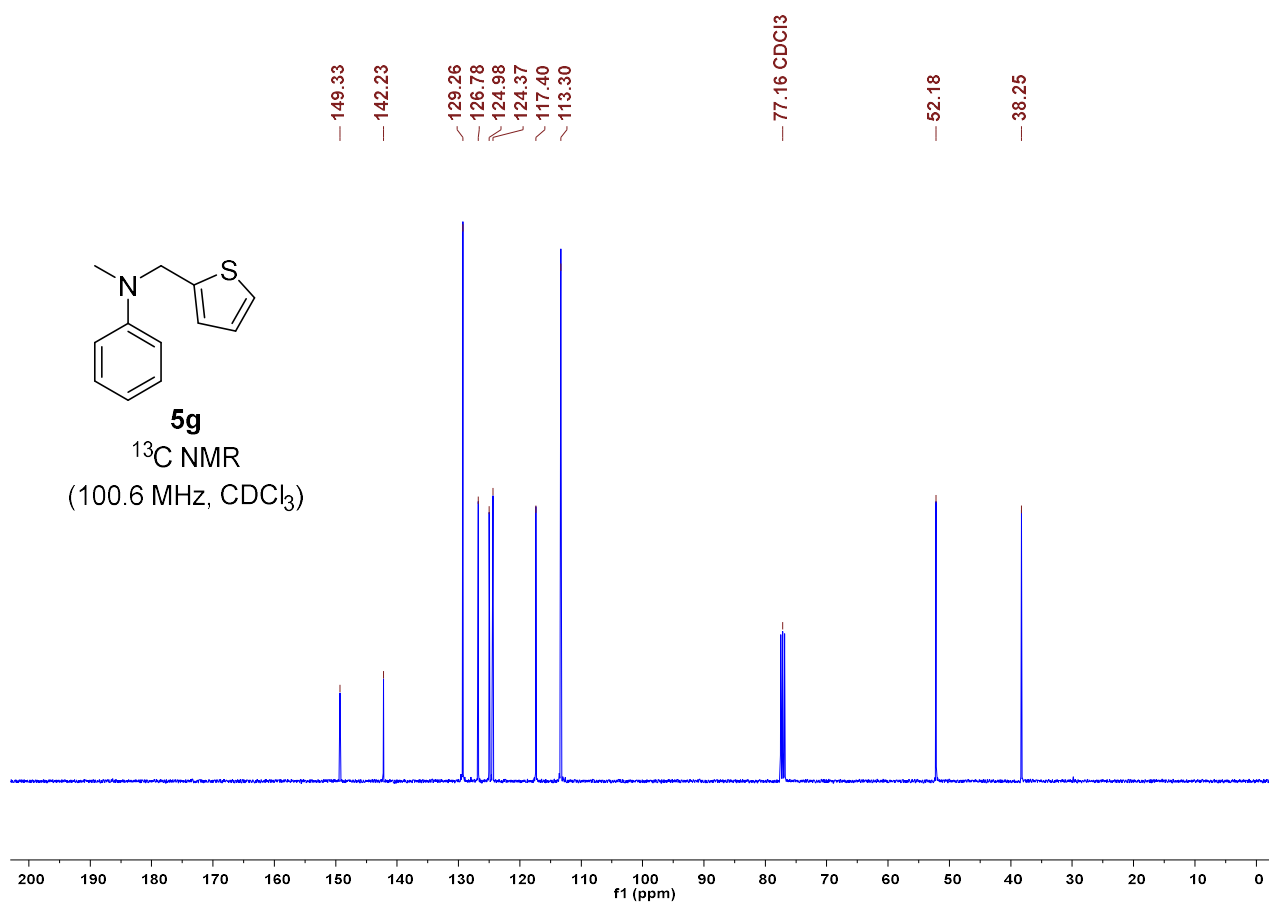
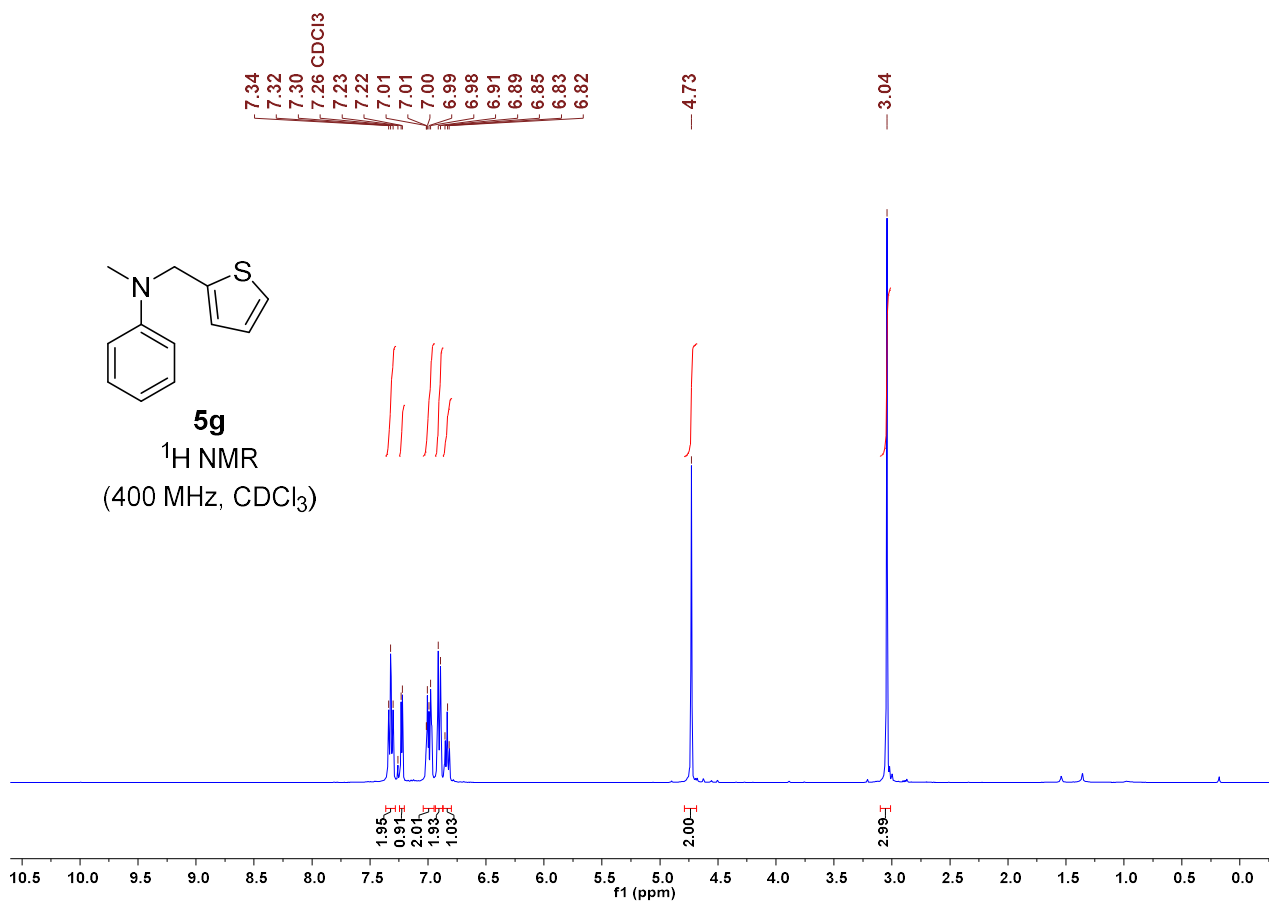


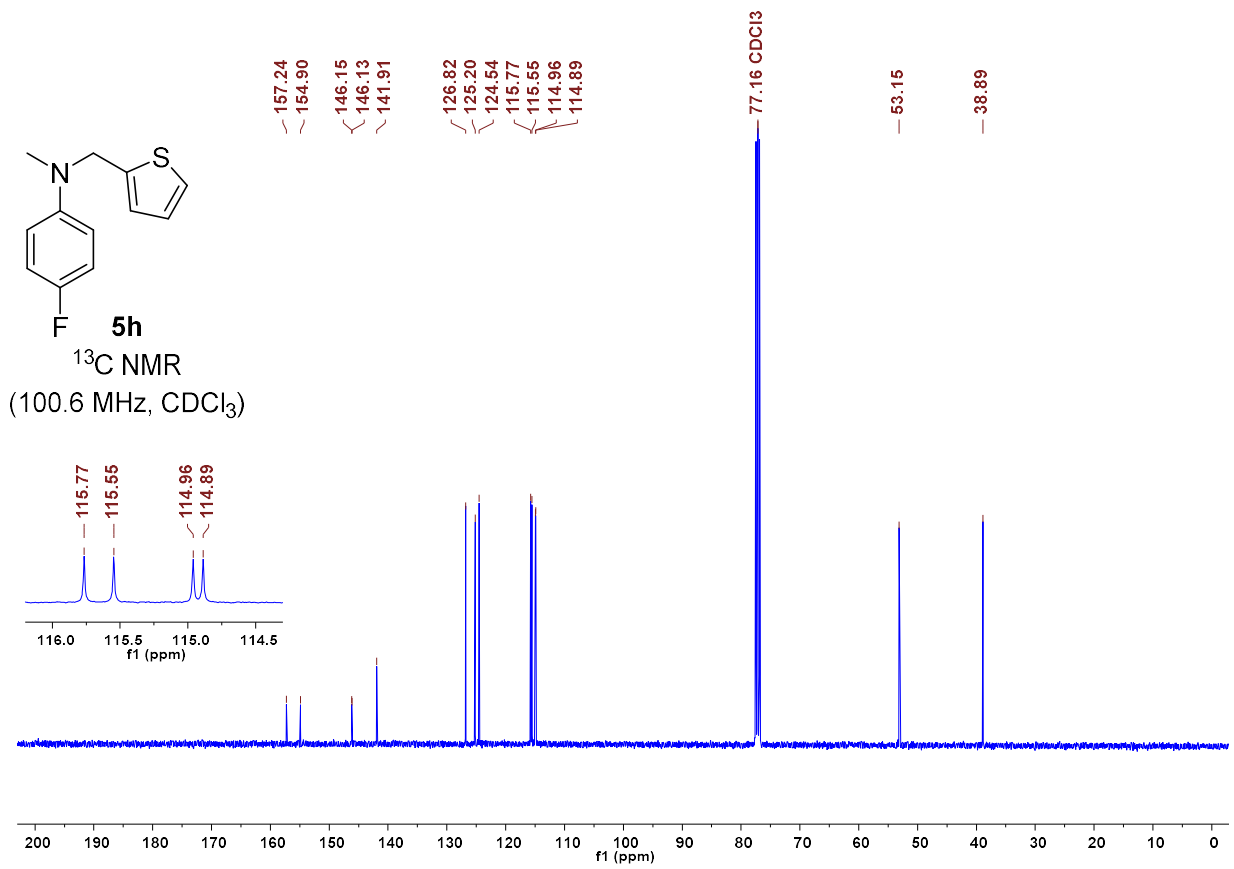
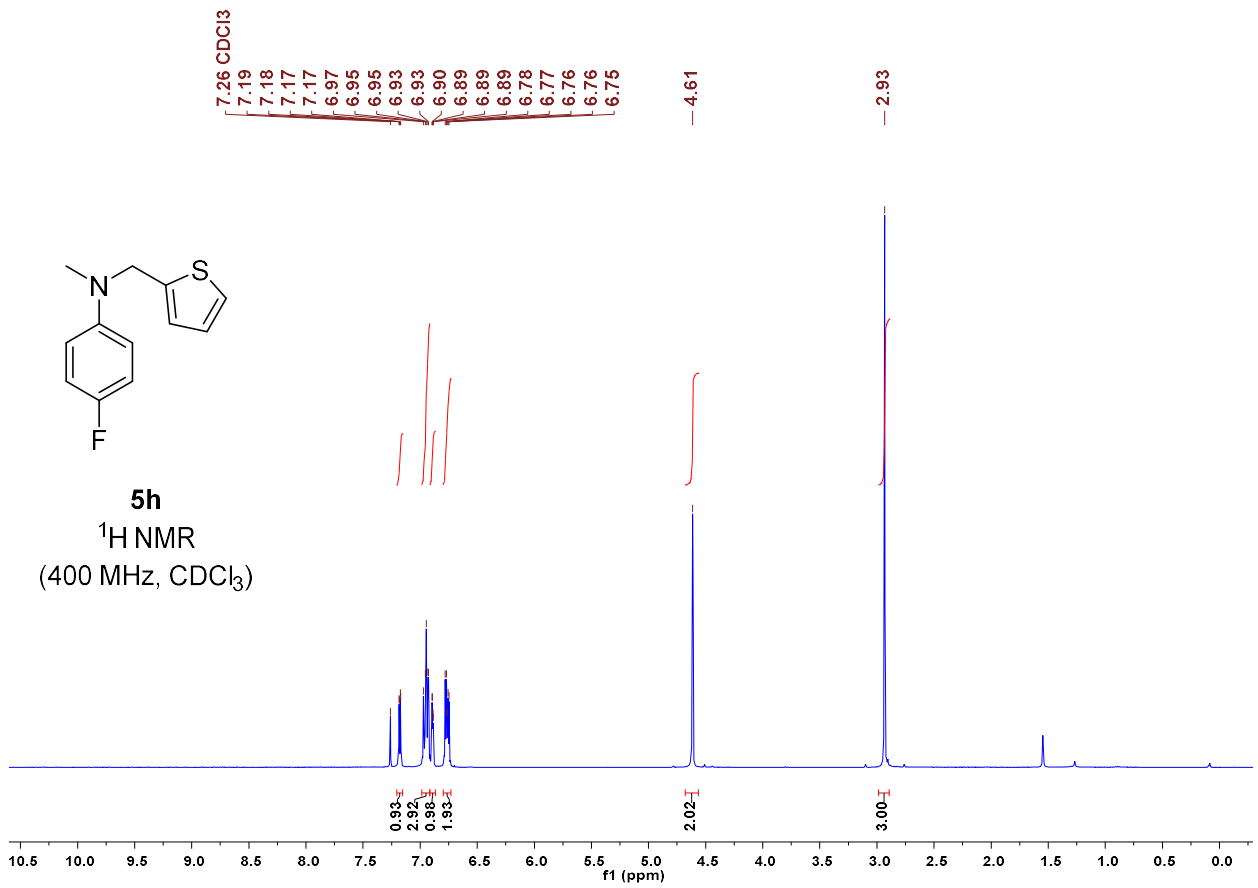


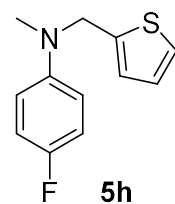




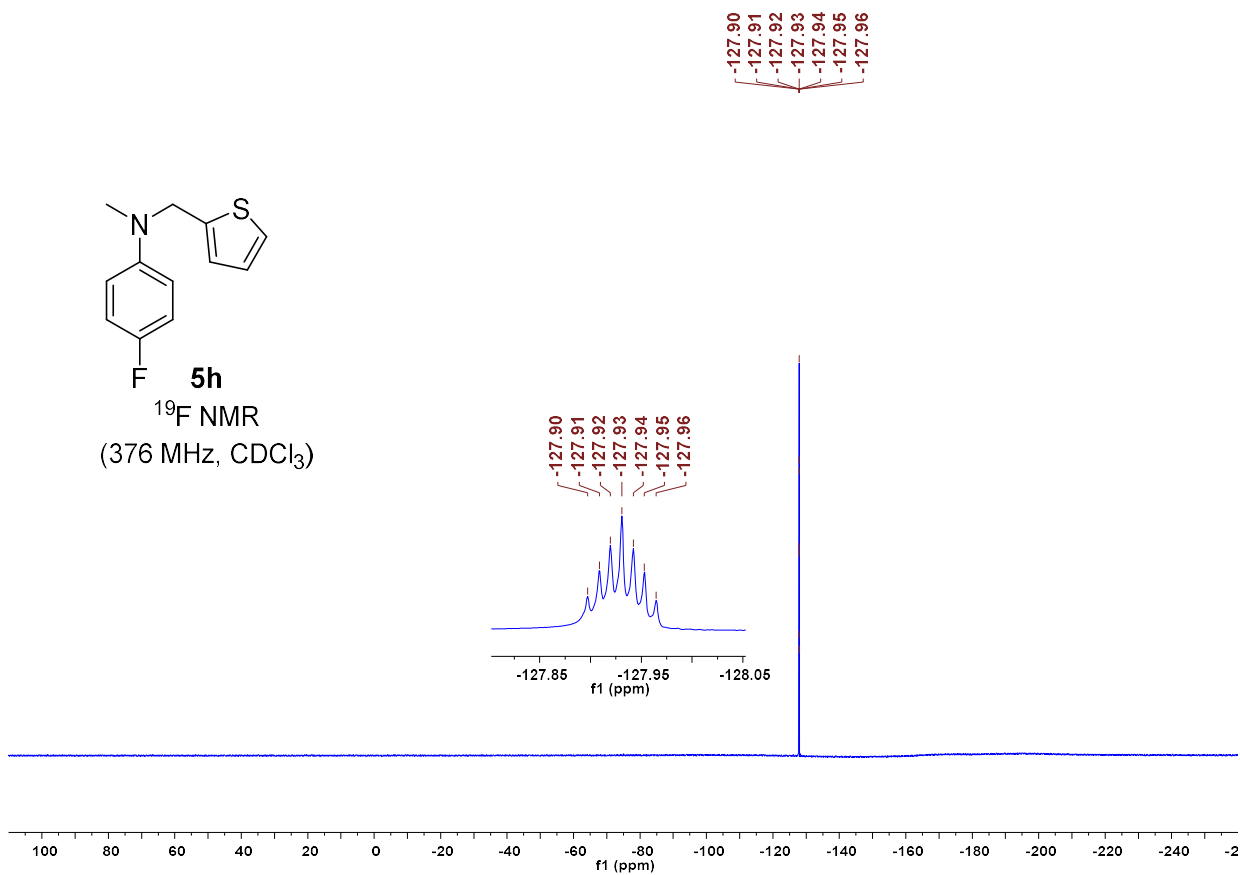


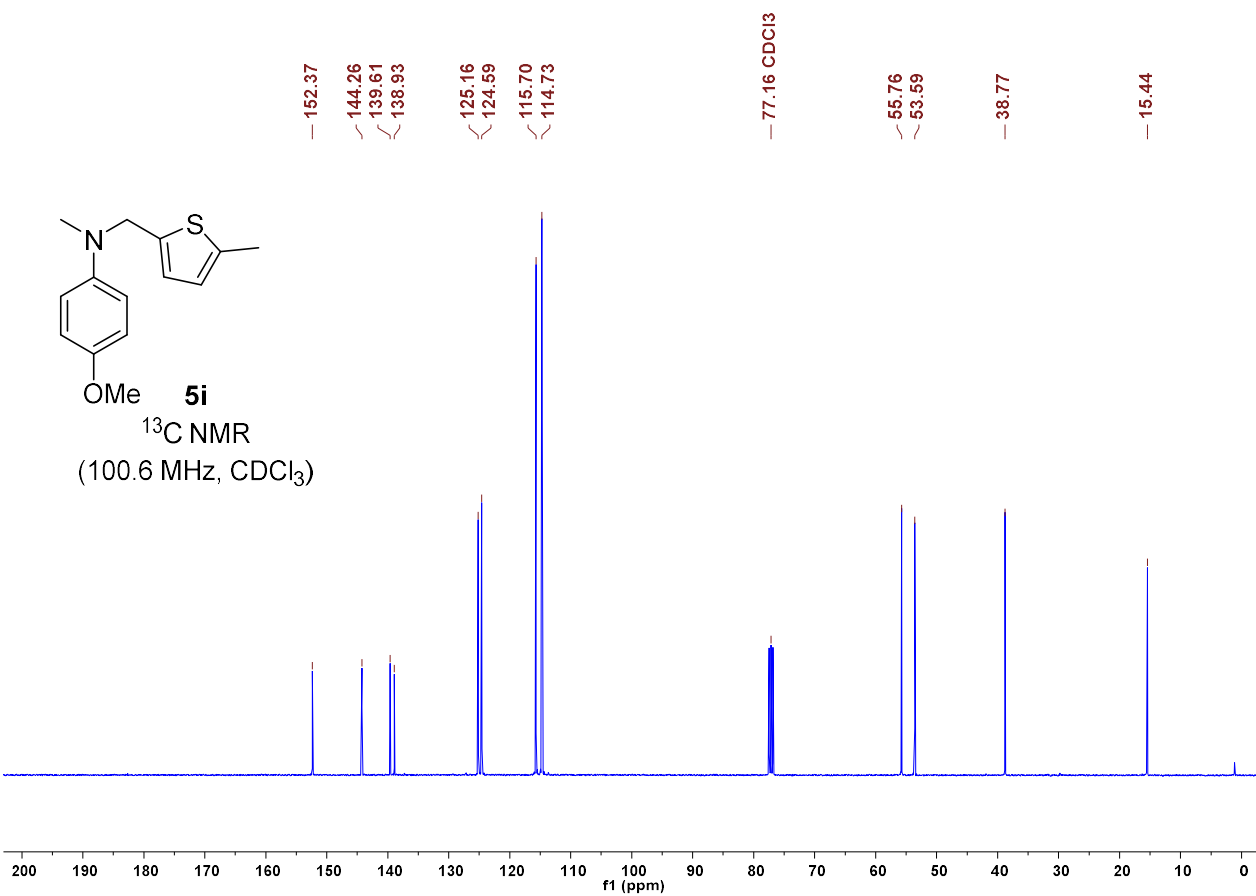
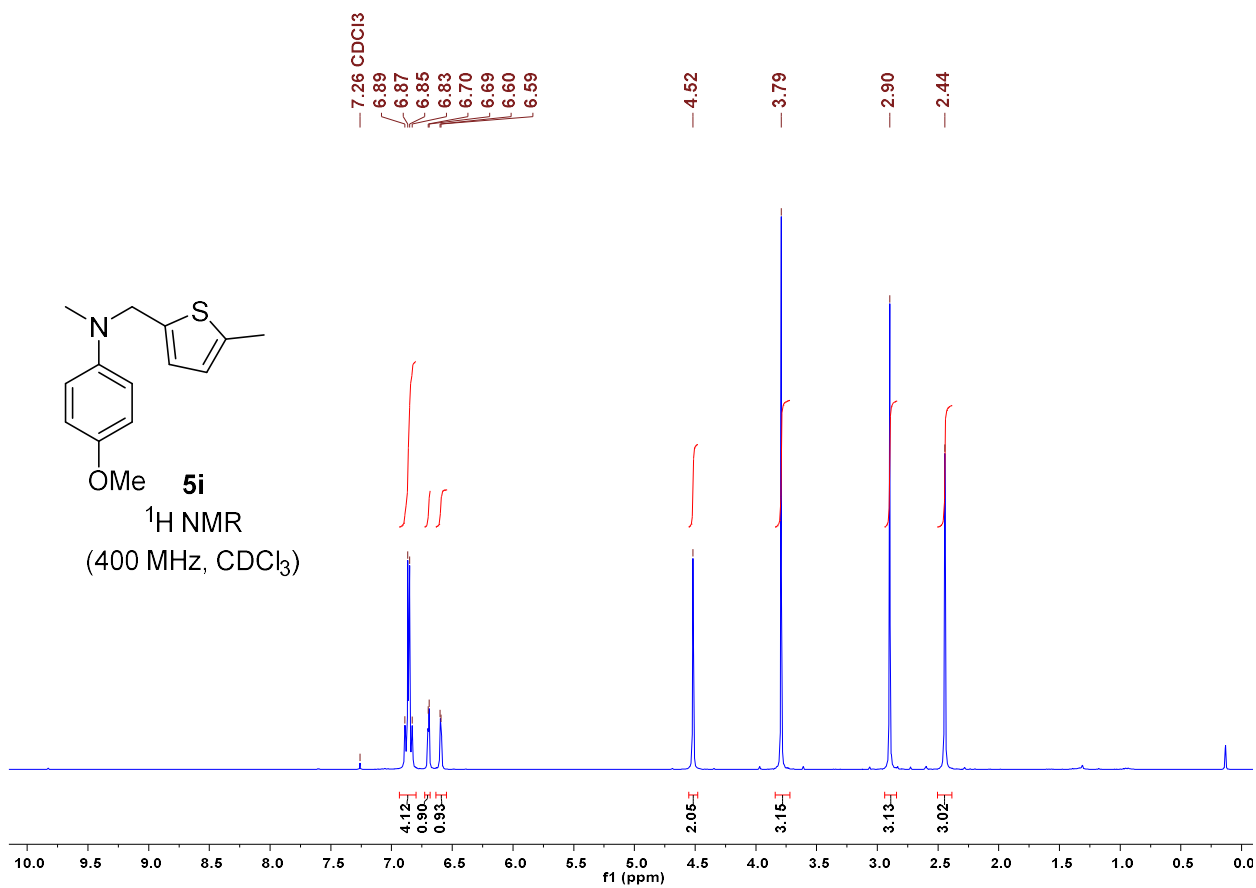


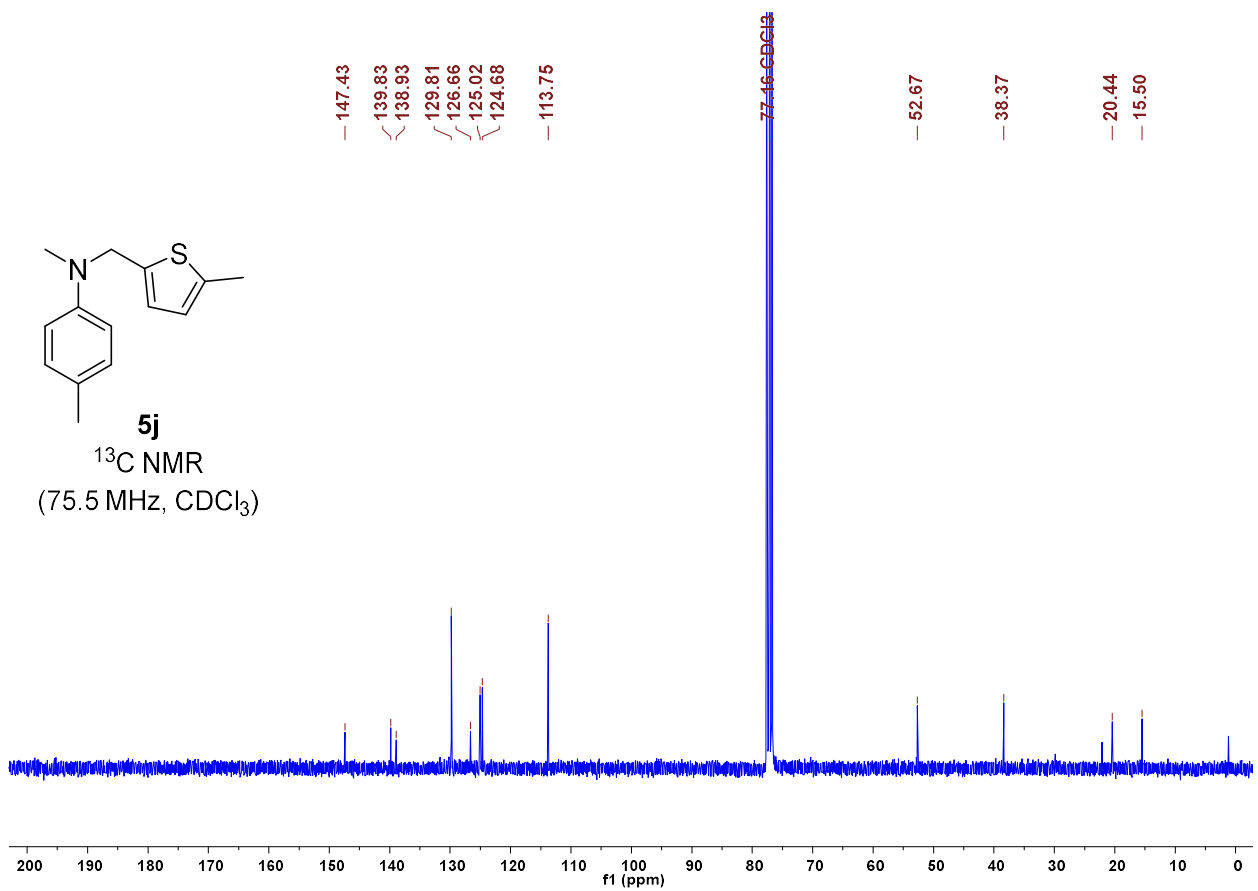
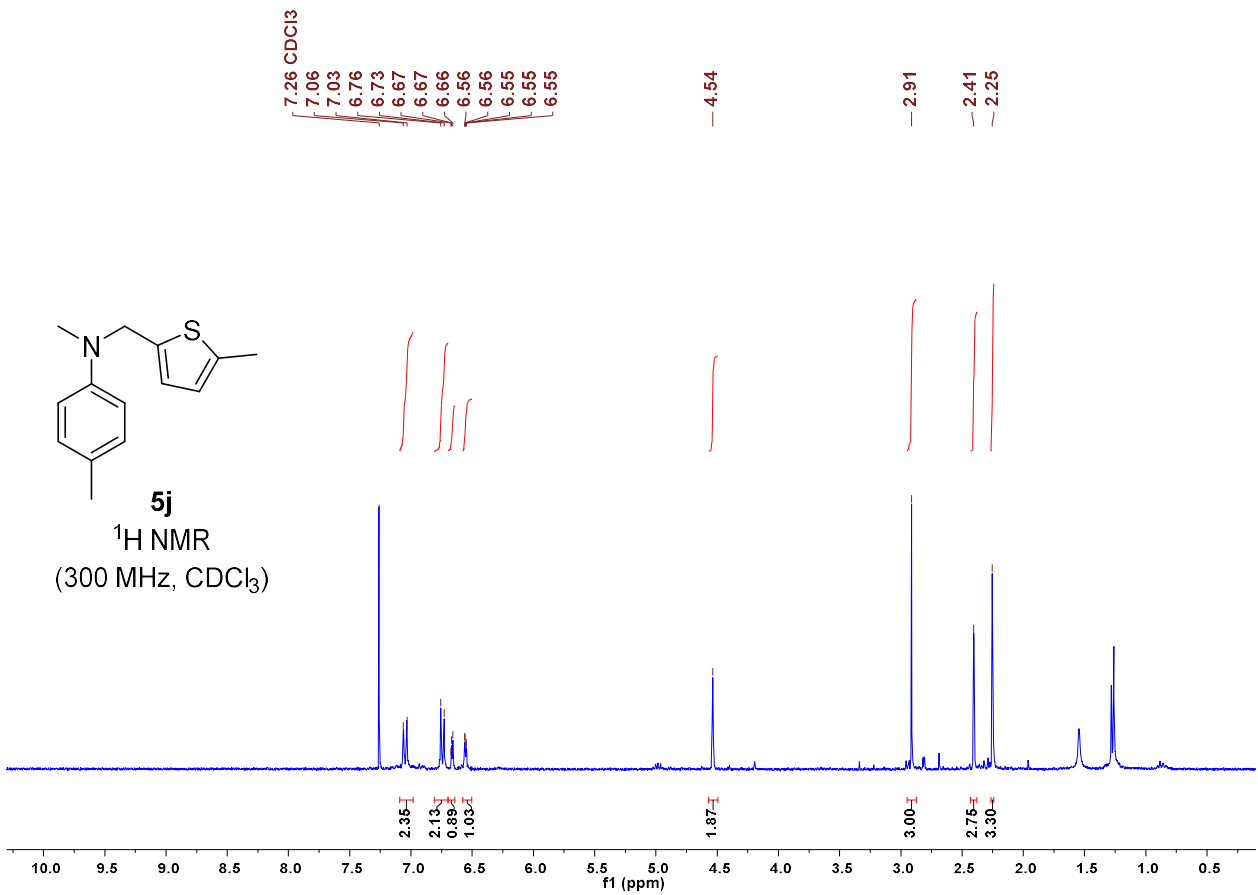


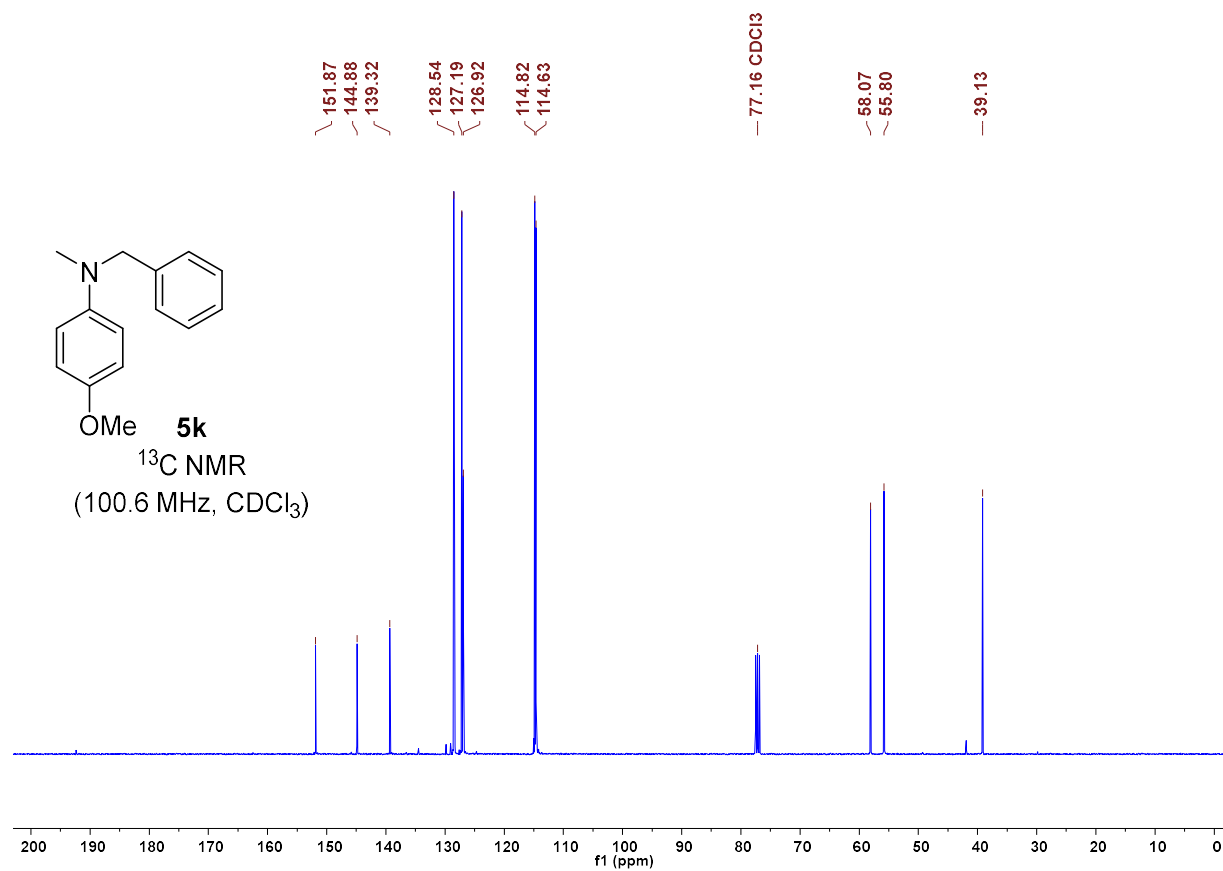
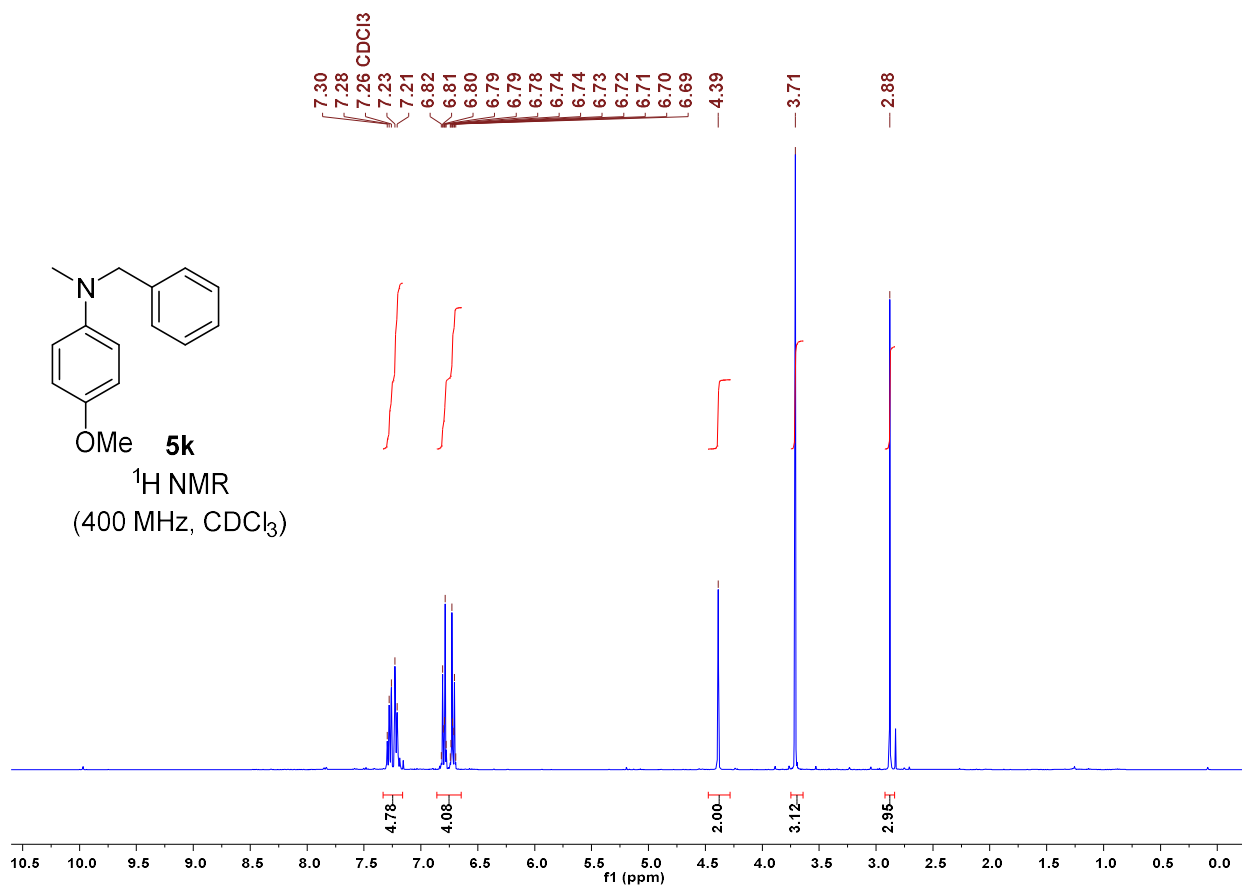


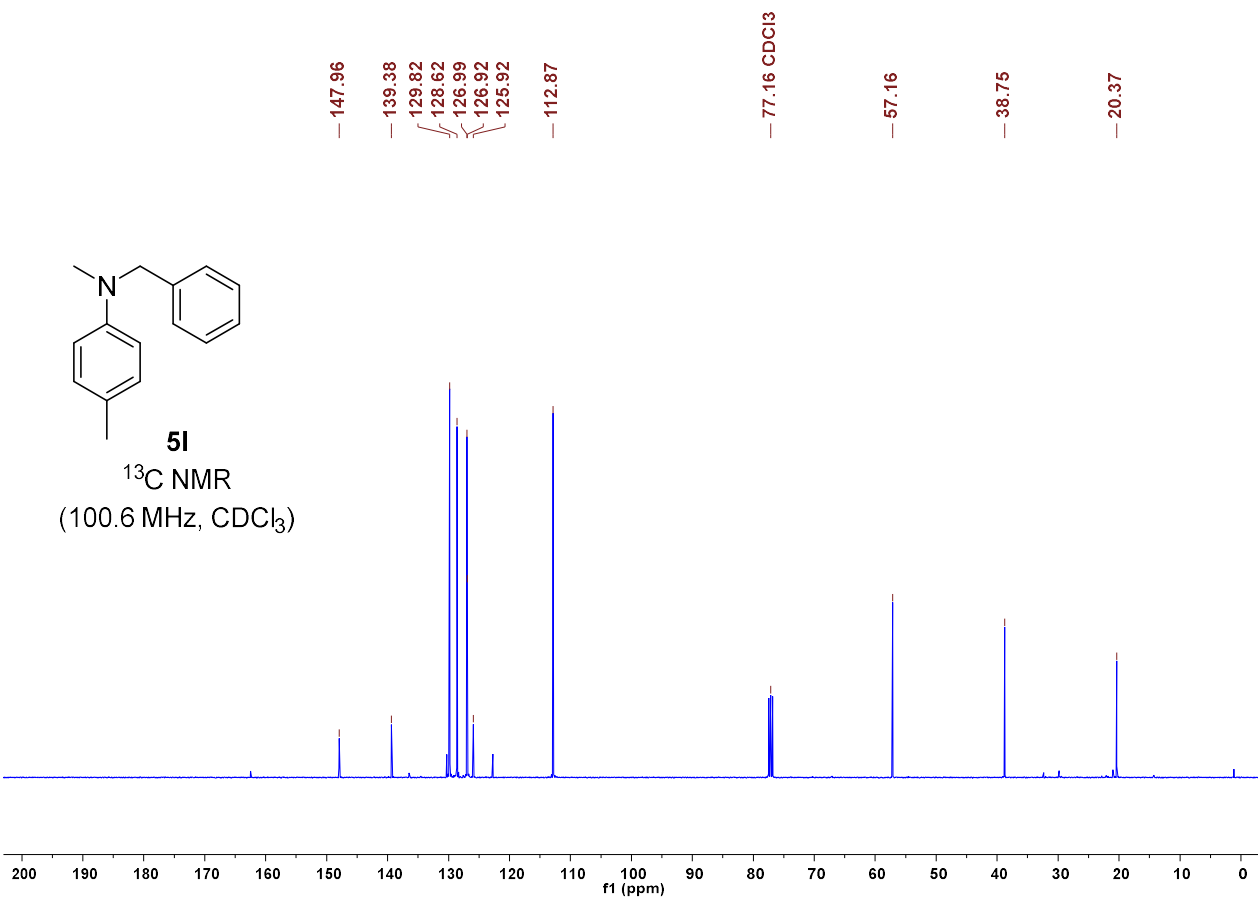
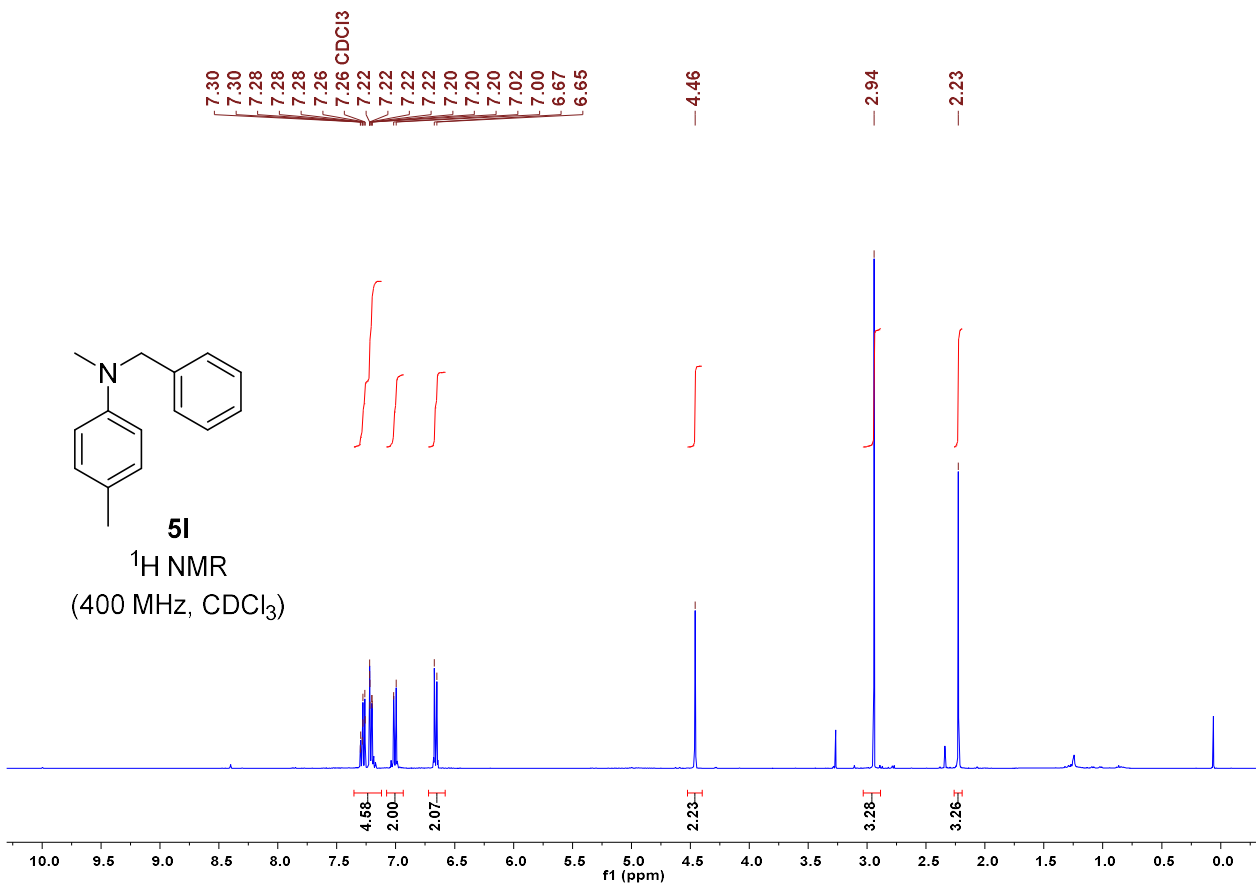
**5h**  
<sup>19</sup>F NMR  
(376 MHz, CDCl<sub>3</sub>)

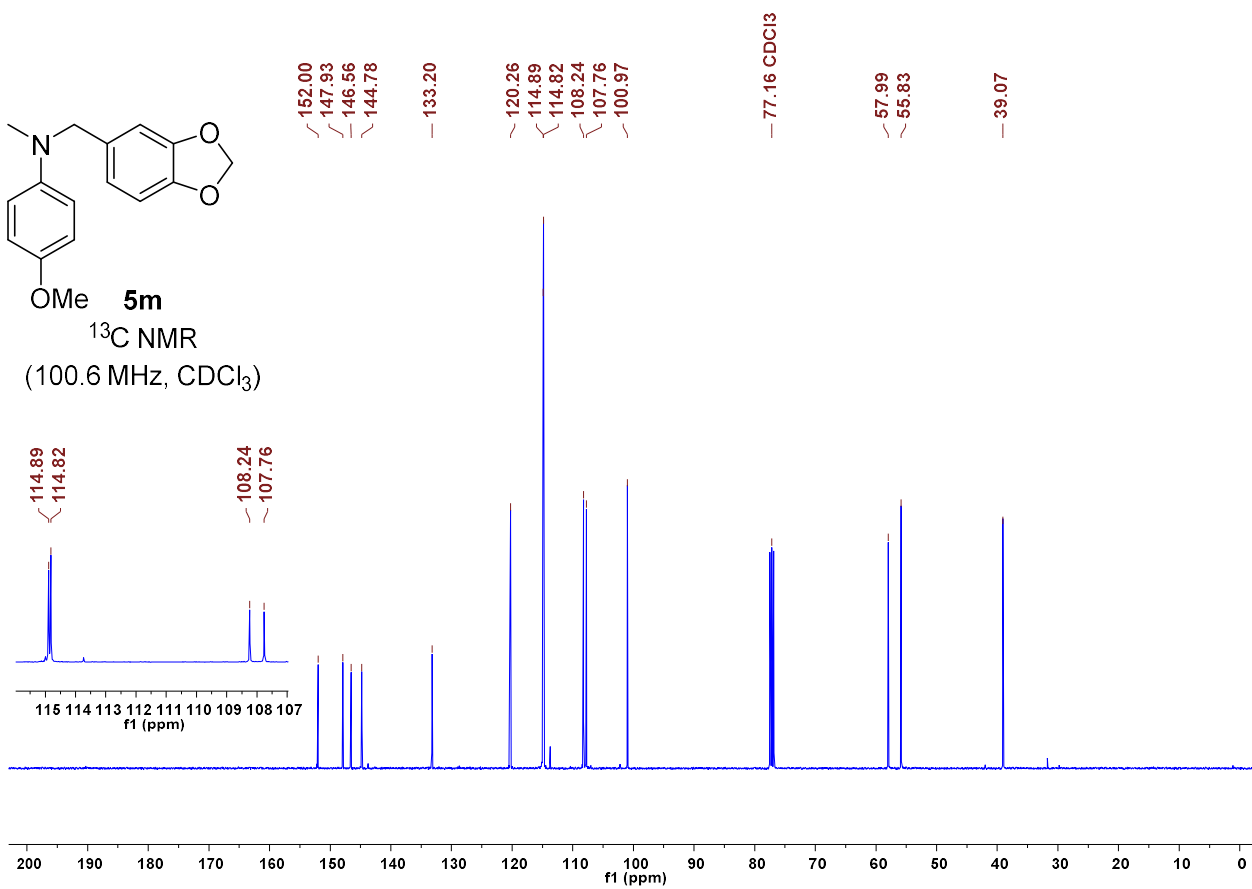
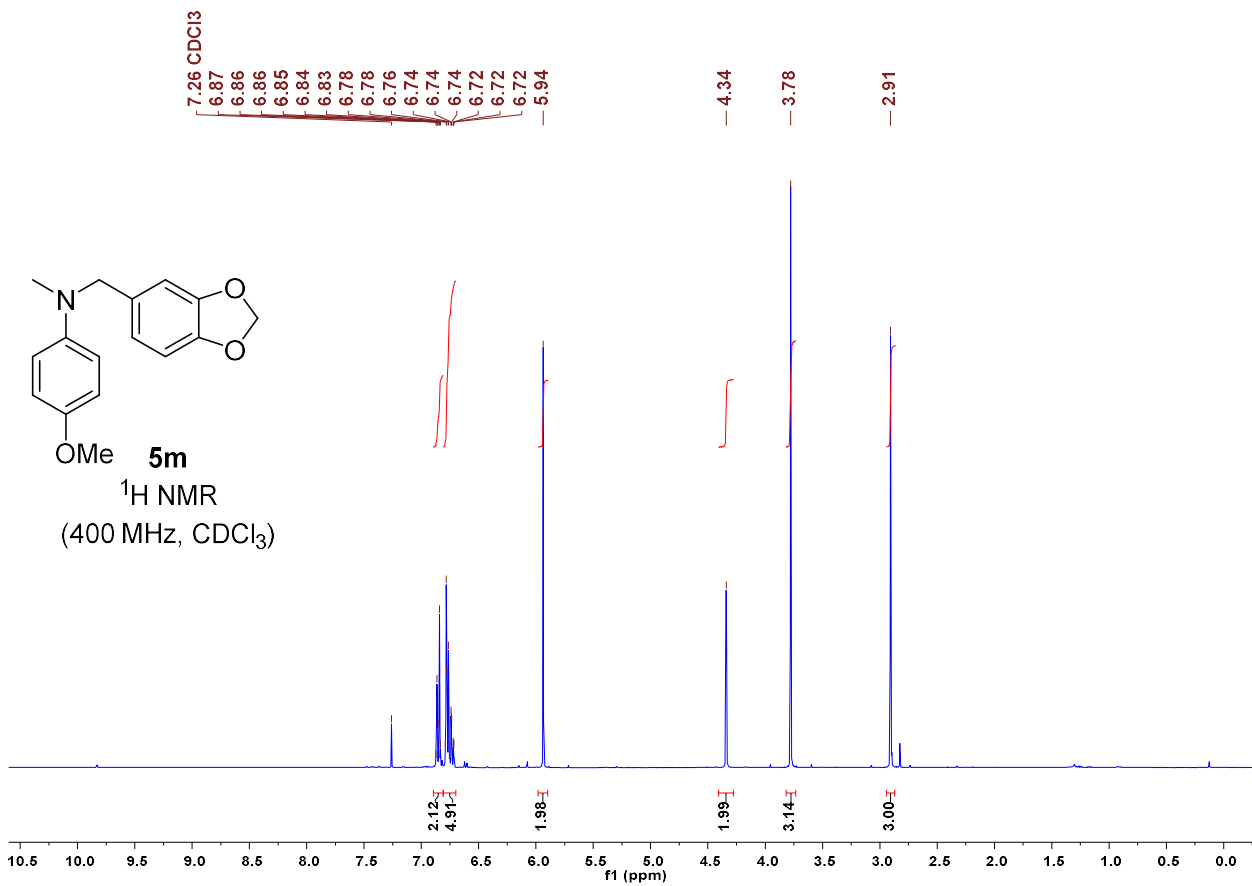


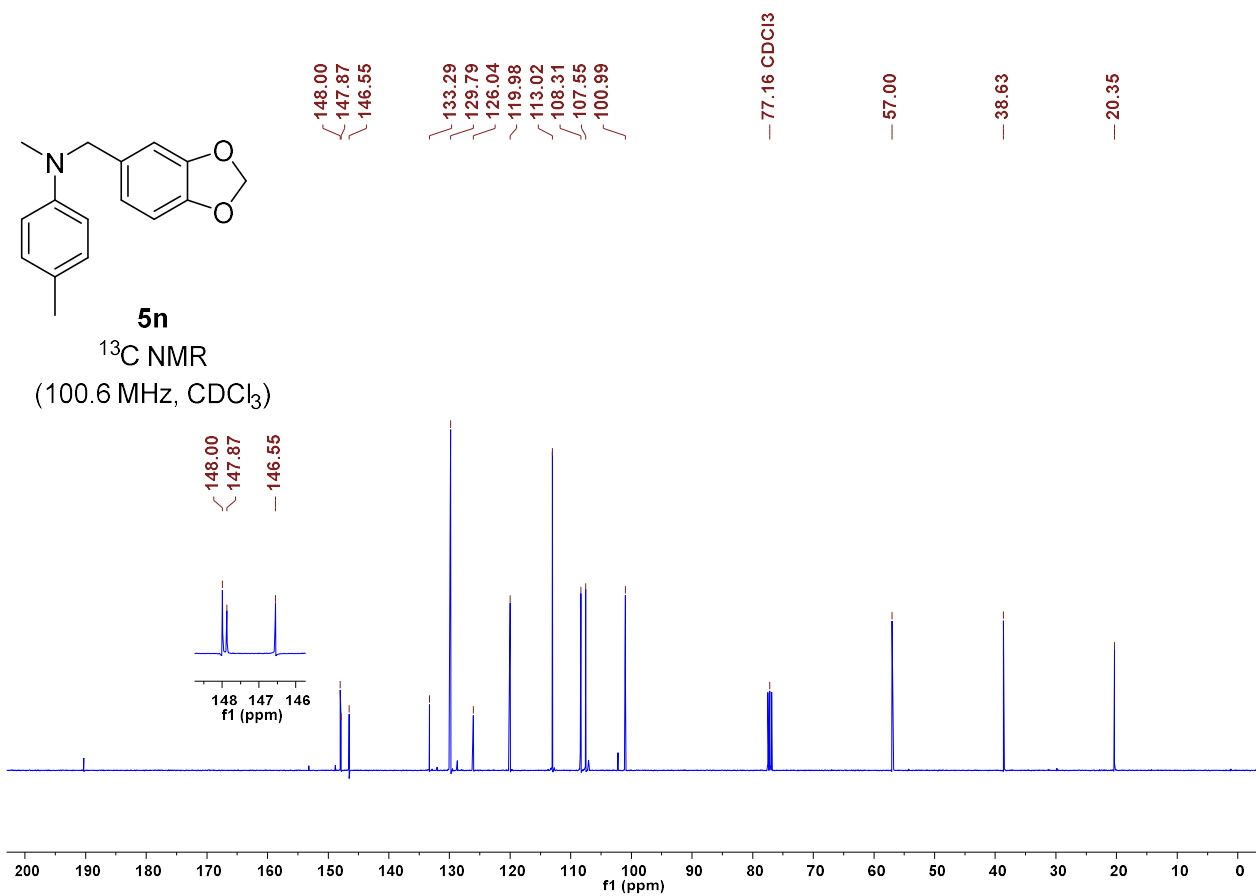
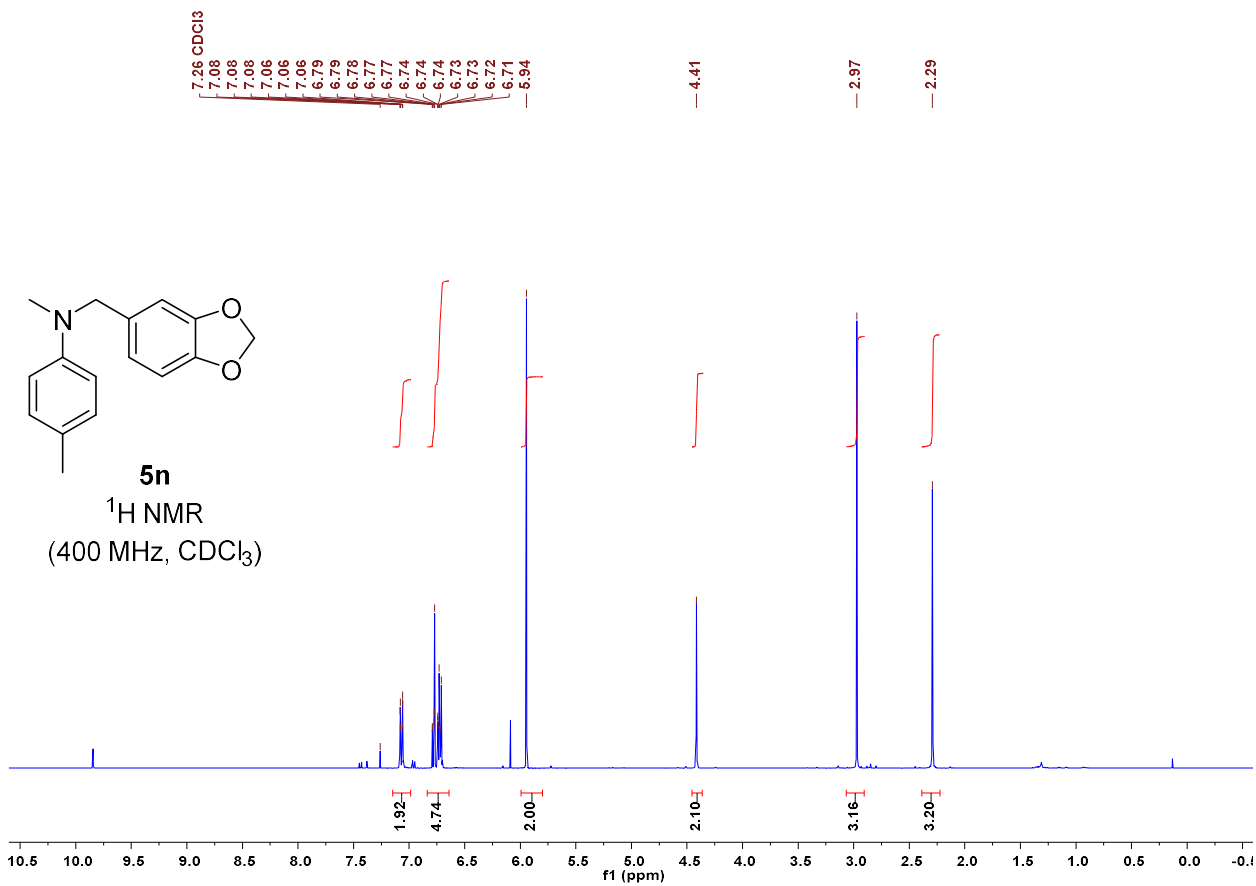


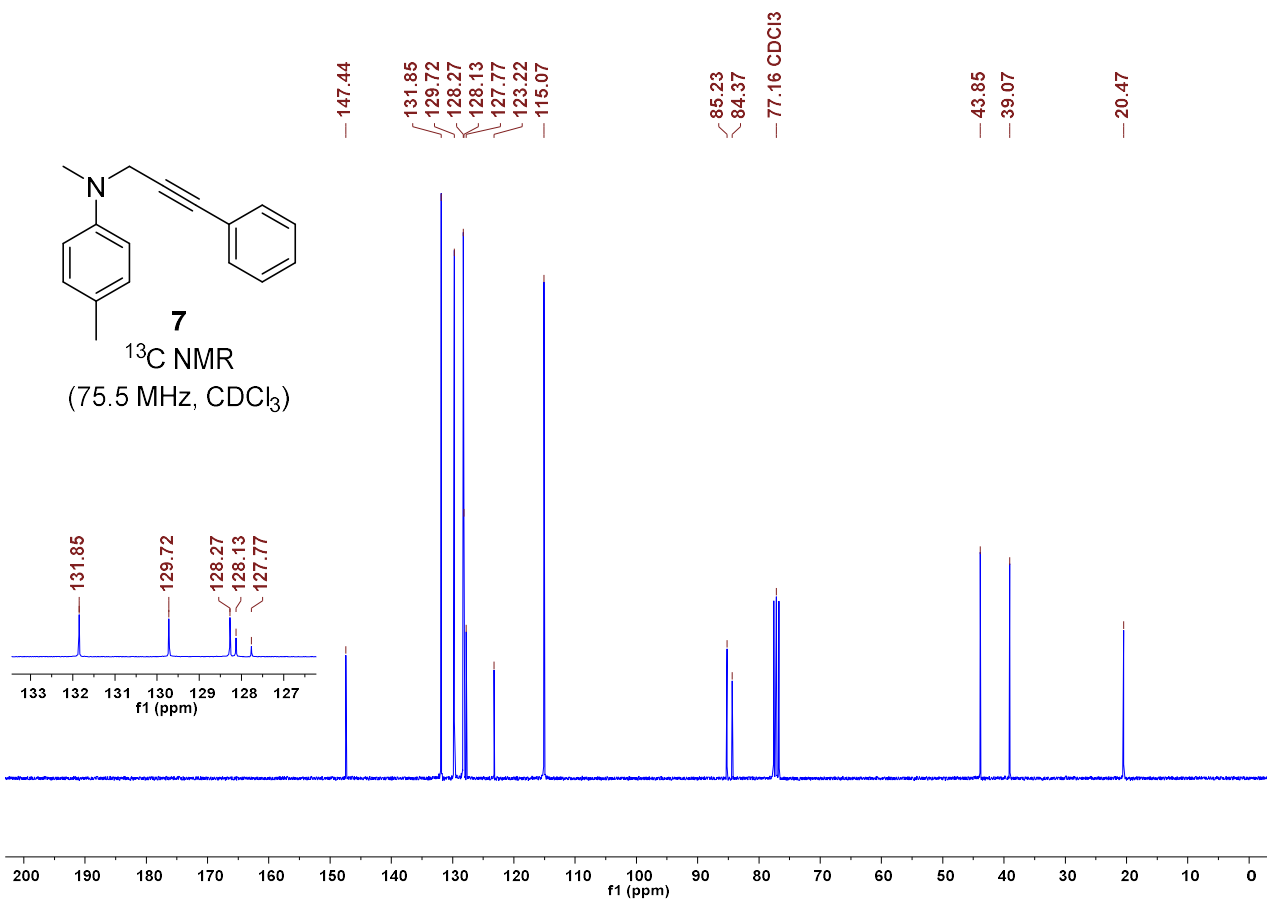
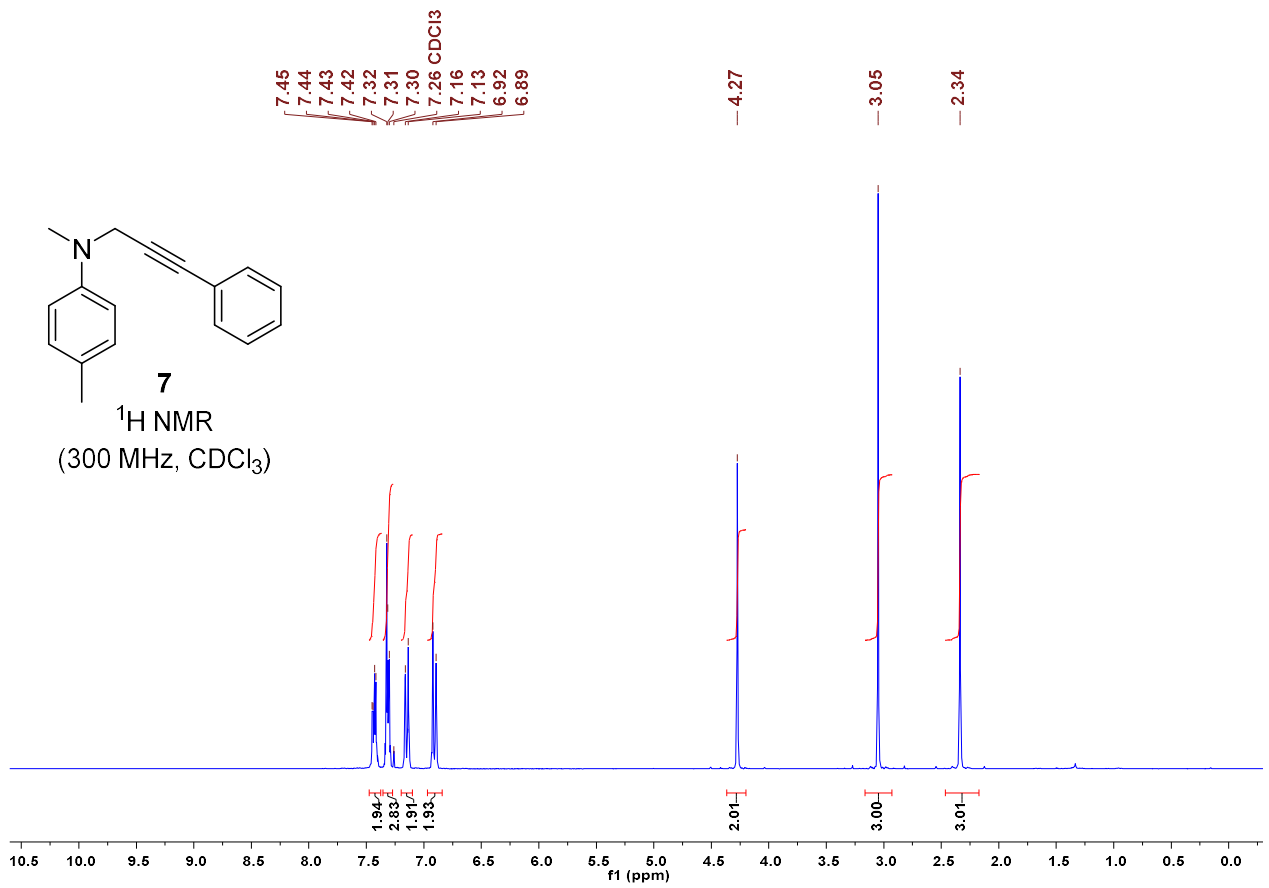


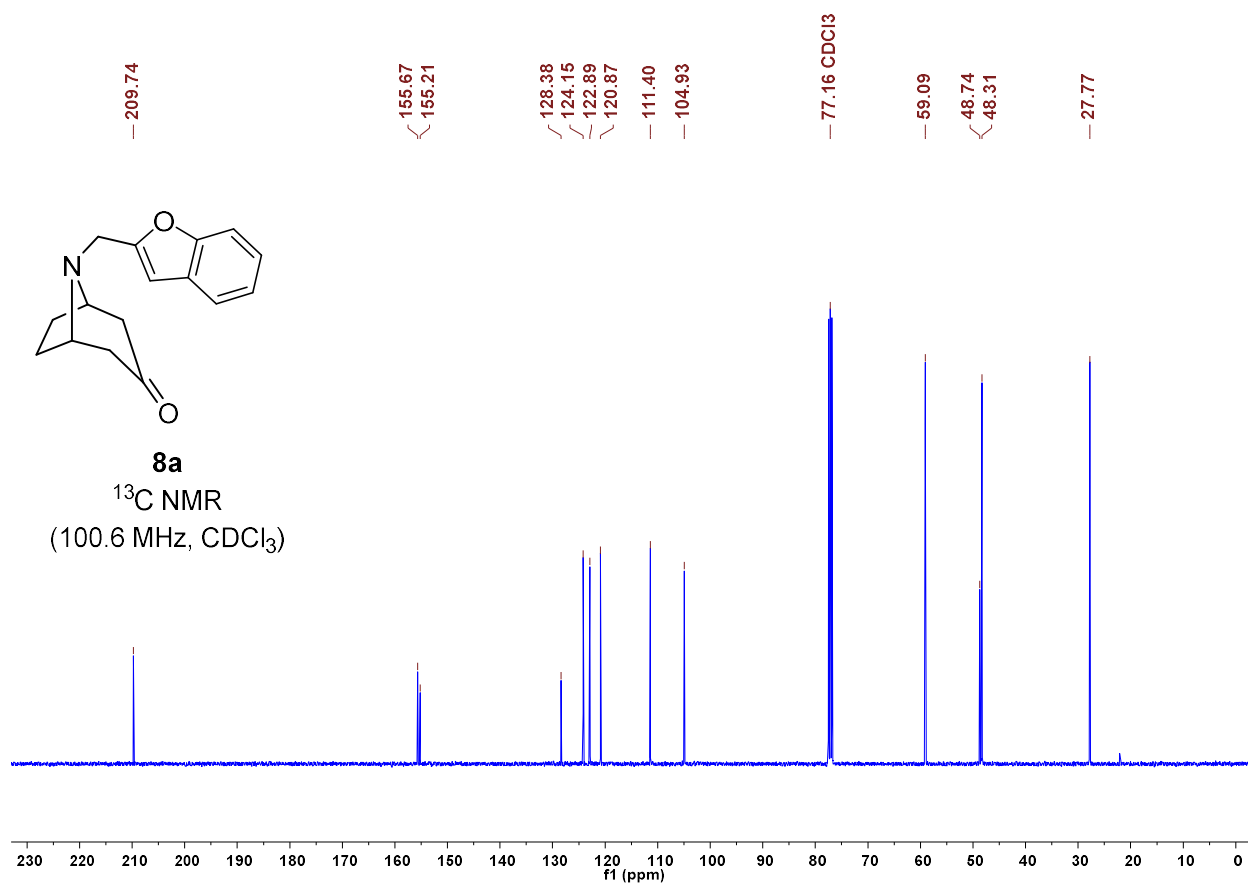
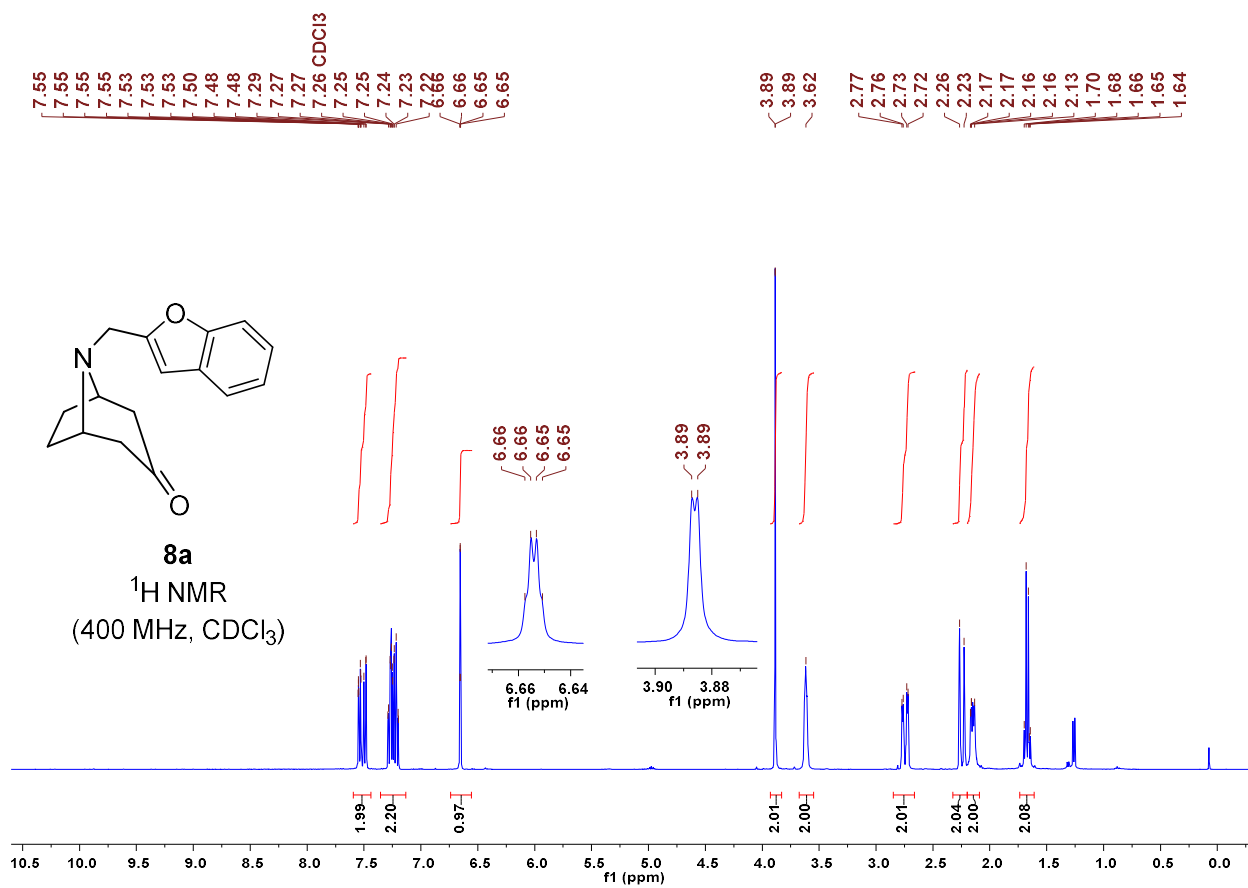


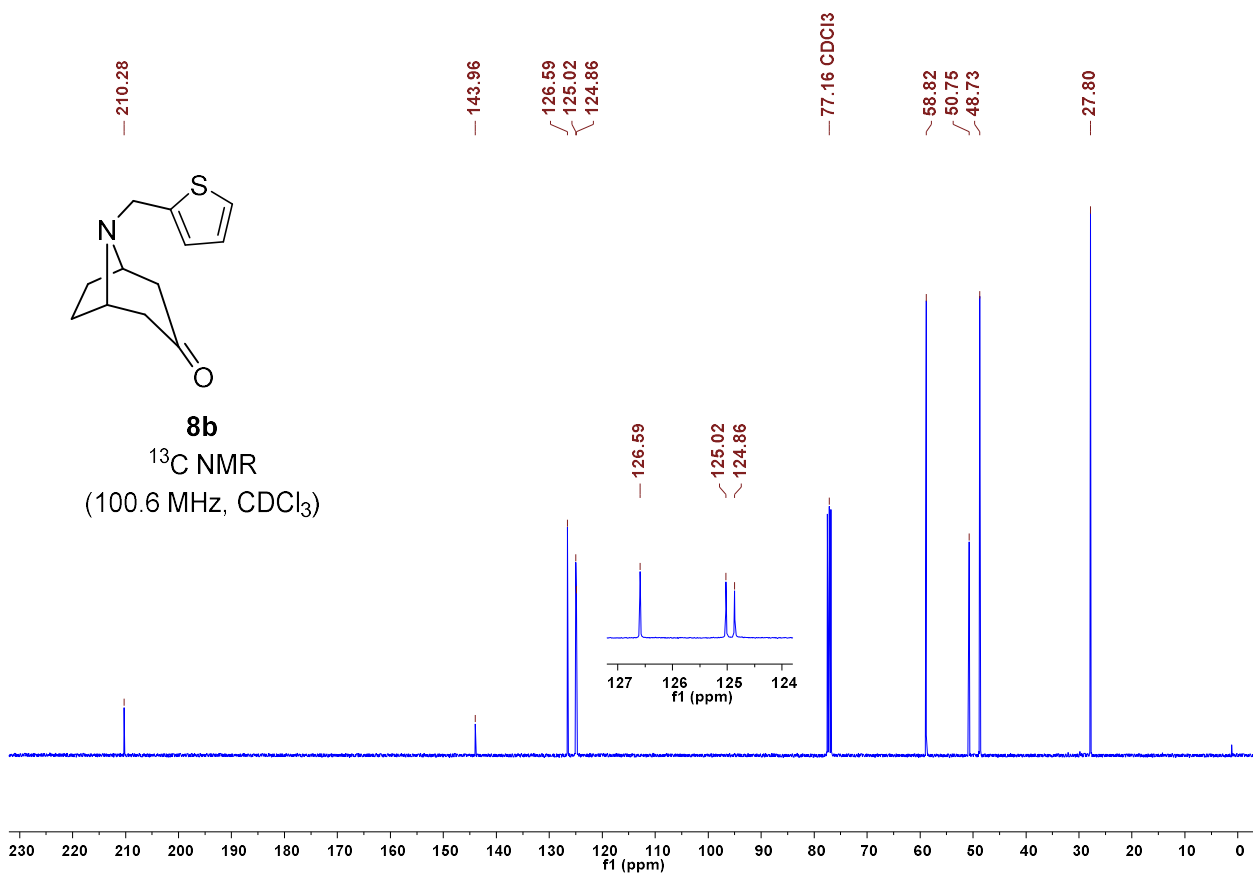
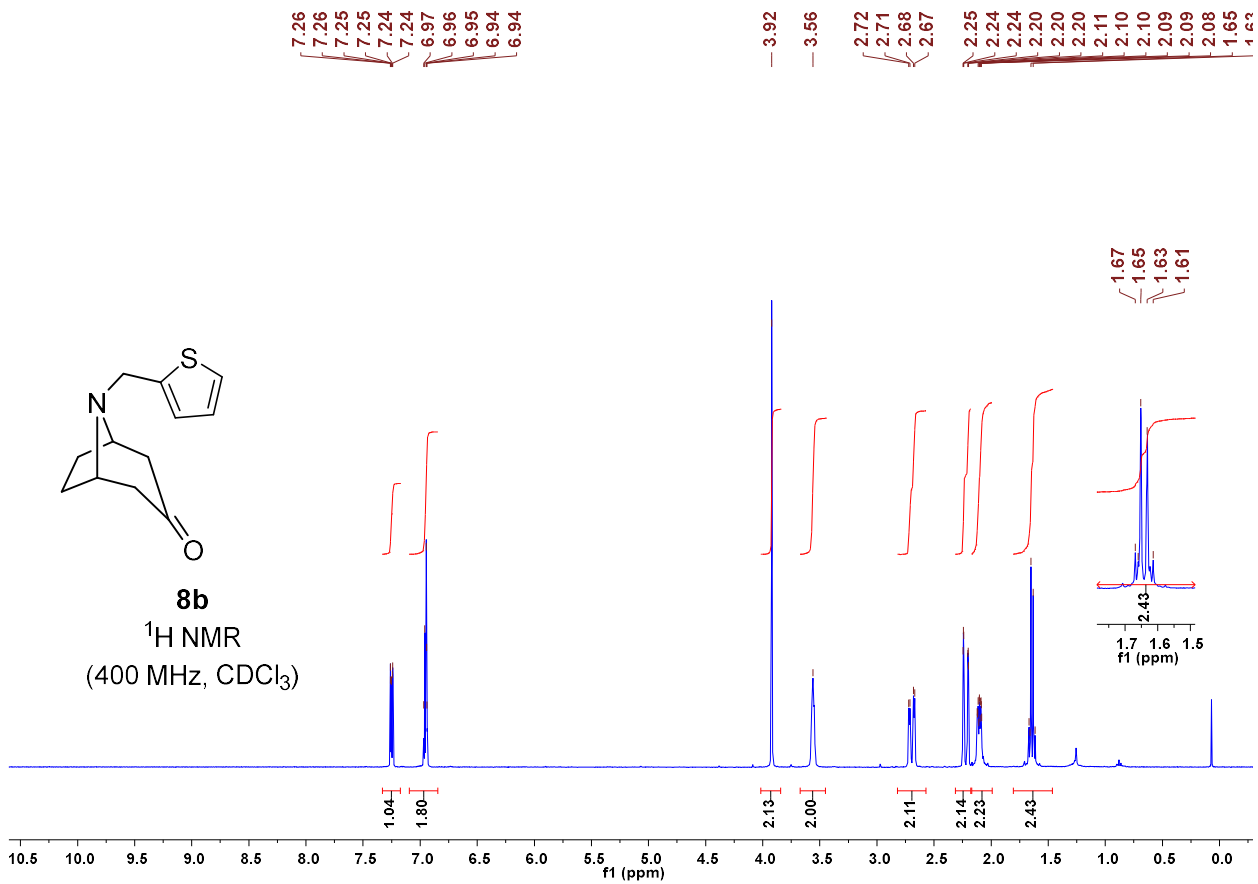










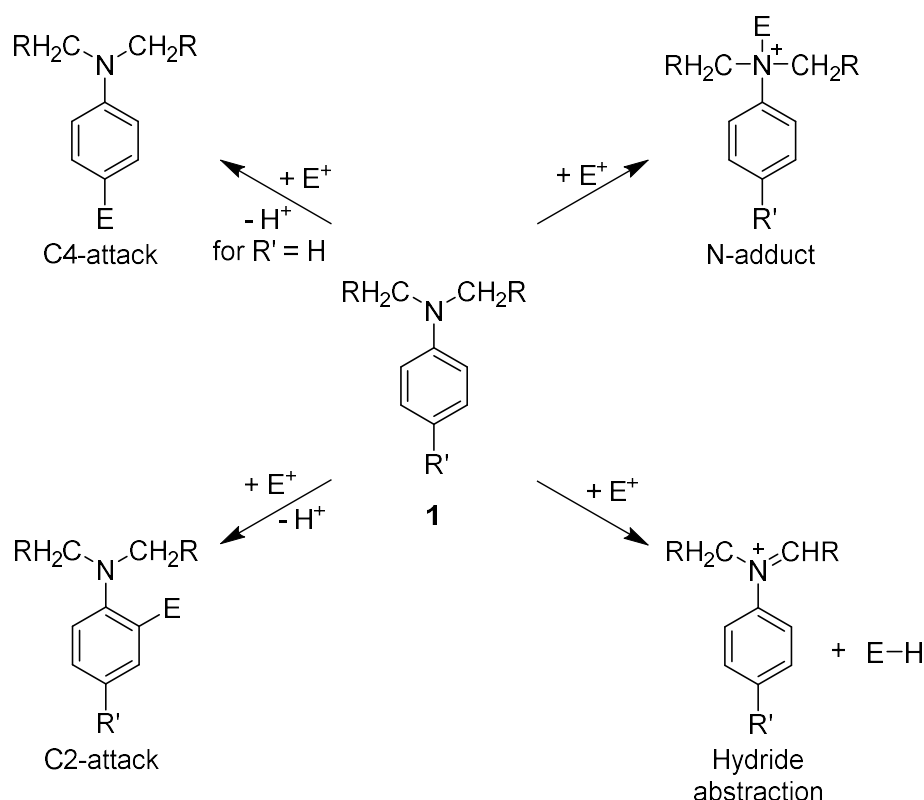


## Chapter 3

# Quantification of the Nucleophilic Reactivities of *N,N*-Dialkylated Anilines

## Introduction

Neutral nitrogen nucleophiles represent a vast and interesting class of nucleophiles, in which a wide variation of properties through structural change is possible, with the nucleophilic center kept constant. *N,N*-Dialkylated anilines (**1**) are ambident nucleophiles.<sup>[1]</sup> When they react with cationic electrophiles, four different reasonable reactions are possible for a nucleophilic attack (Scheme 1). Aside from the attack of the nitrogen atom lone pair, the attack of the carbon ring atoms, C2 and C4, by the electrophile is also possible. Finally, a hydride at the alkyl group might also be abstracted by cationic electrophiles.

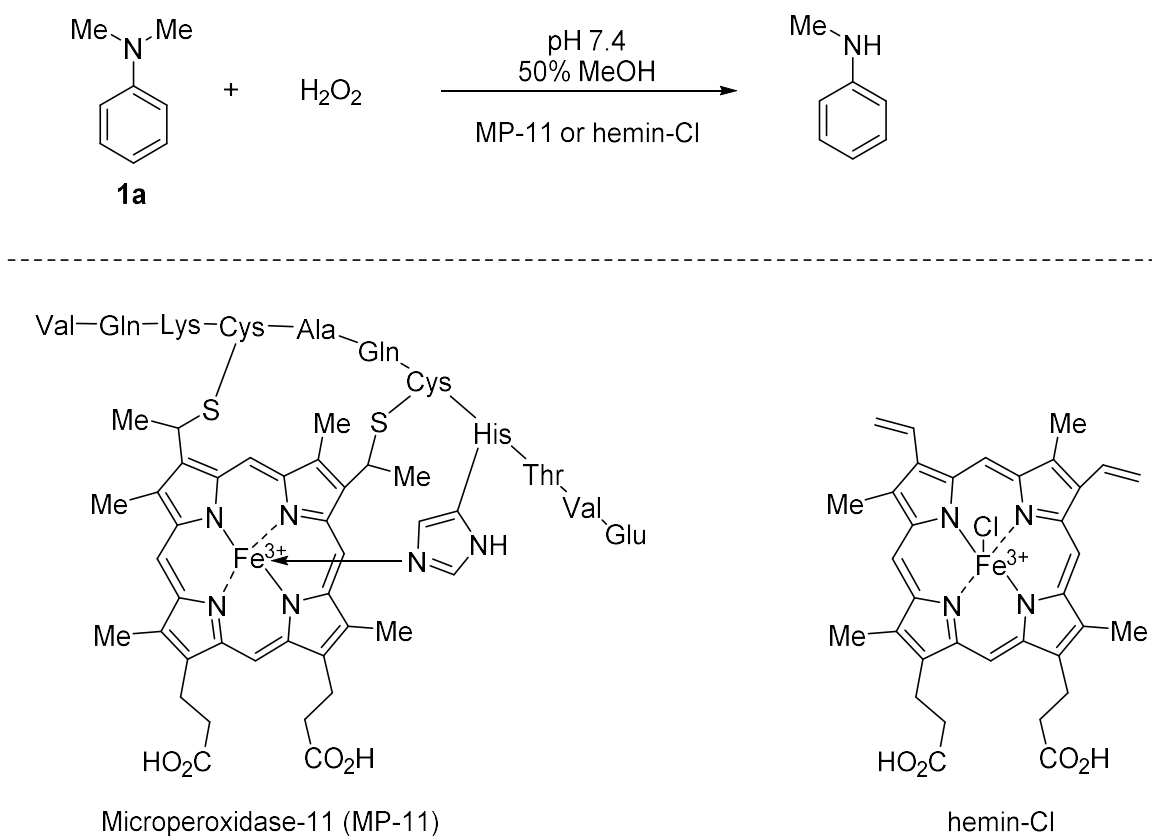


Scheme 1: Possible reactions of *N,N*-dialkylated anilines (**1**) with cationic electrophiles.

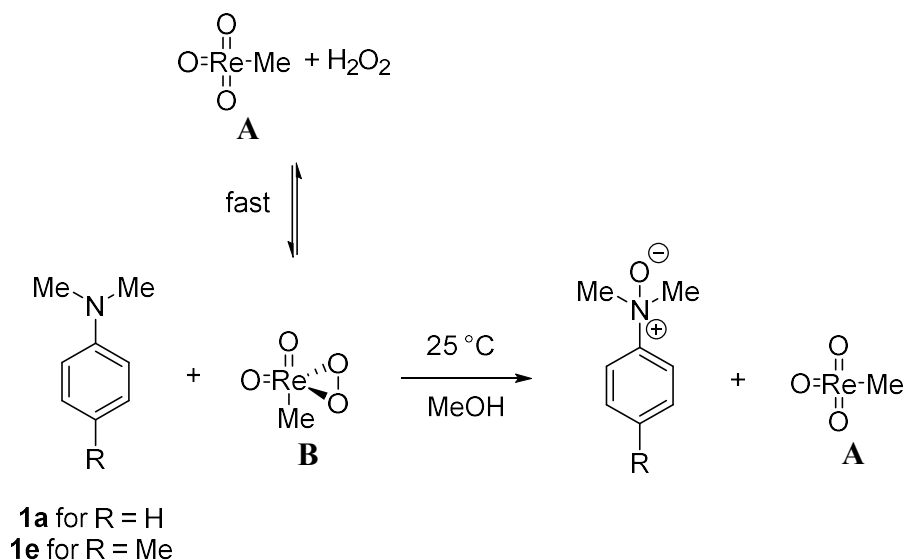
*N,N*-Dialkylated anilines (**1**) are highly important in organic chemistry as they are used as activator for polymerisations<sup>[2]</sup> and for the production of dyes,<sup>[3]</sup> pharmaceuticals and

agricultural chemicals.<sup>[4]</sup> Numerous kinetic studies on the reactivities of amines,<sup>[5]</sup> azoles,<sup>[6]</sup> and pyridines<sup>[7]</sup> have been performed, but kinetic data for the reaction with *N,N*-dialkylated anilines (**1**) is very limited to date.

Hirobe et al studied the conversion of the demethylation of *N,N*-dimethylaniline (**1a**) with hydrogen peroxide in the presence of Microperoxidase-11 (MP-11) and hemin-Cl (Scheme 2). They found full conversion in the presence of MP-11 within 5 min but only 20% conversion with hemin-Cl using the same setup (1 mM H<sub>2</sub>O<sub>2</sub>, 5 mM *N,N*-dimethylaniline (**1a**), 50% methanol, 50 mM sodium phosphate pH 7.4, 10 μM MP-11 or hemin-Cl, respectively). The data points could be fitted ( $k_{\text{obs}} = 4.1 \times 10^{-2} \text{ s}^{-1}$  using MP-11 as catalyst and  $2.1 \times 10^{-3} \text{ s}^{-1}$  for catalysis by hemin-Cl), although only 5 equivalents of **1a** over H<sub>2</sub>O<sub>2</sub> were applied.<sup>[8]</sup>



Scheme 2: Oxidative demethylation of *N,N*-dimethylaniline (**1a**) with hydrogen peroxide, using Microperoxidase-11 (MP-11) or hemin-Cl as a catalyst.



Scheme 3: Reaction of *N,N*-dimethylated anilines (**1**) with H<sub>2</sub>O<sub>2</sub> in the presence of the catalyst methyltrioxorhenium (**A**). The reaction proceeds via the *in situ* formed species **B**.

Another kinetic study of the reaction of hydrogen peroxide with *N,N*-dimethylated anilines (**1**) was performed by Espenson and Zhu (Scheme 3). They studied the oxidation of amines with hydrogen peroxide at 25 °C in methanol in presence of methylrhenium trioxide. Thereby, the 3-methyl-1,2,3-dioxarhenirane 3,3-dioxide MeRe(O)<sub>2</sub>(O<sub>2</sub>) (**B**) is formed *in situ* from methyltrioxorhenium (**A**) and hydrogen peroxide. They obtained the rate constants for the reaction of several *para* substituted *N,N*-dimethylanilines by initial rate experiments in methanol at 25 °C. Evaluation of this data shows a good correlation of the logarithmized second-order rate constants with the  $\sigma_p$  parameter (Table 1 and Figure 1), showing the consistency of the reaction mechanism within the studied amines. The data showed that the reaction is first-order with respect CH<sub>3</sub>ReO<sub>3</sub> and aniline. A zeroth-order dependence on [H<sub>2</sub>O<sub>2</sub>] was found.<sup>[9]</sup>

Table 1: Rate constants of the oxidation of *para*-substituted dimethylanilines at 25.0 °C in methanol.

<i>para</i> substituent	$k_2 \text{ M}^{-1} \text{ s}^{-1}$	$\lg k_2$	$\sigma_p^{[a]}$
CH <sub>3</sub>	24.5	1.39	-0.17
H	18.4	1.26	0
F	12.7	1.10	0.06
Br	8.7	0.94	0.23
NO <sub>2</sub>	1.9	0.28	0.78

[a] Values taken from Ref. [10].

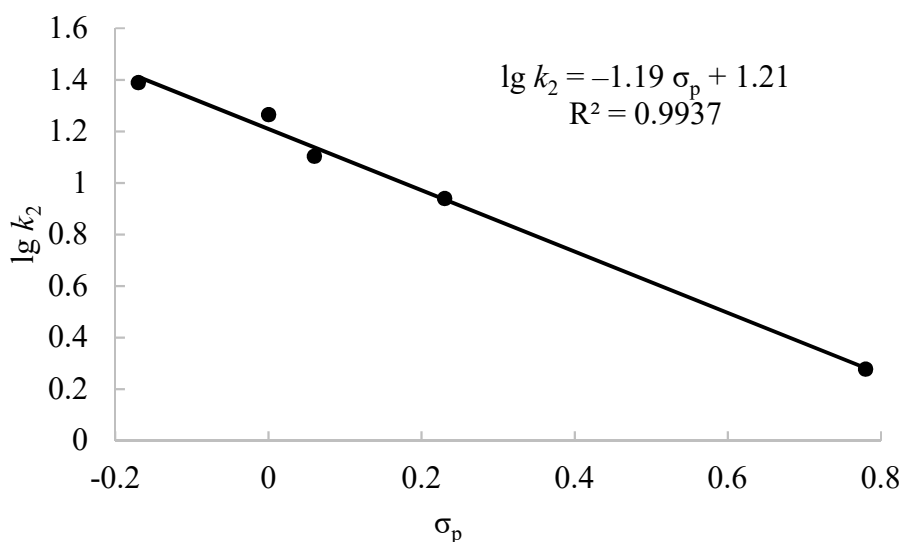
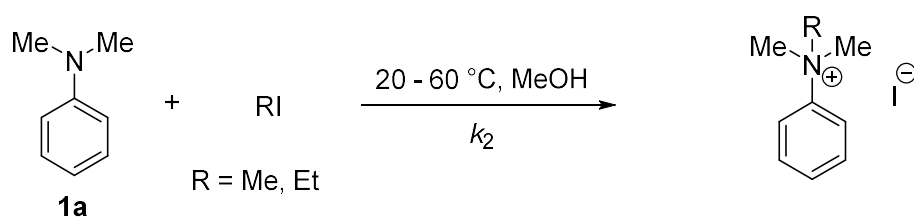
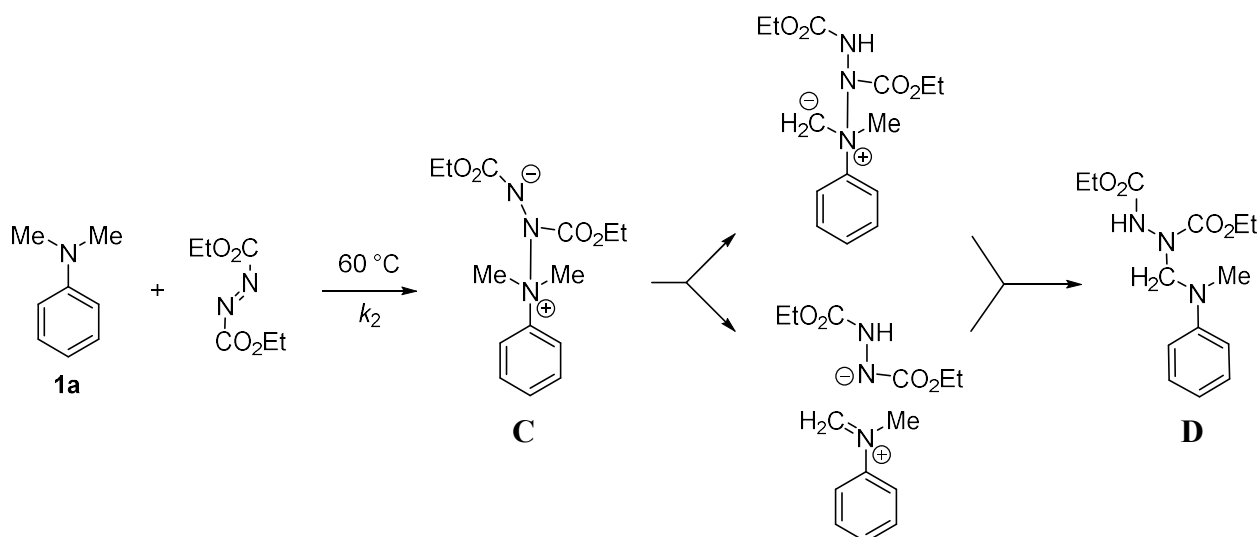


Figure 1: Hammett plot of the oxidation of para-substituted dimethylanilines at 25.0 °C in methanol with data of Table 1.



Scheme 4: Methylation and ethylation of *N,N*-dimethylaniline (**1a**) in methanol at various temperatures.

The methylation and ethylation of *N,N*-dimethylaniline (**1a**) was studied by Reis et al. in methanol at various temperatures, from 20 °C to 60 °C, with methyl iodide and ethyl iodide respectively (Scheme 4). They found a temperature dependent increase of the second-order rate constant by a factor of 22 in the case of the methyl iodide (from  $3.61 \times 10^{-5} \text{ M}^{-1} \text{ s}^{-1}$  to  $8.07 \times 10^{-4} \text{ M}^{-1} \text{ s}^{-1}$ ) and of 33 for the reaction with ethyl iodide (from  $1.68 \times 10^{-5} \text{ M}^{-1} \text{ s}^{-1}$  to  $5.53 \times 10^{-4} \text{ M}^{-1} \text{ s}^{-1}$ ). The Gibbs energy of activation,  $\Delta G^\ddagger$ , was calculated to be 99.2 kJ mol<sup>-1</sup> for the methylation and 106.7 kJ mol<sup>-1</sup> for the ethylation.<sup>[11]</sup>

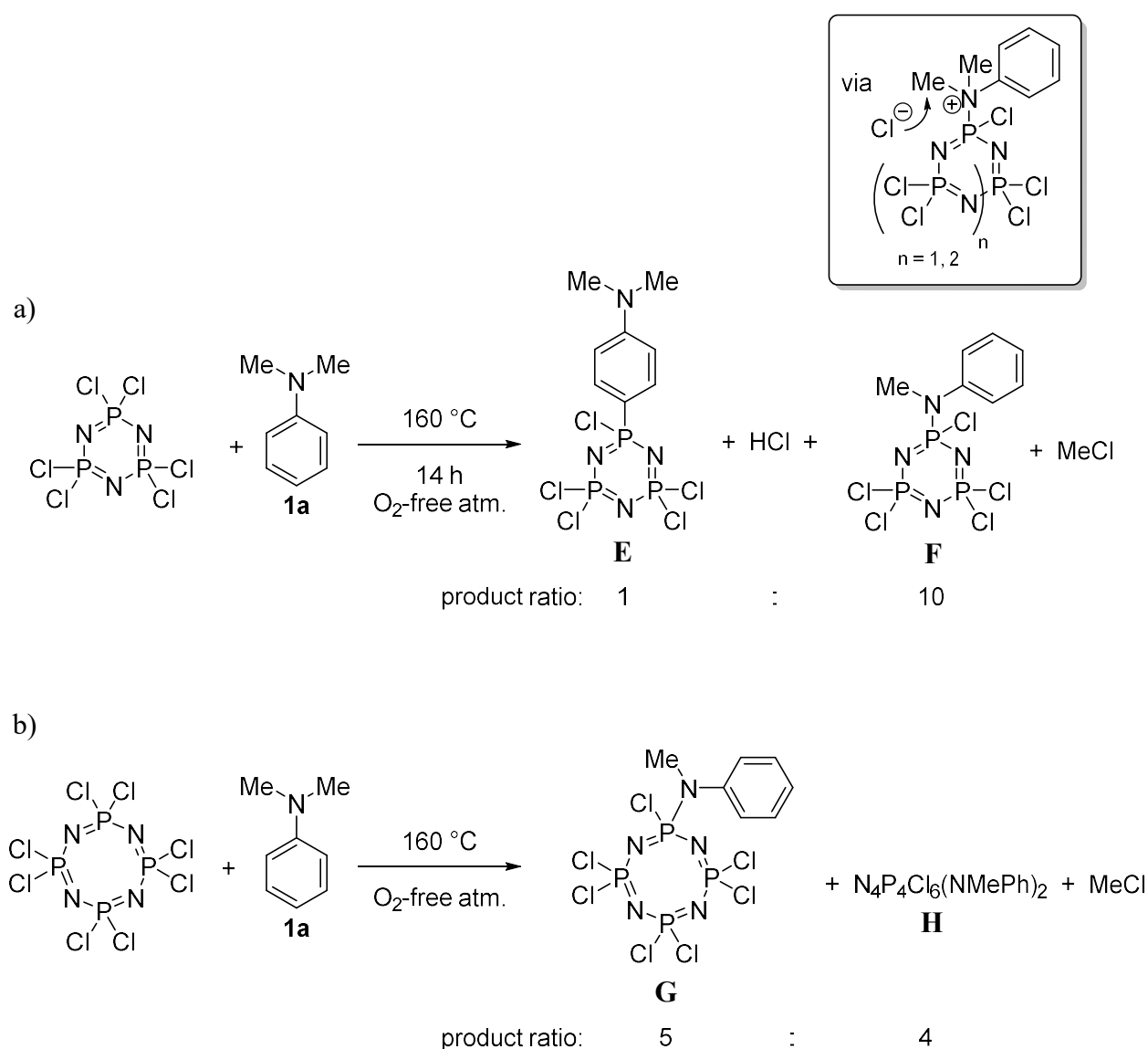


Scheme 5: Reaction of *N,N*-dimethylaniline (**1a**) with diethyl azodicarboxylate. Kinetically measured is the initial attack of the nitrogen atom at the azo moiety, yielding the intermediate **C**. The formation of the isolated product (**D**) was considered via a ylid-rearrangement (top pathway) but was later revised to form via a iminium ion (bottom pathway).<sup>[12]</sup>

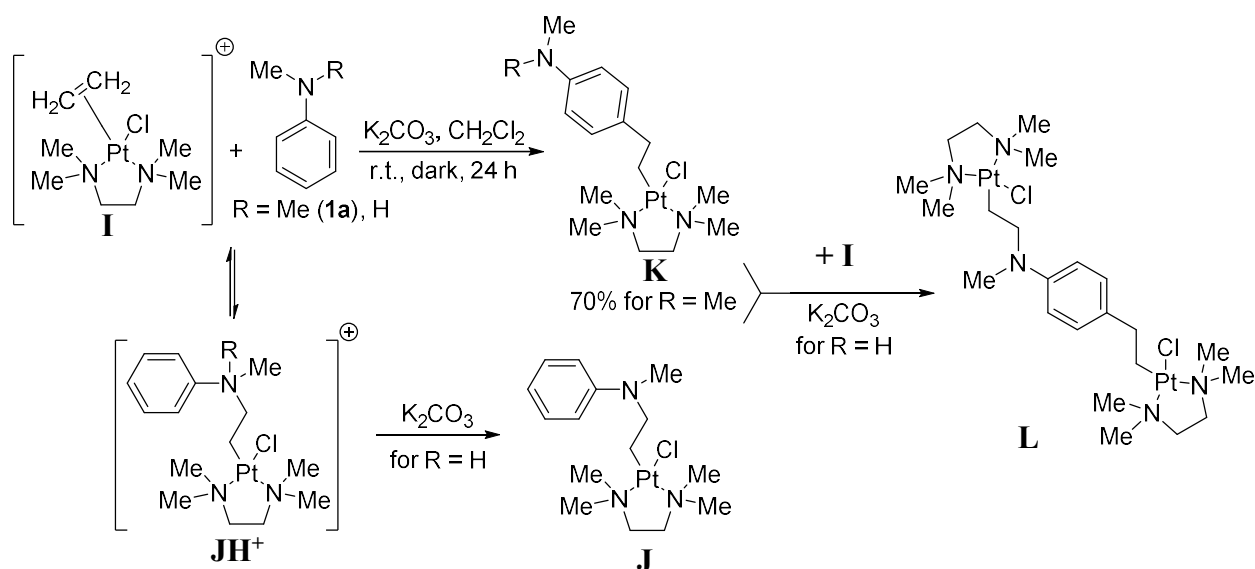
Huisgen and Jakob studied the addition of diethyl azodicarboxylates to *N,N*-dimethylaniline (**1a**) (Scheme 5). They studied the kinetics by iodometric titration in different solvents. By addition of radical inhibitors they excluded a radical mechanism of the reaction. The second-order rate constants  $k_2(60\text{ }^\circ\text{C})$  increases by a factor of 6, changing the solvent from unpolar cyclohexane ( $2.1 \times 10^{-1}\text{ M}^{-1}\text{ s}^{-1}$ ) to the very polar nitrobenzene ( $1.3\text{ M}^{-1}\text{ s}^{-1}$ ). Because of the high solvent polarity dependence, they concluded a polar intermediate and therefore a nucleophilic addition of the *N,N*-dimethylaniline (**1a**) nitrogen atom to the azo moiety (intermediate **C**). They found a strong decrease of the second-order rate constants by electron-withdrawing groups in dioxane at  $60\text{ }^\circ\text{C}$  (from  $3.5 \times 10^{-1}\text{ M}^{-1}\text{ s}^{-1}$  for **1a**, to  $1.4 \times 10^{-2}\text{ M}^{-1}\text{ s}^{-1}$  for *m*-nitro-*N,N*-dimethylaniline and no reaction with *p*-nitro-*N,N*-dimethylaniline), which supports this hypothesis. The formation of the isolated products was supposed to be an ylid-rearrangement (top pathway in Scheme 5), but was revised in 1994, to proceed over an iminium ion as intermediate (bottom pathway in Scheme 5).<sup>[12]</sup>

The ambident reactivity of *N,N*-dialkylated anilines **1** was studied intensively for synthetic use, for example with hexachlorocyclotriphosphazatriene ( $\text{N}_3\text{P}_3\text{Cl}_6$ ) (Scheme 6). Shaw and Cheng observed the C4 substituted product [ $\text{N}_3\text{P}_3\text{Cl}_5(\text{C}_6\text{H}_4\cdot\text{NMe}_2)$ ] (**E**) and the nitrogen-substituted product [ $\text{N}_3\text{P}_3\text{Cl}_5(\text{NMePh})$ ] (**F**), beside hydrochloride and alkylchloride as side products. When reacting  $\text{N}_3\text{P}_3\text{Cl}_6$  with *N,N*-dimethylaniline (**1a**), a conversion of about 60% was achieved within

14 h at 160 °C. The ratio of the carbon- (compound **E**) to the nitrogen-substituted (compound **F**) was found to be 1:10. In contrast, reactions of octachlorocyclotetraphosphazetetrane ( $N_4P_4Cl_8$ ) yield only nitrogen-substituted derivatives but as mono- ( $N_4P_4Cl_7NMePh$ , **G**) and di-substituted ( $N_4P_4Cl_6(NMePh)_2$ , **H**), which might be geminal or nongeminal, in a ratio of 5:4 with a total isolated yield of 85%. Taking the high reaction temperature into account, the formation of nitrogen-substituted products **F**, **G** and **H** may be surprising at the first glance, but the N-attack may become irreversible after fast elimination of the methyl chloride molecule, via a  $S_N2$ -type reaction (inlay in Scheme 6).<sup>[1a]</sup>

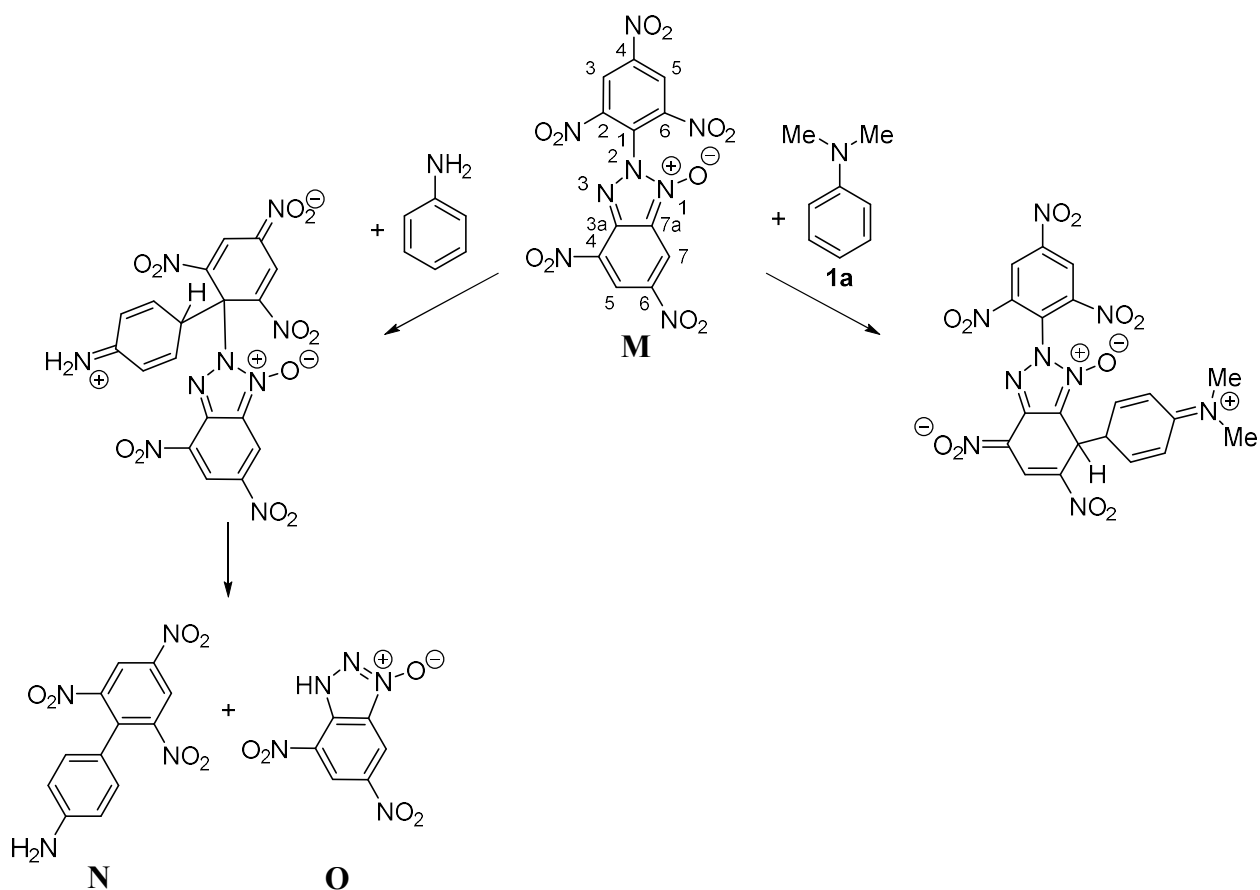


Scheme 6: Ambident reactivity of *N,N*-dimethylaniline (**1a**) when reacting with a) hexachlorocyclotriphosphazatriene ( $N_3P_3Cl_6$ ) and b) octachlorocyclotetraphosphazetetrane ( $N_4P_4Cl_8$ ). An exact structure of the disubstituted product  $N_4P_4Cl_6(NMePh)_2$  (**H**) was not given.<sup>[1a]</sup>



Scheme 7: Cationic palladium olefin complex  $[\text{PtCl}(\eta^2\text{-CH}_2=\text{CH}_2(\text{tmeda}))^+$  (tmeda = *N,N,N',N'*-tetramethyl-1,2-diaminoethane) (**I**) reacting with *N,N*-dimethylaniline (**1a**) or *N*-methylaniline. In case of **1a** only the C4 substituted product **K** was formed, while the reaction with *N*-methylaniline gave a mixture.<sup>[1b]</sup>

Maresca et al. studied the reaction of the cationic palladium olefin complex  $\text{C}_8\text{H}_{21}\text{ClN}_2\text{Pt}^+$  (**I**) with *N,N*-dimethylaniline (**1a**) and *N*-methylaniline. The proposed reaction mechanism with anilines is shown in Scheme 7. With *N*-methylaniline in excess (3 equivalents over **I**), the major product **JH**<sup>+</sup> is formed via nitrogen-attack. Carrying out the reaction in presence of potassium carbonate, the attack of the *para* carbon atom was also observed (minor product **K**, ca. 20% of the reaction products; reaction conditions r.t. and 48 h). *N*-Methylaniline further reacted with another equivalent of  $\text{C}_8\text{H}_{21}\text{ClN}_2\text{Pt}^+$  (**I**) and furnished the C and N substituted product **L**. Carrying out the analogous reaction with *N,N*-dimethylaniline (**1a**) in presence of potassium carbonate, the carbon substituted product **K** was formed, according to the authors, quantitative (70% conversion).<sup>[1b]</sup>



Scheme 8: Reaction of 4,6-dinitro-2-(2,4,6-trinitrophenyl)-2*H*-benzo[*d*][1,2,3]triazole 1-oxide **M** with aniline (left pathway) and *N,N*-dimethylaniline (**1a**) in DMSO-*d*<sub>6</sub> (right pathway).<sup>[1c]</sup>

Renfrow and Strauss studied the reaction of so-called super-electrophiles, namely 1,3,5-trinitrobenzene and 4,6-dinitro-2-(2,4,6-trinitrophenyl)-2*H*-benzo[*d*][1,2,3]triazole 1-oxide (**M**) with aniline and *N,N*-dimethylaniline (**1a**) (Scheme 8). Both amines did not react with 1,3,5-trinitrobenzene in DMSO-*d*<sub>6</sub>, but formed a  $\sigma$ -complex with **M**. Interestingly, with aniline the formation of the Meisenheimer type complex occurred at the picryl ring (carbon C1 of **M** in Scheme 8) and this  $\sigma$ -complex decomposed into 2',4',6'-trinitro-[1,1'-biphenyl]-4-amine (**N**) and 5,7-dinitro-1*H*-benzo[*d*][1,2,3]triazole 3-oxide (**O**). *N,N*-Dimethylaniline (**1a**), however, attacked only at the benzotriazole moiety and formed a stable  $\sigma$ -complex (carbon C7 of **M** in Scheme 8), but no product of the attack of the nitrogen atom was observed.<sup>[1c]</sup>

## The linear free energy relationship – The Mayr-Patz Equation

Elucidating the position of *N,N*-dialkylated anilines **1** in a comprehensive reactivity scale was missing so far. During the recent decades, Mayr et al. have constructed a comprehensive nucleophilicity scale, which is based on the kinetics of reactions of  $\pi$ -,  $n$ -, and  $\sigma$ -nucleophiles with benzhydrylium ions, structurally related quinone methides, and diethyl benzylidenemalonates.<sup>[13]</sup>

The second-order rate constants of these reactions have been described by Equation 1, where  $E$  is an electrophile-specific parameter, and  $N$  and  $s_N$  are solvent dependent nucleophile-specific parameters.<sup>[14]</sup>

$$\lg k_2 (20\text{ }^\circ\text{C}) = s_N (N + E) \quad (1)$$

With this equation, second-order rate constants of nucleophiles with electrophiles can be estimated. Generally, reactions at 20 °C will not occur, if the sum of  $N$  and  $E$  parameter is smaller than  $-5$ , and will react under diffusion control if the sum is higher than 9. The scale covers electrophiles with an  $E$  parameter ranging from  $-25$  to 8 and nucleophiles with a  $N$  parameter ranging from  $-4$  to 30, providing the base for reaction estimations for a wide range of nucleophiles-electrophiles combinations (Figure 2).

The  $N$  and  $s_N$  parameters for *N,N*-dialkylated anilines **1** are not available to date. Related compounds, like primary anilines and aliphatic tertiary amines, were already studied by Mayr et al. (Figure 3) with regard to their nucleophilicity at the nitrogen atom. The  $N$  parameters of aromatic amines vary around 13, those of the aliphatic ones around 18. This reflects the influence of the aromatic ring, lowering the reactivity of the nitrogen atom significantly.

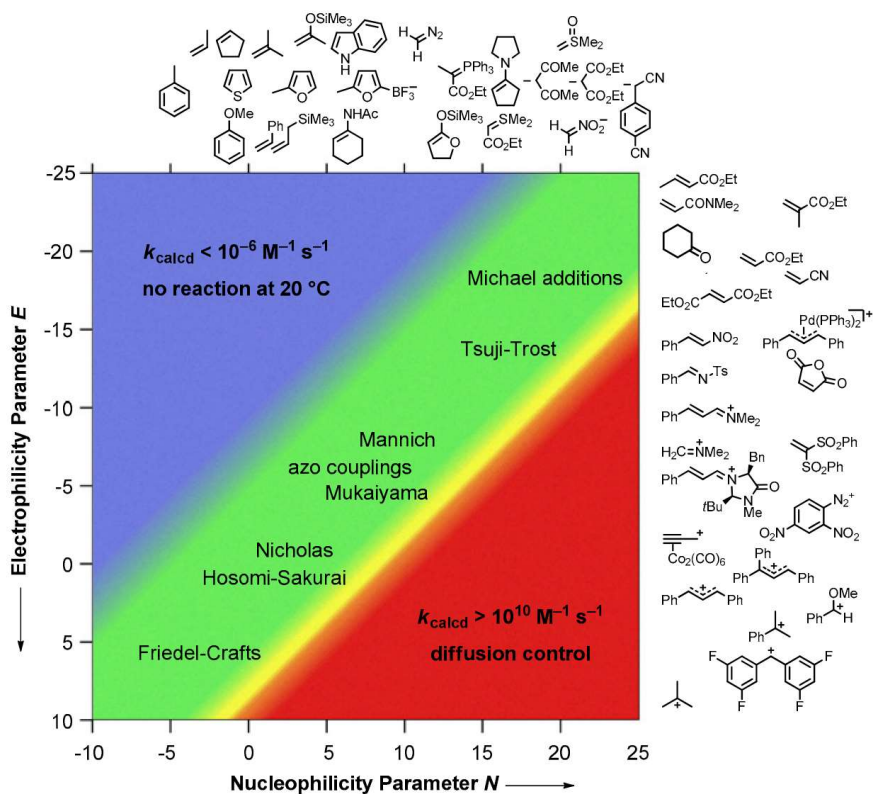


Figure 2: Plot of nucleophilicity parameter  $N$  versus electrophilicity parameter  $E$ , highlighting that many name reactions in organic chemistry are just in the well-defined corridor (green) between “no reaction” (blue) and “diffusion control” (red).

$N = 12.64$	$N = 12.92$	$N = 13.19$	$N = 13.42$	$N = 17.1^{[a]}$	$N = 20.59$	$N = 18.72$	$N = 16.8^{[a]}$
$s_N = (0.68)$	$s_N = (0.60)$	$s_N = (0.69)$	$s_N = (0.60)$	$s_N = (0.52)$	$s_N = (0.52)$	$s_N = (0.52)$	$s_N = (0.52)$

Figure 3: Nucleophile-specific parameters  $N$  and  $s_N$  (in parenthesis) of  $p$ -substituted anilines (left) and aliphatic amines (right) in acetonitrile for the attack of the nitrogen atom. [a]  $N$  parameters estimated with an  $s_N$  parameter of 0.52.<sup>[5g, 5h]</sup>

A variety of arenes have been studied by Mayr et al., for example toluene ( $N$  parameter of  $-4.36$  and  $s_N$  of  $1.77^{[15]}$ ). Comparing the  $\sigma_p^+$  of the methyl group ( $-0.32$ ) with the one of the dimethyl-amino group ( $-1.74$ ) suggests a huge increase of the nucleophilic reactivity of the para-position (C4 carbon). Based on these  $\sigma_p^+$  parameters, a  $N$  parameter of  $5.5$  was estimated for  $N,N$ -dimethylaniline (**1a**) at the C4-position.<sup>[13c]</sup> Comparing this estimated  $N$  parameter with the  $N$  and  $s_N$  parameters of aniline ( $N$  parameter of  $12.64$  and  $s_N$  of  $0.68$  for the attack at the nitrogen atom)<sup>[5g]</sup> and tertiary amines, like 1-methylpiperidine ( $N$  parameter of  $18.72$  and  $s_N$  of

0.52 for the attack at the nitrogen atom)<sup>[5h]</sup> suggests, that the corresponding attack of the nitrogen atom of **1a** is anticipated to be faster than the attack of the C4 carbon. The thereby formed quaternary ammonium salts might be unstable and therefore not isolable. It can be summarized, that a *N* parameter of 5.5 for the C4 carbon and a *N* parameter of 13 for the nitrogen atom of **1a** is expected (Figure 4).

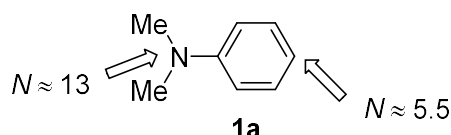
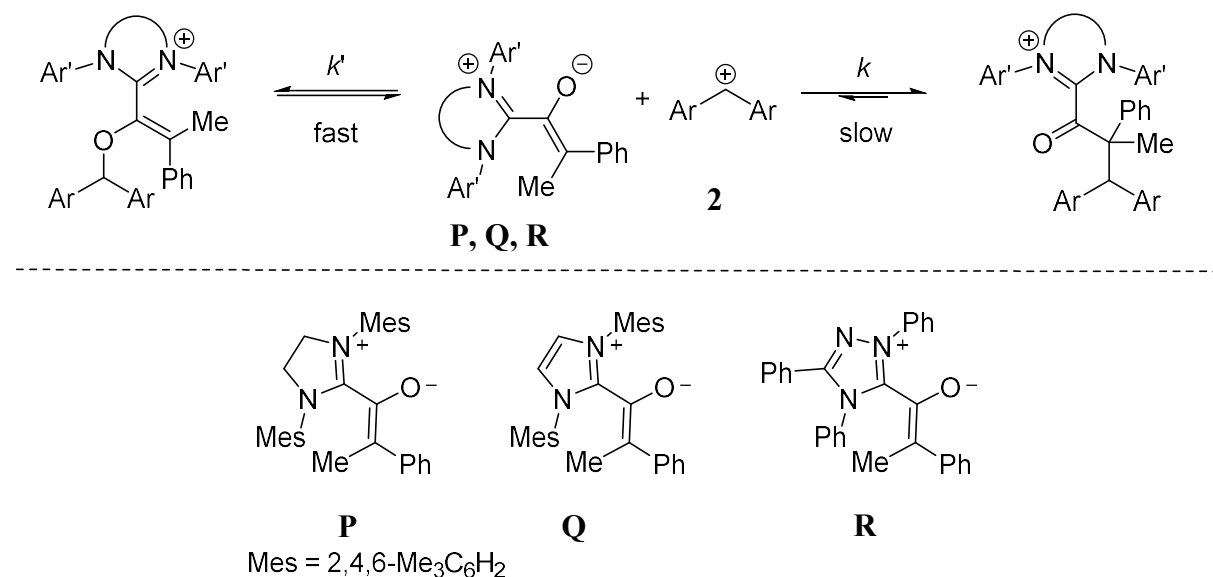


Figure 4: Estimated *N* parameters for the nitrogen and the C4 atom of *N,N*-dimethylaniline (**1a**).

*N,N*-Dialkylated anilines **1** are ambident nucleophiles with four nucleophilic sites (Scheme 1). Ambident reactivity is often analysed with the HSAB (hard and soft acids and bases) principle.<sup>[16]</sup> It was shown, however, that this concept is practically useless, as it is only applicable in around 50% of the cases and hence not better than flipping a coin.<sup>[17]</sup> Therefore there will be no further mention of this concept. In this work the reactivity of *N,N*-dialkylated anilines (**1**) for reactions with carbocations via N-attack, C-attack and hydride transfer will be discussed in terms of kinetic and thermodynamic control.



Scheme 9: Ambident reactivity of azolium-enolates investigated by Mayr and Maji with benzhydrylium ions **2**.<sup>[6e]</sup>

Ambident nucleophiles, like *N,N*-dialkylated anilines **1**, might give complex kinetics. This behaviour was found by Mayr et al. while studying the reactivities of azolium-enolates (Scheme 9). The extraordinary behaviour was explained by the different nucleophilic centers present in the nucleophile. The fast, but incomplete reaction (Figure 5) was assigned to benzhydrylium

attack at the more nucleophilic oxygen-center, the slow reaction to the electrophilic attack at the carbon-center of the enolate. Using the weakly Lewis acidic carbenium ions  $(\text{thq})_2\text{CH}^+$  (bis(1-methyl-1,2,3,4-tetrahydroquinolin-6-yl)methylum) and  $(\text{ind})_2\text{CH}^+$  (bis(1-methylindolin-5-yl)methylum), the formation of the benzhydryl enol ether was irrelevant, and only the attack at the carbon of the azolium enolate was observed. The stronger Lewis acidic  $(\text{dma})_2\text{CH}^+$  (**2b**) reacts first to a large extent to give the benzhydryl enol ether, rearrangement then leads to the thermodynamically more stable product of C-attack. In case of  $(\text{pyr})_2\text{CH}^+$  (**2a**) a borderline situation was found. At low concentrations of the azolium-enolate **R** the equilibrium for the oxygen-attack was shifted to the reactant side, while at high concentrations the oxygen-attack is measurable. In conclusion, the enolate-oxygen atom was attacked 20 times faster by benzhydrylium ions than the carbon atom leading to the thermodynamically more stable products.<sup>[6e]</sup>

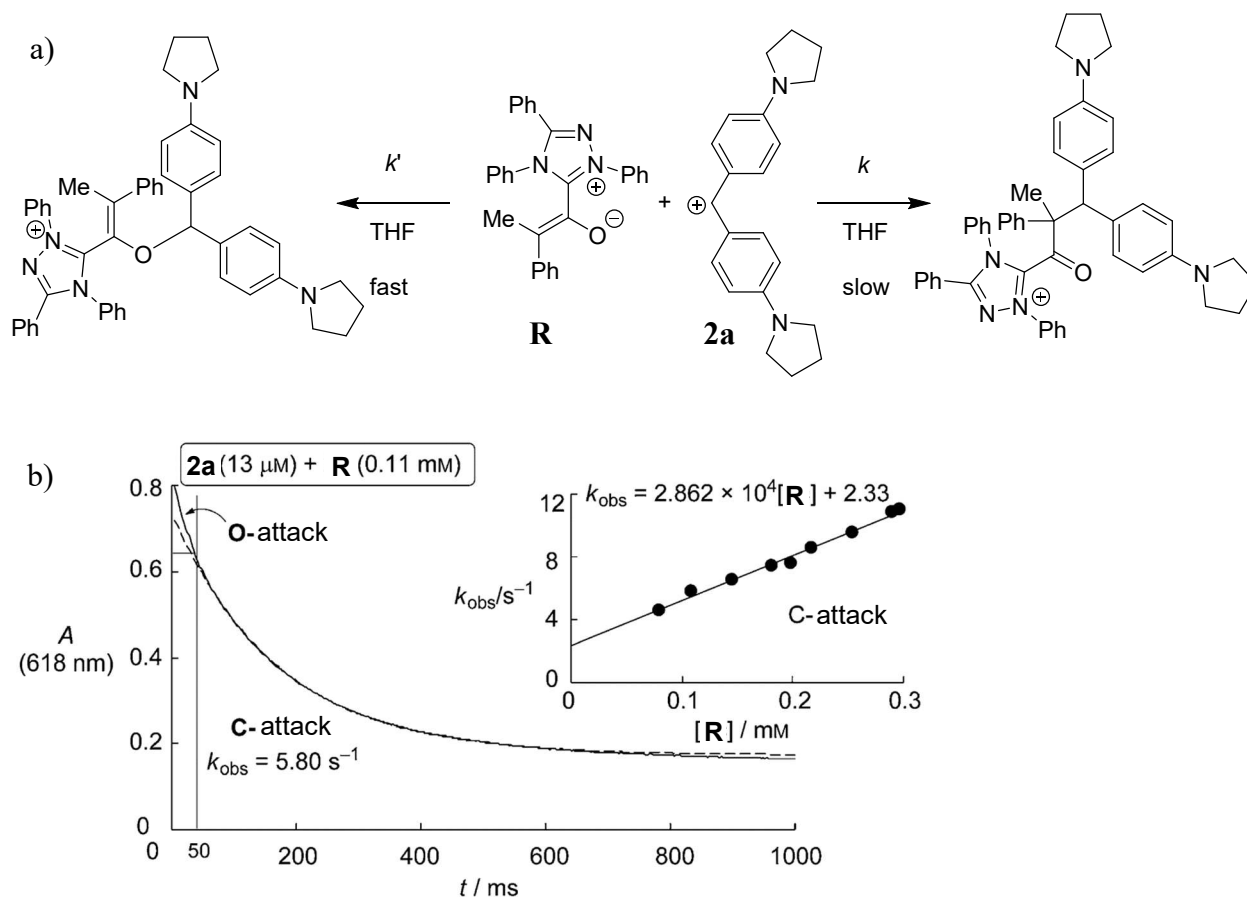
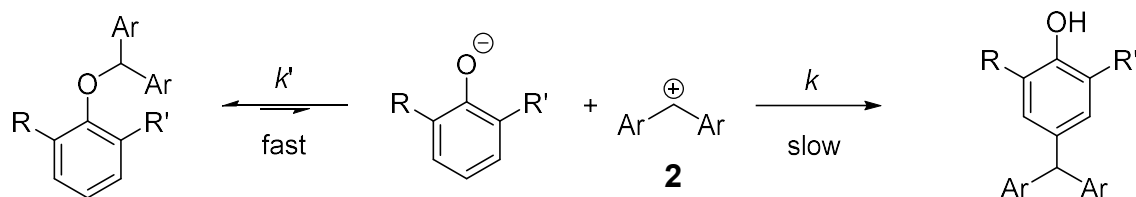
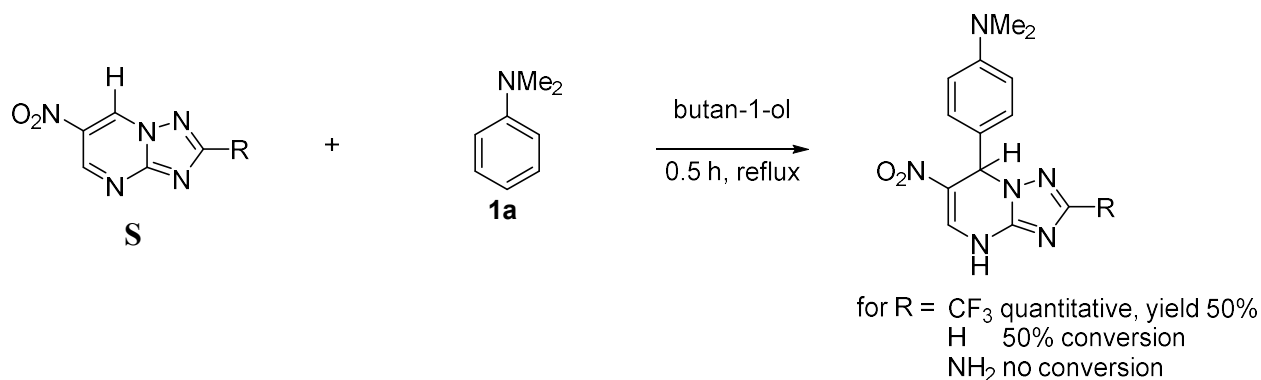


Figure 5: a) Reaction of  $(\text{pyr})_2\text{CH}^+$  (**2a**) with (Z)-2-phenyl-1-(1,3,4-triphenyl-4H-1,2,4-triazol-1-ium-5-yl)prop-1-en-1-olate (**R**). b) Plot of the absorbance  $A$  at 618 nm vs. time for the reaction of **R** ( $c = 1.1 \times 10^{-4} \text{ M}$ ) with **2a** ( $c = 1.3 \times 10^{-5} \text{ M}$ ) in THF at 20 °C with the calculated absorbance for the attack of the C-attack (dashed line;  $k_{\text{obs}} = 5.80 \text{ s}^{-1}$ ). Inlay: Linear correlation of the first-order rate constants  $k_{\text{obs}}$  for the C-attack vs.  $[\text{R}]$ .



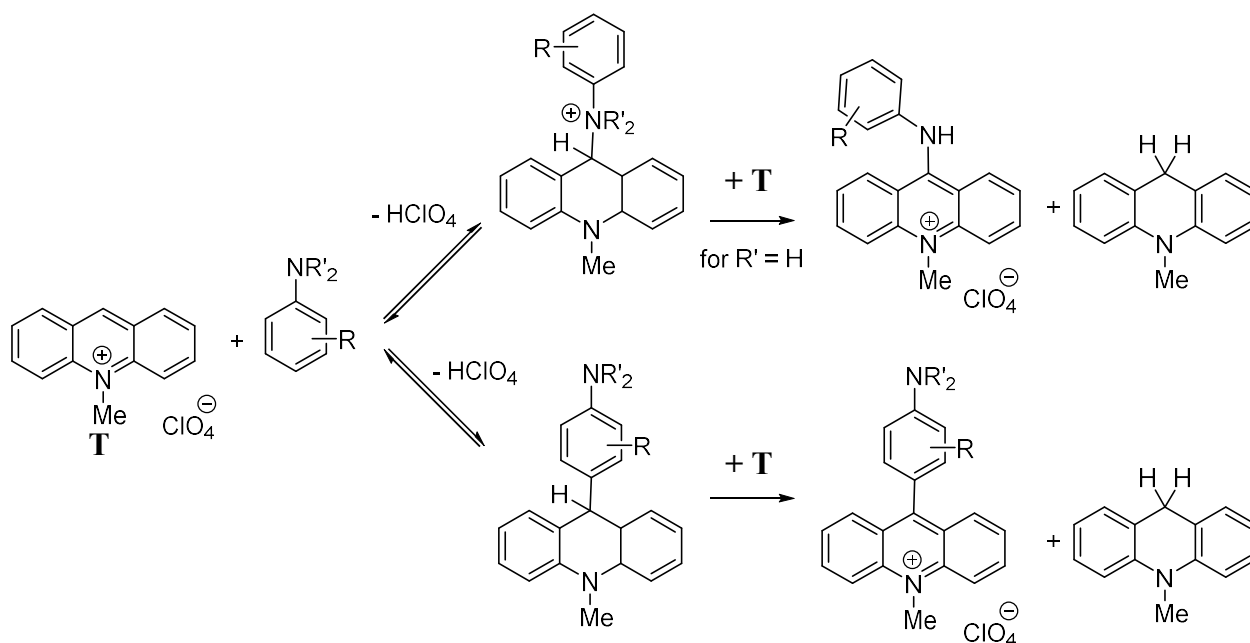
Scheme 10: Ambident reactivity of phenolates investigated by Ofial and co-workers.<sup>[18]</sup>

Ofial et al. investigated the ambident reaction of phenolates with benzhydrylium ions (Scheme 10). They found a fast attack of the phenolate oxygen atom which yielded the benzhydryl ethers as products. This attack is reversible and followed by slow and irreversible attack of the C4 ring carbon of the phenolate. Thus, the oxygen-substituted products of phenolates rearranged to the C4-substituted products. The reactivity of the oxygen atom was measured by UV/Vis spectroscopy. The subsequent isomerisation was studied by <sup>1</sup>H NMR spectroscopy and the second-order rate constants  $k_{2c}$  for reaction at the C4 carbon were derived thereof. An attack of the C2 carbon was not observed.<sup>[18]</sup>



Scheme 11: Reactivity of *N,N*-dimethylaniline (**1a**) under thermodynamic control.<sup>[19]</sup>

A wide range of reactions of electrophiles with substituted anilines and phenols was studied by Chupakhin et al. Reactions of *N,N*-dimethylaniline (**1a**) with electron-deficient arenes in butanol at reflux are shown in Scheme 11. Thus, the reactions are under thermodynamic control. This is reflected by the obtained product. For the reaction of *N,N*-dimethylaniline (**1a**) with azolopyrimidines (**S**) they found quantitative to no conversion, depending on the substituent at the azolopyrimidine (quantitative for R = CF<sub>3</sub>, 50% conversion for R = H, no conversion for R = NH<sub>2</sub>). As expected from the reaction conditions, no reaction product of the attack of the nitrogen atom of the dimethylamino group was found. Correspondingly, no conversion was observed reacting *N,N*-dimethyl-*para*-toluidine (**1e**) with azolopyrimidines (**S**), which was attributed to a steric hindrance of the dimethylamino group.<sup>[19]</sup>



Scheme 12: Ambident reactivity of primary and tertiary anilines in DMSO at 35 °C.<sup>[1d]</sup>

Chupakhin et al. also studied the ambident reactivity of primary and tertiary anilines with the *N*-methylacridinium ion (**T**). With tertiary anilines, a charge transfer complex was obtained with a broad absorption band at 540–580 nm. With a large excess of primary anilines it was possible to shift the equilibrium towards the N-adduct even at room temperature in DMSO. Thus, both species, the N-adduct as well as the C4 substitution product of aniline have been observed, but the ratio is dependent on the rest R of the amine (Scheme 12 and Table 2). In general, the methyl substituents at the nitrogen atom hinder a reaction at the nitrogen atom. Introducing substituents to the aromatic ring influences the ratio of carbon to nitrogen attack. A methyl group in *ortho* position (Table 2, entry 2) gives the C4 attack exclusively, while a methyl group in *meta* position, decreases the ratio to 2:1 (Table 2, entry 3). High yields of the N-adduct were found, if the C4 atom is blocked (Table 2, entry 4+5), but also a substitution at the C2 carbon was observed in the case of *p*-toluidine (Table 2, entry 4).<sup>[1d]</sup>

Table 2: Product ratio of the reactions of *N*-methylacridinium ion (**T**) with anilines in DMSO-*d*<sub>6</sub> at 35°C after 3 h.<sup>[1d]</sup>

Amine	C2 substitution [%]	C4 substitution [%]	N-adduct [%]
Aniline	–	80	20
<i>o</i> -Toluidine	–	100	–
<i>m</i> -Toluidine	–	66	34
<i>p</i> -Toluidine	28	–	72
<i>p</i> -Anisidine	–	–	100

## Project Proposal

Experimental data for the reactivity of *N,N*-dimethylaniline (**1a**) with benzhydrylium ions **2** was not available<sup>[5g, 5h]</sup> and only an estimate of the reactivity at the C4 carbon was made.<sup>[13c]</sup> The four different reaction sites might react parallel with the cationic electrophiles **2** and lead to multi-exponential decays of the monitored absorbance of these. Literature reports on the kinetics of ambident nucleophiles always find a fast and reversible reaction of the electron rich heteroatom with the benzhydrylium ions first, and a slow reaction of a carbon atom, if present.<sup>[5h, 6e, 18]</sup>

Many parameters, like the solvent or the substitution pattern at the *N,N*-dialkylated anilines **1** have effects on the reactivity and the ratio of carbon to nitrogen attack.<sup>[1d]</sup> We therefore decided to study beside *N,N*-dimethylaniline (**1a**), various substitution patterns, to put the experimental results in a broader context. Thus, the effect of alkyl groups on the reactivity of anilines, like ethyl groups (*N,N*-diethylaniline (**1b**)) and of the cyclic five-membered ring (1-phenylpyrrolidine (**1c**)) and six-membered ring (1-phenylpiperidine (**1d**)) were studied. Additionally, the effect of a *para* substitution at the aromatic ring was investigated (*N,N*-dimethyl-*para*-toluidine (**1e**) and *N,N*-dimethyl-*para*-anisidine (**1f**)). As reaction partner, several benzhydrylium ions, with an *E* parameter of around –5, were chosen as reference electrophiles (Table 3 and Figure 6), as the *N* parameter of the C4 carbon of **1a** was estimated to be 5.5 and the *N* parameter of the nitrogen atom can be estimated around 13 (Figure 4).

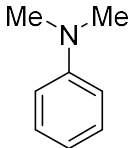
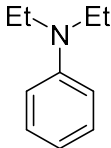
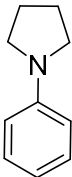
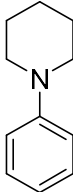
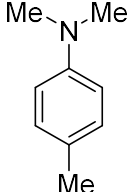
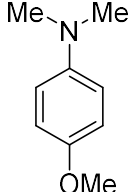
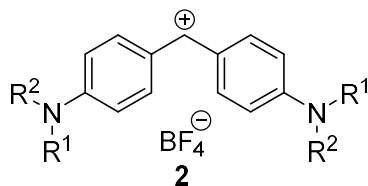
						
	<b>1a</b>	<b>1b</b>	<b>1c</b>	<b>1d</b>	<b>1e</b>	<b>1f</b>
$pK_{aH}(\text{AN}) =$	11.43	12.4 <sup>[a,b]</sup>			12.23	12.74
$pK_{aH}(\text{H}_2\text{O}) =$	5.13 <sup>[a]</sup>	6.56	4.40 <sup>[c]</sup>	5.20 <sup>[d]</sup>	5.60 <sup>[a]</sup>	5.83 <sup>[a]</sup>
$GB_{\text{exp}}^{\text{[b]}} =$	216.7 <sup>[a]</sup>	221.8	218.7	221.4	219.5 <sup>[a]</sup>	220.6 <sup>[a]</sup>

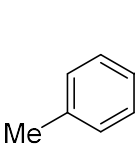
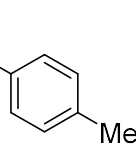
Figure 6: *N,N*-Dimethylaniline (**1a**) and derivatives (**1b–f**) studied with benzhydrylium ions **2** in this work. Gas-phase basicities ( $GB$ ) are in kcal mol<sup>-1</sup> (1 kcal mol<sup>-1</sup> = 4.184 kJ mol<sup>-1</sup>).  $pK_{aH}$  and  $GB_{\text{exp}}$  values were taken from Ref. [20]. [a] Averaged value. [b] Taken from Ref. [21]. [c] Taken from Ref. [22]. [d] Taken from Ref. [23].

The  $pK_a$  values of the anilines **1a–f** do not differ dramatically (Figure 6). In water the most basic one is the *N,N*-diethylaniline (**1b**), the least basic one (more than two  $pK_{aH}$  units less basic) is 1-phenylpyrrolidine (**1c**). The para substituted anilines **1e** and **1f** are, as expected, more basic than the parent compound **1a**, but not as basic as the *N,N*-diethylsubstituted **1b**. Unfortunately,  $pK_{aH}$  values in acetonitrile are not available for all anilines **1a–f**, but a similar trend is found. In the row of **1a**, **1b**, **1e** and **1f**, *N,N*-dimethylaniline (**1a**) is the least basic one, but *N,N*-dimethyl-*para*-anisidine (**1f**) is slightly more basic than *N,N*-diethylaniline (**1b**).

We determined rate and equilibrium constants in polar aprotic solvents, namely in acetonitrile and dichloromethane. If not mentioned otherwise, the solvent used is acetonitrile. For clarity the counter ions of the benzhydrylium ions, which are tetrafluoroborate (BF<sub>4</sub><sup>-</sup>) in case of **2a–g** and bromide (Br<sup>-</sup>) in case of the significantly more reactive **2h**, are mostly omitted (Table 3).

Table 3: Benzhydrylium tetrafluoroborates **2** employed as reference electrophiles in this study.<sup>[24]</sup>



Electrophile	R <sup>1</sup>	R <sup>2</sup>	No.	<i>E</i> parameter	λ <sub>max</sub> [nm] in acetonitrile	λ <sub>max</sub> [nm] in dichloromethane
(pyr) <sub>2</sub> CH <sup>+</sup>	C <sub>4</sub> H <sub>8</sub> (cycl.)		<b>2a</b>	-7.69	612	620
(dma) <sub>2</sub> CH <sup>+</sup>	Me	Me	<b>2b</b>	-7.02	605	613
(mpa) <sub>2</sub> CH <sup>+</sup>	Ph	Me	<b>2c</b>	-5.89	613	623
(mor) <sub>2</sub> CH <sup>+</sup>	C <sub>2</sub> H <sub>4</sub> -O-C <sub>2</sub> H <sub>4</sub> (cycl.)		<b>2d</b>	-5.53	612	621
(dpa) <sub>2</sub> CH <sup>+</sup>	Ph	Ph	<b>2e</b>	-4.72	645	674
(mfa) <sub>2</sub> CH <sup>+</sup>	CH <sub>2</sub> CF <sub>3</sub>	Me	<b>2f</b>	-3.85	586	593
(pfa) <sub>2</sub> CH <sup>+</sup>	CH <sub>2</sub> CF <sub>3</sub>	Ph	<b>2g</b>	-3.14	592	601
(tol) <sub>2</sub> CHBr			<b>2h</b>	3.63 <sup>[a]</sup>	_[b]	_[b]

[a] *E* parameter of the corresponding cation (tol)<sub>2</sub>CH<sup>+</sup>. [b] Not used for photometric studies.

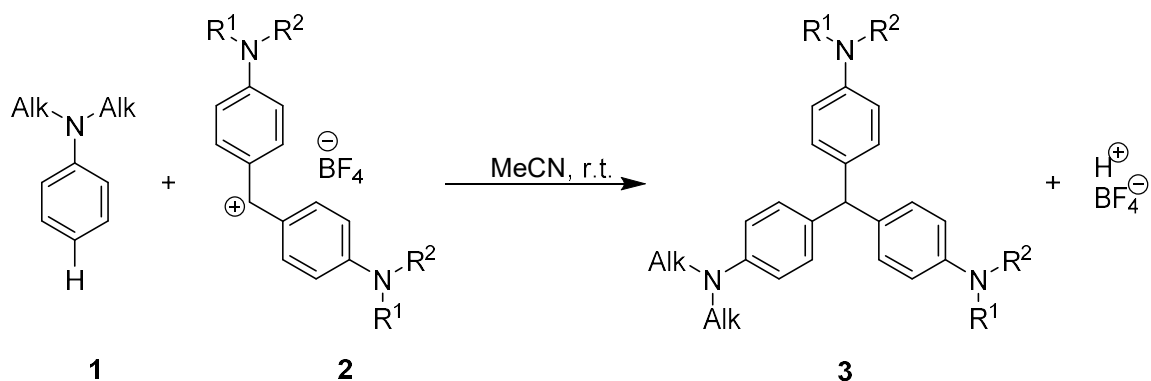
## Results and Discussion

### Product Studies

As outlined in Scheme 1, various products can be formed when *N*-phenyl dialkylamines react with carbocations. Product studies for the reactions of **1** with the reference electrophiles **2** were performed to elucidate the product structures and the selectivity of their formation.

To the deeply blue-coloured solutions of the benzhydrylium ions **2** in dry solvents (acetonitrile or dichloromethane) the anilines **1** were added dropwise in slight excess ( $\approx 1.1$  equiv.). Complete decoloration of the solutions was not achieved, indicating that a small amount of **2** remained in the reaction mixture. After TLC showed no further conversion, the mixture was subjected to basic aqueous workup and purified by flash chromatography. The reactions of **1a**, **1b** and **1d** with the benzhydrylium ions **2b**, **2d** and **2f** furnished triarylmethanes **3** in good yields (Table 4). Though, the reaction conditions had not been optimized. Nevertheless, some significant differences are observed. The reaction of *N,N*-dimethylaniline (**1a**) with  $(\text{dma})_2\text{CH}^+$  (**2b**) furnished the 4,4',4''-methanetriyltris(*N,N*-dimethylaniline) (**3ab**) in good yield in 48 h. Reacting the more reactive benzhydrylium ion  $(\text{mfa})_2\text{CH}^+$  (**2f**) with **1a** furnished the corresponding triarylmethane 4,4'-((4-(dimethylamino)phenyl)methylene)bis(*N*-methyl-*N*-(2,2,2-trifluoroethyl)aniline) (**3af**) also in good yield within 18 h. The reaction of **2f** with 1-phenylpiperidine (**1d**) was completed within 1 h and after aqueous workup the 4,4'-((4-(piperidin-1-yl)phenyl)methylene)bis(*N*-methyl-*N*-(2,2,2-trifluoroethyl)aniline) (**3df**) was isolated as product of the attack of the C4 carbon. Reacting *N,N*-diethylaniline (**1b**) with  $(\text{dma})_2\text{CH}^+$  (**2b**) produced 4,4'-((4-(diethylamino)phenyl)methylene)bis(*N,N*-dimethylaniline) (**3bb**) in good yields but after a reaction time of 5 d. The extraordinary long reaction time is due to total lack of visible decolouration. The reaction was quenched as no further conversion was detected. Aside from the reaction time, the result is equal to the result of the reaction of *N,N*-dimethylaniline (**1a**) with **2b**. Again, using the more reactive cation  $(\text{mor})_2\text{CH}^+$  (**2d**) led to 4-(bis(4-morpholinophenyl)methyl)-*N,N*-diethylaniline (**3bd**) in 24 h. Other reaction products than the triarylmethanes **3** were not observed under these reaction conditions. The isolated powders were slightly blue or violet, or became slightly coloured within a few hours, indicating decomposition of a very small amount of the product. This degradation did not affect the analytical data of the obtained compounds, as the isolated compounds stayed analytically pure over several days.

Table 4: Yields and reaction times of the reactions of *N,N*-dialkylated anilines **1a**, **1b** and **1d** with benzhydrylium ions **2** in acetonitrile at room temperature.



Aniline	Alk	Electrophile	R <sup>1</sup>	R <sup>2</sup>	Reaction time <sup>[a]</sup>	Product, yield <sup>[b]</sup>
<b>1a</b>	Me	(dma) <sub>2</sub> CH <sup>+</sup> ( <b>2b</b> )	Me	Me	48 h	<b>3ab</b> , 70%
<b>1a</b>	Me	(mfa) <sub>2</sub> CH <sup>+</sup> ( <b>2f</b> )	Me	CH <sub>2</sub> CF <sub>3</sub>	18 h	<b>3af</b> , 84% <sup>[c]</sup>
<b>1b</b>	Et	(dma) <sub>2</sub> CH <sup>+</sup> ( <b>2b</b> )	Me	Me	5 d	<b>3bb</b> , 75%
<b>1b</b>	Et	(mor) <sub>2</sub> CH <sup>+</sup> ( <b>2d</b> )	C <sub>2</sub> H <sub>4</sub> -O-C <sub>2</sub> H <sub>4</sub> (cycl.)		24 h	<b>3bd</b> , 84%
<b>1d</b>	C <sub>5</sub> H <sub>10</sub> (cycl.)	(mfa) <sub>2</sub> CH <sup>+</sup> ( <b>2f</b> )	Me	CH <sub>2</sub> CF <sub>3</sub>	1 h	<b>3df</b> , 87%

[a] Reaction conditions not optimized. [b] Isolated yields. [c] Dichloromethane was used as solvent.

## Nucleophilicity of *N,N*-dimethylaniline (**1a**)

The unambiguous results of the product studies encouraged us to investigate the kinetics of these reactions. The reactions of *N,N*-dimethylaniline (**1a**) with benzhydrylium ions **2** were monitored photometrically or by time-resolved  $^1\text{H}$  NMR spectroscopy. The advantage of  $^1\text{H}$  NMR spectroscopy are that relatively high concentrations of reactants are employed, which accelerates the reaction. A disadvantage is the sensitivity of this method, as nearly equimolar ratios of the reaction partners are necessary. Thus, pseudo first-order conditions cannot be applied. Therefore, the rate law for second-order reactions (2) was integrated to Equation 3.

$$\frac{d[\text{P}]}{dt} = -\frac{d[\text{E}^+]}{dt} = k[\text{E}^+][\mathbf{1a}] \quad (2)$$

$$kt = \frac{1}{[\mathbf{1a}]_0 - [\text{E}^+]_0} \ln \frac{[\text{E}^+]_0([\text{E}^+]_t + [\mathbf{1a}]_0 - [\text{E}^+]_0)}{[\mathbf{1a}]_0[\text{E}^+]_t} = Y \quad (3)$$

Exemplary the reaction of *N,N*-dimethylaniline (**1a**) with  $(\text{dma})_2\text{CH}^+ \text{BF}_4^-$  (**2b**) in  $\text{CD}_3\text{CN}$  at 23 °C is shown (Figure 7). The second-order rate constant  $k_2 = 1.18 \times 10^{-2} \text{ M}^{-1} \text{ s}^{-1}$  is the slope of the correlation. In analogy to the product studies, the time-resolved  $^1\text{H}$  NMR spectra clearly show the formation of the *para*-substituted product (see Figure S4 in the Supporting Information).

The same reaction was followed by UV/Vis spectroscopy. For all photometrically studied combinations, *N,N*-dimethylaniline (**1a**) was added in excess ( $> 10$  equivalents) to achieve pseudo-first-order conditions. The pseudo-first-order rate constants  $k_{\text{obs}}$  ( $\text{s}^{-1}$ ) were obtained by least-squares fitting of the monoexponential function  $A_t = A_0 e^{-k_{\text{obs}}t} + C$  to the time-dependent absorbance decays of the electrophiles. Plots of  $k_{\text{obs}}$  versus the nucleophile concentrations were linear for most reactions with the reference electrophiles. The second-order rate constants  $k_2$  ( $\text{M}^{-1} \text{ s}^{-1}$ ) were obtained from the slopes of these plots, according to eq. 4, where  $k_0$  is one or several background reactions, with e.g. the solvent or residual water, which may or may not occur.

$$k_{\text{obs}} = k_2 [\text{Nu}] + k_0 \quad (4)$$

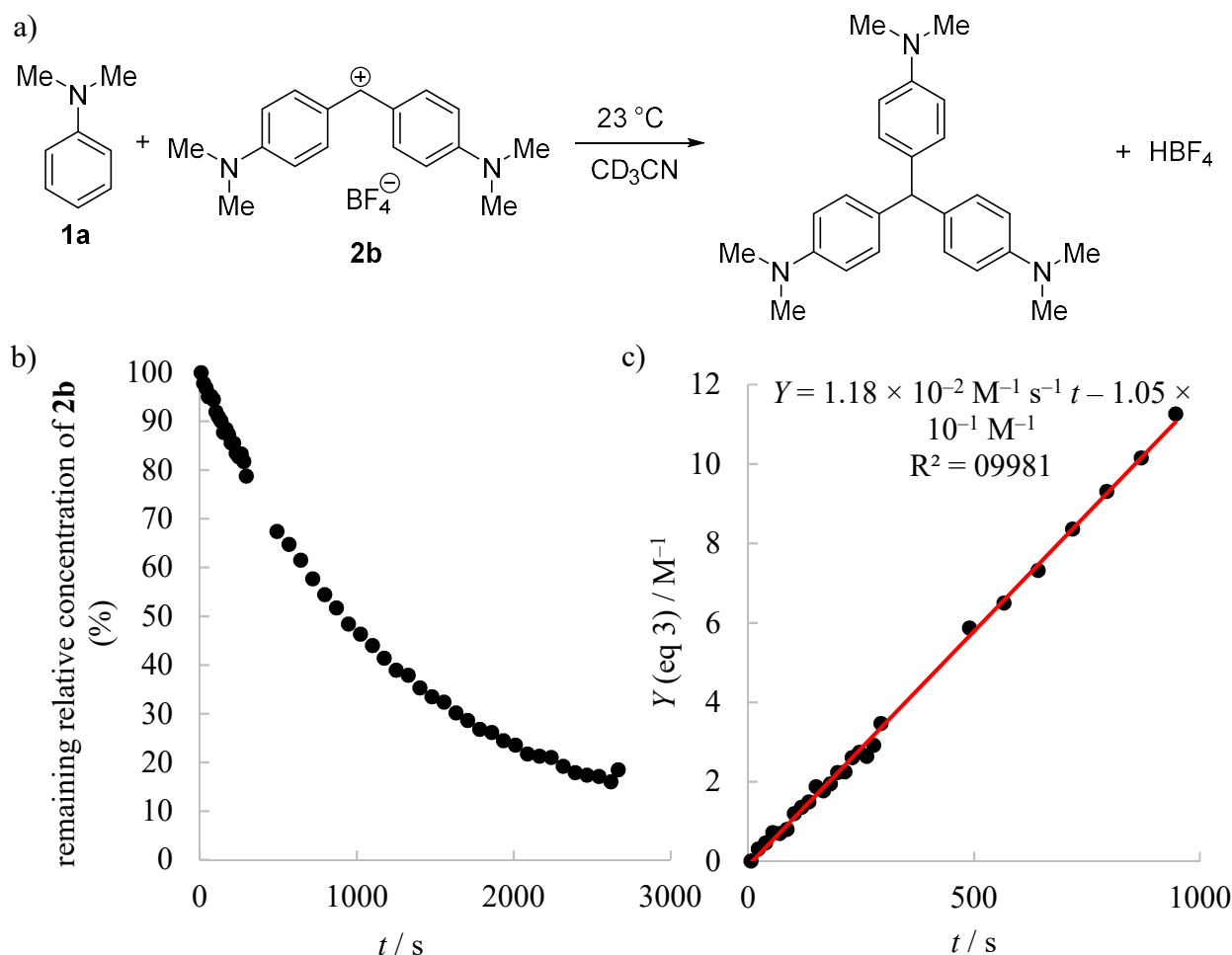


Figure 7: a) Reaction of  $N,N$ -dimethylaniline (**1a**) with  $(dma)_2CH^+ BF_4^-$  (**2b**) in  $CD_3CN$  at  $23\text{ }^\circ C$ . b) Decay of the relative concentration of  $(dma)_2CH^+ BF_4^-$  (**2b**;  $c = 2.32 \times 10^{-2} M$ ) while reacting with  $N,N$ -dimethylaniline (**1a**;  $c = 7.13 \times 10^{-2} M$ ) in  $CD_3CN$  at  $23\text{ }^\circ C$ . c) Determination of the second-order rate constant by plotting time versus  $Y = ([\mathbf{1a}]_0 - [\mathbf{2b}]_0)^{-1} \ln([\mathbf{2b}]_0([\mathbf{2b}]_t + [\mathbf{1a}]_0 - [\mathbf{2b}]_0) / [\mathbf{1a}]_0[\mathbf{2b}]_t)$  ( $k_2 = 1.18 \times 10^{-2} M^{-1} s^{-1}$ , data points up to 50% conversion were used).

Monitoring the absorbance of  $(dma)_2CH^+$  (**2b**) when reacting with **1a** by UV/Vis spectroscopy, an unexpected behaviour was found, as the absorbance of the **2b** drops significantly in the first seconds (Figure 3). Excluding this time range from the fit of the monoexponential function  $A_t = A_0 e^{-k_{obs}t} + C$  the second-order rate constants  $k_2$  were obtained from the slopes of the linear plots of  $k_{obs}$  against the nucleophile concentrations (inlay in Figure 3b), yielding a  $k_2 = 9.91 \times 10^{-3} M^{-1} s^{-1}$ , with is only 16% slower than the  $k_2$  obtained by  $^1H$  NMR spectroscopy at the

slightly elevated temperature ( $k_2 = 1.18 \times 10^{-2} \text{ M}^{-1} \text{ s}^{-1}$  in  $\text{CD}_3\text{CN}$  at  $23 \text{ }^\circ\text{C}$ ). Therefore it can be concluded, that this reaction is the attack of the **1a**'s C4 carbon atom. However, the initial drop of the absorbance could also be evaluated using least-squares fitting of the exponential function  $A_t = A_0 e^{-k_{\text{obs}}t} + C$  to the time-dependent absorbance (Figure 3c). This shows clearly the appearance of a second reaction.

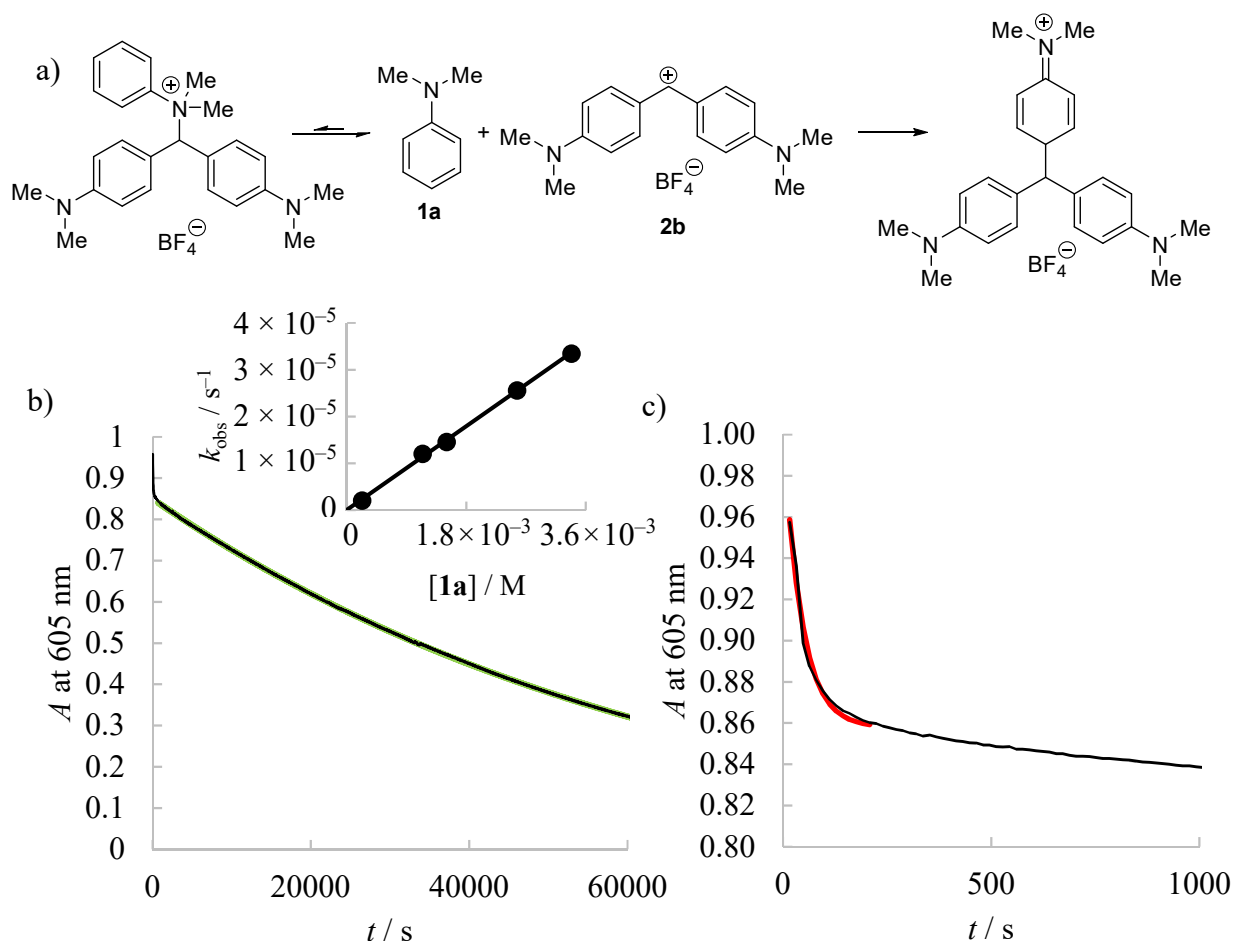


Figure 8: a) Reaction of  $N,N$ -dimethylaniline (**1a**) with  $(\text{dma})_2\text{CH}^+ \text{BF}_4^-$  (**2b**) in  $\text{CH}_3\text{CN}$  at  $20 \text{ }^\circ\text{C}$ . b) Plot of the absorbance  $A$  at 605 nm vs. time for the reaction of  $N,N$ -dimethylaniline (**1a**;  $c = 1.67 \times 10^{-3} \text{ M}$ ) with **2b** ( $c = 1.16 \times 10^{-5} \text{ M}$ ) in acetonitrile at  $20 \text{ }^\circ\text{C}$  with the calculated absorbance (green line;  $k_{\text{obs}} = 1.48 \times 10^{-5} \text{ s}^{-1}$ ). Inlay: The slope of the linear correlation of the first-order rate constants  $k_{\text{obs}}$  with the nucleophile concentrations corresponds to the second-order rate constant  $k_2$  ( $\text{CH}_3\text{CN}$ ,  $20 \text{ }^\circ\text{C}$ ) for the attack of the C4 carbon of **1a** at the carbocation **2b**. Correlation line:  $k_{\text{obs}} = 9.91 \times 10^{-3} \text{ M}^{-1} \text{ s}^{-1} [\mathbf{1a}] + 1.14 \times 10^{-7} \text{ s}^{-1}$ ,  $R^2 = 0.9988$ ). c) Enhancement of the first seconds. A unexpected sudden drop of the absorbance of **2b** is found. It can be described by another monoexponential function (red line;  $A_t = A_0 e^{-k_{\text{obs}}t} + C$  with a  $k_{\text{obs}} = 2.28 \times 10^{-2} \text{ s}^{-1}$ ).

Benzhydrylium ions **2** can react with *N,N*-dimethylaniline (**1a**) at four different reaction sides (Scheme 1). Product mixtures of the attacks at the **1a**'s nitrogen, C2 or C4 atom has been reported in the literature. [1a, 1b, 1d] To clarify the regioselectivity of the reactions, Florian Achraimer from the Zipse group performed quantum mechanics calculations at B2PLYP-D3(FC)/G3MP2large//M06-2X/6-31+G(d) level of theory of the reactions of carbocations **2** with *N,N*-dimethylaniline (**1a**) in the gas phase. The reaction of *N,N*-dimethylaniline (**1a**) with three different electrophiles was studied: two benzhydrylium ions **2x** (R = H) and **2b** (R = NMe<sub>2</sub>) and the prop-2-yl cation **2y**, as a sterically more demanding alternative to the methyl cation (Figure 9).

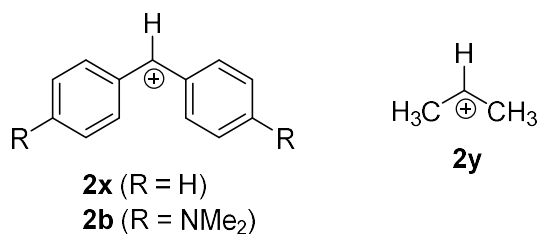


Figure 9: Carbocations **2b**, **2x** and **2y** used for quantum-chemical studies.

As expected the most exothermic reaction enthalpies were obtained for the reaction of the prop-2-yl cation (**2y**; black bars in Figure 10) with the nitrogen of the *N,N*-dimethylaniline (**1a**) ( $\langle\Delta H_{\text{N}}\rangle = -267.6 \text{ kJ mol}^{-1}$ ), followed by addition to the *para* position ( $\langle\Delta H_{\text{para}}\rangle = -248.2 \text{ kJ mol}^{-1}$ ). A similar trend is observed for the parent benzhydrylium ion **2x** (red bars in Figure 10) with reaction enthalpies of  $\langle\Delta H_{\text{N}}\rangle = -119.0 \text{ kJ mol}^{-1}$  for the attack of the nitrogen atom and  $\langle\Delta H_{\text{para}}\rangle = -102.2 \text{ kJ mol}^{-1}$  for addition to the *para* position of **1a**.

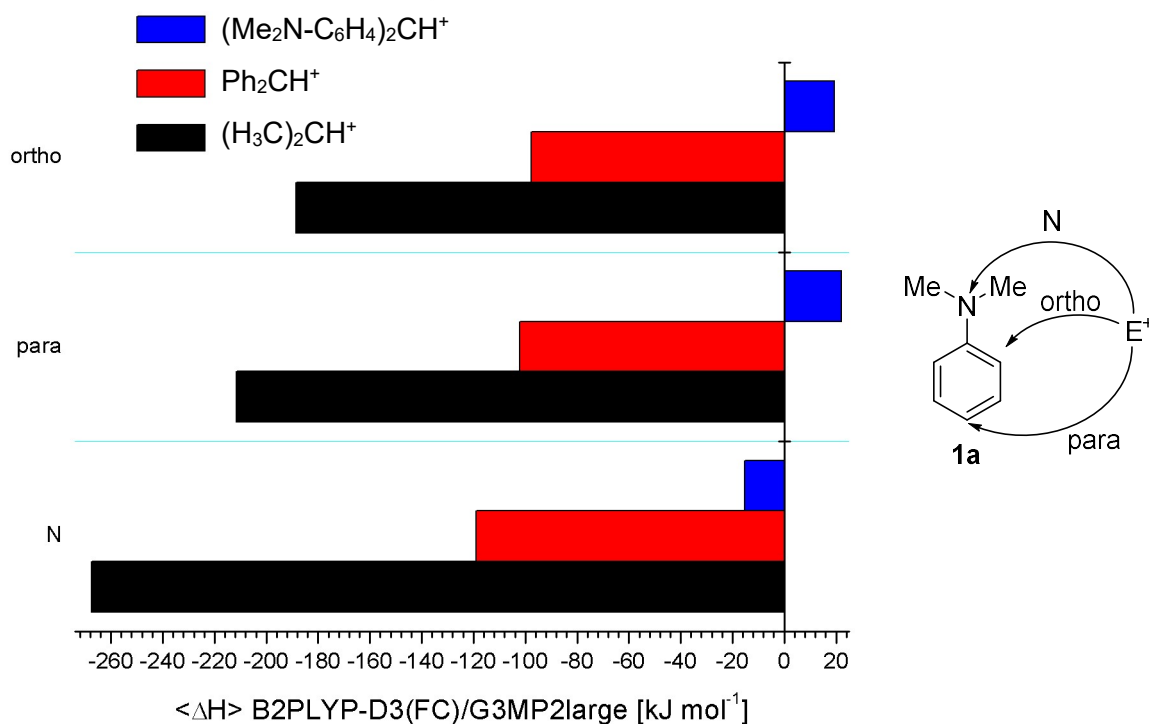


Figure 10: Reaction enthalpies of *N,N*-dimethylaniline (**1a**) with carbocations ( $E^+$ ) **2x** (red), **2b** (blue) and **2y** (black) at B2PLYP-D3(FC)/G3MP2large//M06-2X/6-31+G(d) level of theory in the gas phase for the reaction at the C2 carbon (“ortho”), the C4 carbon (“para”) and the nitrogen atom (“N”) of *N,N*-dimethylaniline (**1a**).

Interestingly, the calculations for  $(dma)_2CH^+$  (**2b**) show positive reaction enthalpies for the formation of the C–C bound adduct at the *para* position ( $\langle \Delta H_{para} \rangle = +22.1 \text{ kJ mol}^{-1}$ ). This reflects the increased stability of the reactant electrophile. Inclusion of implicit solvation using a continuum model (SMD/B3LYP/6-31G(d)) with dichloromethane or acetonitrile as respective solvent show smaller reaction enthalpies compared to the gas phase (Figure 11). The reaction enthalpies in acetonitrile are even smaller than those obtained in dichloromethane. Negative reaction enthalpies were found for the reaction of **1a** with **2x**, but no change of the thermochemical results with the cation  $(dma)_2CH^+$  (**2b**). The gap between the theoretical studies and the experimental results is most probably due to high stability of the re-aromatised product **3ab**. The experimentally confirmed exclusive formation of the product resulting from the attack of the C4 atom of **1a** at the electrophiles proves the occurrence of this reaction (Table 4, entry 1). The reaction enthalpies for the formation of the product **3ab** have not been calculated.

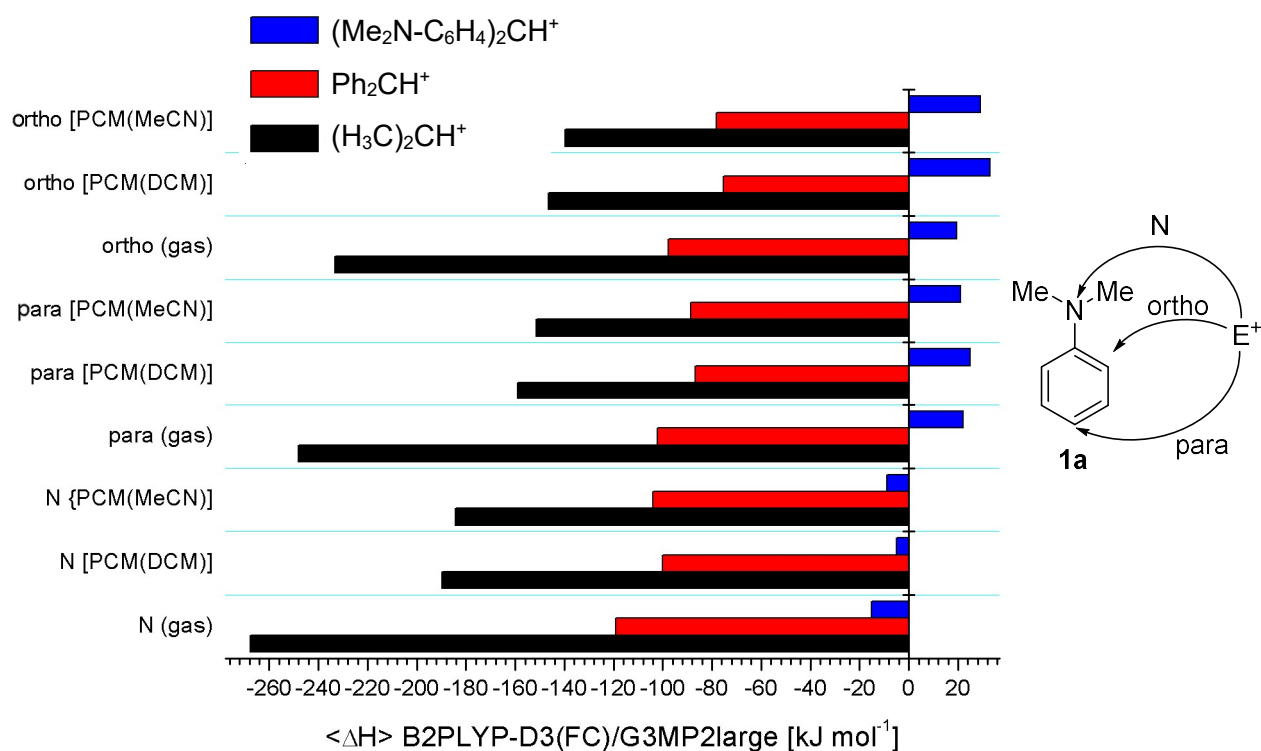


Figure 11: Boltzmann-averaged reaction enthalpies for the reaction of *N,N*-dimethylaniline (**1a**) with carbocations ( $E^+$ ) **2x** (red), **2b** (blue) and **2y** (black) applying an implicit solvation model (SMD/B3LYP/6-31G(d)).

In conclusion, the smallest reaction enthalpies of *N,N*-dimethylaniline (**1a**) with (dma)<sub>2</sub>CH<sup>+</sup> (**2b**) was found for the attack of the nitrogen atom. The attack at the *ortho* and *para* carbon atom was found to be less favourable. The C2 position is statistically represented twice, but still energetically not favourable. A product of the attack of the C2 carbon was not found in the product studies. The abstraction of a hydride was not calculated, but all time-resolved <sup>1</sup>H NMR spectra of reaction mixtures of *N,N*-dialkylated anilines **1a–c** with benzhydrylium cations **2a+b** did not indicate products originating from hydride transfer. The calculations support, therefore, an initial reaction of the nitrogen atom of **1a** at carbocations and a slower attack of the C4 carbon atom.

Therefore, we suggest in line with the literature,<sup>[5h, 6e, 18]</sup> that the first decay of the benzhydrylium ion **2** absorbance represents the attack of the electron rich nitrogen at the benzhydryl ion **2**, leading to an instable ammonium intermediate. The slower reaction is the attack of the C4 carbon atom of the aromatic ring. The attack of the C2 carbon atom was excluded due to the steric demand, the calculations shown above and the absence of a C2 substituted product in the product studies. After the formation of a Wheland complex via the

attack of the carbon atom, a proton is released. This may protonate the formed product **3** as well as a free aniline **1a**. This protonation does not affect the kinetic analysis, as only up to one equivalent of **1a** can be protonated and a huge excess of **1a** ( $> 10$  equivalents over the electrophile **2**) is used. Thus, pseudo-first-order conditions are ensured during the entire reaction time. A hydride shift was also excluded, as the resulting diarylmethane would be stable but was not observed, neither in the product studies, nor in the time-resolved  $^1\text{H}$  NMR spectroscopic studies.

After evaluation of the time-dependence absorption of the benzhydrylium ions **2** when reacting with *N,N*-dimethylaniline (**1a**), the second-order rate constants  $k_2$  of the attack of the nitrogen or C4 atom were obtained from the slopes of the linear plots of  $k_{\text{obs}}$  vs. **[1a]** (Figure 12) and are listed in Table 5.

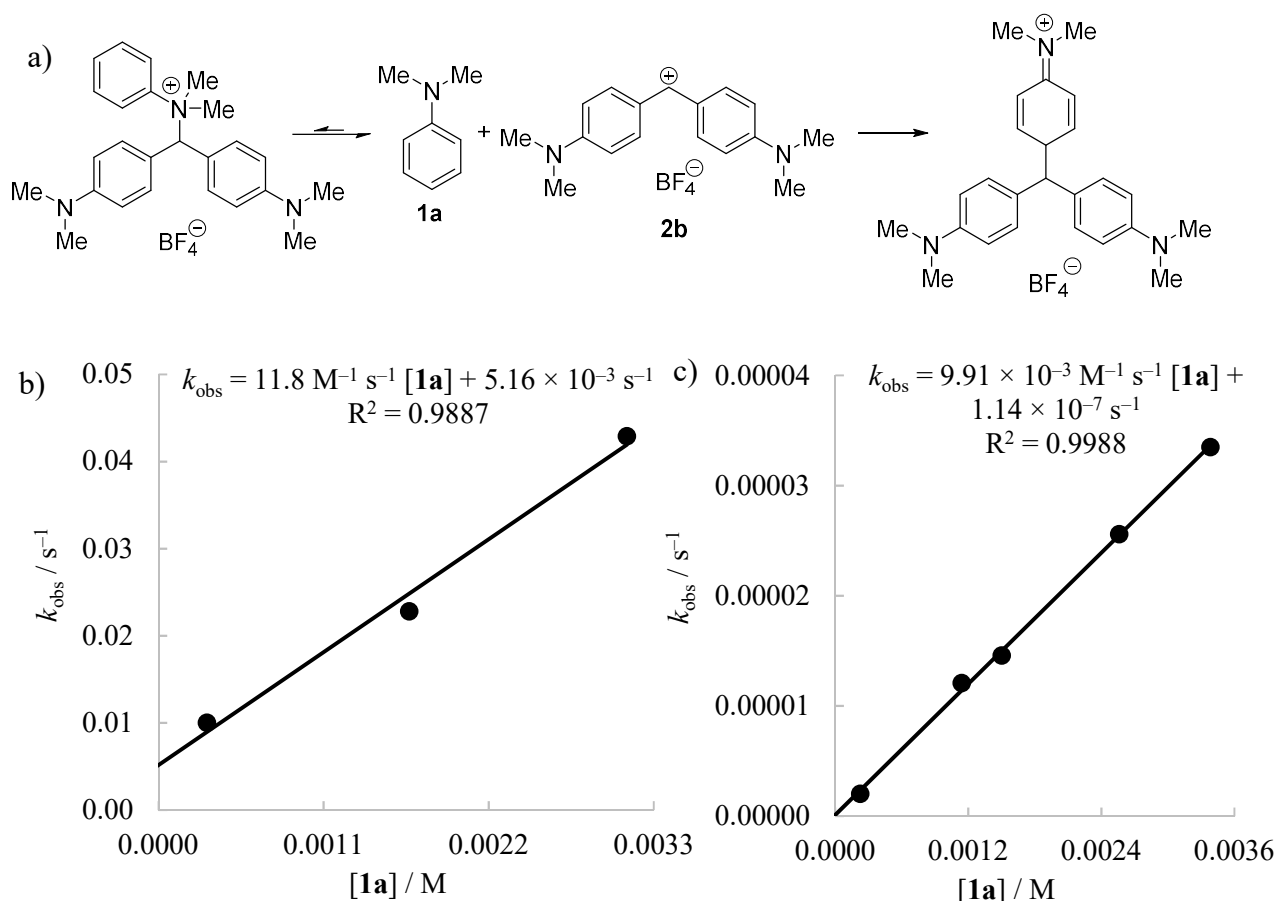
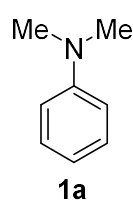


Figure 12: a) Reaction of *N,N*-dimethylaniline (**1a**) with  $(\text{dma})_2\text{CH}^+ \text{BF}_4^-$  (**2b**) in  $\text{CH}_3\text{CN}$  at  $20^\circ\text{C}$ . The slope of the linear correlation of the first-order rate constants  $k_{\text{obs}}$  with the nucleophile concentrations corresponds to the second-order rate constant  $k_2$  ( $\text{CH}_3\text{CN}$ ,  $20^\circ\text{C}$ ) for the attack at the carbocation **2b** b) of the nitrogen atom of **1a** and c) of the C4 carbon of **1a**.

Table 5: Second-order rate constants ( $k_2$ , 20 °C) for the reactions of benzhydrylium tetrafluoroborates **2** with *N,N*-dimethylaniline (**1a**) in acetonitrile and resulting  $N$  and  $s_N$  parameters.

Nucleophile	Solvent	Reaction Site	$N$ ( $s_N$ )	Reference electrophile	$E$ parameter	$k_2$ (M <sup>-1</sup> s <sup>-1</sup> )	lg $k_2$
 <p><b>1a</b></p>	MeCN	C4	5.83 (1.69)	(pyr) <sub>2</sub> CH <sup>+</sup> ( <b>2a</b> )	-7.69	1.01 × 10 <sup>-3</sup>	-3.00
				(dma) <sub>2</sub> CH <sup>+</sup> ( <b>2b</b> )	-7.02	9.91 × 10 <sup>-3</sup>	-2.00
				(dma) <sub>2</sub> CH <sup>+</sup> ( <b>2b</b> )	-7.02	1.18 × 10 <sup>-2</sup>	-1.93 <sup>[a, b]</sup>
				(mpa) <sub>2</sub> CH <sup>+</sup> ( <b>2c</b> )	-5.89	9.39 × 10 <sup>-1</sup>	-0.03
				(mor) <sub>2</sub> CH <sup>+</sup> ( <b>2d</b> )	-5.53	1.97	0.29
				(dpa) <sub>2</sub> CH <sup>+</sup> ( <b>2e</b> )	-4.72	89.7	1.95
				(mfa) <sub>2</sub> CH <sup>+</sup> ( <b>2f</b> )	-3.85	27.6	1.44 <sup>[a]</sup>
				(pfa) <sub>2</sub> CH <sup>+</sup> ( <b>2g</b> )	-3.14	504	2.70 <sup>[a]</sup>
				(dma) <sub>2</sub> CH <sup>+</sup> ( <b>2b</b> )	-7.02	11.5	1.06
				(mor) <sub>2</sub> CH <sup>+</sup> ( <b>2d</b> )	-5.53	260	2.41
	MeCN	N	8.49 (0.79)	(dpa) <sub>2</sub> CH <sup>+</sup> ( <b>2e</b> )	-4.72	1.51 × 10 <sup>3</sup>	3.18
				(mfa) <sub>2</sub> CH <sup>+</sup> ( <b>2f</b> )	-3.85	5.53 × 10 <sup>3</sup>	3.74
				(pfa) <sub>2</sub> CH <sup>+</sup> ( <b>2g</b> )	-3.14	1.12 × 10 <sup>4</sup>	4.05

[a] Excluded from the determination of  $N$  and  $s_N$  parameter. [b] Measured at 23 °C by <sup>1</sup>H NMR spectroscopy.

The second-order rate constants  $k_2$  correlate linearly with the electrophilicity parameters  $E$  of the benzhydrylium cations **2**, as claimed by eq. 1 (Figure 13). The  $N$  and  $s_N$  parameters of *N,N*-dimethylaniline (**1a**) were derived as the intercepts on the abscissa ( $N = -E$  at  $\log k_2 = 0$ ;  $N = 8.49$  for the attack of the nitrogen atom and  $N = 5.83$  for the attack of the C4 ring carbon) and the slopes of these correlations ( $s_N = 0.79$  for the attack of the nitrogen atom and  $s_N = 1.69$  for the attack of the C4 ring carbon) reflecting the susceptibilities of *N,N*-dimethylaniline (**1a**) toward changes of the reactivities of the electrophiles. The second-order rate constants of the reactions with (mfa)<sub>2</sub>CH<sup>+</sup> (**2f**) and (pfa)<sub>2</sub>CH<sup>+</sup> (**2g**) were not used to derive the  $N$  and  $s_N$  parameters as they differ dramatically from the correlation line, as the attack of the nitrogen and the carbon atom cannot be separated for the kinetic evaluation.

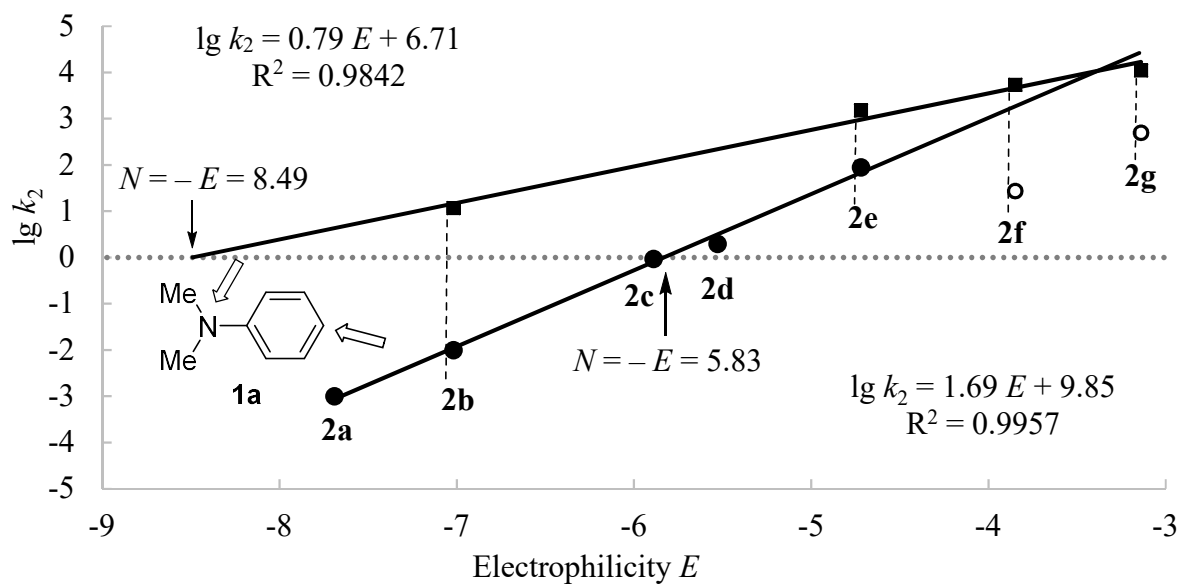


Figure 13: Correlation of the logarithmized second-order rate constants  $\lg k_2$  (MeCN, 20 °C) for the reactions of *N,N*-dimethylaniline (**1a**) at the nitrogen atom (squares) and the C4 ring carbon (circles) with the electrophiles **2** with their respective electrophilicity parameters  $E$ . The  $N$  parameters were derived as the intercepts on the abscissa (stroked line,  $N = -E$  at  $\lg k_2 = 0$ ;  $N = 8.49$  for the attack of the nitrogen atom and  $N = 5.83$  for the attack of the C4 ring carbon), the  $s_N$  parameters are the slopes of the correlation line ( $s_N = 0.79$  for the attack of the nitrogen atom and  $s_N = 1.69$  for the attack of the C4 ring carbon). The open symbols were not used for the calculation of the correlation line.

The reactivities of aliphatic tertiary amines were studied by Mayr et al. in acetonitrile and dichloromethane.<sup>[5h]</sup> Qualitatively, the thermodynamic stabilities of the quaternary ammonium salts in acetonitrile were found to decrease for a given benzhydrylium ion from the cyclic tertiary amines, like *N*-methylpiperidine or *N*-methylnorpholine, to the non-cyclic trialkylated amine  $\text{NEt}_3$ . The formation of ammonium salts from benzhydrylium ions and tertiary amines in dichloromethane was found to be thermodynamically even less favourable than in acetonitrile. However, it was neither possible to determine the equilibrium constants, nor were any aromatic amines studied in that work.<sup>[5h]</sup> It is therefore not surprising, that it was neither possible to isolate nor observe by NMR spectroscopic methods quaternary ammonium salts in this work.

## Nucleophilicity of *N,N*-diethylaniline (**1b**)

Analogous to the reaction of  $(\text{dma})_2\text{CH}^+ \text{BF}_4^-$  (**2b**) with *N,N*-dimethylaniline (**1a**) the time-resolved  $^1\text{H}$  NMR spectra of the reaction of  $(\text{pyr})_2\text{CH}^+ \text{BF}_4^-$  (**2a**) with *N,N*-diethylaniline (**1b**) showed the formation of the *para*-substituted product (Figure 14). The second-order rate constant  $k_2 = 7.17 \times 10^{-4} \text{ M}^{-1} \text{ s}^{-1}$  were obtained from the linear correlation of  $Y$  vs.  $t$  according to eq. 3 (Figure 14c).

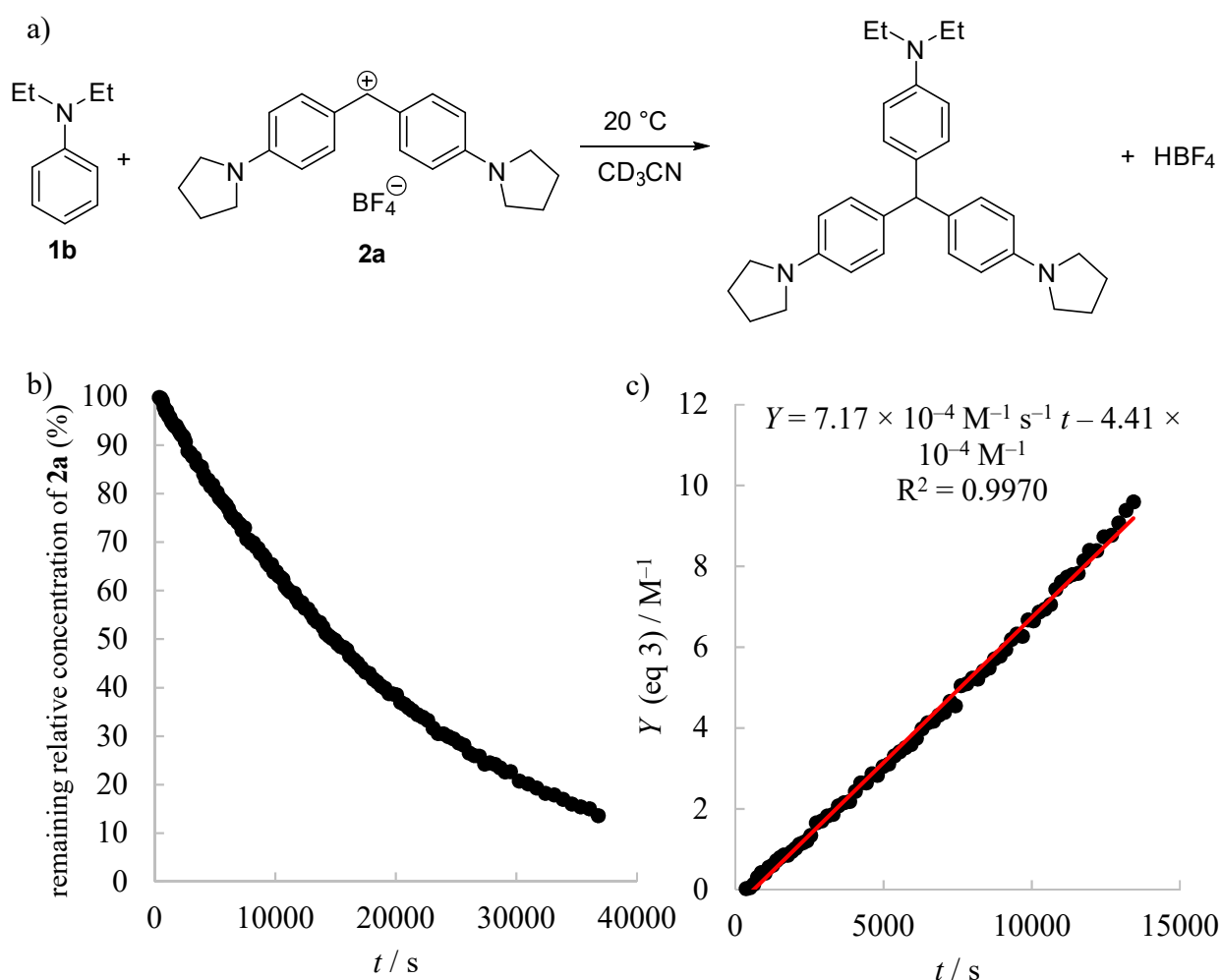


Figure 14: a) Reaction of *N,N*-diethylaniline (**1b**) with  $(\text{pyr})_2\text{CH}^+ \text{BF}_4^-$  (**2a**) in  $\text{CD}_3\text{CN}$  at  $20^\circ\text{C}$ . b) Decay of the relative concentration of  $(\text{pyr})_2\text{CH}^+ \text{BF}_4^-$  (**2a**;  $c = 3.65 \times 10^{-2} \text{ M}$ ) while reacting with *N,N*-diethylaniline (**1b**;  $c = 7.48 \times 10^{-2} \text{ M}$ ) in  $\text{CD}_3\text{CN}$  at  $20^\circ\text{C}$ . c) Determination of the second-order rate constant by plotting time versus  $Y = ([\mathbf{1b}]_0 - [\mathbf{2a}]_0)^{-1} \ln([\mathbf{2a}]_0([\mathbf{2a}]_t + [\mathbf{1b}]_0 - [\mathbf{2a}]_0) / [\mathbf{1b}]_0[\mathbf{2a}]_t)$  ( $k_2 = 7.17 \times 10^{-4} \text{ M}^{-1} \text{ s}^{-1}$ , data points up to 50% conversion were used).

When photometric UV/Vis spectroscopy was applied to monitor the reactions of benzhydrylium ions **2** with **1b**, again a bisexponential decay was found, indicating the occurrence of two different reactions (Figure 15).

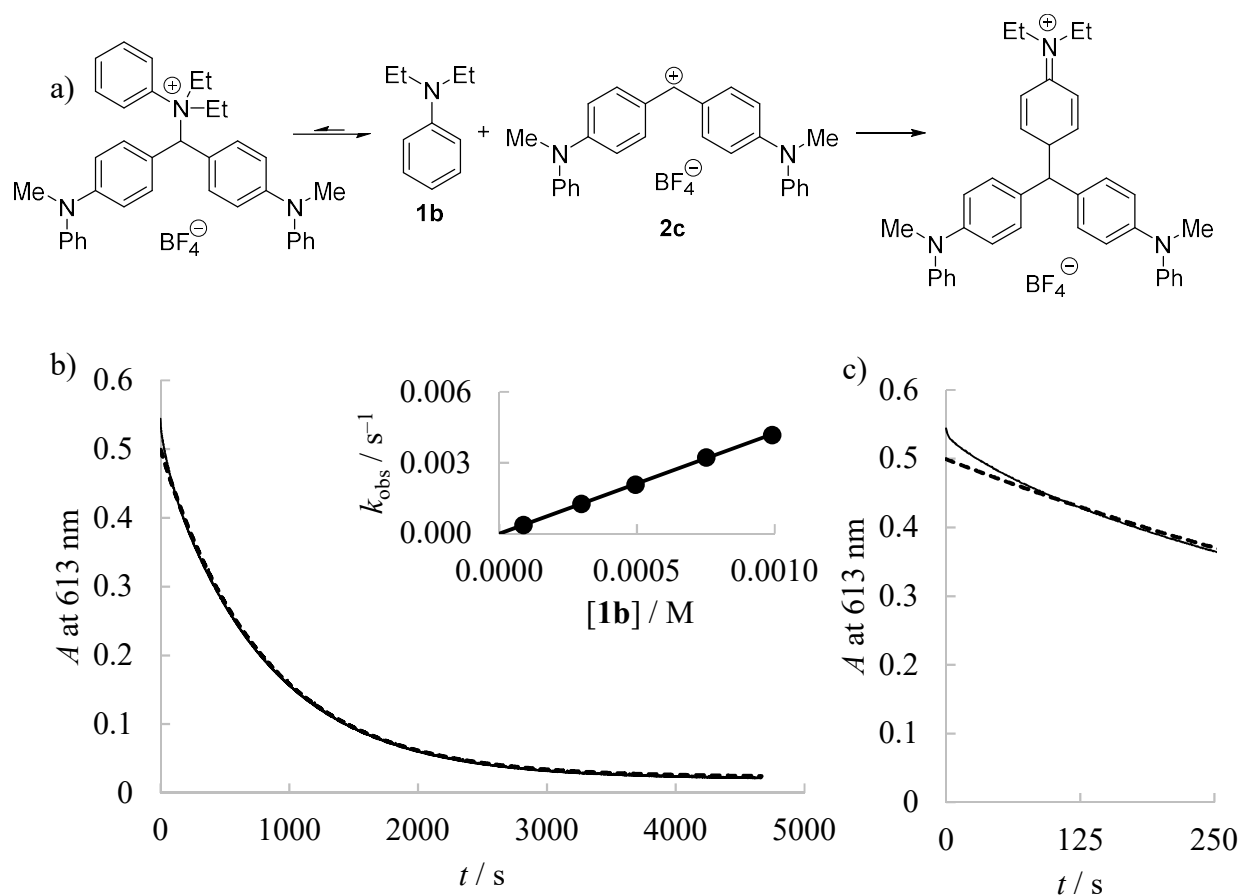
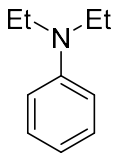


Figure 15: a) Reaction of *N,N*-diethylaniline (**1b**) with  $(\text{mpa})_2\text{CH}^+ \text{BF}_4^-$  (**2c**) in  $\text{CH}_3\text{CN}$  at 20 °C. b) Plot of the absorbance  $A$  at 613 nm vs. time for the reaction of *N,N*-diethylaniline (**1b**) ( $c = 2.97 \times 10^{-4}$  M) with **2c** ( $c = 9.25 \times 10^{-6}$  M) in acetonitrile at 20 °C with the calculated decay (dashed line). Plot of the first-order rate constants  $k_{\text{obs}}$  vs. the concentration of **1b** (inlay, correlation line  $k_{\text{obs}} = 4.24 \text{ M}^{-1} \text{ s}^{-1} [\text{1b}] + 1.34 \times 10^{-6} \text{ s}^{-1}$ ,  $R^2 = 0.9997$ ). c) Enhancement of the first seconds, showing the significant deviation between measured and absorbance calculated for the attack of the C4 carbon.

Thus, the results were analogous to the reactions of *N,N*-dimethylaniline (**1a**) with benzhydrylium ions **2**. A fast but reversible attack of the nitrogen atom and slow but irreversible attack of the C4 carbon of **1b** at the cationic electrophiles. The second-order rate constants for these attacks are listed in Table 6.

Table 6: Second-order rate constants ( $k_2$ , 20 °C) for the reactions of benzhydrylium tetrafluoroborates **2** with *N,N*-diethylaniline (**1b**) in acetonitrile and resulting  $N$  and  $s_N$  parameters.

Nucleophile	Solvent	Reaction Site	$N$ ( $s_N$ )	Reference electrophile	$E$ parameter	$k_2$ (M <sup>-1</sup> s <sup>-1</sup> )	lg $k_2$
 <b>1b</b>	MeCN	C4	6.28 (1.64)	(pyr) <sub>2</sub> CH <sup>+</sup> ( <b>2a</b> )	-7.69	$7.17 \times 10^{-4}$	-3.14 <sup>[a]</sup>
				(dma) <sub>2</sub> CH <sup>+</sup> ( <b>2b</b> )	-7.02	$2.50 \times 10^{-1}$	-0.60 <sup>[a]</sup>
				(mpa) <sub>2</sub> CH <sup>+</sup> ( <b>2c</b> )	-5.89	4.24	0.63
				(mor) <sub>2</sub> CH <sup>+</sup> ( <b>2d</b> )	-5.53	17.9	1.25
				(dpa) <sub>2</sub> CH <sup>+</sup> ( <b>2e</b> )	-4.72	354	2.55
		N	(dma) <sub>2</sub> CH <sup>+</sup> ( <b>2b</b> )	-7.69	80.7	1.91	
			(mor) <sub>2</sub> CH <sup>+</sup> ( <b>2d</b> )	-7.02	$1.23 \times 10^3$	3.09	
			(mfa) <sub>2</sub> CH <sup>+</sup> ( <b>2f</b> )	-3.85	$7.95 \times 10^3$	3.90	

[a] Excluded from the determination of  $N$  and  $s_N$  parameter due to significant deviations.

The  $N$  and  $s_N$  parameters are again obtained by linear correlation of the logarithmized second-order rate constants lg  $k_2$  with the electrophilicity parameters  $E$  of the benzhydrylium ions **2** (Figure 16). The  $s_N$  parameter for the attack of the C4 atom of **1b** is almost identical to that for the attack of the C4 atom of **1a** ( $s_N = 1.69$ ), showing the consistency of this method. However, **1b** is more reactive than **1a**, for the attack of the nitrogen (**1a**:  $N = 8.49$   $s_N = 0.79$ ) as well as for the attack of the C4 carbon (**1a**:  $N = 5.83$   $s_N = 1.69$ ). This shows the inductive effect of the ethyl groups compared to the methyl groups, which is also reflected by the higher basicity of **1b** in comparison to **1a** (Figure 6).

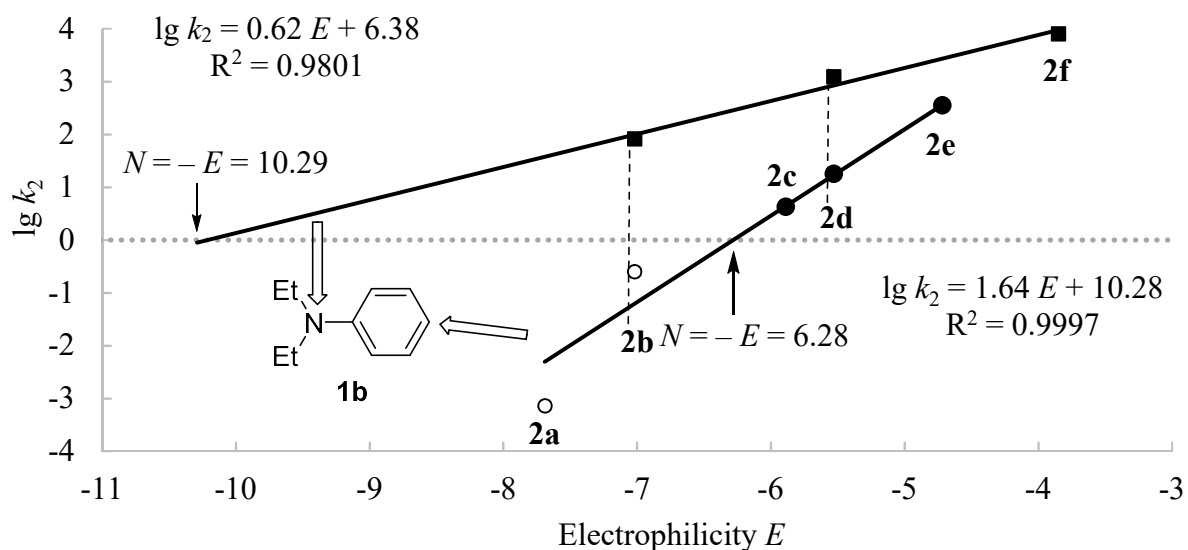


Figure 16: Correlation of the logarithmized rate constants  $\lg k_2$  (MeCN, 20 °C) for the reactions of *N,N*-diethylaniline (**1b**) at the nitrogen atom (squares) and the C4 ring carbon (circles) with the electrophiles **2** with their electrophilicity parameters  $E$ . The  $N$  parameter was derived as the intercept on the abscissa (stroked line,  $N = -E$  at  $\lg k_2 = 0$ ;  $N = 10.29$  for the attack of the nitrogen atom and  $N = 6.28$  for the attack of the C4 ring carbon), the  $s_N$  parameter is the slope of the correlation line ( $s_N = 0.62$  for the attack of the nitrogen atom and  $s_N = 1.64$  for the attack of the C4 ring carbon). The open symbols were not used for the calculation of the correlation line.

## Nucleophilicity of *N,N*-dimethylaniline (**1a**) and *N,N*-diethylaniline (**1b**) in dichloromethane

Monitoring the reactions of benzhydrylium ions **2a–f** with *N,N*-dimethylaniline (**1a**) in dichloromethane by UV/Vis photometry, again a bisexponential decay was observed. The attack of the nitrogen atom of **1a** at the cations **2** in dichloromethane could be evaluated analogous as in the case of acetonitrile. However, for the correlation of the first-order rate constants  $k_{\text{obs}}$  against **[1a]** upward curvatures (Figure 17a) instead of a linear correlation was obtained. This indicates a rate-determining proton transfer subsequent to the attack of **1a**'s C4 atom on the benzhydrylium ion **2**, in which a second molecule **1a** acts as Brønsted base. As the direct determination of  $k_2$  from the slopes of the plots of  $k_{\text{obs}}$  versus **[1a]** was not possible in these cases, the method of evaluation for these kinetics had to be changed.

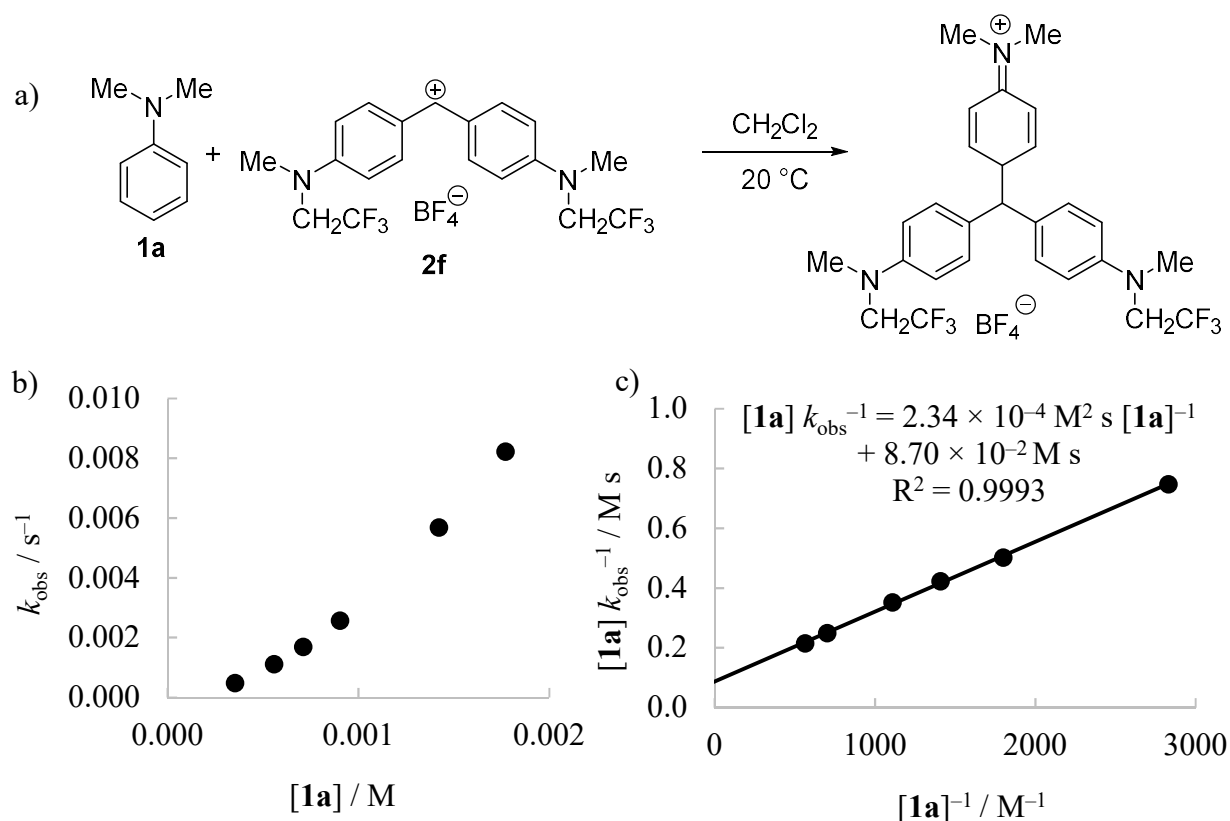


Figure 17: a) Reaction of *N,N*-dimethylaniline (**1a**) with  $(\text{mfa})_2\text{CH}^+ \text{BF}_4^-$  (**2f**) in  $\text{CH}_2\text{Cl}_2$  at  $20^\circ\text{C}$ . Plot of b)  $k_{\text{obs}}$  versus **[1a]** and c)  $[1a]k_{\text{obs}}^{-1}$  versus  $1/[1a]$  for the reaction of **1a** with  $(\text{mfa})_2\text{CH}^+$  (**2f**) in dichloromethane at  $20^\circ\text{C}$ .

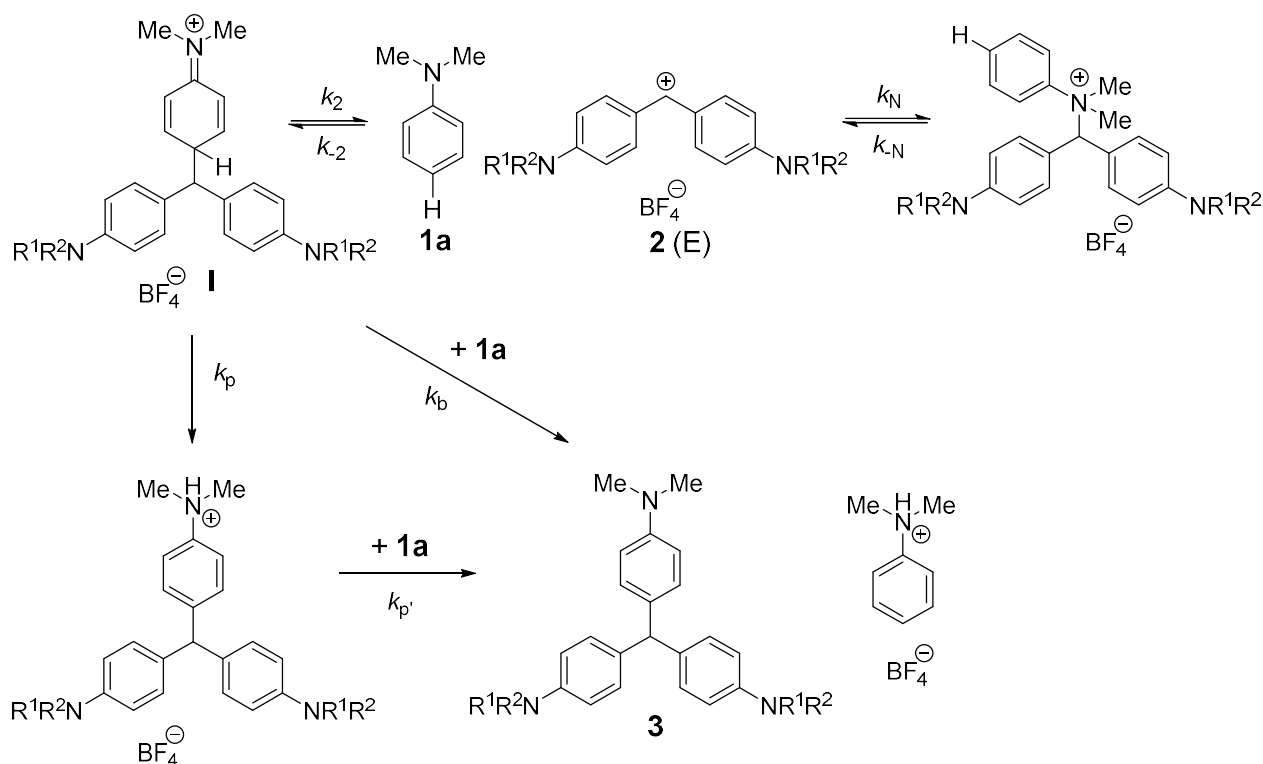


Figure 18: Reaction of *N,N*-dimethylaniline (**1a**) with benzhydrylium ion (**2**, E) in dichloromethane. The rate determining step is shifted from the initial attack of the C4 carbon to the proton transfer  $k_b$  and  $k_p$ , respectively. At high nucleophile concentrations, the direct proton-transfer ( $k_p$ ) as well as the proton-transfer after the irreversible formation of the carbon-carbon bond ( $k_p'$ ) can be neglected. A steady-state concentration for the intermediate **I** is assumed.

For the reactions of *N,N*-dimethylaniline (**1a**) with benzhydrylium ions **2a–f** in dichloromethane, the proton transfer becomes rate determining and the measured  $k_{\text{obs}}$  values do not correlate linearly with  $[\mathbf{1a}]$  anymore (Figure 18). The kinetics follow therefore the rate law of Equation 5, which is derived in the Supporting Information; it can be rewritten as Equation 6 (on page 253).<sup>[25]</sup>

$$k_{\text{obs}} = \frac{k_2 k_b [\mathbf{1a}]^2}{k_{-2} + k_b} \quad (5)$$

$$\frac{[\mathbf{1a}]}{k_{\text{obs}}} = \frac{1}{k_2} + \frac{k_{-2}}{k_2 k_b [\mathbf{1a}]} \quad (6)$$

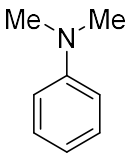
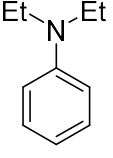
Indeed, the plots of  $[\mathbf{1a}]/k_{\text{obs}}$  versus  $1/[\mathbf{1a}]$  were found to be linear for the reactions of **1a** with **2a–f** in dichloromethane (Figure 17b), which shows that the formalism holds for these cases in a wide range of concentrations of **1a**. At higher concentrations of **1a** again a linear correlation

between  $k_{\text{obs}}$  and **1a** is found and Equation 6 simplifies to Equation 4, as the second term tends to zero. The same is true for a very slow, negligible reverse reaction.

The effect of the proton transfer becoming the rate determining step only occurred in dichloromethane, not in acetonitrile, in which the proton can also be stabilized by the solvent. The effect did also not occur, using the about one  $pK_{\text{aH}}$  unit more basic nucleophile *N,N*-diethylaniline (**1b**;  $pK_{\text{a}}$  in acetonitrile of **1a** = 11.43, of **1b** = 12.4, Figure 6).<sup>[20-21]</sup>

Second-order rate constants for the reactions of **1a** and **1b** with the reference electrophiles **2** in dichloromethane are collected in Table 7.

Table 7: Second-order rate constants ( $k_2$ , 20 °C) for the reactions of benzhydrylium tetrafluoroborates **2** with tertiary alkylated anilines **1a** and **1b** in dichloromethane and resulting  $N$  and  $s_N$  parameters.

Nucleophile	Solvent	Reaction Site	$N$ ( $s_N$ )	Reference electrophile	$E$ parameter	$k_2$ ( $\text{M}^{-1} \text{s}^{-1}$ )	$\lg k_2$			
 <b>1a</b>	CH <sub>2</sub> Cl <sub>2</sub>	C4	5.01 (1.22)	(pyr) <sub>2</sub> CH <sup>+</sup> ( <b>2a</b> )	-7.69	$2.72 \times 10^{-4}$	-3.57			
				(dma) <sub>2</sub> CH <sup>+</sup> ( <b>2b</b> )	-7.02	$3.70 \times 10^{-3}$	-2.43			
				(mpa) <sub>2</sub> CH <sup>+</sup> ( <b>2c</b> )	-5.89	$2.11 \times 10^{-1}$	-0.68			
				(mor) <sub>2</sub> CH <sup>+</sup> ( <b>2d</b> )	-5.53	$3.40 \times 10^{-1}$	-0.47			
				(dpa) <sub>2</sub> CH <sup>+</sup> ( <b>2e</b> )	-4.72	2.99	0.48			
				(mfa) <sub>2</sub> CH <sup>+</sup> ( <b>2f</b> )	-3.85	11.5	1.06			
		N	(mpa) <sub>2</sub> CH <sup>+</sup> ( <b>2c</b> )	-5.89	60.7	1.78				
			(mfa) <sub>2</sub> CH <sup>+</sup> ( <b>2f</b> )	-3.85	476	2.68				
			 <b>1b</b>	CH <sub>2</sub> Cl <sub>2</sub>	C4	4.92 (1.30)	(pyr) <sub>2</sub> CH <sup>+</sup> ( <b>2a</b> )	-7.69	$2.98 \times 10^{-4}$	-3.53 <sup>[b]</sup>
							(dma) <sub>2</sub> CH <sup>+</sup> ( <b>2b</b> )	-7.02	$4.61 \times 10^{-3}$	-2.34
(mor) <sub>2</sub> CH <sup>+</sup> ( <b>2d</b> )	-5.53	$6.12 \times 10^{-2}$					-1.21			
(dpa) <sub>2</sub> CH <sup>+</sup> ( <b>2e</b> )	-4.72	$8.14 \times 10^{-1}$					-0.09			
(pfa) <sub>2</sub> CH <sup>+</sup> ( <b>2g</b> )	-3.14	529					2.72			

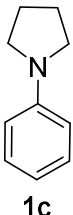
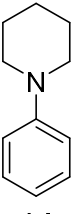
[a] Excluded from the determination of  $N$  and  $s_N$  parameter. [b] Measured at 23 °C.

[c] Inaccurate due to the limited amount of available data points.

## Nucleophilicity of tertiary cyclic aryl amines 1-phenylpyrrolidine (1c) and 1-phenylpiperidine (1d)

Similar to the diethyl-substituted aniline (**1b**), 1-phenylpyrrolidine (**1c**) shows a bisexponential decay when reacting with benzhydrylium ions **2** in acetonitrile. For the reactions with (mfa)<sub>2</sub>CH<sup>+</sup> (**2f**) and (pfa)<sub>2</sub>CH<sup>+</sup> (**2g**) the *k*<sub>2</sub> values for the attack of the nitrogen atom could be evaluated (Table 8). The *N* and *s<sub>N</sub>* parameters were obtained analogously to the *N,N*-dialkylated anilines **1a-c** (Figure 21). For the attack of the nitrogen atom of 1-phenylpyrrolidine (**1c**) a *N* parameter of 9.87 and a slope parameter of 0.55 were determined. These are similar to the parameters of the N-attack of **1b** (*N* = 10.29 and *s<sub>N</sub>* = 0.62). **1c**'s C4 carbon is less reactive (*N* = 6.13 and *s<sub>N</sub>* = 1.63) and has a reactivity in between of the parameters of the C4-attack of **1a** (*N* = 5.83 and *s<sub>N</sub>* = 1.69) and **1b** (*N* = 6.28 and *s<sub>N</sub>* = 1.64). The similarity of the *s<sub>N</sub>* parameters found for the of the *N,N*-dialkylated anilines **1a-c** of 1.66±0.03 for the C4-attack and 0.67±0.12 for the N-attack shows the consistency of these results.

Table 8: Second-order rate constants (*k*<sub>2</sub>, 20 °C) for the reactions of benzhydrylium ions **2** with tertiary alkylated anilines **1c** and **1d** in acetonitrile and the resulting *N* and *s<sub>N</sub>* parameters.

Nucleophile	Solvent	Reaction Site	<i>N</i> ( <i>s<sub>N</sub></i> )	Reference electrophile	<i>E</i> parameter	<i>k</i> <sub>2</sub> (M <sup>-1</sup> s <sup>-1</sup> )	lg <i>k</i> <sub>2</sub>
 <b>1c</b>	MeCN	C4	6.13 (1.63)	(pyr) <sub>2</sub> CH <sup>+</sup> ( <b>2a</b> )	-7.69	2.72 × 10 <sup>-3</sup>	-2.57
				(mor) <sub>2</sub> CH <sup>+</sup> ( <b>2d</b> )	-5.53	9.91	1.00
				(dpa) <sub>2</sub> CH <sup>+</sup> ( <b>2e</b> )	-4.72	186	2.27
		N	9.87 <sup>[a]</sup> (0.55)	(mfa) <sub>2</sub> CH <sup>+</sup> ( <b>2f</b> )	-3.85	2.08 × 10 <sup>3</sup>	3.32
				(pfa) <sub>2</sub> CH <sup>+</sup> ( <b>2g</b> )	-3.14	5.15 × 10 <sup>3</sup>	3.71
 <b>1d</b>	MeCN	N <sup>[b]</sup>	10.65 (0.79)	(dma) <sub>2</sub> CH <sup>+</sup> ( <b>2b</b> )	-7.02	773	2.89
				(mor) <sub>2</sub> CH <sup>+</sup> ( <b>2d</b> )	-5.53	9.71 × 10 <sup>3</sup>	3.99
				(mfa) <sub>2</sub> CH <sup>+</sup> ( <b>2f</b> )	-3.85	1.87 × 10 <sup>5</sup>	5.27
				(pfa) <sub>2</sub> CH <sup>+</sup> ( <b>2g</b> )	-3.14	9.34 × 10 <sup>5</sup>	5.97

[a] Inaccurate due to the limited amount of available data points. [b] The C4 substitution was found as the only product (see Table 4, entry 5).

For 1-phenylpiperidine (**1d**) a totally different behaviour was observed. In contrast to **1c**, reactions of **1d** with (mfa)<sub>2</sub>CH<sup>+</sup> (**2f**) followed monoexponential decays and showed full

conversions over the whole concentration range. As for the *N,N*-dialkylated anilines **1a–c** when reacting with **2** only small conversions by the attack of the nitrogen atom were observed (Figure 3c and Figure 15c), we originally expected the observation of the attack of the **1d**'s C4 carbon. Also in the reaction of **1d** with (dma)<sub>2</sub>CH<sup>+</sup> (**2b**), only monoexponential decays were found. However, nearly full conversion was only observed for high concentrations of **1d** (Figure 19).

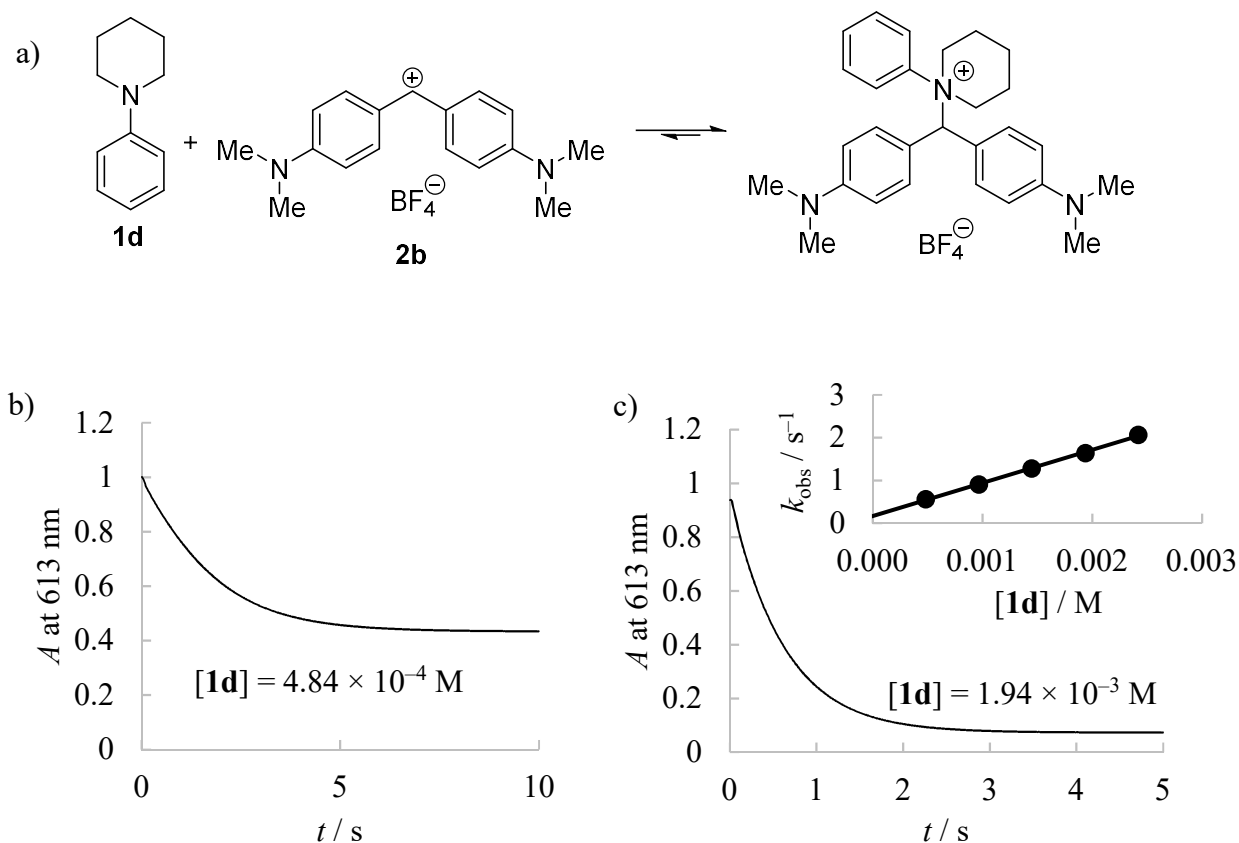
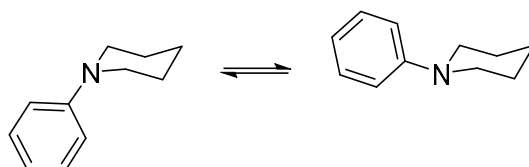


Figure 19: a) Reaction of 1-phenylpiperidine (**1d**) with (dma)<sub>2</sub>CH<sup>+</sup> BF<sub>4</sub><sup>-</sup> (**2b**) in CH<sub>3</sub>CN at 20 °C. Plot of the absorbance at 613 nm vs. time for the reaction of 1-phenylpiperidine (**1d**) with (dma)<sub>2</sub>CH<sup>+</sup> (**2b**) in acetonitrile at 20 °C at low and at high concentrations of **1d**.  $[\mathbf{2b}]_0 = 7.23 \times 10^{-6} \text{ M}$  with b)  $[\mathbf{1d}] = 4.84 \times 10^{-4} \text{ M}$  and c)  $[\mathbf{1d}] = 1.94 \times 10^{-3} \text{ M}$ . The linear dependence of  $[\mathbf{1d}]$  vs.  $k_{\text{obs}}$  is given over the whole concentration range (inlay). Regression line  $k_{\text{obs}} = 773 \text{ M}^{-1} \text{ s}^{-1} [\text{Nu}] + 0.17 \text{ s}^{-1}$ ,  $R^2 = 0.9984$ .

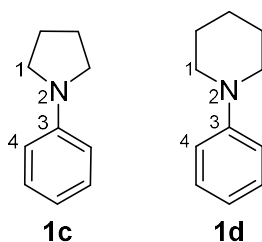
The existence of an equilibrium in the reactions of **1d** with **2b** already indicates a reversible reaction, most likely, due to the attack of the nitrogen atom. The linear dependence of  $k_{\text{obs}}$  vs. [**1d**] holds for the full concentration range, revealing no change in the reaction mechanism. The second-order rate constants are listed in Table 8. Evaluation of the  $k_2$  values according to eq. 1, gave a  $N$  and  $s_N$ -parameter of 10.65 and 0.79 respectively (Figure 21), similar to the parameters found for the attacks of the nitrogen atom in the  $N,N$ -dialkylated anilines **1a–c** ( $N$  parameters and in parenthesis  $s_N$ -parameter for the attack of the nitrogen atom: **1a** 8.49 (0.79), **1b** 10.29 (0.62) and **1c** 9.87 (0.55)). These obtained parameters are also similar to the parameters obtained for the N-attack of other primary anilines and tertiary amines, studied by Mayr et al.<sup>[5g, 5h]</sup> The sharp contrast to the behavior of 1-phenylpyrrolidine (**1c**) can be rationalised by taking the three-dimensional shape of the molecule into account (Scheme 13).



Scheme 13: Conformers of 1-phenylpiperidine (**1d**). Axial (left) and equatorial (right).<sup>[26]</sup>

Theoretical studies revealed a ratio of equatorial to axial position of the phenyl ring of about 9:1 (Eq:Ax = 92:8 (B3LYP), 87:13 (B3LYP-GD3), 84:16 (M06-2X), 83:17 (MP2/6-311G\*\*) and 76:24 (MP2/cc-pVTZ)),<sup>[26]</sup> which is in good agreement with the experimental gas-phase electron diffraction data of 90(10):10(10).<sup>[26]</sup> The geometrical presentation of these conformers shows a pyramidal conformation at the nitrogen atom, whereas the minor axial conformer is pseudo trigonal planar.<sup>[26]</sup> Sophia Schwarz calculated the geometries of the conformers of the substrates **1c** and **1d** as well as for isopropyl cation adducts at the nitrogen and the C4 atom.<sup>[27]</sup> The conformation analysis was performed using the Avogadro program package. The energetically most stable conformers were used as starting structures for a geometry optimization at B3LYP/6-31++G(3df,2p) level of theory using the Gaussian09 program package. A subsequent frequency analysis was performed to verify the minimum structures and to obtain the thermal corrections to the enthalpies and Gibbs free energies at 298 K (Table 10). In this analysis, the axial minor conformer was not considered.

Table 9: Optimized structures of 1-phenylpyrrolidine (**1c**) and 1-phenylpiperidine (**1d**) (first line), as well as after the reaction with isopropyl cation at the nitrogen (second line) and the C4 carbon atom (third line) (gas phase, 298 K). The dihedral angle is the angle between the two intersecting planes through the atom C1, N2, C3 and N2, C3, C4, respectively.



	Structure of <b>1c</b> and dihedral angle $\alpha$ [ $^{\circ}$ ] at the nitrogen atom	Structure of <b>1d</b> and dihedral angle $\alpha$ [ $^{\circ}$ ] at the nitrogen atom
reactant	 180.00	 141.82
N-adduct	 118.90	 117.91
C4-adduct	 179.74	 176.55

The differences in reactivity at the nitrogen atoms of **1c** and **1d**, can be rationalized with the different structural features. The higher reactivity at the nitrogen atom of the piperidino compounds compared to pyrrolidino analogues can be explained by the higher *p*-character of the nitrogen lone-pair in a five-membered ring compared with a six-membered ring. Quantum chemical calculations by Robert Mayer at the SMD(MeCN)/M06-2X/6-31+G(d,p) level confirmed the geometrical differences of **1c** compared to **1d** (Figure 20).

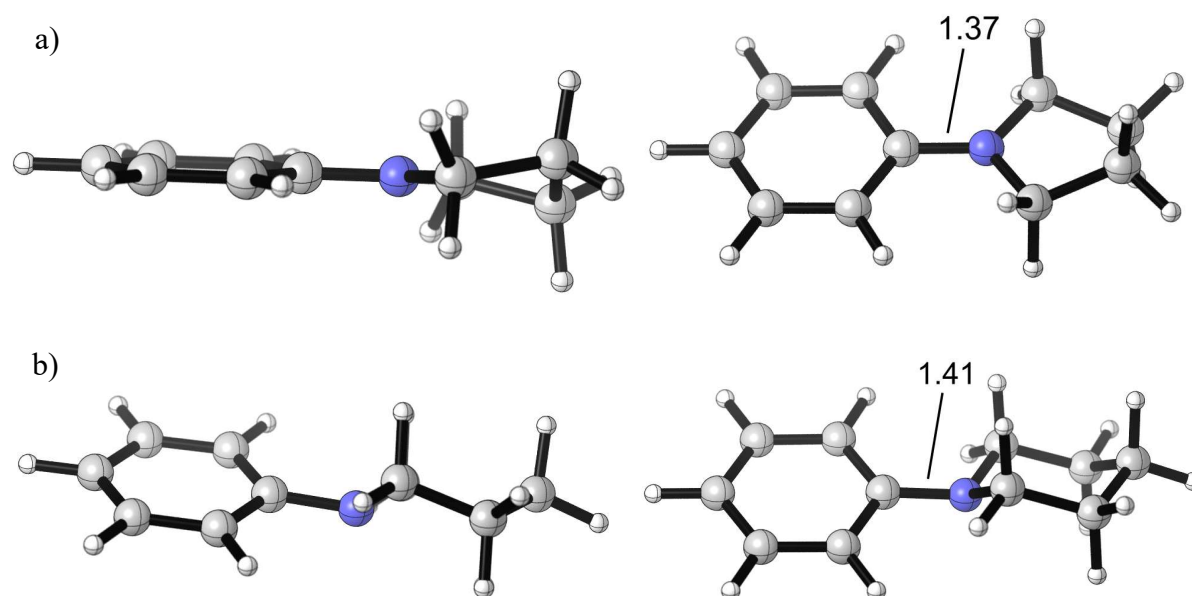
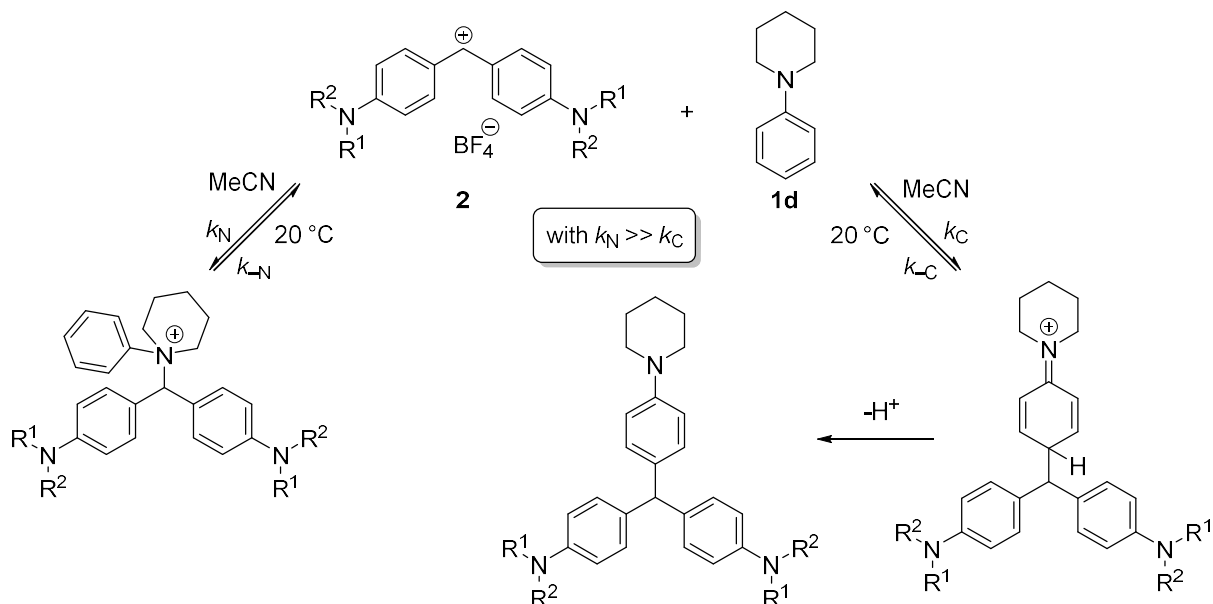


Figure 20: Conformers of a) 1-phenylpyrrolidine (**1c**) and b) 1-phenylpiperidine (**1d**) calculated at the SMD(MeCN)/M06-2X/6-31+G(d,p) level of theory. The out-of-plane distances were calculated for the distance of the nitrogen atom and the plane defined by the three carbon atoms bond to the nitrogen atom. The out-of-plane distance of the nitrogen atom is 0 Å for **1c** and of 0.352 Å for **1d** (left). The bond length of the C1 ring carbon to the nitrogen atom is 1.37 Å for **1c** and 1.41 Å for **1d** (right).

The distance of the nitrogen atom from the plane defined by the three carbon atoms directly bound to the nitrogen atom, was calculated. **1c** is perfectly planar with an out-of-plane distance of the N atom of 0 Å, whereas the N atom of **1d** is 0.352 Å out of the defined plane. The bond length of the C1 ring carbon to the nitrogen atom is 1.37 Å for **1c** and 1.41 Å for **1d**. This clearly shows a higher double bond character for **1c** which lowers the reactivity at the nitrogen atom compared to **1d**, but increases the reactivity at the C4 carbon atom of **1c** compared to **1d**. Nevertheless, in the reaction of **1d** with (mfa)<sub>2</sub>CH<sup>+</sup> (**2f**), not the N-adduct was the isolated product, but the tri-aryl methane, as a product of the attack of the C4 at the aniline ring (Table 4, entry 5). The proposed reaction mechanism for the reactions of **1d** with benzhydrylium ions

**2** is, therefore, similar to the reaction mechanism of the *N,N*-dialkylated anilines **1a–c**. A fast but reversible attack of the nitrogen atom, and a slow but irreversible attack of the carbon atom (Scheme 14). The rate constants for the isomerisation of the N-adduct to the C4 substituted product, were not obtained, however.



Scheme 14: Reaction mechanism for the reactions of 1-phenylpiperidine (**1d**) with benzhydrylium ions **2** in MeCN at 20 °C.

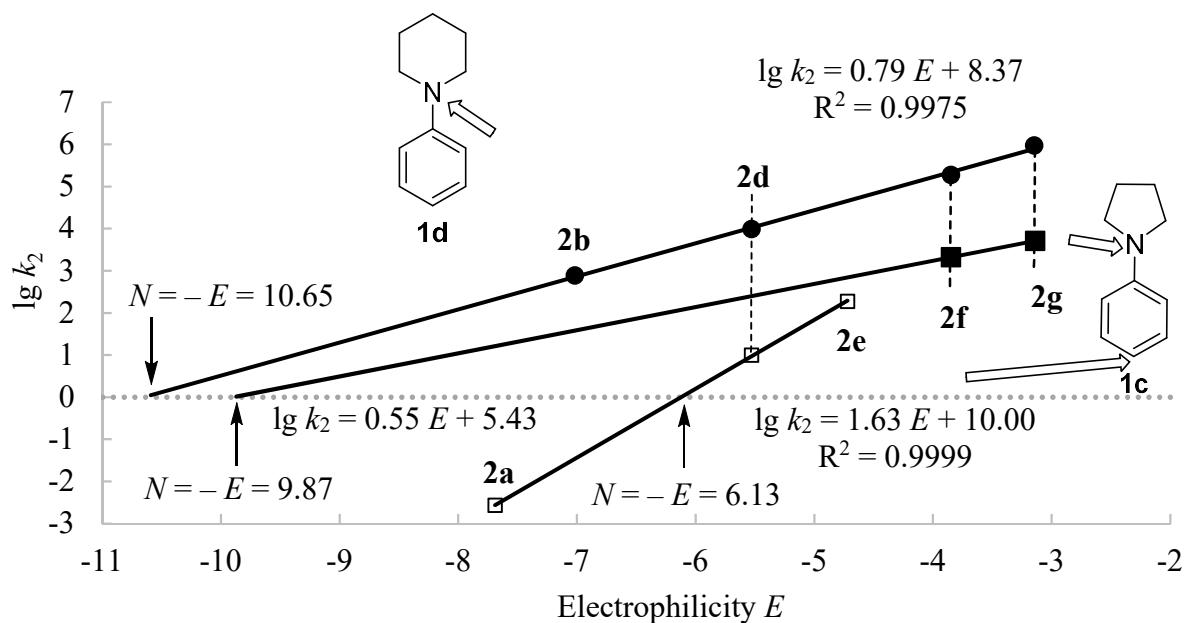
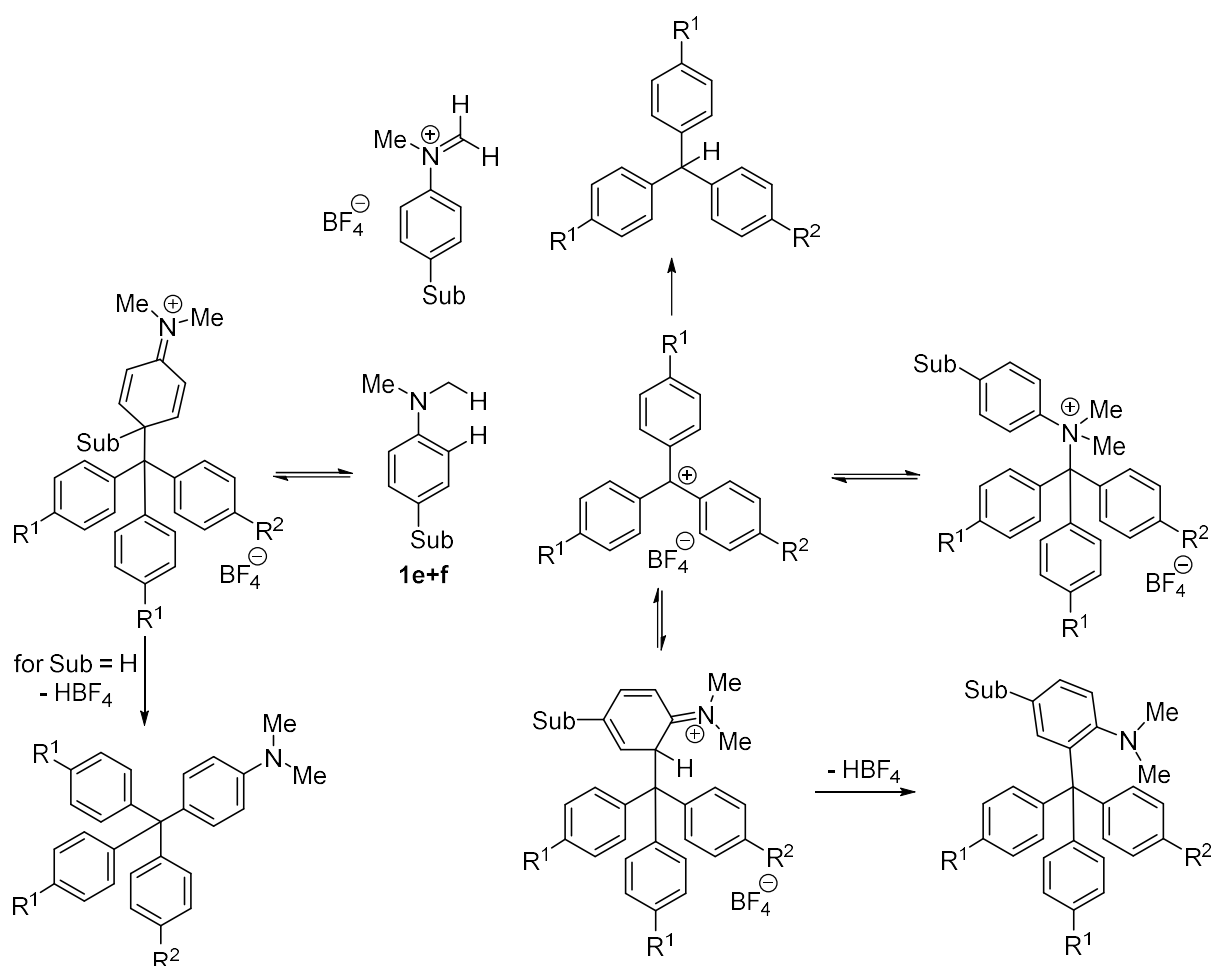


Figure 21: Correlation of the logarithmized second-order rate constants for the reactions of reference benzhydrylium ions **2** with 1-phenylpyrrolidine (**1c**, filled squares) and 1-phenylpiperidine (**1d**, circles) at the nitrogen atom and at the C4 of 1-phenylpyrrolidine (**1c**, open squares) in acetonitrile at 20 °C. The  $N$  parameters were derived as the intercepts on the abscissa (stroked line,  $N = -E$  at  $\lg k_2 = 0$ ;  $N = 10.65$  for the attack of the nitrogen atom of **1d** and  $N = 9.87$  for the attack of the nitrogen atom of **1c** and  $N = 6.13$  for the attack of the C4 ring carbon of **1c**), the  $s_N$  parameters are the slopes of the correlation lines ( $s_N = 0.79$  for the attack of the nitrogen atom of **1d** and  $s_N = 0.55$  for the attack of the nitrogen atom of **1c** and  $s_N = 1.63$  for the attack of the C4 ring carbon of **1c**).

## Abstraction of hydride from the CH<sub>3</sub> group in $\alpha$ -position of the nitrogen atom

So far, we discussed the reactions of *N,N*-dialkylated anilines **1** with benzhydrylium ions **2** at the nitrogen atom and at the C<sub>4</sub> ring carbon. Another possible reaction is the abstraction of hydride from the CH<sub>3</sub> group in  $\alpha$ -position of the nitrogen atom. The synthetic use of the activation of this C–H bond was already shown in chapter 2 of this work.

In 2015, Ofial summarized the use of tritylium ions as a complementary probe to benzhydrylium ions for examining ambident nucleophilicity and demonstrated their impact on the determination of nucleophilicities of *n*-nucleophiles or hydride donors.<sup>[28]</sup> However, beside the hydride abstraction, an attack of the tritylium ions at the nitrogen atom of **1** or the C<sub>4</sub> carbon is also possible (Scheme 15).



Scheme 15: Mechanistic scenario for the reactions of tritylium ions with *N,N*-dimethylaniline (**1a**), and *N,N*-dimethyl-*para*-toluidine (**1e**) in acetonitrile. The rest R<sup>1</sup> = OMe and R<sup>2</sup> = H or OMe.

We performed some preliminary experiments. The time-resolved  $^1\text{H}$  NMR spectra show clearly the formation of the tris(4-methoxyphenyl)methane by a resonance at around 5.5 ppm, what proves the abstraction of a hydride (see Figure S4 in the Supporting Information). The second-order rate constants were obtained from the formation of tris(4-methoxyphenyl)methane (Figure 22; for time-resolved  $^1\text{H}$  NMR spectra see Supporting Information). The results are shown in Table 10.

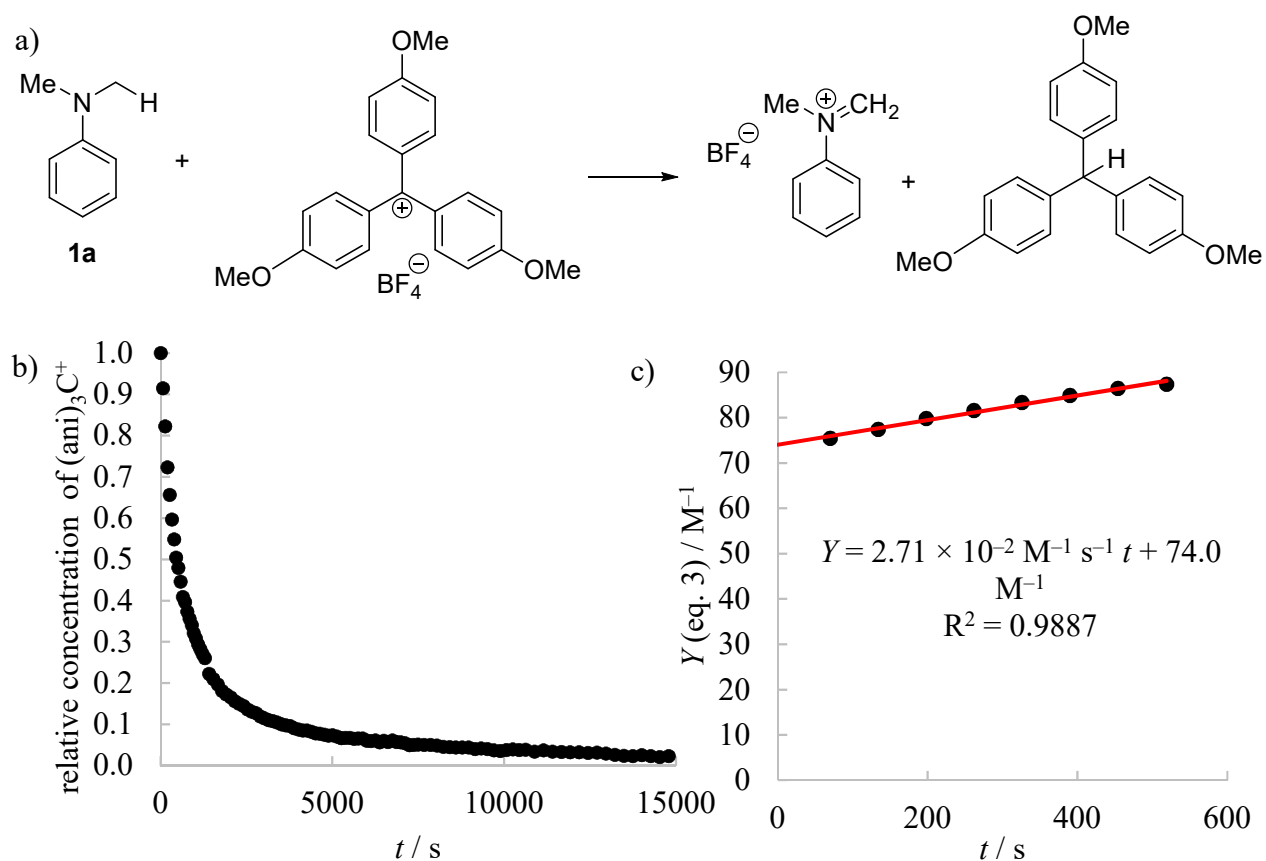
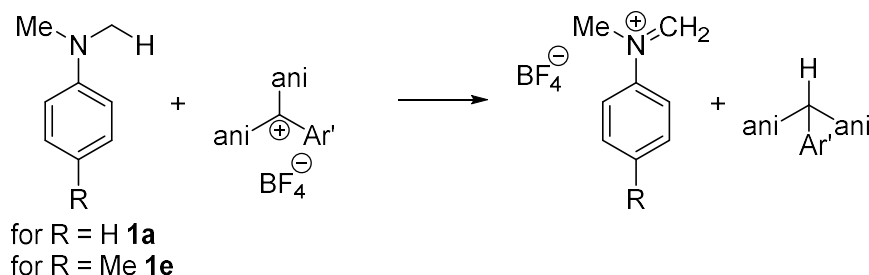


Figure 22: a) Reaction of  $N,N$ -dimethylaniline (**1a**) with  $(\text{ani})_3\text{C}^+ \text{BF}_4^-$  in  $\text{CD}_3\text{CN}$  at  $20^\circ\text{C}$ .  $\text{ani} = p\text{-MeOC}_6\text{H}_4$ . b) Decay of the relative concentration of  $(\text{ani})_3\text{C}^+ \text{BF}_4^-$  ( $c = 4.93 \times 10^{-2} \text{ M}$ ) while reacting with  $N,N$ -dimethylaniline (**1a**;  $c = 1.03 \times 10^{-1} \text{ M}$ ) in  $\text{CD}_3\text{CN}$  at  $20^\circ\text{C}$ . b) Determination of the second-order rate constant by plotting time versus  $Y = ([\mathbf{1a}]_0 - [(\text{ani})_3\text{C}^+]_0)^{-1} \ln([(\text{ani})_3\text{C}^+]_0 [(\text{ani})_3\text{C}^+]_t + [\mathbf{1a}]_0 - [(\text{ani})_3\text{C}^+]_0) / [\mathbf{1a}]_0 [(\text{ani})_3\text{C}^+]_t$ ) ( $k_2 = 2.71 \times 10^{-2} \text{ M}^{-1} \text{ s}^{-1}$ , data points up to 50% conversion were used).

Table 10: Second-order rate constant ( $k_2$ , 20 °C) for the reactions of  $(\text{ani})_2\text{Ar}'\text{C}^+$  with  $N,N$ -dimethylaniline (**1a**) in acetonitrile. The rest  $\text{ani} = p\text{-MeOC}_6\text{H}_4$  and  $\text{Ar}' = \text{Ph}$  or  $\text{ani}$ .



Nucleophile	Proposed Reaction Side	Solvent	$N(S_N)$ parameter	Reference Electro-ophile	$E$ parameter	$k_2$ ( $\text{M}^{-1} \text{s}^{-1}$ )	$\lg k_2$
 <b>1a</b>	$\alpha\text{-C-H}$	aceto- nitrile	1.48	$(\text{ani})_3\text{C}^+$	-4.35	$2.71 \times 10^{-2[\text{b}]}$	-1.56
			$(0.54)^{[\text{a}]}$	$(\text{ani})_2\text{PhC}^+$	-3.04	$1.42 \times 10^{-1[\text{c}]}$	-0.85
 <b>1e</b>	$\alpha\text{-C-H}$	aceto- nitrile	-	$(\text{ani})_3\text{C}^+$	-4.35	$4.78 \times 10^{-3[\text{b,d}]}$	-2.32

[a] Inaccurate due to limited available data points. [b] Obtained by time-resolved  $^1\text{H}$  NMR spectroscopy. [c] Reaction side of the electrophile might be at the central carbon of  $(\text{ani})_2\text{PhC}^+$  or at the C4 of the phenyl ring.<sup>[29]</sup> [d] At 23 °C.

Monitoring the reaction of  $(\text{ani})_2\text{PhC}^+$  with  $N,N$ -dimethylaniline (**1a**) photometrically via UV/Vis spectroscopy at 497 nm, a bisexponential decay is observed (Figure 23). Due to the steric demand of the tritylium ion, reactions at the C<sub>4</sub> or even C<sub>2</sub> carbons are unlikely. For the synthesis of tetraarylmethanes high temperatures are reported ( $> 90^\circ\text{C}$ ),<sup>[30]</sup> which allows us to exclude these reactions.

Though the attack of nitrogen is sterically demanding, this attack is the most reasonable one, as the nitrogen atom is the reaction center with the highest reactivity present in  $N,N$ -dimethylaniline (**1a**) in acetonitrile (Table 5).

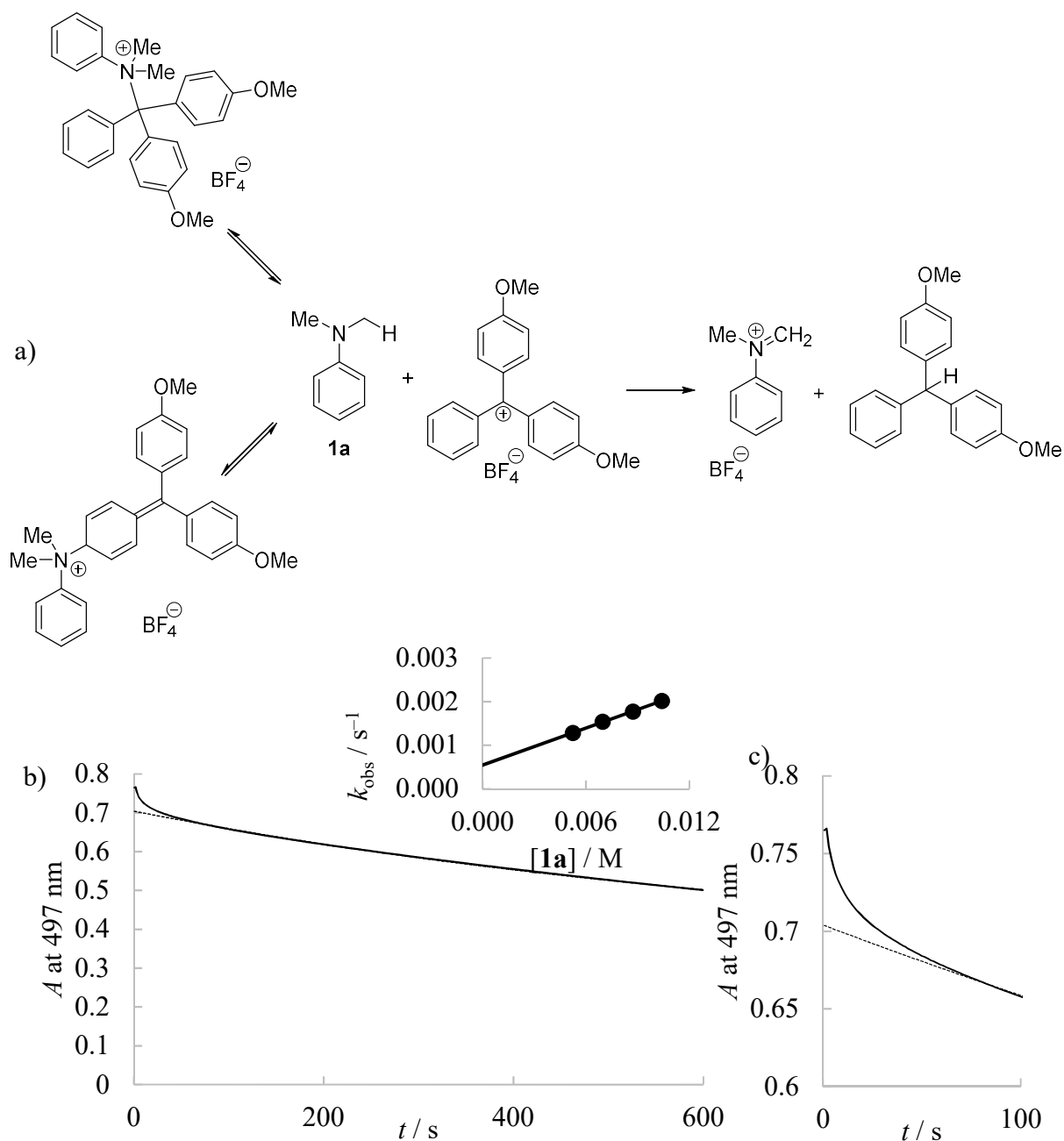


Figure 23: a) Reaction of  $N,N$ -dimethylaniline (**1a**) with  $(\text{ani})_2\text{PhC}^+\text{BF}_4^-$  in  $\text{CH}_3\text{CN}$  at  $20^\circ\text{C}$ . b) Plot of the absorbance  $A$  at 497 nm vs. time for the reaction of  $N,N$ -dimethylaniline ( $[\mathbf{1a}] = 5.22 \times 10^{-3} \text{ M}$ ) with  $(\text{ani})_2\text{PhC}^+$  ( $[(\text{ani})_2\text{PhC}^+]_0 = 2.72 \times 10^{-5} \text{ M}$ ) in acetonitrile at  $20^\circ\text{C}$ .  $\text{ani} = p\text{-MeOC}_6\text{H}_4$ . A  $k_{\text{obs}} = 1.28 \times 10^{-3} \text{ s}^{-1}$  was obtained by least-squares fitting of the exponential function  $A_t = A_0 e^{-k_{\text{obs}}t} + C$  to the time-dependent absorbance for the data points of 50-600 s. The calculated decay is shown as dashed line. Plot of the first-order rate constants  $k_{\text{obs}}$  vs. the concentration of **1a** (inlay, correlation line  $k_{\text{obs}} = 1.42 \times 10^{-1} \text{ M}^{-1} \text{ s}^{-1} [\mathbf{1a}] + 5.44 \times 10^{-4} \text{ s}^{-1}$ ,  $R^2 = 0.9994$ ). c) Enhancement of the first seconds, showing the significant deviation between measured and calculated absorbance for  $t < 80$  s.

The obtained experimental results should be treated with caution, as only a limited amount of data points is available. Nevertheless, the observed reaction is significantly slower than the attack of the C4 carbon. The benzhydrylium ion  $(\text{dpa})_2\text{CH}^+$  (**2e**) ( $E$  parameter of  $-4.72$ ) is of similar reactivity as the tritylium ion  $(\text{ani})_3\text{C}^+$  ( $E$  parameter of  $-4.35$ ), but the observed reaction is 3310 times slower when reacting  $(\text{ani})_3\text{C}^+$  with **1a**. The reaction of **1a** with  $(\text{ani})_2\text{PhC}^+$  is 6 times faster than the reaction with  $(\text{ani})_3\text{C}^+$ , resulting into a  $N$  parameter of 1.48 and a  $S_N$  parameter of 0.54. Comparing the second-order rate constants of the reaction of **1a** and **1e** with  $(\text{ani})_3\text{C}^+$ , the latter is nearly 20 times slower.

This shows the importance of the reaction partner design for a selective hydride abstraction, as done in Chapter 2 of this work about the C–H bond functionalisation at N-CH<sub>3</sub> groups of anilines derivatives with azodicarboxylates.

## Reactions of benzhydrylium ions **2** with the *para*-substituted *N,N*-dimethylanilines *N,N*,4-trimethylaniline (**1e**) and the 4-methoxy-*N,N*-dimethylaniline (**1f**)

Monitoring the reaction of *N,N*-dialkylated anilines **1a–c** with benzhydrylium ions **2**, via UV/Vis spectroscopy gave bisexponential decays. This complicates the kinetic evaluation. In contrast, reacting 1-phenylpiperidine (**1d**) with **2** only the attack of the nitrogen atom was observed. However, the isolated product of these reactions is the substitution at the C4 carbon. To get further insights on the reactivity of *N,N*-dialkylated anilines **1**, and stable and isolable products of the N-adduct, we investigated the reactions of *para*-substituted *N,N*-dimethylanilines, namely the *N,N*,4-trimethylaniline (**1e**) and the 4-methoxy-*N,N*-dimethylaniline (**1f**). The substituent patterns of **1e** and **1f** were chosen, as an enhancement of reactivity and stability of the formed N-adducts was expected through their electron donating effect. In addition the *para* position of the phenyl ring is blocked in **1e** and **1f**.

The kinetics investigations revealed again a bisexponential decay for the reactions of **1e** or **1f** with the benzhydrylium ions **2b** and **2d–g**. Analogous to the *N,N*-dialkylated anilines **1–c**, a fast but reversible reaction and a slow reaction was found. For the reaction of 4-methoxy-*N,N*-

dimethylaniline (**1f**) with  $(\text{mor})_2\text{CH}^+$  (**2d**) in acetonitrile the second-order rate constant for the fast reaction is  $278 \text{ M}^{-1} \text{ s}^{-1}$  and for the slow reaction  $9.02 \text{ M}^{-1} \text{ s}^{-1}$  (Figure 24).

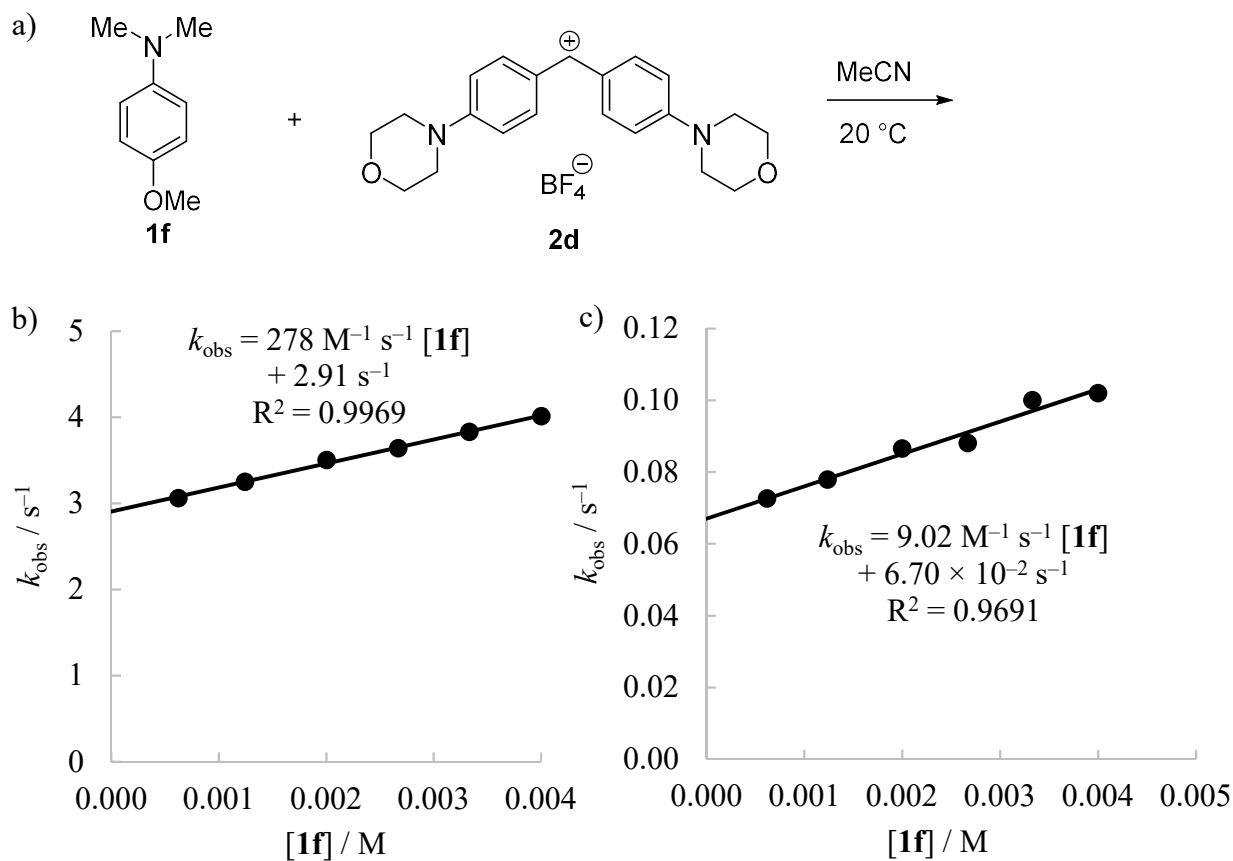


Figure 24: a) Reaction of 4-methoxy-*N,N*-dimethylaniline (**1f**) with  $(\text{mor})_2\text{CH}^+$  (**2d**) in  $\text{CH}_3\text{CN}$  at  $20 \text{ }^\circ\text{C}$ . b+c) Plots of the obtained first-order rate constants  $k_{\text{obs}}$  from the reaction of 4-methoxy-*N,N*-dimethylaniline (**1f**) with  $(\text{mor})_2\text{CH}^+$  (**2d**) versus  $[\mathbf{1f}]$ . b) Second-order rate constant  $k_2 = 278 \text{ M}^{-1} \text{ s}^{-1}$  for the fast reaction, c) Second-order rate constant  $k_2 = 9.02 \text{ M}^{-1} \text{ s}^{-1}$  for the slow reaction.

When reacting *N,N*-dimethyl-*para*-toluidine ( $[1\mathbf{e}] = 8.79 \times 10^{-4} \text{ M}$ ) with  $(\text{pfa})_2\text{CH}^+$  ( $[2\mathbf{g}]_0 = 1.76 \times 10^{-5} \text{ M}$ ) in acetonitrile at  $20^\circ\text{C}$ , within seconds the formation of two equilibria was observed. A first equilibrium is reached after ca. 0.2 s, while a second equilibrium is reached after around 25 s (Figure 25). The observed first-order rate constants  $k_{\text{obs}}$  correlated linearly with  $[1\mathbf{e}]$ . A second-order rate constant for the fast reaction of  $2.89 \text{ M}^{-1} \text{ s}^{-1}$  and for the slow reaction of  $260 \text{ M}^{-1} \text{ s}^{-1}$  was obtained (see Table S57 and S59 in the Supporting Information). However, the reactions could also be induced by a trace impurity of the investigated batches of  $1\mathbf{e}$  and  $1\mathbf{f}$ .

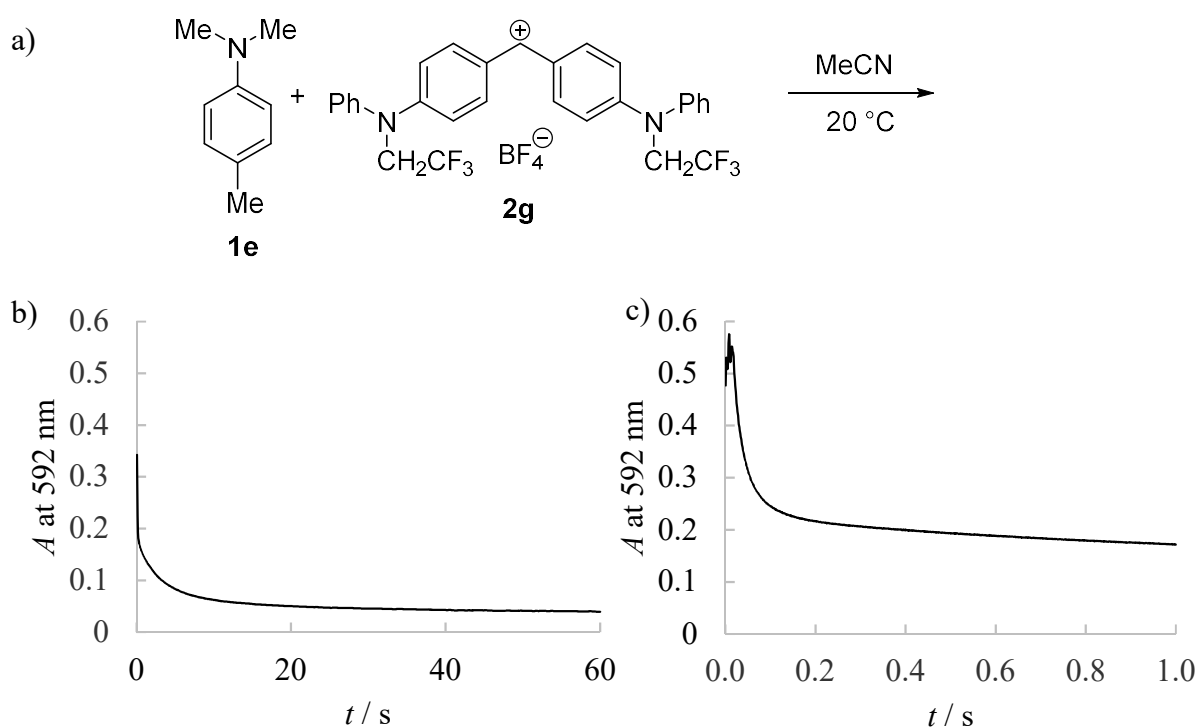
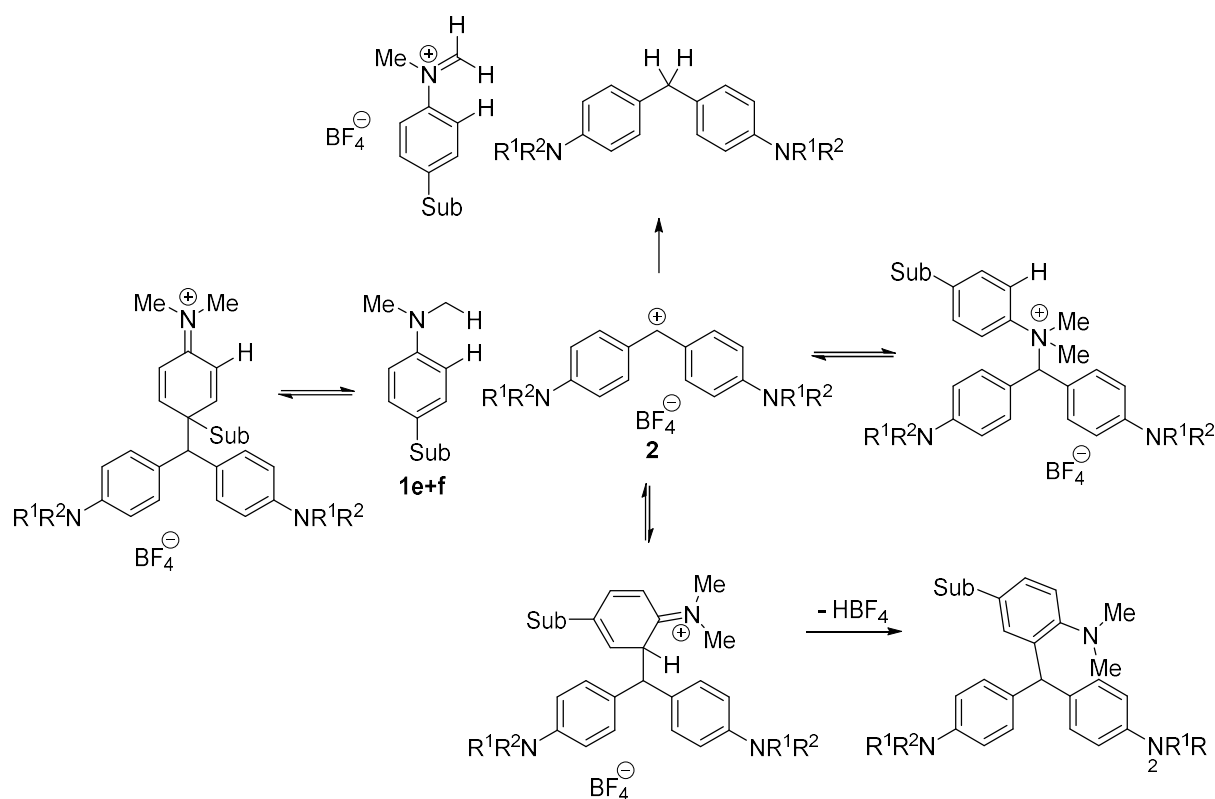


Figure 25: a) *N,N*-dimethyl-*para*-toluidine (**1e**) reacting with  $(\text{pfa})_2\text{CH}^+$  (**2g**) in acetonitrile at  $20^\circ\text{C}$ . a+b) Plot of the absorbance at 592 nm vs. time for the reaction of *N,N*-dimethyl-*para*-toluidine ( $[1\mathbf{e}] = 8.79 \times 10^{-4} \text{ M}$ ) with  $(\text{pfa})_2\text{CH}^+$  ( $[2\mathbf{g}]_0 = 1.76 \times 10^{-5} \text{ M}$ ) in acetonitrile at  $20^\circ\text{C}$ . a) One data point per 60 ms, revealing an equilibrium reached at about 25 s. b) One data point per 1 ms, revealing a second equilibrium reached at about 0.2 s.

The abstraction of a hydride is not reversible and not as fast as the monitored reactions. Thus, the hydride abstraction can be excluded for the monitored reactions. Most reasonable is therefore a fast attack of the nitrogen atom and a slow attack of a ring carbon. A disadvantage of the UV/Vis spectroscopy is that only the absorption and concentration of free benzhydrylium ion **2** can be followed. Direct rearrangements are not visible. Thus, the results should be treated as preliminary and further studies have to be performed to clarify the exact reaction mechanism.

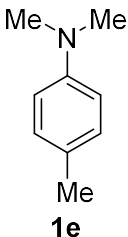
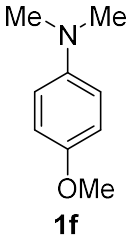
The proposed general reaction scheme is shown in Scheme 16. As the second-order rate constants of the fast reaction, as well as the obtained  $N$  and  $s_N$  parameters (Table 11), are in the same range as for the nitrogen attack of the tertiary anilines **1a–c**, we suggest a fast reaction at the nitrogen atom.

An abstraction of a hydride is possible, but as shown for the reaction of *N,N*-dimethyl-*para*-toluidine (**1e**) with  $(\text{ani})_3\text{C}^+$  ( $E = -4.35$ ) several orders of magnitude slower than the reaction observed with  $(\text{mor})_2\text{CH}^+$  (**2d**;  $E = -5.53$ ) and  $(\text{pfa})_2\text{CH}^+$  (**2g**;  $E = -3.14$ ) (Table 10, entry 3 and Table 11, entry 1 and 2). The slower reaction could be an attack of a ring carbon. As the N-adduct as well as the Wheland complex, formed by an attack of the C4 carbon, are unstable, the even slower reaction at the C2 carbon might take place.



Scheme 16: Proposed general reaction scheme for the reaction of *para*-substituted *N,N*-dimethylanilines *N,N*-dimethyl-*para*-toluidine (**1e**) and *N,N*-dimethyl-*para*-anisidine (**1f**).

Table 11: Second-order rate constants ( $k_2$ , 20 °C) for the reactions of benzhydrylium tetrafluoroborates **2** with tertiary alkylated anilines *N,N*-dimethyl-*para*-toluidine (**1e**) and *N,N*-dimethyl-*para*-anisidine (**1f**) in acetonitrile and resulting  $N$  and  $s_N$  parameters.

Nucleophile	Proposed Reaction Side	$N$ ( $s_N$ )	Reference electrophile	$E$ parameter	$k_2$ ( $M^{-1} s^{-1}$ )	$\lg k_2$
 <b>1e</b>	C2/C4	n.d.	(mor) <sub>2</sub> CH <sup>+</sup> ( <b>2d</b> )	-5.53	260	2.42
			(pfa) <sub>2</sub> CH <sup>+</sup> ( <b>2g</b> )	-3.14	99.5	1.99
	N	12.16 (0.50)	(mor) <sub>2</sub> CH <sup>+</sup> ( <b>2d</b> )	-5.53	$1.64 \times 10^3$	3.22
			(dpa) <sub>2</sub> CH <sup>+</sup> ( <b>2e</b> )	-4.72	$6.76 \times 10^3$	3.83
			(pfa) <sub>2</sub> CH <sup>+</sup> ( <b>2g</b> )	-3.14	$2.89 \times 10^4$	4.46
 <b>1f</b>	C2/C4	n.d.	(mor) <sub>2</sub> CH <sup>+</sup> ( <b>2d</b> )	-5.53	9.03	0.96
	N	9.71 (0.58)	(mor) <sub>2</sub> CH <sup>+</sup> ( <b>2d</b> )	-5.53	278	2.44
			(pfa) <sub>2</sub> CH <sup>+</sup> ( <b>2g</b> )	-3.14	$6.59 \times 10^3$	3.82

For the attack of the C4 carbon of **1a** at (mfa)<sub>2</sub>CH<sup>+</sup> (**2f**) and (pfa)<sub>2</sub>CH<sup>+</sup> (**2g**) in acetonitrile, the obtained second-order rate constants deviate significantly from the correlation line of  $\lg k_2$  vs. Electrophilicity parameter  $E$  of the applied benzhydrylium ions **2**. Similarly the linear free energy relationship (Equation 1) is not applicable of the attack of the C4 carbon of **1e** at (pfa)<sub>2</sub>CH<sup>+</sup> (**2g**) and thus, a  $N$  and  $s_N$  parameter could not be derived for this reaction side. However, for the attack of the nitrogen atom of **1e** and **1f**, the logarithmized second-order rate constants  $\lg k_2$  correlate linearly with the Electrophilicity parameter  $E$  of the applied benzhydrylium ions **2** (Figure 26).

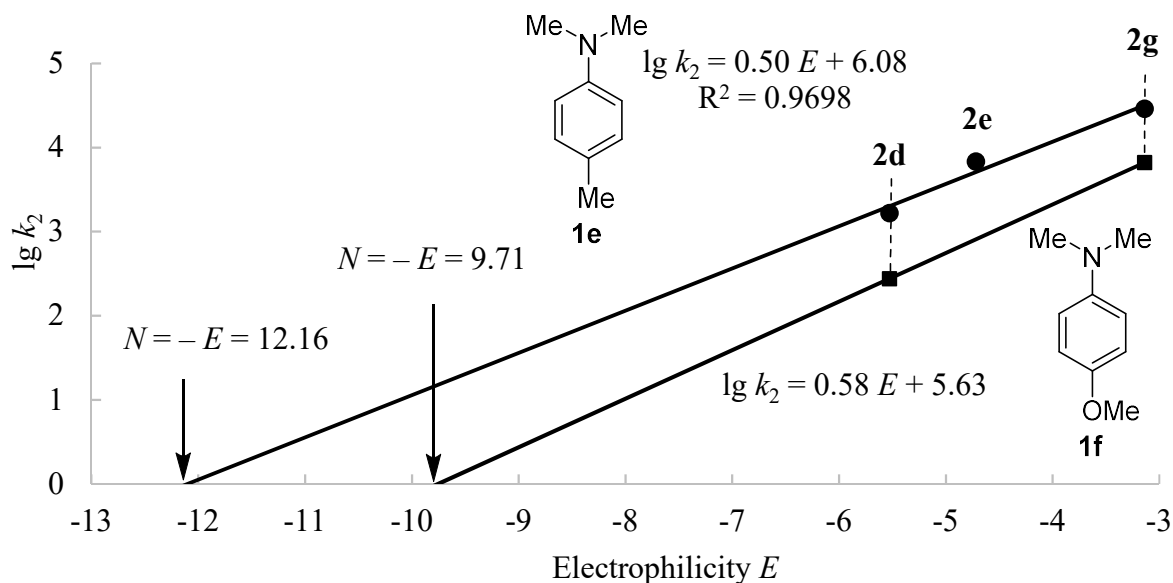
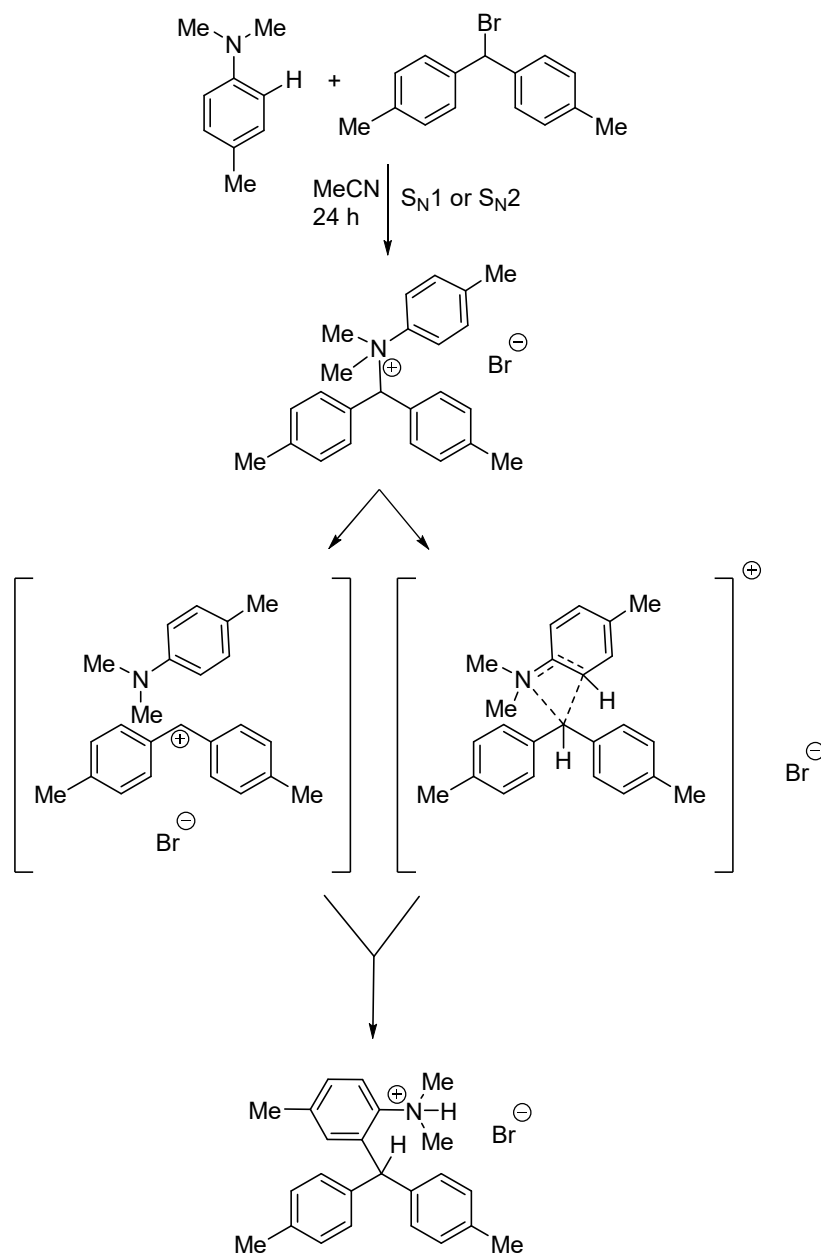


Figure 26: Correlation of the logarithmized second-order rate constants  $\lg k_2$  for the reactions of *N,N*-dimethyl-*para*-toluidine (**1e**, circles) and 4-methoxy-*N,N*-dimethylaniline (**1f**, squares) at the nitrogen atom with the electrophiles **2** in acetonitrile with their electrophilicity parameters  $E$ . The  $N$  parameter are derived as the intercepts on the abscissa ( $N = -E$  at  $\log k_2 = 0$ ;  $N = 12.16$  for the attack of the nitrogen atom of **1e** and  $N = 9.71$  for the attack of the nitrogen atom of **1f**), the  $s_N$  parameters are the slopes of the correlation lines ( $s_N = 0.50$  for the attack of the nitrogen atom of **1e** and  $s_N = 0.58$  for the attack of the nitrogen atom of **1f**).

The attack of the anilines C2 carbon at the benzhydrylium ions **2** seems unlikely, but the proof of principle is shown by reacting **1e** with  $(\text{tol})_2\text{CHBr}$  (**2h**,  $E$  parameter of the corresponding cation  $(\text{tol})_2\text{CH}^+$  is  $+3.63$ ) to the *ortho*-substituted product 2-(di-*p*-tolylmethyl)-*N,N*,4-trimethylbenzenammonium bromide (Figure 27).  $(\text{Tol})_2\text{CH}^+$  is way more reactive than all the other benzhydrylium ions used for the kinetic studies. It is reasonable to assume a first attack of the carbocation at the nitrogen atom, followed by a slow concerted or stepwise rearrangement to the nearby C2 carbon atom (Scheme 17).



Scheme 17: Proposed mechanism of the reaction of *N,N*-dimethyl-*para*-toluidine (**1e**) with *o*-tolyl bromide (**2h**). The formation of the N-adduct might either take place at the free benzhydrylium ion or follow a S<sub>N</sub>2-type mechanism. The N-adduct degenerates by a stepwise (left reaction pathway) or concerted (right reaction pathway) rearrangement.

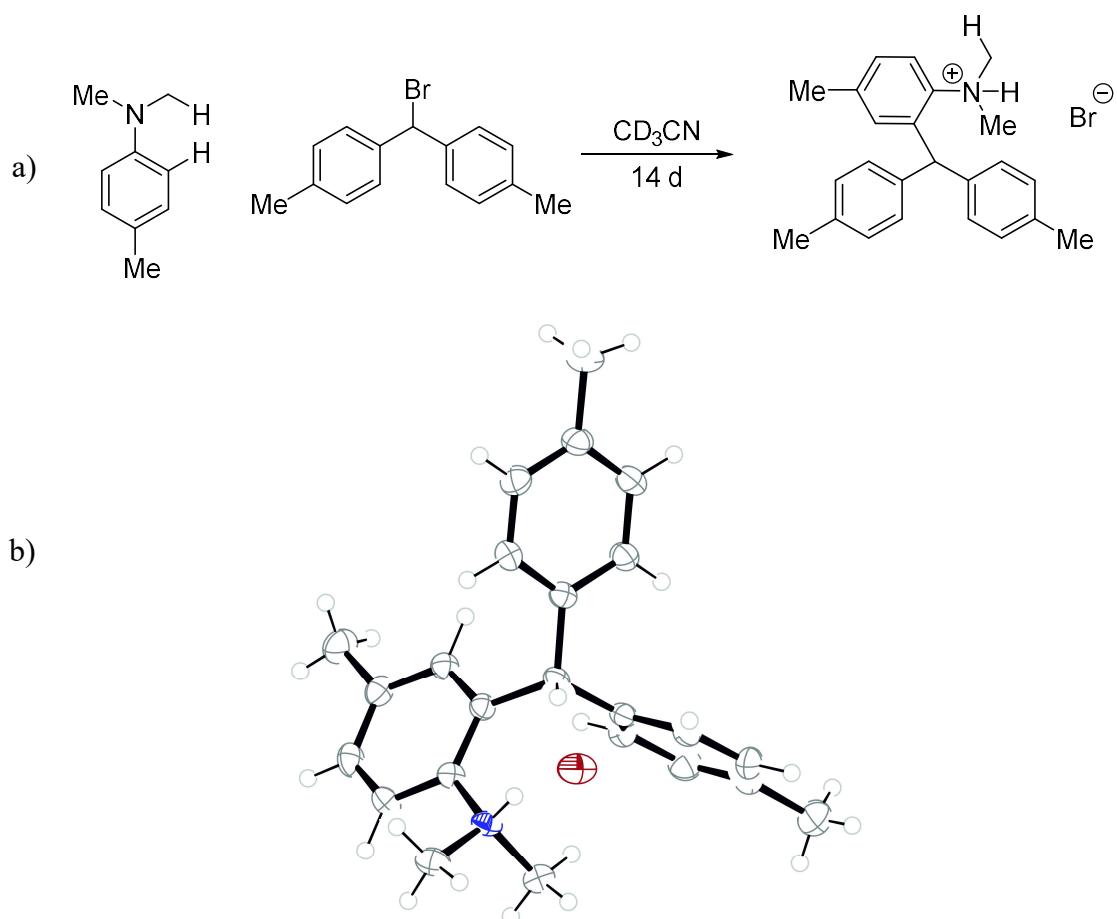


Figure 27: a) Reaction of *N,N*-dimethyl-*para*-toluidine (**1e**) with (tol)<sub>2</sub>CHBr (**2h**) in CD<sub>3</sub>CN at 23 °C. b) X-ray crystal structure (ORTEP protection) of the reaction product 2-(di-*p*-tolylmethyl)-*N,N*,4-trimethylbenzenammonium bromide, which crystallized within 14 days. The asymmetric unit contains two formula units, one selected molecule is presented. Thermal ellipsoids are drawn at the 50% probability level.<sup>[31]</sup>

## Conclusion

The second-order rate constants ( $k_2$ ) for the reactions of *N,N*-dialkylated anilines **1** with benzhydrylium ions **2** were studied in acetonitrile and dichloromethane. In most cases a bisexponential decay of the time-dependent absorbance of the electrophiles **2** was observed. This is due to a fast, but reversible attack of the nitrogen atom and a slow but irreversible attack of the C4 carbon atom at the benzhydrylium ions **2**. Nucleophilicity parameters for the attack of the nitrogen atom were obtained for all *N,N*-dialkylated anilines **1a–f**. For the nucleophiles *N,N*-dimethylaniline (**1a**), *N,N*-diethylaniline (**1b**) and 1-phenylpyrrolidine (**1c**) the reactivity of the C4 carbon was also determined. As 1-phenylpiperidine (**1d**) yields the N-adduct quantitatively and rearranges to the thermodynamic stable triarylmethane the reactivity at the C4 carbon could not be determined. Product studies were performed with the nucleophiles **1a,b+d** and triarylmethanes were obtained as product of the attack of *N,N*-dialkylated anilines at the C4 carbon. The *para*-substituted compounds *N,N*-dimethyl-*para*-toluidine (**1e**) and *N,N*-dimethyl-*para*-anisidine (**1f**) also showed a fast reaction at the nitrogen atom. The formed quaternary ammonium salts are unstable and a subsequent reaction occurs, which could not be clarified within this work. The attack of the nitrogen atom of the amines **1a–f**, as well as the attack of the C4 carbon of amines **1a–c**, follows the linear free energy relationship (Equation 1). The measured rate constants correlated linearly with the electrophilicity parameters of the respective electrophile (Figure 13), allowing us to derive their nucleophilicity parameters  $N$  and  $s_N$  for at least one reaction center of each investigated aniline **1** (Figure 28). The nucleophilic reactivities of the studied *N,N*-dialkylated anilines **1** for the attack of the C4 carbon are very similar in acetonitrile and dichloromethane, respectively. For the attack at the nitrogen atom they cover a range of nearly 4 orders of magnitude. For the abstraction of a hydride from the methyl group in  $\alpha$ -position of the nitrogen atom a  $N$  parameter of 1.48 and  $s_N$  parameter of 0.54 was found.

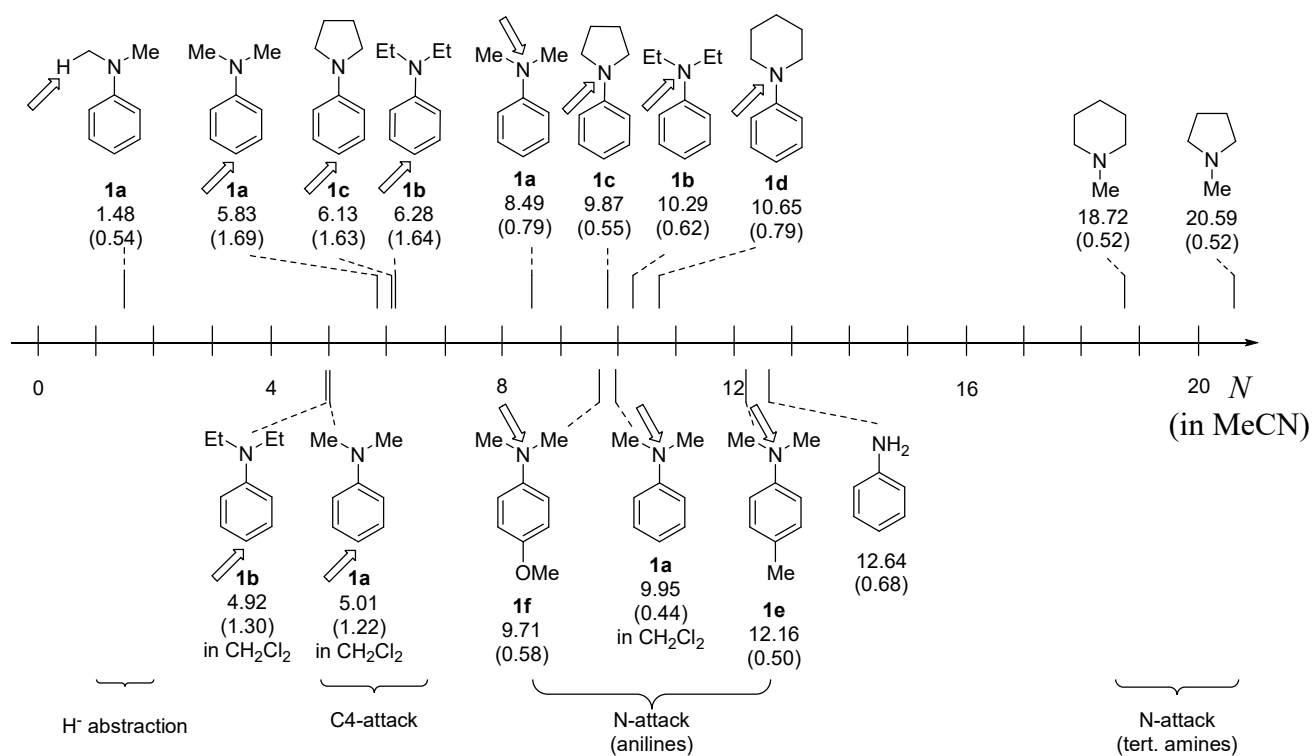


Figure 28:  $N$  and  $s_N$  parameters of the  $N,N$ -dialkylated anilines **1** studied in this work. As comparison the  $N$  and  $s_N$  parameters of aniline (taken from Ref. [5g]) and tertiary aliphatic amines (taken from Ref. [5h]) are depicted.

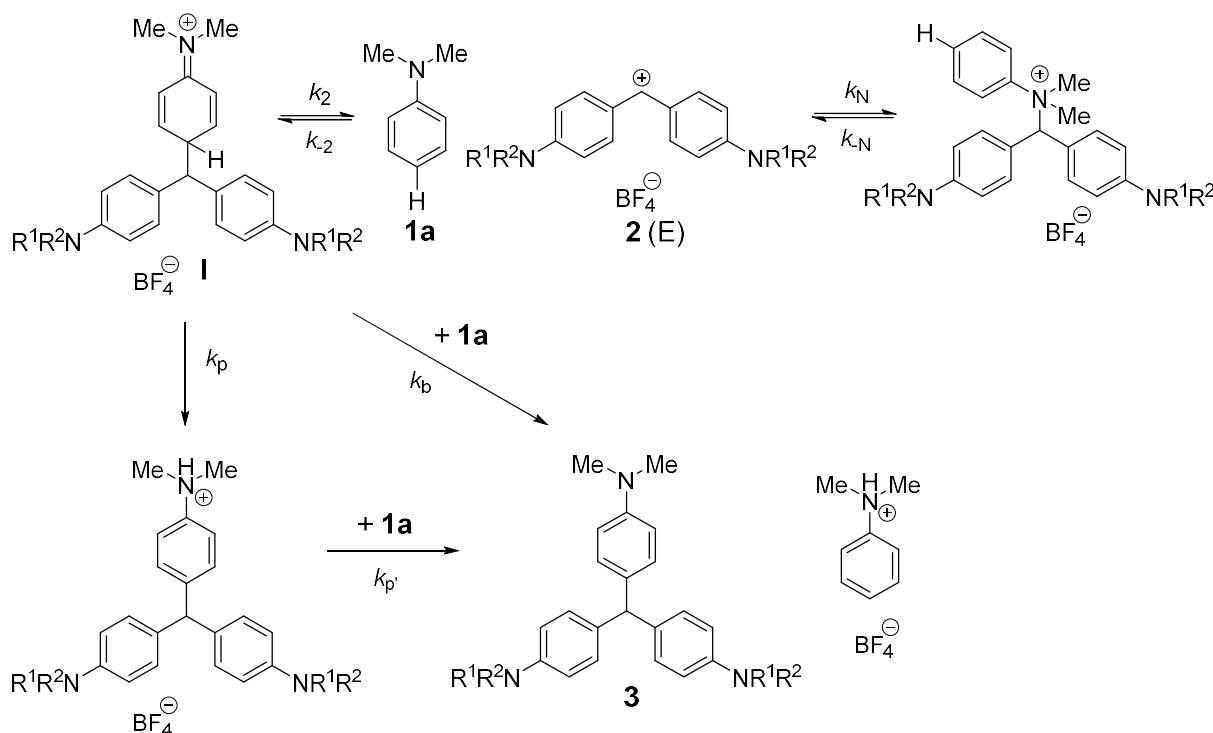
## References

- [1] a) C. Y. Cheng, R. A. Shaw, *J. Chem. Soc. Perkin Trans. 1* **1976**, 1739-1745; b) C. R. Barone, R. Cini, S. d. Pinto, N. G. Di Masi, L. Maresca, G. Natile, G. Tamasi, *Inorg. Chim. Acta* **2010**, 363, 205-212; c) E. Buncel, R. A. Renfrow, M. J. Strauss, *Can. J. Chem.* **1983**, 61, 1690-1691; d) O. N. Chupakhin, V. N. Charushin, E. O. Sidorov, G. L. Rusinov, *J. Org. Chem. USSR* **1977**, 15, 206-214.
- [2] a) A. Pfeil, *EP2532636* **2012**, A2; b) T. Bürgel, *EP2518033* **2012**, A2.
- [3] P. Grieb, *Chem. Ber.* **1877**, 10, 528.
- [4] a) *National Toxicology Program. Toxicology and Carcinogenesis Studies of N,N-Dimethylaniline (CAS No. 121-69-7) in F344/N Rats and B6C3F1 Mice (Gavage Studies). TR No. 360. U.S. Department of Health and Human Services, Public Health Service, National Institutes of Health, Bethesda, MD, 1989*; b) M. Sittig, *Handbook of Toxic and Hazardous Chemicals and Carcinogens 2nd edn*, Noyes Publications, Park Ridge, NJ, **1985**; c) *U.S. Department of Health and Human Services. Hazardous Substances Data Bank (HSDB, online database). National Toxicology Information Program, National Library of Medicine, Bethesda, MD, 1993*; d) J. E. Amoores, E. Hautala, *J. Appl. Toxicol.* **1983**, 3, 272-290.
- [5] a) C. F. Bernasconi, M. Panda, *J. Org. Chem.* **1987**, 52, 3042-3050; b) J. P. Richard, T. L. Amyes, T. Vontor, *J. Am. Chem. Soc.* **1992**, 114, 5626-5634; c) B. Varghese, S. Kothari, K. K. Banerji, *Int. J. Chem. Kinet.* **1999**, 31, 245-252; d) J. P. Richard, M. M. Toteva, J. Crueiras, *J. Am. Chem. Soc.* **2000**, 122, 1664-1674; e) M. R. Crampton, T. A. Emokpae, C. Isanbor, *J. Phys. Org. Chem.* **2006**, 19, 75-80; f) E. N. Wiedemann, F. A. Mandl, I. D. Blank, C. Ochsenfeld, A. R. Ofial, S. A. Sieber, *ChemPlusChem* **2015**, 80, 1673-1679; g) F. Brotzel, Y. C. Chu, H. Mayr, *J. Org. Chem.* **2007**, 72, 3679-3688; h) J. Ammer, M. Baidya, S. Kobayashi, H. Mayr, *J. Phys. Org. Chem.* **2010**, 23, 1029-1035.
- [6] a) C. K. M. Heo, J. W. Bunting, *J. Chem. Soc. Perkin Trans. 2* **1994**, 2279-2290; b) A. A. Matveev, A. N. Vdovichenko, A. F. Popov, L. M. Kapkan, A. Y. Chervinskii, V. N. Matvienko, *Russ. J. Org. Chem.* **1995**, 31, 1646-1649; c) T. B. Phan, M. Breugst, H. Mayr, *Angew. Chem. Int. Ed.* **2006**, 45, 3869-3874; d) M. Baidya, F. Brotzel, H. Mayr, *Org. Biomol. Chem.* **2010**, 8, 1929-1935; e) B. Maji, H. Mayr, *Angew. Chem.* **2013**, 125, 11370-11374.
- [7] a) E. M. Arnett, R. Reich, *J. Am. Chem. Soc.* **1980**, 102, 5892-5902; b) Y. Kondo, R. Uematsu, Y. Nakamura, S. Kusabayashi, *J. Chem. Soc. Perkin Trans. 2* **1998**, 1219-1224; c) S.-D. Yoh, D.-Y. Cheong, O.-S. Lee, *J. Phys. Org. Chem.* **2003**, 16, 63-68; d) F. Brotzel, B. Kempf, T. Singer, H. Zipse, H. Mayr, *Chem. Eur. J.* **2007**, 13, 336-345.
- [8] T. Mashino, S. Nakamura, M. Hirobe, *Tetrahedron Lett.* **1990**, 31, 3163-3166.
- [9] Z. Zhu, J. H. Espenson, *J. Org. Chem.* **1995**, 60, 1326-1332.
- [10] C. Hansch, A. Leo, R. W. Taft, *Chem. Rev.* **1991**, 91, 165-195.
- [11] António J. I. Alfaia, António R. T. Calado, João Carlos R. Reis, *Eur. J. Org. Chem.* **2000**, 3627-3631.
- [12] a) R. Huisgen, F. Jakob, *Justus Liebigs Ann. Chem.* **1954**, 590, 37-54; b) R. Huisgen, American Chemical Society, Washington DC, **1994**, pp. 51-52.
- [13] a) H. Mayr, T. Bug, M. F. Gotta, N. Hering, B. Irrgang, B. Janker, B. Kempf, R. Loos, A. R. Ofial, G. Remennikov, H. Schimmel, *J. Am. Chem. Soc.* **2001**, 123, 9500-9512; b) R. Lucius, R. Loos, H. Mayr, *Angew. Chem.* **2002**, 114, 97-102; c) H. Mayr, B. Kempf, A. R. Ofial, *Acc. Chem. Res.* **2003**, 36, 66-77; d) H. Mayr, A. R. Ofial, *Pure Appl. Chem.* **2005**, 77, 1807-1821; e) D. Richter, N. Hampel, T. Singer, A. R. Ofial, H. Mayr, *Eur. J. Org. Chem.* **2009**, 3203-3211; f) For a comprehensive listing of

- nucleophilicity parameters  $N$ ,  $s_N$  and electrophilicity parameters  $E$ , see <http://www.cup.uni-muenchen.de/oc/mayr/DBintro.html>.
- [14] a) H. Mayr, M. Patz, *Angew. Chem. Int. Ed.* **1994**, *33*, 938-957; *Angew. Chem.* **1994**, *106*, 990-1010.
- [15] J. Ammer, C. Nolte, H. Mayr, *J. Am. Chem. Soc.* **2012**, *134*, 13902-13911.
- [16] a) R. G. Pearson, *J. Am. Chem. Soc.* **1963**, *85*, 3533-3539; b) R. G. Pearson, *Science* **1966**, *151*, 172-177; c) R. G. Pearson, *J. Am. Chem. Soc.* **1967**, *89*, 1827-1836.
- [17] H. Mayr, M. Breugst, A. R. Ofial, *Angew. Chem.* **2011**, *123*, 6598-6634.
- [18] R. J. Mayer, M. Breugst, N. Hampel, A. R. Ofial, H. Mayr, *J. Org. Chem.* **2019**, *84*, 8837-8858.
- [19] G. L. Rusinov, A. A. Tumashov, T. L. Pilicheva, O. N. Chupakhin, *Russ. J. Org. Chem.* **1991**, *27*, 1100-1105.
- [20] I. Kaljurand, R. Lilleorg, A. Murumaa, M. Mishima, P. Burk, I. Koppel, I. A. Koppel, I. Leito, *J. Phys. Org. Chem.* **2013**, *26*, 171-181.
- [21] Y. E. Zevatskii, D. V. Samoilov, *Russ. J. Org. Chem.* **2009**, *44*, 1737.
- [22] L. C. Craig, R. M. Hixon, *J. Am. Chem. Soc.* **1931**, *53*, 4367-4372.
- [23] E. Folkers, O. Runquist, *J. Org. Chem.* **1964**, *29*, 830-832.
- [24] R. J. Mayer, N. Hampel, P. Mayer, A. R. Ofial, H. Mayr, *Eur. J. Org. Chem.* **2019**, 412-421.
- [25] T. A. Nigst, A. Antipova, H. Mayr, *J. Org. Chem.* **2012**, *77*, 8142-8155.
- [26] S. A. Shlykov, T. D. Phien, Y. Gao, P. M. Weber, *J. Mol. Struct.* **2017**, *1132*, 3-10.
- [27] S. Schwarz, LMU München (München), **2016**.
- [28] a) S. Minegishi, H. Mayr, *J. Am. Chem. Soc.* **2003**, *125*, 286-295; b) A. R. Ofial, *Pure Appl. Chem.* **2015**, *87*, 341-351; c) X. Chen, Y. Tan, G. Berionni, A. R. Ofial, H. Mayr, *Chem. Eur. J.* **2014**, *20*, 11069-11077.
- [29] a) P. S. M. R. Heck, S. Winstein, *Tetrahedron Lett.* **1964**, *5*, 2033-2036; b) S. Fukuzumi, K. Ohkubo, J. Otera, *J. Org. Chem.* **2001**, *66*, 1450-1454.
- [30] a) D. Su, F. M. Menger, *Tetrahedron Lett.* **1997**, *38*, 1485-1488; b) S. Zhang, B.-S. Kim, C. Wu, J. Mao, P. J. Walsh, *Nat. Commun.* **2017**, *8*, 14641; c) T. J. Zimmermann, T. J. J. Müller, *Synthesis* **2002**, 1157-1162.
- [31] X-ray crystal structure was measured and solved by Prof. Dr. K. Karaghiosoff.

## Quantification of the Nucleophilic Reactivities of *N,N*-Dialkylated Anilines

### 1. Derivation of Equation 6 of the main chapter



Scheme S1: Reaction of *N,N*-dimethylaniline (**1a**, **Nu**) with benzhydrylium ion (**2**, **E**) in dichloromethane.

The reaction of *N,N*-dimethylaniline (**1a**, **Nu**) with benzhydrylium ion (**2**, **E**) in dichloromethane speeds up disproportionately with the nucleophiles concentration. This indicates the shift of the rate-determining step from the attack of the carbon atom towards the proton transfer, due to the increased concentration of base. Therefore, the reaction pathway had to be reconsidered (Scheme S1).

For the further discussion,  $k_{p'}$  is irrelevant, as the carbon-carbon bond is already formed irreversibly. The change of the concentration of the zwitterionic intermediate **I** can be expressed by equation S1.

$$\frac{d[\mathbf{I}]}{dt} = k_2[\mathbf{E}][\mathbf{Nu}] - k_{-2}[\mathbf{I}] - k_b[\mathbf{I}][\mathbf{Nu}] - k_p[\mathbf{I}] \quad (\text{S1})$$

The rate law can be expressed by equations S2 and S3 if we assume a steady-state concentration for the intermediate **I**.

$$-\frac{d[\mathbf{E}]}{dt} = \frac{k_2[\mathbf{E}][\mathbf{Nu}](k_b[\mathbf{Nu}] + k_p)}{k_{-2} + k_b[\mathbf{Nu}] + k_p} \quad (\text{S2})$$

$$k_{\text{obs}} = \frac{k_2[\mathbf{Nu}](k_b[\mathbf{Nu}] + k_p)}{k_{-2} + k_b[\mathbf{Nu}] + k_p} \quad (\text{S3})$$

At high nucleophile concentrations, the direct proton-transfer ( $k_p$ ) can be neglected, and eq (S3) is reduced to eq (S4) which can be rewritten as eq (S5).

$$k_{\text{obs}} = \frac{k_2 k_b [\mathbf{Nu}]^2}{k_{-2} + k_b [\mathbf{Nu}]} \quad (\text{S4})$$

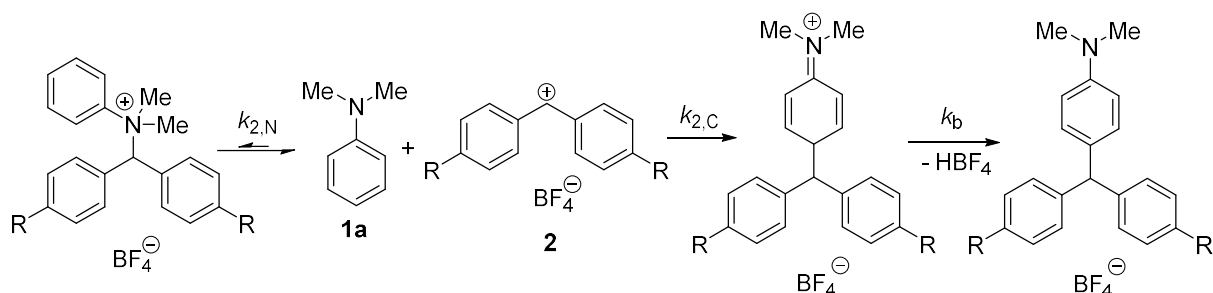
$$\frac{[\mathbf{Nu}]}{k_{\text{obs}}} = \frac{1}{k_2} + \frac{k_{-2}}{k_2 k_b [\mathbf{Nu}]} \quad (\text{S5})$$

Second-order rate constants for the C-N-bond formation ( $k_2$ ) were obtained as the reciprocal intercepts of plots of  $[\mathbf{Nu}]/k_{\text{obs}}$  versus  $1/[\mathbf{Nu}]$ .

At very high nucleophile concentrations where  $k_{-2} \ll k_b[\mathbf{Nu}]$ , eq (S4) is reduced to eq (S6) resulting in a linear dependence between rate and nucleophile concentration.

$$k_{\text{obs}} = k_2[\mathbf{Nu}] \quad (\text{S6})$$

## 2. Theoretical Studies by Florian Achrainer and Hendrik Zipse



Scheme S2: Reaction of benzhydrylium ions of type **2** with *N,N*-dimethylaniline (**1a**). R = H or NMe<sub>2</sub>.

The different possibilities of attack were already discussed in the main chapter, but in a general view (Scheme S2). To clarify the reaction observed by the first decay, Florian Achrainer from the Zipse group performed theoretical calculations at B2PLYP-D3(FC)/G3MP2large//M06-2X/6-31+G(d) level of theory to quantify the regioselectivity of the reactions of carbon cations shown in Figure S1 with *N,N*-dimethylaniline (**1a**). The reaction enthalpies of *N,N*-dimethylaniline (**1a**) with carbocations **2x**, **2b** and **2y** (Figure S1) has been discussed in the main chapter.

Three different electrophiles were included: two benzhydrylium ions **2x** (R = H) and **2b** (R = NMe<sub>2</sub>) and the prop-2-yl cation **2y**, which was chosen for its small steric demand, as a sterically more demanding alternative to the methyl cation (Figure S1).

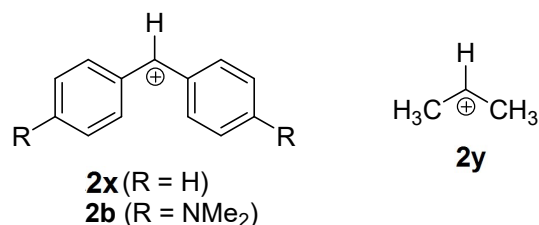


Figure S1: Carbocations **2b**, **2x** and **2y** used for quantum-chemical studies.

Even though their formation from dimethylaniline and benzhydryl cations is endothermic, **4b** and **5b** represent bound adducts at M06-2X/6-31+G(d) level characterized by a typical bond length of 162 to 164 pm. Mulliken charge analysis confirms this result since most of the positive charge of the benzhydrylium ion is transferred to the aniline moiety (see Figure S2).

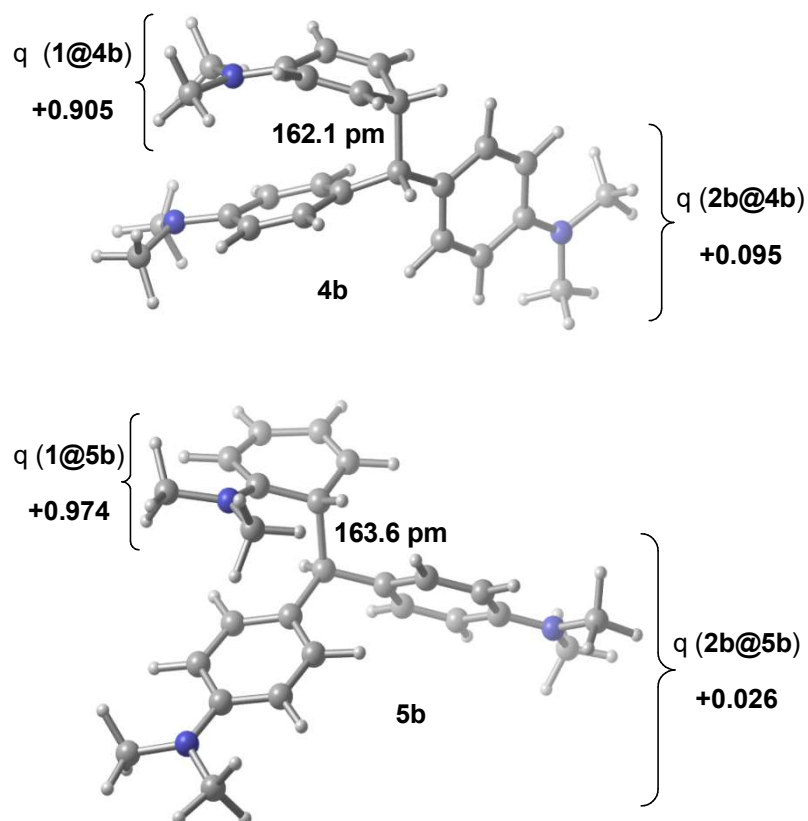


Figure S2: M06-2X/6-31+G(d) optimized structures of the most stable *ortho* and *para* adducts of **1** and **2b**, together with cumulative Mulliken charges  $q$  of the reactants in the adduct, respectively.

The structure of N-alkylated adduct **3b** is highly dependent on the employed theory and basis set (Figure S3). Optimization at the M06-2X/6-31+G(d) level yields the expected N-adduct with a comparatively long C-N bond and 45% cation to aniline charge transfer. Optimization with other hybrid DFT methods (B3LYP, B98) with exclusion of diffuse functions or dispersion corrections failed to locate the covalent adduct and gave in contrast the non-bonded ion-dipole complex **3b-CT** with moderate charge transfer character.

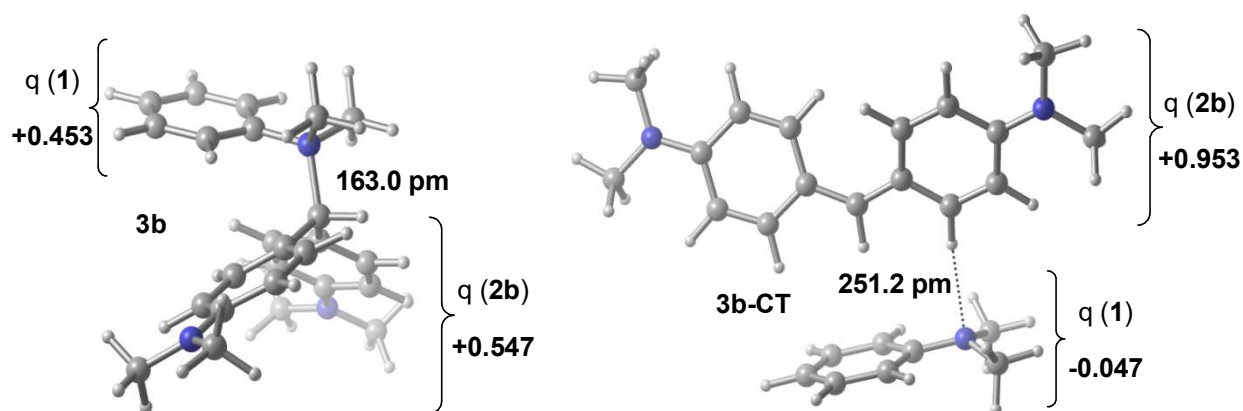


Figure S3: Comparison of optimization of the N-adducts **3b** at M06-2X/6-31+G(d) (left) and its charge-transfer complex **3b-CT** at B3LYP/6-31G(d,p) level of theory (right).

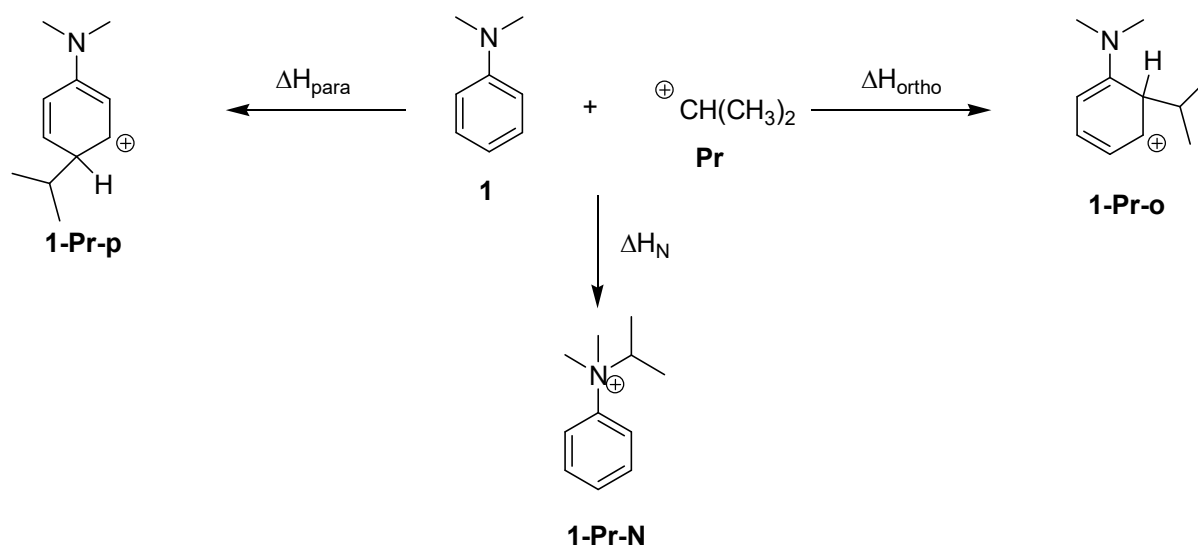
### 3. Additional information on the quantum-chemical calculations

All stationary points have been optimized at M06-2X/6-31+G(d) level of theory<sup>[1]</sup> with initial coordinates from the MM3\* force field as implemented in *MacroModel* (*Schrödinger* program package).<sup>[2]</sup> Thermal corrections at 298.15 K have been calculated at the same level using the rigid rotor/harmonic oscillator model. Dispersion interactions of the aromatic  $\pi$  system have been included using *Grimme's* corrected B2PLYP-D3(FC)<sup>[3]</sup> approach in combination with the G3MP2large basis set and M06-2X/6-31+G(d) geometries. The related methyl cation affinities (MCA) of Lewis-basic organocatalysts have recently been validated and MP2(FC)/6-31+G(2d,p)//B98/6-31G(d) calculations were identified as method of choice for the correct thermodynamic prediction.<sup>[4]</sup> Recently, Lewis acidities of benzhydrylium ions have been correlated with quantum chemically calculated acidities at B3LYP/6-311++G(3df,2pd)//B3LYP/6-31G(d,p) level.<sup>[5]</sup> The passage from gas to liquid phase has been accomplished by employing a polarizable continuum model (PCM)<sup>[6]</sup> with dichloromethane or acetonitrile as the solvent, respectively. The solvent model density (SMD)<sup>[7]</sup> with a combination of B3LYP theory and 6-31G(d) basis set in a single-point approach has been used to calculate  $\Delta G_{\text{solv}}$  at 298.15 K. Boltzmann-averaged enthalpies of n conformers are obtained by **eq. 1**:

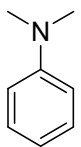
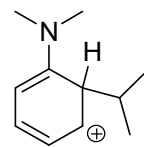
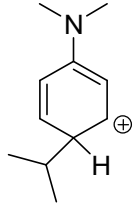
$$w_i = \frac{\exp\left(\frac{-\Delta H_{298}}{R T}\right)}{\sum_{i=1}^n \frac{-\Delta H_{298}}{R T}}$$
$$\langle H_{298} \rangle = \sum_{i=1}^n w_i H_i \quad (1)$$

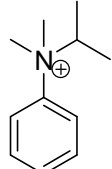
B2PLYP-D3 theory is implemented in *Gaussian09 Rev. D.01*. All other calculations have been performed with *Gaussian09 Rev. C.01*.<sup>[8]</sup>

All stationary points have been optimized at B3LYP/6-311++G(3df,2p) level of theory. Thermal corrections at 298.15 K have been calculated at the same level using the rigid rotor/harmonic oscillator model. The related methyl cation affinities (MCA) of Lewis-basic organocatalysts have recently been validated and MP2(FC)/6-31+G(2d,p)//B98/6-31G(d) was identified as method of choice.<sup>[4]</sup> The passage from gas to liquid phase has been accomplished by employing a polarizable continuum model (PCM)<sup>[9]</sup> with dichloromethane as the respective solvent. The solvent model density (SMD) with a combination of B3LYP theory and 6-31G(d) basis set in a single-point approach has been used to calculate  $\Delta G_{\text{solv}}$  at 298.15 K.<sup>[7]</sup> All calculations have been performed with *Gaussian09*, Rev. C.01.<sup>[8]</sup>



**Table S1:** Energies and enthalpies of considered reactants at 298.15 K in the gas phase (in Hartree).

					
<b>B3LYP/6-311++G(3df,2p)</b>	E	-366.3386909	-118.2522846	(a) -484.6663348 (b) -484.6706123	-484.6793837
	H			(a) -484.382012 (b) -484.386290	
		-366.156034	-118.158537	<H> -484.3862325	-484.395227
				<H <sub>sol</sub> > -484.4667417	
MP2(FC)/6-31+G(2d,p)// B98/6-31G(d)	E	-365.1545403	-117.8244049	(a) -483.2360494 (b) -483.2387679	-483.2434280
	H			(a) -482.9499439 (b) -482.9527495	
		-364.9707267	-117.7299161	<H> -482.9525922	-482.9576194
				<H <sub>sol</sub> > -483.0331020	
SMD/B3LYP/6-31G(d)// B3LYP/6-311++G(3df,2p) <b>CH<sub>2</sub>Cl<sub>2</sub></b>	$\Delta G_{\text{solv}}$	-0.0128604	-0.1007954	(a) -0.0803335 (b) -0.0804769	-0.0795845

		
B3LYP/6-311++G(3df,2p)	E	-484.6798423
	H	-484.394414
MP2(FC)/6-31+G(2d,p)// B98/6-31G(d)	E	-483.2642558
	H	-482.9772275
SMD/B3LYP/6-31G(d)// B3LYP/6-311++G(3df,2p) <b>CH<sub>2</sub>Cl<sub>2</sub></b>	$\Delta G_{\text{solv}}$	-0.0837119

**Table S2:** Reaction enthalpies of the electrophilic addition of the 2-propyl cation (**Pr**) to aniline **1** (in kJ mol<sup>-1</sup>).

	<sup>+</sup> CH(CH <sub>3</sub> ) <sub>2</sub>		
	$\Delta H_{\text{ortho}}$	$\Delta H_{\text{para}}$	$\Delta H_{\text{N}}$
B3LYP/6-311++G(3df,2p)	-188.15	-211.76	-209.63
MP2(FC)/6-31+G(2d,p)// B98/6-31G(d)	-661.49	-674.69	-726.17
B3LYP + $\Delta G_{\text{solv}}$	-101.12	-122.31	-131.01
MP2 + $\Delta G_{\text{solv}}$	-574.47	-585.24	-647.55

**Table S3:** Ratio prediction of rate constants obtained using the Arrhenius equation  $k = \exp(-\Delta\Delta H/RT)$ .

<sup>+</sup> CH(CH <sub>3</sub> ) <sub>2</sub>				
	$\Delta\Delta H_{ortho}$	$\Delta\Delta H_{para}$	$\Delta\Delta H_N$	$k_{ortho} : k_{para} : k_N$
<b>B3LYP/6-311++G(3df,2p)</b>	<b>+23.61</b>	<b>0.0</b>	<b>+2.13</b>	<b>7.3 10<sup>-5</sup> : 1 : 0.42</b>
MP2(FC)/6-31+G(2d,p)// B98/6-31G(d)	+64.68	+51.48	0.0	n/a
<b>B3LYP + <math>\Delta G_{solv}</math></b>	<b>+29.89</b>	<b>+8.70</b>	<b>0.0</b>	<b>5.8 10<sup>-6</sup> : 0.030 : 1</b>
MP2 + $\Delta G_{solv}$	73,08	+62.31	0.0	n/a

Structure of all stationary points (optimized at B3LYP/6-311++G(3df,2p) level)

**1**

```
1\1\GINC-S2\FOpt\RB3LYP\6-311++G(2df,2p)\C8H11N1\ROOT\06-Nov-2014\0\#\#
P B3LYP/6-311++G(2df,2p) opt freq pop=nbo\Dimethylanilin\0,1\C,-1.00
78817339,-1.0879625507,-0.0019371419\C,0.0974673419,-0.7909678155,-0.7
904117641\C,0.6790032659,0.4685203183,-0.7677099492\C,0.1723016686,1.4
856717478,0.0655502606\C,-0.9588099502,1.1771926583,0.8473675648\C,-1.
5272426422,-0.087927267,0.8116888606\H,-1.4570791061,-2.0707572405,-0.
0261717151\H,0.5169620296,-1.5477085963,-1.4408649673\H,1.5314553622,0
.6565885911,-1.4013150548\H,-1.3990143336,1.9246891631,1.4884307347\H,
-2.3935051117,-0.2883672254,1.42905212\N,0.7700361622,2.7360639846,0.1
231075089\C,0.0936380944,3.8182519234,0.8113233294\H,0.7210049208,4.70
51183374,0.7814026566\H,-0.8762091132,4.0691179015,0.362459363\H,-0.07
53463495,3.5722214429,1.8607013733\C,1.7820003657,3.08777669,-0.853983
8199\H,2.1563115125,4.0841217827,-0.6344653247\H,2.6293165844,2.402151
1485,-0.8068598753\H,1.4006484121,3.0838516258,-1.8833177693\Version=
AM64L-G09RevC.01\State=1-A\HF=-366.3386909\RMSD=7.395e-09\RMSF=1.495e-
05\Dipole=0.2730638,0.7487442,-0.0516745\Quadrupole=-0.5375901,2.32321
34,-1.7856233,1.4412896,-3.0026985,1.2316527\PG=C01 [X(C8H11N1)]\@
```

**Pr**

```
1\1\GINC-S1\FOpt\RB3LYP\6-311++G(2df,2p)\C3H7(1+)\FLORIAN\07-Nov-2014\
0\#\# P B3LYP/6-311++G(2df,2p) opt freq pop=nbo\Propyl cation\1,1\C,-1
.2685053739,-0.1936388223,-0.032333106\H,-1.2088076472,-1.2777637889,-
0.0362727165\H,-1.8613323173,0.2208286434,-0.853918009\H,-1.8526228729
,0.1260757266,0.8619090832\C,-0.0231403921,0.4937360799,0.1462021886\H
,-0.0299335938,1.5737793876,-0.0011401846\C,1.2302519253,-0.1053480244
,0.5002795686\H,1.1837715704,-1.1493974264,0.7947620645\H,1.8119690376
,-0.0299904891,-0.447863648\H,1.8166188839,0.5213638736,1.1797147793\
Version=AM64L-G09RevC.01\State=1-A\HF=-118.2522846\RMSD=2.491e-09\RMSF
=5.355e-06\Dipole=-0.0019497,0.3106269,-0.0424004\Quadrupole=3.30594,-
1.1147124,-2.1912275,0.1058398,0.5755916,-0.1458447\PG=C01 [X(C3H7)]\@
```

## 1-Pr-p

```
1\1\GINC-S2\FOpt\RB3LYP\6-311++G(2df,2p)\C11H18N1(1+)\ROOT\08-Nov-2014
\0\#\#P B3LYP/6-311++G(2df,2p) opt freq pop=nbo\Dimethylanilin + para
Propyl\1,1\C,-0.6656171196,-0.8649687722,3.483306362\C,0.6825820899,-
0.667312087,2.9049024195\C,1.2809443344,0.5314801452,2.7952878337\C,0.
616649444,1.7371335522,3.2372472206\C,-0.7101771376,1.6098367102,3.796
4723777\C,-1.2934840249,0.4047693851,3.9134116302\H,-1.2975381466,-1.2
723944578,2.6769495028\H,1.2009850998,-1.5424085788,2.5361517245\H,-1.
2271633433,2.4868270608,4.1501846172\H,-2.2810924045,0.3403744557,4.35
38773375\N,1.2021923216,2.9177691761,3.1292286367\C,0.5034079326,4.175
2137898,3.4428001628\H,1.00284259,4.9830223177,2.918359267\H,-0.527434
1502,4.140047896,3.106184615\H,0.5351305601,4.3785487282,4.5135686039\
C,2.5990213452,3.0661308198,2.6877191043\H,2.9685551132,4.022804405,3.
0414216224\H,3.2237943378,2.2853627597,3.1090157915\H,2.6648482588,3.0
444315904,1.5995485081\H,2.2557050172,0.5975926071,2.3401923073\C,-0.7
318126073,-1.9742233271,4.6079249116\H,-1.7776580072,-1.9846114058,4.9
24285769\C,0.1354174813,-1.622363482,5.8180650559\H,1.1960454697,-1.61
54397553,5.5618213219\H,-0.1179179841,-0.6489396078,6.2388847876\H,-0.
0043809616,-2.3643518548,6.6032187461\C,-0.3998590374,-3.3598114434,4.
0519975549\H,-0.5760269139,-4.1140998298,4.8180705236\H,-1.0200644617,
-3.6139615575,3.1917306471\H,0.6465844644,-3.4458496798,3.7567981576\
Version=AM64L-G09RevC.01\State=1-A\HF=-484.6793837\RMSD=6.356e-09\RMSF
=4.209e-06\Dipole=0.3710081,1.5125463,-0.5056579\Quadrupole=-3.0550379
,14.0388717,-10.9838338,7.3647174,-4.5820339,-3.6071376\PG=C01 [X(C11H
18N1)]\@
```

## 1-Pr-o\_a

```
1\1\GINC-S3\FOpt\RB3LYP\6-311++G(2df,2p)\C11H18N1(1+)\FLORIAN\08-Nov-2
014\0\#\#P B3LYP/6-311++G(2df,2p) opt freq pop=nbo\Dimethylanilin + or
tho Propyl\1,1\C,-0.4523503689,-0.928793185,3.3298258235\C,0.81222170
99,-0.7869085047,2.9092521746\C,1.5841346644,0.4789023661,3.0884376435
\C,0.7257553575,1.6751167863,3.3997345081\C,-0.5497091606,1.431655596,
3.9999756172\C,-1.1079951509,0.1922909651,3.9406677732\H,-0.9778753216
,-1.8676673264,3.2352927742\H,1.3566941644,-1.6198480369,2.4843850239\
H,-1.1225697677,2.2433914541,4.4161309622\H,-2.1037112981,0.0557438774
,4.34266757\H,2.1710836011,0.6481163646,2.1867373399\N,1.1132429357,2.
9134882654,3.1451192775\C,0.3101900258,4.0702435678,3.5858287095\H,0.8
897703666,4.9712986142,3.4183327464\H,-0.6162325571,4.1350519785,3.015
9525006\H,0.0836455561,3.9999145291,4.6461386858\C,2.2527878308,3.2915
97278,2.2998955\H,3.004791336,3.8091833229,2.892267072\H,2.7062954434,
2.4322974267,1.8268041336\H,1.888916576,3.9686339457,1.5282244502\C,2.
6758791883,0.1904522127,4.2414818166\H,3.0876639411,-0.7764672965,3.94
65115062\C,3.8271541085,1.1953263378,4.2397387586\H,3.5125915667,2.184
8706311,4.5715612856\H,4.5890576023,0.8563916907,4.9414354898\H,4.3030
059084,1.2825923796,3.2634231175\C,2.0742883544,0.044375745,5.63834537
96\H,1.2432414173,-0.6574247681,5.6663803907\H,2.8390715004,-0.3302634
005,6.3179113367\H,1.7312744097,1.0007034434,6.0345399627\Version=AM6
4L-G09RevC.01\State=1-A\HF=-484.6663348\RMSD=4.159e-09\RMSF=1.617e-05\
Dipole=-0.2892876,0.7970231,-0.4847538\Quadrupole=0.7371816,7.0183263,
-7.7555078,0.8246703,-2.1444514,-1.9097662\PG=C01 [X(C11H18N1)]\@
```

## 1-Pr-o\_b

```
1\1\GINC-S3\FOpt\RB3LYP\6-311++G(2df,2p)\C11H18N1(1+)\FLORIAN\08-Nov-2
014\0\#P B3LYP/6-311++G(2df,2p) opt freq pop=nbo\Dimethylanilin + or
tho Propyl\1,1\C,-0.4328983477,-1.4662527396,0.3836631526\C,0.6526935
297,-0.7560583329,0.0459981714\C,0.6103889582,0.3797137072,-0.91949600
05\C,-0.6849059978,0.5013275366,-1.681424214\C,-1.8254518945,-0.210589
633,-1.2024738492\C,-1.6916443195,-1.1487269395,-0.2252423378\H,-0.379
7160938,-2.266679496,1.1070404757\H,1.6105003954,-0.9641924723,0.50126
22033\H,-2.7930585094,-0.0552795102,-1.6496155827\H,-2.5712695839,-1.6
968232057,0.0871220097\H,1.4275924989,0.2277320411,-1.62939342\N,-0.77
68072864,1.263821623,-2.7580831293\C,-2.0658541365,1.4696660093,-3.444
0267473\H,-1.9289611762,2.2240480685,-4.2106706721\H,-2.4038469745,0.5
470062045,-3.914357598\H,-2.8205584568,1.8222605663,-2.7456134337\C,0.
3576267993,1.9094600567,-3.4298911411\H,0.2760711833,2.9922977387,-3.3
41314352\H,1.305877299,1.5912587051,-3.0181678605\H,0.3265281243,1.644
7255532,-4.4856999028\C,0.958776999,1.7517920572,-0.1749566112\H,0.876
3132112,2.5224018234,-0.9419219101\C,-0.0261824119,2.0961737487,0.9433
537161\H,0.0146327763,1.3722930718,1.7565016762\H,0.2288472164,3.06961
18148,1.360814189\H,-1.05606054,2.1532083975,0.5918286839\C,2.40532706
58,1.7486997526,0.3233445546\H,3.1133042882,1.4938223498,-0.4664234873
\H,2.6641826257,2.7422404097,0.6879950228\H,2.5540168583,1.0561046834,
1.1511088645\Version=AM64L-G09RevC.01\State=1-A\HF=-484.6706123\RMSD=
1.763e-09\RMSF=7.740e-06\Dipole=-0.4598949,0.0254534,-1.0524287\Quadru
pole=0.0441129,-2.9322414,2.8881286,2.678513,4.1055155,-6.9706196\PG=C
01 [X(C11H18N1)]\@
```

## 1-Pr-N

```
1\1\GINC-S2\FOpt\RB3LYP\6-311++G(2df,2p)\C11H18N1(1+)\ROOT\08-Nov-2014
\0\#P B3LYP/6-311++G(2df,2p) opt freq pop=nbo\Dimethylanilin + N Pro
pyl\1,1\C,-0.4317234349,-0.9919661536,3.1891769388\C,0.6324455046,-0.
8091460738,2.3136139199\C,1.3302752294,0.3904968252,2.2975736308\C,0.9
616050127,1.4145177816,3.1657903196\C,-0.0997365139,1.2416041931,4.043
3030342\C,-0.7932883581,0.0337633588,4.0489337403\H,0.9240216065,-1.59
90101998,1.6361232494\H,-0.4105368138,2.0123348457,4.728626569\H,-1.61
86211972,-0.0937508601,4.734825291\N,1.7395275898,2.708294845,3.118987
8328\C,1.1471027536,3.7608959175,4.0122316717\H,1.7268823889,4.6690293
208,3.8982115953\H,0.1237508683,3.9479693472,3.7041921381\H,1.17350271
29,3.4369246606,5.0448046371\C,1.6670204431,3.2475531311,1.7072417115\
H,2.0746232898,4.2513048623,1.6861540328\H,2.2304680176,2.606030466,1.
0401140463\H,0.6241566176,3.2640552372,1.4071619896\H,2.149409451,0.50
24207608,1.6030809599\H,-0.9736316625,-1.9267938,3.1983872895\C,3.2377
524265,2.4263894959,3.5210234993\H,3.5332534153,1.6681689461,2.8007577
968\C,4.136744879,3.6450243655,3.3528287488\H,5.1567891344,3.321182919
3,3.5561992885\H,4.1345293567,4.0567547326,2.346834179\H,3.9104732068,
4.4358999618,4.065980641\C,3.3316874358,1.8442370773,4.9246911075\H,4.
350962835,1.489250194,5.0693758017\H,3.1422925447,2.5901859815,5.69520
46634\H,2.6674913504,0.9971835205,5.0754740662\Version=AM64L-G09RevC.
01\State=1-A\HF=-484.6798423\RMSD=1.389e-09\RMSF=8.164e-06\Dipole=0.40
79701,1.0749272,-0.1814547\Quadrupole=0.2900068,4.2372296,-4.5272364,5
.7319083,-2.0470951,1.1889562\PG=C01 [X(C11H18N1)]\@
```

## 4. General remarks

### Materials

Commercially available acetonitrile (H<sub>2</sub>O content < 50 ppm) was used without further purification. Dichloromethane was successively treated with concentrated sulfuric acid, water, 10% NaHCO<sub>3</sub> solution, and water. After drying with CaCl<sub>2</sub>, it was freshly distilled over CaH<sub>2</sub> under exclusion of moisture (N<sub>2</sub> atmosphere). The reference electrophiles used in this work were synthesized according to literature procedures.<sup>[10]</sup>

The alkylated anilines were synthesized following the procedure of Bieber et al. from the corresponding free anilines.<sup>[11]</sup>

### NMR spectroscopy

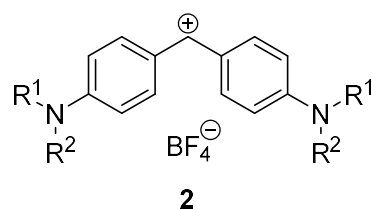
In the <sup>1</sup>H and <sup>13</sup>C NMR spectra chemical shifts are given in ppm and refer to tetramethylsilane ( $\delta_{\text{H}} = 0.00$ ,  $\delta_{\text{C}} = 0.0$ ), to CD<sub>3</sub>CN ( $\delta_{\text{H}} = 1.94$ ,  $\delta_{\text{C}} = 1.3$ ), [D<sub>6</sub>]-DMSO ( $\delta_{\text{H}} = 2.50$ ,  $\delta_{\text{C}} = 39.5$ ) or to CDCl<sub>3</sub> ( $\delta_{\text{H}} = 7.26$ ,  $\delta_{\text{C}} = 77.0$ ),<sup>[12]</sup> as internal standards. The coupling constants are given in Hz. For reasons of simplicity, the <sup>1</sup>H NMR signals of AA'BB'-spin systems of *p*-disubstituted aromatic rings are treated as doublets. Signal assignments are based on additional COSY, gHSQC, and HMBC experiments.

### Kinetics

As the reactions of colored benzhydrylium ions **2** (Table S1) with colorless *N,N*-dialkylated anilines **1** yielded colorless products (or products with a different absorption range than the reactants), the reactions could be followed by UV-Vis spectroscopy. For fast reactions ( $t_{1/2} < 60$  s), the kinetics were monitored using stopped-flow techniques. The temperature of all solutions was kept constant at  $20.0 \pm 0.1$  °C by using a circulating bath thermostat. In all runs the concentration of the colorless compound was at least 10 times higher than the concentration of the colored compound, resulting in pseudo-first-order kinetics with an exponential Decay of the relative concentration of the minor compound. First-order rate constants  $k_{\text{obs}}$  were obtained by least-squares fitting of the exponential function  $A(t) = A_0 \exp(-k_{\text{obs}} t) + C$  to the time-dependent absorbances. The second-order rate constants  $k_2$  were obtained from the slopes of the linear plots of  $k_{\text{obs}}$  against the concentration of the excess components.

The reaction was monitored at the  $\lambda_{\max}$  published by Mayr et al. in 2001 (Table S4).<sup>[13]</sup> Some  $\lambda_{\max}$  were revised by Mayr et al. in 2019.<sup>[14]</sup>

**Table S4:** Benzhydrylium ions **2** employed as reference electrophiles in this study with  $\lambda_{\max}$  published by Mayr et al. in 2001.<sup>[13]</sup>



Electrophile	R <sup>1</sup>	R <sup>2</sup>	No.	<i>E</i>	$\lambda_{\max}$ [nm] in acetonitrile	$\lambda_{\max}$ [nm] in dichloromethane
(pyr) <sub>2</sub> CH <sup>+</sup>	C <sub>4</sub> H <sub>8</sub> (cycl.)		<b>2a</b>	-7.69	612	620
(dma) <sub>2</sub> CH <sup>+</sup>	Me	Me	<b>2b</b>	-7.02	606 <sup>[a]</sup>	612 <sup>[a]</sup>
(mpa) <sub>2</sub> CH <sup>+</sup>	Ph	Me	<b>2c</b>	-5.89	613	622 <sup>[a]</sup>
(mor) <sub>2</sub> CH <sup>+</sup>	C <sub>2</sub> H <sub>4</sub> -O-C <sub>2</sub> H <sub>4</sub> (cycl.)		<b>2d</b>	-5.53	612	620 <sup>[a]</sup>
(dpa) <sub>2</sub> CH <sup>+</sup>	Ph	Ph	<b>2e</b>	-4.72	644 <sup>[a]</sup>	672 <sup>[a]</sup>
(mfa) <sub>2</sub> CH <sup>+</sup>	CH <sub>2</sub> CF <sub>3</sub>	Me	<b>2f</b>	-3.85	586	593
(pfa) <sub>2</sub> CH <sup>+</sup>	CH <sub>2</sub> CF <sub>3</sub>	Ph	<b>2g</b>	-3.14	592	601
(tol) <sub>2</sub> CH <sup>+</sup>			<b>2h</b>	3.63 <sup>[b]</sup>	_[c]	_[c]

[a] Revised in Ref. [14]. For  $\lambda_{\max}$  See Table 3 in the main chapter. [b] *E* parameter of the corresponding cation (tol)<sub>2</sub>CH<sup>+</sup>. [c] Not used for photometric studies.

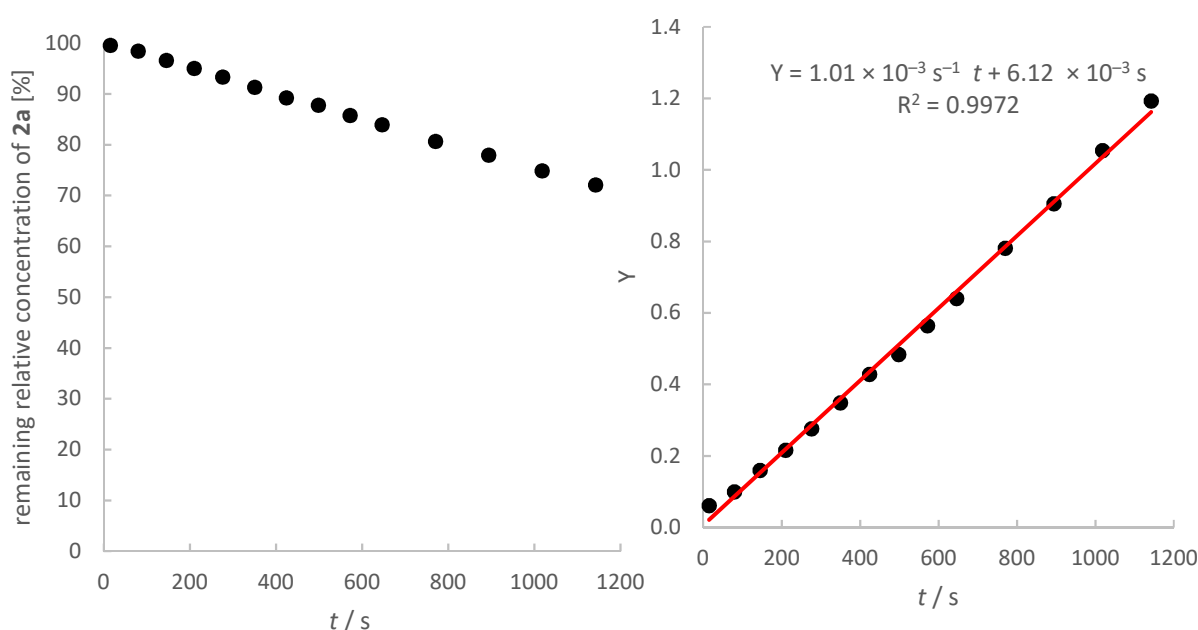
## 5. Reactions of *N,N*-dimethylaniline (1a) with benzhydrylium ions 2 in CH<sub>3</sub>CN at 20 °C

### 5.1 Reactions of *N,N*-dimethylaniline (1a) with benzhydrylium ions 2 at the C4 carbon in CH<sub>3</sub>CN at 20 °C

**Table S5:** Reaction of *N,N*-dimethylaniline (1a) with (pyr)<sub>2</sub>CH<sup>+</sup> BF<sub>4</sub><sup>-</sup> (2a) in CD<sub>3</sub>CN (20 °C, <sup>1</sup>H NMR spectroscopy).

[E] <sub>0</sub> (M)	[Nu] <sub>0</sub> (M)	[Nu] <sub>0</sub> /[E] <sub>0</sub>	<i>k</i> <sub>2</sub> (M <sup>-1</sup> s <sup>-1</sup> )
1.53 × 10 <sup>-1</sup>	3.04 × 10 <sup>-1</sup>	1.98	1.01 × 10 <sup>-3</sup>

$$k_2 (20\text{ °C}) = 1.01 \times 10^{-3} \text{ M}^{-1} \text{ s}^{-1}$$

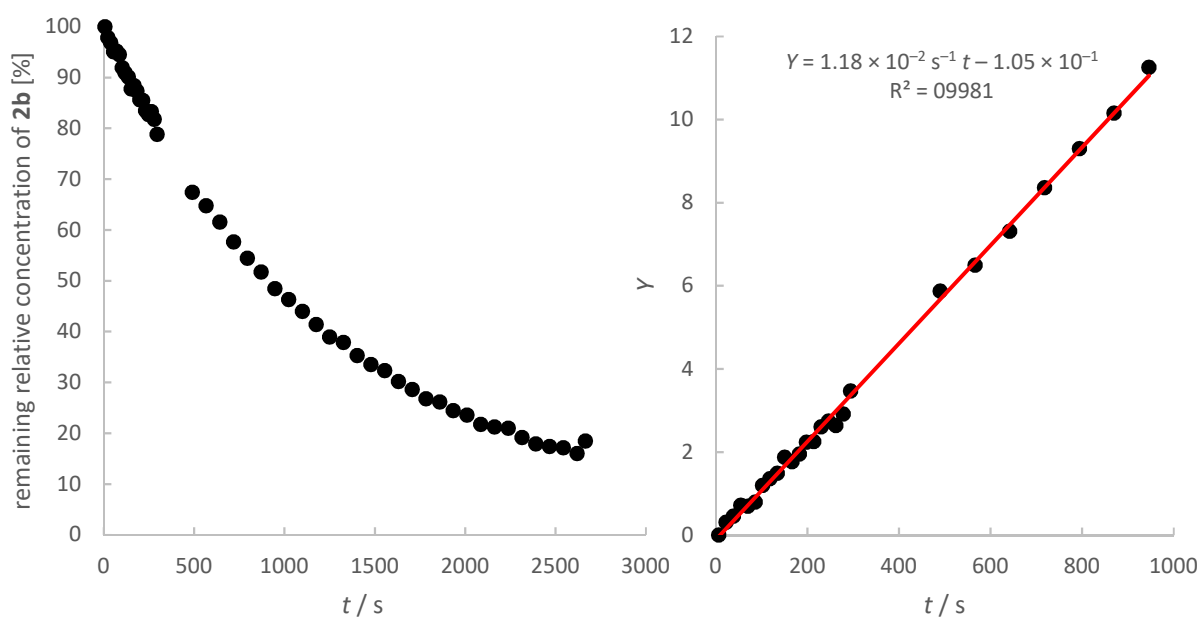


Decay of the relative concentration of (pyr)<sub>2</sub>CH<sup>+</sup> BF<sub>4</sub><sup>-</sup> while reacting with *N,N*-dimethylaniline (1a) in CD<sub>3</sub>CN at 20 °C (left). Determination of the second order rate constant by plotting time versus  $Y = ([\text{Nu}]_0 - [\text{E}]_0)^{-1} \ln([\text{E}]_0([\text{E}]_t + [\text{Nu}]_0 - [\text{E}]_0) / [\text{Nu}]_0[\text{E}]_t)$  ( $k_2 = 1.01 \times 10^{-3} \text{ M}^{-1} \text{ s}^{-1}$ , all data points were used (27% conversion); right).

**Table S6:** Reaction of *N,N*-dimethylaniline (**1a**) with (dma)<sub>2</sub>CH<sup>+</sup> BF<sub>4</sub><sup>-</sup> (**2b**) in CD<sub>3</sub>CN (23 °C, <sup>1</sup>H NMR spectroscopy).

[E] <sub>0</sub> (M)	[Nu] <sub>0</sub> (M)	[Nu] <sub>0</sub> /[E] <sub>0</sub>	<i>k</i> <sub>2</sub> (M <sup>-1</sup> s <sup>-1</sup> )
2.32 × 10 <sup>-2</sup>	7.13 × 10 <sup>-2</sup>	3.07	1.18 × 10 <sup>-2</sup>

$$k_2 (23 \text{ }^\circ\text{C}) = 1.18 \times 10^{-2} \text{ M}^{-1} \text{ s}^{-1}$$



Decay of the relative concentration of (dma)<sub>2</sub>CH<sup>+</sup> BF<sub>4</sub><sup>-</sup> (**2b**) while reacting with *N,N*-dimethylaniline (**1a**) in CD<sub>3</sub>CN at 23 °C (left). Determination of the second order rate constant by plotting time versus  $Y = ([Nu]_0 - [E]_0)^{-1} \ln([E]_0([E]_t + [Nu]_0 - [E]_0) / [Nu]_0[E]_t)$  ( $k_2 = 1.18 \times 10^{-2} \text{ M}^{-1} \text{ s}^{-1}$ , data points up to 50% conversion were used; right).

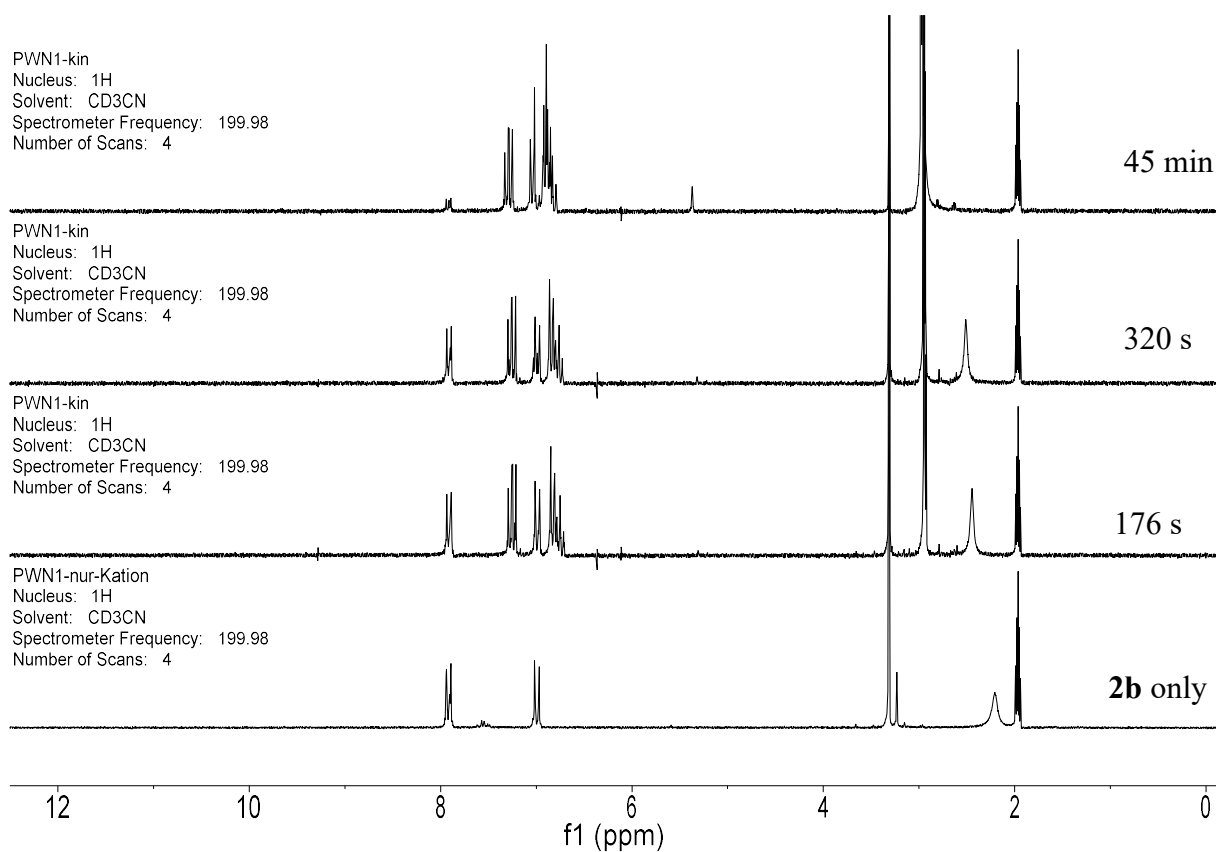
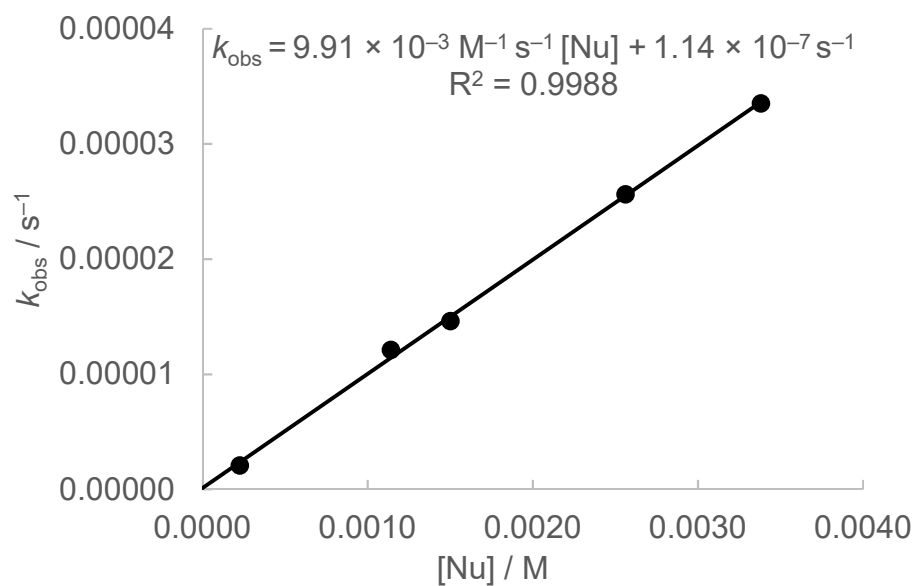


Figure S4: Time-resolved  $^1\text{H}$  NMR spectra of the reaction of *N,N*-dimethylaniline (**1a**) with  $(\text{dma})_2\text{CH}^+ \text{BF}_4^-$  (**2b**) in  $\text{CD}_3\text{CN}$  at 23 °C. The resonance at 5.36 ppm clearly proves the formation of the triarylmethane **3ab**.

**Table S7:** Reaction of **1a** with (dma)<sub>2</sub>CH<sup>+</sup> BF<sub>4</sub><sup>-</sup> (**2b**) in MeCN (20 °C, conventional UV/Vis, detection at 605 nm).

[E] <sub>0</sub> (M)	[Nu] <sub>0</sub> (M)	[Nu] <sub>0</sub> /[E] <sub>0</sub>	<i>k</i> <sub>obs</sub> (s <sup>-1</sup> )
1.14 × 10 <sup>-5</sup>	2.25 × 10 <sup>-4</sup>	19.7	2.06 × 10 <sup>-6</sup>
9.58 × 10 <sup>-6</sup>	1.14 × 10 <sup>-3</sup>	119	1.21 × 10 <sup>-5</sup>
1.16 × 10 <sup>-5</sup>	1.50 × 10 <sup>-3</sup>	129	1.46 × 10 <sup>-5</sup>
9.71 × 10 <sup>-6</sup>	2.56 × 10 <sup>-3</sup>	263	2.56 × 10 <sup>-5</sup>
1.08 × 10 <sup>-5</sup>	3.38 × 10 <sup>-3</sup>	312	3.35 × 10 <sup>-5</sup>

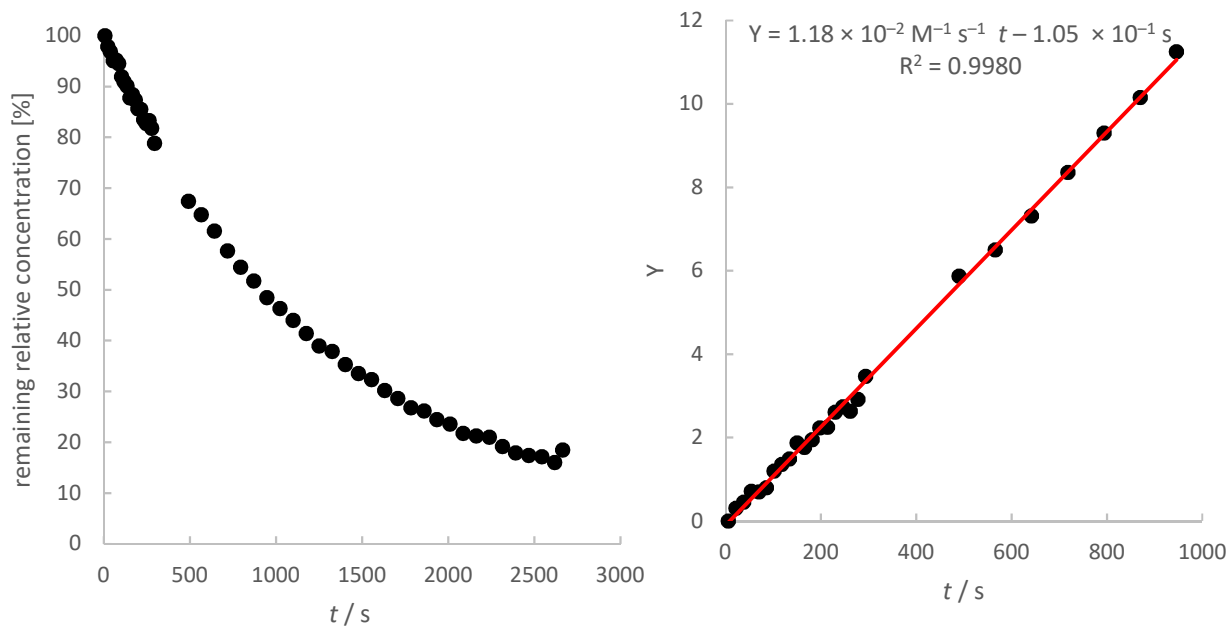
$$k_2 (20\text{ °C}) = 9.91 \times 10^{-3} \text{ M}^{-1} \text{ s}^{-1}$$



**Table S8:** Reaction of *N,N*-dimethylaniline (**1a**) with (dma)<sub>2</sub>CH<sup>+</sup> BF<sub>4</sub><sup>-</sup> (**2b**) in CD<sub>3</sub>CN (23 °C, <sup>1</sup>H NMR spectroscopy).

[E] <sub>0</sub> (M)	[Nu] <sub>0</sub> (M)	[Nu] <sub>0</sub> /[E] <sub>0</sub>	<i>k</i> <sub>2</sub> (M <sup>-1</sup> s <sup>-1</sup> )
2.32 × 10 <sup>-2</sup>	7.13 × 10 <sup>-2</sup>	3.07	1.18 × 10 <sup>-2</sup>

$$k_2 (23 \text{ }^\circ\text{C}) = 1.18 \times 10^{-2} \text{ M}^{-1} \text{ s}^{-1}$$



Decay of the relative concentration of (pyr)<sub>2</sub>CH<sup>+</sup> BF<sub>4</sub><sup>-</sup> while reacting with *N,N*-dimethylaniline (**1a**) in CD<sub>3</sub>CN at 23 °C (left). Determination of the second order rate constant by plotting time versus  $Y = ([Nu]_0 - [E]_0)^{-1} \ln([E]_0([E]_t + [Nu]_0 - [E]_0) / [Nu]_0[E]_t)$  ( $k_2 = 1.18 \times 10^{-2} \text{ M}^{-1} \text{ s}^{-1}$ , data points up to 50% conversion were used; right).

**Table S9:** Reaction of **1a** with  $(\text{mpa})_2\text{CH}^+ \text{BF}_4^-$  in MeCN (20 °C, conventional UV/Vis, detection at 612 nm).

$[\text{E}]_0$ (M)	$[\text{Nu}]_0$ (M)	$[\text{Nu}]_0/[\text{E}]_0$	$k_{\text{obs}}$ ( $\text{s}^{-1}$ )
$9.78 \times 10^{-6}$	$1.06 \times 10^{-4}$	10.8	$1.40 \times 10^{-4}$
$9.98 \times 10^{-6}$	$4.49 \times 10^{-4}$	44.9	$4.79 \times 10^{-4}$
$9.53 \times 10^{-6}$	$6.86 \times 10^{-4}$	71.9	$6.96 \times 10^{-4}$
$9.87 \times 10^{-6}$	$8.87 \times 10^{-4}$	89.9	$8.72 \times 10^{-4}$

$$k_2 (20\text{ °C}) = 9.39 \times 10^{-1} \text{ M}^{-1} \text{ s}^{-1}$$

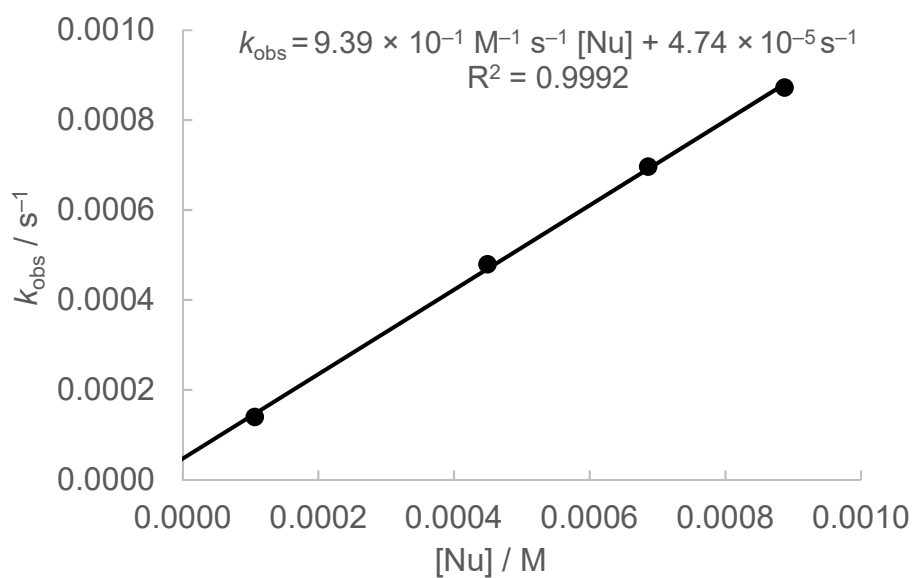


**Table S10:** Reaction of **1a** with (mor)<sub>2</sub>CH<sup>+</sup> BF<sub>4</sub><sup>-</sup> in MeCN (20 °C, conventional UV/Vis, detection at 612 nm).

[E] <sub>0</sub> (M)	[Nu] <sub>0</sub> (M)	[Nu] <sub>0</sub> /[E] <sub>0</sub>	k <sub>obs</sub> (s <sup>-1</sup> )
1.65 × 10 <sup>-5</sup>	8.33 × 10 <sup>-4</sup>	50.4	1.94 × 10 <sup>-3</sup>
1.62 × 10 <sup>-5</sup>	1.63 × 10 <sup>-3</sup>	101	3.83 × 10 <sup>-3</sup>
1.64 × 10 <sup>-5</sup>	1.98 × 10 <sup>-3</sup>	121	4.45 × 10 <sup>-3</sup>
1.59 × 10 <sup>-5</sup>	2.40 × 10 <sup>-3</sup>	151	5.12 × 10 <sup>-3</sup>
1.63 × 10 <sup>-5</sup>	3.28 × 10 <sup>-3</sup>	202	6.83 × 10 <sup>-3</sup>

$$k_2 (20\text{ }^\circ\text{C}) = 1.97 \times 10^{-1} \text{ M}^{-1} \text{ s}^{-1}$$

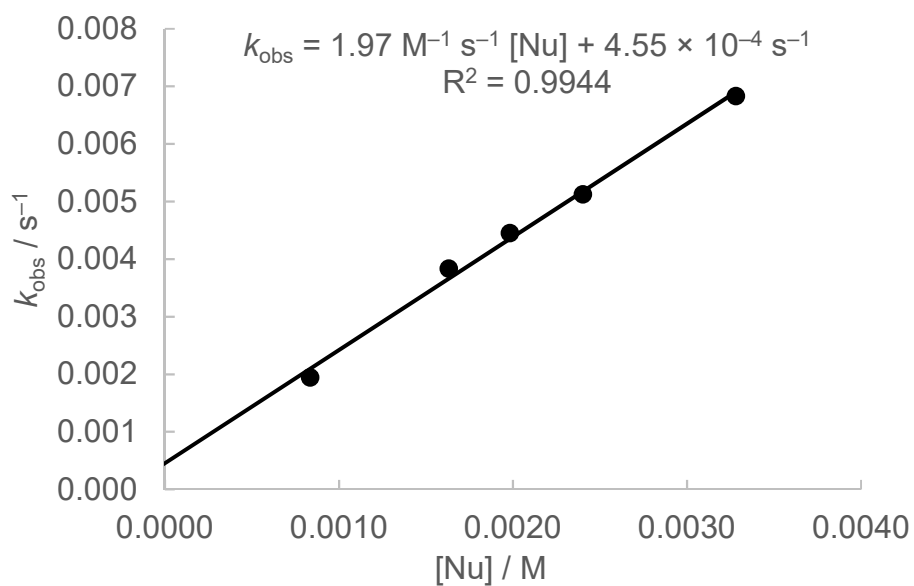


**Table S11:** Reaction of **1a** with  $(\text{dpa})_2\text{CH}^+ \text{BF}_4^-$  in MeCN (20 °C, conventional UV/Vis, detection at 644 nm).

$[\text{E}]_0$ (M)	$[\text{Nu}]_0$ (M)	$[\text{Nu}]_0/[\text{E}]_0$	$k_{\text{obs}}$ ( $\text{s}^{-1}$ )
$1.46 \times 10^{-5}$	$1.34 \times 10^{-4}$	9.18	$1.31 \times 10^{-2}$
$1.54 \times 10^{-5}$	$4.51 \times 10^{-4}$	29.3	$3.89 \times 10^{-2}$
$1.42 \times 10^{-5}$	$7.27 \times 10^{-4}$	51.4	$7.00 \times 10^{-2}$
$1.41 \times 10^{-5}$	$1.03 \times 10^{-3}$	73.4	$9.34 \times 10^{-2}$
$1.48 \times 10^{-5}$	$1.35 \times 10^{-3}$	91.7	$1.21 \times 10^{-1}$

$$k_2 (20 \text{ }^\circ\text{C}) = 89.7 \text{ M}^{-1} \text{ s}^{-1}$$

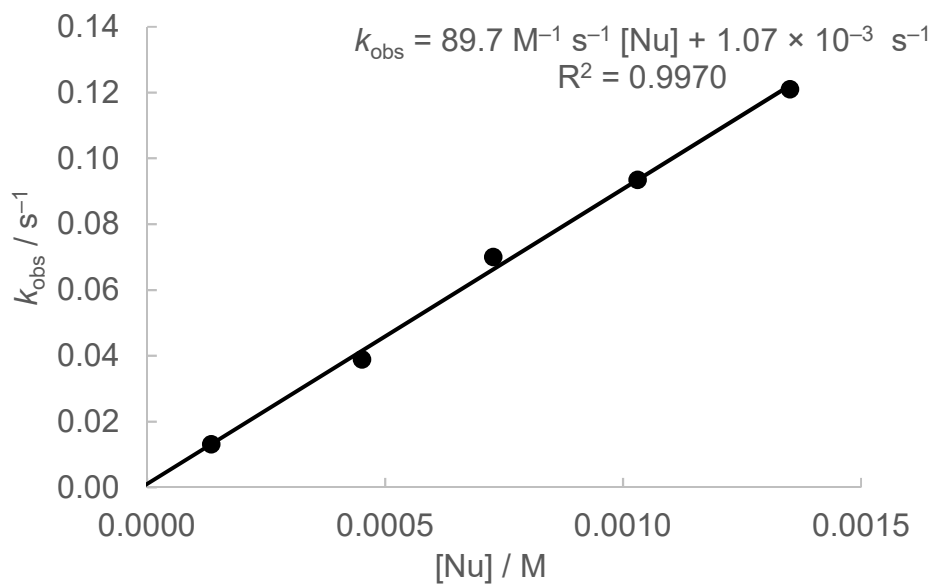


**Table S12:** Reaction of **1a** with  $(\text{mfa})_2\text{CH}^+ \text{BF}_4^-$  in MeCN (20 °C, conventional UV/Vis, detection at 586 nm).

$[\text{E}]_0$ (M)	$[\text{Nu}]_0$ (M)	$[\text{Nu}]_0/[\text{E}]_0$	$k_{\text{obs}}$ ( $\text{s}^{-1}$ )
$1.80 \times 10^{-5}$	$1.89 \times 10^{-4}$	10.5	$5.55 \times 10^{-3}$
$1.81 \times 10^{-5}$	$3.79 \times 10^{-4}$	20.9	$1.15 \times 10^{-2}$
$1.87 \times 10^{-5}$	$5.47 \times 10^{-4}$	29.3	$1.60 \times 10^{-2}$
$1.71 \times 10^{-5}$	$6.80 \times 10^{-4}$	39.8	$2.01 \times 10^{-2}$
$1.79 \times 10^{-5}$	$8.99 \times 10^{-4}$	50.2	$2.48 \times 10^{-2}$
$1.78 \times 10^{-5}$	$1.12 \times 10^{-3}$	62.9	$3.18 \times 10^{-2}$

$$k_2 (20 \text{ }^\circ\text{C}) = 27.6 \text{ M}^{-1} \text{ s}^{-1}$$

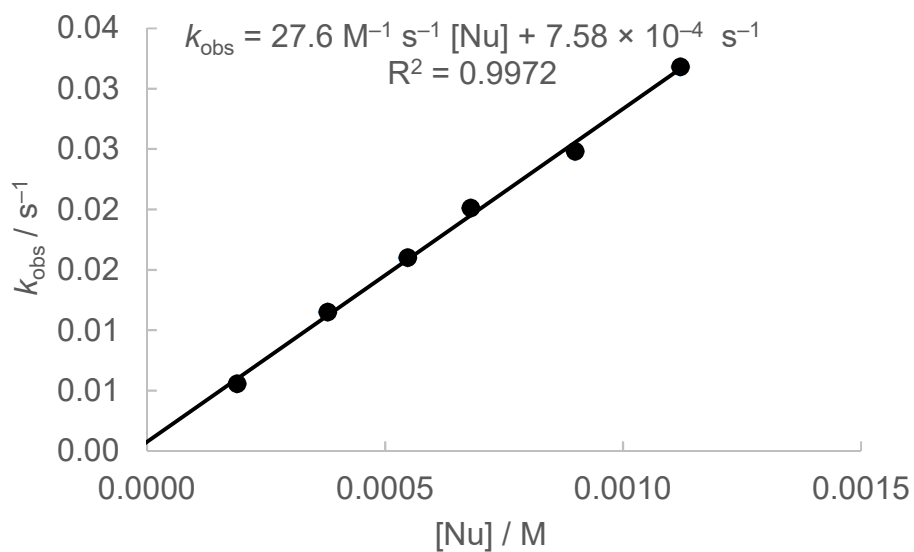
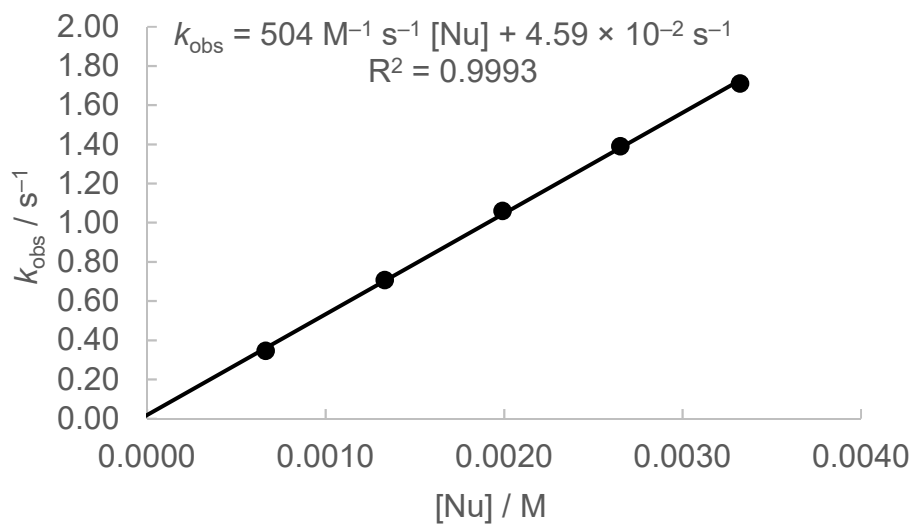


**Table S13:** Reaction of *N,N*-dimethylaniline (**1a**) with (mfa)<sub>2</sub>CH<sup>+</sup> BF<sub>4</sub><sup>-</sup> (**2f**) in MeCN (20 °C, stopped-flow, detection at 592 nm).

[E] <sub>0</sub> (M)	[Nu] <sub>0</sub> (M)	[Nu] <sub>0</sub> /[E] <sub>0</sub>	<i>k</i> <sub>obs</sub> (s <sup>-1</sup> )
2.32 × 10 <sup>-5</sup>	6.63 × 10 <sup>-4</sup>	28.6	3.46 × 10 <sup>-1</sup>
2.32 × 10 <sup>-5</sup>	1.33 × 10 <sup>-3</sup>	57.3	7.06 × 10 <sup>-1</sup>
2.32 × 10 <sup>-5</sup>	1.99 × 10 <sup>-3</sup>	85.8	1.06
2.32 × 10 <sup>-5</sup>	2.65 × 10 <sup>-3</sup>	114	1.39
2.32 × 10 <sup>-5</sup>	3.32 × 10 <sup>-3</sup>	143	1.71

$$k_2 (20\text{ }^\circ\text{C}) = 504\text{ M}^{-1}\text{ s}^{-1}$$



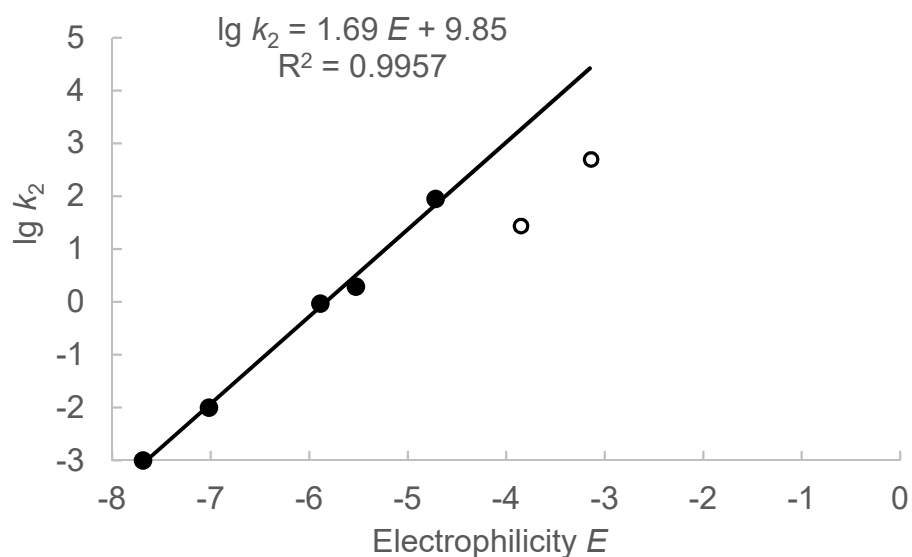
Determination of reactivity parameters  $N$  and  $s_N$  for  $N,N$ -dimethylaniline (**1a**) in MeCN at the C4 carbon atom

**Table S14:** Rate constants for the reactions of  $N,N$ -dimethylaniline (**1a**) with reference electrophiles (20 °C).

Electrophile	$E$ -Parameter	$k_2$ ( $M^{-1} s^{-1}$ )	$\lg k_2$
(pyr) <sub>2</sub> CH <sup>+</sup> ( <b>2a</b> )	-7.69	$1.01 \times 10^{-3}$	-3.00
(dma) <sub>2</sub> CH <sup>+</sup> ( <b>2b</b> )	-7.02	$9.91 \times 10^{-3}$	-2.00
(dma) <sub>2</sub> CH <sup>+</sup> ( <b>2b</b> )	-7.02	$1.20 \times 10^{-2}$	-1.92 <sup>[a, b]</sup>
(mpa) <sub>2</sub> CH <sup>+</sup> ( <b>2c</b> )	-5.89	$9.39 \times 10^{-1}$	-0.03
(mor) <sub>2</sub> CH <sup>+</sup> ( <b>2d</b> )	-5.53	1.97	0.29
(dpa) <sub>2</sub> CH <sup>+</sup> ( <b>2e</b> )	-4.72	89.7	1.95
(mfa) <sub>2</sub> CH <sup>+</sup> ( <b>2f</b> )	-3.85	27.6	1.44 <sup>[a, c]</sup>
(pfa) <sub>2</sub> CH <sup>+</sup> ( <b>2g</b> )	-3.14	504	2.70 <sup>[a, d]</sup>

[a] Values not considered for the depicted linear correlation. [b] Measured at 23 °C.

$$N = 5.83, s_N = 1.69$$



## 5.2 Reactions of *N,N*-dimethylaniline (1a) with benzhydrylium ions 2 at the nitrogen in CH<sub>3</sub>CN at 20 °C

**Table S15:** Reaction of *N,N*-dimethylaniline (1a) with (dma)<sub>2</sub>CH<sup>+</sup> BF<sub>4</sub><sup>-</sup> (2b) in MeCN (20 °C, stopped-flow, detection at 606 nm).

[E] <sub>0</sub> (M)	[Nu] <sub>0</sub> (M)	[Nu] <sub>0</sub> /[E] <sub>0</sub>	<i>k</i> <sub>obs</sub> (s <sup>-1</sup> )
1.14 × 10 <sup>-5</sup>	3.21 × 10 <sup>-4</sup>	28.2	1.00 × 10 <sup>-2</sup>
1.16 × 10 <sup>-5</sup>	1.67 × 10 <sup>-3</sup>	144	2.28 × 10 <sup>-2</sup>
1.09 × 10 <sup>-5</sup>	3.12 × 10 <sup>-3</sup>	286	4.29 × 10 <sup>-2</sup>

$$k_2 (20\text{ °C}) = 11.8\text{ M}^{-1}\text{ s}^{-1}$$

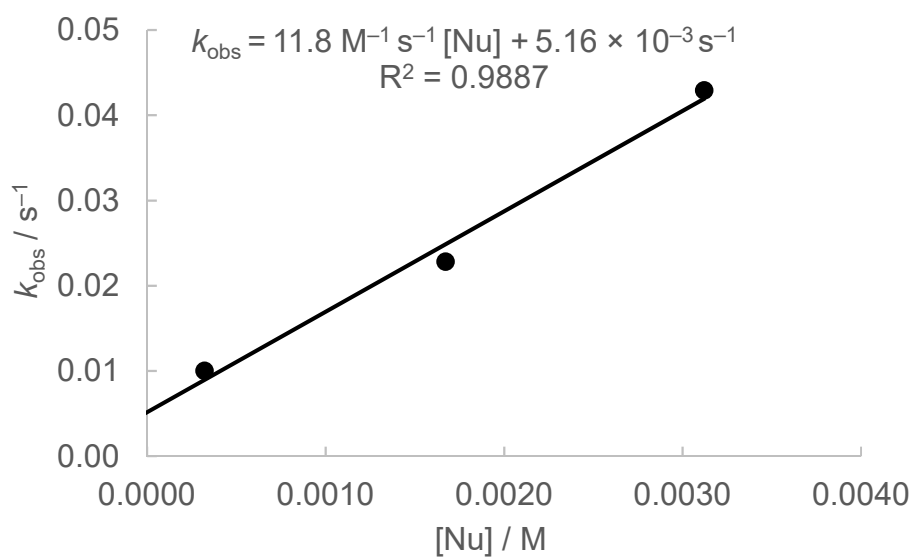


**Table S16:** Reaction of *N,N*-dimethylaniline (**1a**) with (dpa)<sub>2</sub>CH<sup>+</sup> BF<sub>4</sub><sup>-</sup> (**2e**) in MeCN (20 °C, stopped-flow, detection at 644 nm).

[E] <sub>0</sub> (M)	[Nu] <sub>0</sub> (M)	[Nu] <sub>0</sub> /[E] <sub>0</sub>	<i>k</i> <sub>obs</sub> (s <sup>-1</sup> )
5.10 × 10 <sup>-5</sup>	1.47 × 10 <sup>-3</sup>	28.8	8.94
5.10 × 10 <sup>-5</sup>	1.96 × 10 <sup>-3</sup>	38.4	9.61
5.10 × 10 <sup>-5</sup>	2.45 × 10 <sup>-3</sup>	48.0	10.5
5.10 × 10 <sup>-5</sup>	2.94 × 10 <sup>-3</sup>	57.6	11.1
5.10 × 10 <sup>-5</sup>	3.42 × 10 <sup>-3</sup>	67.1	11.9
5.10 × 10 <sup>-5</sup>	3.91 × 10 <sup>-3</sup>	76.7	12.6

$$k_2 (20\text{ }^\circ\text{C}) = 1.50 \times 10^3 \text{ M}^{-1} \text{ s}^{-1}$$

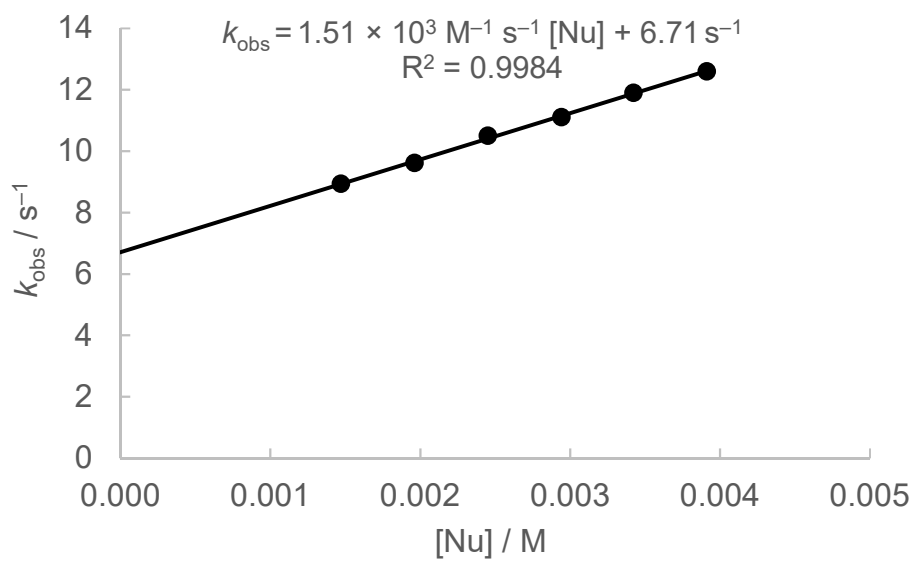
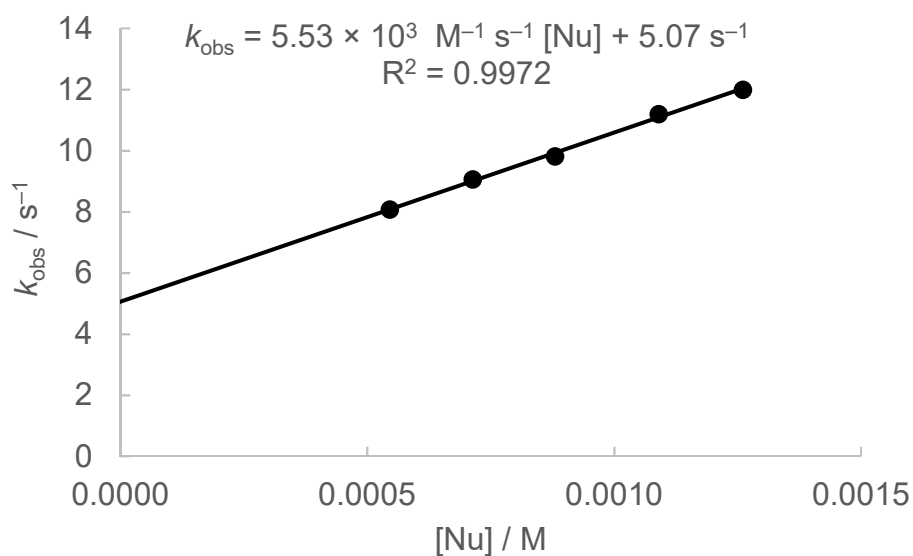


**Table S17:** Reaction of *N,N*-dimethylaniline (**1a**) with (mfa)<sub>2</sub>CH<sup>+</sup> BF<sub>4</sub><sup>-</sup> (**2f**) in MeCN (20 °C, stopped-flow, detection at 586 nm).

[E] <sub>0</sub> (M)	[Nu] <sub>0</sub> (M)	[Nu] <sub>0</sub> /[E] <sub>0</sub>	<i>k</i> <sub>obs</sub> (s <sup>-1</sup> )	<i>A</i> <sub>0</sub>	<i>A</i> <sub>equil.</sub>	<i>A</i> / <i>A</i> <sub>0</sub>
1.80 × 10 <sup>-5</sup>	5.45 × 10 <sup>-4</sup>	30.3	8.08	0.82	0.63	1.31
1.80 × 10 <sup>-5</sup>	7.13 × 10 <sup>-4</sup>	39.6	9.06	0.86	0.56	1.55
1.80 × 10 <sup>-5</sup>	8.80 × 10 <sup>-4</sup>	48.9	9.82	0.81	0.47	1.73
1.80 × 10 <sup>-5</sup>	1.09 × 10 <sup>-3</sup>	60.6	11.2	0.76	0.40	1.92
1.80 × 10 <sup>-5</sup>	1.26 × 10 <sup>-3</sup>	70.0	12.0	0.70	0.32	2.18

$$k_2 (20\text{ }^\circ\text{C}) = 5.53 \times 10^3 \text{ M}^{-1} \text{ s}^{-1}$$



$$K (20\text{ }^\circ\text{C}) = 318 \text{ M}^{-1}$$

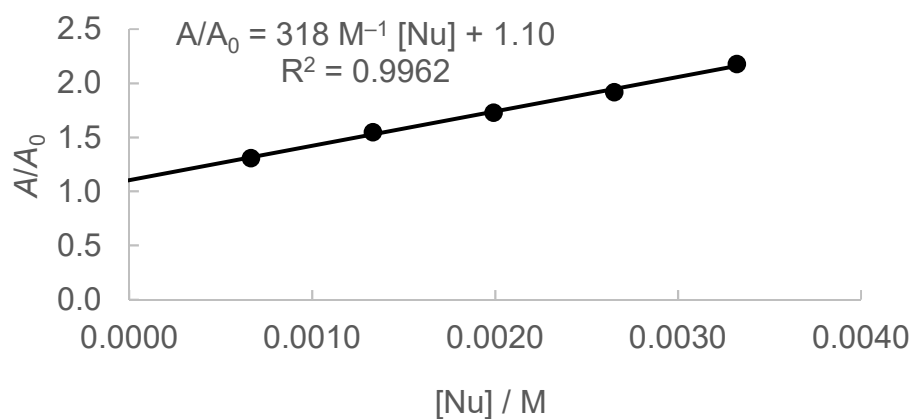
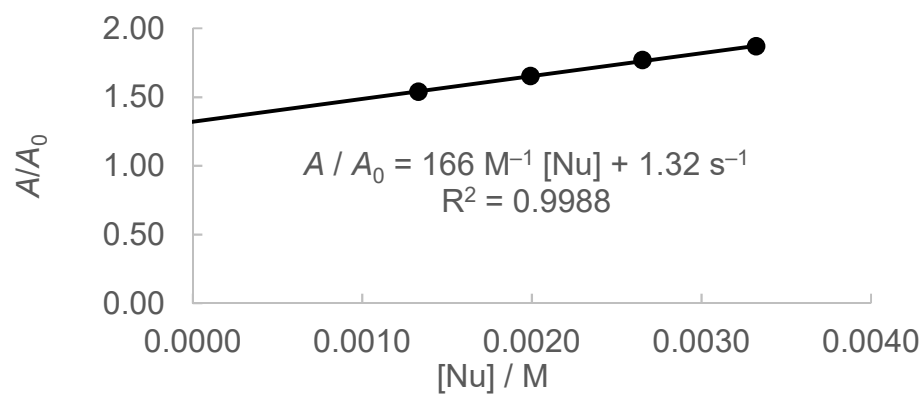


**Table S18:** Reaction of *N,N*-dimethylaniline (**1a**) with (pfa)<sub>2</sub>CH<sup>+</sup> BF<sub>4</sub><sup>-</sup> (**2g**) in MeCN (20 °C, stopped-flow, detection at 592 nm).

[E] <sub>0</sub> (M)	[Nu] <sub>0</sub> (M)	[Nu] <sub>0</sub> /[E] <sub>0</sub>	<i>k</i> <sub>obs</sub> (s <sup>-1</sup> ) <sup>[a]</sup>	<i>A</i> <sub>0</sub>	<i>A</i> <sub>equil.</sub>	<i>A</i> / <i>A</i> <sub>0</sub>
2.32 × 10 <sup>-5</sup>	1.33 × 10 <sup>-4</sup>	57.3	n.d.	1.29	0.84	1.54
2.32 × 10 <sup>-5</sup>	1.99 × 10 <sup>-4</sup>	85.8	n.d.	1.38	0.84	1.65
2.32 × 10 <sup>-5</sup>	2.65 × 10 <sup>-3</sup>	114	n.d.	1.36	0.77	1.77
2.32 × 10 <sup>-5</sup>	3.32 × 10 <sup>-3</sup>	143	n.d.	1.31	0.70	1.87

[a] Too little datapoints were observed to evaluate a *k*<sub>obs</sub>.

$$K (20\text{ °C}) = 166\text{ M}^{-1}$$

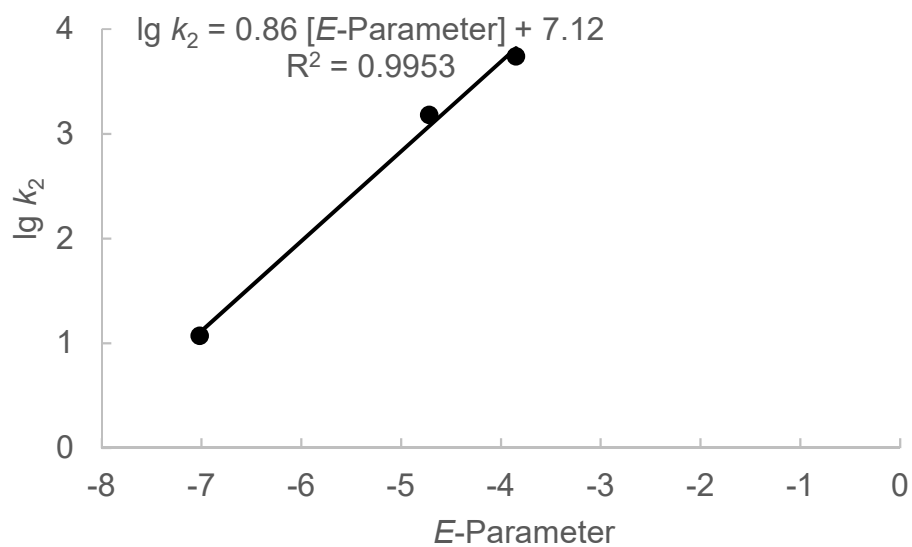


Determination of reactivity parameters  $N$  and  $s_N$  for  $N,N$ -dimethylaniline (**1a**) in MeCN for the reaction at the nitrogen atom

**Table S19:** Rate constants for the reactions of **1a** with reference electrophiles (20 °C).

Electrophile	$E$ -Parameter	$k_2$ ( $M^{-1} s^{-1}$ )	$\lg k_2$
(dma) <sub>2</sub> CH <sup>+</sup> ( <b>2b</b> )	-7.02	11.8	1.07
(dpa) <sub>2</sub> CH <sup>+</sup> ( <b>2e</b> )	-4.72	$1.51 \times 10^3$	3.18
(mfa) <sub>2</sub> CH <sup>+</sup> ( <b>2f</b> )	-3.85	$5.53 \times 10^3$	3.74

$N = 8.28$ ,  $s_N = 0.86$

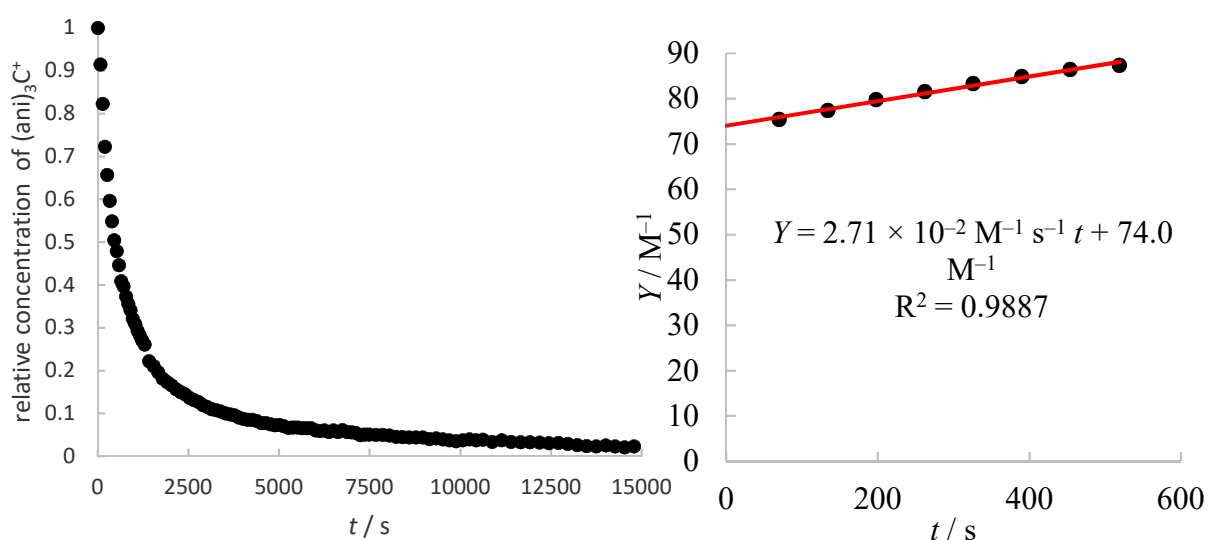


## 6. Reactions of *N,N*-dimethylaniline (**1a**) with tritylium ions in acetonitrile at 20 °C

**Table S20:** Reaction of *N,N*-dimethylaniline (**1a**) with  $(\text{ani})_3\text{CH}^+ \text{BF}_4^-$  in  $\text{CD}_3\text{CN}$  (20 °C,  $^1\text{H}$  NMR spectroscopy). The rest ani = *p*-MeOC<sub>6</sub>H<sub>4</sub>.

$[\text{E}]_0$ (M)	$[\text{Nu}]_0$ (M)	$[\text{Nu}]_0/[\text{E}]_0$	$k_2$ ( $\text{M}^{-1} \text{s}^{-1}$ )
$4.93 \times 10^{-2}$	$1.03 \times 10^{-1}$	2.09	$2.71 \times 10^{-2}$

$$k_2 (20 \text{ °C}) = 2.71 \times 10^{-2} \text{ M}^{-1} \text{ s}^{-1}$$

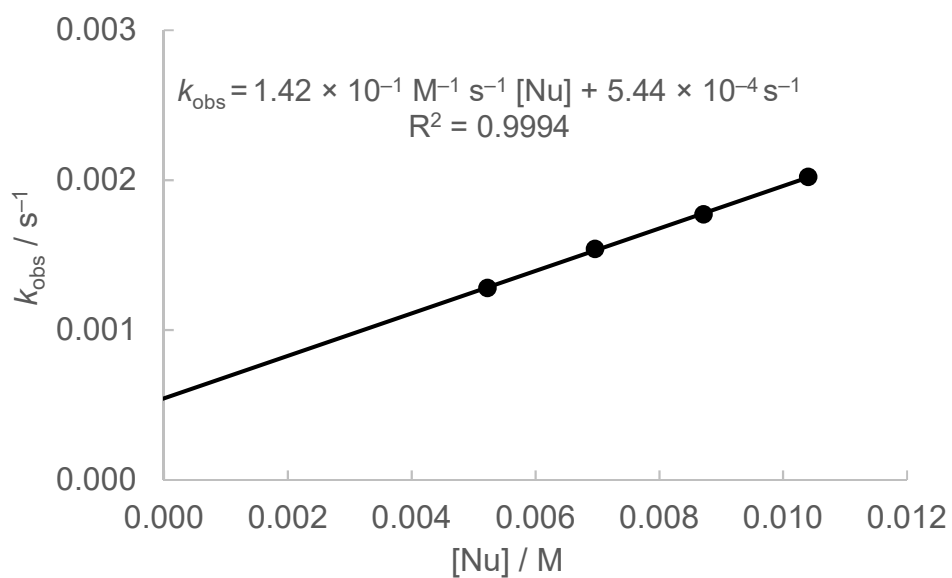


Decay of the relative concentration of  $(\text{ani})_3\text{C}^+ \text{BF}_4^-$  while reacting with *N,N*-dimethylaniline (**1a**) in  $\text{CD}_3\text{CN}$  at 20 °C (left). Determination of the second order rate constant by plotting time versus  $Y = ([\text{Nu}]_0 - [\text{E}]_0)^{-1} \ln([\text{E}]_0([\text{E}]_t + [\text{Nu}]_0 - [\text{E}]_0) / [\text{Nu}]_0[\text{E}]_t)$  ( $k_2 = 2.71 \times 10^{-2} \text{ M}^{-1} \text{ s}^{-1}$ , data points up to 50% conversion were used; right).

**Table S21:** Reaction of *N,N*-dimethylaniline (**1a**) with (ani)<sub>2</sub>PhC<sup>+</sup> BF<sub>4</sub><sup>-</sup> in acetonitrile (20 °C, stopped flow, detection at 497 nm). The rest ani = *p*-MeOC<sub>6</sub>H<sub>4</sub>.

[E] <sub>0</sub> (M)	[Nu] <sub>0</sub> (M)	[Nu] <sub>0</sub> /[E] <sub>0</sub>	<i>k</i> <sub>obs</sub> (s <sup>-1</sup> )
2.72 × 10 <sup>-5</sup>	5.22 × 10 <sup>-3</sup>	192	1.28 × 10 <sup>-3</sup>
2.72 × 10 <sup>-5</sup>	6.96 × 10 <sup>-3</sup>	256	1.54 × 10 <sup>-3</sup>
2.72 × 10 <sup>-5</sup>	8.71 × 10 <sup>-3</sup>	320	1.77 × 10 <sup>-3</sup>
2.72 × 10 <sup>-5</sup>	1.04 × 10 <sup>-2</sup>	382	2.02 × 10 <sup>-3</sup>

$$k_2 (20\text{ °C}) = 1.42 \times 10^{-1} \text{ M}^{-1} \text{ s}^{-1}$$



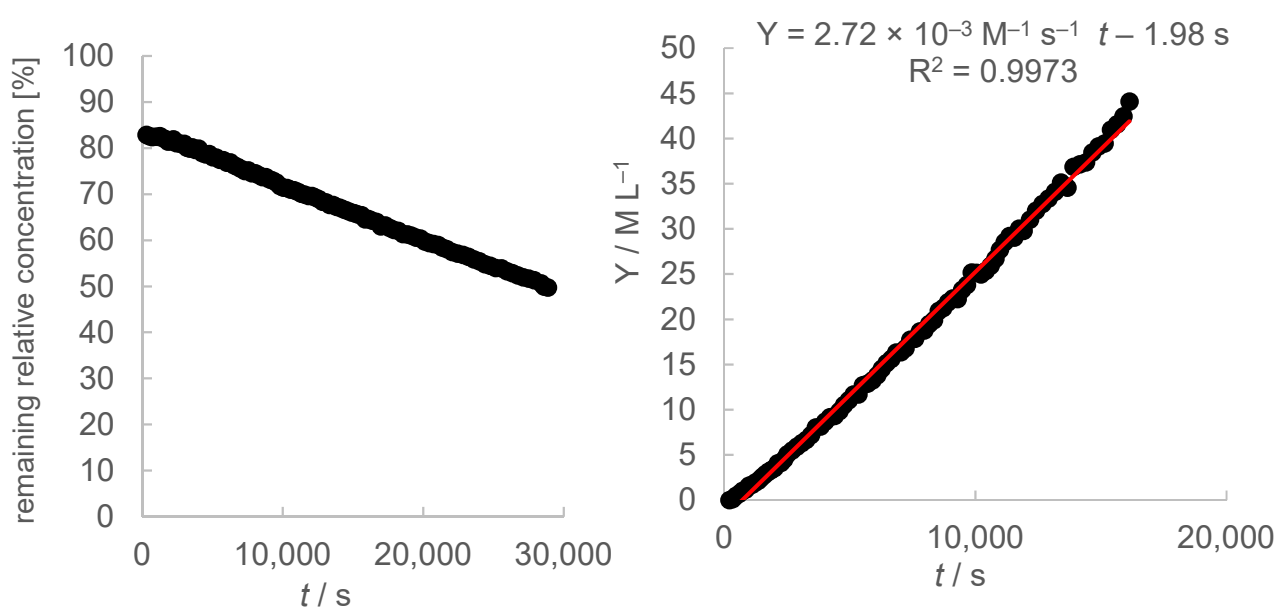
## 7. Reactions of *N,N*-dimethylaniline (1a) with benzhydrylium ions 2 in dichloromethane at 20 °C.

### 7.1 Reactions of *N,N*-dimethylaniline (1a) with benzhydrylium ions 2 at the C4 carbon in dichloromethane at 20 °C

**Table S22:** Reaction of *N,N*-dimethylaniline (**1a**) with (pyr)<sub>2</sub>CH<sup>+</sup> BF<sub>4</sub><sup>-</sup> (**2a**) in CD<sub>2</sub>Cl<sub>2</sub> (20 °C, <sup>1</sup>H NMR spectroscopy).

[E] <sub>0</sub> (M)	[Nu] <sub>0</sub> (M)	[Nu] <sub>0</sub> /[E] <sub>0</sub>	<i>k</i> <sub>2</sub> (M <sup>-1</sup> s <sup>-1</sup> )
2.04 × 10 <sup>-2</sup>	4.17 × 10 <sup>-2</sup>	2.04	2.72 × 10 <sup>-3</sup>

$$k_2 (20\text{ °C}) = 2.72 \times 10^{-3} \text{ M}^{-1} \text{ s}^{-1}$$



Decay of the relative concentration of (pyr)<sub>2</sub>CH<sup>+</sup> BF<sub>4</sub><sup>-</sup> while reacting with *N,N*-dimethylaniline (**1a**) in CD<sub>2</sub>Cl<sub>2</sub> at 20 °C (left). Determination of the second order rate constant by plotting time versus  $Y = ([\text{Nu}]_0 - [\text{E}]_0)^{-1} \ln([\text{E}]_0([\text{E}]_t + [\text{Nu}]_0 - [\text{E}]_0) / [\text{Nu}]_0[\text{E}]_t)$  ( $k_2 = 2.72 \times 10^{-3} \text{ M}^{-1} \text{ s}^{-1}$ , data points up to 50% conversion were used; right).

**Table S23:** Reaction of *N,N*-dimethylaniline (**1a**) with (mpa)<sub>2</sub>CH<sup>+</sup> BF<sub>4</sub><sup>-</sup> (**2c**) in dichloromethane (20 °C, conventional UV/Vis, detection at 622 nm).

[E] <sub>0</sub> (M)	[Nu] <sub>0</sub> (M)	[Nu] <sub>0</sub> /[E] <sub>0</sub>	<i>k</i> <sub>obs</sub> (s <sup>-1</sup> )	[Nu] <sub>0</sub> <sup>-1</sup> (M <sup>-1</sup> )	[Nu] <sub>0</sub> <i>k</i> <sub>obs</sub> <sup>-1</sup> (M s)
1.75 × 10 <sup>-5</sup>	4.39 × 10 <sup>-3</sup>	251	5.36 × 10 <sup>-4</sup>	228	8.19
1.81 × 10 <sup>-5</sup>	3.77 × 10 <sup>-3</sup>	208	4.35 × 10 <sup>-4</sup>	265	8.67
1.78 × 10 <sup>-5</sup>	1.60 × 10 <sup>-3</sup>	89.9	1.02 × 10 <sup>-4</sup>	625	15.7
1.79 × 10 <sup>-5</sup>	1.08 × 10 <sup>-3</sup>	60.3	5.70 × 10 <sup>-5</sup>	926	18.9

$$k_2 (20\text{ °C}) = 2.11 \times 10^{-1} \text{ M}^{-1} \text{ s}^{-1}$$

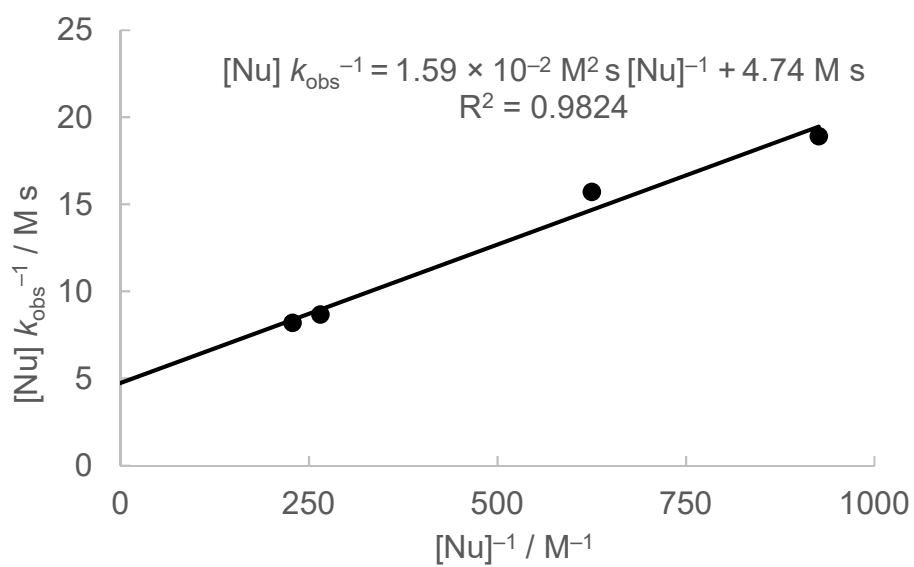


**Table S24:** Reaction of *N,N*-dimethylaniline (**1a**) with (mor)<sub>2</sub>CH<sup>+</sup> BF<sub>4</sub><sup>-</sup> (**2d**) in dichloromethane (20 °C, conventional UV/Vis, detection at 620 nm).

[E] <sub>0</sub> (M)	[Nu] <sub>0</sub> (M)	[Nu] <sub>0</sub> /[E] <sub>0</sub>	<i>k</i> <sub>obs</sub> (s <sup>-1</sup> )	[Nu] <sub>0</sub> <sup>-1</sup> (M <sup>-1</sup> )	[Nu] <sub>0</sub> <i>k</i> <sub>obs</sub> <sup>-1</sup> (M s)
9.98 × 10 <sup>-6</sup>	2.01 × 10 <sup>-3</sup>	201	2.83 × 10 <sup>-4</sup>	498	7.10
9.83 × 10 <sup>-6</sup>	1.54 × 10 <sup>-3</sup>	157	2.09 × 10 <sup>-4</sup>	649	7.37
9.34 × 10 <sup>-6</sup>	1.04 × 10 <sup>-3</sup>	111	9.94 × 10 <sup>-5</sup>	962	10.5
1.02 × 10 <sup>-5</sup>	5.19 × 10 <sup>-4</sup>	50.9	2.94 × 10 <sup>-5</sup>	1.93 × 10 <sup>3</sup>	17.7

$$k_2 (20\text{ °C}) = 3.40 \times 10^{-1} \text{ M}^{-1} \text{ s}^{-1}$$

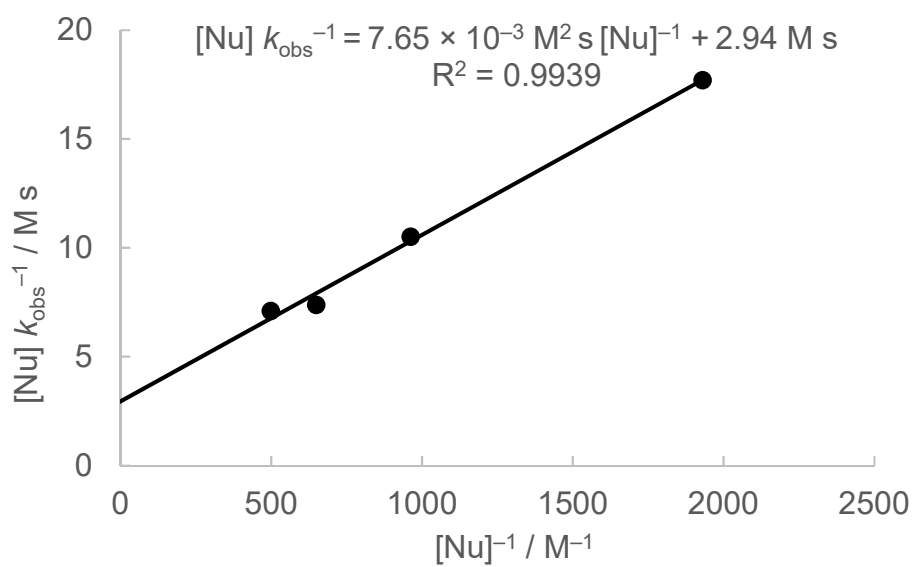


**Table S25:** Reaction of *N,N*-dimethylaniline (**1a**) with (dpa)<sub>2</sub>CH<sup>+</sup> BF<sub>4</sub><sup>-</sup> (**2e**) in dichloromethane (20 °C, conventional UV/Vis, detection at 672 nm).

[E] <sub>0</sub> (M)	[Nu] <sub>0</sub> (M)	[Nu] <sub>0</sub> /[E] <sub>0</sub>	<i>k</i> <sub>obs</sub> (s <sup>-1</sup> )	[Nu] <sub>0</sub> <sup>-1</sup> (M <sup>-1</sup> )	[Nu] <sub>0</sub> <i>k</i> <sub>obs</sub> <sup>-1</sup> (M s)
3.12 × 10 <sup>-5</sup>	3.29 × 10 <sup>-4</sup>	10.5	3.85 × 10 <sup>-4</sup>	3.04 × 10 <sup>3</sup>	8.55 × 10 <sup>-1</sup>
2.96 × 10 <sup>-5</sup>	1.13 × 10 <sup>-3</sup>	38.2	2.27 × 10 <sup>-3</sup>	885	4.98 × 10 <sup>-1</sup>
2.84 × 10 <sup>-5</sup>	1.42 × 10 <sup>-3</sup>	50.0	3.15 × 10 <sup>-3</sup>	704	4.51 × 10 <sup>-1</sup>
3.16 × 10 <sup>-5</sup>	1.91 × 10 <sup>-3</sup>	60.4	4.54 × 10 <sup>-3</sup>	524	4.21 × 10 <sup>-1</sup>
3.13 × 10 <sup>-5</sup>	2.10 × 10 <sup>-3</sup>	67.1	5.06 × 10 <sup>-3</sup>	476	4.15 × 10 <sup>-1</sup>

$$k_2 (20\text{ }^\circ\text{C}) = 2.99\text{ M}^{-1}\text{ s}^{-1}$$

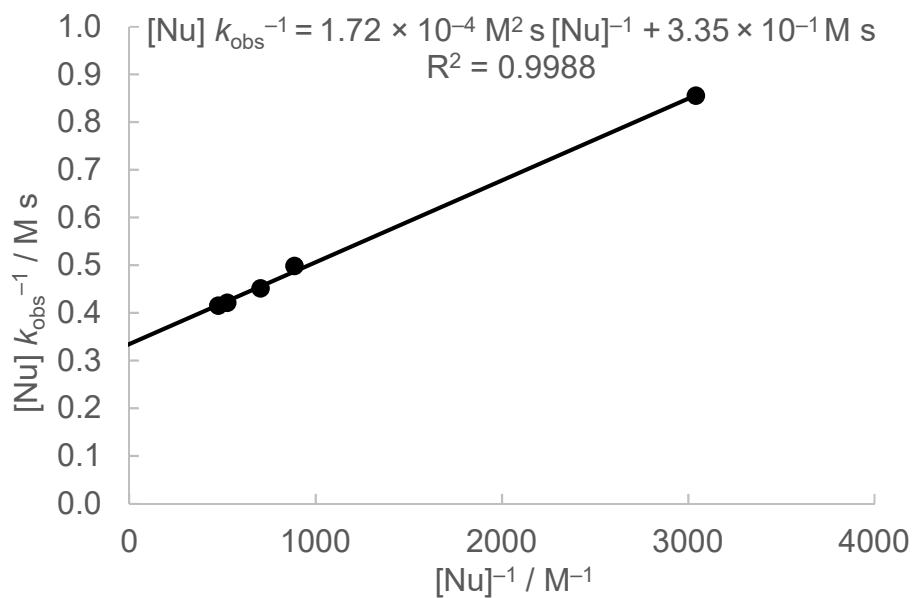
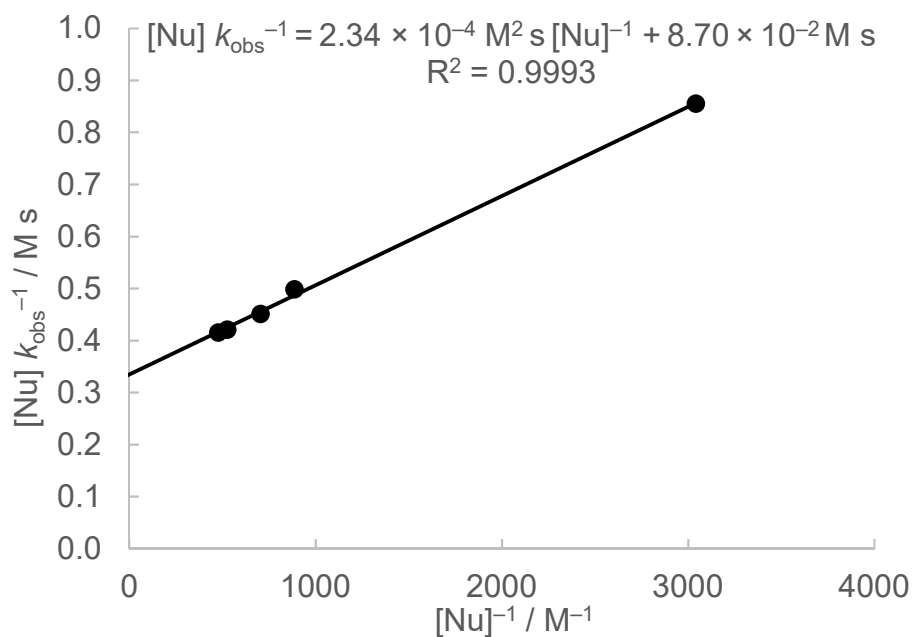


**Table S26:** Reaction of **1a** with  $(\text{mfa})_2\text{CH}^+ \text{BF}_4^-$  (**2f**) in dichloromethane (20 °C, conventional UV/Vis, detection at 593 nm).

$[\text{E}]_0$ (M)	$[\text{Nu}]_0$ (M)	$[\text{Nu}]_0/[\text{E}]_0$	$k_{\text{obs}}$ ( $\text{s}^{-1}$ )	$[\text{Nu}]_0^{-1}$ ( $\text{M}^{-1}$ )	$[\text{Nu}]_0 k_{\text{obs}}^{-1}$ (M s)
$1.79 \times 10^{-5}$	$3.53 \times 10^{-4}$	19.7	$4.72 \times 10^{-4}$	$2.83 \times 10^3$	$7.48 \times 10^{-1}$
$1.80 \times 10^{-5}$	$5.57 \times 10^{-4}$	30.9	$1.11 \times 10^{-3}$	$1.80 \times 10^3$	$5.02 \times 10^{-1}$
$1.80 \times 10^{-5}$	$7.10 \times 10^{-4}$	39.4	$1.68 \times 10^{-3}$	$1.41 \times 10^3$	$4.23 \times 10^{-1}$
$1.75 \times 10^{-5}$	$9.02 \times 10^{-4}$	51.5	$2.56 \times 10^{-3}$	$1.11 \times 10^3$	$3.52 \times 10^{-1}$
$1.74 \times 10^{-5}$	$1.42 \times 10^{-3}$	81.6	$5.68 \times 10^{-3}$	704	$2.50 \times 10^{-1}$
$1.74 \times 10^{-5}$	$1.77 \times 10^{-3}$	102	$8.22 \times 10^{-3}$	565	$2.15 \times 10^{-1}$

$$k_2 (20 \text{ }^\circ\text{C}) = 11.5 \text{ M}^{-1} \text{ s}^{-1}$$

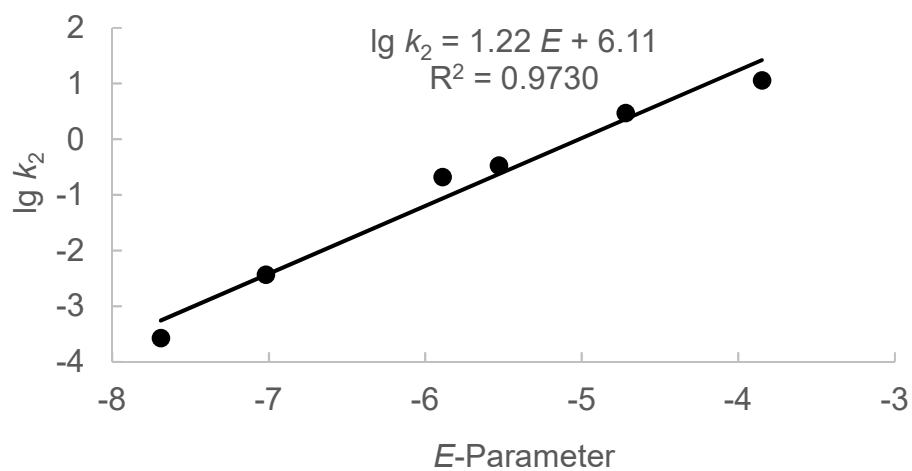


Determination of reactivity parameters  $N$  and  $s_N$  for  $N,N$ -dimethylaniline (**1a**) in dichloromethane at the C4 carbon atom

**Table S27:** Rate constants for the reactions of  $N,N$ -dimethylaniline (**1a**) with reference electrophiles (20 °C).

Electrophile	$E$ -Parameter	$k_2$ ( $M^{-1} s^{-1}$ )	$\lg k_2$
(pyr) <sub>2</sub> CH <sup>+</sup> ( <b>2a</b> )	-7.69	$2.72 \times 10^{-4}$	-3.57
(dma) <sub>2</sub> CH <sup>+</sup> ( <b>2b</b> )	-7.02	$3.70 \times 10^{-3}$	-2.43
(mpa) <sub>2</sub> CH <sup>+</sup> ( <b>2c</b> )	-5.89	$2.11 \times 10^{-1}$	$-6.76 \times 10^{-1}$
(mor) <sub>2</sub> CH <sup>+</sup> ( <b>2d</b> )	-5.53	$3.40 \times 10^{-1}$	$-4.69 \times 10^{-1}$
(dpa) <sub>2</sub> CH <sup>+</sup> ( <b>2e</b> )	-4.72	2.99	$4.76 \times 10^{-1}$
(mfa) <sub>2</sub> CH <sup>+</sup> ( <b>2f</b> )	-3.85	11.5	1.06

$N = 5.01, s_N = 1.22$

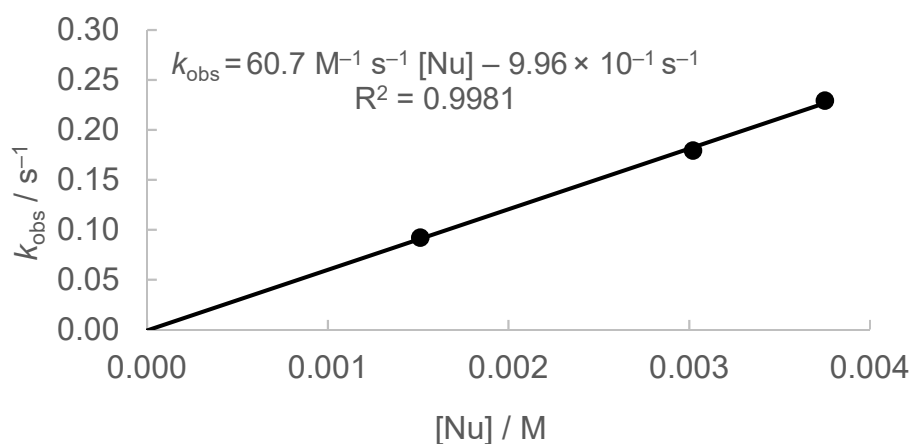


## 7.2 Reactions of *N,N*-dimethylaniline (1a) with benzhydrylium ions 2 at the nitrogen in dichloromethane at 20 °C

**Table S28:** Reaction of 1a with (mpa)<sub>2</sub>CH<sup>+</sup> BF<sub>4</sub><sup>-</sup> (2f) in dichloromethane (20 °C, stopped-flow, detection at 622 nm).

[E] <sub>0</sub> (M)	[Nu] <sub>0</sub> (M)	[Nu] <sub>0</sub> /[E] <sub>0</sub>	<i>k</i> <sub>obs</sub> (s <sup>-1</sup> )
1.50 × 10 <sup>-5</sup>	1.51 × 10 <sup>-3</sup>	101	9.18 × 10 <sup>-2</sup>
1.50 × 10 <sup>-5</sup>	3.02 × 10 <sup>-3</sup>	201	1.79 × 10 <sup>-1</sup>
1.50 × 10 <sup>-5</sup>	3.75 × 10 <sup>-3</sup>	250	2.29 × 10 <sup>-1</sup>

$$k_2 (20\text{ °C}) = 60.7\text{ M}^{-1}\text{ s}^{-1}$$

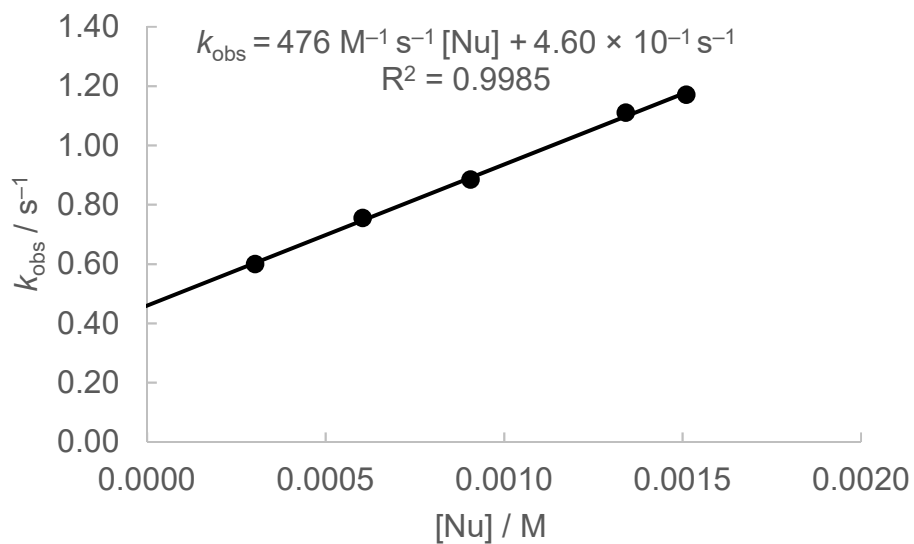


[a] The negative intercept with the abscissa is due to slow/incomplete mixing of the reactants in comparison with the fast reaction.

**Table S29:** Reaction of **1a** with  $(\text{mfa})_2\text{CH}^+ \text{BF}_4^-$  (**2f**) in dichloromethane (20 °C, stopped-flow, detection at 593 nm).

$[\text{E}]_0$ (M)	$[\text{Nu}]_0$ (M)	$[\text{Nu}]_0/[\text{E}]_0$	$k_{\text{obs}}$ ( $\text{s}^{-1}$ )
$1.50 \times 10^{-5}$	$3.02 \times 10^{-4}$	20.1	$6.00 \times 10^{-1}$
$1.50 \times 10^{-5}$	$6.03 \times 10^{-4}$	40.2	$7.55 \times 10^{-1}$
$1.50 \times 10^{-5}$	$9.05 \times 10^{-4}$	60.3	$8.84 \times 10^{-1}$
$1.50 \times 10^{-5}$	$1.34 \times 10^{-3}$	89.3	1.11
$1.50 \times 10^{-5}$	$1.51 \times 10^{-3}$	101	1.17

$$k_2 (20 \text{ }^\circ\text{C}) = 476 \text{ M}^{-1} \text{ s}^{-1}$$

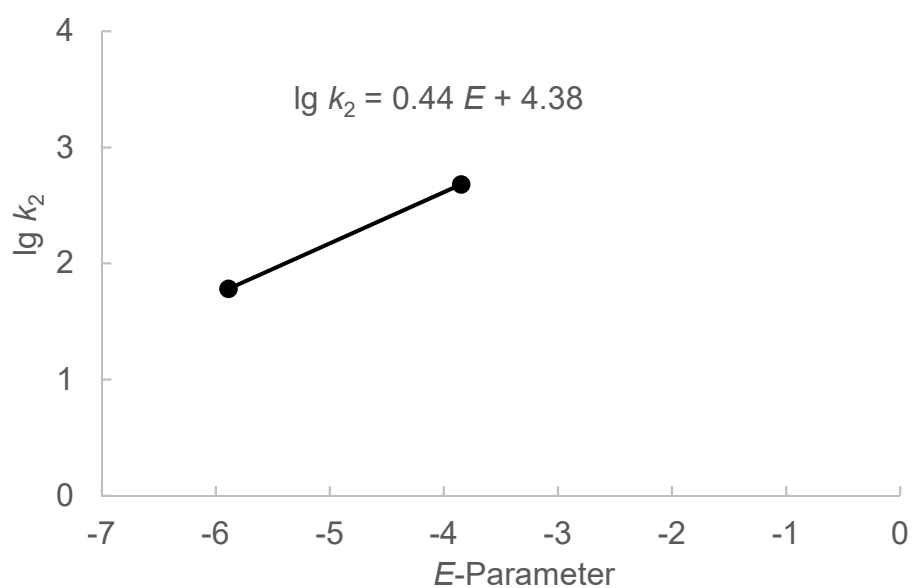


Determination of reactivity parameters  $N$  and  $s_N$  for  $N,N$ -dimethylaniline (**1a**) in dichloromethane at the nitrogen atom

**Table S30:** Rate constants for the reactions of **1a** with reference electrophiles (20 °C).

Electrophile	$E$ -Parameter	$k_2$ ( $M^{-1} s^{-1}$ )	$\lg k_2$
(mpa) <sub>2</sub> CH <sup>+</sup> ( <b>2c</b> )	-5.89	60.7	1.78
(mfa) <sub>2</sub> CH <sup>+</sup> ( <b>2f</b> )	-3.85	476	2.68

$N = 9.95, s_N = 0.44$



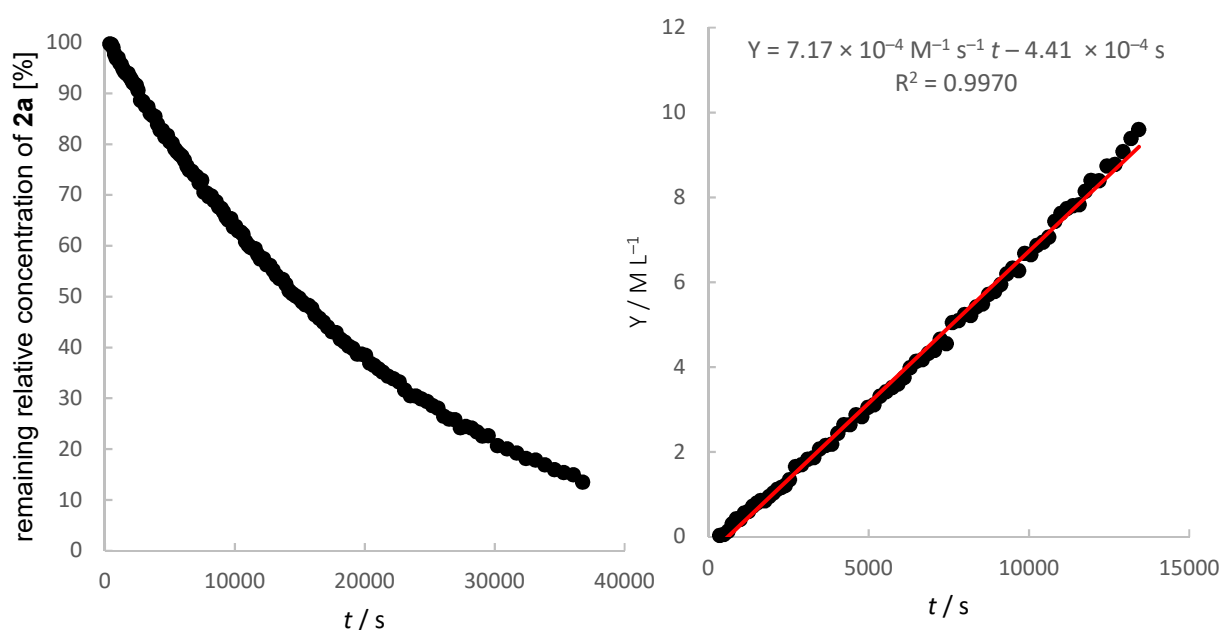
## 8. Reactions of *N,N*-diethylaniline (**1b**) with benzhydrylium ions **2** in acetonitrile at 20 °C

### 8.1 Reactions of *N,N*-diethylaniline (**1b**) with benzhydrylium ions **2** at the C4 carbon in acetonitrile at 20 °C

**Table S31:** Reaction of *N,N*-diethylaniline (**1b**) with (pyr)<sub>2</sub>CH<sup>+</sup> BF<sub>4</sub><sup>-</sup> (**2a**) in CD<sub>3</sub>CN (20 °C, <sup>1</sup>H NMR spectroscopy).

[E] <sub>0</sub> (M)	[Nu] <sub>0</sub> (M)	[Nu] <sub>0</sub> /[E] <sub>0</sub>	<i>k</i> <sub>2</sub> (M <sup>-1</sup> s <sup>-1</sup> )
3.65 × 10 <sup>-2</sup>	7.48 × 10 <sup>-2</sup>	2.05	7.17 × 10 <sup>-4</sup>

$$k_2 (20\text{ °C}) = 7.17 \times 10^{-4} \text{ M}^{-1} \text{ s}^{-1}$$



Decay of the relative concentration of (pyr)<sub>2</sub>CH<sup>+</sup> BF<sub>4</sub><sup>-</sup> (**2a**) while reacting with *N,N*-diethylaniline (**1b**) in CD<sub>3</sub>CN at 20 °C (left). Determination of the second order rate constant by plotting time versus  $Y = ([\text{Nu}]_0 - [\text{E}]_0)^{-1} \ln([\text{E}]_0([\text{E}]_t + [\text{Nu}]_0 - [\text{E}]_0) / [\text{Nu}]_0[\text{E}]_t)$  ( $k_2 = 7.17 \times 10^{-4} \text{ M}^{-1} \text{ s}^{-1}$ , data points up to 50% conversion were used; right).

**Table S32:** Reaction of **1b** with  $(\text{dma})_2\text{CH}^+ \text{BF}_4^-$  (**2b**) in MeCN (20 °C, stopped-flow, detection at 606 nm).

$[\text{E}]_0$ (M)	$[\text{Nu}]_0$ (M)	$[\text{Nu}]_0/[\text{E}]_0$	$k_{\text{obs}}$ ( $\text{s}^{-1}$ )
$8.90 \times 10^{-6}$	$9.53 \times 10^{-5}$	10.7	$3.13 \times 10^{-5}$
$1.24 \times 10^{-5}$	$1.51 \times 10^{-4}$	12.2	$4.71 \times 10^{-5}$
$9.97 \times 10^{-6}$	$2.36 \times 10^{-4}$	23.7	$7.13 \times 10^{-5}$
$9.94 \times 10^{-6}$	$4.94 \times 10^{-4}$	49.7	$1.32 \times 10^{-4}$

$$k_2 (20 \text{ }^\circ\text{C}) = 2.50 \times 10^{-1} \text{ M}^{-1} \text{ s}^{-1}$$

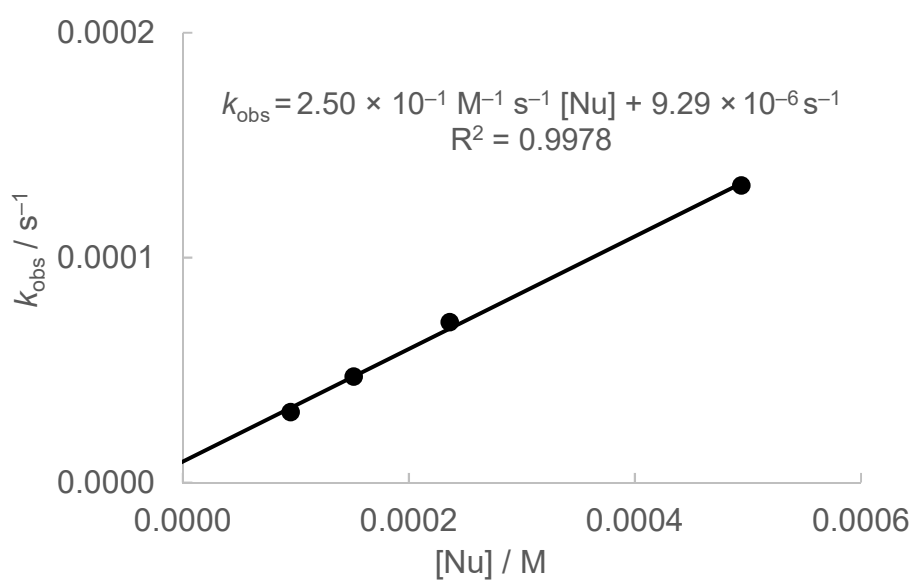


**Table S33:** Reaction of **1b** with  $(\text{mpa})_2\text{CH}^+ \text{BF}_4^-$  (**2c**) in MeCN (20 °C, stopped-flow, detection at 613 nm).

$[\text{E}]_0$ (M)	$[\text{Nu}]_0$ (M)	$[\text{Nu}]_0/[\text{E}]_0$	$k_{\text{obs}}$ ( $\text{s}^{-1}$ )
$8.84 \times 10^{-6}$	$8.69 \times 10^{-5}$	9.84	$3.70 \times 10^{-4}$
$9.25 \times 10^{-6}$	$2.97 \times 10^{-4}$	32.1	$1.26 \times 10^{-3}$
$9.31 \times 10^{-6}$	$4.94 \times 10^{-4}$	53.1	$2.08 \times 10^{-3}$
$9.83 \times 10^{-6}$	$7.51 \times 10^{-4}$	76.4	$3.23 \times 10^{-3}$
$9.82 \times 10^{-6}$	$9.90 \times 10^{-4}$	101	$4.18 \times 10^{-3}$

$$k_2 (20 \text{ }^\circ\text{C}) = 4.24 \text{ M}^{-1} \text{ s}^{-1}$$

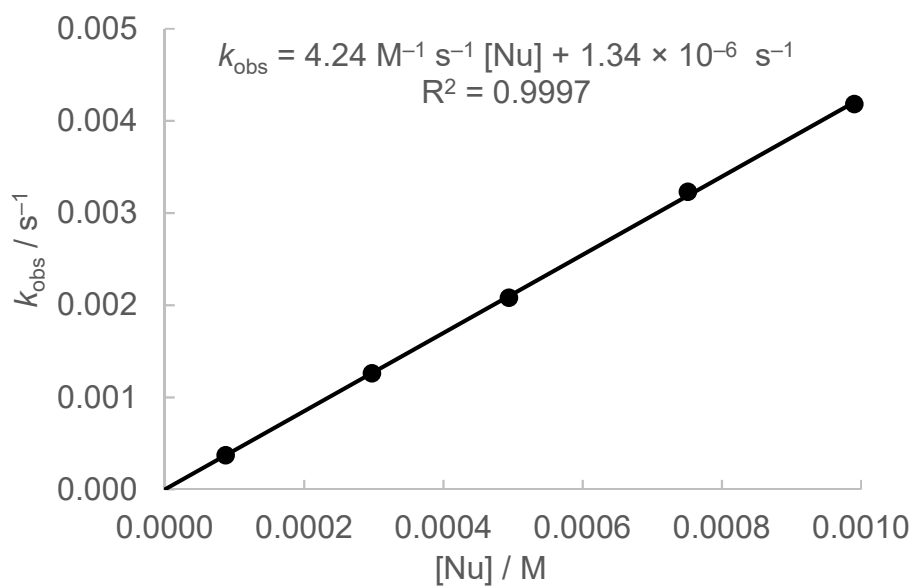


**Table S34:** Reaction of **1b** with (mor)<sub>2</sub>CH<sup>+</sup> BF<sub>4</sub><sup>-</sup> (**2d**) in MeCN (20 °C, conventional UV/Vis, detection at 612 nm).

[E] <sub>0</sub> (M)	[Nu] <sub>0</sub> (M)	[Nu] <sub>0</sub> /[E] <sub>0</sub>	k <sub>obs</sub> (s <sup>-1</sup> )
1.13 × 10 <sup>-5</sup>	6.49 × 10 <sup>-4</sup>	57.4	6.20 × 10 <sup>-2</sup>
1.13 × 10 <sup>-5</sup>	1.30 × 10 <sup>-3</sup>	115	7.14 × 10 <sup>-2</sup>
1.13 × 10 <sup>-5</sup>	1.95 × 10 <sup>-3</sup>	172	8.53 × 10 <sup>-2</sup>

$$k_2 (20\text{ °C}) = 17.9 \times 10^{-1} \text{ M}^{-1} \text{ s}^{-1}$$

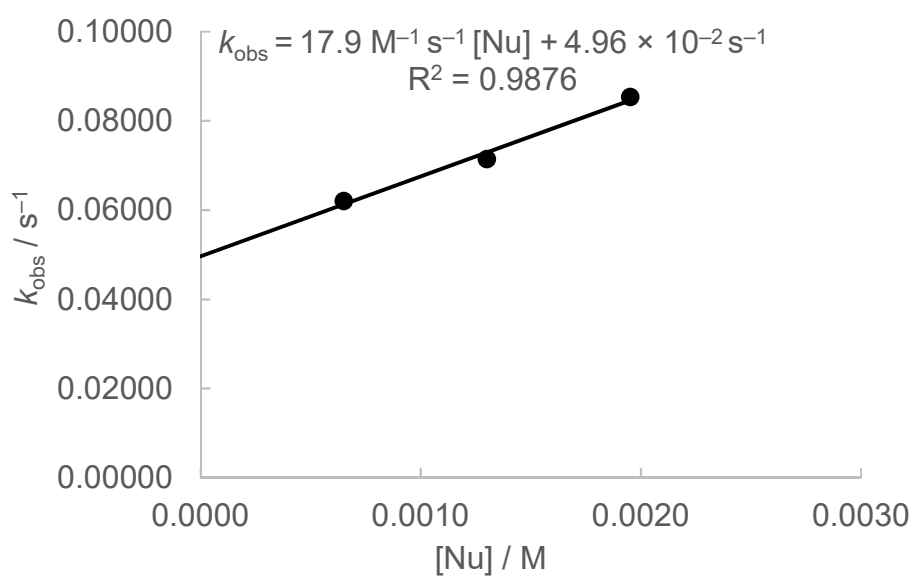
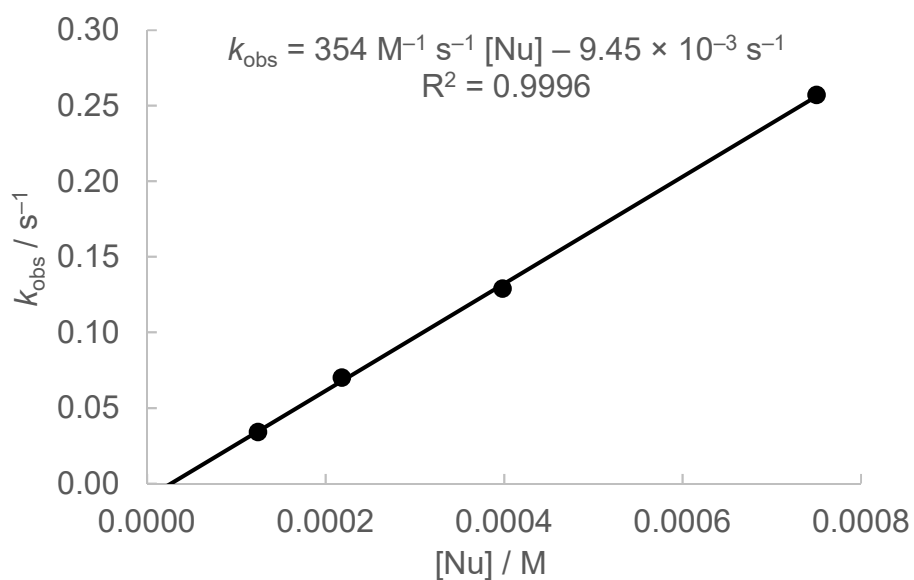


**Table S35:** Reaction of **1b** with  $(\text{dpa})_2\text{CH}^+ \text{BF}_4^-$  (**2e**) in MeCN (20 °C, conventional UV/Vis, detection at 644 nm).

$[\text{E}]_0$ (M)	$[\text{Nu}]_0$ (M)	$[\text{Nu}]_0/[\text{E}]_0$	$k_{\text{obs}}$ ( $\text{s}^{-1}$ )
$1.38 \times 10^{-5}$	$1.24 \times 10^{-4}$	9.01	$3.40 \times 10^{-2}$
$1.57 \times 10^{-5}$	$2.18 \times 10^{-4}$	13.9	$7.00 \times 10^{-2}$
$1.45 \times 10^{-5}$	$3.98 \times 10^{-4}$	27.5	$1.29 \times 10^{-1}$
$1.43 \times 10^{-5}$	$7.50 \times 10^{-4}$	52.6	$2.57 \times 10^{-1}$

$$k_2 (20 \text{ }^\circ\text{C}) = 354 \text{ M}^{-1} \text{ s}^{-1}$$



[a] The negative intercept with the abscissa is due to slow/incomplete mixing of the reactants in comparison with the fast reaction.

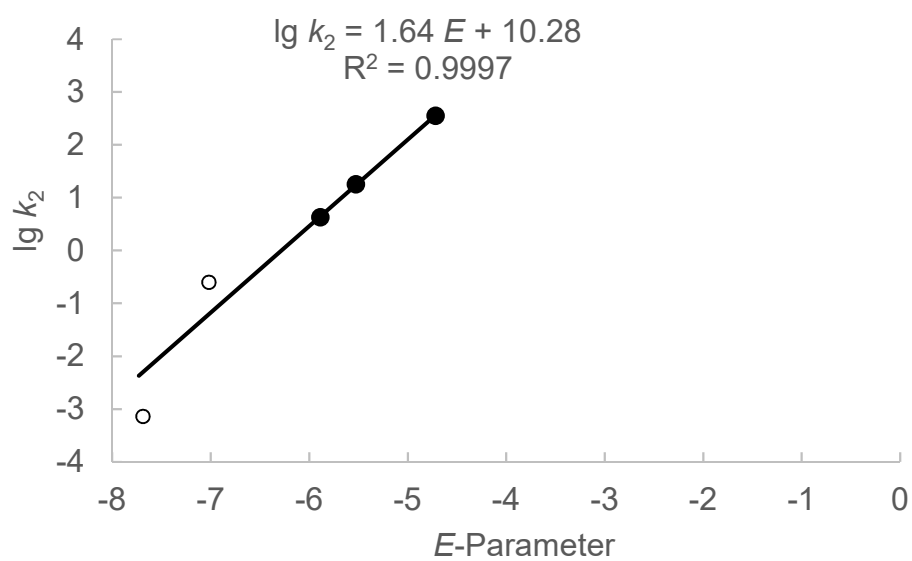
Determination of reactivity parameters  $N$  and  $s_N$  for  $N,N$ -diethylaniline (**1b**) in MeCN

**Table S36:** Rate constants for the reactions of  $N,N$ -diethylaniline (**1b**) with reference electrophiles (20 °C).

Electrophile	$E$ -Parameter	$k_2$ ( $M^{-1} s^{-1}$ )	$\lg k_2$
(pyr) <sub>2</sub> CH <sup>+</sup> ( <b>2a</b> )	-7.69	$7.17 \times 10^{-4}$	-3.14 <sup>[a]</sup>
(dma) <sub>2</sub> CH <sup>+</sup> ( <b>2b</b> )	-7.02	$2.50 \times 10^{-1}$	-0.60 <sup>[a]</sup>
(mpa) <sub>2</sub> CH <sup>+</sup> ( <b>2c</b> )	-5.89	4.24	0.63
(mor) <sub>2</sub> CH <sup>+</sup> ( <b>2d</b> )	-5.53	17.9	1.25
(dpa) <sub>2</sub> CH <sup>+</sup> ( <b>2e</b> )	-4.72	354	2.55

[a] Not considered for the correlation.

$N = 6.28$ ,  $s_N = 1.64$



## 8.2 Reactions of *N,N*-diethylaniline (**1b**) with benzhydrylium ions **2** at the nitrogen atom in acetonitrile at 20 °C

**Table S37:** Reaction of **1b** with (dma)<sub>2</sub>CH<sup>+</sup> BF<sub>4</sub><sup>-</sup> (**2b**) in MeCN (20 °C, conventional UV/Vis, detection at 606 nm).

[E] <sub>0</sub> (M)	[Nu] <sub>0</sub> (M)	[Nu] <sub>0</sub> /[E] <sub>0</sub>	<i>k</i> <sub>obs</sub> (s <sup>-1</sup> )
8.90 × 10 <sup>-6</sup>	9.53 × 10 <sup>-5</sup>	10.7	1.64 × 10 <sup>-2</sup>
9.97 × 10 <sup>-6</sup>	2.36 × 10 <sup>-4</sup>	23.7	2.50 × 10 <sup>-2</sup>
9.94 × 10 <sup>-6</sup>	4.94 × 10 <sup>-4</sup>	49.7	4.81 × 10 <sup>-2</sup>

$$k_2 (20\text{ °C}) = 80.7\text{ M}^{-1}\text{ s}^{-1}$$

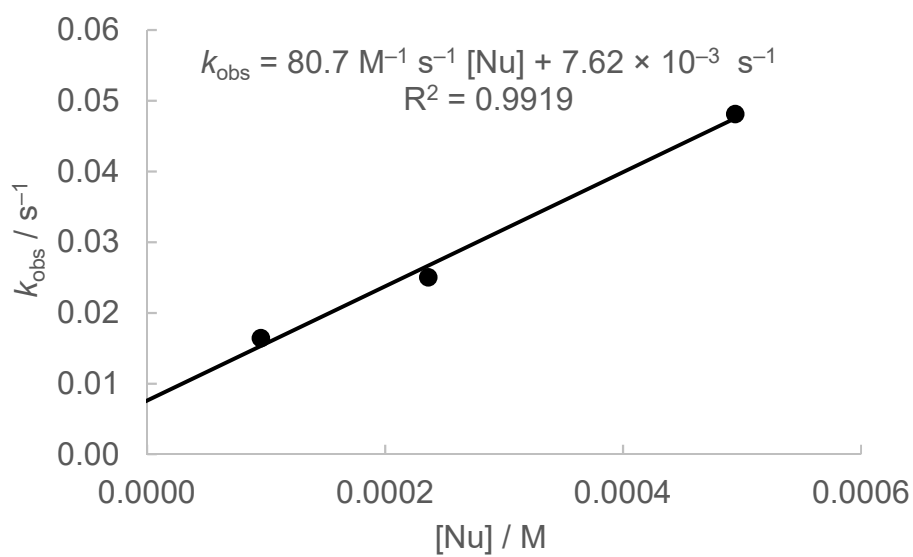


**Table S38:** Reaction of **1b** with (mor)<sub>2</sub>CH<sup>+</sup> BF<sub>4</sub><sup>-</sup> (**2d**) in MeCN (20 °C, stopped-flow, detection at 612 nm).

[E] <sub>0</sub> (M)	[Nu] <sub>0</sub> (M)	[Nu] <sub>0</sub> /[E] <sub>0</sub>	k <sub>obs</sub> (s <sup>-1</sup> )
1.13 × 10 <sup>-5</sup>	9.74 × 10 <sup>-4</sup>	86.2	3.30
1.13 × 10 <sup>-5</sup>	1.62 × 10 <sup>-3</sup>	143	4.03
1.13 × 10 <sup>-5</sup>	1.95 × 10 <sup>-3</sup>	172	4.52

$$k_2 (20\text{ }^\circ\text{C}) = 1.23 \times 10^3 \text{ M}^{-1} \text{ s}^{-1}$$

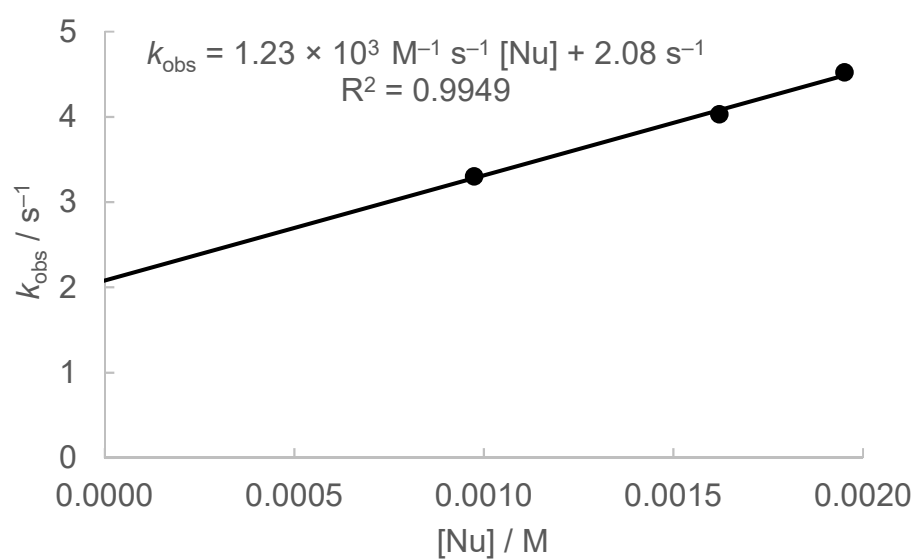
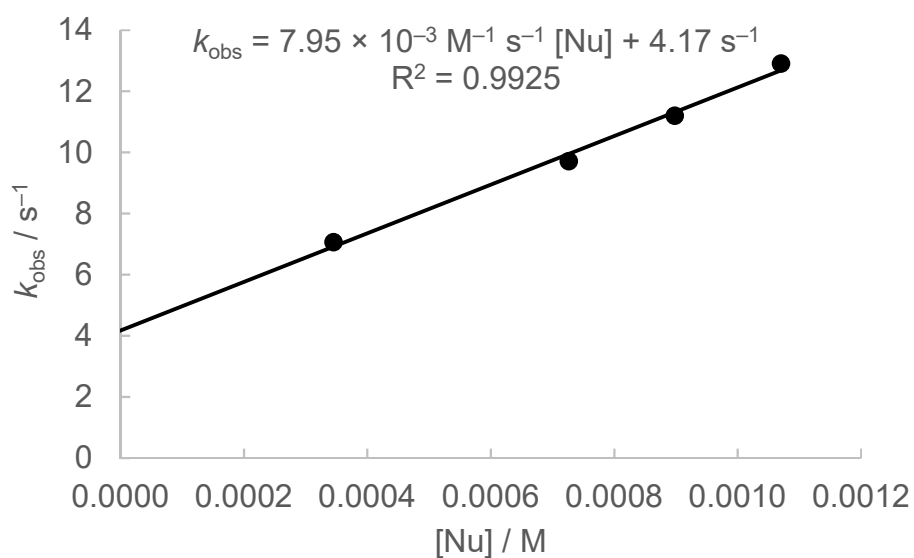


**Table S39:** Reaction of **1b** with  $(\text{mfa})_2\text{CH}^+ \text{BF}_4^-$  (**2f**) in MeCN (20 °C, stopped-flow, detection at 586 nm).

$[\text{E}]_0$ (M)	$[\text{Nu}]_0$ (M)	$[\text{Nu}]_0/[\text{E}]_0$	$k_{\text{obs}}$ ( $\text{s}^{-1}$ )
$1.49 \times 10^{-5}$	$3.45 \times 10^{-4}$	23.2	7.06
$1.49 \times 10^{-5}$	$7.26 \times 10^{-4}$	48.7	9.71
$1.49 \times 10^{-5}$	$8.98 \times 10^{-4}$	60.3	11.2
$1.49 \times 10^{-5}$	$1.07 \times 10^{-3}$	71.8	12.9

$$k_2 (20 \text{ }^\circ\text{C}) = 7.95 \times 10^3 \text{ M}^{-1} \text{ s}^{-1}$$

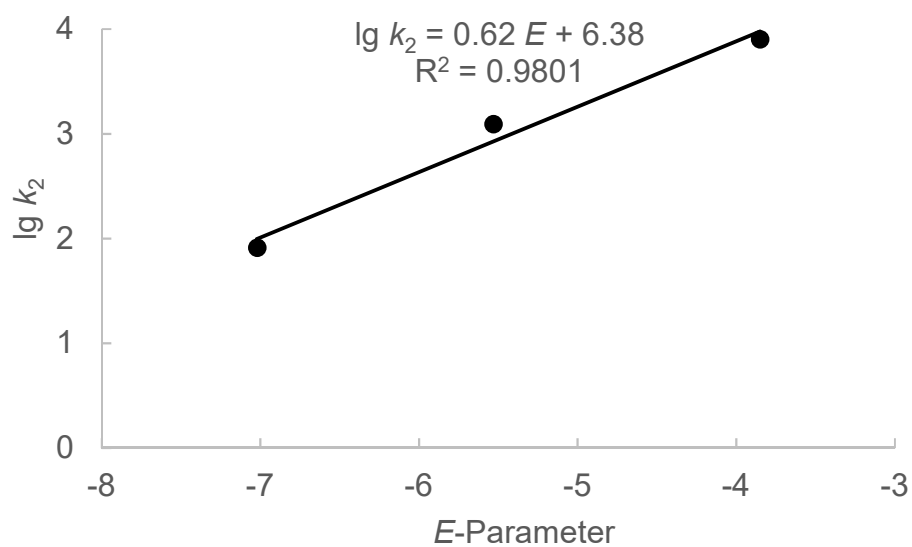


Determination of reactivity parameters  $N$  and  $s_N$  for  $N,N$ -diethylaniline (**1b**) in MeCN at 20 °C at the nitrogen atom.

**Table S40:** Rate constants for the reactions of **1b** with reference electrophiles (20 °C).

Electrophile	$E$ -Parameter	$k_2$ ( $M^{-1} s^{-1}$ )	$\lg k_2$
(dma) <sub>2</sub> CH <sup>+</sup> ( <b>2b</b> )	-7.02	80.7	1.91
(mor) <sub>2</sub> CH <sup>+</sup> ( <b>2d</b> )	-5.53	$1.23 \times 10^3$	3.09
(mfa) <sub>2</sub> CH <sup>+</sup> ( <b>2f</b> )	-3.85	$7.95 \times 10^3$	3.90

$N = 10.29$ ,  $s_N = 0.62$

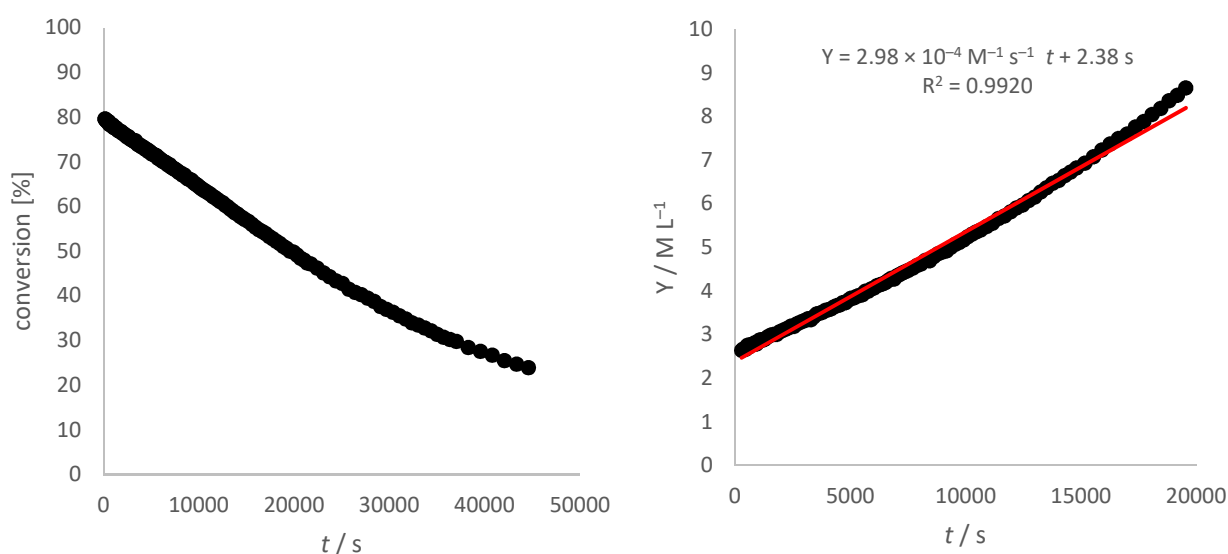


## 9. Reactions of *N,N*-diethylaniline (**1b**) with benzhydrylium ions **2** at the C4 carbon in dichloromethane at 20 °C.

**Table S41:** Reaction of *N,N*-diethylaniline (**1b**) with (pyr)<sub>2</sub>CH<sup>+</sup> BF<sub>4</sub><sup>-</sup> (**2a**) in CD<sub>2</sub>Cl<sub>2</sub> (23 °C, <sup>1</sup>H NMR spectroscopy).

[E] <sub>0</sub> (M)	[Nu] <sub>0</sub> (M)	[Nu] <sub>0</sub> /[E] <sub>0</sub>	<i>k</i> <sub>2</sub> (M <sup>-1</sup> s <sup>-1</sup> )
4.65 × 10 <sup>-2</sup>	9.35 × 10 <sup>-2</sup>	2.01	2.98 × 10 <sup>-4</sup>

$$k_2 (23 \text{ °C}) = 2.98 \times 10^{-4} \text{ M}^{-1} \text{ s}^{-1}$$

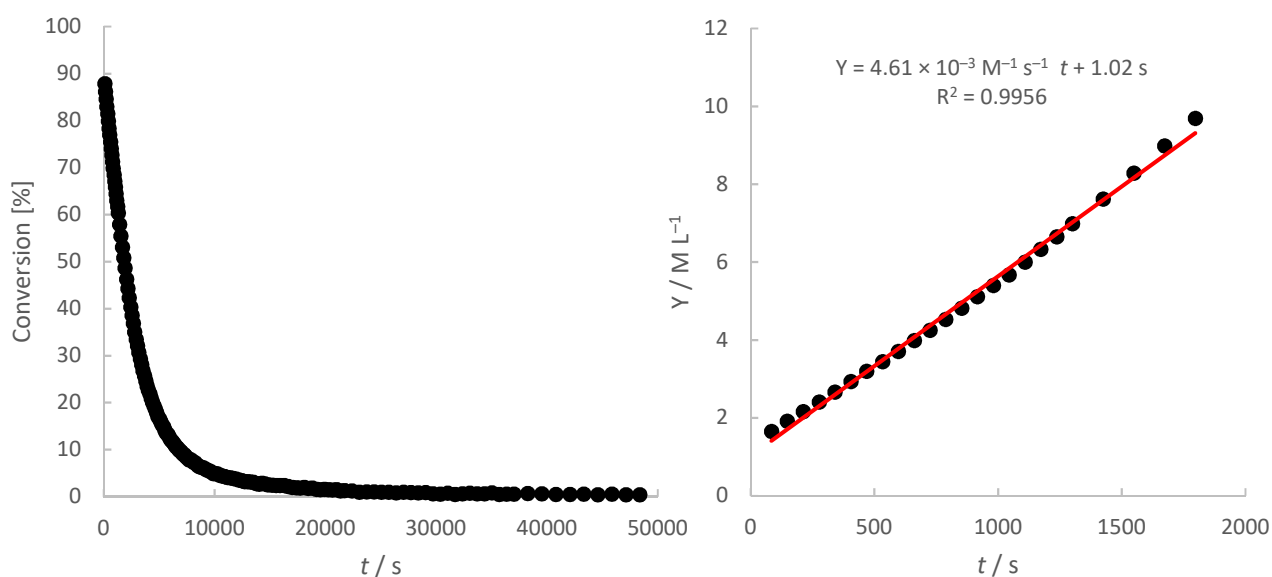


Decay of the relative concentration of (pyr)<sub>2</sub>CH<sup>+</sup> BF<sub>4</sub><sup>-</sup> (**2a**) while reacting with *N,N*-diethylaniline (**1b**) in CD<sub>2</sub>Cl<sub>2</sub> at 23 °C (left). Determination of the second order rate constant by plotting time versus  $Y = ([\text{Nu}]_0 - [\text{E}]_0)^{-1} \ln([\text{E}]_0([\text{E}]_t + [\text{Nu}]_0 - [\text{E}]_0) / [\text{Nu}]_0[\text{E}]_t)$  ( $k_2 = 2.98 \times 10^{-4} \text{ M}^{-1} \text{ s}^{-1}$ , data points up to 50% conversion were used; right).

**Table S42:** Reaction of *N,N*-diethylaniline (**1b**) with (dma)<sub>2</sub>CH<sup>+</sup> BF<sub>4</sub><sup>-</sup> (**2b**) in CD<sub>2</sub>Cl<sub>2</sub> (20 °C, <sup>1</sup>H NMR spectroscopy).

[E] <sub>0</sub> (M)	[Nu] <sub>0</sub> (M)	[Nu] <sub>0</sub> /[E] <sub>0</sub>	<i>k</i> <sub>2</sub> (M <sup>-1</sup> s <sup>-1</sup> )
3.88 × 10 <sup>-2</sup>	8.10 × 10 <sup>-2</sup>	2.09	4.61 × 10 <sup>-3</sup>

$$k_2 (20\text{ °C}) = 4.61 \times 10^{-3} \text{ M}^{-1} \text{ s}^{-1}$$



Decay of the relative concentration of (dma)<sub>2</sub>CH<sup>+</sup> BF<sub>4</sub><sup>-</sup> (**2b**) while reacting with *N,N*-diethylaniline (**1b**) in CD<sub>2</sub>Cl<sub>2</sub> at 20 °C (left). Determination of the second order rate constant by plotting time versus  $Y = ([\text{Nu}]_0 - [\text{E}]_0)^{-1} \ln([\text{E}]_0([\text{E}]_t + [\text{Nu}]_0 - [\text{E}]_0) / [\text{Nu}]_0[\text{E}]_t)$  ( $k_2 = 4.61 \times 10^{-3} \text{ M}^{-1} \text{ s}^{-1}$ , data points up to 50% conversion were used; right).

**Table S43:** Reaction of *N,N*-diethylaniline (**1b**) with (mor)<sub>2</sub>CH<sup>+</sup> BF<sub>4</sub><sup>-</sup> (**2d**) in dichloromethane (20 °C, conventional UV/Vis, detection at 620 nm).

[E] <sub>0</sub> (M)	[Nu] <sub>0</sub> (M)	[Nu] <sub>0</sub> /[E] <sub>0</sub>	<i>k</i> <sub>obs</sub> (s <sup>-1</sup> )
2.10 × 10 <sup>-5</sup>	1.07 × 10 <sup>-3</sup>	51.0	9.11 × 10 <sup>-5</sup>
2.15 × 10 <sup>-5</sup>	1.48 × 10 <sup>-3</sup>	68.8	1.16 × 10 <sup>-4</sup>
2.13 × 10 <sup>-5</sup>	2.05 × 10 <sup>-3</sup>	96.2	1.51 × 10 <sup>-4</sup>
2.08 × 10 <sup>-5</sup>	3.08 × 10 <sup>-3</sup>	148	2.14 × 10 <sup>-4</sup>

$$k_2 (20\text{ °C}) = 6.12 \times 10^{-2} \text{ M}^{-1} \text{ s}^{-1}$$

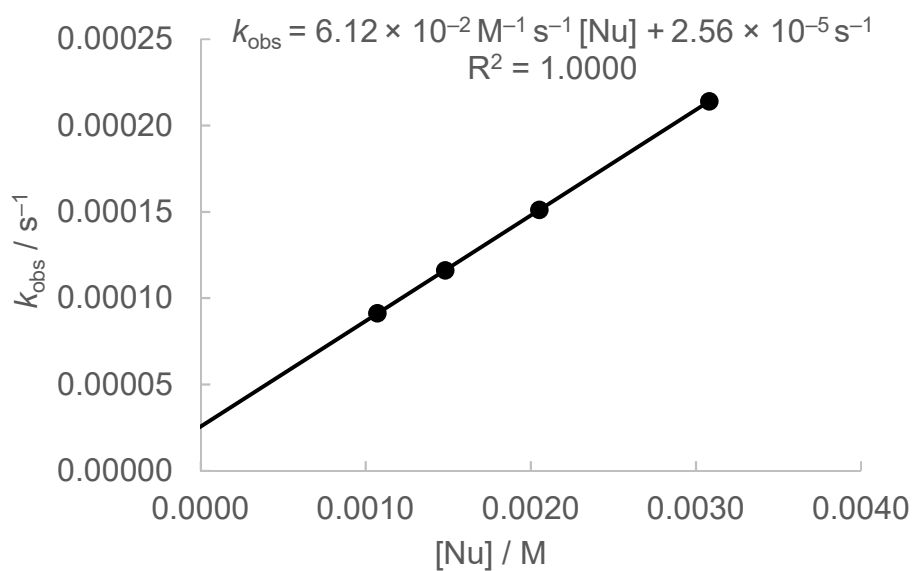


**Table S44:** Reaction of **1b** with  $(\text{dpa})_2\text{CH}^+ \text{BF}_4^-$  (**2e**) in dichloromethane (20 °C, conventional UV/Vis, detection at 672 nm).

$[\text{E}]_0$ (M)	$[\text{Nu}]_0$ (M)	$[\text{Nu}]_0/[\text{E}]_0$	$k_{\text{obs}}$ ( $\text{s}^{-1}$ )
$1.59 \times 10^{-5}$	$1.69 \times 10^{-4}$	10.6	$3.21 \times 10^{-4}$
$2.56 \times 10^{-5}$	$4.80 \times 10^{-4}$	18.8	$5.04 \times 10^{-4}$
$1.50 \times 10^{-5}$	$7.60 \times 10^{-4}$	50.7	$8.17 \times 10^{-4}$
$1.55 \times 10^{-5}$	$1.06 \times 10^{-3}$	68.4	$1.01 \times 10^{-3}$
$2.48 \times 10^{-5}$	$1.49 \times 10^{-3}$	60.1	$1.38 \times 10^{-3}$

$$k_2 (20 \text{ }^\circ\text{C}) = 8.14 \times 10^{-1} \text{ M}^{-1} \text{ s}^{-1}$$

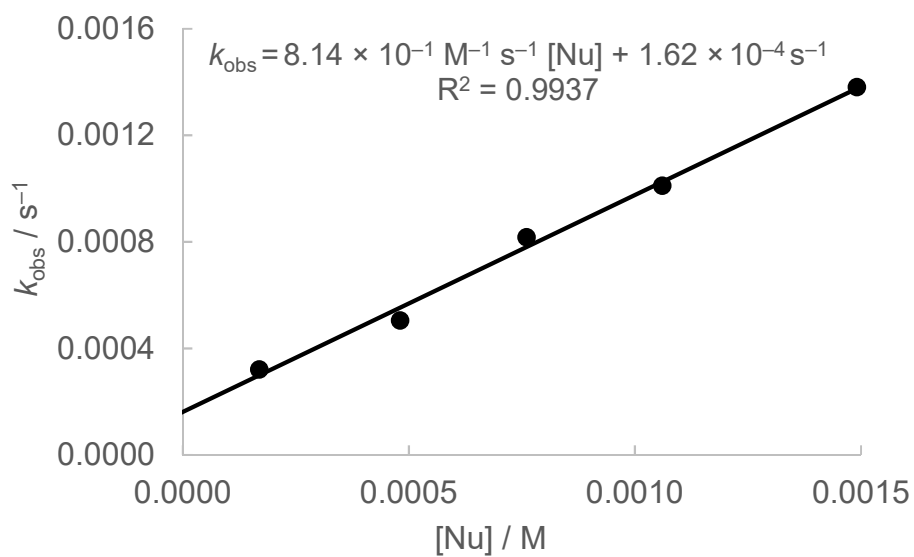
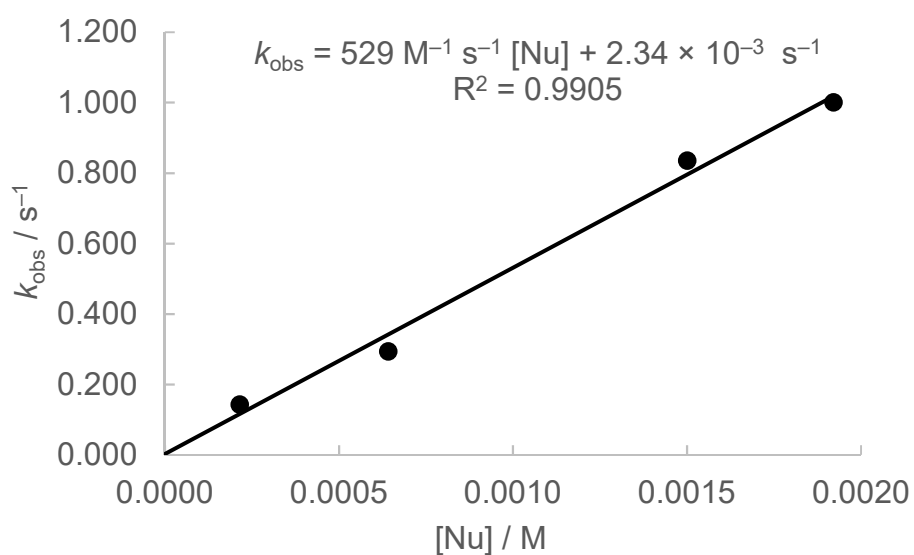


**Table S45:** Reaction of **1b** with (pfa)<sub>2</sub>CH<sup>+</sup> BF<sub>4</sub><sup>-</sup> (**2g**) in dichloromethane (20 °C, stopped-flow, detection at 601 nm).

[E] <sub>0</sub> (M)	[Nu] <sub>0</sub> (M)	[Nu] <sub>0</sub> /[E] <sub>0</sub>	<i>k</i> <sub>obs</sub> (s <sup>-1</sup> )
1.55 × 10 <sup>-5</sup>	2.14 × 10 <sup>-4</sup>	13.8	1.42 × 10 <sup>-1</sup>
1.55 × 10 <sup>-5</sup>	6.41 × 10 <sup>-4</sup>	41.4	2.93 × 10 <sup>-1</sup>
1.55 × 10 <sup>-5</sup>	1.50 × 10 <sup>-3</sup>	96.8	8.35 × 10 <sup>-1</sup>
1.55 × 10 <sup>-5</sup>	1.92 × 10 <sup>-3</sup>	124	1.00

$$k_2 (20\text{ }^\circ\text{C}) = 529\text{ M}^{-1}\text{ s}^{-1}$$



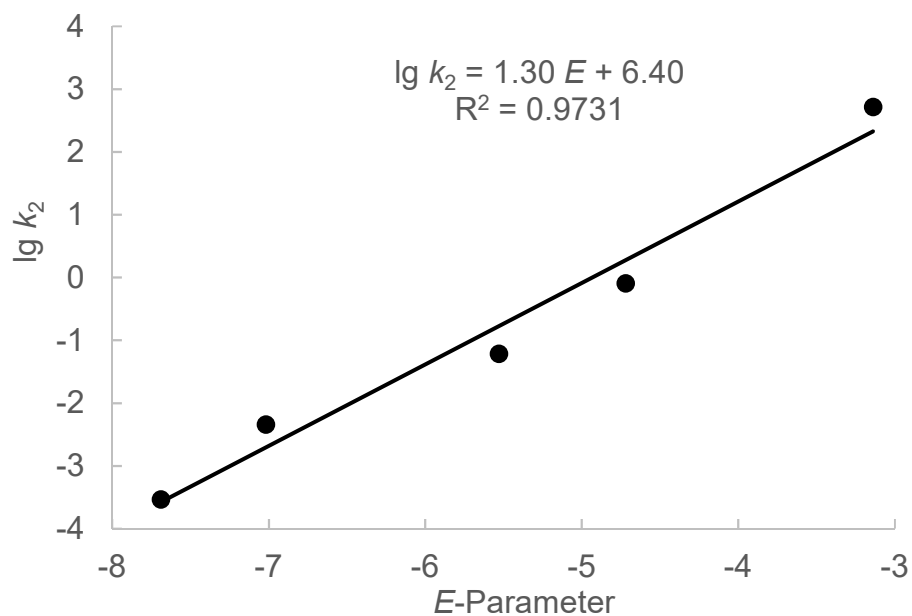
Determination of reactivity parameters  $N$  and  $s_N$  for  $N,N$ -diethylaniline (**1b**) in dichloromethane at 20 °C at the C4 carbon atom.

**Table S46:** Rate constants for the reactions of  $N,N$ -diethylaniline (**1b**) with reference electrophiles (20 °C).

Electrophile	$E$ -Parameter	$k_2$ ( $M^{-1} s^{-1}$ )	$\lg k_2$
(pyr) <sub>2</sub> CH <sup>+</sup> ( <b>2a</b> )	-7.69	$2.98 \times 10^{-4}$ [a]	-3.53
(dma) <sub>2</sub> CH <sup>+</sup> ( <b>2b</b> )	-7.02	$4.61 \times 10^{-3}$	-2.34
(mor) <sub>2</sub> CH <sup>+</sup> ( <b>2d</b> )	-5.53	$6.12 \times 10^{-2}$	-1.21
(dpa) <sub>2</sub> CH <sup>+</sup> ( <b>2e</b> )	-4.72	$8.14 \times 10^{-1}$	-0.09
(pfa) <sub>2</sub> CH <sup>+</sup> ( <b>2g</b> )	-3.14	529	2.72

[a] Measured at 23 °C.

$N = 4.92$ ,  $s_N = 1.30$



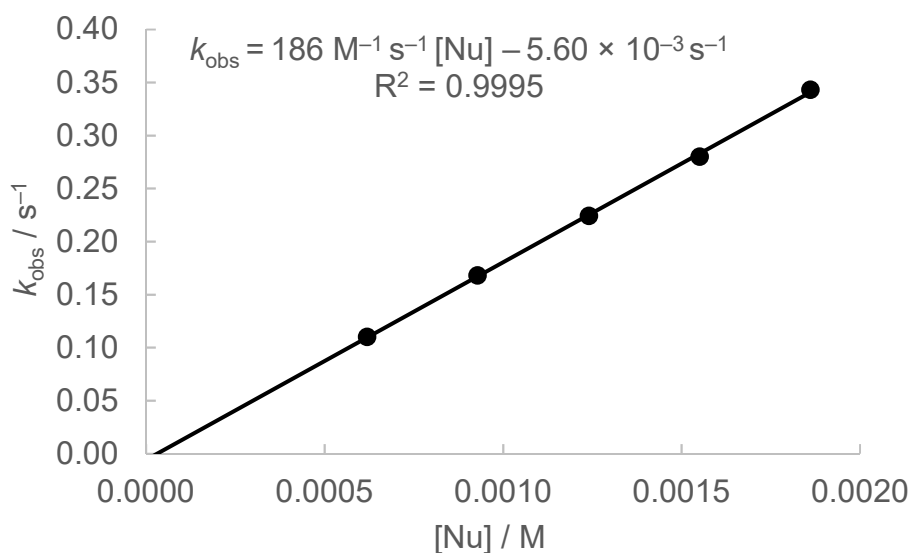
## 10. Reactions of 1-phenylpyrrolidine (1c) with benzhydrylium ions 2 in acetonitrile at 20 °C.

### 10.1 Reactions of 1-phenylpyrrolidine (1c) with benzhydrylium ions 2 at the C4 carbon in acetonitrile at 20 °C

**Table S47:** Reaction of 1-phenylpyrrolidine (1c) with (dpa)<sub>2</sub>CH<sup>+</sup> BF<sub>4</sub><sup>-</sup> (2e) in MeCN (20 °C, stopped-flow, detection at 644 nm).

[E] <sub>0</sub> (M)	[Nu] <sub>0</sub> (M)	[Nu] <sub>0</sub> /[E] <sub>0</sub>	k <sub>obs</sub> (s <sup>-1</sup> )
1.88 × 10 <sup>-5</sup>	6.18 × 10 <sup>-4</sup>	33.0	1.10 × 10 <sup>-1</sup>
1.88 × 10 <sup>-5</sup>	9.28 × 10 <sup>-4</sup>	49.4	1.68 × 10 <sup>-1</sup>
1.88 × 10 <sup>-5</sup>	1.24 × 10 <sup>-3</sup>	65.9	2.24 × 10 <sup>-1</sup>
1.88 × 10 <sup>-5</sup>	1.55 × 10 <sup>-3</sup>	82.4	2.80 × 10 <sup>-1</sup>
1.88 × 10 <sup>-5</sup>	1.86 × 10 <sup>-3</sup>	98.9	3.43 × 10 <sup>-1</sup>

$$k_2 (20 \text{ }^\circ\text{C}) = 186 \text{ M}^{-1} \text{ s}^{-1}$$



[a] The negative intercept with the abscissa is due to slow/incomplete mixing of the reactants in comparison with the fast reaction.

**Table S48:** Reaction of 1-phenylpyrrolidine (**1c**) with (mor)<sub>2</sub>CH<sup>+</sup> BF<sub>4</sub><sup>-</sup> (**2d**) in MeCN (20 °C, stopped-flow, detection at 612 nm).

[E] <sub>0</sub> (M)	[Nu] <sub>0</sub> (M)	[Nu] <sub>0</sub> /[E] <sub>0</sub>	<i>k</i> <sub>obs</sub> (s <sup>-1</sup> )
1.91 × 10 <sup>-5</sup>	6.18 × 10 <sup>-4</sup>	32.4	6.75 × 10 <sup>-3</sup>
1.91 × 10 <sup>-5</sup>	9.28 × 10 <sup>-4</sup>	48.6	9.51 × 10 <sup>-3</sup>
1.91 × 10 <sup>-5</sup>	1.24 × 10 <sup>-3</sup>	64.8	1.26 × 10 <sup>-2</sup>
1.91 × 10 <sup>-5</sup>	1.55 × 10 <sup>-3</sup>	81.0	1.58 × 10 <sup>-2</sup>
1.91 × 10 <sup>-5</sup>	1.86 × 10 <sup>-3</sup>	97.2	1.90 × 10 <sup>-2</sup>

$$k_2 (20\text{ }^\circ\text{C}) = 9.91\text{ M}^{-1}\text{ s}^{-1}$$

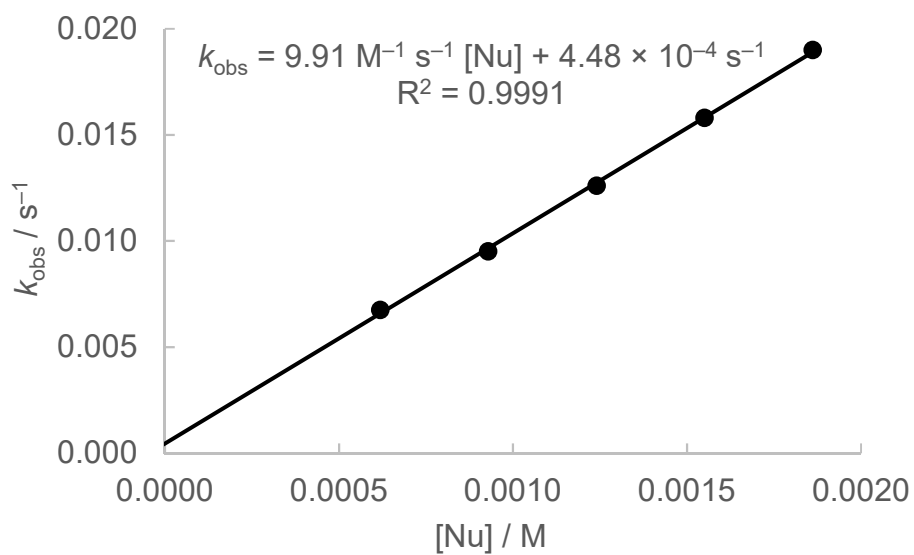
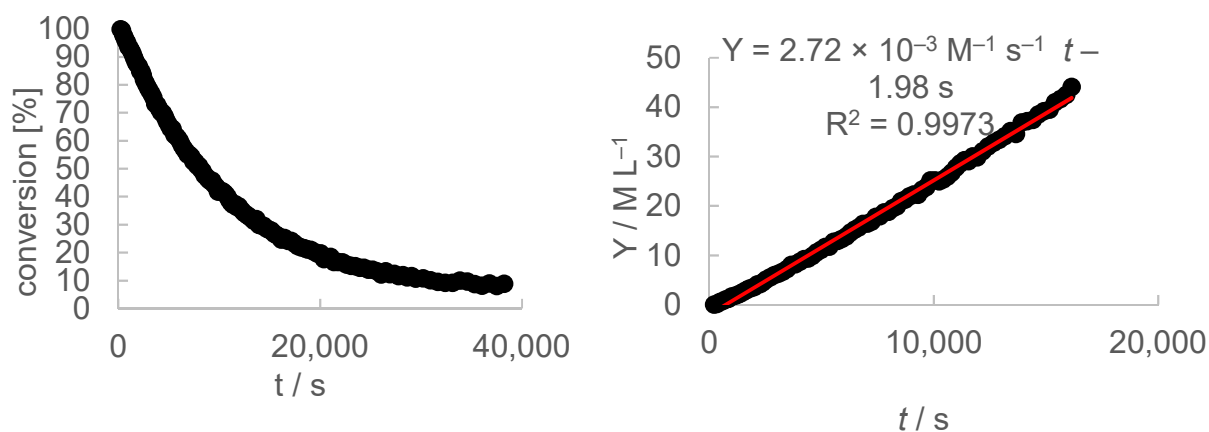


**Table S49:** Reaction of 1-phenylpyrrolidine (**1c**) with (pyr)<sub>2</sub>CH<sup>+</sup> BF<sub>4</sub><sup>-</sup> (**2a**) in CD<sub>3</sub>CN (20 °C, <sup>1</sup>H NMR spectroscopy).

[E] <sub>0</sub> (M)	[Nu] <sub>0</sub> (M)	[Nu] <sub>0</sub> /[E] <sub>0</sub>	k <sub>2</sub> (M <sup>-1</sup> s <sup>-1</sup> )
2.04 × 10 <sup>-2</sup>	4.17 × 10 <sup>-2</sup>	2.04	2.72 × 10 <sup>-3</sup>

$$k_2 (20\text{ °C}) = 2.72 \times 10^{-3} \text{ M}^{-1} \text{ s}^{-1}$$



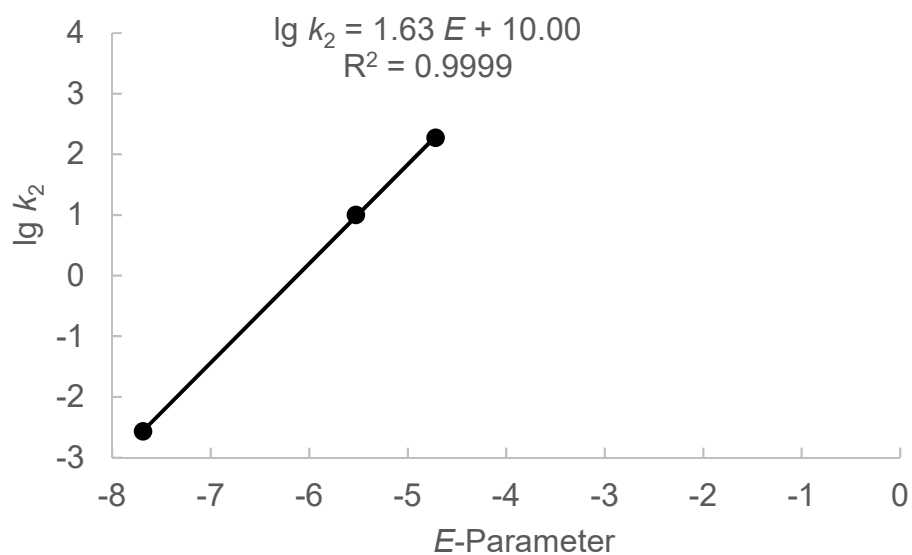
Decay of the relative concentration of (pyr)<sub>2</sub>CH<sup>+</sup> BF<sub>4</sub><sup>-</sup> while reacting with 1-phenylpyrrolidine (**1c**) in CD<sub>3</sub>CN at 20 °C (left). Determination of the second order rate constant by plotting time versus  $Y = ([\text{Nu}]_0 - [\text{E}]_0)^{-1} \ln([\text{E}]_0([\text{E}]_t + [\text{Nu}]_0 - [\text{E}]_0) / [\text{Nu}]_0[\text{E}]_t)$  ( $k_2 = 2.72 \times 10^{-3} \text{ M}^{-1} \text{ s}^{-1}$ , data points up to 50% conversion were used; right).

Determination of reactivity parameters  $N$  and  $s_N$  for 1-phenylpyrrolidine (**1c**) in MeCN

**Table S50:** Rate constants for the reactions of 1-phenylpyrrolidine (**1c**) with reference electrophiles (20 °C).

Electrophile	$E$ -Parameter	$k_2$ ( $M^{-1} s^{-1}$ )	$\lg k_2$
(pyr) <sub>2</sub> CH <sup>+</sup> ( <b>2a</b> )	-7.69	$2.72 \times 10^{-3}$	-2.57
(mor) <sub>2</sub> CH <sup>+</sup> ( <b>2d</b> )	-5.53	9.91	1.00
(dpa) <sub>2</sub> CH <sup>+</sup> ( <b>2e</b> )	-4.72	186	2.27

$N = 6.13$ ,  $s_N = 1.63$



## 10.2 Reactions of 1-phenylpyrrolidine (1c) with benzhydrylium ions 2 at the nitrogen atom in acetonitrile at 20 °C

**Table S51:** Reaction of 1-phenylpyrrolidine (1c) with (mfa)<sub>2</sub>CH<sup>+</sup> BF<sub>4</sub><sup>-</sup> (2f) in MeCN (20 °C, stopped-flow, detection at 586 nm).

[E] <sub>0</sub> (M)	[Nu] <sub>0</sub> (M)	[Nu] <sub>0</sub> /[E] <sub>0</sub>	k <sub>obs</sub> (s <sup>-1</sup> )
8.06 × 10 <sup>-6</sup>	3.62 × 10 <sup>-4</sup>	44.9	9.19
8.06 × 10 <sup>-6</sup>	7.24 × 10 <sup>-4</sup>	89.8	9.88
8.06 × 10 <sup>-6</sup>	9.05 × 10 <sup>-4</sup>	112	10.3
8.06 × 10 <sup>-6</sup>	1.09 × 10 <sup>-3</sup>	135	10.7

$$k_2 (20\text{ °C}) = 2.08 \times 10^3 \text{ M}^{-1} \text{ s}^{-1}$$

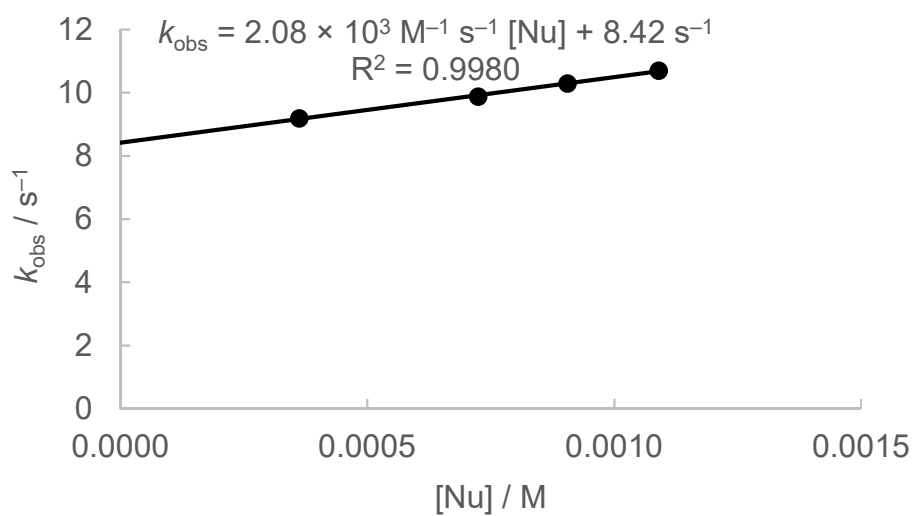
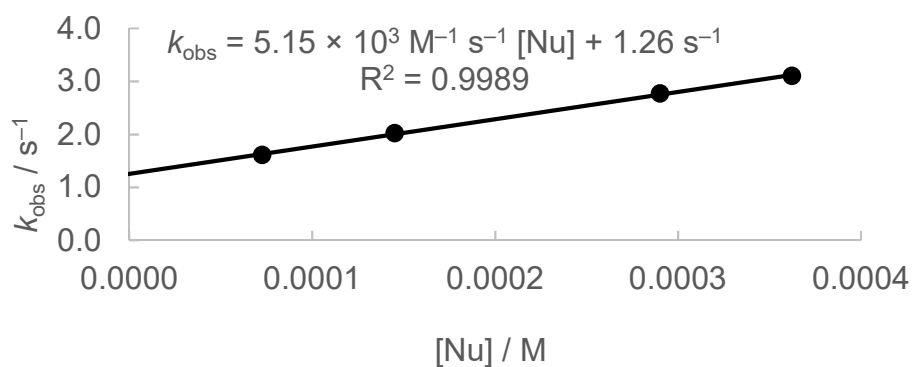


**Table S52:** Reaction of **1c** with (pfa)<sub>2</sub>CH<sup>+</sup> BF<sub>4</sub><sup>-</sup> (**2g**) in MeCN (20 °C, stopped-flow, detection at 592 nm).

[E] <sub>0</sub> (M)	[Nu] <sub>0</sub> (M)	[Nu] <sub>0</sub> /[E] <sub>0</sub>	<i>k</i> <sub>obs</sub> (s <sup>-1</sup> )
8.86 × 10 <sup>-6</sup>	7.24 × 10 <sup>-5</sup>	8.2	1.61
8.86 × 10 <sup>-6</sup>	1.45 × 10 <sup>-4</sup>	16.4	2.02
8.86 × 10 <sup>-6</sup>	2.90 × 10 <sup>-4</sup>	32.7	2.77
8.86 × 10 <sup>-6</sup>	3.62 × 10 <sup>-4</sup>	40.9	3.10

$$k_2 (20\text{ }^\circ\text{C}) = 5.15 \times 10^3 \text{ M}^{-1} \text{ s}^{-1}$$

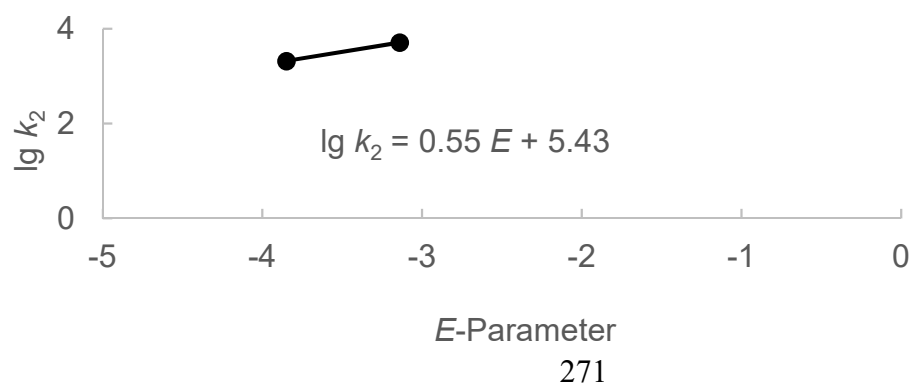


Determination of reactivity parameters *N* and *s<sub>N</sub>* for 1-phenylpyrrolidine (**1c**) in MeCN

**Table S53:** Rate constants for the reactions of 1-phenylpyrrolidine (**1c**) with reference electrophiles at the nitrogen atom (20 °C).

Electrophile	<i>E</i> -Parameter	<i>k</i> <sub>2</sub> (M <sup>-1</sup> s <sup>-1</sup> )	lg <i>k</i> <sub>2</sub>
(mfa) <sub>2</sub> CH <sup>+</sup> ( <b>2f</b> )	-3.85	2.08 × 10 <sup>3</sup>	3.32
(pfa) <sub>2</sub> CH <sup>+</sup> ( <b>2g</b> )	-3.14	5.15 × 10 <sup>3</sup>	3.71

$$N = 9.87, s_N = 0.55$$



## 11. Reactions of 1-phenylpiperidine (1d) with benzhydrylium ions 2 at the nitrogen atom in CH<sub>3</sub>CN at 20 °C.

**Table S54:** Reaction of 1-phenylpiperidine (**1d**) with (dma)<sub>2</sub>CH<sup>+</sup> BF<sub>4</sub><sup>-</sup> (**2b**) in MeCN (20 °C, stopped-flow, detection at 606 nm).

[E] <sub>0</sub> (M)	[Nu] <sub>0</sub> (M)	[Nu] <sub>0</sub> /[E] <sub>0</sub>	k <sub>obs</sub> (s <sup>-1</sup> )
7.23 × 10 <sup>-6</sup>	4.84 × 10 <sup>-4</sup>	66.9	5.61 × 10 <sup>-1</sup>
7.23 × 10 <sup>-6</sup>	9.68 × 10 <sup>-4</sup>	134	9.12 × 10 <sup>-1</sup>
7.23 × 10 <sup>-6</sup>	1.45 × 10 <sup>-3</sup>	201	1.28
7.23 × 10 <sup>-6</sup>	1.94 × 10 <sup>-3</sup>	268	1.64
7.23 × 10 <sup>-6</sup>	2.42 × 10 <sup>-3</sup>	335	2.07

$$k_2 (20\text{ °C}) = 773\text{ M}^{-1}\text{ s}^{-1}$$

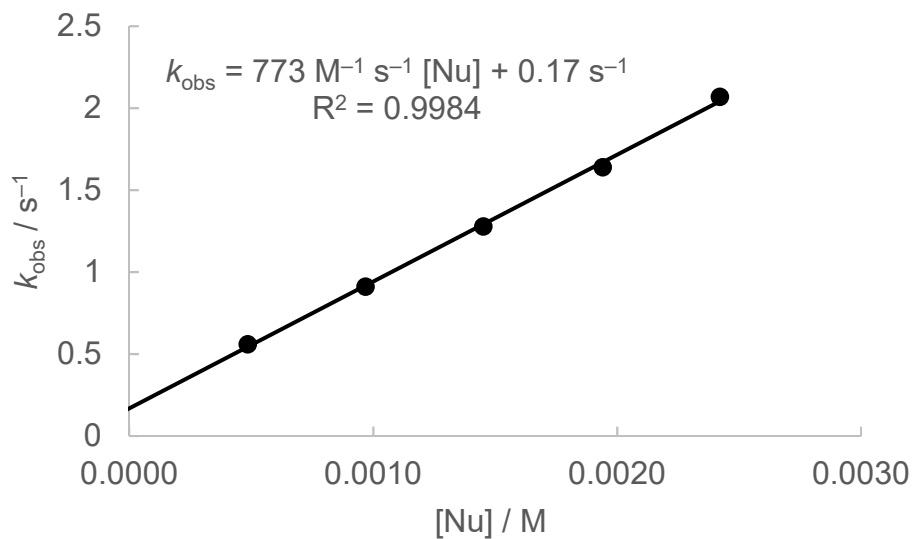
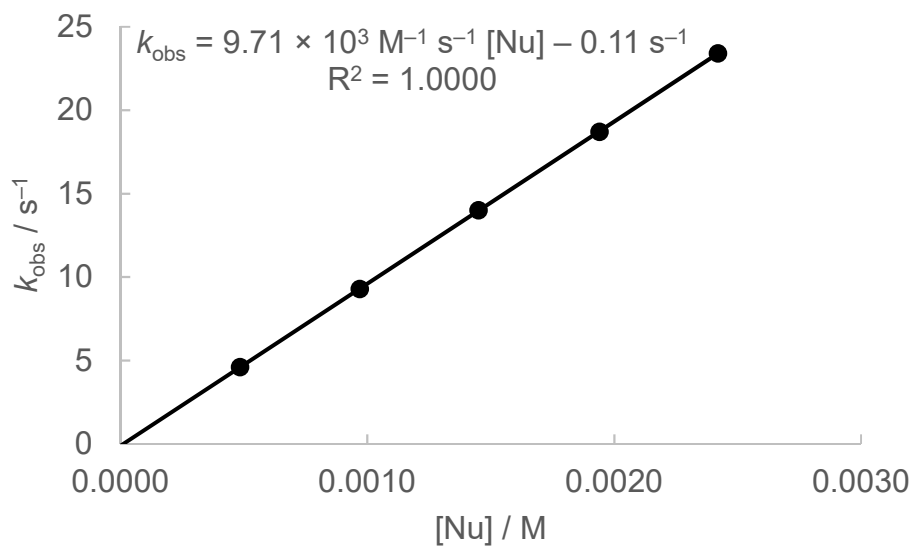


**Table S55:** Reaction of 1-phenylpiperidine (**1d**) with (mor)<sub>2</sub>CH<sup>+</sup> BF<sub>4</sub><sup>-</sup> (**2d**) in MeCN (20 °C, stopped-flow, detection at 612 nm).

[E] <sub>0</sub> (M)	[Nu] <sub>0</sub> (M)	[Nu] <sub>0</sub> /[E] <sub>0</sub>	<i>k</i> <sub>obs</sub> (s <sup>-1</sup> )
9.90 × 10 <sup>-6</sup>	4.84 × 10 <sup>-4</sup>	48.9	4.59
9.90 × 10 <sup>-6</sup>	9.68 × 10 <sup>-4</sup>	97.7	9.28
9.90 × 10 <sup>-6</sup>	1.45 × 10 <sup>-3</sup>	147	14.0
9.90 × 10 <sup>-6</sup>	1.94 × 10 <sup>-3</sup>	196	18.7
9.90 × 10 <sup>-6</sup>	2.42 × 10 <sup>-3</sup>	244	23.4

$$k_2 (20\text{ °C}) = 9.71 \times 10^3 \text{ M}^{-1} \text{ s}^{-1}$$

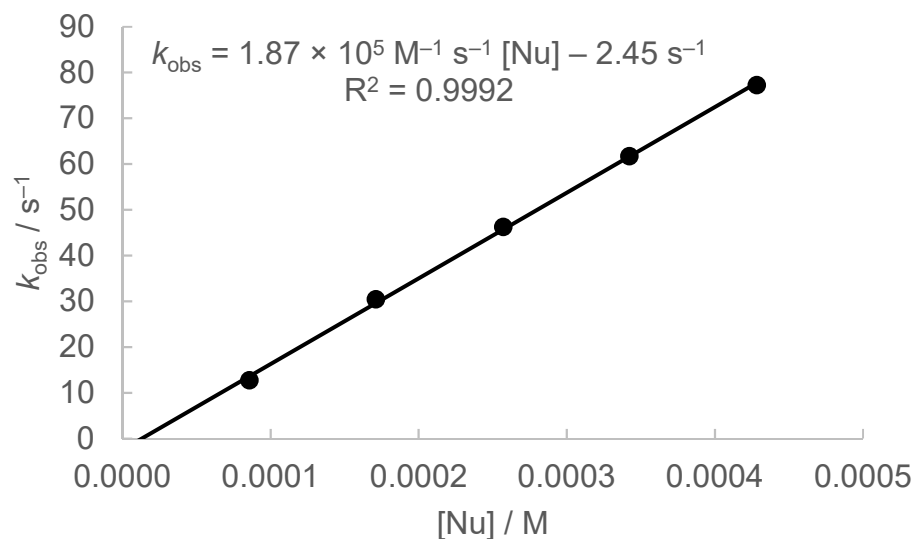


[a] The negative intercept with the abscissa is due to slow/incomplete mixing of the reactants in comparison with the fast reaction.

**Table S56:** Reaction of 1-phenylpiperidine (**1d**) with (mfa)<sub>2</sub>CH<sup>+</sup> BF<sub>4</sub><sup>-</sup> (**2f**) in MeCN (20 °C, stopped-flow, detection at 586 nm).

[E] <sub>0</sub> (M)	[Nu] <sub>0</sub> (M)	[Nu] <sub>0</sub> /[E] <sub>0</sub>	<i>k</i> <sub>obs</sub> (s <sup>-1</sup> )
8.40 × 10 <sup>-6</sup>	8.56 × 10 <sup>-5</sup>	10.2	12.7
8.40 × 10 <sup>-6</sup>	1.71 × 10 <sup>-4</sup>	20.4	30.4
8.40 × 10 <sup>-6</sup>	2.57 × 10 <sup>-4</sup>	30.6	46.2
8.40 × 10 <sup>-6</sup>	3.42 × 10 <sup>-4</sup>	40.8	61.7
8.40 × 10 <sup>-6</sup>	4.28 × 10 <sup>-4</sup>	50.9	77.2

$$k_2 (20\text{ °C}) = 1.87 \times 10^5 \text{ M}^{-1} \text{ s}^{-1}$$

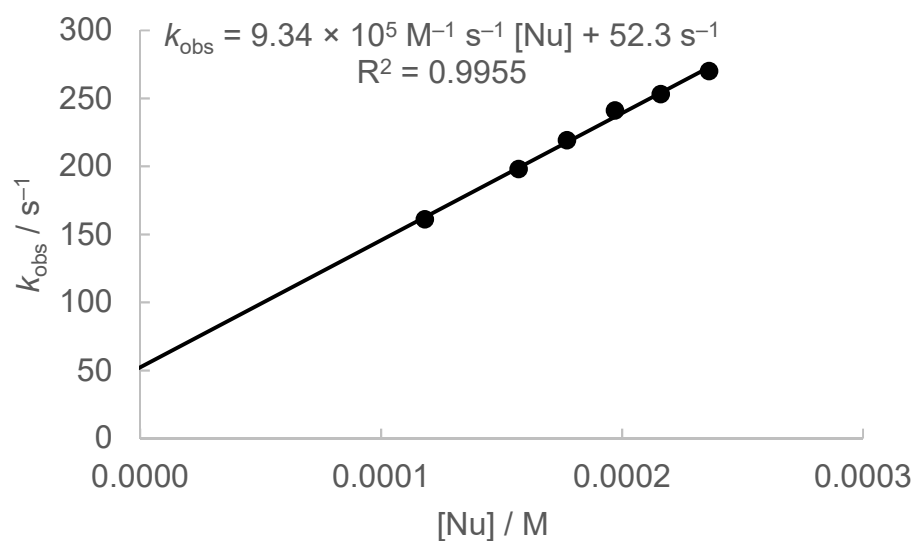


[a] The negative intercept with the abscissa is due to slow/incomplete mixing of the reactants in comparison with the fast reaction.

**Table S57:** Reaction of 1-phenylpiperidine (**1d**) with (pfa)<sub>2</sub>CH<sup>+</sup> BF<sub>4</sub><sup>-</sup> (**2g**) in MeCN (20 °C, stopped-flow, detection at 591 nm).

[E] <sub>0</sub> (M)	[Nu] <sub>0</sub> (M)	[Nu] <sub>0</sub> /[E] <sub>0</sub>	k <sub>obs</sub> (s <sup>-1</sup> )
8.80 × 10 <sup>-6</sup>	1.18 × 10 <sup>-4</sup>	13.4	161
8.80 × 10 <sup>-6</sup>	1.57 × 10 <sup>-4</sup>	17.9	198
8.80 × 10 <sup>-6</sup>	1.77 × 10 <sup>-4</sup>	20.1	219
8.80 × 10 <sup>-6</sup>	1.97 × 10 <sup>-4</sup>	22.4	241
8.80 × 10 <sup>-6</sup>	2.16 × 10 <sup>-4</sup>	24.6	253
8.80 × 10 <sup>-6</sup>	2.36 × 10 <sup>-4</sup>	26.8	270

$$k_2 (20\text{ }^\circ\text{C}) = 9.34 \times 10^5 \text{ M}^{-1} \text{ s}^{-1}$$

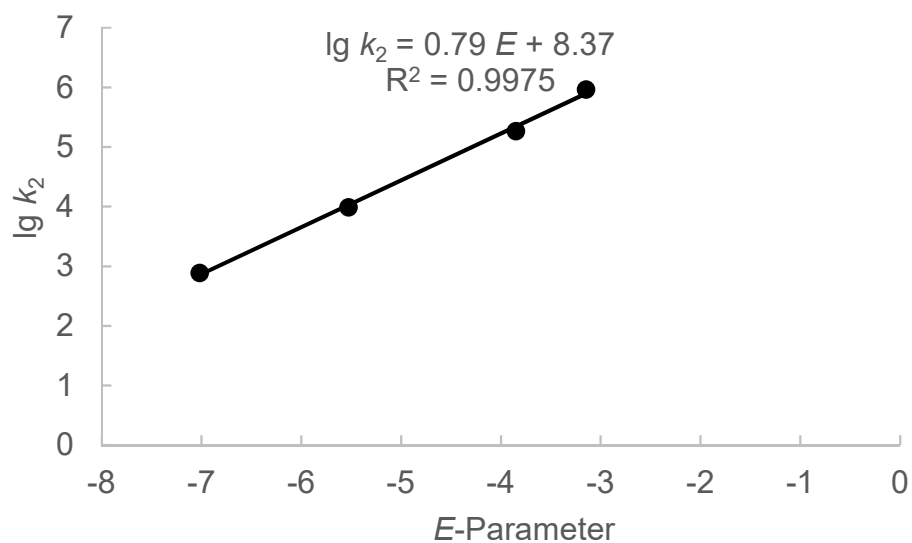


Determination of reactivity parameters  $N$  and  $s_N$  for 1-phenylpiperidine (**1d**) in MeCN at 20 °C at the nitrogen atom.

**Table S58:** Rate constants for the reactions of 1-phenylpiperidine (**1d**) with reference electrophiles (20 °C).

Electrophile	$E$ -Parameter	$k_2$ ( $M^{-1} s^{-1}$ )	$\lg k_2$
(dma) <sub>2</sub> CH <sup>+</sup> ( <b>2b</b> )	-7.02	773	2.89
(mor) <sub>2</sub> CH <sup>+</sup> ( <b>2d</b> )	-5.53	$9.71 \times 10^3$	3.99
(mfa) <sub>2</sub> CH <sup>+</sup> ( <b>2f</b> )	-3.85	$1.87 \times 10^5$	5.27
(pfa) <sub>2</sub> CH <sup>+</sup> ( <b>2g</b> )	-3.15	$9.34 \times 10^5$	5.97

$N = 10.65$ ,  $s_N = 0.79$



## 12. Reactions of *N,N*-dimethyl-*para*-toluidine (1e) with benzhydrylium ions 2 in acetonitrile at 20 °C

### 12.1 Reactions of *N,N*-dimethyl-*para*-toluidine (1e) with benzhydrylium ions 2 at the nitrogen atom in acetonitrile at 20 °C

**Table S59:** Reaction of *N,N*-dimethyl-*para*-toluidine (1e) with (mor)<sub>2</sub>CH<sup>+</sup> BF<sub>4</sub><sup>-</sup> (2d) in acetonitrile (20 °C, stopped-flow, detection at 612 nm).

[E] <sub>0</sub> (M)	[Nu] <sub>0</sub> (M)	[Nu] <sub>0</sub> /[E] <sub>0</sub>	<i>k</i> <sub>obs</sub> (s <sup>-1</sup> )
1.11 × 10 <sup>-5</sup>	4.91 × 10 <sup>-4</sup>	44.3	8.86 × 10 <sup>-1</sup>
1.11 × 10 <sup>-5</sup>	6.88 × 10 <sup>-4</sup>	62.1	1.44
1.11 × 10 <sup>-5</sup>	8.84 × 10 <sup>-4</sup>	79.8	1.74
1.11 × 10 <sup>-5</sup>	1.47 × 10 <sup>-3</sup>	133	2.57

$$k_2 (20 \text{ °C}) = 1.64 \times 10^3 \text{ M}^{-1} \text{ s}^{-1}$$

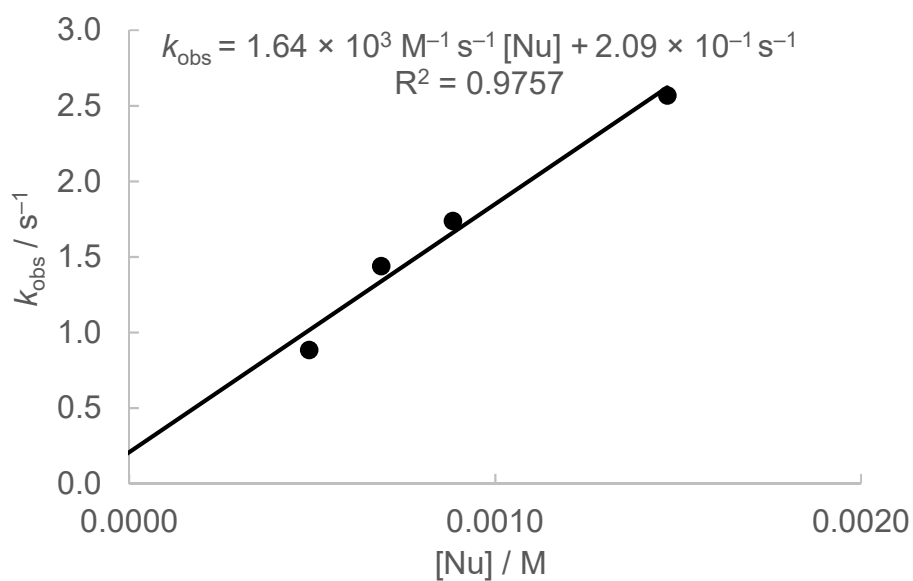


**Table S60:** Reaction of *N,N*-dimethyl-*para*-toluidine (**1e**) with (dpa)<sub>2</sub>CH<sup>+</sup> BF<sub>4</sub><sup>-</sup> (**2e**) in MeCN (20 °C, stopped-flow, detection at 644 nm).

[E] <sub>0</sub> (M)	[Nu] <sub>0</sub> (M)	[Nu] <sub>0</sub> /[E] <sub>0</sub>	<i>k</i> <sub>obs</sub> (s <sup>-1</sup> )
1.22 × 10 <sup>-5</sup>	2.95 × 10 <sup>-4</sup>	24.2	9.09
1.22 × 10 <sup>-5</sup>	4.91 × 10 <sup>-4</sup>	40.3	9.94
1.22 × 10 <sup>-5</sup>	1.08 × 10 <sup>-3</sup>	88.5	14.6
1.22 × 10 <sup>-5</sup>	1.47 × 10 <sup>-3</sup>	120	16.7

$$k_2 (20\text{ }^\circ\text{C}) = 6.76 \times 10^3 \text{ M}^{-1} \text{ s}^{-1}$$

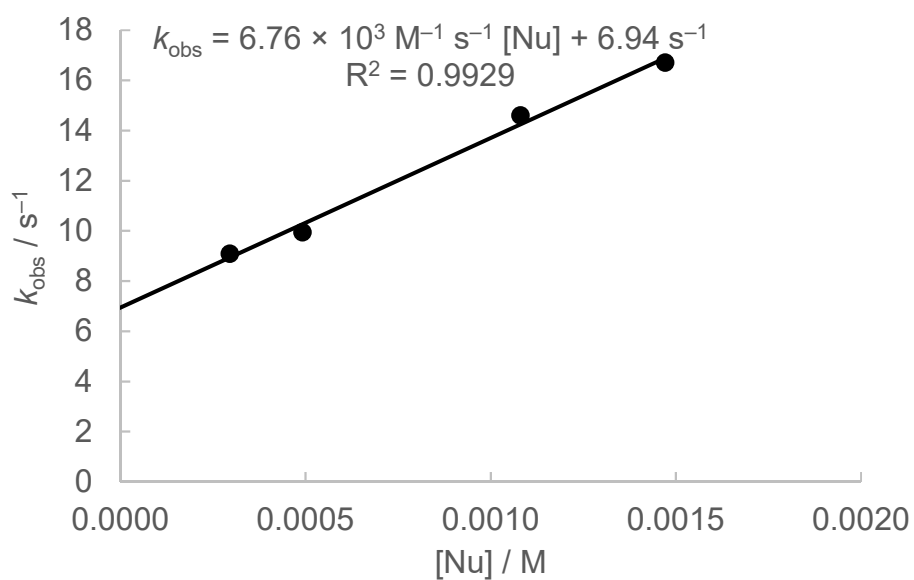
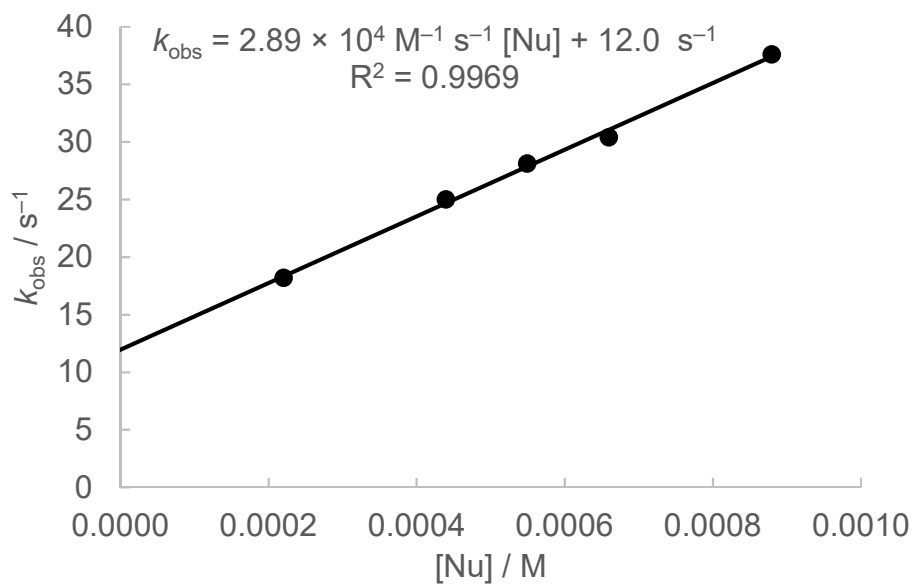


**Table S61:** Reaction of *N,N*-dimethyl-*para*-toluidine (**1e**) with (pfa)<sub>2</sub>CH<sup>+</sup> BF<sub>4</sub><sup>-</sup> (**2g**) in MeCN (20 °C, stopped-flow, detection at 592 nm).

[E] <sub>0</sub> (M)	[Nu] <sub>0</sub> (M)	[Nu] <sub>0</sub> /[E] <sub>0</sub>	<i>k</i> <sub>obs</sub> (s <sup>-1</sup> )
1.76 × 10 <sup>-5</sup>	2.20 × 10 <sup>-4</sup>	12.5	18.2
1.76 × 10 <sup>-5</sup>	4.39 × 10 <sup>-4</sup>	24.9	25.0
1.76 × 10 <sup>-5</sup>	5.49 × 10 <sup>-4</sup>	31.2	28.1
1.76 × 10 <sup>-5</sup>	6.59 × 10 <sup>-4</sup>	37.4	30.4
1.76 × 10 <sup>-5</sup>	8.79 × 10 <sup>-4</sup>	49.9	37.6

$$k_2 (20\text{ °C}) = 2.89 \times 10^4 \text{ M}^{-1} \text{ s}^{-1}$$

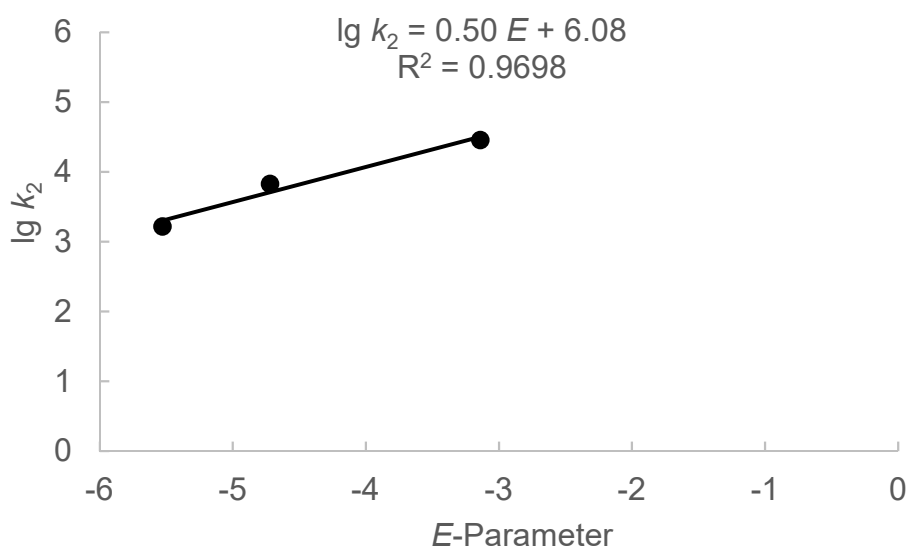


Determination of reactivity parameters  $N$  and  $s_N$  for  $N,N$ -dimethyl-*para*-toluidine (**1e**) in MeCN at 20 °C at the nitrogen atom.

**Table S62:** Rate constants for the reactions of  $N,N$ -dimethyl-*para*-toluidine (**1e**) with reference electrophiles (20 °C).

Electrophile	$E$ -Parameter	$k_2$ ( $M^{-1} s^{-1}$ )	$\lg k_2$
(mor) <sub>2</sub> CH <sup>+</sup> ( <b>2d</b> )	-5.53	$1.64 \times 10^3$	3.22
(dpa) <sub>2</sub> CH <sup>+</sup> ( <b>2e</b> )	-4.72	$6.76 \times 10^3$	3.83
(pfa) <sub>2</sub> CH <sup>+</sup> ( <b>2g</b> )	-3.14	$2.89 \times 10^4$	4.46

$N = 12.16$ ,  $s_N = 0.50$



## 12.2 Subsequent reactions of *N,N*-dimethyl-*para*-toluidine (**1e**) with benzhydrylium ions **2** after the attack at the nitrogen atom in acetonitrile at 20 °C

**Table S63:** Reaction of *N,N*-dimethyl-*para*-toluidine (**1e**) with (mfa)<sub>2</sub>CH<sup>+</sup> BF<sub>4</sub><sup>-</sup> (**2f**) in acetonitrile (20 °C, stopped-flow, detection at 586 nm).

[E] <sub>0</sub> (M)	[Nu] <sub>0</sub> (M)	[Nu] <sub>0</sub> /[E] <sub>0</sub>	<i>k</i> <sub>obs</sub> (s <sup>-1</sup> )
9.05 × 10 <sup>-6</sup>	6.43 × 10 <sup>-4</sup>	71.0	3.71 × 10 <sup>-1</sup>
9.05 × 10 <sup>-6</sup>	9.64 × 10 <sup>-4</sup>	107	4.77 × 10 <sup>-1</sup>
9.05 × 10 <sup>-6</sup>	1.29 × 10 <sup>-3</sup>	143	5.09 × 10 <sup>-1</sup>
9.05 × 10 <sup>-6</sup>	1.64 × 10 <sup>-3</sup>	181	6.29 × 10 <sup>-1</sup>
9.05 × 10 <sup>-6</sup>	1.96 × 10 <sup>-3</sup>	217	7.25 × 10 <sup>-1</sup>

$$k_2 (20\text{ °C}) = 260\text{ M}^{-1}\text{ s}^{-1}$$

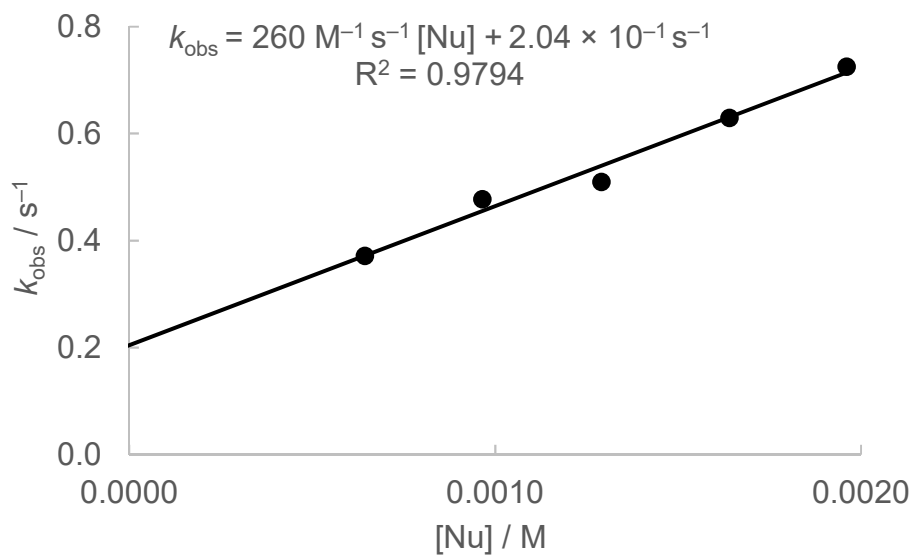
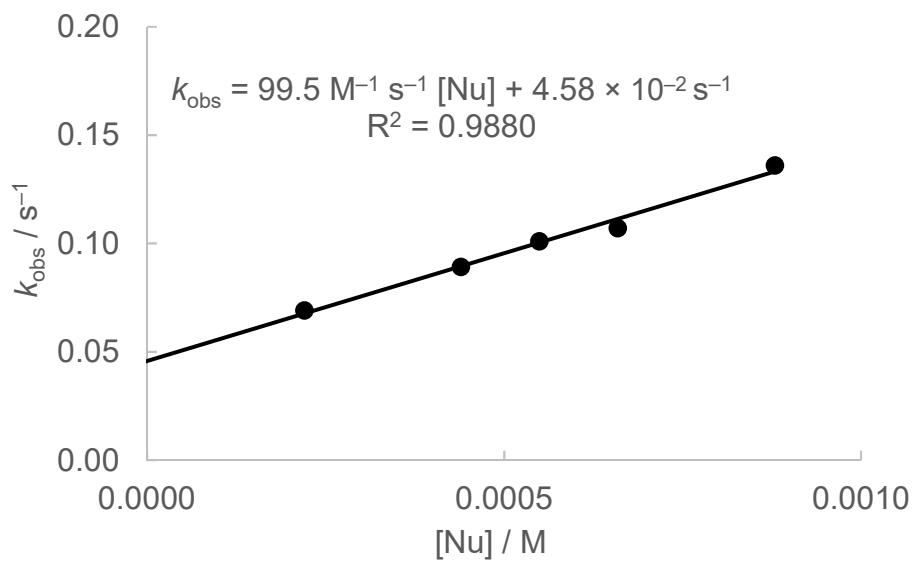


**Table S64:** Reaction of *N,N*-dimethyl-*para*-toluidine (**1e**) with (pfa)<sub>2</sub>CH<sup>+</sup> BF<sub>4</sub><sup>-</sup> (**2g**) in MeCN (20 °C, stopped-flow, detection at 592 nm).

[E] <sub>0</sub> (M)	[Nu] <sub>0</sub> (M)	[Nu] <sub>0</sub> /[E] <sub>0</sub>	<i>k</i> <sub>obs</sub> (s <sup>-1</sup> )
1.76 × 10 <sup>-5</sup>	2.20 × 10 <sup>-4</sup>	12.5	6.91 × 10 <sup>-2</sup>
1.76 × 10 <sup>-5</sup>	4.39 × 10 <sup>-4</sup>	24.9	8.91 × 10 <sup>-2</sup>
1.76 × 10 <sup>-5</sup>	5.49 × 10 <sup>-4</sup>	31.2	1.01 × 10 <sup>-1</sup>
1.76 × 10 <sup>-5</sup>	6.59 × 10 <sup>-4</sup>	37.4	1.07 × 10 <sup>-1</sup>
1.76 × 10 <sup>-5</sup>	8.79 × 10 <sup>-4</sup>	49.9	1.36 × 10 <sup>-1</sup>

$$k_2 (20\text{ }^\circ\text{C}) = 99.5\text{ M}^{-1}\text{ s}^{-1}$$

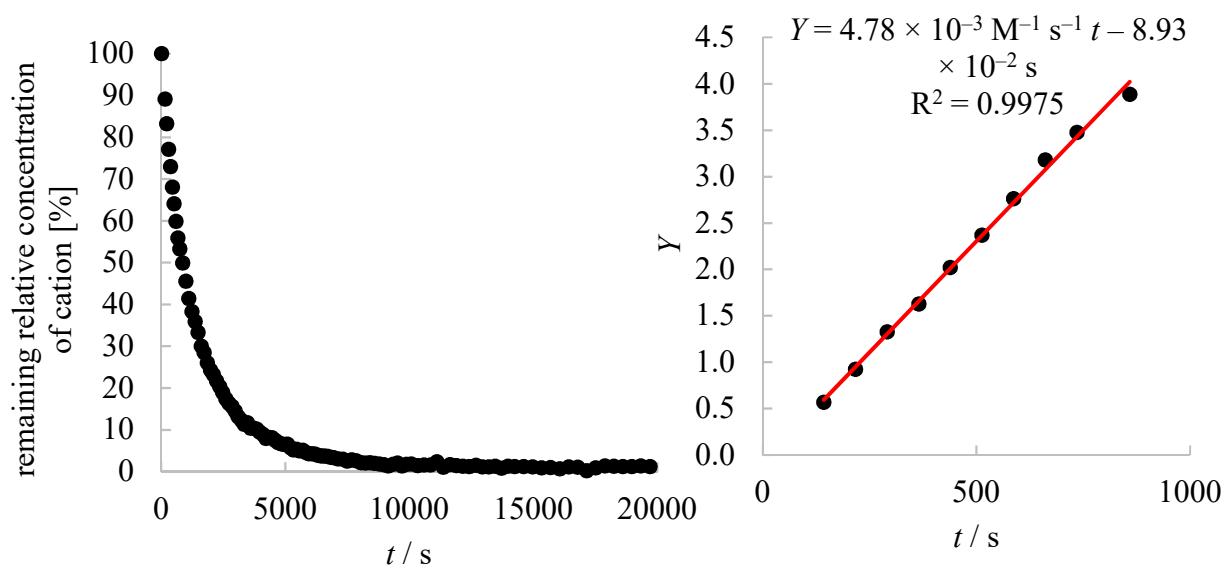


### 13. Reactions of *N,N*-dimethyl-*para*-toluidine (**1e**) with tritylium ions in acetonitrile

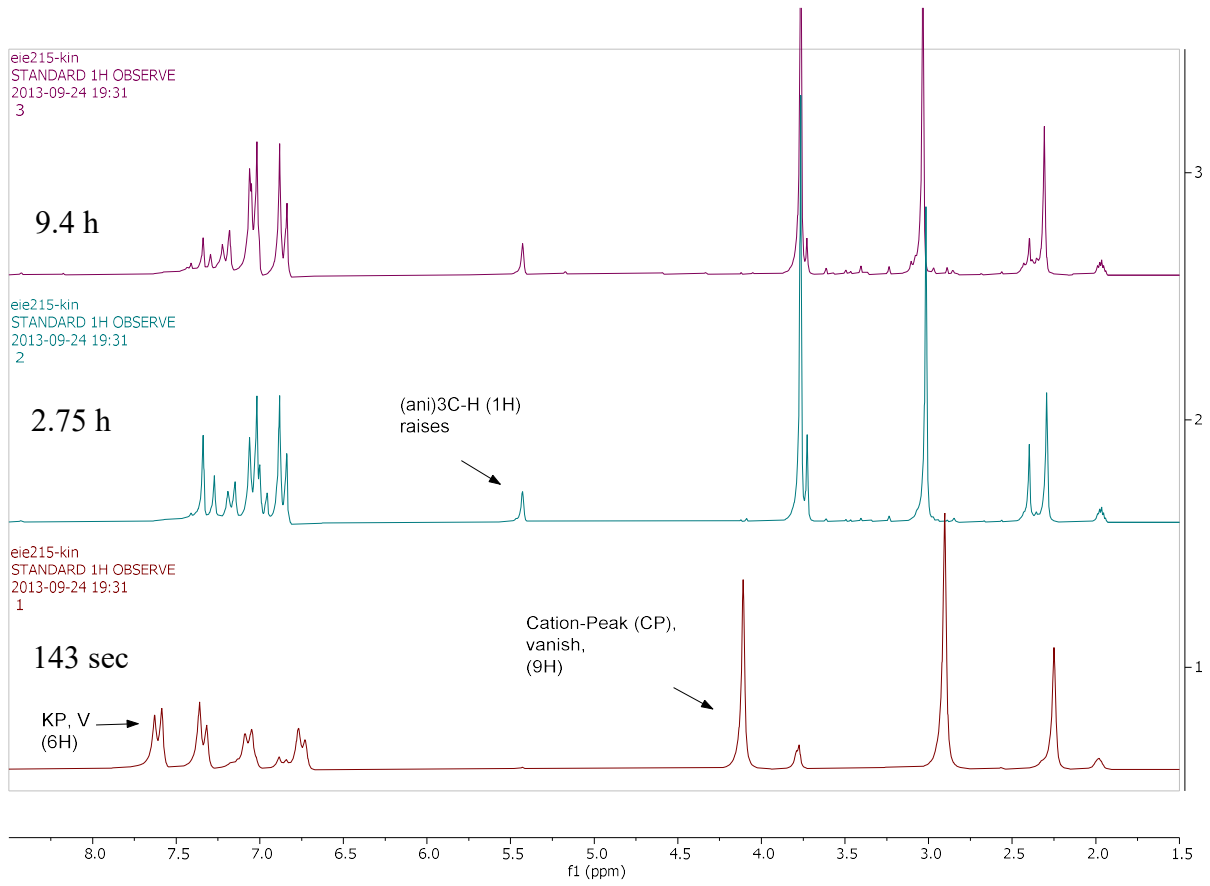
**Table S65:** Reaction of *N,N*-dimethyl-*para*-toluidine (**1e**) with  $(\text{ani})_3\text{C}^+ \text{BF}_4^-$  in  $\text{CD}_3\text{CN}$  (23 °C,  $^1\text{H}$  NMR spectroscopy). The rest ani = *p*-MeOC<sub>6</sub>H<sub>4</sub>.

$[\text{E}]_0$ (M)	$[\text{Nu}]_0$ (M)	$[\text{Nu}]_0/[\text{E}]_0$	$k_2$ ( $\text{M}^{-1} \text{s}^{-1}$ )
$1.00 \times 10^{-1}$	$2.08 \times 10^{-1}$	2.08	$4.78 \times 10^{-3}$

$$k_2 (23 \text{ °C}) = 4.78 \times 10^{-3} \text{M}^{-1} \text{s}^{-1}$$



Decay of the relative concentration of  $(\text{ani})_3\text{C}^+ \text{BF}_4^-$  while reacting with *N,N*-dimethyl-*para*-toluidine (**1e**) in  $\text{CD}_3\text{CN}$  at 23 °C (left). Determination of the second order rate constant by plotting time versus  $Y = ([\text{Nu}]_0 - [\text{E}]_0)^{-1} \ln([\text{E}]_0([\text{E}]_t + [\text{Nu}]_0 - [\text{E}]_0) / [\text{Nu}]_0[\text{E}]_t)$  ( $k_2 = 4.78 \times 10^{-3} \text{M}^{-1} \text{s}^{-1}$ , data points up to 50% conversion were used; right).



## 14. Reactions of *N,N*-dimethyl-*para*-anisidine (1f) with benzhydrylium ion 2 in acetonitrile at 20 °C.

### 14.1 Reactions of *N,N*-dimethyl-*para*-anisidine (1f) with benzhydrylium ions 2 at the nitrogen atom in acetonitrile at 20 °C

**Table S66:** Reaction of *N,N*-dimethyl-*para*-anisidine (1f) with (mor)<sub>2</sub>CH<sup>+</sup> BF<sub>4</sub><sup>-</sup> (2d) in acetonitrile (20 °C, stopped-flow, detection at 612 nm).

[E] <sub>0</sub> (M)	[Nu] <sub>0</sub> (M)	[Nu] <sub>0</sub> /[E] <sub>0</sub>	<i>k</i> <sub>obs</sub> (s <sup>-1</sup> )
1.23 × 10 <sup>-5</sup>	6.22 × 10 <sup>-4</sup>	50.6	3.06
1.23 × 10 <sup>-5</sup>	1.24 × 10 <sup>-3</sup>	101	3.25
1.23 × 10 <sup>-5</sup>	2.00 × 10 <sup>-3</sup>	163	3.50
1.23 × 10 <sup>-5</sup>	2.67 × 10 <sup>-3</sup>	217	3.64
1.23 × 10 <sup>-5</sup>	3.33 × 10 <sup>-3</sup>	271	3.83
1.23 × 10 <sup>-5</sup>	4.00 × 10 <sup>-3</sup>	325	4.01

$$k_2 (20\text{ °C}) = 278\text{ M}^{-1}\text{ s}^{-1}$$

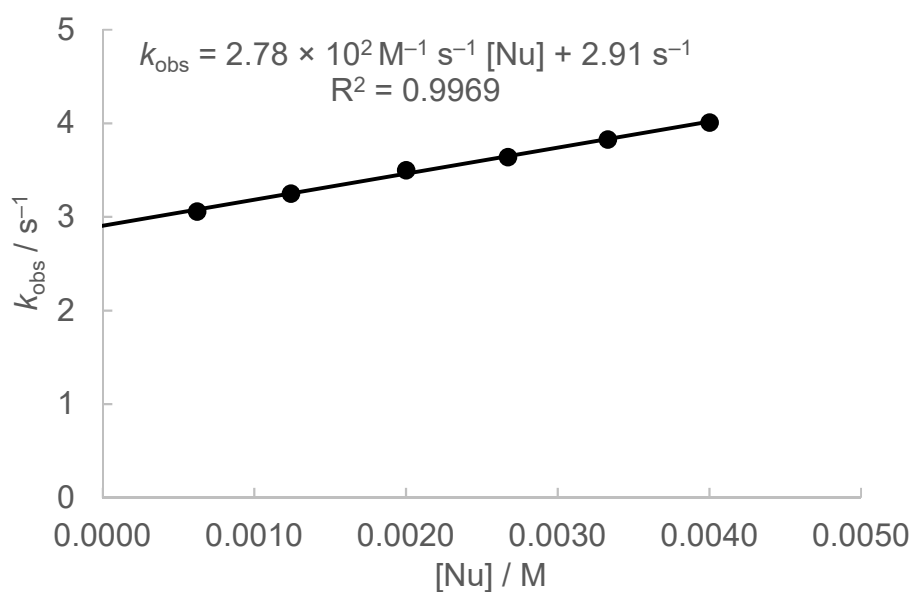
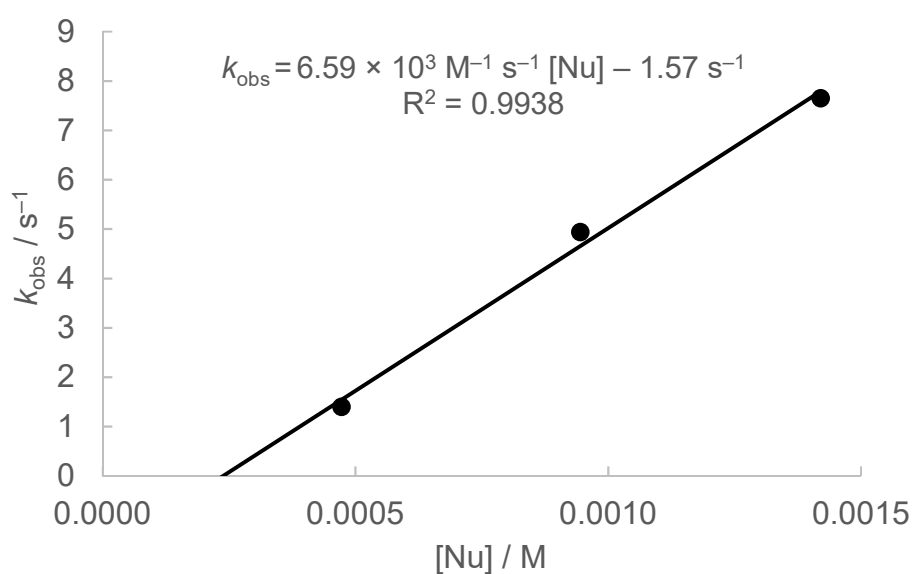


**Table S67:** Reaction of *N,N*-dimethyl-*para*-anisidine (**1f**) with (pfa)<sub>2</sub>CH<sup>+</sup> BF<sub>4</sub><sup>-</sup> (**2g**) in MeCN (20 °C, stopped-flow, detection at 592 nm).

[E] <sub>0</sub> (M)	[Nu] <sub>0</sub> (M)	[Nu] <sub>0</sub> /[E] <sub>0</sub>	<i>k</i> <sub>obs</sub> (s <sup>-1</sup> )
1.70 × 10 <sup>-5</sup>	4.72 × 10 <sup>-4</sup>	27.8	1.40
1.70 × 10 <sup>-5</sup>	9.44 × 10 <sup>-4</sup>	55.5	4.94
1.70 × 10 <sup>-5</sup>	1.42 × 10 <sup>-3</sup>	83.5	7.65

$$k_2 (20\text{ °C}) = 6.59 \times 10^3 \text{ M}^{-1} \text{ s}^{-1}$$



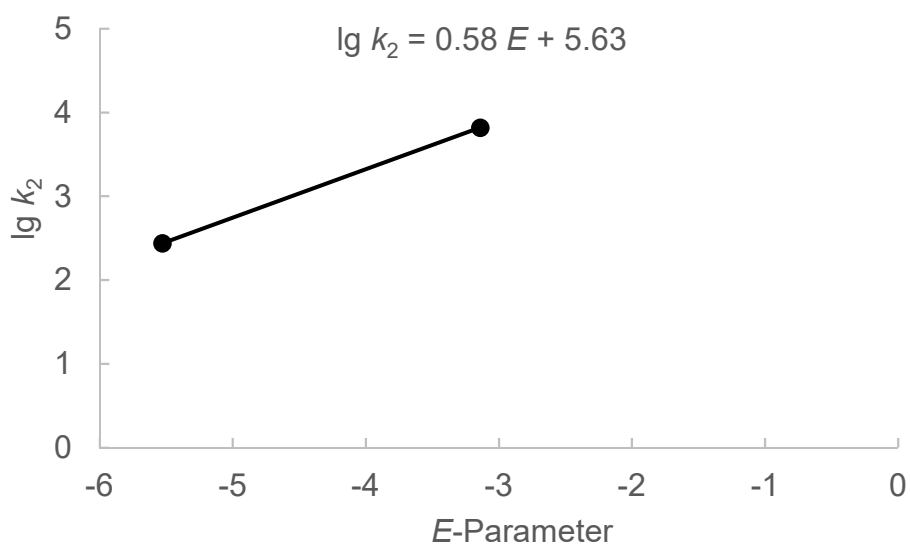
[a] The negative intercept with the abscissa is due to slow/incomplete mixing of the reactants in comparison with the fast reaction.

Determination of reactivity parameters  $N$  and  $s_N$  for  $N,N$ -dimethyl-*para*-anisidine (**1f**) in MeCN at 20 °C at the nitrogen atom.

**Table S68:** Rate constants for the reactions of  $N,N$ -dimethyl-*para*-anisidine (**1f**) with reference electrophiles (20 °C).

Electrophile	$E$ -Parameter	$k_2$ ( $M^{-1} s^{-1}$ )	$\lg k_2$
(mor) <sub>2</sub> CH <sup>+</sup> ( <b>2d</b> )	-5.53	278	2.44
(pfa) <sub>2</sub> CH <sup>+</sup> ( <b>2g</b> )	-3.14	$6.59 \times 10^3$	3.82

$N = 9.71$ ,  $s_N = 0.58$

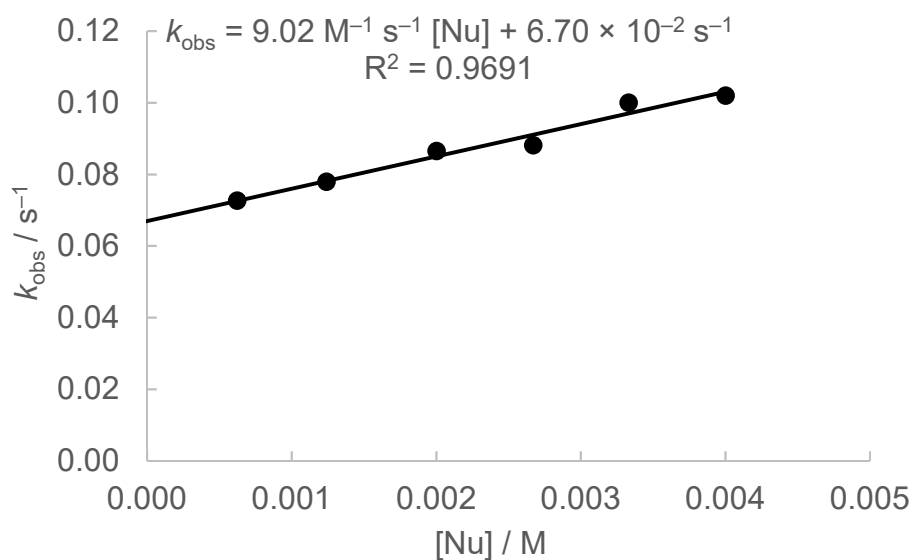


## 14.2 Subsequent reactions of *N,N*-dimethyl-*para*-anisidine (1f) with benzhydrylium ions 2 after the attack at the nitrogen atom in acetonitrile at 20 °C

**Table S69:** Reaction of *N,N*-dimethyl-*para*-anisidine (1f) with (mor)<sub>2</sub>CH<sup>+</sup> BF<sub>4</sub><sup>-</sup> (2d) in acetonitrile (20 °C, stopped-flow, detection at 612 nm).

[E] <sub>0</sub> (M)	[Nu] <sub>0</sub> (M)	[Nu] <sub>0</sub> /[E] <sub>0</sub>	<i>k</i> <sub>obs</sub> (s <sup>-1</sup> )
1.23 × 10 <sup>-5</sup>	6.22 × 10 <sup>-4</sup>	50.6	7.26 × 10 <sup>-2</sup>
1.23 × 10 <sup>-5</sup>	1.24 × 10 <sup>-3</sup>	101	7.79 × 10 <sup>-2</sup>
1.23 × 10 <sup>-5</sup>	2.00 × 10 <sup>-3</sup>	163	8.65 × 10 <sup>-2</sup>
1.23 × 10 <sup>-5</sup>	2.67 × 10 <sup>-3</sup>	217	8.81 × 10 <sup>-2</sup>
1.23 × 10 <sup>-5</sup>	3.33 × 10 <sup>-3</sup>	271	1.00 × 10 <sup>-1</sup>
1.23 × 10 <sup>-5</sup>	4.00 × 10 <sup>-3</sup>	325	1.02 × 10 <sup>-1</sup>

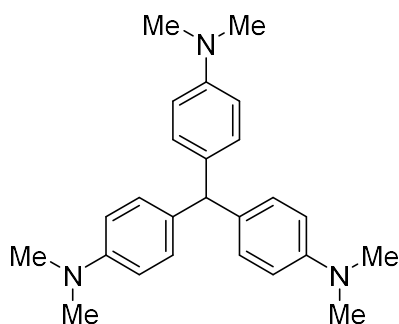
$$k_2 (20\text{ °C}) = 9.02\text{ M}^{-1}\text{ s}^{-1}$$



## 15. Products of the reaction of *N,N*-dialkylated anilines **1** with benzhydryl ions **2**

### General Procedure 1 (GP1):

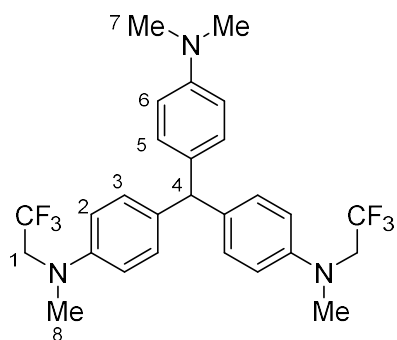
To a solution of **2** in dry MeCN or dichloromethane (5 mL) was added **1** dropwise and stirred at room temperature for the indicated time. The reaction mixtures did not decolorize completely. After reaction completeness was indicated by TLC, NaOH solution (2 M, 10 mL) was added and extracted with dichloromethane (3x 10 mL). The combined organic layers were evaporated and purified by flush chromatography (gradient i-hexane/acetone = 1:0 to 5:1) yielded in slightly colored powders.



According to GP1 *N,N*-dimethylaniline (**1a**, 32.6 mg, 0.269 mmol) and **2b** (81.6 mg, 0.240 mmol) in dry MeCN (5 mL) yielded 4,4',4''-methanetriyltris(*N,N*-dimethylaniline) (63.0 mg, 0.169 mmol, 70%) as slightly violet powder.

<sup>1</sup>H and <sup>13</sup>C NMR is according to literature.<sup>[15]</sup>

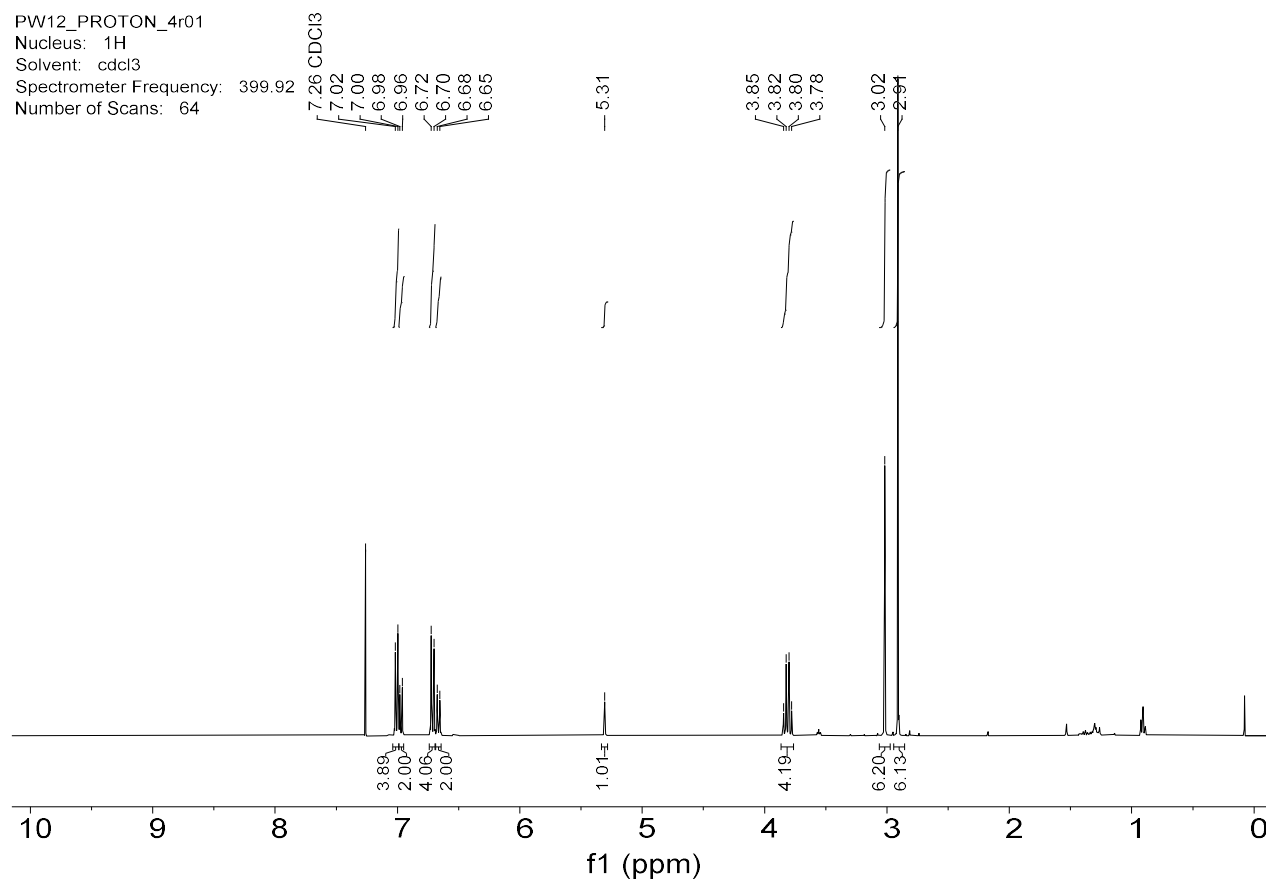
Elemental Analysis: calcd for [C<sub>25</sub>H<sub>31</sub>N<sub>3</sub>]: C: 80.39, H: 8.37, N: 11.25; found: C: 80.47, H: 8.56, N: 11.26.



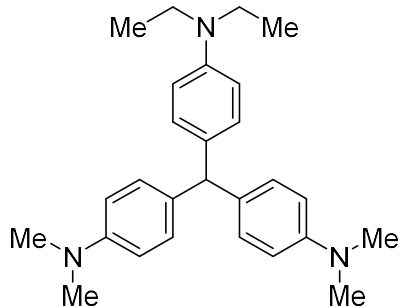
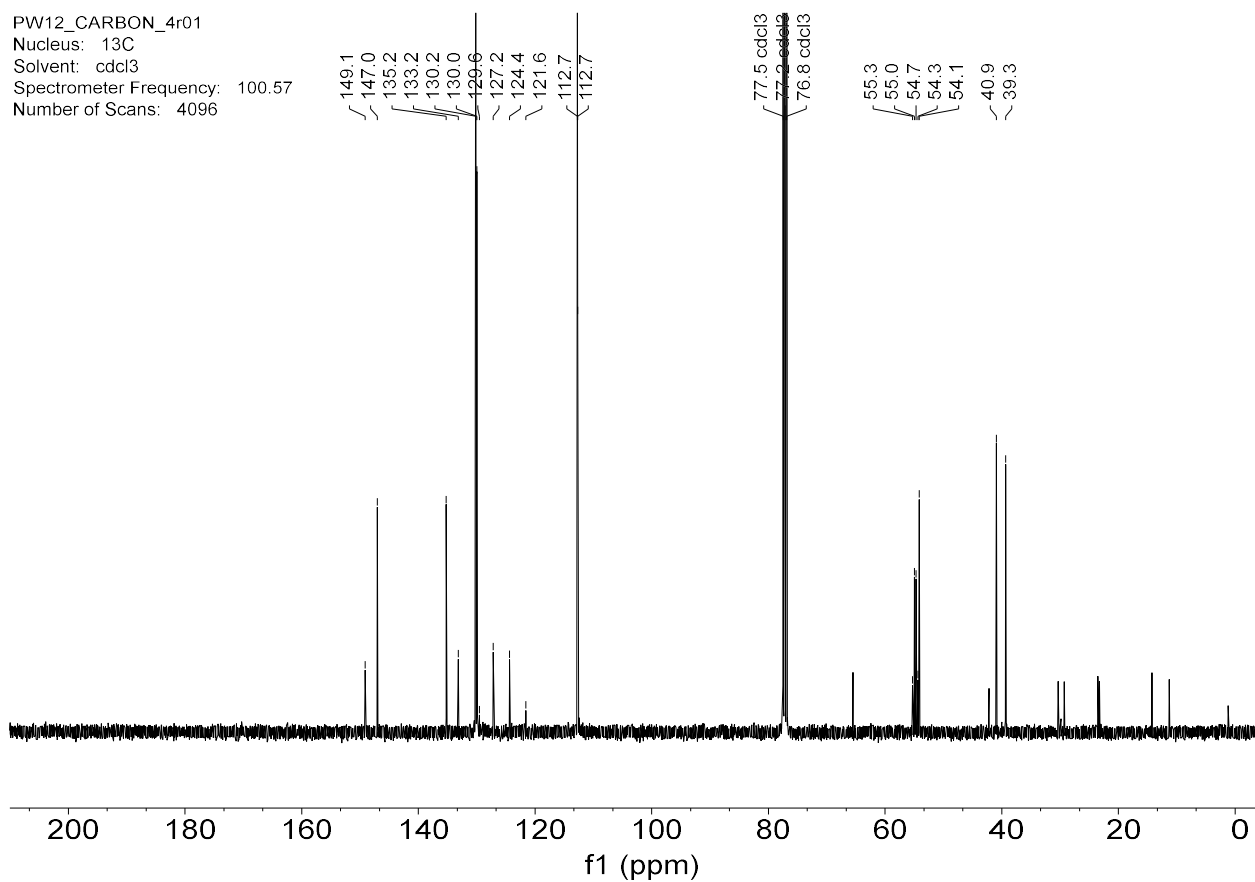
According to GP1 *N,N*-dimethylaniline (**1a**, 22.1 mg, 0.182 mmol) and **2f** (78.0 mg, 0.164 mmol) in dry dichloromethane (5 mL) yielded 4,4'-((4-(dimethylamino)phenyl)methylene)bis(*N*-methyl-*N*-(2,2,2-trifluoroethyl)aniline) (70.0 mg, 0.137 mmol, 84%) as slightly bluish powder.

$^1\text{H}$  NMR (400 MHz, Chloroform-*d*)  $\delta$  7.01 (d,  $J = 8.3$  Hz, 4H, 3-H), 6.97 (d,  $J = 8.3$  Hz, 2H, 5-H), 6.71 (d,  $J = 8.8$  Hz, 4H, 2-H), 6.66 (d,  $J = 8.8$  Hz, 2H, 6-H), 5.31 (s, 1H, 4-H), 3.81 (q,  $J = 9.0$  Hz, 4H, 1-H), 3.02 (s, 6H, 8-H), 2.91 (s, 6H, 7-H).

$^{13}\text{C}$  NMR (101 MHz, Chloroform-*d*)  $\delta$  149.1 (q,  $\text{CNMe}_2$ ), 147.0 (q,  $\text{CNMeCH}_2\text{CF}_3$ ), 135.2 (q,  $2 \times \text{C}_{\text{arom}}$ ), 133.2 (q,  $1 \times \text{C}_{\text{arom}}$ ), 130.2 (3-C), 130.0 (5-C), 125.8 (q,  $J = 282.7$  Hz,  $\text{CF}_3$ ), 112.7 (6-C and 2-C), 54.8 (q,  $J = 32.6$  Hz,  $\text{CH}_2\text{CF}_3$ ), 54.1 (4-C), 40.9 (7-C), 39.3 (8-C).



PW12\_CARBON\_4r01  
 Nucleus: 13C  
 Solvent: cdcl3  
 Spectrometer Frequency: 100.57  
 Number of Scans: 4096

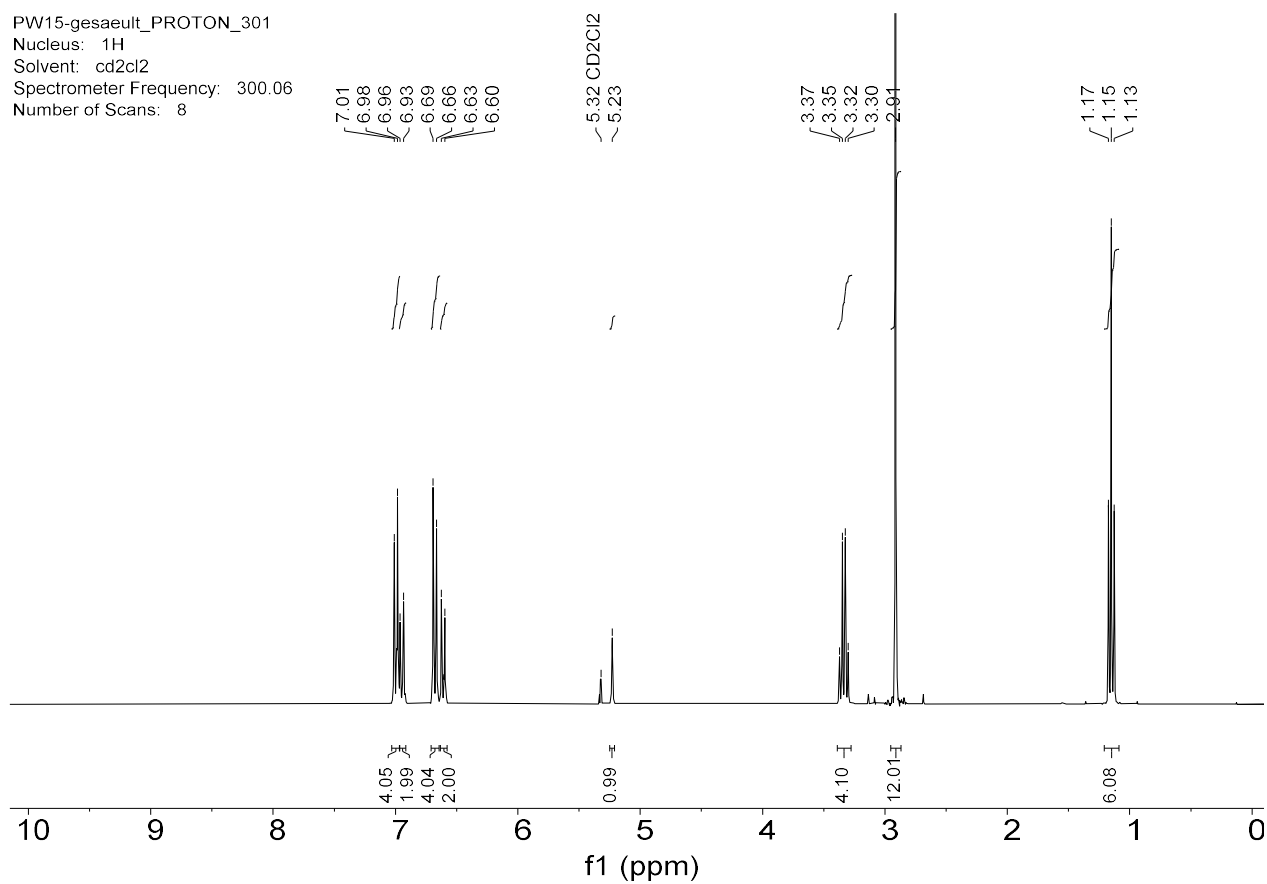


According to GP1 *N,N*-diethylaniline (**1b**, 53.9 mg, 0.361 mmol) and **2b** (110.0 mg, 0.323 mmol) in dry MeCN (5 mL) yielded after five days 4,4'-((4-(diethylamino)phenyl)methylene)bis(*N,N*-dimethylaniline) (97.0 mg, 0.242 mmol, 75%) as slightly bluish powder.

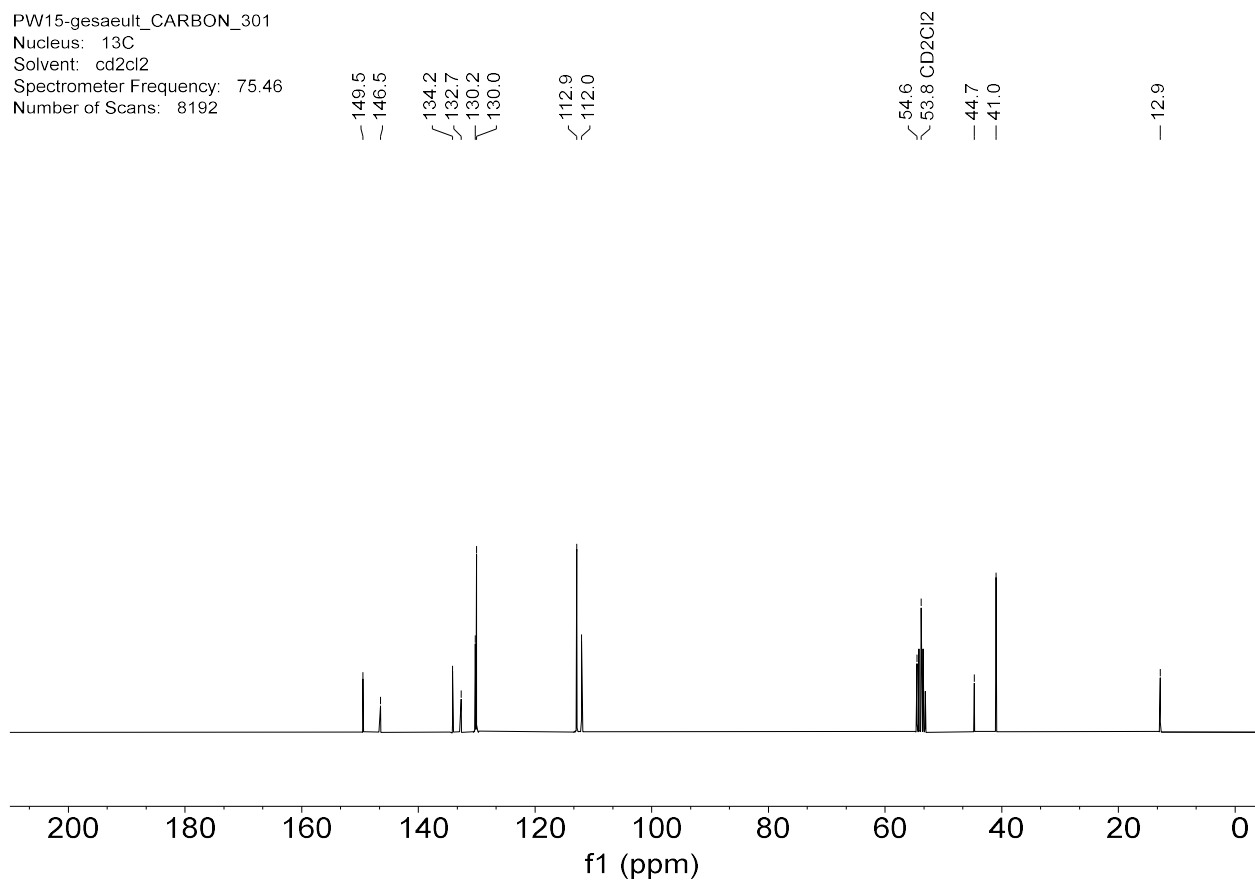
$^1\text{H}$  NMR (300 MHz, Methylene Chloride- $d_2$ )  $\delta$  7.00 (d,  $J = 8.3$  Hz, 4H), 6.95 (d,  $J = 8.3$  Hz, 2H), 6.68 (d,  $J = 8.9$  Hz, 4H), 6.61 (d,  $J = 8.9$  Hz, 2H), 5.23 (s, 1H), 3.34 (q,  $J = 7.0$  Hz, 4H), 2.91 (s, 12H), 1.15 (t,  $J = 7.0$  Hz, 6H).

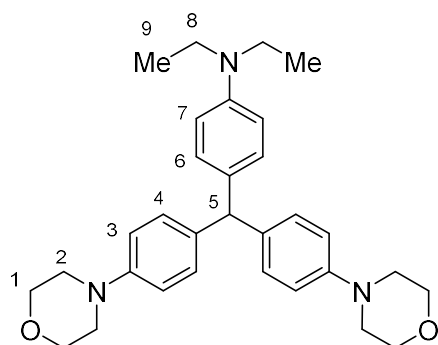
$^{13}\text{C}$  NMR (75 MHz, Methylene Chloride- $d_2$ )  $\delta$  149.5, 146.5, 134.2, 132.7, 130.2, 130.0, 112.9, 112.0, 54.6 (superimposed), 44.7, 41.0, 12.9.

PW15-gesaeult\_PROTON\_301  
Nucleus: 1H  
Solvent: cd2cl2  
Spectrometer Frequency: 300.06  
Number of Scans: 8



PW15-gesaeult\_CARBON\_301  
Nucleus: 13C  
Solvent: cd2cl2  
Spectrometer Frequency: 75.46  
Number of Scans: 8192





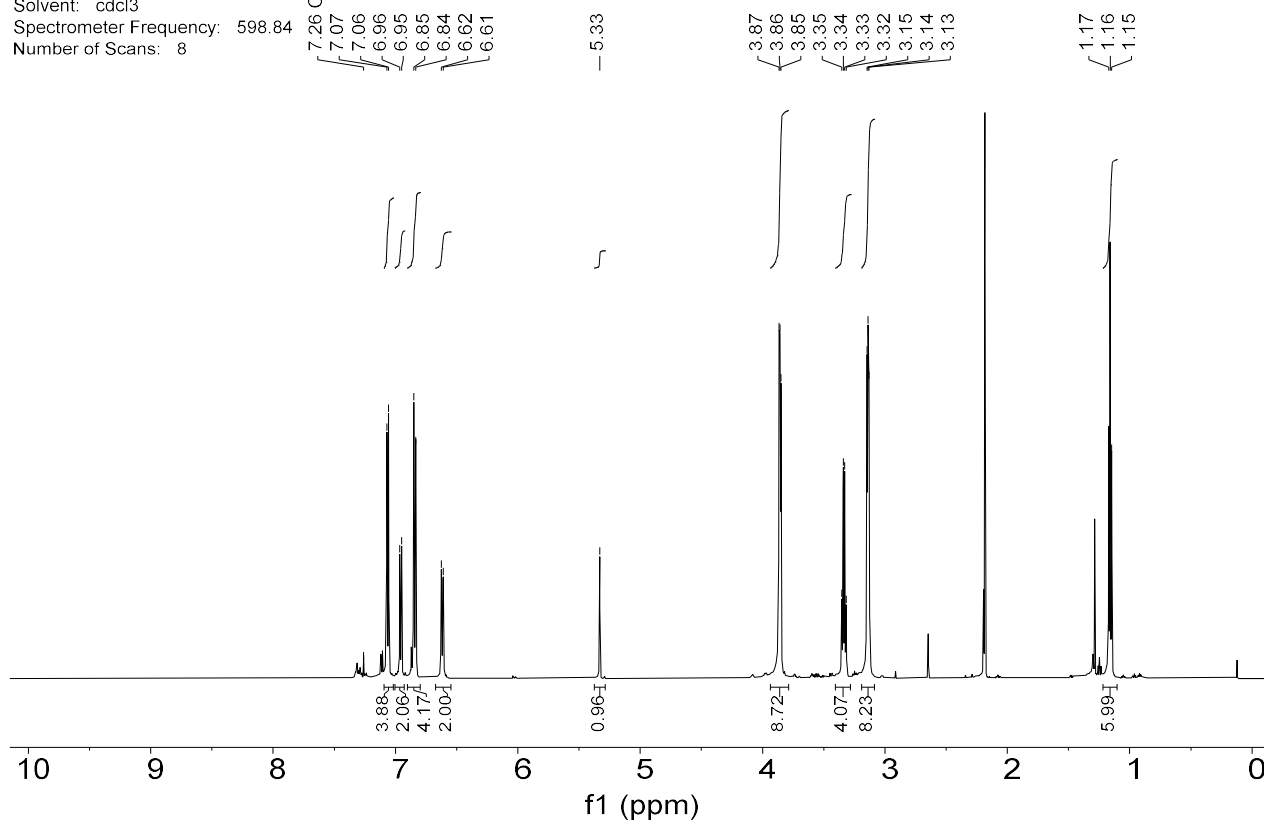
According to GP1 *N,N*-diethylaniline (**1b**, 33.0 mg, 0.221 mmol) and **2d** (93.8 mg, 0.221 mmol) in dry MeCN (5 mL) yielded after 24 h 4-(bis(4-morpholinophenyl)methyl)-*N,N*-diethylaniline (90.0 mg, 0.185 mmol, 84%) as slightly bluish powder.

$^1\text{H}$  NMR (599 MHz, Chloroform-*d*)  $\delta$  7.06 (d,  $J = 8.7$  Hz, 4H, 4-H), 6.96 (d,  $J = 8.8$  Hz, 2H, 6-H), 6.84 (d,  $J = 8.4$  Hz, 4H, 7-H), 6.62 (d,  $J = 8.7$  Hz, 2H, 3-H), 5.33 (s, 1H, 5-H), 3.94 – 3.79 (m, 8H, 1-H), 3.33 (q,  $J = 7.1$  Hz, 4H, 8-H), 3.19 – 3.09 (m, 8H, 2-H), 2.18 (s, 3H), 1.16 (t,  $J = 7.0$  Hz, 6H, 9-H). The additional resonance at  $\delta = 2.16$  ppm is caused by trace amounts of acetone.

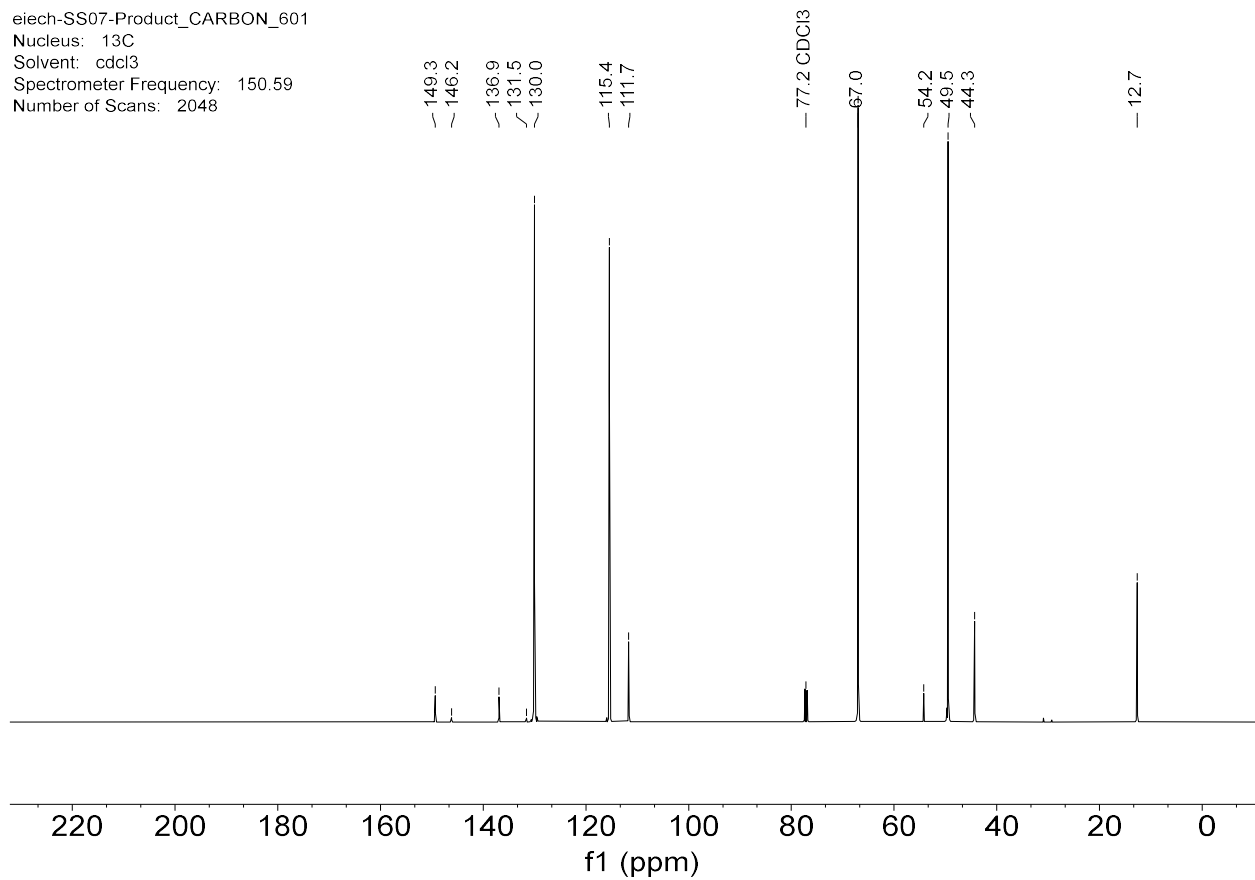
$^{13}\text{C}$  NMR (151 MHz, Chloroform-*d*)  $\delta$  149.3 (q), 146.2 (q), 136.9 (q), 131.5 (q), 130.0 (superimposed 4-C, 6-C), 115.4 (3-C), 111.7 (7-C), 67.0 (1-C), 54.2 (5-C), 49.5 (2-C), 44.3 (8-C), 12.7 (9-C).

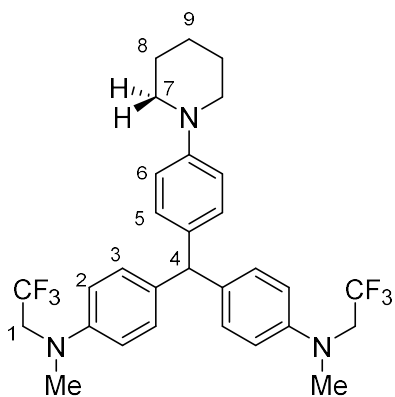
HR-MS (EI):  $m/z$  calcd for  $[\text{C}_{31}\text{H}_{39}\text{N}_3\text{O}_2]^+$  485.3037 found: 485.3034.

eiach-SS07-Product\_PROTON\_6013  
Nucleus: 1H  
Solvent: cdcl3  
Spectrometer Frequency: 598.84  
Number of Scans: 8



eiach-SS07-Product\_CARBOON\_601  
Nucleus: 13C  
Solvent: cdcl3  
Spectrometer Frequency: 150.59  
Number of Scans: 2048



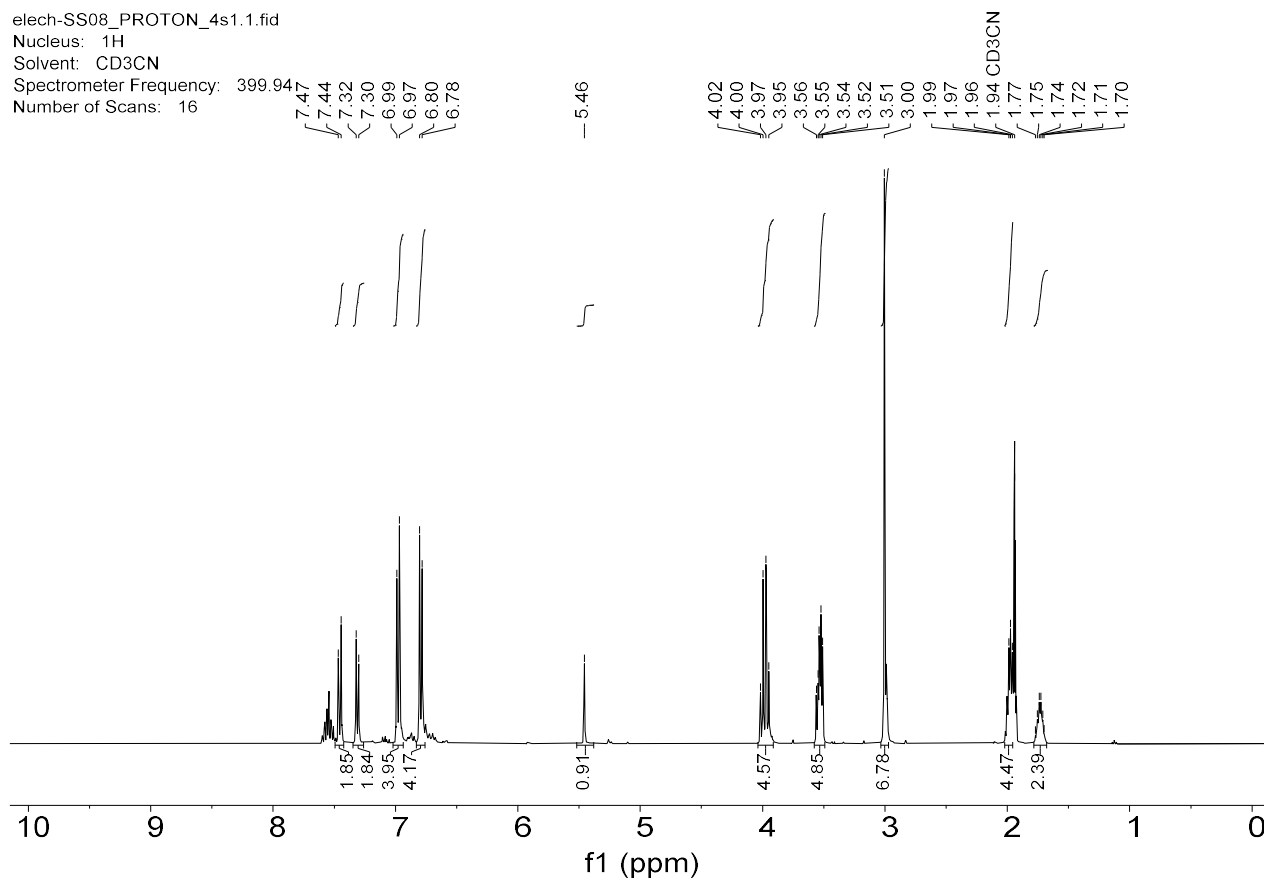


According to GP1 1-phenylpiperidine (**1d**, 3.7 mg, 0.023 mmol) and **2f** (11.0 mg, 0.023 mmol) in dry MeCN (5 mL) yielded after 1 h 4,4'-((4-(piperidin-1-yl)phenyl)methylene)bis(*N*-methyl-*N*-(2,2,2-trifluoroethyl)aniline) (10.9 mg, 0.020 mmol, 87%) as blue powder.

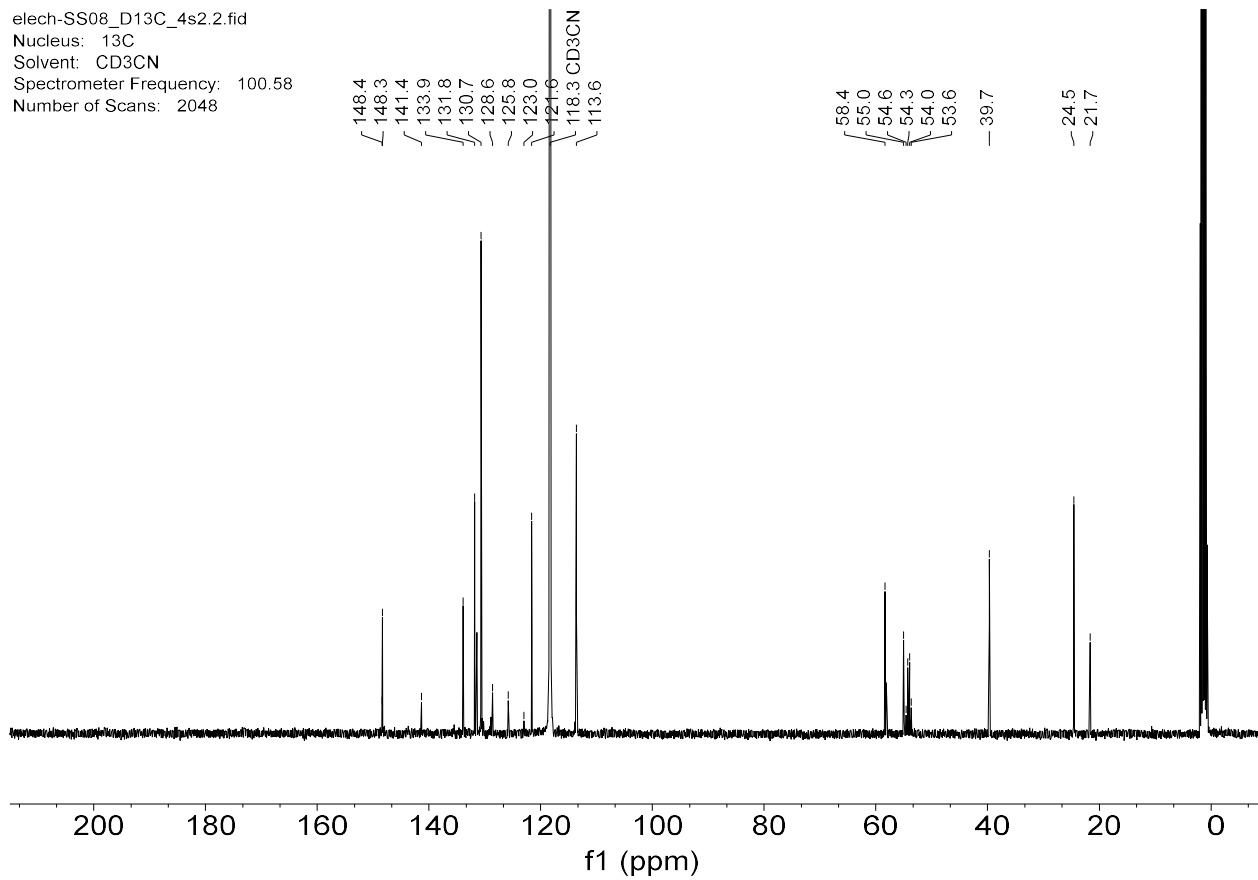
$^1\text{H}$  NMR (400 MHz, Acetonitrile- $d_3$ )  $\delta$  7.46 (d,  $J$  = 8.8 Hz, 2H, 5-H), 7.31 (d,  $J$  = 8.5 Hz, 2H, 6-H), 6.98 (d,  $J$  = 8.6 Hz, 4H, 3-H), 6.79 (d,  $J$  = 8.9 Hz, 4H, 2-H), 5.46 (s, 1H, 4-H), 3.98 (q,  $J$  = 9.3 Hz, 4H, 1-H), 3.59 – 3.49 (m, 4H, 7-H), 3.00 (s, 6H,  $\text{CH}_3$ ), 2.03 – 1.95 (m, 4H, 8-H), 1.73 (h,  $J$  = 5.0, 4.3 Hz, 2H, 9-H).

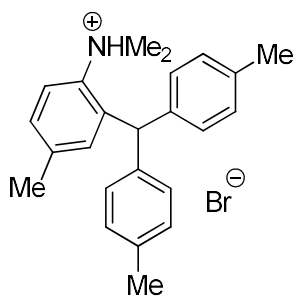
$^{13}\text{C}$  NMR (101 MHz, Acetonitrile- $d_3$ )  $\delta$  148.4 (q), 148.3 (q), 141.4 (q), 133.9 (q), 131.8 (6-C), 131.4, 130.7 (3-C), 127.2 (q,  $J$  = 282.7 Hz,  $\text{CF}_3$ ), 121.6 (5-C), 113.6 (2-C), 58.4 (7-C), 55.0 (4-C), 54.1 (q,  $J$  = 31.9 Hz, 1-C), 39.7 ( $\text{CH}_3$ ), 24.5 (8-C), 21.7 (9-C).

elech-SS08\_PROTON\_4s1.1.fid  
Nucleus: 1H  
Solvent: CD3CN  
Spectrometer Frequency: 399.94  
Number of Scans: 16



elech-SS08\_D13C\_4s2.2.fid  
Nucleus: 13C  
Solvent: CD3CN  
Spectrometer Frequency: 100.58  
Number of Scans: 2048





4,4'-(Bromomethylene)bis(methylbenzene) (22.0 mg, 80.7  $\mu\text{mol}$ ) was solved in  $\text{CD}_3\text{-CN}$  (1 mL) and *N,N*-dimethyl-*para*-toluidine (11.0 mg, 81.4  $\mu\text{mol}$ ) was added and the reaction was monitored by time-resolved  $^1\text{H}$  NMR spectroscopy. The solution became turbid within 1 d. After two weeks 2-(di-*p*-tolylmethyl)-*N,N*,4-trimethylbenzenaminium bromide crystallized suitable for X-ray diffraction analysis. The solvent was decanted and the crystals dried under high vacuum (25.1 mg, 61.2  $\mu\text{mol}$ , 76%).

$^1\text{H}$  NMR (400 MHz,  $\text{DMSO-}d_6$ )  $\delta$  7.70 (s, 1H,  $\text{C}_{\text{Aryl}}\text{H}$ ), 7.26 (s, 1H,  $\text{C}_{\text{Aryl}}\text{H}$ ), 7.13 (d,  $J = 7.7$  Hz, 4H,  $\text{C}_{\text{Aryl}}\text{H}$ ), 6.95 (d,  $J = 7.9$  Hz, 4H,  $\text{C}_{\text{Aryl}}\text{H}$ ), 6.81 (s, 1H,  $\text{C}_{\text{Aryl}}\text{H}$ ), 6.24 (s, 1H,  $\text{Ar}_3\text{CH}$ ), 4.58 (s, 1H,  $\text{NH}$ ), 2.91 (s, 6H,  $\text{NCH}_3$ ), 2.27 (s, 6H  $\text{CH}_3$ ), 2.22 (s, 3H,  $\text{CH}_3$ ).

$^{13}\text{C}$  NMR (201 MHz,  $\text{DMSO-}d_6$ )  $\delta$  139.0 (q), 135.8 (q), 131.4 (q), 129.0 (superimposed,  $\text{C}_{\text{Aryl}}\text{H}$ ), 121.1 (q), 47.6 ( $\text{Ar}_3\text{CH}$ ), 47.0, 20.7 ( $\text{CH}_3$ ), 20.6 ( $\text{CH}_3$ ).

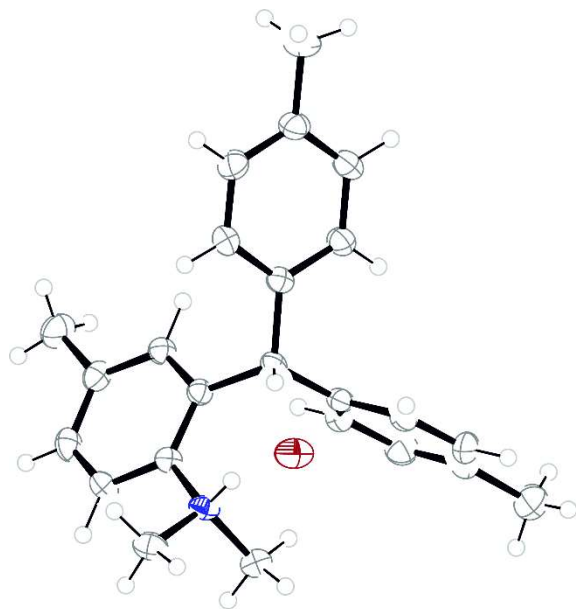
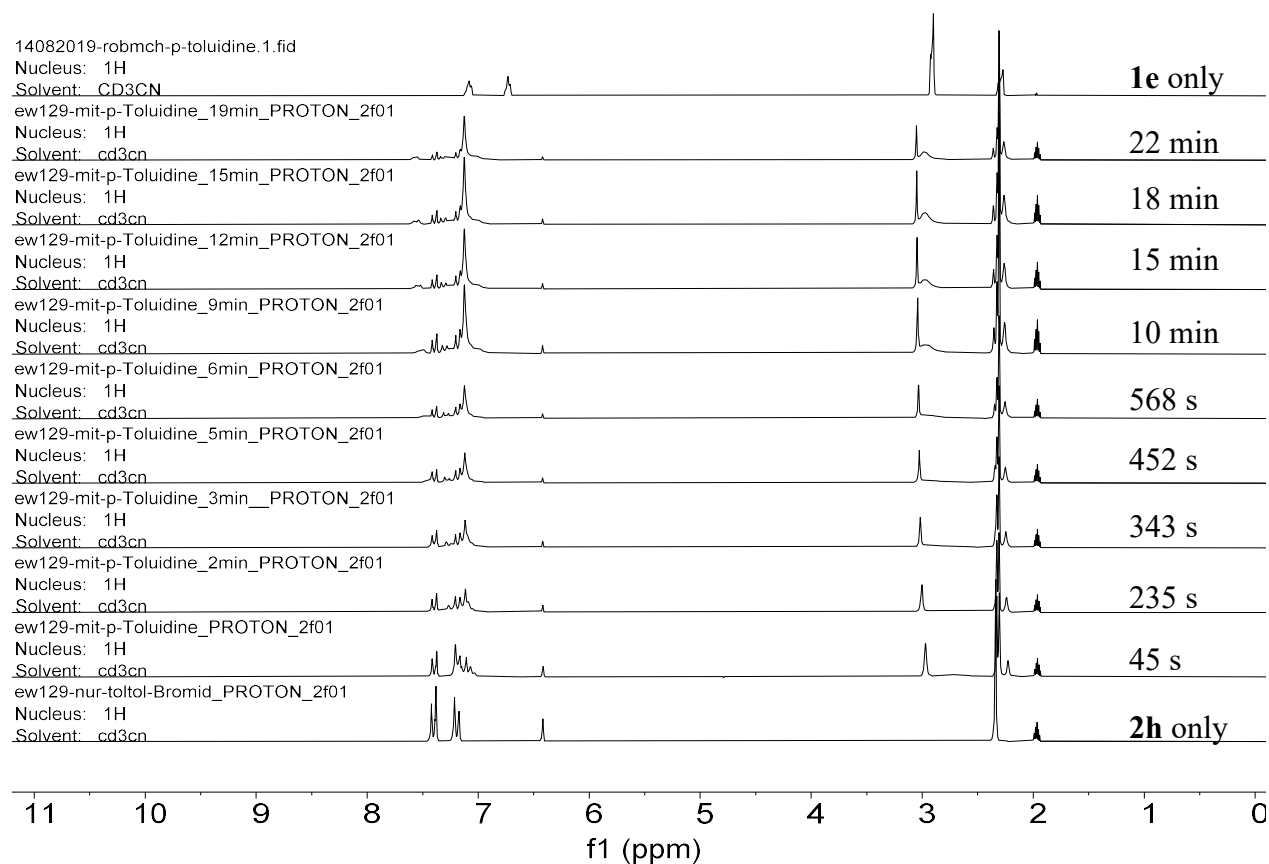
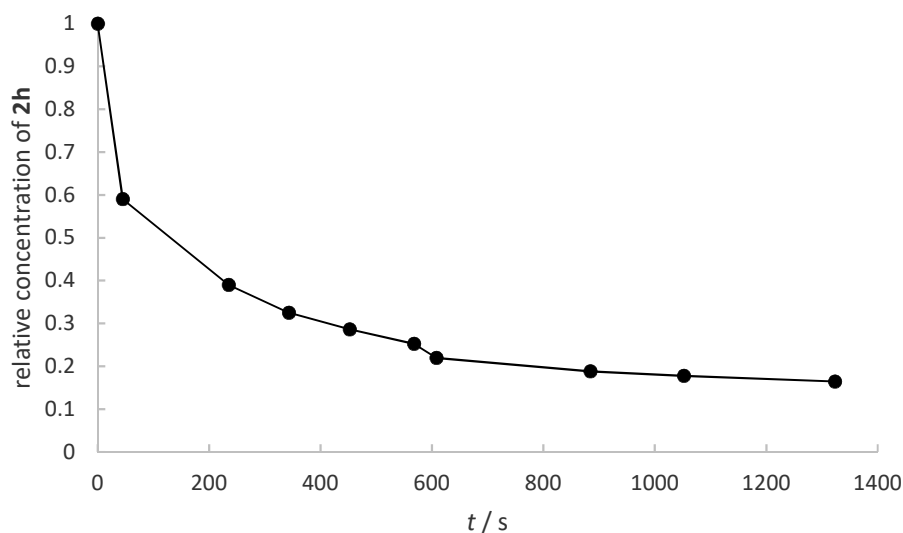
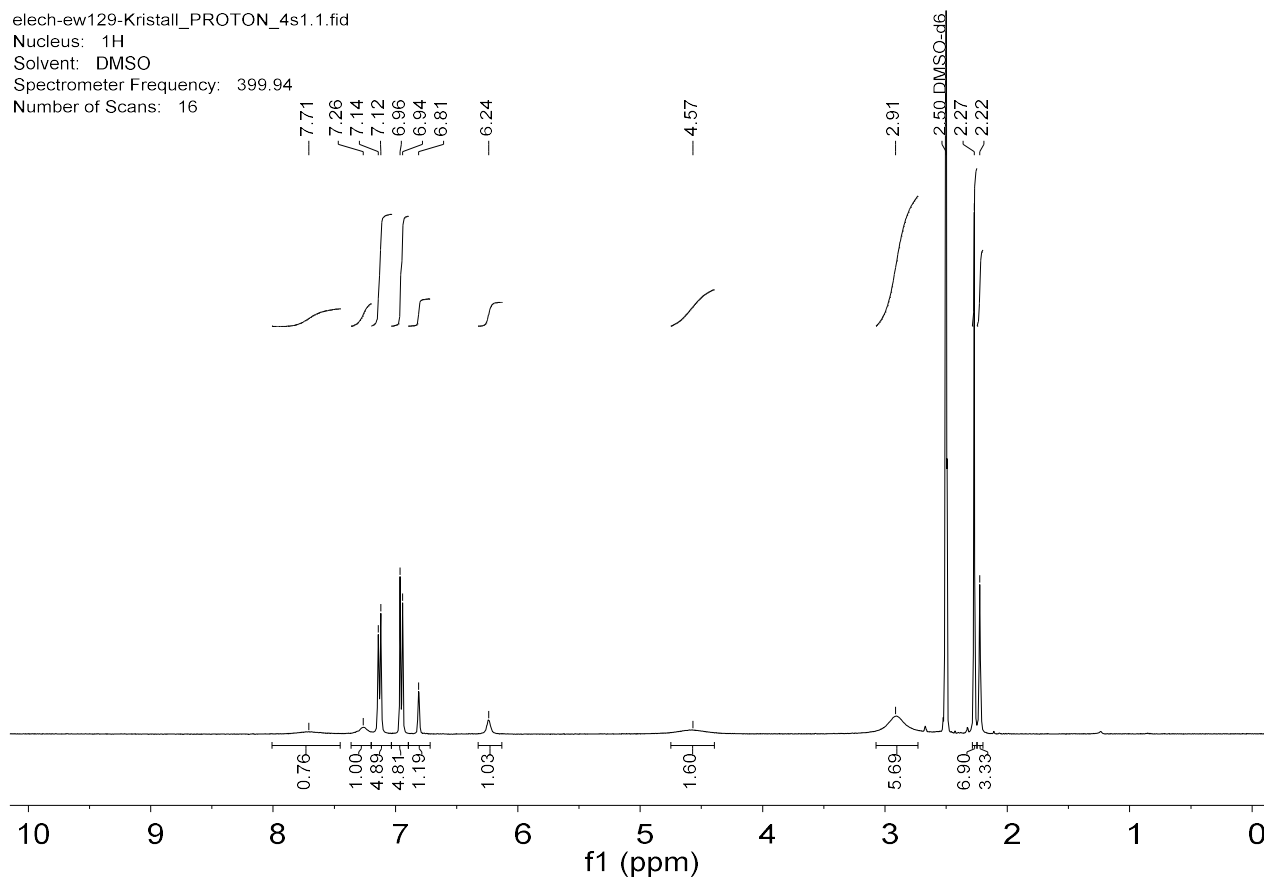


Figure S5: X-ray structure of 2-(di-*p*-tolylmethyl)-*N,N*,4-trimethylbenzenaminium bromide. Shown is one from two symmetric units. Thermal ellipsoids are drawn at the 50% probability level.

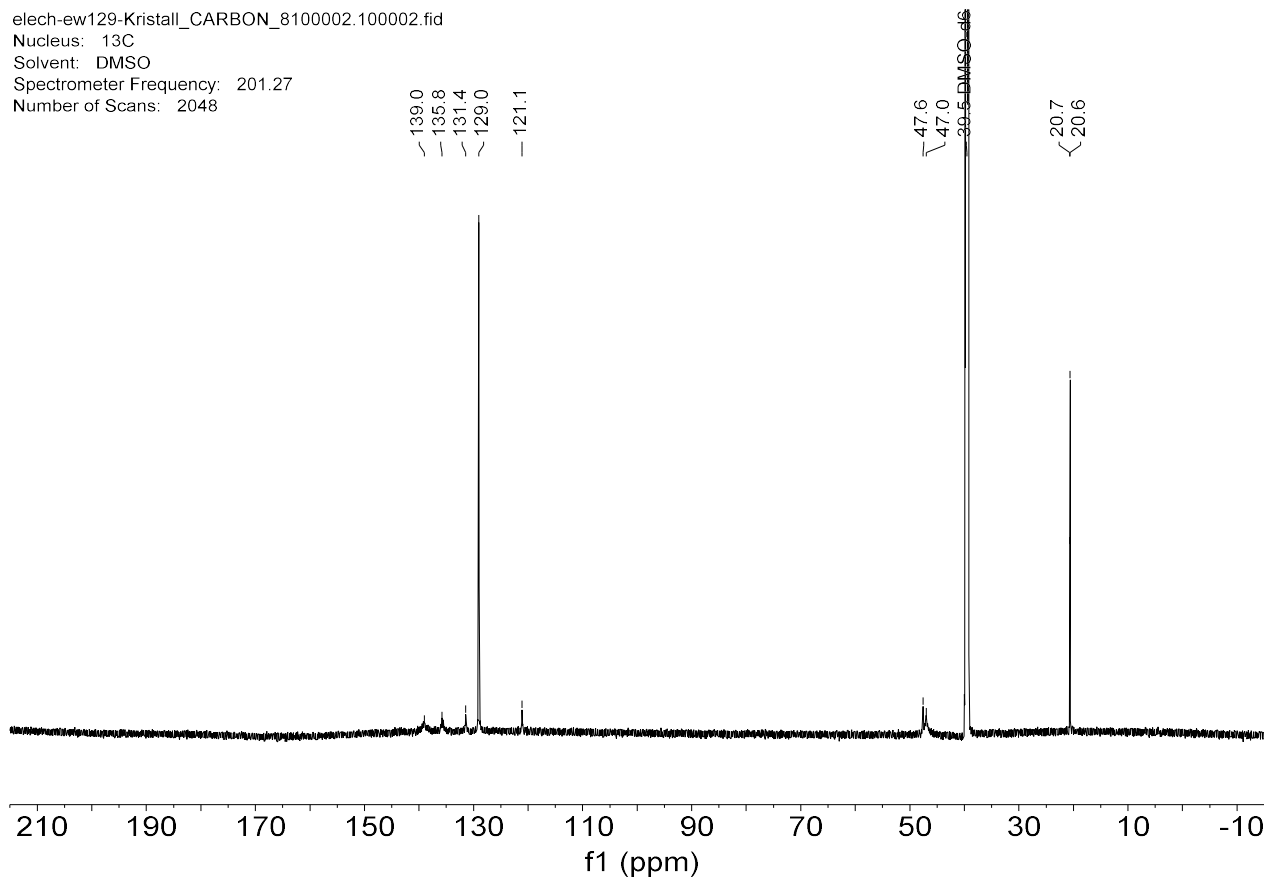
The remaining relative concentration of **2h** was determined by following the integral of the resonance at 6.40 ppm and normalizing it to the integral of the resonances of the solvent ( $\text{CD}_x\text{H}_y\text{CN}$ , q at 1.94 ppm) as reference.  $[\text{4,4'-(bromomethylene)bis(methylbenzene)}]_0 \approx 80.7\text{mM}$ ,  $[\text{N,N-dimethyl-para-toluidine}]_0 \approx 81.4\text{ mM}$ . All  $^1\text{H}$  NMR spectra were measured at 200 MHz.



elech-ew129-Kristall\_PROTON\_4s1.1.fid  
Nucleus: 1H  
Solvent: DMSO  
Spectrometer Frequency: 399.94  
Number of Scans: 16



elech-ew129-Kristall\_CARBON\_8100002.100002.fid  
Nucleus: 13C  
Solvent: DMSO  
Spectrometer Frequency: 201.27  
Number of Scans: 2048



## 16. References

- [1] D. G. Truhlar, Y. Zhao, *Theor. Chem. Acc.* **2008**, *120*, 215-241.
- [2] *Schrödinger, MACROMODEL 9.7 2009.*
- [3] a) S. Ehrlich, L. Goerigk, S. Grimme, *J. Comp. Chem.* **2011**, *32*, 1456-1465; b) L. Goerigk, S. Grimme, *J. Chem. Theory Comp.* **2011**, *7*, 291-309.
- [4] a) Y. Wei, T. Singer, H. Mayr, G. N. Sastry, H. Zipse, *J. Comp. Chem.* **2008**, *29*, 291-297; b) C. Lindner, B. Maryasin, F. Richter, H. Zipse, *J. Phys. Org. Chem.* **2010**, *23*, 1036-1042.
- [5] H. Mayr, J. Ammer, M. Baidya, B. Maji, T. A. Nigst, A. R. Ofial, T. Singer, *J. Am. Chem. Soc.* **2015**, *137*, 2580-2599.
- [6] J. Tomasi, B. Mennucci, R. Cammi, *Chem. Rev.* **2005**, *105*, 2999-3094.
- [7] A. V. Marenich, C. J. Cramer, D. G. Truhlar, *J. Phys. Chem. B* **2009**, *113*, 6378-6396.
- [8] Gaussian 09, Revision C.01 or Revision D.01, M. J. Frisch, G. W. Trucks, H. B. Schlegel, G. E. Scuseria, M. A. Robb, J. R. Cheeseman, G. Scalmani, V. Barone, G. A. Petersson, H. Nakatsuji, X. Li, M. Caricato, A. Marenich, J. Bloino, B. G. Janesko, R. Gomperts, B. Mennucci, H. P. Hratchian, J. V. Ortiz, A. F. Izmaylov, J. L. Sonnenberg, D. Williams-Young, F. Ding, F. Lipparini, F. Egidi, J. Goings, B. Peng, A. Petrone, T. Henderson, D. Ranasinghe, V. G. Zakrzewski, J. Gao, N. Rega, G. Zheng, W. Liang, M. Hada, M. Ehara, K. Toyota, R. Fukuda, J. Hasegawa, M. Ishida, T. Nakajima, Y. Honda, O. Kitao, H. Nakai, T. Vreven, K. Throssell, J. A. Montgomery, Jr., J. E. Peralta, F. Ogliaro, M. Bearpark, J. J. Heyd, E. Brothers, K. N. Kudin, V. N. Staroverov, T. Keith, R. Kobayashi, J. Normand, K. Raghavachari, A. Rendell, J. C. Burant, S. S. Iyengar, J. Tomasi, M. Cossi, J. M. Millam, M. Klene, C. Adamo, R. Cammi, J. W. Ochterski, R. L. Martin, K. Morokuma, O. Farkas, J. B. Foresman, D. J. Fox, Gaussian, Inc., Wallingford CT, 2016.
- [9] a) M. Cossi, V. Barone, R. Cammi, J. Tomasi, *Chem. Phys. Lett.* **1996**, *255*, 327-335; b) B. Mennucci, J. Tomasi, *J. Chem. Phys.* **1997**, *106*, 5151-5158.
- [10] a) R. Lucius, R. Loos, H. Mayr, *Angew. Chem.* **2002**, *114*, 97-102; b) D. Richter, N. Hampel, T. Singer, A. R. Ofial, H. Mayr, *Eur. J. Org. Chem.* **2009**, 3203-3211; c) O. Kaumanns, R. Lucius, H. Mayr, *Chem. Eur. J.* **2008**, *14*, 9675-9682.
- [11] R. A. da Silva, I. H. S. Estevam, L. W. Bieber, *Tetrahedron Lett.* **2007**, *48*, 7680-7682.
- [12] H. E. Gottlieb, V. Kotlyar, A. Nudelman, *J. Org. Chem.* **1997**, *62*, 7512-7515.
- [13] H. Mayr, T. Bug, M. F. Gotta, N. Hering, B. Irrgang, B. Janker, B. Kempf, R. Loos, A. R. Ofial, G. Remennikov, H. Schimmel, *J. Am. Chem. Soc.* **2001**, *123*, 9500-9512.
- [14] R. J. Mayer, N. Hampel, P. Mayer, A. R. Ofial, H. Mayr, *Eur. J. Org. Chem.* **2019**, 412-421.
- [15] SDDBS No. 5993HSP-43-212, *National Institute of Advanced Industrial Science and Technology (AIST)* **1999**.